

Advances in the research of diabetic retinopathy, volume III

Edited by

Mohd Imtiaz Nawaz and Sara Rezzola

Published in

Frontiers in Endocrinology



FRONTIERS EBOOK COPYRIGHT STATEMENT

The copyright in the text of individual articles in this ebook is the property of their respective authors or their respective institutions or funders. The copyright in graphics and images within each article may be subject to copyright of other parties. In both cases this is subject to a license granted to Frontiers.

The compilation of articles constituting this ebook is the property of Frontiers.

Each article within this ebook, and the ebook itself, are published under the most recent version of the Creative Commons CC-BY licence. The version current at the date of publication of this ebook is CC-BY 4.0. If the CC-BY licence is updated, the licence granted by Frontiers is automatically updated to the new version.

When exercising any right under the CC-BY licence, Frontiers must be attributed as the original publisher of the article or ebook, as applicable.

Authors have the responsibility of ensuring that any graphics or other materials which are the property of others may be included in the CC-BY licence, but this should be checked before relying on the CC-BY licence to reproduce those materials. Any copyright notices relating to those materials must be complied with.

Copyright and source acknowledgement notices may not be removed and must be displayed in any copy, derivative work or partial copy which includes the elements in question.

All copyright, and all rights therein, are protected by national and international copyright laws. The above represents a summary only. For further information please read Frontiers' Conditions for Website Use and Copyright Statement, and the applicable CC-BY licence.

ISSN 1664-8714
ISBN 978-2-8325-6437-0
DOI 10.3389/978-2-8325-6437-0

About Frontiers

Frontiers is more than just an open access publisher of scholarly articles: it is a pioneering approach to the world of academia, radically improving the way scholarly research is managed. The grand vision of Frontiers is a world where all people have an equal opportunity to seek, share and generate knowledge. Frontiers provides immediate and permanent online open access to all its publications, but this alone is not enough to realize our grand goals.

Frontiers journal series

The Frontiers journal series is a multi-tier and interdisciplinary set of open-access, online journals, promising a paradigm shift from the current review, selection and dissemination processes in academic publishing. All Frontiers journals are driven by researchers for researchers; therefore, they constitute a service to the scholarly community. At the same time, the *Frontiers journal series* operates on a revolutionary invention, the tiered publishing system, initially addressing specific communities of scholars, and gradually climbing up to broader public understanding, thus serving the interests of the lay society, too.

Dedication to quality

Each Frontiers article is a landmark of the highest quality, thanks to genuinely collaborative interactions between authors and review editors, who include some of the world's best academicians. Research must be certified by peers before entering a stream of knowledge that may eventually reach the public - and shape society; therefore, Frontiers only applies the most rigorous and unbiased reviews. Frontiers revolutionizes research publishing by freely delivering the most outstanding research, evaluated with no bias from both the academic and social point of view. By applying the most advanced information technologies, Frontiers is catapulting scholarly publishing into a new generation.

What are Frontiers Research Topics?

Frontiers Research Topics are very popular trademarks of the *Frontiers journals series*: they are collections of at least ten articles, all centered on a particular subject. With their unique mix of varied contributions from Original Research to Review Articles, Frontiers Research Topics unify the most influential researchers, the latest key findings and historical advances in a hot research area.

Find out more on how to host your own Frontiers Research Topic or contribute to one as an author by contacting the Frontiers editorial office: frontiersin.org/about/contact

Advances in the research of diabetic retinopathy, volume III

Topic editors

Mohd Imtiaz Nawaz — King Saud University, Saudi Arabia

Sara Rezzola — University of Brescia, Italy

Citation

Nawaz, M. I., Rezzola, S., eds. (2025). *Advances in the research of diabetic retinopathy, volume III*. Lausanne: Frontiers Media SA. doi: 10.3389/978-2-8325-6437-0

Table of contents

- 05 **Editorial: Advances in the research of diabetic retinopathy, volume III**
Mohd Imtiaz Nawaz and Sara Rezzola
- 08 **Discriminating early-stage diabetic retinopathy with subjective and objective perimetry**
Faran Sabeti, Joshua P. van Kleeef, Rakesh M. Iyer, Corinne F. Carle, Christopher J. Nolan, Rong Hui Chia and Ted Maddess
- 20 **Vascular changes of the choroid and their correlations with visual acuity in diabetic retinopathy**
Ruixia Jing, Xiubin Sun, Jimin Cheng, Xue Li and Zhen Wang
- 29 **Association between AST/ALT ratio and diabetic retinopathy risk in type 2 diabetes: a cross-sectional investigation**
Xianhua Li, Wenqing Hao, Sen Lin and Nailong Yang
- 37 **Unveiling the molecular complexity of proliferative diabetic retinopathy through scRNA-seq, AlphaFold 2, and machine learning**
Jun Wang, Hongyan Sun, Lisha Mou, Ying Lu, Zijing Wu, Zuhui Pu and Ming-ming Yang
- 50 **Causal association of circulating metabolites with diabetic retinopathy: a bidirectional Mendelian randomization analysis**
Bo Li, Xu Zhao, Wanrun Xie, Zhenzhen Hong, Ye Cao, Yan Ding and Yi Zhang
- 58 **The L-shape relationship between hemoglobin, albumin, lymphocyte, platelet score and the risk of diabetic retinopathy in the US population**
Ranran Ding, Yusong Zeng, Zhimei Wei, Zitong He, Zhixin Jiang, Jinguo Yu and Caiyun You
- 67 **Correlation between vessel density and thickness in the retina and choroid of severe non-proliferative diabetic retinopathy patients**
Kai He, Selena Wei-Zhang, Ziqi Li, Parhat Kaysar, Tianjing Yang, Zhiyong Sun, Wei Zhou and Hua Yan
- 74 **Levels of asymmetric dimethylarginine in plasma and aqueous humor: a key risk factor for the severity of fibrovascular proliferation in proliferative diabetic retinopathy**
Xinyang Guo, Wei Jin and Yiqiao Xing
- 83 **Cell and molecular targeted therapies for diabetic retinopathy**
Shivakumar K. Reddy, Vasudha Devi, Amritha T. M. Seetharaman, S. Shailaja, Kumar M. R. Bhat, Rajashekhar Gangaraju and Dinesh Upadhy

- 99 **Transcriptome analysis combined with Mendelian randomization screening for biomarkers causally associated with diabetic retinopathy**
Junyi Liu, Jinghua Li, Yongying Tang, Kunyi Zhou, Xueying Zhao, Jie Zhang and Hong Zhang
- 115 **Relationship of fibroblast growth factor 21, Klotho, and diabetic retinopathy: a meta-analysis**
Yanhua Jiang, Weilai Zhang, Yao Xu, Xiandong Zeng and Xin Sun
- 123 **Association between rest-activity rhythm and diabetic retinopathy among US middle-age and older diabetic adults**
Zhijie Wang, Mengai Wu, Haidong Li and Bin Zheng
- 133 **Effects of mesenchymal stromal cells and human recombinant Nerve Growth Factor delivered by bioengineered human corneal lenticule on an innovative model of diabetic retinopathy**
Letizia Pelusi, Jose Hurst, Nicola Detta, Caterina Pipino, Alessia Lamolinara, Gemma Conte, Rodolfo Mastropasqua, Marcello Allegretti, Nadia Di Pietrantonio, Tiziana Romeo, Mona El Zarif, Mario Nubile, Laura Guerricchio, Sveva Bollini, Assunta Pandolfi, Sven Schnichels and Domitilla Mandatori
- 148 **Genetically mimicked effects of thyroid dysfunction on diabetic retinopathy risk: a 2-sample univariable and multivariable Mendelian randomization study**
Junlin Ouyang, Ling Zhou, Qing Wang and Wei Yan
- 158 **Recent advances and applications of optical coherence tomography angiography in diabetic retinopathy**
Qing Zhang, Di Gong, Manman Huang, Zhentao Zhu, Weihua Yang and Gaoen Ma



OPEN ACCESS

EDITED AND REVIEWED BY
Åke Sjöholm,
Gävle Hospital, Sweden

*CORRESPONDENCE
Mohd Imtiaz Nawaz
✉ mnawaz@ksu.edu.sa

RECEIVED 14 May 2025

ACCEPTED 16 May 2025

PUBLISHED 28 May 2025

CITATION

Nawaz MI and Rezzola S (2025) Editorial:
Advances in the research of diabetic
retinopathy, volume III.
Front. Endocrinol. 16:1628562.
doi: 10.3389/fendo.2025.1628562

COPYRIGHT

© 2025 Nawaz and Rezzola. This is an open-access article distributed under the terms of the [Creative Commons Attribution License \(CC BY\)](#). The use, distribution or reproduction in other forums is permitted, provided the original author(s) and the copyright owner(s) are credited and that the original publication in this journal is cited, in accordance with accepted academic practice. No use, distribution or reproduction is permitted which does not comply with these terms.

Editorial: Advances in the research of diabetic retinopathy, volume III

Mohd Imtiaz Nawaz^{1,2*} and Sara Rezzola³

¹Department of Ophthalmology, College of Medicine, King Saud University, Riyadh, Saudi Arabia, ²Dr. Nasser Al-Rashid Research Chair in Ophthalmology, Abdulaziz University Hospital, Riyadh, Saudi Arabia, ³Department of Molecular and Translational Medicine, University of Brescia, Brescia, Italy

KEYWORDS

diabetic retinopathy (DR), biomarkers, Mendelian randomization (MR) analysis, optical coherence tomography angiography (OCTA), predictive risk model, therapeutic targets

Editorial on the Research Topic

Advances in the research of diabetic retinopathy, volume III

Diabetic Retinopathy (DR) is a major neurovascular disorder of the retina that causes serious vision loss in the working-age population worldwide. The long-term effects of diabetes mellitus initiate multiple dysregulated metabolic pathways in the retina. Subsequently, the onset and progression of DR engage the simultaneous involvements of early neurodegenerative events, oxidative stress, inflammation, and angiogenesis, finally culminating in irreversible fibrotic changes (1, 2).

Surprisingly, the appearance of clinical manifestation of DR takes several years, making the early detection and the diagnosis difficult for clinicians. In addition, current treatment interventions for advanced proliferative DR (PDR) – including vitreous hemorrhage, macular edema, formation of the epiretinal membrane, and retinal neovascularization – are also limited. Among available treatment strategies, vitrectomy and laser photocoagulation represent the traditional approach for managing PDR-associated vision-threatening conditions (3). Moreover, breakthroughs in understanding the starring role of major angiogenic mediator Vascular Endothelial Growth Factor (VEGF) in the initiation and progression of DR-associated pathogenesis have led to the development of anti-VEGF drugs (e.g., pegaptanib, bevacizumab, ranibizumab, and aflibercept/VEGF Trap-Eye) as therapies for PDR management (1, 3). Indeed, VEGF is considered a key players in the pathophysiological mechanisms underlying PDR. Unfortunately, each treatment strategy has its limitations. Likewise, vitrectomy and laser photocoagulation are invasive and destructive procedures. Similarly, anti-VEGF drugs or corticosteroids are limited by short duration of action, a poor response in a significant percentage of patients, and the presence of adverse side effects (4, 5). Additionally, interventions for early-stage DR are also inadequate.

Thus, thinking outside the box to improve our knowledge of DR pathogenesis and corresponding management strategies, future research should (i) re-evaluate existing and/or explore new molecular and pathophysiological pathways, possibly at different stages of the disease; (ii) develop innovative approaches for early detection and cost-effective strategies, with the aim to manage DR at its earliest stage, rather than waiting for the onset of non-manageable forms of vision-threatening lesions.

Given the overwhelming success of the previous two editions of the Research Topic *Advances in the Research of Diabetic Retinopathy* (6, 7), and the ongoing research advancements in the field, we launched *Volume III* of the edition. The goal was to compile a dossier highlighting new and exciting experimental evidence to advance the understanding of retinal vascular damage and its underlying cellular and molecular mechanisms.

In response to this purpose, *Volume III* attracted numerous exciting original articles and reviews. Notably, the volume includes several contributions discussing emerging therapeutic strategies for DR managing.

In this frame, a significant work by [Sabeti et al.](#) developed a sensitive functional test to investigate the effects of early-stage DR on visual function across the central and peripheral retina, using two multifocal pupillographic objective perimetry (mfPOP) stimulus methods. The results of this study demonstrate the utility and advantage of mfPOP in detecting early changes in visual function in type 2 diabetes (T2D) patients.

Other methods, including meta-analysis, multivariable Mendelian randomization (MR) analysis, application of advanced machine learning, and cross-sectional retrospective investigations, represent alternative strategies for predicting correlations between molecular variables and the degree of DR in T2D patients.

Using meta-analysis, [Jiang et al.](#) and [Ouyang et al.](#) demonstrated significant associations between fibroblast growth factor 21 (FGF21) or thyroid dysfunction and DR, respectively. Fully characterizing their role may significantly contribute to understanding the pathogenesis of DR.

In a study by [Wang et al.](#), the molecular complexity of PDR was unveiled employing single-cell RNA sequencing (scRNA-seq), AlphaFold 2, and machine learning methods. This study deepened our understanding of oxidative stress-related genes - ALKBH1, PSIP1, and ATP13A2 - which could serve as biomarkers and enhance both diagnostic and therapeutic strategies for PDR.

Similarly, bioinformatic analysis of a public database may offer another tool to gain novel insight into potential biomarkers that may play a role in DR pathogenesis. For instance, [Liu et al.](#) identified three genes (OSER1, HIPK2, and DDRGK1) as potential biomarkers in DR pathogenesis. The value of these types of studies lies also in their potential to assist pharmaceutical companies in rapidly identifying biomarker-targeting strategies for DR management.

Remarkably, researchers have also been working tirelessly to identify correlations between novel molecular variables and DR progression. In this context, a cross-sectional study led by [Ding et al.](#), demonstrated that the HALP score obtained by measuring the serum levels of hemoglobin, albumin, lymphocyte, and platelet, has an L-shaped correlation with the risk of DR. In addition, based on the well-known roles of Aspartate aminotransferase (AST) and Alanine aminotransferase (ALT) in metabolic and inflammatory processes, a study reported a positive association between the AST/ALT ratio and presence of DR, suggesting that clinical scores may contribute to early detection, risk stratification, and timely interventions in DR patients ([Li et al.](#)).

Even though the retina is a highly metabolically active tissue, there is still a significant gap in study about the relationship between

metabolites and the initiation and progression of DR. In an attempt to fill some gap in this area, [Li et al.](#) utilized open-access genome-wide association studies (GWAS) database to identify potential metabolites involved in the pathogenesis of DR. This Mendelian randomization study suggests that 9 metabolites were negatively associated with the risk of DR, while two metabolites, i.e., 5-hydroxymethyl-2-furoylcarnitine and the glutamate-to-alanine ratio, may be associated with an increased risk of DR.

A real-world study by [Guo et al.](#) investigated arginine pathway metabolites by utilizing plasma and aqueous humor samples from PDR patients. This study showed that among the arginine pathway metabolites (L-arginine, asymmetric dimethylarginine (ADMA), L-ornithine, and L-citrulline) ADMA levels were elevated both in plasma and aqueous humor compared to the control patients, positively correlating with the severity of fibrovascular proliferation in PDR. These findings indicate that ADMA could represent a risk factor for severe PDR. Thus, future research assessing the impact of modulating ADMA levels on PDR development is warranted.

Recent advances in scanning optical coherence tomography angiography (OCTA), a non-invasive imaging technique, suggests its potential as valuable clinical tool for detecting early diabetes-induced retinal and choroidal microvasculature changes in DR patients. In this frame, a review article by [Zhang et al.](#) discussed in detail the OCTA's imaging principles, its applications in detecting DR lesions, and its diagnostic advantages over fundus fluorescein angiography.

Further supporting the clinical usefulness of OCTA, [Jing et al.](#) demonstrated that a decrease in the choroidal vascularity index (CVI) over the course of diabetes correlates with visual impairment, indicating that CVI could serve as a reliable imaging biomarker to monitor the progression of DR. Similarly, [He et al.](#) showed a decrease in retinal and choroidal thickness as well as vessel density (VD), with a strong correlation between tissue thickness and VD in patients with non-PDR. In conclusion, these and other similar studies highlight the significance of OCTA-derived parameters as a predictive indicator of the severity of DR, providing a promising strategy for the early diagnosis and intervention of DR.

As stated above, several therapeutic approaches have been developed over the years to manage DR. In this context, [Reddy et al.](#) critically reviewed the benefits and limitations of existing DR management strategies. Among emerging treatments, cell-based therapies, for instance transplantation or cell engineering, are gaining interest as new approaches. For example, [Pelusi et al.](#) evaluated the effects of mesenchymal stromal cells (MSCs) derived from human amniotic fluids (hAFSCs) and recombinant human nerve growth factor (rhNGF), delivered via bioengineered human corneal lenticule (hCL) in an *ex vivo* porcine neuroretinal explant model exposed to high glucose (HG). Their findings suggest that hAFSCs and rhNGF can modulate key molecular mechanisms involved in DR, and that bioengineered hCLs may represent a promising platform for ocular drug delivery. In addition, the use of porcine neuroretinal explants treated with HG could be a useful model to reproduce *ex vivo* DR pathophysiology.

Finally, several studies have demonstrated that changes in the environment around or lifestyle modifications can alter circadian rhythm that could, in turn, accelerate diabetes-related complications. Accordingly, data from a recent study by Wang et al. suggests that maintaining a more regular sleep-activity cycle might mitigate the risk of DR development. Thus, beyond conventional clinical strategies, promoting a circadian rhythm stability and increasing diurnal activity may effectively mitigate the risk of progression of DR and diabetes-associated complications at large in a non-pharmacological manner.

In conclusion, *Volume III* of this Research Topic offers new insights and novel valuable data toward understanding the early retinal vascular damage and the pathological mechanism underlying the onset and progression of DR. The use of a high-end predictive models could provide a wealth of knowledge into the early assessment and pathological grading of DR. Furthermore, contributions focused on the identification and characterization of novel potential biomarkers could open new therapeutic avenues for the management of DR.

The editors of this Research Topic believe that the collection of articles presented in this volume represents a valuable addition to the existing body of clinical and basic research on DR. However, as scientific knowledge evolves without boundaries, the editors encourage more interdisciplinary research aimed at improving early diagnosis of the disease and developing of cost-effective treatment strategies for the management of DR.

Author contributions

MN: Supervision, Validation, Conceptualization, Writing – review & editing, Writing – original draft. SR: Conceptualization, Writing – review & editing, Validation.

References

1. Nawaz IM, Rezzola S, Cancarini A, Russo A, Costagliola C, Semeraro F, et al. Human vitreous in proliferative diabetic retinopathy: Characterization and translational implications. *Prog Retin Eye Res.* (2019) 72:100756. doi: 10.1016/j.preteyeres.2019.03.002
2. Wei L, Sun X, Fan C, Li R, Zhou S, Yu H. The pathophysiological mechanisms underlying diabetic retinopathy. *Front Cell Dev Biol.* (2022) 10:963615. doi: 10.3389/fcell.2022.963615
3. Sadikan MZ, Abdul Nasir NA. Diabetic retinopathy: emerging concepts of current and potential therapy. *Naunyn Schmiedeberg Arch Pharmacol.* (2023) 396(12):3395–406. doi: 10.1007/s00210-023-02599-y
4. Kieran MW, Kalluri R, Cho YJ. The VEGF pathway in cancer and disease: responses, resistance, and the path forward. *Cold Spring Harb Perspect Med.* (2012) 2:a006593. doi: 10.1101/cshperspect.a006593
5. van Wijngaarden P, Qureshi SH. Inhibitors of vascular endothelial growth factor (VEGF) in the management of neovascular age-related macular degeneration: a review of current practice. *Clin Exp Optom.* (2008) 91:427–37. doi: 10.1111/j.1444-0938.2008.00305.x
6. Chakrabarti S, Lanza M, Siddiqui K. Editorial: Advances in the research of diabetic retinopathy. *Front Endocrinol (Lausanne).* (2022) 13:1038056. doi: 10.3389/fendo.2022.1038056
7. Nawaz MI. Editorial: Advances in the research of diabetic retinopathy, volume II. *Front Endocrinol (Lausanne).* (2023) 14:1281490. doi: 10.3389/fendo.2023.1281490

Acknowledgments

This work was supported by the Nasser Al-Rasheed Research Chair in Ophthalmology, Department of Ophthalmology, College of Medicine, King Saud University, Riyadh, Saudi Arabia and by a Fondazione Cariplo “Giovani Ricercatori” Grant to SR.

Conflict of interest

The authors declare that the research was conducted in the absence of any commercial or financial relationships that could be construed as a potential conflict of interest.

The author(s) declared that they were an editorial board member of Frontiers, at the time of submission. This had no impact on the peer review process and the final decision.

Generative AI statement

The author(s) declare that no Generative AI was used in the creation of this manuscript.

Publisher's note

All claims expressed in this article are solely those of the authors and do not necessarily represent those of their affiliated organizations, or those of the publisher, the editors and the reviewers. Any product that may be evaluated in this article, or claim that may be made by its manufacturer, is not guaranteed or endorsed by the publisher.



OPEN ACCESS

EDITED BY

Sara Rezzola,
University of Brescia, Italy

REVIEWED BY

Jason C. Park,
University of Illinois Chicago, United States
Catarina Mateus,
Polytechnic Institute of Porto, Portugal

*CORRESPONDENCE

Faran Sabeti
✉ faran.sabeti@canberra.edu.au

RECEIVED 06 November 2023

ACCEPTED 13 December 2023

PUBLISHED 08 January 2024

CITATION

Sabeti F, van Kleef JP, Iyer RM, Carle CF,
Nolan CJ, Chia RH and Maddess T (2024)
Discriminating early-stage diabetic
retinopathy with subjective
and objective perimetry.
Front. Endocrinol. 14:1333826.
doi: 10.3389/fendo.2023.1333826

COPYRIGHT

© 2024 Sabeti, van Kleef, Iyer, Carle, Nolan,
Chia and Maddess. This is an open-access
article distributed under the terms of the
[Creative Commons Attribution License \(CC BY\)](#).
The use, distribution or reproduction in other
forums is permitted, provided the original
author(s) and the copyright owner(s) are
credited and that the original publication in
this journal is cited, in accordance with
accepted academic practice. No use,
distribution or reproduction is permitted
which does not comply with these terms.

Discriminating early-stage diabetic retinopathy with subjective and objective perimetry

Faran Sabeti^{1,2*}, Joshua P. van Kleef¹, Rakesh M. Iyer³,
Corinne F. Carle¹, Christopher J. Nolan^{3,4}, Rong Hui Chia⁵
and Ted Maddess¹

¹Eccles Institute for Neuroscience, The John Curtin School of Medical Research, The Australian National University, Canberra, ACT, Australia, ²Discipline of Optometry, Faculty of Health, University of Canberra, Canberra, ACT, Australia, ³Department of Endocrinology, The Canberra Hospital, Garran, ACT, Australia, ⁴School of Medicine and Psychology, The Australian National University, Canberra, ACT, Australia, ⁵School of Medicine, University of Western Australia, Crawley, WA, Australia

Introduction: To prevent progression of early-stage diabetic retinopathy, we need functional tests that can distinguish multiple levels of neural damage before classical vasculopathy. To that end, we compared multifocal pupillographic objective perimetry (mfPOP), and two types of subjective automated perimetry (SAP), in persons with type 2 diabetes (PwT2D) with either no retinopathy (noDR) or mild to-moderate non-proliferative retinopathy (mmDR).

Methods: Both eyes were assessed by two mfPOP test methods that present stimuli within either the central $\pm 15^\circ$ (OFA15) or $\pm 30^\circ$ (OFA30), each producing per-region sensitivities and response delays. The SAP tests were 24-2 Short Wavelength Automated Perimetry and 24-2 Matrix perimetry.

Results: Five of eight mfPOP global indices were significantly different between noDR and mmDR eyes, but none of the equivalent measures differed for SAP. Per-region mfPOP identified significant hypersensitivity and longer delays in the peripheral visual field, verifying earlier findings. Diagnostic power for discrimination of noDR vs. mmDR, and normal controls vs. PwT2D, was much higher for mfPOP than SAP. The mfPOP per-region delays provided the best discrimination. The presence of localized rather than global changes in delay ruled out iris neuropathy as a major factor.

Discussion: mfPOP response delays may provide new surrogate endpoints for studies of interventions for early-stage diabetic eye damage.

KEYWORDS

multifocal, type 2 diabetes, diabetic retinopathy, objective perimetry, subjective perimetry, multifocal methods

Introduction

The incidence of type 2 diabetes (T2D) has been rising globally (1), and diabetic retinopathy is a common microvascular complication of this condition. It has been estimated that 10% of persons with diabetes for 15 years or more will develop severe visual impairment, which ultimately affects 90% of persons with diabetes (2, 3). In light of the potential vision loss in the working population, the ability to identify eyes at risk of progression in a clinical setting gains significance (4). It has now been well established by our laboratory and others that changes in visual function occur before the onset of vasculopathy (5–15), suggesting that damage to the neural retina may occur early in the progression to retinopathy, possibly identifying at-risk eyes. This has also been confirmed histologically, with degeneration of retinal glia and neurons occurring before microvascular changes (16, 17). Possible therapeutics, like fenofibrate (18, 19) or candesartan (20), might be provided if we can quantify this early damage accurately enough to manage treatment.

It has been reported that short-wavelength automated perimetry (SWAP) can identify eyes with diabetic macular oedema (DMO) and retinal vasculopathy (21, 22). Matrix perimetry has also been shown to identify functional impairment before the onset of retinopathy (23). The subjective nature of such perimetry methods gives rise to high rates of fixation losses, false positives, and false negatives (24, 25). Such problems reduce the sensitivity and specificity of these methods, lowering their diagnostic utility in the clinic. Standard perimetry also suffers poor reproducibility, related to their tiny stimuli which only test around 0.5% of the assessed visual-field area (26). Objective methods that avoid these problems have been employed, including multifocal electroretinograms (mfERGs) and visual-evoked potentials (mfVEPs) (27, 28). However, these methods require long setup times (29) and have exhibited high inter-subject variability (30). Also, the diagnostic power of these methods in diabetic persons who show no retinopathy is poor (31).

Multifocal pupillographic objective perimetry (mfPOP) measures relative change in pupil responses to many concurrently presented visual-field stimuli providing rapid, objective, and non-invasive visual field testing. The method tracks the severity of retinal dysfunction consistent with the degree of retinal vascular abnormalities in persons with diabetes (9, 11, 32–34). Previously, we have reported that per-region response delays were more informative than per-region sensitivity in persons with T2D (PwT2D), easily discriminating eyes with and without retinopathy (9, 11, 32). mfERG studies have also indicated that abnormalities in regional response delays are diagnostic (14). Delay mfPOP data were also more informative than sensitivity data in persons with type 1 diabetes who had early-stage DR (33). That study found a strong association between metabolic and tissue injury factors such as body mass index (BMI), glycosylated hemoglobin (HbA1c), and creatinine. MfPOP delays are also a good marker of progression or improvement of DMO, and better than Matrix perimetry (32, 34). A recent review of 44 functional and structural measures from 23 studies indicates that mfPOP measures are significantly better at

discriminating normal controls from persons with diabetes without evidence of classical retinopathy (31).

In this study, we investigated the effects of early-stage diabetic retinopathy on visual function across the central and peripheral retina with two mfPOP stimulus methods. Secondary objectives were to determine if changes in mfPOP responses could identify severity of non-proliferative diabetic retinopathy (NPDR) among PwT2D and compare the diagnostic capacity of mfPOP against SWAP and Matrix perimetric testing. The strength of this study is the evaluation of retinal dysfunction in early stages of DR before the onset of retinal vasculopathy with a head-to-head comparison of subjective and objective measures of retinal sensitivity measured on the same patients on the same day.

Methods

Subjects

A total of 35 subjects (mean age \pm SD, 57.5 \pm 11.0 years, 14 female) with T2D were recruited from The Canberra Hospital Endocrinology Department. Exclusion criteria included best corrected visual acuity (BCVA) lower than 6/9; intraocular pressure >21 mmHg; distance refraction outside \pm 5D, cylinder refraction >2D; pregnancy; medications that may affect retinal sensitivity or iris function; and evidence of non-diabetes-related systemic, ocular, or neurological disease that may influence retinal responses. Ethics approval was given by the ACT Health Human Research Committee (eth.7.07.667), and the study complied with the Declaration of Helsinki. All subjects provided informed consent in writing prior to experimentation.

Relevant medical information including duration of diabetes, BMI, systolic and diastolic blood pressure, recent HbA1c, lipid profile, and estimated glomerular filtration rate (eGFR) was recorded. Additional diabetes complications testing included measurement of skin autofluorescence, as a marker of tissue advanced glycation end-product (AGE) accumulation using an AGE reader (DiagnOptics, Groningen, The Netherlands) and biothesiometer testing (Bio-Medical Instrument Company, Newbury, Ohio, USA) to assess peripheral neuropathy. Blood glucose levels (BGL) were measured by a finger-prick point-of-care test after the ophthalmic testing was finished.

All patients underwent a single eye examination including a detailed history, a series of eye tests including BCVA determined using an ETDRS logMAR chart, 24-2 SWAP SITA Fast strategy (Humphrey Field Analyzer; Carl Zeiss Meditec, Inc., Dublin, CA), frequency doubling technology (Matrix) perimetry 24-2 ZEST strategy (Carl Zeiss Meditec, Dublin, Calif.), and optical coherence tomography (Spectralis, HRA+OCT; Heidelberg Engineering, Heidelberg, Germany). Both SWAP and MATRIX perimetry tested the central 24 degrees of the visual field with 54 test stimuli presented to each eye centered on the same locations. Most tests were conducted on the same day unless reasons like fatigue suggested otherwise. When SWAP and Matrix were done on the same day, SWAP was done first as subjects generally find it more

taxing. When the tests were done on different days, the order was randomized. Subjects also underwent fundus photography to determine the presence and severity of NPDR based on the Early Treatment of Diabetic Retinopathy Study (ETDRS) scoring system (35). Grading was performed independently by a single ophthalmologist who was masked to the participant's identities. The eyes of each diabetic patient were subsequently separated into two groups: no NPDR (ETDRS 10; $n = 42$ eyes) and mild/moderate NPDR (ETDRS 34 or 45; $n = 28$ eyes).

mfPOP stimuli and data acquisition

All subjects underwent mfPOP testing with a prototype of the FDA-cleared ObjectiveFIELD Analyzer (OFA; Konan Medical USA, Irvine, CA) which produces perimetric measures of mean defects (MD), pattern standard deviations (PSD), per-region total deviations (TDs), and pattern deviations (PDs), all relative to the OFA's normative data. These measures are like those with the same names in standard automated perimetry. The acronyms and their

definitions those used on for SWAP and Matrix perimetry. Briefly, the TDs are the differences (deviations) from normative data at each visual field location. Negative decibel values indicate poor sensitivity. The PDs are the TDs with the 86th percentile of the TD values subtracted off to compensate for global biases in subject performance. The MD is the mean of the TDs, and the PSD is the standard deviation (SD) of the TDs. In fact, for the HFA and Matrix perimeters, both have spatial weights applied before the mean or SD are calculated. The weights give less emphasis to peripheral locations. The OFA has TDs (and their derived measures) for response delay, that is, the differences from normal delay at each test region.

To compare central to peripheral response characteristics, two OFA stimulus protocols were used to cover either the central $\pm 30^\circ$ (OFA30, Figures 1A, B) or $\pm 15^\circ$ (OFA15, Figure 1D) of the visual field. Both protocols had yellow stimuli with a maximum luminance of 150 cd/m² and 288 cd/m² for OFA30 and OFA15, respectively, and were presented on 10 cd/m² yellow backgrounds. The order of OFA protocol testing was randomized. The exact luminance of each test region was designed to elicit the same amplitude of response in

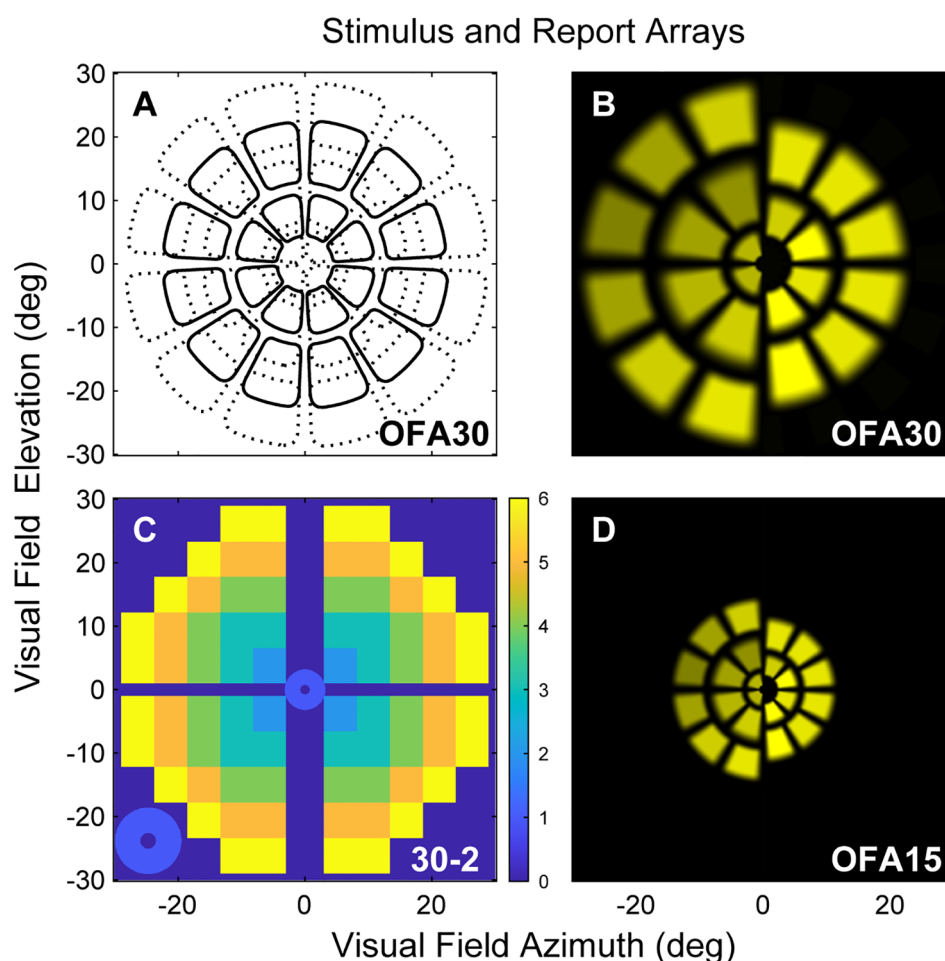


FIGURE 1

(A) Low luminance contours of the OFA30 stimuli showing their slightly overlapping five rings. (B) The left and right halves of rings 1,3,5 and 2,4 to show the luminance balancing of the test stimuli. (C) OFA response data, sensitivity, and delay TDs and PDs were mapped onto a 30-2 pattern with and extra four central regions to create six rings as a function of eccentric (color calibration bar at right). (D) Is similar to B but shows stimuli of the OFA15 method illustrating its test regions are scaled by a factor of 0.5 compared with OFA30.

a normal person, so-called luminance balancing (36). The edges of the individual stimuli were blurred to minimize the effects of misrefraction, but trial lenses were used (37). The pseudo-randomly presented stimuli were each shown for a duration of 33 ms at an average interval of 4 s per region, yielding an aggregate presentation rate of 22/s. Each region was thus tested 90 times. Stimulus duration was 6 min in total, divided into nine segments of 40-s duration with brief resting periods between segments to minimize fatigue.

The stimuli were spatially and temporally sparse, meaning that no overlapping regions were presented simultaneously (38). A newer stimulus presentation method was employed in this study, namely, the *clustered volleys* technique, which greatly enhances the signal-to-noise ratio (39). This method has demonstrated greater power in clinical experiments compared to older mfPOP methods (40), and we have now updated our protocols to utilize these more advanced techniques.

Subjects were asked to fixate on a central red cross, which was adjusted to the patient's habitual distance of eye deviation before each test. The two different stimulus protocols were presented dichoptically on two LCD screens at 60 frames/s. Fusion of the displays into a cyclopean view was assisted by the presentation of a dim starburst radial pattern in the background and a thin pale vertical line passing through the point of fixation. The protocols tested both eyes independently and concurrently, with both pupils recorded. Therefore, both direct and consensual responses were measured at 44 locations per visual field (Figure 1).

A circle was fitted in real time around the pupil to measure its diameter. Parts of the pupil extending 3 mm above the center were not measured to allow for mild ptosis. Blinks and fixation losses were detected by continuous monitoring, and any data recorded during these events was discarded. If the data loss exceeded 15%, the 40-s segment was repeated. This only occurs in around 1 in 200 tests.

Data analysis

Data analysis was performed using MATLAB (2020b MathWorks Inc., Natick, MA). Pupil diameter was normalized to the average pupil diameter during testing for each subject. We used a non-linear regression method to estimate the pupil responses for each region from the raw pupillary waveforms (9). The per-region response amplitudes were then logarithmically transformed to decibels (dB) to stabilize the variance. Time to peak responses for each test region (per-region delays) were also recorded in milliseconds (ms). Direct and consensual responses were recorded from each eye producing 176 response estimates for each participant (2 eyes \times 2 responses per region \times 44 regions = 176), providing 176 per-region sensitivities and 176 delays. These were further transformed to a 30-2 pattern for reporting purposes using a method we have used before providing six rings of reported values (Figure 1C) (41). As discussed above, the OFA software produced summary statistics that are standard in perimetry, including MD, PSD, TDs, and PDs.

We explored effects upon OFA TDs and PDs of factors like age, sex, ETDRS severity, HbA1c levels, and visual field eccentricity. We

used linear mixed effects models (the MATLAB *fitlme* function) to account for factors like the multiple regions within-eye, or eyes within subject, as required. For these models, the intercept (reference value) was the response of male subjects with ETDRS severity 10 (no retinopathy). When age was fitted, it was in decades (10 years) and was referenced to the mean age so it would not affect the intercept. Similar models examined determinants of MD and PSD data.

We compared the diagnostic performance of the perimetric tests utilizing receiver operating characteristic (ROC) analysis. For that, we took eyes of severity ETDRS 10 to be the control eyes (noDR) and examined discrimination of those eyes from eyes scored as ETDRS 34 and 45 (mild-to-moderate NPDR, mmDR). Our earlier studies of early-DR (11) have provided standardized effect sizes around 1.47. Using that and G*Power 3.1.9.7 (University of Kiel, Germany) showed that for an unequal t-test and a target p-value of 0.01, we had a power of 0.99 for a study group size of 22. For each perimeter type, the normative template was the median of the threshold values at each location across control eyes. We felt that more complex normative models that might consider factors like age and sex were not justified given our sample size. In any case, our main interest was the relative diagnostic performance of the different methods. We compared the area under the ROC curves (AUROC) calculated for each of the means of the *first- to twentieth-worst* deviations from normal fields for both amplitudes and delays (9). Here, we report the AUROC values for the six worst regions, since that provided close to the highest AUROC for all methods. For OFA results, we also compared discrimination of 85 matched normal controls of the OFA database (54.8 ± 12.2 years, 49 females) with eyes of the 35 PwT2D subjects (57.5 ± 11.0 years, 14 females).

Results

Participant data

A summary of the subject demographics is presented in Table 1. Between diabetes patient subgroups (noDR and mmDR), the only significant demographic difference was duration of diabetes. There was no significant difference in blood test parameters, biomarkers of diabetic tissue damage (eGFR, AGE, Biothesiometry), or basic optical coherence tomography parameters like the mean macular thickness or retinal nerve fiber layer (RNFL) thickness.

Mean defects and pattern standard deviations

Table 2 examines the mean defect (MD) and pattern standard deviations (PSD) for each perimetry test. There were more values for OFA given the two tests, OFA15 and OFA30, had MD and PSD data for both sensitivities and delays. We examined differences using unpaired t-tests. The only significant differences were for both the OFA15 and OFA30 sensitivities and delays.

TABLE 1 Clinical and demographic information of the persons with diabetes (mean \pm SD).

| Measure | No NPDR OU ETDRS 10 | Mild/Mod NPDR OD or OS ETDRS 34, 45 |
|---|---------------------------|---|
| Subjects | 18 | 17 |
| Age (years) | 55.6 \pm 11.6 | 59.6 \pm 10.2 |
| Sex (% male) | 14/18 (77) | 7/17 (41) |
| Duration of diabetes (years) | 10.5 \pm 6.2 | 18.1 \pm 9.0* |
| HbA _{1c} current (mmol/mol) | 8.3 \pm 1.7 | 8.7 \pm 1.9 |
| HbA _{1c} 5-year mean (mmol/mol) | 8.2 \pm 1.2 | 8.9 \pm 1.7 |
| BMI | 34.3 \pm 4.9 | 31.4 \pm 5.5 |
| Systolic BP | 133.9 \pm 17.1 | 130.9 \pm 12.1 |
| Diastolic BP | 81.3 \pm 11.0 | 76.4 \pm 9.9 |
| Total cholesterol (mmol/L) | 4.12 \pm 0.93 | 4.73 \pm 0.9 |
| Triglycerides (mmol/L) | 2.25 \pm 1.43 | 2.59 \pm 1.4 |
| HDL-cholesterol | 1.09 \pm 0.4 | 1.04 \pm 0.9 |
| LDL-cholesterol | 2.09 \pm 0.8 | 2.39 \pm 1.1 |
| Biothesiometry | 16.8 \pm 12.4 | 22.4 \pm 14.5 |
| AGE reading | 2.60 \pm 0.7 | 2.80 \pm 0.6 |
| BVCA (LogMAR) | 0.00 \pm 0.1 | 0.10 \pm 0.2 |
| OCT central 1 mm Macular thickness (μ m) | 280 \pm 27.1 | 279 \pm 31.2 |
| OCT peripapillary Mean RNFL thickness (μ m) | 0.94 \pm 10.4 | 1.01 \pm 22.9 |

*Refers to statistically significant difference ($p < 0.05$) between DR groups.

TABLE 2 Mean defect (MD) and pattern standard deviations (PSD) of the eyes of the PwT2D (mean \pm SD).

| | No NPDR ETDRS 10 | Mild/Mod NPDR ETDRS 34 or 45 |
|--------------------------------|---------------------|---------------------------------|
| Eyes | 42 | 28 |
| Matrix MD (dB) | -0.63 \pm 2.7 | -1.12 \pm 3.0 |
| Matrix PSD (dB) | 2.88 \pm 0.9 | 3.00 \pm 0.8 |
| SWAP MD (dB) | -2.37 \pm 3.8 | -2.44 \pm 3.7 |
| SWAP PSD (dB) | 3.19 \pm 0.7 | 3.31 \pm 1.0 |
| OFA OFA15 Sensitivity MD (dB) | -6.52 \pm 7.7 | -10.7 \pm 9.0* |
| OFA OFA30 Sensitivity MD (dB) | -4.46 \pm 7.7 | -9.19 \pm 6.3** |
| OFA OFA15 Sensitivity PSD (dB) | 6.70 \pm 1.4 | 6.52 \pm 1.6 |
| OFA OFA30 Sensitivity PSD (dB) | 6.60 \pm 1.6 | 6.28 \pm 1.7 |
| OFA OFA15 Delay MD (ms) | 39.8 \pm 27.4 | 59.9 \pm 7.4* |
| OFA OFA30 Delay MD (ms) | 46.3 \pm 28.8 | 70.7 \pm 24.5** |
| OFA OFA15 Delay PSD (ms) | 29.4 \pm 27.5 | 27.5 \pm 7.4 |
| OFA OFA30 Delay PSD (ms) | 27.9 \pm 5.84 | 34.1 \pm 15.8* |

Statistically significant differences between DR groups: * $p \leq 0.02$, ** $p \leq 0.002$.

We used the demographic data of **Table 1** to examine which of those variables might determine OFA mean defects (MDs) using multivariate mixed effect models (fitting eyes within subjects). We examined both the OFA for sensitivity and delay data. The results for OFA15 and OFA30 were very similar, so we only present the model data for OFA30 variables reporting some significant independent effects (**Table 3**). Only BGL and ETDRS 43 were significant for sensitivity MDs. For delay MDs, the BGL on the day, 5-year mean HbA_{1c}, BMI, and biothesiometry were significant. Biothesiometry was not significant for the OFA15 data.

OFA total deviations and pattern deviations

We next examined how the OFA data varied across the visual field. As an initial analysis, we simply took the means of the TDs across eyes in each of the two categories: noDR and mmDR (**Figure 2**). In these plots, the yellow background corresponds to the expected TD levels for normal controls, i.e., 0, cooler/darker tones represent abnormality as shown on the calibration bars. On average, the more severe eyes showed more extreme changes relative to normal. Peripheral damage was more evident for OFA30 fields (e.g., **Figure 2H**).

With that information in mind, we examined the independent effects determining the TDs using linear mixed effects models (Methods). **Table 4** shows the results for the sensitivity TDs for OFA15 (**Table 4A**) and OFA30 (**Table 4B**). We fitted the six rings of the 30-2 report (**Figure 1C**) as factors to examine the effect of visual field eccentricity, as indicated by **Figure 2**. For both models, the intercept combines the central ring 1 (**Figure 1C**), of male eyes (of the average age) and retinopathy level ETDRS 10 (noDR).

For OFA15, this was -6.90 ± 0.97 dB (relative to the OFA normative data), indicating some global suppression. Response sensitivity was more suppressed in females (-2.57 ± 0.27 dB); however, it increased with age by 2.10 ± 0.12 dB/decade. ETDRS 35 and 43 further suppressed global sensitivity by around -3 dB to -6 dB. The outer rings 4 and 5 showed significant relative hypersensitivity of 1.6 to 1.8 dB (both $p \leq 0.033$). Ring 6 was marginally significantly hypersensitive ($p = 0.071$). For OFA30, there were no significant effects of eccentricity but the outcomes for age, and ETDRS levels 35 and 45 were like those of OFA15.

Table 5 shows the same model fitted to the OFA delay TDs. The intercepts for OFA15 and OFA30 indicated that ETDRS 10 had mean delays of 42.9 ± 3.97 ms and 35.5 ± 3.17 ms, respectively (relative to the OFA normative data). Female responses were slower than males in both tests at 11.1 ± 1.24 and 24.1 ± 1.1 ms slower, respectively ($p < 0.001$). Age was only significant for OFA30, increasing by 2.56 ± 0.44 ms/decade of age ($p < 0.001$). ETDRS 35 eyes were 22 to 27 ms slower relative to ETDRS 10 (both $p < 0.001$). ETDRS 43 eyes produced faster than average delays (-5.98 ± 1.73 ms) for OFA15 and slower than average for OFA30 (4.06 ± 1.51 ms), both $p < 0.007$. The peripheral rings 5 and 6 of OFA30 were slower by 15 ms to 23 ms relative to central ring 1 (both $p < 0.001$).

We fitted the same models to the PDs. These showed few interesting significant effects except for OFA30 delays whose PDs

TABLE 3 Demographic variables determining OFA30 sensitivity and delay mean defect (MD) data.

| A. Sensitivity MDs (db) | | | | |
|-------------------------|----------|-------|--------|---------|
| Name | Estimate | SE | t-stat | p-value |
| (Intercept) | −8.05 | 6.073 | −1.33 | 0.190 |
| ETDRS 35 | −2.71 | 2.155 | −1.26 | 0.214 |
| ETDRS 43 | −7.74 | 2.905 | −2.66 | 0.010* |
| BGL | −0.65 | 0.265 | −2.44 | 0.018* |
| HbA1c 5yr | 0.99 | 0.819 | 1.21 | 0.233 |
| BMI | 0.04 | 0.179 | 0.21 | 0.831 |
| Biothesiometry | 0.10 | 0.068 | 1.44 | 0.154 |
| B. Delay MDs (ms) | | | | |
| Name | Estimate | SE | t-stat | p-value |
| (Intercept) | 55.9 | 16.61 | 3.36 | 0.001* |
| ETDRS 35 | 9.45 | 6.125 | 1.54 | 0.128 |
| ETDRS 43 | −16.2 | 8.826 | −1.83 | 0.072 |
| BGL | 2.86 | 0.716 | 4.00 | 0.000* |
| HbA1c 5yr | −5.04 | 2.248 | −2.24 | 0.028* |
| BMI | −2.24 | 0.514 | −4.35 | <0.001* |
| Biothesiometry | 0.62 | 0.191 | 3.25 | 0.002* |

Statistically significant ($p \leq 0.05$) differences are denoted with *.

showed very similar results to the TD results for rings 5 and 6 of Table 5 (to within 0.5 ms for each).

Diagnostic power

To investigate the diagnostic performance of the total deviations (TDs) from the various stimulus protocols across diabetic groups, we utilized ROC analysis (Methods). Figure 3 shows that response delay TDs (blue) were more diagnostic than those for sensitivities (yellow) especially when the discrimination was between noDR and mmDR: labeled as (noDR cf mmDR) on the x-axis. SWAP, Matrix, and OFA sensitivity-based TDs performed similarly poorly with AUROCs around 60%. OFA15 and OFA30 delays performed similarly well for the noDR/mmDR comparison at $84.0 \pm 3.98\%$ and $82.9 \pm 4.06\%$, respectively. That was remarkable given such early disease stages were being compared. When mild/moderate eyes were compared with 85 normal control eyes from the OFA normative data (Cont cf mmDR in Figure 3 x-axis labels), performance improved somewhat for delays at $86.1 \pm 2.59\%$ and $84.9 \pm 3.00\%$ and for OFA15 and OFA30, but more so for sensitivities at $80.0 \pm 3.77\%$ and $79.3 \pm 3.81\%$. Interestingly sensitivities performed best for the Cont cf. mmDR comparisons relative to noDR eye comparisons.

Discussion

To our knowledge, this study is the first report of a head-to-head comparison of both subjective and objective measures of PwT2D against structural changes in the retina and optic nerve. Our results showed significant differences between the NPDR subgroups for OFA MDs and PSDs but not for SWAP or Matrix perimetry MDs or PSDs. Except for duration of disease, there were no differences in the clinical and demographic data of our two subgroups (Table 1). An earlier study using older mfPOP methods found correlations with complications screening variables like those of Table 1 (33).

The results for OFA and Matrix are consistent with progression analysis of persons with mild DMO, where OFA metrics, but not Matrix, tracked changes in macular thickness (32, 34). A study by Montesanto et al. (15) showed significant loss relative to normal controls using Matrix; however, in our calculation using the published data, the AUROC was only around 60% (31). Other reports have shown no significant change in SWAP mean deviations in PwT2D (8, 42). A study with an achromatic Medmont perimeter showed that persons with no to mild NPDR but who had peripheral neuropathy showed statistically significant peripheral visual field loss (43).

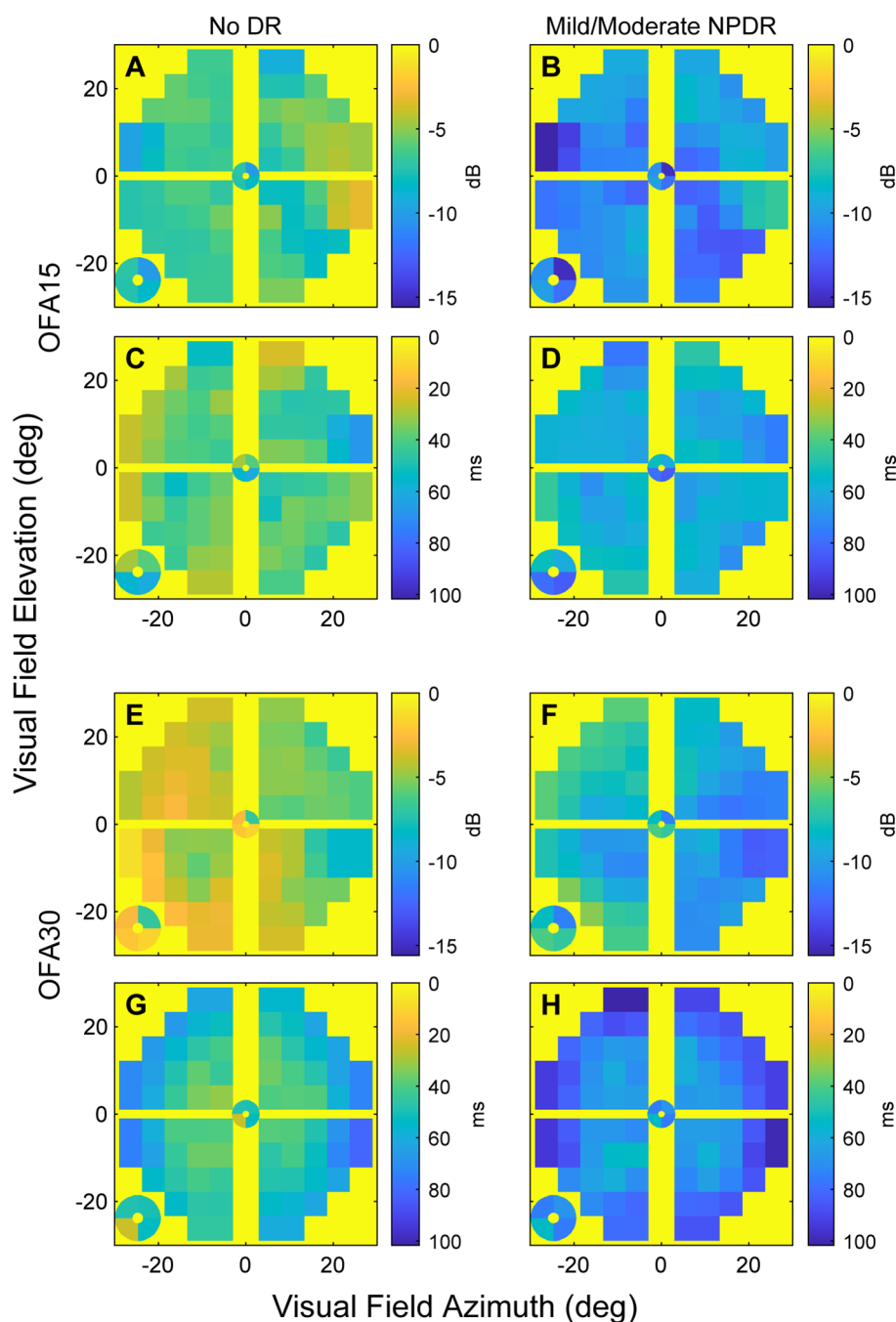


FIGURE 2

The mean sensitivity and delay TD data for OFA15 (A–D) and OFA30 (E–H). The means were computed at each 30–2 field location across the ETDRS 10 eyes (noDR, A, C, E, G), and ETDRS 34 and 45 eyes (mDR, B, D, F, H). From the top down, the rows alternate: sensitivities, delays, sensitivities, delays (n.b. the calibration bar units of dB and ms). Before taking the means, right-eye data were flipped to left eye format; hence, the figures have the nasal field on the right. The four small central locations are magnified and presented at the bottom left of each panel. Generally, mDR eyes (B, D, F, H) showed more severe changes than those with noDR. Peripheral damage appeared to be more evident for OFA30 fields.

As in previous OFA studies of diabetes (9, 11, 32, 44), peripheral retinal features like peripheral hypersensitivity and delay changes were evident (Tables 4, 5). Strictly, the hypersensitivity for rings 4 to 6 for OFA15 (Table 4) were relative to the intercept, but in those rings of OFA15 an average of 1.28 regions/field were flagged as hypertensive at $p \leq 0.05$, but only for ETDRS 10 and 35 eyes. The TDs in those regions averaged $+15.0 \pm 1.9$ dB. These features are

seen in both early-stage diabetic eye damage and age-related macular degeneration (AMD) when measured by multifocal VEPs and mfPOP on the same day in diabetes and AMD (44). Modestly hypersensitive regions have also been observed in three OFA studies of early-stage AMD (40, 45, 46). In exudative AMD, those OFA peripheral measures can also predict good outcomes from (47), or the need for (43), anti-vascular endothelial growth factor (anti-

TABLE 4 Outcomes of linear mixed effects models showing the significant determinants of the OFA sensitivity total deviations (TDs) for: A) the OFA15 test, B) the OFA30 test.

| A | | OFA15 sensitivities | | |
|-------------|----------|---------------------|--------|---------|
| Name | Estimate | SE | t-stat | p-value |
| (Intercept) | −6.90 | 0.696 | −9.92 | <0.001* |
| Female | −2.57 | 0.269 | −9.54 | <0.001* |
| Age | 2.10 | 0.116 | 18.1 | <0.001* |
| Ring 2 | 0.45 | 0.970 | 0.47 | 0.640 |
| Ring 3 | 1.27 | 0.792 | 1.60 | 0.109 |
| Ring 4 | 1.80 | 0.767 | 2.35 | 0.019* |
| Ring 5 | 1.60 | 0.751 | 2.14 | 0.033* |
| Ring 6 | 1.34 | 0.741 | 1.80 | 0.071 |
| ETDRS 35 | −3.23 | 0.293 | −11.0 | <0.001* |
| ETDRS 43 | −6.42 | 0.400 | −16.0 | <0.001* |
| B | | OFA30 sensitivities | | |
| Name | Estimate | SE | t-stat | p-value |
| (Intercept) | −3.21 | 0.792 | −4.06 | <0.001* |
| Female | −0.22 | 0.269 | −0.80 | 0.422 |
| Age | 1.77 | 0.118 | 15.0 | <0.001* |
| Ring 2 | −1.33 | 1.103 | −1.21 | 0.227 |
| Ring 3 | −1.27 | 0.901 | −1.42 | 0.157 |
| Ring 4 | −1.38 | 0.872 | −1.58 | 0.113 |
| Ring 5 | −1.07 | 0.854 | −1.26 | 0.209 |
| Ring 6 | −0.66 | 0.842 | −0.79 | 0.432 |
| ETDRS 35 | −4.07 | 0.295 | −13.8 | <0.001* |
| ETDRS 43 | −7.13 | 0.404 | −17.7 | <0.001* |

Statistically significant ($p \leq 0.05$) differences are denoted with *.

The units are dB except for Age in dB/decade. The Intercept is for males of the mean age and ETDRS 10 and central Ring 1 of the 30-2 pattern (Figure 1C). Negative sensitivities are lower than for ETDRS 10.

VEGF) treatment. Thus, peripheral hypersensitivity may be a feature of the early development of retinal diseases more generally. PwT2D have been reported to have MD values around 3 to 4 dB on SWAP perimetry (8). Unfortunately, unlike OFA, no form of standard automated perimetry reports the significance of any regions of hypersensitivity. In addition, the patchy distribution of damage is consistent with the observed per-region changes being afferent defects as we have shown before (9). Previous OFA studies of diabetes had reported features suggestive of peripheral hypersensitivity (9, 11, 32, 44) due to observation of faster than normal delays peripherally (32). Both may be markers for earlier-stage disease.

An interesting feature of the per-region delays was that the more peripheral rings of the larger OFA30 stimuli showed delays that were 15 to 22 ms slower ($p < 0.001$) than the inner rings. The inner rings of OFA30 correspond to the whole of the OFA15 stimulus, and OFA15 showed no significant delays as a function of stimulus ring. Iris neuropathy would mimic a global change in

delay, i.e., the same change for all test regions. The slower responses to stimuli applied to rings 5 and 6 of OFA30 cannot therefore be due to iris neuropathy given that OFA15 and OFA30 were tested on the same day and in randomized order. It is possible that some of the effects of ETDRS 35 and 43 could be attributed to iris neuropathy but in the case of OFA15, ETDRS 43 eyes were 5.98 ± 1.73 ms quicker than the normative data ($p = 0.001$), whereas in the same eyes on the same day, they were slower for OFA30 by 4.06 ± 1.51 ms ($p = 0.007$). Here, we report (Table 5) that for the two stimuli, female PwT2D produced longer response delays than males by 11.1 ± 1.24 ms ($p < 0.001$) and 24.1 ± 1.12 ms ($p < 0.001$). This may be attributed to the small sample size. Among the 85 control subjects, we took the per-subject means (giving one delay per subject) and a simple linear model indicated that males had 19.9 ± 5.09 ms (mean \pm SE) longer response delays ($p = 0.0002$). Thus, this may be a real effect that requires further study.

For OFA30, biothesiometry was mildly associated with an increased delay MD ($p = 0.002$, Table 3B) but was not associated

TABLE 5 Outcomes of linear mixed effects models showing the significant determinants of the OFA Delay Total Deviations (TDs) for: A) the OFA15 test, B) the OFA30 test.

| A | | OFA15 delays | | |
|-------------|----------|--------------|--------|---------|
| Name | Estimate | SE | t-Stat | p-Value |
| (Intercept) | 42.9 | 3.97 | 10.8 | <0.001* |
| Female | 11.1 | 1.24 | 8.95 | <0.001* |
| Age | −0.27 | 0.50 | −0.55 | 0.584 |
| Ring 2 | −6.29 | 5.49 | −1.15 | 0.252 |
| Ring 3 | −6.10 | 4.48 | −1.36 | 0.173 |
| Ring 4 | −6.11 | 4.34 | −1.41 | 0.159 |
| Ring 5 | −7.12 | 4.25 | −1.67 | 0.094 |
| Ring 6 | −7.16 | 4.19 | −1.71 | 0.088 |
| ETDRS 35 | 27.6 | 1.27 | 21.7 | <0.001* |
| ETDRS 43 | −5.98 | 1.73 | −3.45 | 0.001* |
| B | | OFA30 delays | | |
| Name | Estimate | SE | t-stat | p-value |
| (Intercept) | 35.3 | 3.17 | 11.1 | <0.001* |
| Female | 24.1 | 1.12 | 21.7 | <0.001* |
| Age | 2.56 | 0.44 | 5.86 | <0.001* |
| Ring 2 | −2.17 | 4.39 | −0.49 | 0.621 |
| Ring 3 | −2.82 | 3.59 | −0.79 | 0.431 |
| Ring 4 | 2.65 | 3.47 | 0.76 | 0.446 |
| Ring 5 | 15.3 | 3.40 | 4.48 | <0.001* |
| Ring 6 | 22.7 | 3.35 | 6.78 | <0.001* |
| ETDRS 35 | 22.3 | 1.10 | 20.2 | <0.001* |
| ETDRS 43 | 4.06 | 1.51 | 2.69 | 0.007* |

Statistically significant ($p \leq 0.05$) differences are denoted with *.

The units are ms except for Age in ms/decade. The Intercept is as for Table 2. Positive delays are longer than for ETDRS 10.

with changed sensitivity (Table 3A). Biothesiometry readings were not associated with either sensitivity or delay MD changes for OFA15 (not shown). BMI similarly reduced delay by -2.24 ms per BMI unit ($p < 0.001$). eGFR was not significant for sensitivity or delay for either test (not shown). Overall, metabolic/tissue-damage variables that might be linked to iris neuropathy tended not to add to global delays. By contrast, large changes in global sensitivity and delay were associated with ETDRS 10 (the intercept in Tables 3–5).

As in previous OFA studies of early-stage diabetic eye damage, AUROCs were high (9, 11) and focal changes in response delays were among the most informative measures. Those are correlated with changes in retinal thickness in DMO (32). Here, none of the SWAP, Matrix, or OFA sensitivities produced useable diagnostic power when the noDR and mmDR groups were compared (Figure 3). When compared with normal controls, sensitivities were almost as effective as delays. A recent review of 44

functional and structural measures from 23 studies, which examined diagnostic power for discriminating noDR eyes from control eyes using a range of structural and functional methods, found median AUROCs around 89% for OFA and 60% to 70% for the other methods ($p < 0.0001$). That review included a recent OFA study of young persons with type 1 diabetes, and the overall median value across nine measures from four OFA studies was 89% (31). That included a recent study using new fifth-generation OFA stimuli which test both eyes in <90 s (48). Similar results using the same method have been published for early-stage AMD (49). That rapid test is ideal for testing children and infirm persons.

The high diagnostic power of OFA methods may mean they could be useful for managing DR with newer treatments. Candesartan shows promise in the prevention of earlier-stage retinopathy in T2D patients (20). Fenofibrate is also gaining recognition as a therapy with potential to prevent progression and

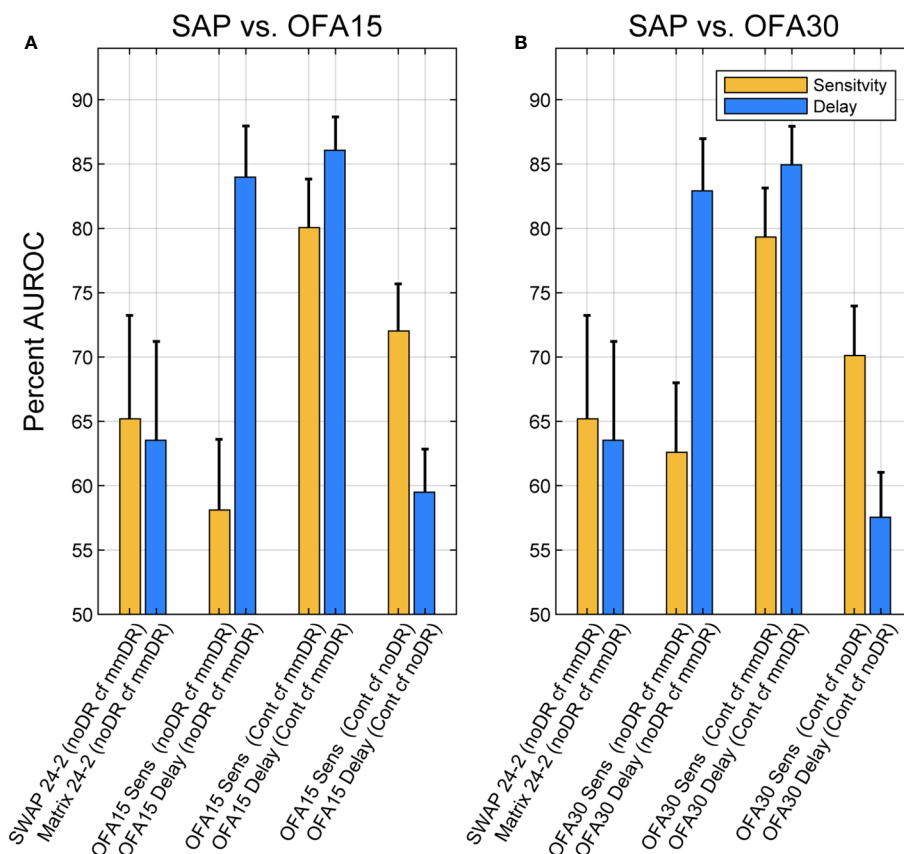


FIGURE 3

Areas under receiver operating characteristic (AUROCs) expressed as percentages for different comparisons of Total Deviations outputs. Blue bars are for delay data, and yellow are for sensitivity data (legend). AUROC of 50% represents chance classification, and an AUC of 100% represents perfect discrimination. The x-axis labels of each plot give the test: SWAP 24-2, Matrix 24-2, OFA15, or OFA30 for Sensitivities (Sens) or Times-to-peak (Delay). The leftmost four comparisons were for discriminating ETDRS 10 eyes from the Mild to Moderate NPDR eyes (ETDRS 34 and 45): (noDR cf mmDR). The rightmost four comparisons were between normal control eyes (Cont) and ETDRS 34 and 45 eyes (mmDR), or Control cf. ETDRS 10 (noDR). The leftmost pair of yellow and blue bars give AUROCs for SWAP and Matrix 24-2 tests. The SAP versus OFA15 (A) and OFA30 (B) methods performed similarly, with delays performing better except for the (Cont cf noDR) comparison where sensitivity was better. The error bars represent SEM.

even reverse earlier stages of DR in T2D (18, 19). Clearly, additional new treatments that target earlier stages of diabetic eye disease are needed and these will need monitoring tools for preclinical early-stage disease and new clinical endpoints. Functional measures are more likely than structural to be able to provide surrogate endpoints that are acceptable to regulatory authorities.

The limitations of our study were the relatively small number of subjects with mild/mod NPDR. Also, patients may have been fatigued during SAP testing due to the series of tests that were conducted at each visit, which may have affected reliability of those tests. Furthermore, OFA test reproducibility was not examined in this study; however, good reproducibility of mfPOP has been demonstrated previously in T2D (9) and glaucoma (50).

The results of this study demonstrate the utility and advantage of mfPOP in detecting changes in visual function in T2D. This

study is the first to complete a direct comparison between objective vs. subjective measures of visual field sensitivity corresponding to varying retinopathy severities. Small-scale longitudinal studies suggest the findings of our cross-sectional studies translate into ability to track disease progression (32, 34), with similar results in AMD (43). With the advent of novel interventions in early DR, more sensitive methods for identifying eyes at risk of progression to the sight threatening stages of DR are needed. The ability to test children with the same rapid tests that adults use (48) might assist in the management of T1D.

Data availability statement

The raw data supporting the conclusions of this article will be made available by the authors, without undue reservation.

Ethics statement

The studies involving humans were approved by ACT Health Human Research Committee (eth.7.07.667). The studies were conducted in accordance with the local legislation and institutional requirements. The participants provided their written informed consent to participate in this study.

Author contributions

FS: Conceptualization, Data curation, Formal Analysis, Writing – original draft, Writing – review & editing. JK: Formal Analysis, Writing – review & editing. RI: Data curation, Supervision, Writing – review & editing. CC: Data curation, Methodology, Writing – review & editing. CN: Conceptualization, Data curation, Supervision, Writing – review & editing. RC: Data curation, Writing – original draft. TM: Conceptualization, Formal Analysis, Writing – review & editing.

Funding

The author(s) declare financial support was received for the research, authorship, and/or publication of this article. NHMRC

1028560, ARC CE0561903, Our Health in Our Hands (OHIOH) ANU intramural grant.

Acknowledgments

Part of these data was presented in an abstract at an Association for Research in Vision and Ophthalmology meeting.

Conflict of interest

TM, JK, CC and FS could earn royalty income from the sale of the OFA.

The remaining authors declare that the research was conducted in the absence of any commercial or financial relationships that could be construed as a potential conflict of interest.

Publisher's note

All claims expressed in this article are solely those of the authors and do not necessarily represent those of their affiliated organizations, or those of the publisher, the editors and the reviewers. Any product that may be evaluated in this article, or claim that may be made by its manufacturer, is not guaranteed or endorsed by the publisher.

References

- Whiting DR, Guariguata L, Weil C, Shaw J. IDF Diabetes Atlas: Global estimates of the prevalence of diabetes for 2011 and 2030. *Diabetes Res Clin Practice* (2011) 94 (3):311–21. doi: 10.1016/j.diabres.2011.10.029
- Glover SJ, Burgess PI, Cohen DB, Harding SP, Hofland HW, Zijlstra EE, et al. Prevalence of diabetic retinopathy, cataract and visual impairment in patients with diabetes in sub-Saharan Africa. *Br J Ophthalmol* (2012) 96(2):156–61. doi: 10.1136/bjo.2010.196071
- Sundling V, Platou CG, Jansson RW, Bertelsen G, Wollo E, Gulbrandsen P. Retinopathy and visual impairment in diabetes, impaired glucose tolerance and normal glucose tolerance: the Nord-Trøndelag Health Study (the HUNT study). *Acta Ophthalmol* (2012) 90(3):237–43. doi: 10.1111/j.1755-3768.2010.01998.x
- Centers for Disease Control. *National diabetes fact sheet*. U.S. Atlanta: Department of Human Services (2005).
- Lobefalo L, Verrotti A, Mastropasqua L, Della Loggia G, Cherubini V, Morgese G, et al. Blue-on-yellow and achromatic perimetry in diabetic children without retinopathy. *Diabetes Care* (1998) 21(11):2003–6. doi: 10.2337/diacare.21.11.2003
- Afrashi F, Erakgun T, Kose S, Ardic K, Montes J. Blue-on-yellow perimetry versus achromatic perimetry in type 1 diabetes patients without retinopathy. *Diabetes Res Clin Pract* (2003) 61(1):7–11. doi: 10.1016/S0168-8227(03)00082-2
- Stavrou EP, Wood JM. Central visual field changes using flicker perimetry in type 2 diabetes mellitus. *Acta Ophthalmol Scand* (2005) 83(5):574–80. doi: 10.1111/j.1600-0420.2005.00527.x
- Nitta K, Saito Y, Kobayashi A, Sugiyama K. Influence of clinical factors on blue-on-yellow perimetry for diabetic patients without retinopathy: comparison with white-on-white perimetry. *Retina* (2006) 26(7):797–802. doi: 10.1097/01.iae.0000244263.98642.61
- Bell A, James AC, Kolic M, Essex RW, Maddess T. Dichoptic multifocal pupillometry reveals afferent visual field defects in early type 2 diabetes. *Invest Ophthalmol Vis Sci* (2010) 51(1):602–8. doi: 10.1167/iops.09-3659
- Jackson GR, Scott IU, Quillen DA, Walter LE, Gardner TW. Inner retinal visual dysfunction is a sensitive marker of non-proliferative diabetic retinopathy. *Br J Ophthalmol* (2012) 96(5):699–703. doi: 10.1136/bjophthalmol-2011-300467
- Sabeti F, Nolan CJ, James AC, Jenkins A, Maddess T. Multifocal pupillometry identifies changes in visual sensitivity according to severity of diabetic retinopathy in type 2 diabetes. *Invest Ophthalmol Vis Sci* (2015) 56(8):4504–13. doi: 10.1167/iops.15-16712
- Gella L, Raman R, Kulothungan V, Saumya Pal S, Ganesan S, Sharma T. Retinal sensitivity in subjects with type 2 diabetes mellitus: Sankara Nethralaya Diabetic Retinopathy Epidemiology and Molecular Genetics Study (SN-DREAMS II, Report No. 4). *Br J Ophthalmol* (2016) 100(6):808–13. doi: 10.1136/bjophthalmol-2015-307064
- Joltikov KA, de Castro VM, Davila JR, Anand R, Khan SM, Farbman N, et al. Multidimensional functional and structural evaluation reveals neuroretinal impairment in early diabetic retinopathy. *Invest Ophthalmol Vis Sci* (2017) 58(6):BIO277–BIO90. doi: 10.1167/iops.17-21863
- McAnany JJ, Park JC. Temporal frequency abnormalities in early-stage diabetic retinopathy assessed by electroretinography. *Invest Ophthalmol Vis Sci* (2018) 59 (12):4871–9. doi: 10.1167/iops.18-25199
- Montesano G, Ometto G, Higgins BE, Das R, Graham KW, Chakravarthy U, et al. Evidence for structural and functional damage of the inner retina in diabetes with no diabetic retinopathy. *Invest Ophthalmol Vis Sci* (2021) 62(3):35. doi: 10.1167/iops.62.3.35
- Fletcher EL, Phipps JA, Ward MM, Puthussery T, Wilkinson-Berka JL. Neuronal and glial cell abnormality as predictors of progression of diabetic retinopathy. *Curr Pharm Des* (2007) 13(26):2699–712. doi: 10.2174/138161207781662920
- Joltikov KA, Sesi CA, de Castro VM, Davila JR, Anand R, Khan SM, et al. Disorganization of retinal inner layers (DRIL) and neuroretinal dysfunction in early diabetic retinopathy. *Invest Ophthalmol Vis Sci* (2018) 59(13):5481–6. doi: 10.1167/iops.18-24955
- Group AS and Group AES, Chew EY, Ambrosius WT, Davis MD, Danis RP, et al. Effects of medical therapies on retinopathy progression in type 2 diabetes. *N Engl J Med* (2010) 363(3):233–44. doi: 10.1056/NEJMoa1001288
- Keech AC, Mitchell P, Summanen PA, O'Day J, Davis TM, Moffitt MS, et al. Effect of fenofibrate on the need for laser treatment for diabetic retinopathy (FIELD study): a randomised controlled trial. *Lancet* (2007) 370(9600):1687–97. doi: 10.1016/S0140-6736(07)61607-9
- Chaturvedi N, Porta M, Klein R, Orchard T, Fuller J, Parving HH, et al. Effect of candesartan on prevention (DIRECT-Prevent 1) and progression (DIRECT-Protect 1) of retinopathy in type 1 diabetes: randomised, placebo-controlled trials. *Lancet* (2008) 372(9647):1394–402. doi: 10.1016/S0140-6736(08)61412-9

21. Agardh E, Stjernquist H, Heijl A, Bengtsson B. Visual acuity and perimetry as measures of visual function in diabetic macular oedema. *Diabetologia* (2006) 49 (1):200–6. doi: 10.1007/s00125-005-0072-8
22. Bengtsson B, Heijl A, Agardh E. Visual fields correlate better than visual acuity to severity of diabetic retinopathy. *Diabetologia* (2005) 48(12):2494–500. doi: 10.1007/s00125-005-0001-x
23. Parravano M, Oddone F, Mineo D, Centofanti M, Borboni P, Lauro R, et al. The role of Humphrey Matrix testing in the early diagnosis of retinopathy in type 1 diabetes. *Br J Ophthalmol* (2008) 92(12):1656–60. doi: 10.1136/bjo.2008.143057
24. Alencar LM, Medeiros FA. The role of standard automated perimetry and newer functional methods for glaucoma diagnosis and follow-up. *Indian J Ophthalmol* (2011) 59(Suppl1):S53–8. doi: 10.4103/0301-4738.73694
25. Liu S, Lam S, Weinreb RN, Ye C, Cheung CY, Lai G, et al. Comparison of standard automated perimetry, frequency-doubling technology perimetry, and short-wavelength automated perimetry for detection of glaucoma. *Invest Ophthalmol Visual Sci* (2011) 52(10):7325–31. doi: 10.1167/iov.11-7795
26. Numata T, Maddess T, Matsumoto C, Okuyama S, Hashimoto S, Nomoto H, et al. Exploring test-retest variability using high-resolution perimetry. *Trans Vis Sci Tech* (2017) 6(5(8)):1–9. doi: 10.1167/tvst.6.5.8
27. Fortune B, Schneck ME, Adams AJ. Multifocal electroretinogram delays reveal local retinal dysfunction in early diabetic retinopathy. *Invest Ophthalmol Visual Sci* (1999) 40(11):2638–51.
28. Chan H-I, Ng Y-f, Chu P-w. Applications of the multifocal electroretinogram in the detection of glaucoma. *Clin Exp Optomet* (2011) 94(3):247–58. doi: 10.1111/j.1444-0938.2010.00571.x
29. Bjerre A, Grigg JR, Parry NR, Henson DB. Test-retest variability of multifocal visual evoked potential and SITA standard perimetry in glaucoma. *Invest Ophthalmol Visual Sci* (2004) 45(11):4035–40. doi: 10.1167/iov.04-0099
30. Klistorner A, Graham SL. Objective perimetry in glaucoma. *Ophthalmology* (2000) 107(12):2283–99. doi: 10.1016/S0161-6420(00)00367-5
31. Rai BB, van Kleef JP, Sabeti F, Vlieger R, Suominen H, Maddess T. Early diabetic eye damage: comparing detection methods using diagnostic power. *Survey Ophthalmol* (2023). doi: 10.1016/j.survophthal.2023.09.002. [Epub ahead of print].
32. Rai BB, Maddess T, Carle CF, Rohan EMF, van Kleef JP, Barry RC, et al. Comparing objective perimetry, matrix perimetry, and regional retinal thickness in early diabetic macular oedema. *Trans Vis Sci Tech* (2021) 10(32):1–12. doi: 10.1167/tvst.10.13.32
33. Sabeti F, Carle CF, Nolan C, Jenkins A, James AC, Baker L, et al. Multifocal pupillographic objective perimetry for assessment of early diabetic retinopathy and generalised diabetes-related tissue injury in persons with type 1 diabetes. *BMC Ophthalmol* (2022) 22(116):1–13. doi: 10.1186/s12886-022-02382-2
34. Sabeti F, Rai BB, van Kleef JP, Carle CF, Rohan EMF, Essex RW, et al. Objective perimetry identifies functional progression and recovery in mild Diabetic Macular Oedema. *PLoS One* (2023). Final Revision. doi: 10.1371/journal.pone.0287319. [Epub ahead of print].
35. Group ETDRSR. Fundus photographic risk factors for progression of diabetic retinopathy: ETDRS report number 12. *Ophthalmology* (1991) 98(5):823–33.
36. Carle CF, James AC, Kolic M, Essex RW, Maddess T. Luminance and colour variant pupil perimetry in glaucoma. *Clin Experiment Ophthalmol* (2014) 42(9):815–24. doi: 10.1111/ceo.12346
37. Phillips S, Stark L. Blur: a sufficient accommodative stimulus. *Doc Ophthalmol* (1977) 43(1):65–89. doi: 10.1007/BF01569293
38. James AC, Ruseckaite R, Maddess T. Effect of temporal sparseness and dichoptic presentation on multifocal visual evoked potentials. *Visual Neurosci* (2005) 22(01):45–54. doi: 10.1017/S0952523805221053
39. Carle CF, James AC, Sabeti F, Kolic M, Essex RW, Chean C, et al. Clustered Volleys stimulus presentation for multifocal objective perimetry. *Trans Vis Sci Tech* (2022) 11(2):1–10. doi: 10.1167/tvst.11.2.5
40. Sabeti F, Maddess T, Essex RW, Saikal A, James AC, Carle CF. Multifocal pupillography in early age-related macular degeneration. *Optom Vis Sci* (2014) 91 (8):904–15. doi: 10.1097/OPX.0000000000000319
41. Sabeti F, Lane J, Rohan EMF, Rai BB, Essex RW, McKone E, et al. Correlation of central versus peripheral macular structure-function with acuity in age-related macular degeneration. *Transl Vis Sci Technol* (2021) 10(2):1–12. doi: 10.1167/tvst.10.2.10
42. Nomura R, Terasaki H, Hirose H, Miyake Y. Blue-on-yellow perimetry to evaluate S cone sensitivity in diabetics. *Ophthalmic Res* (2000) 32(2-3):69–72. doi: 10.1159/000055592
43. Rai BB, Essex RW, Sabeti F, Maddess T, Rohan EMF, van Kleef JP, et al. An objective perimetry study of central versus peripheral sensitivities and delays in age-related macular degeneration. *Trans Vis Sci Tech* (2021) 10(14(24)):1–14. doi: 10.1167/tvst.10.14.24
44. Sabeti F, James AC, Carle CF, Essex RW, Bell A, Maddess T. Comparing multifocal pupillographic objective perimetry (mfPOP) and multifocal visual evoked potentials (mfVEP) in retinal diseases. *Sci Rep* (2017) 7:45847. doi: 10.1038/srep45847
45. Sabeti F, Maddess T, Essex RW, James AC. Multifocal pupillographic assessment of age-related macular degeneration. *Optom Vis Sci* (2011) 88(12):1477–85. doi: 10.1097/OPX.0b013e318235af61
46. Rosli Y, Bedford SM, James AC, Maddess T. Photopic and scotopic multifocal pupillographic responses in age-related macular degeneration. *Vision Res* (2012) 69:42–8. doi: 10.1016/j.visres.2012.07.019
47. Sabeti F, Maddess T, Essex RW, James AC. Multifocal pupillography identifies ranibizumab-induced changes in retinal function for exudative age-related macular degeneration. *Invest Ophthalmol Vis Sci* (2012) 53(1):253–60. doi: 10.1167/iov.11-8004
48. Maddess T, Rohan EMF, Rai BB, Carle CF, Nolan CJ, Sabeti F, et al. *Diagnostic power of rapid objective perimetry in young people with Type 1 Diabetes*. New Orleans, USA: IOVS-ARVO (2023).
49. Rai BB, Sabeti F, Carle CF, Rohan EMF, van Kleef JP, Essex RW, et al. Rapid objective testing of visual function matched to the ETDRS-grid, and its diagnostic power in AMD. *Ophthalmol Sci* (2022) 2(2.100143):1–9. doi: 10.1016/j.xops.2022.100143
50. Maddess T, van Kleef JP, Kolic M, Essex RW, Sarac O, Carle CF. *Comparing macular and wide-field objective perimetry*. Amsterdam: World Glaucoma Association (2021).



OPEN ACCESS

EDITED BY
Sara Rezzola,
University of Brescia, Italy

REVIEWED BY
Changzheng Chen,
Renmin Hospital of Wuhan University, China
Sudhanshu Kumar Bharti,
Patna University, India

*CORRESPONDENCE
Zhen Wang
✉ zwang@sdfmu.edu.cn

RECEIVED 24 October 2023
ACCEPTED 08 February 2024
PUBLISHED 23 February 2024

CITATION
Jing R, Sun X, Cheng J, Li X and Wang Z
(2024) Vascular changes of the choroid
and their correlations with visual acuity
in diabetic retinopathy.
Front. Endocrinol. 15:1327325.
doi: 10.3389/fendo.2024.1327325

COPYRIGHT
© 2024 Jing, Sun, Cheng, Li and Wang. This is
an open-access article distributed under the
terms of the [Creative Commons Attribution
License \(CC BY\)](#). The use, distribution or
reproduction in other forums is permitted,
provided the original author(s) and the
copyright owner(s) are credited and that the
original publication in this journal is cited, in
accordance with accepted academic
practice. No use, distribution or reproduction
is permitted which does not comply with
these terms.

Vascular changes of the choroid and their correlations with visual acuity in diabetic retinopathy

Ruixia Jing¹, Xiubin Sun², Jimin Cheng³,
Xue Li¹ and Zhen Wang^{3*}

¹Jinan Central Hospital, Shandong First Medical University & Shandong Academy of Medical Sciences, Jinan, China, ²Department of Biostatistics, School of Public Health, Cheeloo College of Medicine, Shandong University, Jinan, China, ³Department of Ophthalmology, Central Hospital Affiliated to Shandong First Medical University, Jinan, China

Objective: To investigate changes in the choroidal vasculature and their correlations with visual acuity in diabetic retinopathy (DR).

Methods: The cohort was composed of 225 eyes from 225 subjects, including 60 eyes from 60 subjects with healthy control, 55 eyes from 55 subjects without DR, 46 eyes from 46 subjects with nonproliferative diabetic retinopathy (NPDR), 21 eyes from 21 subjects with proliferative diabetic retinopathy (PDR), and 43 eyes from 43 subjects with clinically significant macular edema (CSME). Swept-source optical coherence tomography (SS-OCT) was used to image the eyes with a 12-mm radial line scan protocol. The parameters for 6-mm diameters of region centered on the macular fovea were analyzed. Initially, a custom deep learning algorithm based on a modified residual U-Net architecture was utilized for choroidal boundary segmentation. Subsequently, the SS-OCT image was binarized and the Niblack-based automatic local threshold algorithm was employed to calibrate subfoveal choroidal thickness (SFCT), luminal area (LA), and stromal area (SA) by determining the distance between the two boundaries. Finally, the ratio of LA and total choroidal area (SA + LA) was defined as the choroidal vascularity index (CVI). The choroidal parameters in five groups were compared, and correlations of the choroidal parameters with age, gender, duration of diabetes mellitus (DM), glycated hemoglobin (HbA1c), fasting blood sugar, SFCT and best-corrected visual acuity (BCVA) were analyzed.

Results: The CVI, SFCT, LA, and SA values of patients with DR were found to be significantly lower compared to both healthy patients and patients without DR ($P < 0.05$). The SFCT was significantly higher in NPDR group compared to the No DR group ($P < 0.001$). Additionally, the SFCT was lower in the PDR group compared to the NPDR group ($P = 0.014$). Furthermore, there was a gradual decrease in CVI with progression of diabetic retinopathy, reaching its lowest value in the PDR group. However, the CVI of the CSME group exhibited a marginally closer proximity to that of the NPDR group. The multivariate regression analysis revealed a positive correlation between CVI and the duration of DM as well as LA ($P < 0.05$). The results of both univariate and multivariate regression analyses demonstrated a significant positive correlation between CVI and BCVA ($P = 0.003$).

Conclusion: Choroidal vascular alterations, especially decreased CVI, occurred in patients with DR. The CVI decreased with duration of DM and was correlated with visual impairment, indicating that the CVI might be a reliable imaging biomarker to monitor the progression of DR.

KEYWORDS

diabetes mellitus, diabetic retinopathy, optical coherence tomography, choroidal vascular index, visual acuity

1 Introduction

By 2045, it is expected that the number of adults worldwide with diabetes mellitus (DM) will exceed 700 million (1). Diabetic retinopathy (DR), which is the most prevalent microvascular complication of DM, remains a leading cause of blindness among the working population (2, 3). It has been reported that approximately one-third of DM patients suffer from DR (4).

The deterioration of vision caused by DR is a prevalent risk factor for permanent blindness in patients with DM (5). Nonproliferative diabetic retinopathy (NPDR) is characterized by asymptomatic microvascular changes or retinal microleakage, which can eventually progress to proliferative diabetic retinopathy (PDR) or diabetic macular edema (DME) as DM advances (6, 7). Therefore, the importance of early diagnosis of DR and the study of its risk factors cannot be ignored.

There was a certain relationship between DR and choroidal thickness (CT) (8). Research conducted by Wang et al. (9) revealed that CT plays a crucial role in the development of DR. Optical coherence tomography (OCT), widely recognized as a valuable non-invasive imaging technique, can be utilized for choroid imaging (10). OCT-derived CT has been proposed as a quantitative index for evaluating choroidal structure and function. Several studies conducted in the past decade have analyzed changes in CT thickness in patients with DR, but the results obtained vary. Some reports showed thinning of CT, while others show no change or even thickening. However, these studies were limited to investigating only CT (11–15). Recently, other choroidal vascular parameters such as the choroidal vascular index (CVI) and the choroidal luminal area (LA) have been reported in age-related macular degeneration (AMD), pathological myopia (PM), and other diseases related to the choroid (16–19). There were also studies that showed a relationship between CVI and the progression of DR, but all of them had limitations. Kim et al. only focused on studying CVI in the 1,500 μm area of the fovea, while Gupta et al. utilized spectral domain optical coherence tomography (SD-OCT) (20, 21).

In this study, we employed the residual U-Net deep learning algorithm, which has been previously reported, to automatically segment and quantify CT and choroidal vasculature in swept source optical coherence tomography (SS-OCT) images (16, 22, 23). We

analyzed the correlation between choroidal vascular changes and DR to provide new insights into the prevention and treatment of DR.

Headings: CVI correlations with visual acuity in DR.

2 Methods

2.1 Study design

This was a retrospective study approved by the Ethics Review Committee of the Central Hospital affiliated with Shandong First Medical University, which followed the basic principles of the Declaration of Helsinki. As this was a retrospective study, written informed consent was waived by the Ethics Review Board. All analytical data has been anonymized.

2.2 Patients

This study included a total of 165 patients (165 eyes) with type 2 DM and 60 healthy patients (60 eyes) who underwent SS-OCT examination at the Department of Ophthalmology, Central Hospital Affiliated to Shandong First Medical University from September 2022 to September 2023. The diagnosis of type 2 DM was based on the criteria set by the American Diabetes Association (24).

Inclusion criteria: Age >18 years. Exclusion criteria: (1) Refractive error > +3.0 D or refractive error < - 3.0 D (spherical equivalent (SE)); (2) Hypertension; (3) Ocular trauma; (4) Retinal laser photocoagulation; (5) Intraocular surgery; (6) Intravitreal injection; (7) Presence of other retinal diseases, such as AMD, retinal arteriovenous occlusion, or neurodegenerative disease; (8) Glaucoma; (9) Hypertrophic choroidal pigment epitheliopathy, such as central serous chorioretinopathy; (10) History of inflammation; (11) Refractive media opacification affecting fundus examination.

2.3 Ophthalmologic examination

Demographic information, comprehensive medical history, and ophthalmic history were recorded during the initial visit. All

patients underwent a comprehensive eye examination, which included measurements of Snellen best-corrected visual acuity (BCVA), intraocular pressure (IOP), autorefractometry, slit lamp biomicroscopy, dilated fundus examination, fundus photography, and SS-OCT.

2.4 Acquiring and analyzing OCT images

The SS-OCT (VG200S; SVision Imaging, Henan, China) device with a central wavelength of 1050 nm was used for OCT imaging. The scanning speed was 100,000 A-scans/s. The axial optical resolution was 3.8 μm , and the axial digital resolution was 2.0 μm . The maximum scanning depth of the posterior segment was 9 mm. To obtain two transverse lines passing through the fovea, a radial line scan measuring 12 mm in length was performed. In order to thoroughly examine changes in choroidal vascular around the macula, we analyzed cross-sectional images within a radius of 6 mm centered on the fovea. The examinations were conducted by an experienced ophthalmic technologist, with a minimum signal strength requirement of 4 as recommended by the manufacture.

Before conducting image analysis, we used Bennett's formula ($t = p \times q \times s$) to correct the OCT image and eliminate the influence of axial length (AL) on image size, based on previous studies (25–27). Here, t represents the actual scan length, p denotes the magnification factor of the OCT imaging system, q refers to the eye-related magnification factor, and s represents the raw measurement value of the OCT imaging system.

We utilized deep learning techniques to automatically quantify choroidal parameters within a circular region with a diameter of 6.0 mm, using the macular fovea as the central point. The choroidal boundary was automatically segmented in all images using deep learning algorithms based on the modified residual U-Net method.

Residual U-Net, a residual unit used as a replacement for the traditional convolution unit, was employed in deep networks. It has been observed that residual U-Net can achieve better performance with fewer parameters compared to traditional methods. The thickness between the retinal pigment epithelium (RPE) layer and the junction of the choroid and sclera is defined as CT. After binarizing the OCT images, we applied Niblack's automatic local threshold algorithm to calibrate both the LA and stromal area (SA). The choroidal vascular index (CVI) was defined as the ratio of LA to the total choroidal area (SA + LA) (Figure 1).

2.5 Basic information and laboratory tests

The study collected data from medical records, including factors such as age, gender, duration of DM, glycated hemoglobin (HbA1c), fasting blood sugar, and body mass index (BMI). Age was defined as the age at the first visit. The duration of DM was defined as the time from the diagnosis of DM to the first eye examination. Fasting blood sugar and HbA1c were recorded as the most recent results in the case system, and BMI was calculated by dividing weight (kg) by height squared (m).

2.6 Patient screening and grouping

Healthy patients were defined as controls. The DM patients were initially classified into four groups (No DR, NPDR, PDR, and CSME) by two retinal specialists independently (R. J. and X. L.) based on the International DR Staging Criteria (28). In case of disagreement between the two retinal specialists, a more senior retinal specialist (Z. W.) made the final decision. One eye of each patient was randomly selected for analysis during the study.

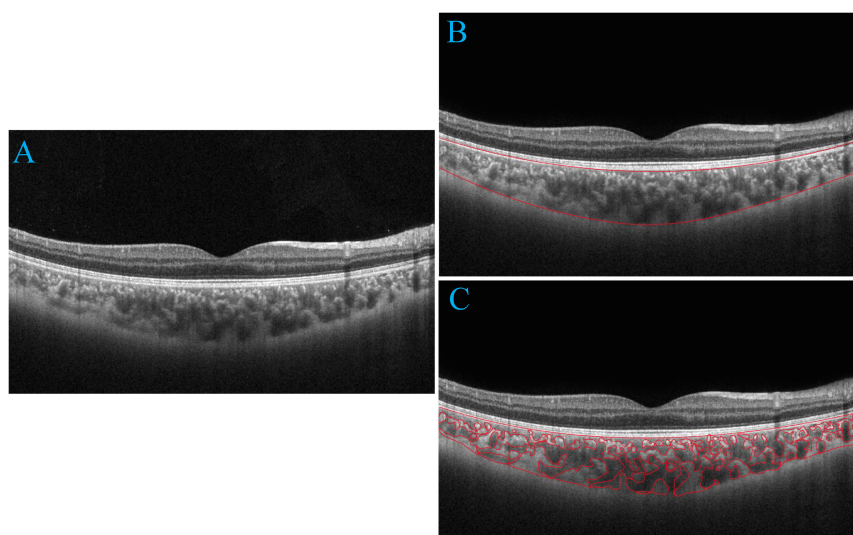


FIGURE 1

Progression of choroidal image segmentation. The original SS-OCT image (A). Segmentation of the choroidal area (B). Overlay of the region of interest created after performing image binarization on the SS-OCT image (C).

2.7 Statistical analysis

The Statistical Package for the Social Sciences (version 26.0, IBM SPSS) was used for data analysis. When appropriate, study data were reported as mean \pm standard deviation (SD), median (interquartile range, IQR), frequencies, or percentages. The Shapiro-Wilk test was employed to assess whether quantitative variables followed a normal distribution. Data that adhered to a normal distribution were described using mean \pm SD. Data that exhibited a skewed distribution were presented as median (IQR). Fisher's exact test was utilized to analyze categorical variables. For normally distributed data, one-way analysis of variance (ANOVA) was applied. The Kruskal-Wallis test was used for analyzing skewed data. Univariate and multivariate linear regression analyses were conducted to investigate the factors influencing choroidal characteristics. Results with a *P* value less than 0.05 were considered statistically significant.

3 Results

3.1 Basic patient characteristics

A total of 225 eyes were included in this study, which were divided into 5 groups: healthy controls (group 1, *n*=60), No DR (group 2, *n*=55), NPDR (group 3, *n*=46), PDR (group 4, *n*=21), and CSME (group 5, *n*=43). The demographic, ocular, and systemic

characteristics of the patients were presented in Table 1. A total of 165 patients with type 2 DM were included in this study, including 101 females and 64 males, with a mean age of 56.67 ± 6.22 years. The mean duration of DM was 9.16 ± 4.03 years. There were no significant differences in age and gender within the study group. DM duration ($P < 0.001$), BMI ($P = 0.034$), HbA1c ($P < 0.001$), and fasting blood sugar ($P < 0.001$) showed significant differences between each DR group. BCVA logMAR was significantly lower in CSME compared to the other study groups ($P < 0.001$). BCVA logMAR did not differ between No DR and NPDR ($P = 0.041$). BCVA logMAR showed slight difference between NPDR and PDR ($P = 0.728$). Systolic blood pressure, IOP, and SE did not show significant differences among the study groups ($P > 0.05$).

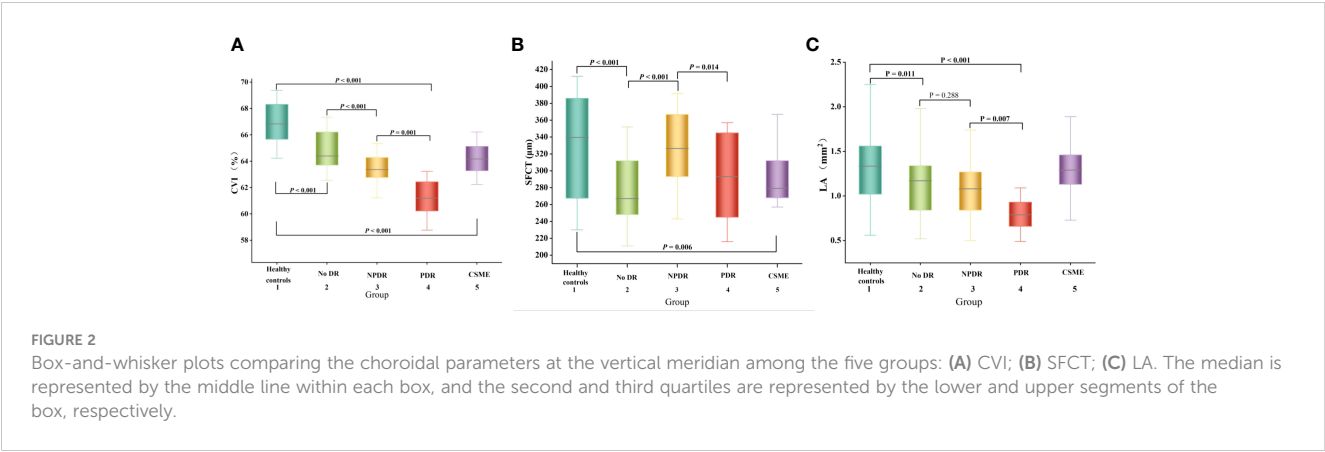
3.2 Subfoveal choroidal thickness and CVI

The SFCT measurement results of each group were shown in Figure 2B. The SFCT values for groups 1-5 were $331.67 \pm 58.43\mu\text{m}$, $278.36 \pm 41.48\mu\text{m}$, $326.57 \pm 45.12\mu\text{m}$, $291.29 \pm 48.94\mu\text{m}$, and $297.23 \pm 42.40\mu\text{m}$, respectively. The thickness of SFCT in the eyes of patients with DM was found to be thinner compared to that in healthy controls ($P < 0.05$). Notably, the SFCT in the No DR group was significantly lower than both the healthy controls group ($P < 0.001$) and the NPDR group ($P < 0.001$). Additionally, the SFCT in the PDR group was significantly lower than that in the NPDR group ($P = 0.014$). These findings indicated that SFCT was

TABLE 1 Demographic and clinical characteristics of the eyes (*n* = 225).

| Variables | Healthy controls (<i>n</i> = 60) | No DR (<i>n</i> = 55) | NPDR (<i>n</i> = 46) | PDR (<i>n</i> = 21) | CSME (<i>n</i> = 43) | <i>P</i> value |
|---|--------------------------------------|---------------------------|--------------------------|-------------------------|--------------------------|---------------------|
| No. of eyes | 60 | 55 | 46 | 21 | 43 | |
| Age, years, median (IQR) | 54.50 (46-69) | 56 (46-49) | 55 (47-69) | 54 (47-69) | 56 (47-69) | 0.204* |
| Sex, <i>n</i> (%) | | | | | | 0.347 [†] |
| Female | 36 | 31 | 29 | 14 | 27 | |
| Male | 24 | 24 | 17 | 7 | 16 | |
| BMI (Kg/m ²), median (IQR) | 21.55 (19.5-24.6) | 22.4 (19.8-24.9) | 23.1 (19.8-34.0) | 23.0 (19.7-24.6) | 23 (19.6-25.6) | < 0.001* |
| DM duration, year, median (IQR) | | 5 (1-12) | 10 (7-15) | 15 (9-18) | 11 (6-15) | < 0.001* |
| HbA1c, %, median (IQR) | | 6.1 (5.2-6.8) | 7 (6.5-7.5) | 7.8 (6.8-8.8) | 7.2 (6.0-8.0) | < 0.001* |
| Fasting blood sugar, mmol/L, median (IQR) | | 7.5 (7.0-9.1) | 7.9 (7.0-9.0) | 8.6 (7.6-9.0) | 8.2 (7.1-10.2) | < 0.001* |
| Systolic BP, mmHg, median (IQR) | | 117 (105-138) | 115.5 (106-135) | 123 (107-129) | 118 (108-127) | 0.595* |
| Diastolic BP, mmHg, median (IQR) | | 68 (62-76) | 65.5 (60-76) | 65 (63-72) | 64 (60-71) | < 0.001* |
| RAAS inhibitors, use, <i>n</i> , % | | 10.9% | 17.39% | 52.38% | 34.88% | <0.001 [†] |
| Ophthalmologic examination | | | | | | |
| BCVA, logMAR, median (IQR) | 0.1 (0-0.3) | 0.1 (0-0.4) | 0.1 (0-0.4) | 0.2 (0-0.5) | 0.6 (0.4-0.8) | < 0.001* |
| SE, diopter, median (IQR) | 0.50 (-1.50-1.50) | 0 (-1.50-1.50) | 0 (-1.50-1.00) | 0 (-1.25-1.25) | 0.50 (-1.25-1.50) | 0.066* |
| IOP, mmHg, median (IQR) | 14 (12-17) | 14 (12-17) | 14 (13-17) | 14 (12-17) | 14 (12-17) | 0.195* |

DR, diabetic retinopathy; NPDR, nonproliferative diabetic retinopathy; PDR, proliferative diabetic retinopathy; CSME, clinically significant macular edema; IQR, interquartile range; BMI, body mass index; DM, diabetes mellitus; HbA1c, glycated hemoglobin; BP, blood pressure; RAAS, renin-angiotensin-aldosterone system; BCVA, best-corrected visual acuity; logMAR, logarithm of the minimum angle of resolution; SE, spherical equivalent. IOP, intraocular pressure; *Kruskal-Wallis test; [†]Fisher exact test; *P* with statistical significance is shown in boldface.



significantly thinner in the eyes of DM patients and that PDR patients have even thinner SFCT compared to other DR patients. In the univariate regression analyses, there were no significant associations observed between gender, duration of DM, fasting blood sugar, HbA1c, systolic blood pressure, renin-angiotensin-aldosterone system (RAAS) inhibitor use, spherical equivalent (SE), or intraocular pressure (IOP) and SFCT ($P > 0.05$) (Table 2). However, age showed a significant correlation with SFCT ($P = 0.032$), along with BMI showing a significant correlation as well ($P = 0.007$), and diastolic blood pressure demonstrating a highly significant association with SFCT ($P < 0.001$) (Table 2). Nevertheless, in the multivariate regression analysis only diastolic blood pressure remained significantly correlated with SFCT ($P = 0.001$) (Table 2).

The CVI measurement results of each group are presented in Figure 2A. The CVI values for groups 1-5 were as follows: $66.93 \pm 1.14\%$, $64.85 \pm 1.33\%$, $63.53 \pm 1.04\%$, $61.25 \pm 1.32\%$, and $64.23 \pm 1.04\%$. Notably, the eyes of DM patients exhibited significantly lower CVI compared to healthy controls ($P < 0.001$). Furthermore, the PDR group demonstrated a significantly lower CVI than both the healthy controls group ($P < 0.001$) and NPDR group ($P = 0.001$). These findings indicate a significant reduction in CVI among DM patients, with even lower levels observed in PDR patients. In the univariate linear regression analysis, gender, age, systolic blood pressure, diastolic blood pressure, SE, IOP, and SA did not show significant correlation with CVI ($P > 0.05$). However, BMI, duration of DM, HbA1c, fasting blood sugar, use of RAAS

TABLE 2 Linear regression analyses of factors associated with SFCT.

| Variables | Univariate | | Multivariate | |
|-----------------------------|----------------------|-------------------|----------------------|--------------|
| | Standardized β | P value | Standardized β | P value |
| Age, years | -0.143 | 0.032 | -0.110 | 0.171 |
| Sex, n (%) | -0.043 | -0.521 | - | - |
| Female | | | | |
| Male | | | | |
| BMI (Kg/m ²) | -0.179 | 0.007 | -0.121 | 0.137 |
| DM duration, year | 0.018 | 0.821 | - | - |
| HbA1c, % | 0.029 | 0.701 | - | - |
| Fasting blood sugar, mmol/L | 0.052 | 0.508 | - | - |
| Systolic BP, mmHg | 0.026 | 0.742 | - | - |
| Diastolic BP, mmHg | 0.290 | < 0.001 | -3.306 | 0.001 |
| RAAS inhibitors, use, n, % | -0.032 | 0.679 | - | - |
| Ophthalmologic examination | | | | |
| SE, diopter | -1.09 | 0.102 | - | - |
| IOP, mmHg | -0.071 | 0.292 | - | - |

SFCT, Subfoveal choroidal thickness; BMI, body mass index; DM, diabetes mellitus; HbA1c, glycated hemoglobin; BP, blood pressure; RAAS, renin-angiotensin-aldosterone system; SE, spherical equivalent. IOP, intraocular pressure; P with statistical significance is shown in boldface.

TABLE 3 Linear regression analyses of factors associated with CVI.

| Variables | Univariate | | Multivariate | |
|-----------------------------------|----------------------|--------------|----------------------|--------------|
| | Standardized β | P value | Standardized β | P value |
| Age, years | 0.022 | 0.735 | - | - |
| Sex, n (%) | 0.038 | 0.573 | - | - |
| Female | | | | |
| Male | | | | |
| BMI (Kg/m ²) | -0.278 | < 0.001 | -0.03 | 0.650 |
| DM duration, year | -0.426 | < 0.001 | -0.212 | 0.016 |
| HbA1c, % | -0.391 | < 0.001 | -0.041 | 0.646 |
| Fasting blood sugar, mmol/L | -0.244 | 0.002 | -0.036 | 0.576 |
| Systolic BP, mmHg | -0.046 | 0.554 | - | - |
| Diastolic BP, mmHg | 0.051 | 0.512 | - | - |
| RAAS inhibitors, use, n, % | 0.147 | 0.025 | -0.081 | 0.197 |
| Ophthalmologic examination | | | | |
| SE, diopter | 0.094 | 0.160 | - | - |
| IOP, mmHg | 0.019 | 0.775 | - | - |
| SFCT, μ m | 0.154 | 0.021 | -0.080 | 0.221 |
| SA (mm ²) | -0.003 | 0.968 | - | - |
| LA (mm ²) | 0.25 | < 0.001 | -1.428 | < 0.001 |

CVI, choroidal vascular index; BMI, body mass index; DM, diabetes mellitus; HbA1c, glycated hemoglobin; BP, blood pressure; SFCT, subfoveal choroidal thickness; RAAS, renin-angiotensin-aldosterone system; SE, spherical equivalent. IOP, intraocular pressure; SA, stromal area; LA, luminal area; P with statistical significance is shown in boldface.

inhibitors, SFCT, LA, and CVI were found to be significantly correlated ($P < 0.05$) according to Table 3. The multivariate linear regression analysis revealed that DM duration and LA remained significantly correlated with CVI after adjusting for other variables ($P < 0.05$) as shown in Table 3.

The LA measurement results of each group are presented in Figure 2C. Notably, the PDR group exhibited a significantly lower LA compared to the other DR groups, suggesting an inverse relationship between LA and CVI.

3.3 BCVA logMAR

The BCVA logMAR measurement results of each group were presented in Figure 3. The BCVA logMAR for groups 1-5 were as follows: 0.107 ± 0.107 , 0.145 ± 0.126 , 0.160 ± 0.134 , 0.257 ± 0.133 , and 0.593 ± 0.118 respectively. The BCVA logMAR of PDR patients was significantly worse compared to that of healthy controls ($P < 0.001$).

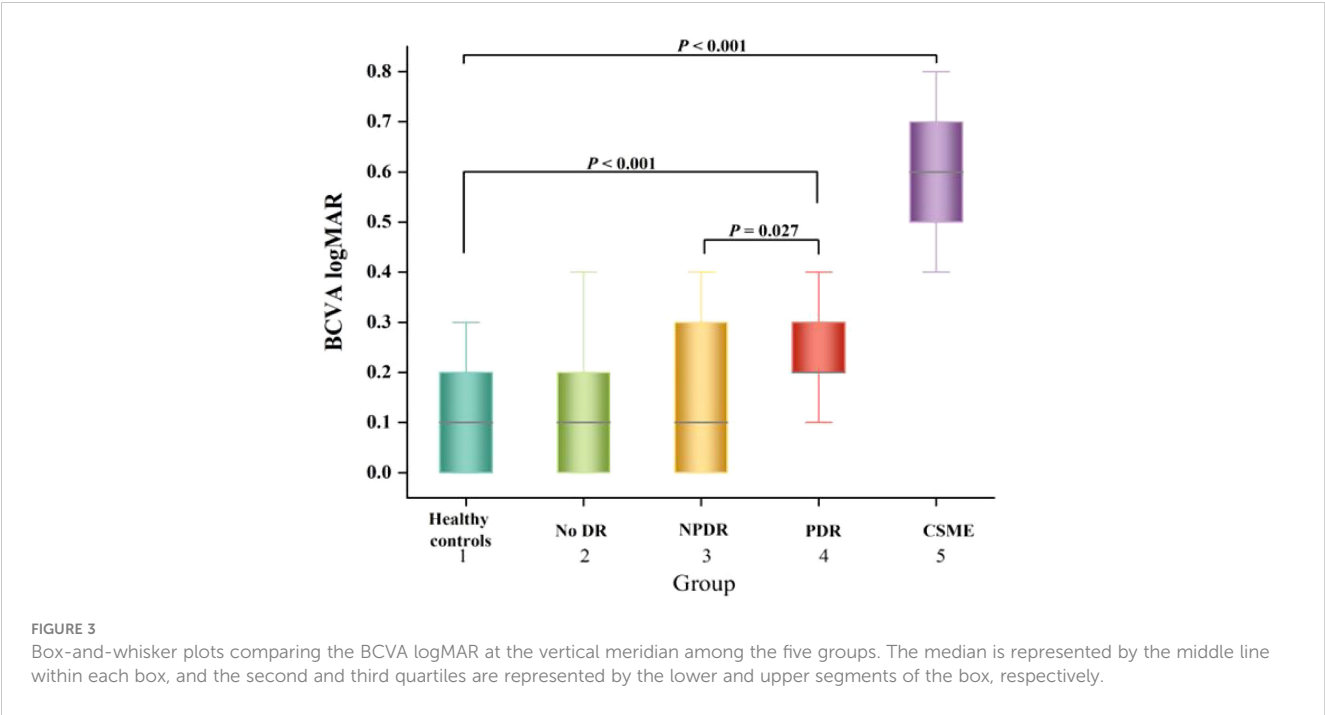
The univariate linear regression analysis revealed a significant association between worse BCVA logMAR and several factors in patients with DR, including older age ($P = 0.006$), longer duration of DM ($P < 0.001$), higher levels of HbA1c ($P = 0.001$), elevated fasting blood sugar levels ($P = 0.002$), thinner SFCT ($P < 0.001$), and reduced choroidal vascularity index values, as shown in Table 4. Eventually, multivariate linear regression analysis revealed significant correlations between BCVA logMAR and age ($P = 0.011$), duration

of DM ($P = 0.012$), fasting blood sugar ($P = 0.011$), and CVI ($P = 0.003$) in patients with DR (Table 4).

4 Discussion

In the present study, SS-OCT was used to evaluate the choroidal structural changes in eyes with DR. The thinning of the choroid found was consistent with previous findings (20, 29). Alterations of the choroidal vasculature in patients with DR was further quantified. We investigated the alterations in choroidal vascular parameters, including CVI, SA, and LA, in both healthy people and patients with DM. In patients with DM, we observed a significant decrease in CVI, LA, and SA in the presence of DR. However, no correlation was found between these parameters and CSME. Furthermore, CVI showed a strong negative association with BCVA, suggesting that patients with lower CVI exhibited poorer visual acuity, which was consistent with previous research findings (30). Consequently, CVI may serve as a reliable biomarker for monitoring the progression of DR; thus, preserving CVI could emerge as a novel clinical objective.

Importantly, the SFCT was found to be thinner in the group without DR compared to healthy controls ($P < 0.001$). However, it was thicker in the NPDR group compared to both the without DR and PDR groups ($P = 0.014$). This suggests that the SFCT initially increases in the early stages of DR and then decreases as the disease



progresses. These findings were consistent with the study conducted by Wang et al. (19). The CVI exhibited a gradual decline with the progression of DR ($P < 0.05$). Nevertheless, multivariate linear regression analysis revealed no significant difference between SFCT and CVI, which contrasted with the findings reported by Kim et al. (20). One possible reason for the discrepancy in research results was the difference in the proximity of the CVI studied. While our study focused on CVI within 6 mm of the fovea, their study examined CVI within 1,500 μm of the fovea. Additionally, they grouped patients with NPDR, whereas we did not. This difference in grouping may also had an impact on the research outcomes.

The influence of HbA1c on CT was still in discussion, which has not been adjusted in most previous CT studies. Unsal et al. (31) and

Kim et al. (32) found a significant correlation between HbA1c and CT, indicating that HbA1c may be a confounding parameter. This study found no correlation between HbA1c and SFCT, which is consistent with the findings of Wang et al. (33). However, our study revealed a significant association between age and BMI with CT. Shao et al. (34) reported that SFCT was significantly associated with BCVA after adjusting for age, sex, AL, and corneal curvature in the normal population. This study further demonstrated that thicker CT was independently associated with better BCVA in DR patients. Therefore, the CT may be a biomarker for visual function in DR patients.

In this study, we observed a significant impact of HbA1c on CVI ($P < 0.001$). However, after adjusting for age, gender, duration of

TABLE 4 Linear regression models based on BCVA.

| Variables | Univariate | | Multivariate | |
|-----------------------------|----------------------|-------------------|----------------------|--------------|
| | Standardized β | P value | Standardized β | P value |
| Age, years | 0.182 | 0.006 | 0.188 | 0.011 |
| Sex, n (%) | 0.005 | 0.08 | - | - |
| Female | | | | |
| Male | | | | |
| DM duration, year | 0.333 | < 0.001 | 0.255 | 0.012 |
| HbA1c, % | 0.262 | 0.001 | 0.153 | 0.117 |
| Fasting blood sugar, mmol/L | 0.241 | 0.002 | 0.190 | 0.011 |
| SFCT, μm | -0.246 | < 0.001 | -0.116 | 0.101 |
| LA (mm^2) | 0.083 | 0.231 | - | - |
| CVI (%) | 0.199 | 0.003 | 0.239 | 0.003 |

BCVA; best-corrected visual acuity; DM, diabetes mellitus; HbA1c, glycated hemoglobin; SFCT, subfoveal choroidal thickness; LA, luminal area; CVI, choroidal vascular index; P with statistical significance is shown in boldface.

DM, fasting blood glucose, and using multivariate regression analyses, we discovered that there was no significant correlation between HbA1c and CVI. This finding was inconsistent with the results of Temel E et al. (35), who reported a negative correlation between HbA1c and CVI. The reason for this difference may be that they did not consider factors such as age, gender, duration of DM.

Previous studies have reported significantly lower CVI in patients with DM and DR (20, 21, 36). However, Kim et al. (20) and Tan et al. (36) did not specifically analyze the changes of CVI in patients with DME. Our study analyzed the changes in CVI in patients with DME as did the study by Gupta et al. (21). Both studies observed a statistically significant decrease in CVI among the DME group when compared to healthy controls. However, our results revealed a higher CVI in the DME group compared to the NPDR and PDR groups, which was not analyzed in their study. Cao et al. (37) found that the loss of choroidal capillaries in the eyes of patients with DM was four times greater than that in nondiabetic patients. The reduction of the choroidal capillary layer (resulting in a decrease in CVI) may contribute to hypoxia in the RPE and outer retinal layer, leading to an upregulation of vascular endothelial growth factor (38). This could also contribute to the deterioration of vision in DR.

In the present study, we found a significant association between worsening BCVA and CVI in DR patients. Multivariate regression analyses revealed that a decrease in CVI was the most relevant factor for visual impairment. Previous studies have not examined the relationship between BCVA and CVI (20, 21). The choroid primarily supplied nutrients and oxygen to the photoreceptors (39). Previous studies have indicated that CT influenced visual impairment caused by photoreceptor degeneration (25). However, our findings showed no significant correlation between BCVA and CT, which was inconsistent with their findings. One possible reason for this discrepancy was that their subjects were patients with PM, who were younger in age, whereas we studied patients with type 2 DM, who were older. In the future, prospective studies with large sample sizes will be needed to investigate whether visual impairment in patients with type 2 DM is influenced by CT.

In this study, CVI was found to be correlated with BCVA, and multivariate regression analyses revealed that a decrease in CVI was the factor most strongly associated with visual impairment. Therefore, we hypothesize that monitoring changes in CVI may provide a reliable parameter for predicting future loss of visual acuity and could serve as a novel target for intervention aimed at preventing the progression of visual impairment in DR.

There were some limitations to this study. Firstly, choroidal parameters were only measured within a 6 mm radius around the macular fovea, but studying larger zones may provide more representative information about CVI. Secondly, some studies have reported diurnal variations in CT obtained by OCT, however, the diurnal variations of choroidal vascular are currently unknown, which may have influenced our results. Thirdly, we included only 21 patients with PDR because we specifically focused on pre-treatment PDR patients, which might have influenced our results. Fourthly, our study of NPDR was not conducted in a graded manner, which may have also influenced our results. Finally, it was important to note that this study was a small retrospective analysis with a limited sample size. The smaller

sample size in this study may have implications on the statistical significance of the analysis results, potentially leading to insufficient power. Furthermore, the generalizability of the findings might be constrained due to the limited sample size. Moreover, a smaller sample size can introduce bias and hinder adequate control for potential confounding factors, thereby impacting the accuracy and reliability of the results. The aforementioned limitations need to be addressed in future research.

5 Conclusions

In conclusion, this study demonstrated that patients with DM, even without DR, exhibited significantly lower CVI compared to healthy controls. Furthermore, alterations in choroidal structure were found to be significantly associated with visual impairment in DR. CVI can be used as a quantitative parameter to evaluate choroidal damage in patients with DR. CVI may serve as a reliable quantitative biomarker for monitoring the progression of DR. Clinicians should closely monitor changes in choroidal vasculature in patients with DR and recognize that preventing a decline in CVI may be an important clinical goal for preventing the progression of DR.

Data availability statement

The original contributions presented in the study are included in the article/supplementary materials. Further inquiries can be directed to the corresponding author.

Ethics statement

The studies involving humans were approved by the Ethics Review Committee of the Central Hospital Affiliated to Shandong First Medical University. The studies were conducted in accordance with the local legislation and institutional requirements. The participants provided their written informed consent to participate in this study.

Author contributions

RJ: Writing – original draft, Writing – review & editing, Investigation, Software. XS: Methodology, Writing – original draft. JC: Methodology, Writing – original draft. XL: Data curation, Methodology, Writing – original draft. ZW: Writing – review & editing.

Funding

The author(s) declare financial support was received for the research, authorship, and/or publication of this article. This study was supported by the Science and Technology Project of Jinan Municipal Health Commission, (2020-4-06). The sponsors and

funding organizations had no role in the design or conduct of this research.

Conflict of interest

The authors declare that the research was conducted in the absence of any commercial or financial relationships that could be construed as a potential conflict of interest.

References

- Zhang R, Dong L, Yang Q, Liu Y, Li H, Zhou W, et al. Prophylactic interventions for preventing macular edema after cataract surgery in patients with diabetes: a bayesian network meta-analysis of randomized controlled trials. *EClinicalMedicine*. (2022) 49:101463. doi: 10.1016/j.eclinm.2022.101463
- Cheung N, Mitchell P, Wong TY. Diabetic retinopathy. *Lancet*. (2010) 376:124–36. doi: 10.1016/S0140-6736(09)62124-3
- Wang W, Lo ACY. Diabetic retinopathy: pathophysiology and treatments. *Int J Mol Sci*. (2018) 19:1816. doi: 10.3390/ijms19061816
- Wong TY, Cheung CM, Larsen M, Sharma S, Simó R. Diabetic retinopathy. *Nat Rev Dis Primers*. (2016) 2:16012. doi: 10.1038/nrdp.2016.12
- Liu T, Lin W, Shi G, Wang W, Feng M, Xie X, et al. Retinal and choroidal vascular perfusion and thickness measurement in diabetic retinopathy patients by the swept-source optical coherence tomography angiography. *Front Med (Lausanne)*. (2022) 9:786708. doi: 10.3389/fmed.2022.786708
- Preethi S, Rajalakshmi AR. Proliferative diabetic retinopathy in typical retinitis pigmentosa. *BMJ Case Rep*. (2015) 2015:bcr2014208589. doi: 10.1136/bcr-2014-208589
- Shah KB, Han DP. Proliferative diabetic retinopathy. *Int Ophthalmol Clin*. (2004) 44:69–84. doi: 10.1097/00004397-200404440-00007
- Hidayat AA, Fine BS. Diabetic choroidopathy. Light and electron microscopic observations of seven cases. *Ophthalmology*. (1985) 92:512–22. doi: 10.1016/S0161-6420(85)34013-7
- Wang W, Li L, Wang J, Chen Y, Kun X, Gong X, et al. Macular choroidal thickness and the risk of referable diabetic retinopathy in type 2 diabetes: a 2-year longitudinal study. *Invest Ophthalmol Vis Sci*. (2022) 63:9. doi: 10.1167/iovs.63.4.9
- Cuenca N, Ortuño-Lizarán I, Sánchez-Sáez X, Kutsyr O, Albertos-Arranz H, Fernández-Sánchez L, et al. Interpretation of OCT and OCTA images from a histological approach: clinical and experimental implications. *Prog Retin Eye Res*. (2020) 77:100828. doi: 10.1016/j.preteyeres.2019.100828
- Lains I, Talcott KE, Santos AR, Marques JH, Gil P, Gil J, et al. Choroidal thickness in diabetic retinopathy assessed with swept-source optical coherence tomography. *Retina*. (2018) 38:173–82. doi: 10.1097/IAE.0000000000001516
- Abadia B, Suñen I, Calvo P, Bartol F, Verdes G, Ferreras A. Choroidal thickness measured using swept-source optical coherence tomography is reduced in patients with type 2 diabetes. *PloS One*. (2018) 13:e0191977. doi: 10.1371/journal.pone.0191977
- Ambiya V, Kumar A, Baranwal VK, Kapoor G, Arora A, Kalra N, et al. Change in subfoveal choroidal thickness in diabetes and in various grades of diabetic retinopathy. *Int J Retina Vitreous*. (2018) 4:34. doi: 10.1186/s40942-018-0136-9
- Tavares Ferreira J, Vicente A, Proença R, Santos BO, Cunha JP, Alves M, et al. Choroidal thickness in diabetic patients without diabetic retinopathy. *Retina*. (2018) 38:795–804. doi: 10.1097/IAE.0000000000001582
- Ohara Z, Tabuchi H, Nakakura S, Yoshizumi Y, Sumino H, Maeda Y, et al. Changes in choroidal thickness in patients with diabetic retinopathy. *Int Ophthalmol*. (2018) 38:279–86. doi: 10.1007/s10792-017-0459-9
- Wang Y, Chen S, Lin J, Chen W, Huang H, Fan X, et al. Vascular changes of the choroid and their correlations with visual acuity in pathological myopia. *Invest Ophthalmol Vis Sci*. (2022) 63:20. doi: 10.1167/iovs.63.12.20
- Koh LHL, Agrawal R, Khandelwal N, Sai Charan L, Chhablani J. Choroidal vascular changes in age-related macular degeneration. *Acta Ophthalmol*. (2017) 95: e597–601. doi: 10.1111/aos.13399
- Rasheed MA, Goud A, Mohamed A, Vupparaboina KK, Chhablani J. Change in choroidal vascularity in acute central serous chorioretinopathy. *Indian J Ophthalmol*. (2018) 66:530–4. doi: 10.4103/ijo.IJO_1160_17
- Kim RY, Chung DH, Kim M, Park YH. Use of choroidal vascularity index for choroidal structural evaluation in central serous chorioretinopathy with choroidal neovascularization. *Retina*. (2020) 40:1395–402. doi: 10.1097/IAE.0000000000002585
- Kim M, Ha MJ, Choi SY, Park YH. Choroidal vascularity index in type-2 diabetes analyzed by swept-source optical coherence tomography. *Sci Rep*. (2018) 8:70. doi: 10.1038/s41598-017-18511-7
- Gupta C, Tan R, Mishra C, Khandelwal N, Raman R, Kim R, et al. Choroidal structural analysis in eyes with diabetic retinopathy and diabetic macular edema-A

Publisher's note

All claims expressed in this article are solely those of the authors and do not necessarily represent those of their affiliated organizations, or those of the publisher, the editors and the reviewers. Any product that may be evaluated in this article, or claim that may be made by its manufacturer, is not guaranteed or endorsed by the publisher.

- novel OCT based imaging biomarker. *PloS One*. (2018) 13:e0207435. doi: 10.1371/journal.pone.0207435
- Zhang H, Yang J, Zhou K, Li F, Hu Y, Zhao Y, et al. Automatic Segmentation and visualization of choroid in OCT with knowledge infused deep learning. *IEEE J BioMed Health Inform*. (2020) 24:3408–20. doi: 10.1109/JBHI.2020.3023144
- Zheng G, Jiang Y, Shi C, Miao H. Deep learning algorithms to segment and quantify the choroidal thickness and vasculature in swept-source optical coherence tomography images. *J Innov Opt Health Sci*. (2021) 14:2140002. doi: 10.1142/S1793545821400022
- American Diabetes Association. 2. Classification and diagnosis of diabetes: standards of medical care in diabetes-2018. *Diabetes Care*. (2018) Suppl 1:S13–27. doi: 10.2337/dc18-S002
- Ye J, Shen M, Huang S, Fan Y, Yao A, Pan C, et al. Visual acuity in pathological myopia is correlated with the photoreceptor myoid and ellipsoid zone thickness and affected by choroid thickness. *Invest Ophthalmol Vis Sci*. (2019) 60:1714–23. doi: 10.1167/iovs.18-26086
- Wang Y, Ye J, Shen M, Yao A, Xue A, Fan Y, et al. Photoreceptor degeneration is correlated with the deterioration of macular retinal sensitivity in high myopia. *Invest Ophthalmol Vis Sci*. (2019) 60:2800–10. doi: 10.1167/iovs.18-26085
- Yang Y, Wang J, Jiang H, Yang X, Feng L, Hu L, et al. Retinal microvasculature alteration in high myopia. *Invest Ophthalmol Vis Sci*. (2016) 57:6020–30. doi: 10.1167/iovs.16-19542
- Wilkinson CP, Ferris FL 3rd, Klein RE, Lee PP, Agardh CD, Davis M, et al. Proposed international clinical diabetic retinopathy and diabetic macular edema disease severity scales. *Ophthalmology*. (2003) 110:1677–82. doi: 10.1016/S0161-6420(03)00475-5
- Abadia B, Bartol-Puyal FA, Calvo P, Verdes G, Isanta C, Pablo LE. Mapping choroidal thickness in patients with type 2 diabetes. *Can J Ophthalmol*. (2020) 55:45–51. doi: 10.1016/j.jcjo.2019.06.009
- Marques JH, Marta A, Castro C, Baptista PM, José D, Almeida D, et al. Choroidal changes and associations with visual acuity in diabetic patients. *Int J Retina Vitreous*. (2022) 8:6. doi: 10.1186/s40942-021-00355-z
- Unsal E, Eltutar K, Zirtioğlu S, Dinçer N, Özdoğan Erkul S, Güngel H. Choroidal thickness in patients with diabetic retinopathy. *Clin Ophthalmol*. (2014) 8:637–42. doi: 10.2147/OPHTH.S59395
- Kim JT, Lee DH, Joe SG, Kim JG, Yoon YH. Changes in choroidal thickness in relation to the severity of retinopathy and macular edema in type 2 diabetic patients. *Invest Ophthalmol Vis Sci*. (2013) 54:3378–84. doi: 10.1167/iovs.12-11503
- Wang W, Liu S, Qiu Z, He M, Wang L, Li Y, et al. Choroidal thickness in diabetes and diabetic retinopathy: a swept source OCT study. *Invest Ophthalmol Vis Sci*. (2020) 61:29. doi: 10.1167/iovs.61.4.29
- Shao L, Xu L, Wei WB, Chen CX, Du KF, Li XP, et al. Visual acuity and subfoveal choroidal thickness: the Beijing Eye Study. *Am J Ophthalmol*. (2014) 158:702–709.e1. doi: 10.1016/j.jajo.2014.05.023
- Temel E, Özcan G, Yanık Ö, Demirel S, Batıoğlu F, Kar İ, et al. Choroidal structural alterations in diabetic patients in association with disease duration, HbA1c level, and presence of retinopathy. *Int Ophthalmol*. (2022) 42:3661–72. doi: 10.1007/s10792-022-02363-w
- Tan KA, Laude A, Yip V, Loo E, Wong EP, Agrawal R. Choroidal vascularity index - a novel optical coherence tomography parameter for disease monitoring in diabetes mellitus? *Acta Ophthalmol*. (2016) 94:e612–6. doi: 10.1111/aos.13044
- Cao J, McLeod S, Merges CA, Luttly GA. Choriocapillaris degeneration and related pathologic changes in human diabetic eyes. *Arch Ophthalmol*. (1998) 116:589–97. doi: 10.1001/archophth.116.5.589
- Shima DT, Adamis AP, Ferrara N, Yeo KT, Yeo TK, Allende R, et al. Hypoxic induction of endothelial cell growth factors in retinal cells: identification and characterization of vascular endothelial growth factor (VEGF) as the mitogen. *Mol Med*. (1995) 1:182–93. doi: 10.1007/BF03401566
- Nickla DL, Wallman J. The multifunctional choroid. *Prog Retin Eye Res*. (2010) 29:144–68. doi: 10.1016/j.preteyeres.2009.12.002



OPEN ACCESS

EDITED BY

Mohd Imtiaz Nawaz,
King Saud University, Saudi Arabia

REVIEWED BY

Rizaldy Taslim Pinzon,
Duta Wacana Christian University, Indonesia
Xinrong Zhang,
Stanford University, United States

*CORRESPONDENCE

Nailong Yang
✉ nailongy@163.com

RECEIVED 26 December 2023

ACCEPTED 15 March 2024

PUBLISHED 03 April 2024

CITATION

Li X, Hao W, Lin S and Yang N (2024)
Association between AST/ALT ratio and
diabetic retinopathy risk in type 2 diabetes: a
cross-sectional investigation.
Front. Endocrinol. 15:1361707.
doi: 10.3389/fendo.2024.1361707

COPYRIGHT

© 2024 Li, Hao, Lin and Yang. This is an open-access article distributed under the terms of the [Creative Commons Attribution License \(CC BY\)](#). The use, distribution or reproduction in other forums is permitted, provided the original author(s) and the copyright owner(s) are credited and that the original publication in this journal is cited, in accordance with accepted academic practice. No use, distribution or reproduction is permitted which does not comply with these terms.

Association between AST/ALT ratio and diabetic retinopathy risk in type 2 diabetes: a cross-sectional investigation

Xianhua Li^{1,2}, Wenqing Hao^{1,2}, Sen Lin³ and Nailong Yang^{1,2*}

¹Department of Endocrinology and Metabolism, The Affiliated Hospital of Qingdao University, Qingdao, China, ²Department of Nursing and Hospital Infection Management, The Affiliated Hospital of Qingdao University, Qingdao, China, ³Department of Endocrinology and Diabetes Department, Shouguang People's Hospital, Weifang, Shandong, China

Objective: This study aimed to explore the association between the aspartate aminotransferase to alanine aminotransferase ratio (AST/ALT ratio) and diabetic retinopathy (DR) in patients with type 2 diabetes.

Methods: In this cross-sectional study, clinical data from 3002 patients with type 2 diabetes admitted to the Department of Endocrinology of our hospital between January 1, 2021, and December 1, 2022, were retrospectively collected. Measurements of AST and ALT were conducted and diabetes-related complications were screened. The association between AST/ALT ratio and diabetic retinopathy was assessed using multivariate logistic regression, and a generalized additive model (GAM) was used to investigate nonlinear relationships. Subgroup analyses and interaction tests were also conducted.

Results: Among the 3002 patients, 1590 (52.96%) were male and 1412 (47.04%) were female. The mean AST/ALT ratio was 0.98 ± 0.32 , ranging from 0.37 (Min) to 2.17 (Max). Diabetic retinopathy was present in 40.47% of the patients. After multivariate adjustments, for each 0.1 unit increase in AST/ALT ratio, the risk of DR increased by 4% (OR = 1.04, 95% CI: 1.01–1.07, $p=0.0053$). Higher AST/ALT ratio quartiles were associated with Higher prevalence of DR (OR vs. Q1: Q4 = 1.34 (CI: 1.03–1.75, $p=0.0303$). The GAM and smoothed curve fit indicated a linear relationship between AST/ALT ratio and DR risk, with no significant interaction effects across different subgroups.

Conclusion: Our study demonstrates a positive correlation between the AST/ALT ratio and diabetic retinopathy risk in type 2 diabetes, suggesting its potential role in assessing DR risk.

KEYWORDS

aspartate aminotransferases, alanine transaminase, diabetic retinopathy, diabetes mellitus, type 2, correlation

1 Introduction

Type 2 diabetes mellitus (T2DM) represents a significant global health challenge, affecting nearly half a billion people worldwide (1). Its prevalence is projected to increase dramatically, marking an escalating public health concern (2, 3). A prevalent microvascular complication of T2DM, diabetic retinopathy (DR), stands as a leading cause of blindness globally (4, 5). In China, the prevalence of DR among diabetic individuals exhibits considerable variation, with estimates ranging from 18.45% to 31.8%. This variation may reflect differences in study methodologies or demographic variations across regions, highlighting the complexity of managing DR within diverse populations (6, 7). Despite advancements in the understanding of DR, significant challenges in its early diagnosis and treatment remain (8, 9).

Liver enzymes, particularly Alanine aminotransferase (ALT) and Aspartate aminotransferase (AST), are emerging as significant markers (10, 11). The AST/ALT ratio, introduced by De Ritis in 1957, is a known indicator of liver function and has been associated with various systemic diseases, including cardiovascular, renal, and oncological conditions (12–15). Recent studies have also linked AST/ALT ratio with gestational diabetes and metabolic syndrome in children, expanding its relevance beyond liver diseases (16, 17). However, the relationship between AST/ALT ratio and DR in T2DM patients remains under-explored.

Considering the roles of AST and ALT in metabolic and inflammatory processes (18–21), investigating their relationship with DR may unveil new proxies for early diagnosis and risk stratification. This is particularly crucial for patients with T2DM, where early detection and accurate risk assessment of DR are essential to prevent severe vision loss (22, 23). Moreover, given the predictive value of the AST/ALT ratio in other systemic diseases (15, 24, 25), exploring its potential association with DR could offer fresh insights into the complexity of T2DM complications and facilitate personalized patient management strategies.

This study aims to address this gap by examining the association between the AST/ALT ratio and DR in T2DM patients. By understanding this relationship, we seek to contribute to the early detection and risk stratification of DR, a crucial step towards improving patient outcomes in T2DM.

2 Methods

2.1 Research setting and population

This single-center, cross-sectional study was conducted at the Endocrinology Department of Qingdao University Affiliated Hospital, between January 1, 2021, and December 1, 2022. Inpatients aged 18 and above, diagnosed with Type 2 Diabetes Mellitus (T2DM) as per the American Diabetes Association's 2021 guidelines, were included. Exclusion criteria were meticulously defined to mitigate potential confounding factors, including:

- Presence of severe systemic or ocular conditions (e.g., uveitis, glaucoma) that could affect the study outcomes.
- Recent ocular treatments or surgeries within the past three months.
- Significant liver diseases or unexplained AST and ALT elevations exceeding 2.5 times the upper limit.
- Use of medications known to affect liver function significantly.
- Malignant neoplasms, due to their profound systemic health impact and potential confounding effect.

Figure 1 illustrates the inclusion and exclusion criteria application.

2.2 Ethics statement

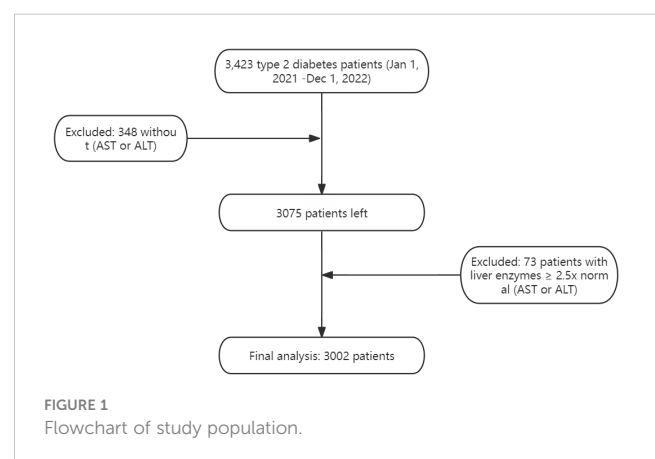
Adhering to the Declaration of Helsinki, informed consent was obtained from all participants. The study received ethical approval from the Ethics Committee of Qingdao University Affiliated Hospital (Approval No. QYFY WZLL 28254).

2.3 Measurement of AST and ALT

Blood samples were collected following an overnight fast to ensure accuracy. AST and ALT were quantified using the Hitachi 7600 analyzer, a method based on kinetic enzyme assay techniques. The established reference ranges were 15–40 U/L for AST and 9–50 U/L for ALT, aligning with clinical standards.

2.4 Diagnosis of diabetic retinopathy

The diagnosis of diabetic retinopathy (DR) in our study was rigorously conducted using a multi-modal imaging approach. Initial assessments involved slit lamp microscopy and optical coherence tomography to identify retinopathy changes during funduscopy examinations. This was followed by confirmatory diagnosis using 45° four-field stereoscopic digital photography with a Carl Zeiss



Fundus Camera, which allowed for the detailed capture of images from both eyes across designated fields, eliminating the need for mydriasis (26).

Experienced ophthalmologists then evaluated these images, classifying DR according to the International Clinical Diabetic Retinopathy Disease Severity Scale into four severity levels. The identification of any severity lesion based on this scale was considered diagnostic of DR (26), ensuring an accurate and comprehensive diagnostic process (27).

2.5 Covariates

2.5.1 Demographic and Clinical Data

Included variables were gender, age, diabetes duration, and complications.

2.5.2 Anthropometrics

Measurements of height, weight, and body mass index (BMI) were conducted, with BMI calculated as weight in kilograms divided by height in meters squared. In aligning with specific regional considerations, we applied the WHO BMI Asian cutoffs to classify participants: <23 as underweight or normal, 23–25 as overweight, and ≥ 25 as obese (28).

2.5.3 Lifestyle Factors

Smoking and alcohol consumption were evaluated, with alcohol consumption defined as intake of 30 g or more weekly for over a year, and smoking defined by a history of 100 or more cigarettes smoked in one's lifetime (29).

2.5.4 Biochemical Analyses

Fasting blood samples enabled creatinine, fasting plasma glucose, liver function tests, HbA1c. All assessments, apart from HbA1c, utilized the Hitachi 7600 analyzer. Fatty liver diagnosis was ultrasound-based (30). Hypertension was identified through blood pressure measurements, following established criteria (31). The eGFR calculation employed the Andrew S. Levey formula (32), with diabetic nephropathy confirmed per KDIGO guidelines when urinary ACR ≥ 30 mg/mmol or eGFR < 60 mL/min/1.73m² (33). Diabetic Peripheral Neuropathy (DPN) Diagnosis: A comprehensive assessment integrated clinical, neurological examinations, and nerve conduction studies, adhering to recognized guidelines (34). DPN diagnosis utilized a structured approach: Clinically Evident DPN: Required at least two positive findings among sensory symptoms, signs, or reflex abnormalities consistent with distal symmetrical polyneuropathy. Abnormal Nerve Conduction Studies: Mandated at least one abnormal parameter (amplitude, latency, F-wave, or nerve conduction velocity) in two or more specific nerves.

2.6 Statistical methods

Continuous variables were reported as means and standard deviations if normally distributed, and medians with interquartile

ranges (IQRs) for skewed distributions. Categorical variables were expressed as percentages. We utilized the Chi-square (χ^2) test for categorical variables, Student's t-test for normally distributed continuous variables, and the Mann-Whitney U test for skewed continuous variables to evaluate differences in diabetic retinopathy status among participants. Additionally, differences among AST/ALT ratio quartiles were analyzed using the χ^2 test for categorical variables, One-Way ANOVA for normally distributed variables, and the Kruskal-Wallis H test for variables with skewed distributions.

The AST/ALT ratio was treated both as a continuous variable, assessed in increments of 0.1 units for a detailed examination of its relationship with diabetic retinopathy (DR) risk, and as a categorical variable through quartile conversion to facilitate group comparisons.

To identify variables potentially associated with diabetic retinopathy (DR), we initially conducted univariate logistic regression analysis. Following this, we employed logistic regression analysis, systematically adjusting for potential confounders across distinct models: Non-adjusted model: No adjustments were applied. Model I: Adjustments were made for essential demographic and clinical factors, including Age, Sex, and Body Mass Index (BMI). Model II: This model provided a comprehensive adjustment for an extended set of variables: Age, Sex, BMI, Duration of Diabetes, Fasting Blood Glucose (FBG), Glycated Hemoglobin (HbA1c), Diabetic Nephropathy (DN), and Diabetic Peripheral Neuropathy (DPN).

To assess non-linear relationships between the AST/ALT ratio and DR risk, Generalized Additive Models (GAM) were utilized. Additionally, subgroup analyses and interaction tests were conducted to investigate the effects of the AST/ALT ratio across different patient subgroups.

Statistical analyses were conducted using R software (The R Foundation) and EmpowerStats (<http://www.empowerstats.com>, X&Y Solutions, Inc., Boston, MA), ensuring the use of robust and reliable tools. Significance was determined by a two-sided P-value of less than 0.05, maintaining a standard criterion for statistical significance.

3 Results

In Table 1, our cross-sectional study included 3002 type 2 diabetes patients, divided into 1787 without diabetic retinopathy (Non-Diabetic Retinopathy group) and 1215 with the condition (Diabetic Retinopathy group). Key differences emerged in demographic and clinical measures.

Significantly, the Diabetic Retinopathy group was older and had a higher proportion of females. The duration of diabetes was notably longer in this group.

Clinically, the Diabetic Retinopathy group showed higher levels of Glycated Hemoglobin (HbA1c) and a significant difference in the AST/ALT ratio, reflecting a potential link to retinopathy severity. Prevalences of hypertension and diabetic nephropathy were also higher in the Diabetic Retinopathy group, underscoring the

TABLE 1 Baseline characteristics of participants.

| | Non-Dia- betic Reti- nopathy (n = 1787) | Diabetic Retinopathy (n = 1215) | P-value |
|---|--|---------------------------------------|---------|
| Age (years old) | 57.20 (13.11) | 61.77 (10.94) | <0.001 |
| Sex, n (%) | | | 0.002 |
| Male | 988 (55.29%) | 602 (49.55%) | |
| Female | 799 (44.71%) | 613 (50.45%) | |
| BMI (kg/m ²) | | | 0.002 |
| <23 | 348 (19.58%) | 290 (24.09%) | |
| 23-25 | 398 (22.40%) | 290 (24.09%) | |
| >=25 | 1031 (58.02%) | 624 (51.83%) | |
| Smoking History, n (%) | | | 0.093 |
| Non-smokers | 1282 (72.02%) | 905 (74.79%) | |
| Smokers | 498 (27.98%) | 305 (25.21%) | |
| Alcohol Consumption History, n (%) | | | 0.518 |
| Non-drinkers | 1326 (74.41%) | 913 (75.45%) | |
| Drinkers | 456 (25.59%) | 297 (24.55%) | |
| Diabetic duration (years) | | | <0.001 |
| <5 | 795 (44.49%) | 250 (20.58%) | |
| 5-10 | 409 (22.89%) | 240 (19.75%) | |
| >=10 | 583 (32.62%) | 725 (59.67%) | |
| FBG (mmol/L) | 7.37 (2.29) | 7.50 (2.84) | 0.165 |
| HbA1c (%) | 8.46 (2.07) | 8.77 (1.94) | <0.001 |
| AST/ALT | 0.94 (0.31) | 1.03 (0.33) | <0.001 |
| eGFR (mL/min per 1.73 m ²) | 96.38 (41.94) | 94.95 (45.38) | 0.383 |
| Hypertension (%) | | | <0.001 |
| No | 858 (48.01%) | 507 (41.73%) | |
| Yes | 929 (51.99%) | 708 (58.27%) | |
| Fatty Liver Disease | | | <0.001 |
| No | 835(46.73%) | 745(61.32%) | |
| Yes | 952(53.27%) | 470(38.68%) | |
| Diabetic nephropathy | | | <0.001 |
| No | 1363 (76.27%) | 750 (61.73%) | |
| Yes | 424 (23.73%) | 465 (38.27%) | |

(Continued)

TABLE 1 Continued

| | Non-Dia- betic Reti- nopathy (n = 1787) | Diabetic Retinopathy (n = 1215) | P-value |
|--------------------------------------|--|---------------------------------------|---------|
| Diabetic peripheral neuropathy | | | <0.001 |
| No | 761 (42.59%) | 239 (19.67%) | |
| Yes | 1026 (57.41%) | 976 (80.33%) | |

Table Results Format: (N) Mean(SD).
FBG, Fasting Blood Glucose; HbA1c, Hemoglobin A1c; AST/ALT, aspartate aminotransferase to alanine aminotransferase; eGFR, Estimated Glomerular Filtration Rate.

comorbidity burden in these patients. In [Supplementary Material 1](#), we present the baseline characteristics of patients with Type 2 Diabetes Mellitus (T2DM), stratified by quartiles of the AST/ALT ratio.

In our preliminary univariate logistic regression analysis ([Table 2](#)), we observed a significant correlation between the AST/ALT ratio and the risk of diabetic retinopathy (DR) in patients with Type 2 Diabetes Mellitus (T2DM). Notably, the AST/ALT ratio, both as a continuous variable (OR: 1.98, 95% CI: 1.61 – 2.42, $p < 0.0001$) and when categorized into quartiles, showed a strong, positive association with DR risk, escalating across quartiles (Q1 as reference: Q2 OR: 1.55, Q3 OR: 1.64, Q4 OR: 2.16; all $p < 0.0001$). Other factors, such as age, female sex, longer diabetes duration, higher HbA1c levels, hypertension, fatty liver disease, diabetic nephropathy, and diabetic peripheral neuropathy, were also significantly associated with increased DR risk.

In our logistic regression analysis, as detailed in [Table 3](#), we systematically adjusted for potential confounders to evaluate the association between the AST/ALT ratio and the risk of diabetic retinopathy (DR) across several models. Analyzing the AST/ALT ratio as a continuous variable, the unadjusted model revealed a significant association (OR: 1.09, 95% CI: 1.07 - 1.12, $p < 0.0001$). The association’s strength was slightly attenuated upon adjusting for age, sex, and BMI in Model I (OR: 1.05, 95% CI: 1.03 - 1.08, $p < 0.0001$). Further adjustments in Model II, incorporating variables such as duration of diabetes, fasting blood glucose, HbA1c, diabetic nephropathy, and diabetic peripheral neuropathy, continued to show a positive association, albeit reduced (OR: 1.04, 95% CI: 1.01 - 1.07, $p = 0.0053$). These findings suggest that the AST/ALT ratio was consistently associated with higher odds of DR in type 2 diabetes, even after accounting for various confounding factors.

When analyzing the AST/ALT ratio as a variable categorized into quartiles, we observed that higher AST/ALT ratio quartiles were associated with an increased prevalence of DR in Model II, illustrating a gradient of risk across quartiles (OR vs. Q1: Q2 = 1.19, 95% CI: 0.92–1.55; Q3 = 1.09, 95% CI: 0.84–1.42; and Q4 = 1.34, 95% CI: 1.03–1.75).

In our study, we utilized generalized additive models (GAM) to explore the potential non-linear relationship between the AST/ALT

TABLE 2 Univariate logistic regression analysis: factors correlated with diabetic retinopathy.

| | Diabetic Retinopathy |
|---|---------------------------|
| Age (years old) | 1.03 (1.03, 1.04) <0.0001 |
| Sex, n (%) | |
| Male | 1.0(Ref) |
| Female | 1.26 (1.09, 1.46) 0.0020 |
| BMI categorial | |
| <23 | 1.0(Ref) |
| 23-25 | 0.87 (0.70, 1.09) 0.2258 |
| >=25 | 0.73 (0.60, 0.87) 0.0007 |
| Smoking History, n (%) | |
| Non-smokers | 1.0(Ref) |
| Smokers | 0.87 (0.73, 1.02) 0.0935 |
| Alcohol Consumption History, n (%) | |
| Non-drinkers | 1.0(Ref) |
| Drinkers | 0.95 (0.80, 1.12) 0.5185 |
| Diabetic duration (years) | |
| <5 | 1.0(Ref) |
| 5-10 | 1.87 (1.51, 2.31) <0.0001 |
| >=10 | 3.95 (3.31, 4.73) <0.0001 |
| HbA1c (%) | 1.08 (1.04, 1.12) 0.0001 |
| FBG (mmol/L) | 1.02 (0.99, 1.05) 0.1654 |
| eGFR (mL/min per 1.73 m ²) | 1.00 (1.00, 1.00) 0.3830 |
| AST/ALT (per 1 change) | 1.98 (1.61, 2.42) <0.0001 |
| AST/ALT quartile | |
| Q1 | 1.0(Ref) |
| Q2 | 1.55 (1.25, 1.92) <0.0001 |
| Q3 | 1.64 (1.32, 2.03) <0.0001 |
| Q4 | 2.16 (1.75, 2.67) <0.0001 |
| Hypertension | |
| No | 1.0(Ref) |
| Yes | 1.29 (1.11, 1.49) 0.0007 |
| Fatty Liver Disease | |
| No | 1.0(Ref) |
| Yes | 0.55 (0.48, 0.64) <0.0001 |
| Diabetic nephropathy | |
| No | 1.0(Ref) |
| Yes | 1.99 (1.70, 2.34) <0.0001 |
| Diabetic peripheral neuropathy | |
| No | 1.0(Ref) |
| Yes | 3.03 (2.56, 3.59) <0.0001 |

OR (95%CI) Pvalue.

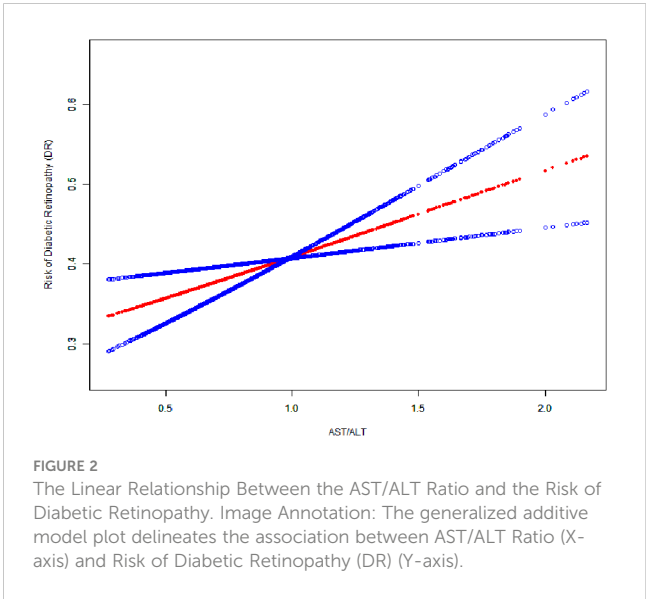
TABLE 3 Relationship between AST/ALT and DR in different models.

| Variable | Non-adjusted OR (95% CI) Pvalue | Adjust I OR (95% CI) Pvalue | Adjust II OR (95% CI) Pvalue |
|--------------------------|---------------------------------|-----------------------------|------------------------------|
| AST/ALT(per 0.1 change) | 1.09 (1.07, 1.12) <0.0001 | 1.05(1.03, 1.08) <0.0001 | 1.04 (1.01, 1.07) 0.0053 |
| AST/ALT subgroups | | | |
| Q1 | 1.0(Ref) | 1.0(Ref) | 1.0(Ref) |
| Q2 | 1.55(1.25,1.92) <0.0001 | 1.34(1.08,1.68) 0.0090 | 1.19(0.92,1.55) 0.1781 |
| Q3 | 1.64(1.32,2.03) <0.0001 | 1.28(1.02,1.60) 0.0340 | 1.09(0.84,1.42) 0.4999 |
| Q4 | 2.16(1.75,2.67) <0.0001 | 1.55(1.23,1.95) 0.0002 | 1.34(1.03,1.75) 0.0303 |

Non-adjusted model adjust for: None.
Adjust I model adjust for: Age; Sex; BMI.
Adjust II model adjust for: Age; Sex; BMI; Diabetic duration; FBG; HbA1c; DN; DPN.

ratio and diabetic retinopathy (DR), given the continuous nature of the AST/ALT ratio as depicted in [Figure 2](#). Our analysis, however, identified a linear relationship between the AST/ALT ratio and DR risk. This finding was determined after comprehensive adjustments for a range of critical variables, including age, sex, body mass index (BMI), duration of diabetes, fasting blood glucose (FBG), Hemoglobin A1c (HbA1c), diabetic nephropathy (DN), and diabetic peripheral neuropathy (DPN).

In our investigation, depicted in [Figure 3](#), we performed stratified analyses to examine the association between the AST/ALT ratio and diabetic retinopathy (DR) risk across diverse subgroups. These subgroups were defined by several key characteristics. The results, illustrated in a forest plot, indicated a consistent association between the AST/ALT ratio and diabetic retinopathy across our subgroups. Notably, this association was



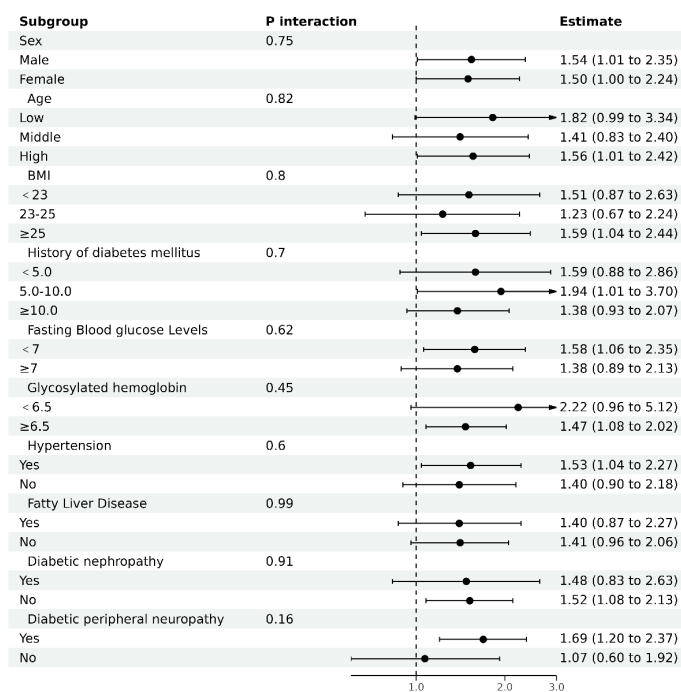


FIGURE 3
The results of subgroup analyses. Analysis adjusted for age, sex, body mass index (BMI), duration of diabetes, fasting blood glucose (FBG), Hemoglobin A1c (HbA1c), diabetic nephropathy (DN), and diabetic peripheral neuropathy (DPN), excluding the variable specific to each subgroup under investigation.

evaluated based on a per 1 unit increase in the AST/ALT ratio. Despite variations in demographic and clinical characteristics, the interaction p-values all exceeded 0.05, suggesting a stable and robust relationship between AST/ALT ratio and diabetic retinopathy risk that is not significantly influenced by these stratifying factors.

4 Discussion

Our study’s primary findings indicate a positive correlation between the AST/ALT ratio and the risk of diabetic retinopathy (DR) in patients with type 2 diabetes. This suggests that patients with higher AST/ALT ratios should be promptly screened for diabetic retinopathy, aiding in the improved management of type 2 diabetic retinopathy. These results provide novel insight into the relationship between liver enzymes and diabetic complications, highlighting the importance of the AST/ALT ratio in the clinical assessment of diabetes patients.

The pathophysiology of DR encompasses oxidative stress, chronic inflammation, and altered metabolic pathways. Intriguingly, the AST/ALT ratio, indicative of changes in liver enzyme levels, is associated with these same pathophysiological factors, including oxidative stress, systemic inflammation, and insulin resistance (35, 36). This association suggests that altered AST/ALT ratios could play a role in the progression of DR.

Further, our findings are in line with other research that highlights the significance of AST/ALT ratios in various diabetic

complications like peripheral neuropathy and nephropathy. These studies underscore the systemic impact of altered liver enzyme levels in diabetes (35, 37).

A notable strength of our study is the use of GAM, which effectively demonstrates the linear relationship between AST/ALT ratios and DR. Through rigorous statistical adjustments and consistent findings across different subgroups, our study suggests that each 0.1 unit increase in the AST/ALT ratio is associated with a 4% increase in the risk of DR.

Additionally, our comprehensive search of the PubMed database did not reveal any similar studies, highlighting the originality of our research. This study preliminarily suggests a potential association between the AST/ALT ratio and diabetic retinopathy (DR), thereby offering a new dimension in understanding possible biomarkers for diabetes and its complications.

However, this study still has some limitations. Being a cross-sectional analysis, it offers associative insights but cannot confirm causality (38). Additionally, the applicability of our results may be restricted to the Chinese population and might not extend to those with AST/ALT ratios beyond the 0.37 to 2.17 range.

In conclusion, our research sheds light on the AST/ALT ratio as a potential indicator associated with the risk of diabetic retinopathy in type 2 diabetes patients. These initial findings suggest that the AST/ALT ratio could be further investigated as a biomarker for assessing DR risk. Such investigations are important to validate these findings and explore the underlying biological mechanisms in more diverse populations and through prospective studies.

5 Conclusion

This study reveals a positive correlation between the AST/ALT ratio and the risk of diabetic retinopathy in type 2 diabetes patients. Further studies are essential to confirm these findings and investigate the underlying mechanisms across diverse populations.

Data availability statement

The raw data supporting the conclusions of this article will be made available by the authors, without undue reservation.

Ethics statement

This research was conducted in accordance with the principles set forth in the Declaration of Helsinki. Informed consent was obtained from all participants. The study received the endorsement of the Ethics Committee of the Affiliated Hospital of Qingdao University (Approval No. QYFY WZLL 28254).

Author contributions

XL: Data curation, Formal analysis, Writing – original draft. WH: Data curation, Supervision, Writing – review & editing. SL: Data curation, Formal analysis, Writing – review & editing. NY: Supervision, Writing – review & editing.

References

1. Sun H, Saeedi P, Karuranga S, Pinkepank M, Ogurtsova K, Duncan BB, et al. IDF Diabetes Atlas: Global, regional and country-level diabetes prevalence estimates for 2021 and projections for 2045. *Diabetes Res Clin Pract.* (2022) 183:109119. doi: 10.1016/j.diabres.2021.109119
2. Lin YK, Gao B, Liu L, Ang L, Mizokami-Stout K, Pop-Busui R, et al. The prevalence of diabetic microvascular complications in China and the USA. *Curr Diabetes Rep.* (2021) 21:16. doi: 10.1007/s11892-021-01387-3
3. Saeedi P, Petersohn I, Salpea P, Malanda B, Karuranga S, Unwin N, et al. Global and regional diabetes prevalence estimates for 2019 and projections for 2030 and 2045: Results from the International Diabetes Federation Diabetes Atlas, 9(th) edition. *Diabetes Res Clin Pract.* (2019) 157:107843. doi: 10.1016/j.diabres.2019.107843
4. Zhang X, Saaddine JB, Chou CF, Cotch MF, Cheng YJ, Geiss LS, et al. Prevalence of diabetic retinopathy in the United States, 2005–2008. *Jama.* (2010) 304:649–56. doi: 10.1001/jama.2010.1111
5. Cai K, Liu YP, Wang D. Prevalence of diabetic retinopathy in patients with newly diagnosed type 2 diabetes: A systematic review and meta-analysis. *Diabetes/metabolism Res Rev.* (2023) 39:e3586. doi: 10.1002/dmrr.3586
6. Zhang X, Huang Y, Xu N, Feng W, Qiao J, Liu M. Low serum dehydroepiandrosterone levels are associated with diabetic retinopathy in patients with type 2 diabetes mellitus. *J Diabetes Invest.* (2023) 14:675–85. doi: 10.1111/jdi.13997
7. Liu J, Hu H, Qiu S, Wang D, Liu J, Du Z, et al. The prevalence and risk factors of diabetic retinopathy: screening and prophylaxis project in 6 provinces of China. *Diabetes Metab syndrome Obes Targets Ther.* (2022) 15:2911–25. doi: 10.2147/DMSO.S378500
8. Vujosevic S, Aldington SJ, Silva P, Hernández C, Scanlon P, Peto T, et al. Screening for diabetic retinopathy: new perspectives and challenges. *Lancet Diabetes Endocrinol.* (2020) 8:337–47. doi: 10.1016/S2213-8587(19)30411-5
9. Kárasón KT, Vo D, Grauslund J, Rasmussen ML. Comparison of different methods of retinal imaging for the screening of diabetic retinopathy: a systematic review. *Acta ophthalmologica.* (2022) 100:127–35. doi: 10.1111/aos.14767
10. Mandato C, Vajro P. Isolated aspartate aminotransferase elevation: Is it liver disease or what else? *Acta paediatrica (Oslo Norway 1992).* (2022) 111:459–61. doi: 10.1111/apa.16213
11. Kulecka M, Wierzbicka A, Paziewska A, Mikula M, Habior A, Janczyk W, et al. A heterozygous mutation in GOT1 is associated with familial macro-aspartate aminotransferase. *J Hepatol.* (2017) 67:1026–30. doi: 10.1016/j.jhep.2017.07.003
12. Schupp T, Rusnak J, Weidner K, Ruka M, Egner-Walter S, Dudda J, et al. Prognostic value of the AST/ALT ratio versus bilirubin in patients with cardiogenic shock. *J Clin Med.* (2023) 12:5275. doi: 10.3390/jcm12165275
13. Liu X, Liu P. Elevated AST/ALT ratio is associated with all-cause mortality in patients with stable coronary artery disease: a secondary analysis based on a retrospective cohort study. *Sci Rep.* (2022) 12:9231. doi: 10.1038/s41598-022-13355-2
14. Liu H, Zha X, Ding C, Hu L, Li M, Yu Y, et al. AST/ALT ratio and peripheral artery disease in a chinese hypertensive population: A cross-sectional study. *Angiology.* (2021) 72:916–22. doi: 10.1177/00033197211004410
15. Zhou J, He Z, Ma S, Liu R. AST/ALT ratio as a significant predictor of the incidence risk of prostate cancer. *Cancer Med.* (2020) 9:5672–7. doi: 10.1002/cam4.3086
16. An R, Ma S, Zhang N, Lin H, Xiang T, Chen M, et al. AST-to-ALT ratio in the first trimester and the risk of gestational diabetes mellitus. *Front Endocrinol.* (2022) 13:1017448. doi: 10.3389/fendo.2022.1017448
17. Çelik N, Ünsal G, Taştanoğlu H. Predictive markers of metabolically healthy obesity in children and adolescents: can AST/ALT ratio serve as a simple and reliable diagnostic indicator? *Eur J Pediatr.* (2023) 183:243–51. doi: 10.1007/s00133-022-02111-v1
18. He Y, Ding F, Yin M, Zhang H, Hou L, Cui T, et al. High serum AST/ALT ratio and low serum INS*PA product are risk factors and can diagnose sarcopenia in middle-aged and older adults. *Front Endocrinol.* (2022) 13:843610. doi: 10.3389/fendo.2022.843610
19. Jiang T, Li Y, Li L, Liang T, Du M, Yang L, et al. Bifidobacterium longum 070103 fermented milk improve glucose and lipid metabolism disorders by regulating gut microbiota in mice. *Nutrients.* (2022) 14:4050. doi: 10.3390/nu14194050

Funding

The author(s) declare that no financial support was received for the research, authorship, and/or publication of this article.

Conflict of interest

The authors declare that the research was conducted in the absence of any commercial or financial relationships that could be construed as a potential conflict of interest.

Publisher's note

All claims expressed in this article are solely those of the authors and do not necessarily represent those of their affiliated organizations, or those of the publisher, the editors and the reviewers. Any product that may be evaluated in this article, or claim that may be made by its manufacturer, is not guaranteed or endorsed by the publisher.

Supplementary material

The Supplementary Material for this article can be found online at: <https://www.frontiersin.org/articles/10.3389/fendo.2024.1361707/full#supplementary-material>

20. Cao C, Zhang X, Yuan J, Zan Y, Zhang X, Xue C, et al. Nonlinear relationship between aspartate aminotransferase to alanine aminotransferase ratio and the risk of prediabetes: A retrospective study based on chinese adults. *Front Endocrinol.* (2022) 13:1041616. doi: 10.3389/fendo.2022.1041616
21. Lin MS, Lin HS, Chang ML, Tsai M-H, Hsieh Y-Y, Lin Y-S, et al. Alanine aminotransferase to aspartate aminotransferase ratio and hepatitis B virus on metabolic syndrome: a community-based study. *Front Endocrinol.* (2022) 13:922312. doi: 10.3389/fendo.2022.922312
22. Muqit MMK, Kourgialis N, Jackson-Degraffenried M, Talukder Z, Khetran ER, Rahman A, et al. Trends in diabetic retinopathy, visual acuity, and treatment outcomes for patients living with diabetes in a fundus photograph-based diabetic retinopathy screening program in Bangladesh. *JAMA network Open.* (2019) 2:e1916285. doi: 10.1001/jamanetworkopen.2019.16285
23. Preston FG, Meng Y, Burgess J, Ferdousi M, Azmi S, Petropoulos IN, et al. Artificial intelligence utilising corneal confocal microscopy for the diagnosis of peripheral neuropathy in diabetes mellitus and prediabetes. *Diabetologia.* (2022) 65:457–66. doi: 10.1007/s00125-021-05617-x
24. Åberg F, Danford CJ, Thiele M, Talbäck M, Rasmussen DN, Jiang ZG, et al. A dynamic aspartate-to-alanine aminotransferase ratio provides valid predictions of incident severe liver disease. *Hepatol Commun.* (2021) 5:1021–35. doi: 10.1002/hep4.1700
25. Wang L, Xu Y, Zhang S, Bibi A, Xu Y, Li T. The AST/ALT ratio (De ritis ratio) represents an unfavorable prognosis in patients in early-stage SFTS: an observational cohort study. *Front Cell infection Microbiol.* (2022) 12:725642. doi: 10.3389/fcimb.2022.725642
26. Wilkinson CP, Ferris FL 3rd, Klein RE, Lee PP, Agardh CD, Davis M, et al. Proposed international clinical diabetic retinopathy and diabetic macular edema disease severity scales. *Ophthalmology.* (2003) 110:1677–82. doi: 10.1016/S0161-6420(03)00475-5
27. Wu Z, Yu S, Kang X, Liu Y, Xu Z, Li Z, et al. Association of visceral adiposity index with incident nephropathy and retinopathy: a cohort study in the diabetic population. *Cardiovasc Diabetol.* (2022) 21:32. doi: 10.1186/s12933-022-01464-1
28. WHO Expert Consultation. Appropriate body-mass index for Asian populations and its implications for policy and intervention strategies. *Lancet (London England).* (2004) 363:157–63. doi: 10.1016/S0140-6736(03)15268-3
29. Yang Q, Xu H, Zhang H, Li Y, Chen S, He D, et al. Serum triglyceride glucose index is a valuable predictor for visceral obesity in patients with type 2 diabetes: a cross-sectional study. *Cardiovasc Diabetol.* (2023) 22:98. doi: 10.1186/s12933-023-01834-3
30. Leivas G, Maraschin CK, Blume CA, Telo GH, Trindade MRM, Trindade EN, et al. Accuracy of ultrasound diagnosis of nonalcoholic fatty liver disease in patients with classes II and III obesity: A pathological image study. *Obes Res Clin Pract.* (2021) 15:461–5. doi: 10.1016/j.orcp.2021.09.002
31. Whelton PK, Flack JM, Jennings G, Schutte A, Wang J, Touyz RM, et al. Editors' Commentary on the 2023 ESH management of arterial hypertension guidelines. *Hypertension (Dallas Tex 1979).* (2023) 80:1795–9. doi: 10.1161/HYPERTENSIONAHA.123.21592
32. Miller WG. Perspective on new equations for estimating glomerular filtration rate. *Clin Chem.* (2021) 67:820–2. doi: 10.1093/clinchem/hvab029
33. Stevens PE, Levin A. Evaluation and management of chronic kidney disease: synopsis of the kidney disease: improving global outcomes 2012 clinical practice guideline. *Ann Internal Med.* (2013) 158:825–30. doi: 10.7326/0003-4819-158-11-201306040-00007
34. Martin CL, Albers JW, Pop-Busui R. Neuropathy and related findings in the diabetes control and complications trial/epidemiology of diabetes interventions and complications study. *Diabetes Care.* (2014) 37:31–8. doi: 10.2337/dc13-2114
35. Xu J, Shi X, Pan Y. The association of aspartate aminotransferase/alanine aminotransferase ratio with diabetic nephropathy in patients with type 2 diabetes. *Diabetes Metab syndrome Obes Targets Ther.* (2021) 14:3831–7. doi: 10.2147/DMSO.S330741
36. Simental-Mendia LE, Rodríguez-Morán M, Gómez-Díaz R, Wachter NH, Rodríguez-Hernández H, Guerrero-Romero F. Insulin resistance is associated with elevated transaminases and low aspartate aminotransferase/alanine aminotransferase ratio in young adults with normal weight. *Eur J Gastroenterol Hepatol.* (2017) 29:435–40. doi: 10.1097/MEG.0000000000000811
37. Yan P, Wu Y, Dan X, Wu X, Tang Q, Chen X, et al. Aspartate aminotransferase/alanine aminotransferase ratio was associated with type 2 diabetic peripheral neuropathy in a Chinese population: A cross-sectional study. *Front Endocrinol.* (2023) 14:1064125. doi: 10.3389/fendo.2023.1064125
38. Savitz DA, Wellenius GA. Can cross-sectional studies contribute to causal inference? It depends. *Am J Epidemiol.* (2023) 192:514–6. doi: 10.1093/aje/kwac037



OPEN ACCESS

EDITED BY

Mohd Imtiaz Nawaz,
King Saud University, Saudi Arabia

REVIEWED BY

Yinan Jiang,
University of Pittsburgh, United States
Ioannis Serafimidis,
Biomedical Research Foundation of the
Academy of Athens (BRFAA), Greece

*CORRESPONDENCE

Ming-ming Yang

✉ ming4622@163.com

Zuhui Pu

✉ zuhuipu@email.szu.edu.cn

[†]These authors have contributed equally to this work

RECEIVED 06 February 2024

ACCEPTED 25 April 2024

PUBLISHED 10 May 2024

CITATION

Wang J, Sun H, Mou L, Lu Y, Wu Z, Pu Z and Yang M-m (2024) Unveiling the molecular complexity of proliferative diabetic retinopathy through scRNA-seq, AlphaFold 2, and machine learning. *Front. Endocrinol.* 15:1382896. doi: 10.3389/fendo.2024.1382896

COPYRIGHT

© 2024 Wang, Sun, Mou, Lu, Wu, Pu and Yang. This is an open-access article distributed under the terms of the [Creative Commons Attribution License \(CC BY\)](#). The use, distribution or reproduction in other forums is permitted, provided the original author(s) and the copyright owner(s) are credited and that the original publication in this journal is cited, in accordance with accepted academic practice. No use, distribution or reproduction is permitted which does not comply with these terms.

Unveiling the molecular complexity of proliferative diabetic retinopathy through scRNA-seq, AlphaFold 2, and machine learning

Jun Wang^{1†}, Hongyan Sun^{2†}, Lisha Mou^{3,4}, Ying Lu^{3,4}, Zijing Wu^{3,4}, Zuhui Pu^{3,4*} and Ming-ming Yang^{2*}

¹Department of Endocrinology, Shenzhen People's Hospital (The Second Clinical Medical College of Jinan University; The First Affiliated Hospital, Southern University of Science and Technology), Shenzhen, China, ²Department of Ophthalmology, Shenzhen People's Hospital (The Second Clinical Medical College, Jinan University; The First Affiliated Hospital, Southern University of Science and Technology), Shenzhen, China, ³Imaging Department, Shenzhen Institute of Translational Medicine, The First Affiliated Hospital of Shenzhen University, Shenzhen Second People's Hospital, Shenzhen, China, ⁴MetaLife Center, Shenzhen Institute of Translational Medicine, Guangdong, Shenzhen, China

Background: Proliferative diabetic retinopathy (PDR), a major cause of blindness, is characterized by complex pathogenesis. This study integrates single-cell RNA sequencing (scRNA-seq), Non-negative Matrix Factorization (NMF), machine learning, and AlphaFold 2 methods to explore the molecular level of PDR.

Methods: We analyzed scRNA-seq data from PDR patients and healthy controls to identify distinct cellular subtypes and gene expression patterns. NMF was used to define specific transcriptional programs in PDR. The oxidative stress-related genes (ORGs) identified within Meta-Program 1 were utilized to construct a predictive model using twelve machine learning algorithms. Furthermore, we employed AlphaFold 2 for the prediction of protein structures, complementing this with molecular docking to validate the structural foundation of potential therapeutic targets. We also analyzed protein-protein interaction (PPI) networks and the interplay among key ORGs.

Results: Our scRNA-seq analysis revealed five major cell types and 14 subcell types in PDR patients, with significant differences in gene expression compared to those in controls. We identified three key meta-programs underscoring the role of microglia in the pathogenesis of PDR. Three critical ORGs (ALKBH1, PSIP1, and ATP13A2) were identified, with the best-performing predictive model demonstrating high accuracy (AUC of 0.989 in the training cohort and 0.833 in the validation cohort). Moreover, AlphaFold 2 predictions combined with molecular docking revealed that resveratrol has a strong affinity for ALKBH1, indicating its potential as a targeted therapeutic agent. PPI network analysis,

revealed a complex network of interactions among the hub ORGs and other genes, suggesting a collective role in PDR pathogenesis.

Conclusion: This study provides insights into the cellular and molecular aspects of PDR, identifying potential biomarkers and therapeutic targets using advanced technological approaches.

KEYWORDS

diabetic retinopathy, single-cell analysis, oxidative stress, AlphaFold 2, NMF, PPI, machine learning, ALKBH1

Introduction

Proliferative diabetic retinopathy (PDR), an advanced stage of diabetic retinopathy, is a leading cause of irreversible blindness in the productive-age population worldwide (1, 2). Characterized by retinal neovascularization leading to severe complications such as neovascular glaucoma, vitreous hemorrhage, and retinal detachment, the pathogenesis of PDR has not been fully elucidated (3, 4). Despite recent advances in imaging and management (5), understanding the underlying molecular mechanisms is crucial for developing effective therapies.

Oxidative stress, which is notably exacerbated in diabetes, plays a pivotal role in PDR pathogenesis (6). It damages mitochondrial structures and DNA in the retinal vasculature, impairing cellular function (7). This stress is a key contributor to neovascular unit insults, underpinning the core pathophysiology of PDR. Additionally, diabetic patients are more susceptible to oxidative stress due to impaired defense mechanisms, further emphasizing the role of oxidative stress in the development and progression of diabetic retinopathy, including PDR (8).

Single-cell RNA sequencing (scRNA-seq) has significantly advanced disease research by providing detailed insights into the cellular and molecular dimensions of various diseases (9, 10). Its ability to dissect gene expression at the individual cell level reveals the intricate cellular landscape of PDR, distinguishing between diseased and healthy states (11). The study carried out by Hu et al. provides valuable insights into the use of scRNA-seq in studying PDR (12). These authors highlighted the application of scRNA-seq for gene expression profiling, identifying cell populations in fibrovascular membranes from PDR patients, and revealing the novel role of microglia in the fibrovascular membrane of PDR. These studies collectively emphasize the significance of scRNA-seq in unraveling the molecular and cellular complexities of

PDR, offering a promising approach for further research and potential therapeutic interventions.

Concurrently, the integration of machine learning algorithms, particularly in predictive modeling, has introduced a new dimension to biomedical research (13, 14). These algorithms, including LASSO, Ridge, and Elastic Net, facilitate the development of predictive models for PDR, thereby increasing the accuracy of diagnoses and informing personalized treatment approaches.

In our study, we combined single-cell sequencing with advanced machine learning methods, as well as Non-negative Matrix Factorization (NMF), to uncover transcriptional and oxidative stress signatures in PDR. Our goal was to pinpoint oxidative stress-related genes (ORGs) that could serve as biomarkers, aiming to enhance the diagnostic and therapeutic landscape of PDR.

Methods

Data processing

ScRNA-seq data from five proliferative diabetic retinopathy (PDR) patients (GSE165784) (12) and three control samples (15) were processed alongside two bulk RNA PDR patient cohorts from the GEO database (cohort 1: GSE160306 (16), 76 samples; cohort 2: GSE102485 (17), 25 samples). Oxidative stress-related genes (ORGs) were identified from the Gene Ontology and PathCards databases.

Single-cell data analysis of PDR patients

The single-cell data of five PDR patients (12) and three healthy controls (15) were analyzed via Seurat (18). We filtered cells based on mitochondrial content (<10%), cell count (>300), and gene number (1000-5000). The t-distributed stochastic neighbor embedding (t-SNE) (19) and 'RunHarmony' functions (20) facilitated visualization and batch effect correction. Cell subtypes were annotated according to cell markers from the original study (12, 15). In the differential expression analysis between microglia and mesenchymal cells in PDR versus control samples, the

Abbreviations: PDR, Proliferative diabetic retinopathy; scRNA-seq, Single-cell RNA sequencing; NMF, Non-negative Matrix Factorization; ORGs, Oxidative stress-related genes; PPI, Protein-protein interaction; CTD, Comparative Toxicogenomics Database.

mitochondrial and ribosomal genes were removed. We used the Wilcoxon signed-rank test to identify significant genes (adjusted P value <0.05, absolute $\log_2FC > 1$).

Non-negative matrix factorization and meta-program detection of microglia in PDR patients

NMF analysis, specifically consensus NMF (cNMF), was applied to microglia in PDR samples, standardizing negative values to zero. After more than 100 iterations, we explored the components (k) ranging from 2 to 10 signatures, determining the optimal component number via a diagnostic plot from the provided tutorial (<https://github.com/dylkot/cNMF>) (21). A two-step gene ranking algorithm was used to identify nonoverlapping gene modules, which were further analyzed for expression patterns using Pearson correlations and hierarchical clustering, revealing three distinct meta-programs.

Establishment of a machine learning-driven predictive ORG model for PDR patients

Twelve machine learning algorithms, including (1) Least Absolute Shrinkage and Selection Operator (LASSO), (2) Ridge, (3) Elastic network (Enet), (4) StepAIC, (5) Support Vector Machines (SVM), (6) GlmBoost, (7) Linear Discriminant Analysis (LDA), (8) Partial Least Squares Regression for Generalized Linear Models (plsRglm), (9) Random Forest (RSF), (10) Generalized Boosted Regression Models (GBMs), (11) XGBoost, (12) Naive Bayes, were utilized to develop a predictive ORG model for PDR. We constructed 109 model combinations, trained initial models with the GSE160306 cohort and validated them with the GSE102485 cohort. Model performance was assessed using the AUC.

Prediction of the structure of proteins

We utilized AlphaFold 2, a tool that has achieved remarkably accurate levels comparable to those obtained through human observation via advanced techniques such as cryoelectron microscopy, for the prediction of protein structures (22). For our specific study objectives, we used AlphaFold 2 to predict the structures of select proteins relevant to our research. We focused on the proteins ALKBH1, PSIP1, and ATP13A2, which play significant roles in the context of PDR. The sequences of these proteins were meticulously retrieved from the NCBI database (23).

Molecular docking analysis

To investigate the binding affinities and interaction patterns of the drug candidates with their targets, we utilized AutoDock Vina 1.2.2, a

software designed for in silico protein–ligand docking (24). The molecular structure of resveratrol was obtained from the PubChem Compound database (<https://pubchem.ncbi.nlm.nih.gov/>) (25). AlphaFold 2 was used to generate the 3D coordinates for ALKBH1. Before docking analysis, all proteins and ligand files were prepared by converting them into PDBQT format. This preparation involved the removal of water molecules and the addition of polar hydrogen atoms to ensure accurate docking simulations. The docking grid box was strategically positioned to encompass the target protein's domain, allowing for unhindered molecular movement within the simulation. The dimensions of the grid box were set to 30 Å × 30 Å × 30 Å, with a grid point spacing of 0.05 nm to capture detailed interaction data. The molecular docking studies were conducted using AutoDock Vina 1.2.2 (<http://autodock.scripps.edu/>).

Protein interaction network analysis of key ORGs

In our study, we investigated protein interactions involving three pivotal ORGs. The use of the STRING database (<https://string-db.org/>) (26), a comprehensive resource, enabled us to compile and amalgamate data on protein–protein interactions (PPIs). Our focus was directed toward interactions with confidence scores surpassing 0.7, a threshold set to ensure the biological relevance and significance of these interactions.

To deepen our analysis and improve its visualization, we transferred the relevant data into Cytoscape (version 3.8.2) (27). Within the Cytoscape environment, we leveraged the capabilities of the cytoHubba plugin. This allowed us to pinpoint and rank the top 10 nodes in the PPI network. The ranking process utilized seven distinct algorithms, each contributing a unique perspective to the analysis. These algorithms included the following: Radiality, which measures the centrality of a node; Maximum Neighborhood Component (MNC), which assesses the largest connected component around a node; Maximum Clique Centrality (MCC), which focuses on the largest clique a node belongs to; Edge Percolated Component (EPC), which evaluates the connectivity and clustering; DMNC, which is the Maximum Neighborhood Component Centrality, a derivative of the MNC; Degree, which counts the number of edges linked to a node; and Closeness, which measures the average distance to other nodes. To synthesize and present our findings, we utilized an UpSet diagram.

Identification of hub genes associated with PDR

To identify the hub genes associated with PDR, we used the Comparative Toxicogenomics Database (CTD, <http://ctdbase.org/>) (28). Utilizing the CTD, we conducted an in-depth analysis to unravel the connections between potential key genes and a spectrum of relevant conditions. This included not only PDR but also a broader scope of related health issues, such as other eye diseases, retinal disorders, vascular diseases, complications arising from diabetes, and diabetes mellitus itself.

Statistical analysis

All the statistical analyses of single cells were performed with R (version 4.3.1). A *P* value less than 0.05 was considered to indicate statistical significance if not explicitly stated.

Results

Analysis of single-cell RNA sequencing data

In this study, we conducted an in-depth analysis of single-cell RNA sequencing data from five patients with proliferative diabetic retinopathy (PDR) (GSE165784) (12) and three healthy controls (15), implementing t-distributed stochastic neighbor embedding (t-SNE) for visualization post-quality control and data normalization. This approach effectively distinguished between cellular clusters of the PDR and control cohorts.

Figure 1A displays the range and individual RNA counts per cell, reflecting successful quality control measures for our sample analysis. We highlighted the 2000 genes with the highest variability across samples in Figure 1B. To further dissect this complexity, we applied linear dimensionality reduction to compute principal components (PCs), as illustrated in Figure 1C. The determination of significant PCs was aided by the integration of both ElbowPlot (Figure 1D) and JackStrawPlot (Figure 1E), setting the stage for more nuanced analyses. The distribution of cells across the PDR and control groups is presented in Figure 1F, with the study encompassing 5 PDR and 3 control samples, as depicted in Figure 1G. A total of 26 clusters were identified across the samples (Figure 1H). Through marker analysis from the original study (12), we classified cells into five primary types: microglia, lymphocytes, myeloid cells, endothelial cells, and mesenchymal cells (Figure 1I). This categorization was further refined, resulting in the identification of 14 distinct subcell types (Figure 1J).

Analysis of gene expression variations and cell-cell interactions in PDR

Our investigation of differential gene expression and intercellular communication within the retinal microenvironment of PDR patients highlighted important findings. We observed pronounced ligand-receptor interactions among various cell types, with notable interactions between microglia and mesenchymal cells, as well as between microglia and endothelial cells (Figures 2A, B). These interactions shed light on the intricate signaling pathways that could be instrumental in the development and progression of PDR, suggesting potential therapeutic targets.

In a detailed analysis of gene expression between microglia and mesenchymal cells in PDR versus control samples, 40 genes were upregulated, and 111 genes were downregulated in both cell types (Figures 2C, D; Supplementary Tables 1–4). The upregulated genes, including FN1, ATP5F1E, B2M, MALAT1, and ATP5MG, and downregulated genes, such as ATP5E, ALDOA, ATP5L, ATP5I,

and C14orf2, indicate a complex regulatory landscape. Furthermore, we revealed nuanced gene expression patterns: GLUL, DAB2, SELENOP, and ALDH1A1 were downregulated in mesenchymal cells but upregulated in microglia (Figure 2E; Supplementary Tables 5, 6), while C12orf75, ITM2C, and CCND1 showed the opposite pattern (Figure 2F; Supplementary Tables 7, 8).

Identification of transcriptional programs in PDR microglia cells using non-negative matrix factorization

In our detailed investigation of specific microglia within PDR samples, we employed the sophisticated technique of NMF to determine the unique transcriptional landscape of these cells. This advanced approach allowed us to systematically catalog various gene modules, which are fundamentally crucial in defining the distinct states of cells. Through this meticulous process, we were able to identify and analyze patterns of gene coexpression within individual PDR samples.

Our comparative analysis across multiple PDR samples was instrumental in revealing recurring gene modules. This aspect of our study was particularly significant because it effectively minimized the impact of technical variations, thereby enhancing the reliability and accuracy of our findings. By focusing on these gene modules, we gained valuable insights into the transcriptional intricacies inherent in PDR microglia.

One of the most noteworthy outcomes of our analysis was the identification of three distinct meta-programs. These meta-programs were discerned and clustered based on their correlation coefficients, providing a clear representation of the transcriptional synergy within microglia. The top-scoring genes of these meta-programs were characterized, as depicted in Figure 3A. Notably, Meta-Program 1 emerged as particularly prominent, exhibiting the highest level of correlation among the three. These results suggest that the genes within Meta-Program 1 are potentially central to the transcriptional identity and function of microglia in the context of PDR.

Elucidation of these meta-programs is important to our understanding of PDR. This study provides a novel perspective on the transcriptional dynamics of microglia, a critical component of disease pathology. This insight not only enhances our understanding of the molecular mechanisms underlying PDR but also opens up new directions for targeted therapeutic strategies aimed at modulating these specific transcriptional programs.

Development and validation of the oxidative stress-related gene predictive model for PDR

To develop a predictive model for PDR based on ORGs, we examined a subset of 15 genes that notably intersected within Meta-Program 1, as illustrated in Figure 3B. We constructed ORG models by twelve diverse machine learning algorithms, including (1) Least Absolute Shrinkage and Selection Operator (LASSO), (2) Ridge, (3) Elastic network (Enet), (4) StepAIC, (5) Support Vector Machines

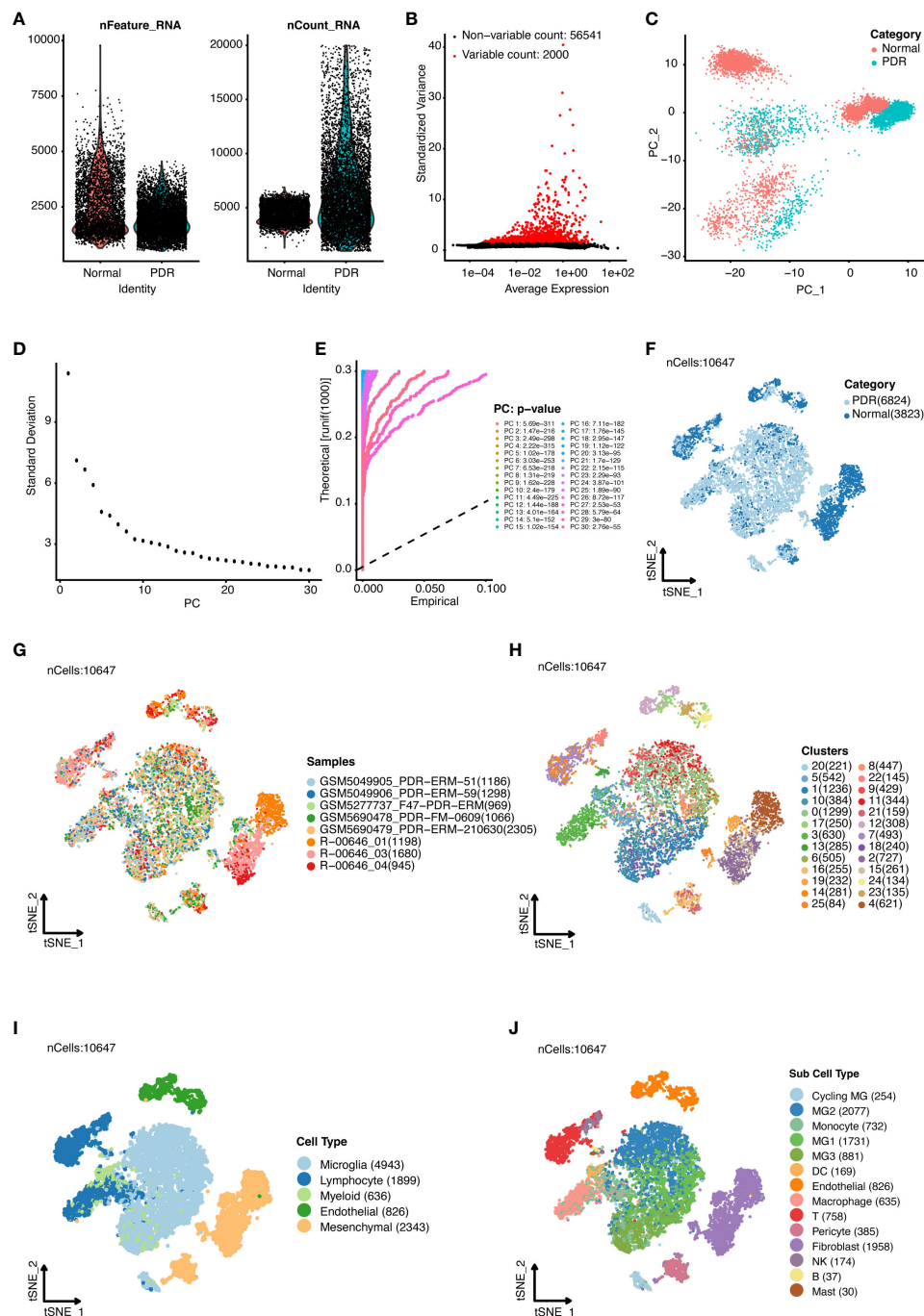


FIGURE 1

Single-cell RNA sequencing analysis of proliferative diabetic retinopathy (PDR) samples compared with normal samples. (A) Quality control of single-cell RNA sequencing data for PDR and normal samples. (B) Identification of highly variable genes. The top 2000 variable genes are shown as red dots. (C) Principal component analysis. Accordingly, we classified the cell groups into two categories. ElbowPlot (D) and JackStrawPlot (E) of principal components. T-distributed stochastic neighbor embedding (t-SNE) analysis of different groups (F), 8 samples (G), 26 clusters (H), five major cell types (I), and 14 subcell types (J).

(SVM), (6) GlmBoost, (7) Linear Discriminant Analysis (LDA), (8) Partial Least Squares Regression for Generalized Linear Models (plsRglm), (9) Random Forest (RSF), (10) Generalized Boosted Regression Models (GBMs), (11) XGBoost, (12) Naive Bayes (Figure 4A). Among the 109 models constructed, the cream of the crop emerged in the form of models based on a sophisticated Stepglm [backward]+RF approach. These standout models

prominently featured three key ORGs, ALKBH1, PSIP1, and ATP13A2, as delineated in Figure 4B. The importance of this model was unmistakably demonstrated in the training cohort (GSE160306), in which an outstanding area under the curve (AUC) of 0.989 was achieved. This exceptional level of predictive accuracy underlines the model's formidable potential as a tool for diagnosing PDR.

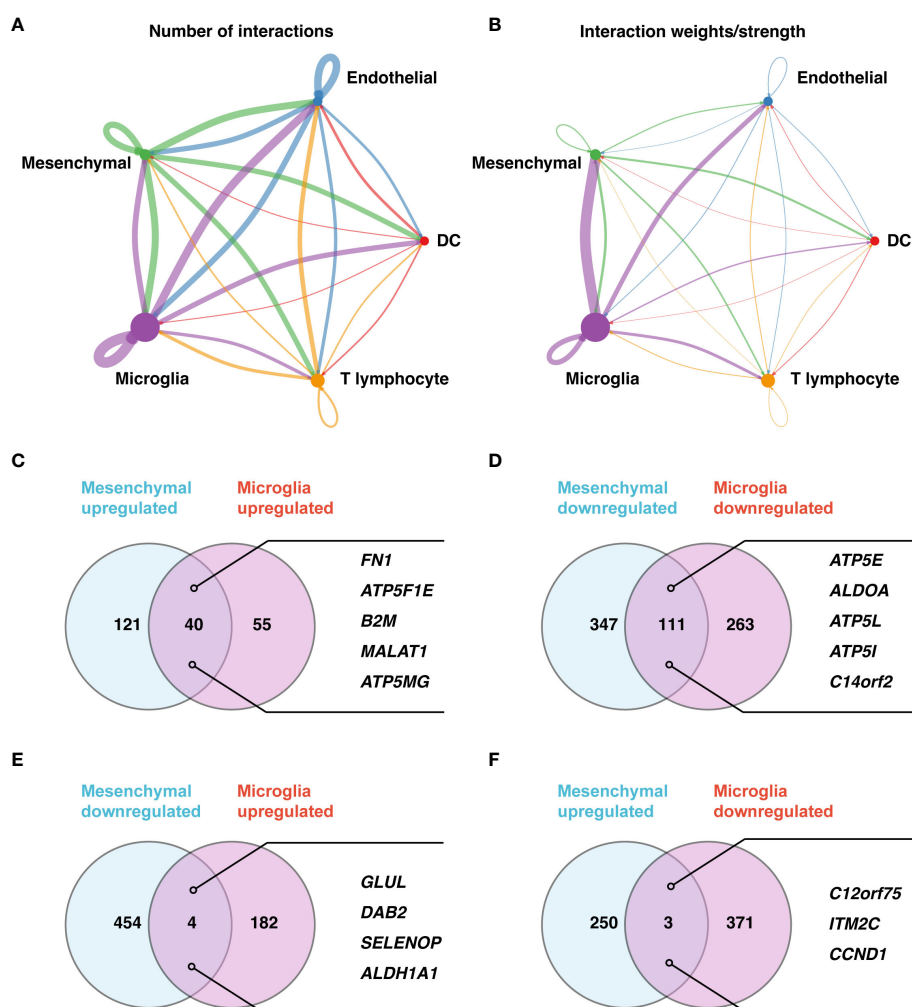


FIGURE 2

Detailed analysis of cell-cell communication and gene expression in PDR. (A, B) Cell-cell communication network maps for five major cell types based on the number of involved genes (A) and interaction weights/strengths (B). (C–F) Gene expression analysis of microglia and mesenchymal cells. Upregulated (C) and downregulated (D) genes in both cell types. (E) Downregulated genes in mesenchymal cells but upregulated genes in microglia. (F) Upregulated genes in mesenchymal cells but downregulated genes in microglia.

To further validate the model's applicability in a clinical setting, we undertook a validation study using an external cohort (GSE102485). The results were encouraging, as the model retained a significant level of diagnostic accuracy, as evidenced by an AUC of 0.833. This performance in an external cohort not only reinforces the model's robustness but also underscores its potential utility as an early detection and ongoing monitoring tool for PDR.

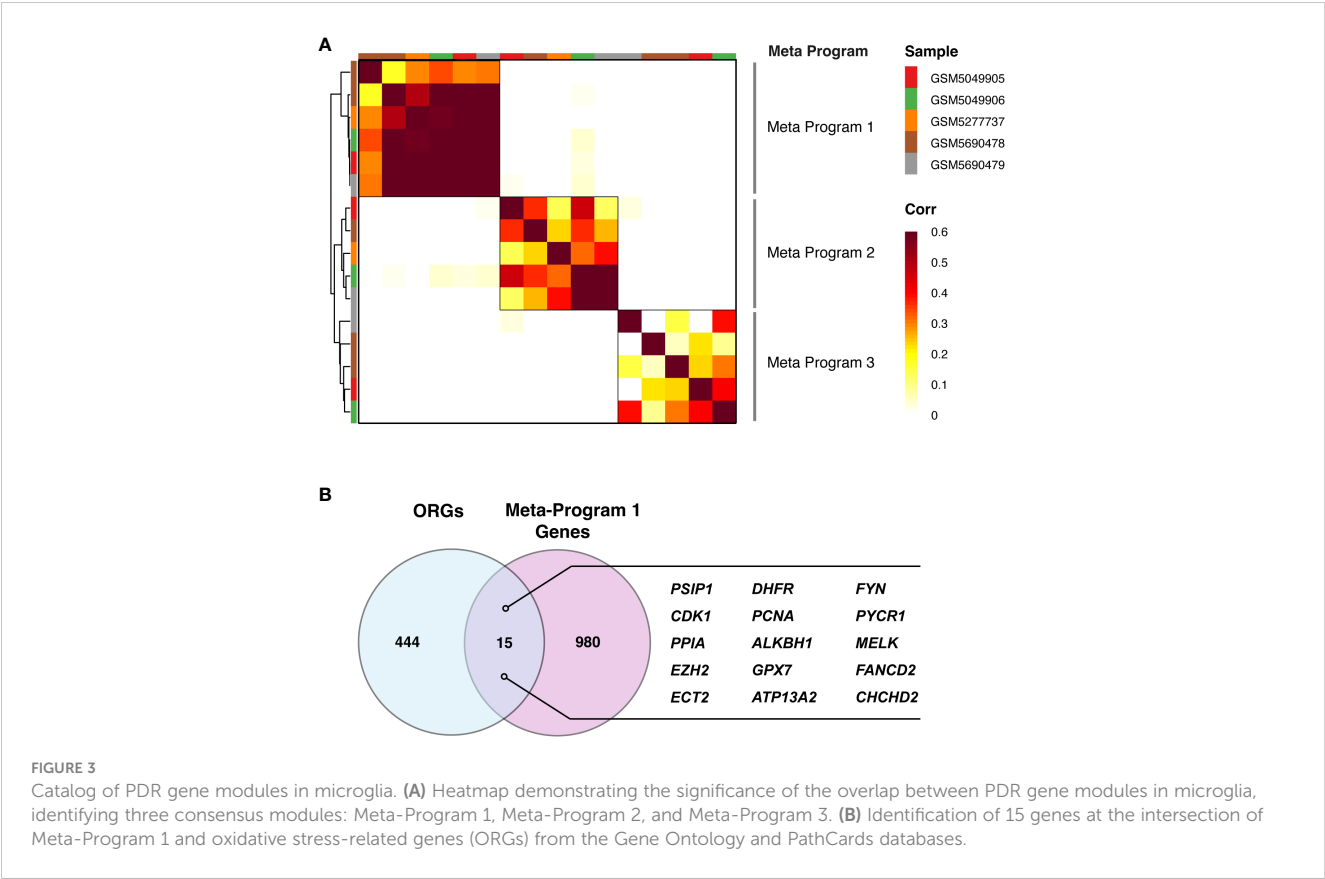
Structural prediction and molecular docking analysis

In our study, we harnessed the ability of AlphaFold 2 technology to predict the complex structures of three pivotal ORGs, ALKBH1, PSIP1, and ATP13A2, as shown in Figure 4C. The predictive confidence for ALKBH1 and ATP13A2 was notably high, whereas PSIP1 demonstrated lower confidence levels and was subsequently not included in further analysis.

Furthermore, to assess the binding affinity of potential therapeutic agents for these targets, we conducted a molecular docking analysis. Specifically, we explored the interaction between ALKBH1 and the candidate drug resveratrol utilizing AutoDock Vina v.1.1.2 for this purpose. The analysis provided insights into the binding modes and calculated the binding energies for the interactions (Figures 5A–C). The derived binding energy for the ALKBH1-resveratrol complex was -6.471 kcal/mol, suggesting a highly stable interaction. This strong and stable binding affinity further underscores the potential therapeutic relevance of targeting ALKBH1 with resveratrol in the context of oxidative stress-related conditions.

Protein interaction analysis of key ORGs in PDR

Next, we explored the protein-protein interactions (PPIs) of these ORGs. For this purpose, we utilized the STRING database,



which is renowned for its extensive protein interaction data. Our focus was on interactions with confidence scores exceeding 0.7, ensuring that only biologically significant and reliable interactions were considered. This selective approach was instrumental in sifting through vast data to identify meaningful connections that could be crucial in the context of PDR.

The PPI network enriched with these curated data was then intricately analyzed using Cytoscape. This platform enabled us to visualize and dissect the complex web of interactions. Using the cytoHubba plugin within Cytoscape, we systematically identified the top 10 nodes in the network utilizing a suite of seven sophisticated algorithms. These included Radiality, Maximum Neighborhood Component (MNC), Maximum Clique Centrality (MCC), EPC (Edge Percolated Component), DMNC (Maximum Neighborhood Component Centrality), Degree, and Closeness, each offering a unique lens to view and understand the network's structure. **Figures 6A, B** depict these findings, revealing a comprehensive map of the interactions.

Furthermore, to emphasize the interconnected nature of these interactions, we constructed an UpSet diagram (**Figure 6C**). This visualization succinctly highlighted the convergence of hub genes across different algorithms, revealing key proteins such as H2AC8, H2BC12, H2AC13, and H2AC16 that were consistently central across all algorithms, as detailed in **Supplementary Table 9**. This representation was instrumental in highlighting the core genes within the network, thereby elucidating their potential collective role in the pathophysiology of PDR.

Integrating comparative toxicogenomics database analysis with PDR research

To complement our protein interaction analysis, we utilized CTD as an instrumental resource. The CTD facilitated the expansion of our study to investigate the connections between our identified hub ORGs and a range of conditions associated with PDR, such as diabetic retinopathy, various eye and retinal diseases, vascular complications, and diabetes mellitus itself. **Figures 7A–F** display these connections, emphasizing the marked correlation between genes *ALKBH1*, *PSIP1*, *ATP13A2*, and the aforementioned conditions, validated by substantial reasoning scores within the CTD. Additionally, we incorporated a “negative control” gene, *PXDNL*, an unrelated ORG, to bolster the conclusiveness of our analysis.

Discussion

Proliferative diabetic retinopathy (PDR) poses a significant challenge in diabetes management and often leads to irreversible blindness. Current treatments such as panretinal photocoagulation have limitations, including potential adverse effects on visual acuity (29). Novel approaches such as CD40-TRAF6 inhibition (30) and anti-IL17A therapy (31) show promise in mouse models but require further clinical validation. These limitations underscore the pressing need for more effective and precise therapeutic strategies.

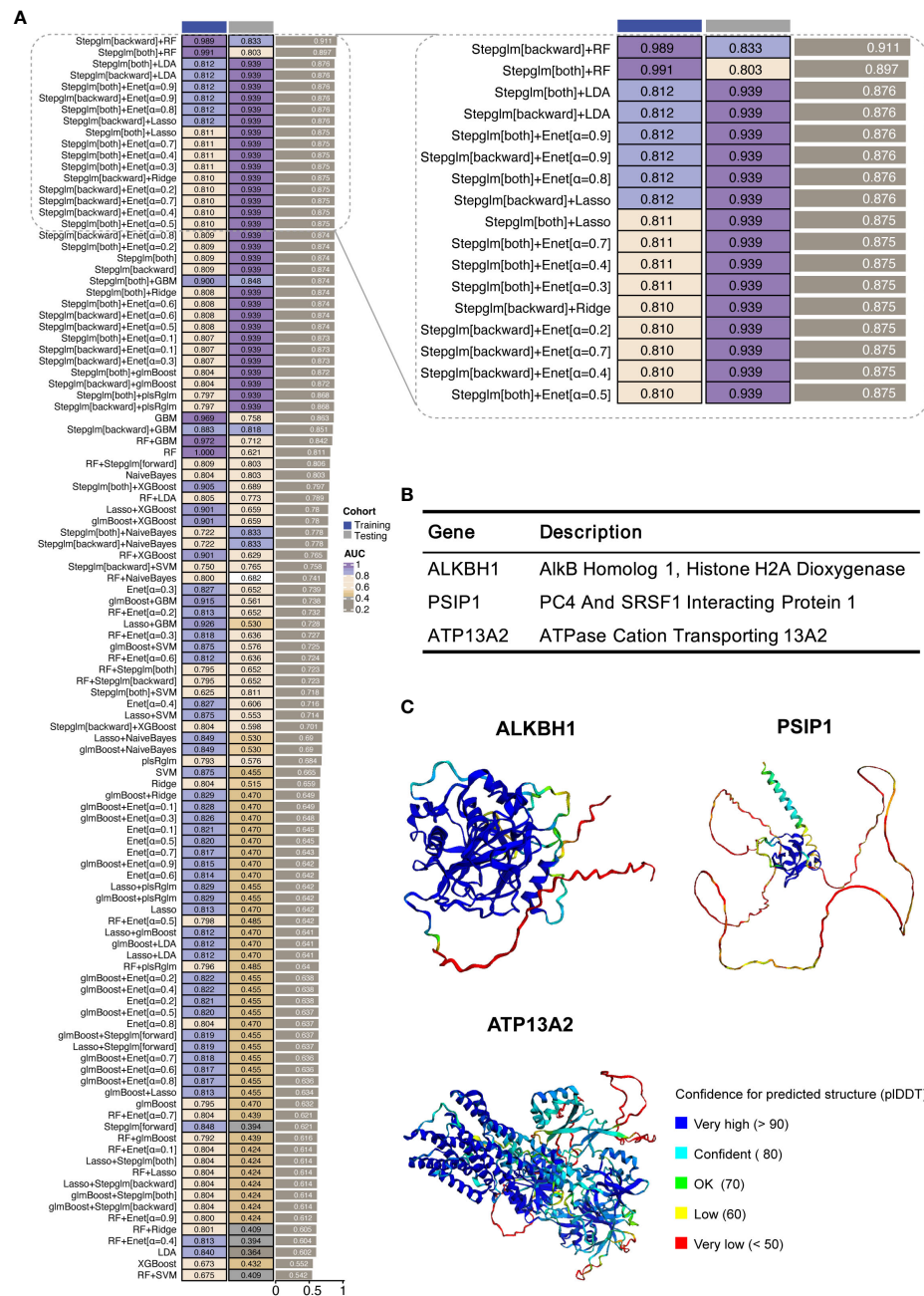


FIGURE 4

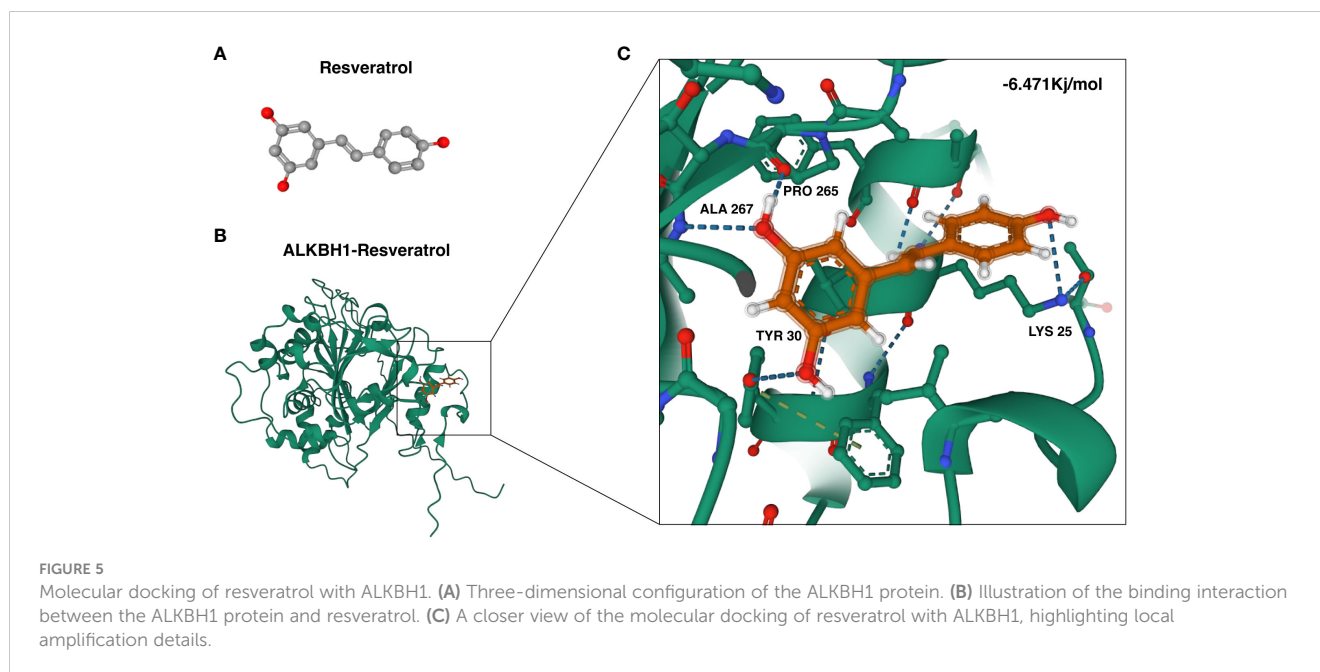
Development of machine learning-derived predictive models. (A) AUC results for combinations of machine learning algorithms in the training and validation cohorts. The training cohort was GSE160306, and the validation cohort was GSE102485. (B) Description of the three hub ORGs included in the highest-performing model. (C) Protein structures of three hub ORGs predicted using AlphaFold 2.

In our study, the integration of single-cell sequencing and Non-negative Matrix Factorization (NMF) was pivotal in revolutionizing our understanding of the transcriptional intricacies in PDR. This advanced methodological approach facilitated in-depth analysis of the disease transcriptional landscape, revealing the existence of specific gene modules and delineating three crucial meta-programs.

Our focused analysis, through the lens of NMF, allowed us to dissect the intricate patterns of gene expression, revealing how different gene modules interact and contribute to the

pathophysiology of PDR. This nuanced understanding of gene modules and their interplay is critical, as it sheds light on the underlying mechanisms that drive the disease. In particular, the discovery of oxidative stress-related genes (ORGs), which are key players within these meta-programs, has been illuminating. This highlights the significant role that oxidative stress, a known factor in diabetic complications, plays in the progression of PDR.

In the context of oxidative stress and its implications for disease pathogenesis, the identification and study of ALKBH enzymes,



particularly ALKBH8, have been pivotal. Previous research has elucidated the role of these enzymes in the intricate regulation of reactive oxygen species (ROS) production and oxidative stress, which are crucial processes in cellular homeostasis and disease development. For example, studies have highlighted the role of ALKBH8 in the development of human bladder cancer, where it contributes to the disease process by downregulating NAD(P)H oxidase-1 (NOX-1) and subsequently activating pathways such as the c-jun NH2-terminal kinase (JNK) and p38 pathways, which are involved in NADPH oxidase 1-dependent ROS production and apoptosis induction (32). Additionally, ALKBH8 has been implicated in the reduction of ROS production through similar mechanisms and in the regulation of selenocysteine protein expression, which serves as a defense against ROS damage in response to oxidative stress (33). These findings collectively underscore the substantial role of ALKBH, particularly ALKBH8, in the regulation of oxidative stress and its relevance to various disease processes.

Similarly, ATP13A2 has been extensively studied for its role in the regulation of cellular responses to oxidative stress. This gene is implicated in protective mechanisms against mitochondrial toxins such as rotenone, which is an environmental risk factor for Parkinson's disease (34). The function of ATP13A2 in mitigating oxidative stress is multifaceted. PSP not only aids in reducing levels of intracellular oxidative damage but also enhances the clearance of oxidatively damaged macromolecules (35). This finding suggested that ATP13A2 plays a significant protective role against oxidative stress, underscoring its importance in maintaining cellular health and preventing damage. Furthermore, the impaired function of ATP13A2 has been directly linked to increased oxidative stress in human neuroblastoma cells, highlighting its critical role in cellular defense mechanisms against oxidative damage (36).

These insights into ALKBH and ATP13A2 provide a deeper understanding of the molecular mechanisms by which oxidative stress influences disease progression and pathology. The significant relationship of these genes with the regulation of oxidative stress emphasizes their potential as therapeutic targets. In the context of PDR, where oxidative stress plays a central role, understanding these mechanisms is crucial. This approach opens potential avenues for targeted therapies that modulate oxidative stress pathways, potentially offering more effective treatment options for conditions such as PDR and beyond.

Therefore, elucidating the roles of ALKBH and ATP13A2 in oxidative stress regulation not only enhances our understanding of the cellular response to oxidative challenges but also positions these genes as key players in the development of novel therapeutic strategies for diseases where oxidative stress is a contributing factor.

Incorporating the AlphaFold 2 technology (22) into our research represents an innovation in our study. AlphaFold 2, an advanced protein structure prediction tool developed by DeepMind, has revolutionized the field of structural biology. Its ability to predict protein structures with unprecedented accuracy provides invaluable insights into the functional mechanisms of proteins at the molecular level.

In the context of our study on PDR, the application of AlphaFold 2 allowed us to predict the structures of key ORGs, namely, ALKBH1, PSIP1, and ATP13A2. This capability is crucial because it provides a deeper understanding of protein configurations and their potential interactions, which are often pivotal in determining their functional roles in cellular processes. The structural insights gained from AlphaFold 2 significantly augmented our understanding of protein–protein interactions (PPIs) and the molecular pathways in which these ORGs are involved. The ability to visualize the precise structure of these

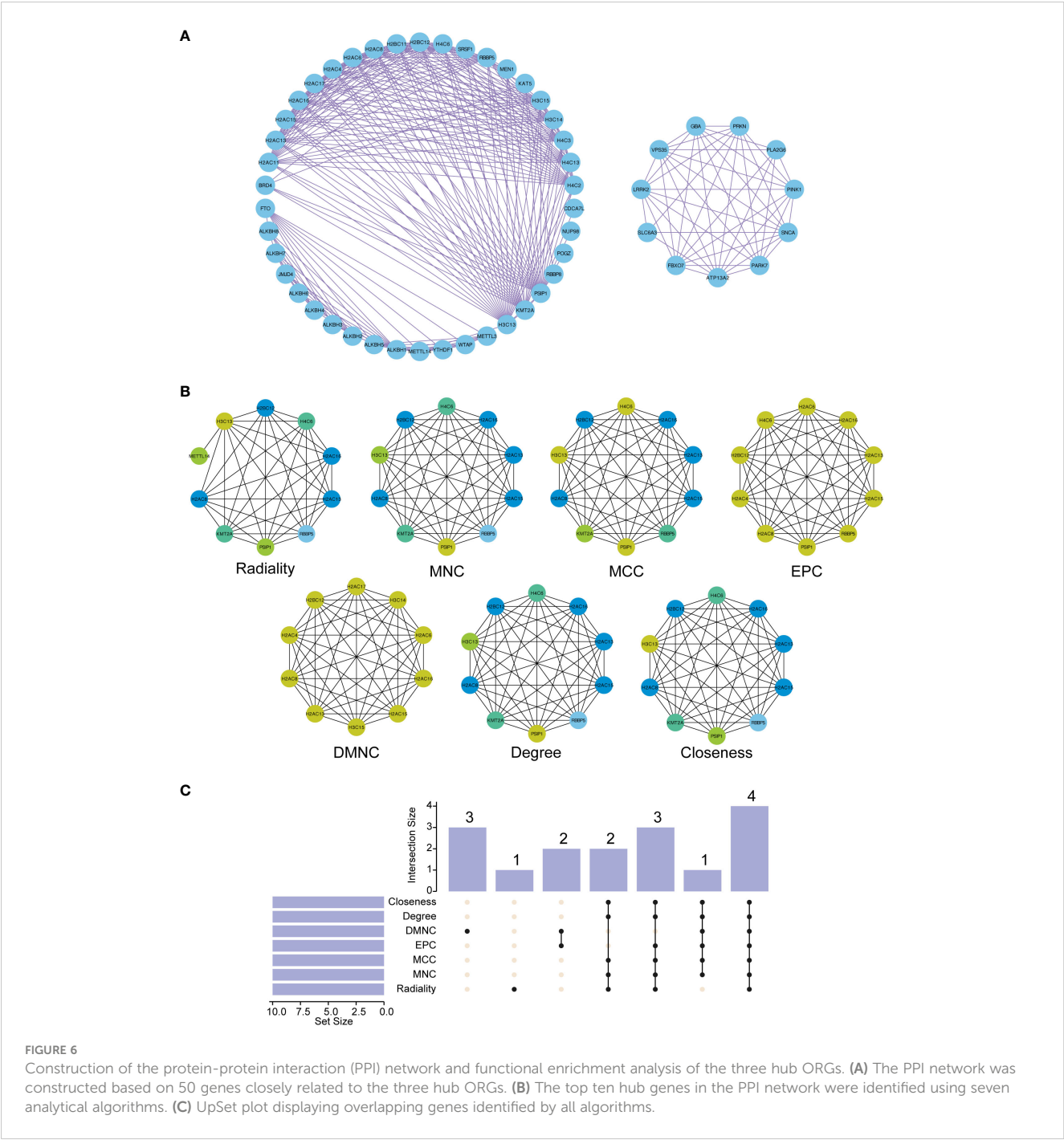


FIGURE 6 Construction of the protein-protein interaction (PPI) network and functional enrichment analysis of the three hub ORGs. **(A)** The PPI network was constructed based on 50 genes closely related to the three hub ORGs. **(B)** The top ten hub genes in the PPI network were identified using seven analytical algorithms. **(C)** UpSet plot displaying overlapping genes identified by all algorithms.

proteins aids in elucidating their functional domains, interaction sites, and potential binding mechanisms, which are essential for elucidating their roles in the pathogenesis of PDR. Furthermore, the application of the AlphaFold 2 in our study sets a precedent for future research on diabetic retinopathy and other related diseases. By enabling a more accurate prediction of protein structures, new possibilities are available for the development of targeted therapeutic interventions, as structural insights are crucial for drug design and discovery.

Our findings resonate with and build upon existing related research in the field, such as the notable work of Hu et al., which focused on the involvement of microglia in PDR (12). This alignment with the findings of previous studies not only validates our findings but also adds a new dimension to our collective understanding of the disease. By contextualizing our results within the broader scientific narrative, we underscore the importance of oxidative stress in PDR pathogenesis and open potential avenues for targeted therapeutic interventions.

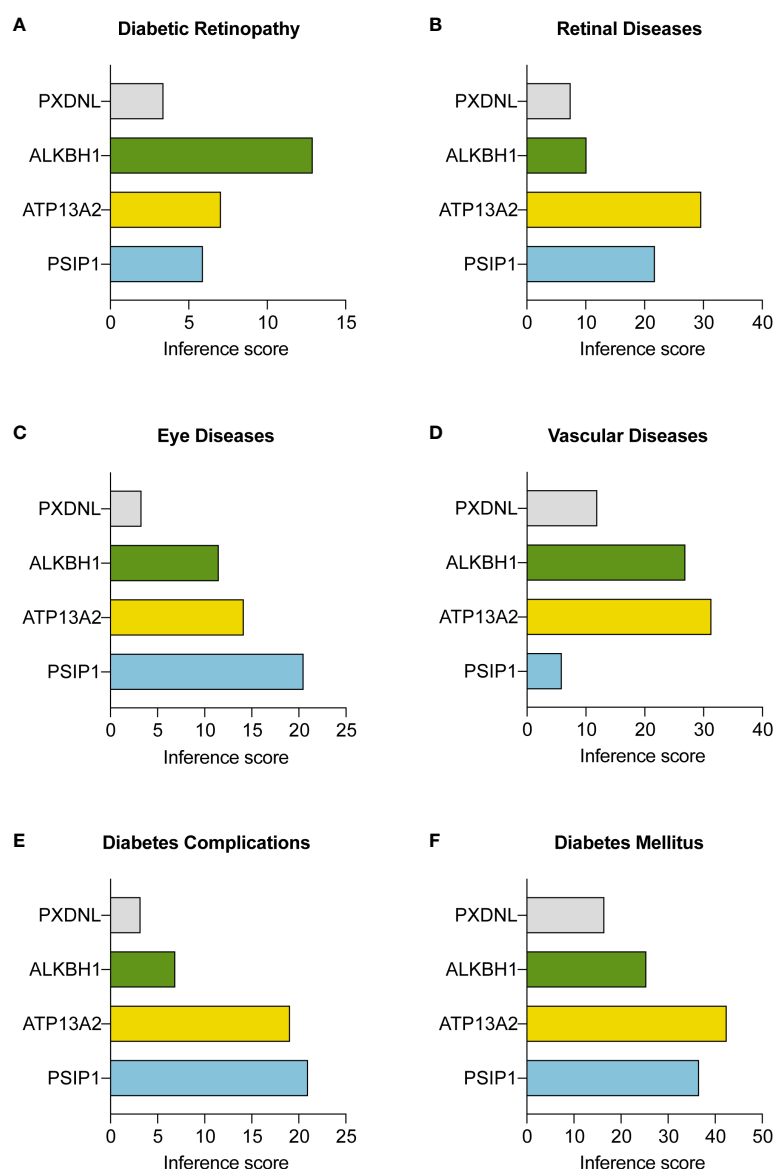


FIGURE 7

Interactions between three key ORGs and the negative control gene PXDNL across various disease conditions. The analysis was conducted with the Comparative Toxicogenomics Database (CTD; <http://ctdbase.org/>). The inference scores between the three hub ORGs and (A) diabetic retinopathy, (B) retinal diseases, (C) eye diseases, (D) vascular diseases, (E) diabetes complications, and (F) diabetes mellitus are shown in bar plots.

There are limitations to this study. While our bioinformatics approach has provided significant insights into potential key players in DR pathogenesis, we recognize that the identification of ALKBH1, ATP13A2, and PSIP1 as potential biomarkers or therapeutic targets is preliminary and necessitates further experimental validation.

In conclusion, our study marks progress in molecular biology and disease research through the application of technologies such as AlphaFold 2, single-cell sequencing, machine learning and NMF. This methodological synergy has not only enriched our understanding of the molecular landscape of PDR but also highlighted the importance of ORGs in its pathogenesis. Our research underscores the value of harnessing advanced technologies to explore disease mechanisms and therapeutic innovations.

Data availability statement

The original contributions presented in the study are included in the article/[Supplementary Materials](#), further inquiries can be directed to the corresponding author/s.

Ethics statement

Ethical approval was not required for the study involving humans in accordance with the local legislation and institutional requirements. Written informed consent to participate in this study was not required from the participants or the participants' legal

guardians/next of kin in accordance with the national legislation and the institutional requirements.

Author contributions

JW: Writing – original draft, Writing – review & editing. HS: Writing – original draft, Writing – review & editing. LM: Formal analysis, Writing – original draft. YL: Formal analysis, Writing – original draft. ZW: Formal analysis, Writing – original draft. ZP: Conceptualization, Writing – review & editing. M-MY: Methodology, Writing – review & editing.

Funding

The author(s) declare financial support was received for the research, authorship, and/or publication of this article. This study was supported in part by the Shenzhen Science and Technology Program (No. JCYJ20220818102603007, GCZX2015043017281705) and the General Project of the Shenzhen Natural Science Foundation (No. JCYJ20210324113808023 and JCYJ20220530152813030).

References

- Li H, Niu Y, Rong A, Yang B, Xu W, Cui H. Effect of adjunctive intravitreal conbercept injection at the end of 25G vitrectomy on severe proliferative diabetic retinopathy: 6-month outcomes of a randomised controlled trial. *Ophthalmol Ther.* (2023) 12:1173–80. doi: 10.1007/s40123-023-00664-6
- González-Cortés JH, Gonzalez-Cantu JE, Sudhakar A, Hernández-Da Mota SE, Bilgic A, Garza-Chavarria JA, et al. *Treatment Algorithm in Proliferative Diabetic Retinopathy - From Protocols to the Real World.* (London, UNITED KINGDOM: IntechOpen Limited) (2022). doi: 10.5772/intechopen.99843.
- She X, Zou C, Zheng Z. Differences in vitreous protein profiles in patients with proliferative diabetic retinopathy before and after ranibizumab treatment. *Front Med.* (2022) 9:776855. doi: 10.3389/fmed.2022.776855
- Nakao S, Kaizu Y, Horie J, Wada I, Arima M, Fukuda Y, et al. Volumetric three-dimensional optical coherence tomography angiography of retinal neovascularization in proliferative diabetic retinopathy. *Retinal cases Brief Rep.* (2023) 17:315–20. doi: 10.1097/icb.0000000000001183
- Pandit S, Ho AC, Yonekawa Y. Recent advances in the management of proliferative diabetic retinopathy. *Curr Opin Ophthalmol.* (2023) 34:232–6. doi: 10.1097/icu.0000000000000946
- Liu S, Ju Y, Gu P. Experiment-based interventions to diabetic retinopathy: present and advances. *Int J Mol Sci.* (2022) 23:7005. doi: 10.3390/ijms23137005
- Kowluru RA, Mohammad G. Mitochondrial fragmentation in a high homocysteine environment in diabetic retinopathy. *Antioxidants.* (2022) 11:365. doi: 10.3390/antiox11020365
- Ozturk Kurt HP, Karagöz ÖzenDS, Genç İ, Erdem MA, Demirağ MD. Comparison of selenium levels between diabetic patients with and without retinopathy. *J Surg Med.* (2023) 1:58–62. doi: 10.28982/josam.7673
- Hwang B, Lee JH, Bang D. Single-cell RNA sequencing technologies and bioinformatics pipelines. *Exp Mol Med.* (2018) 50:1–14. doi: 10.1038/s12276-018-0071-8
- Chen G, Ning B, Shi T. Single-cell rna-seq technologies and related computational data analysis. *Front Genet.* (2019) 10:317. doi: 10.3389/fgene.2019.00317
- Papalexi E, Satija R. Single-cell RNA sequencing to explore immune cell heterogeneity. *Nat Rev Immunol.* (2018) 18:35–45. doi: 10.1038/nri.2017.76
- Hu Z, Mao X, Chen M, Wu X, Zhu T, Liu Y, et al. Single-cell transcriptomics reveals novel role of microglia in fibrovascular membrane of proliferative diabetic retinopathy. *Diabetes.* (2022) 71:762–73. doi: 10.2337/db21-0551
- Prelaj A, Miskovic V, Zanitti M, Trovo F, Genova C, Viscardi G, et al. Artificial Intelligence for predictive biomarker discovery in immuno-oncology: a systematic review. *Ann Oncol.* (2023) 35:29–65. doi: 10.1016/j.annonc.2023.10.125
- Addala V, Newell F, Pearson JV, Redwood A, Robinson BW, Creaney J, et al. Computational immunogenomic approaches to predict response to cancer immunotherapies. *Nat Rev Clin Oncol.* (2023) 21:28–46. doi: 10.1038/s41571-023-00830-6
- Cowan CS, Renner M, De Gennaro M, Gross-Scherf B, Goldblum D, Hou Y, et al. Cell types of the human retina and its organoids at single-cell resolution. *Cell.* (2020) 182:1623–1640.e34. doi: 10.1016/j.cell.2020.08.013
- Becker K, Klein H, Simon E, Viollet C, Haslinger C, Leparç G, et al. In-depth transcriptomic analysis of human retina reveals molecular mechanisms underlying diabetic retinopathy. *Sci Rep.* (2021) 11:10494. doi: 10.1038/s41598-021-88698-3
- Li Y, Chen D, Sun L, Wu Y, Zou Y, Liang C, et al. Induced expression of VEGFC, ANGPT, and EFNB2 and their receptors characterizes neovascularization in proliferative diabetic retinopathy. *Invest Ophthalmol Vis Sci.* (2019) 60:4084–96. doi: 10.1167/iovs.19-26767
- Hao Y, Hao S, Andersen-Nissen E, Mauck WM, Zheng S, Butler A, et al. Integrated analysis of multimodal single-cell data. *Cell.* (2021) 184:3573–3587.e29. doi: 10.1016/j.cell.2021.04.048
- Laurens van der M, Hinton G. Visualizing Data using t-SNE. *Mach Learn Res.* (2008) 9:2579–605. Available at: <https://jmlr.org/papers/v9/vandermaaten08a.html>.
- Korsunsky I, Millard N, Fan J, Slowikowski K, Zhang F, Wei K, et al. Fast, sensitive and accurate integration of single-cell data with Harmony. *Nat Methods.* (2019) 16:1289–96. doi: 10.1038/s41592-019-0619-0
- Kotliar D, Veres A, Nagy MA, Tabrizi S, Hodis E, Melton DA, et al. Identifying gene expression programs of cell-type identity and cellular activity with single-cell RNA-Seq. *Elife.* (2019) 8:e43803. doi: 10.7554/eLife.43803
- Tunyasuvunakool K, Adler J, Wu Z, Green T, Zielinski M, Židek A, et al. Highly accurate protein structure prediction for the human proteome. *Nature.* (2021) 596:590–6. doi: 10.1038/s41586-021-03828-1
- NCBI Resource Coordinators, Agarwala R, Barrett T, Beck J, Benson DA, Bollin C, et al. Database resources of the national center for biotechnology information. *Nucleic Acids Res.* (2018) 46:D8–D13. doi: 10.1093/nar/gkx1095
- Morris GM, Huey R, Olson AJ. Using AutoDock for ligand-receptor docking. *Curr Protoc Bioinf.* (2008). doi: 10.1002/0471250953.bi0814s24
- Wang Y, Bryant SH, Cheng T, Wang J, Gindulyte A, Shoemaker BA, et al. PubChem bioAssay: 2017 update. *Nucleic Acids Res.* (2017) 45:D955–63. doi: 10.1093/nar/gkw1118
- von Mering C, Huynen M, Jaeggi D, Schmidt S, Bork P, Snel B. STRING: a database of predicted functional associations between proteins. *Nucleic Acids Res.* (2003) 31:258–61. doi: 10.1093/nar/gkg034

Conflict of interest

The authors declare that the research was conducted in the absence of any commercial or financial relationships that could be construed as a potential conflict of interest.

Publisher's note

All claims expressed in this article are solely those of the authors and do not necessarily represent those of their affiliated organizations, or those of the publisher, the editors and the reviewers. Any product that may be evaluated in this article, or claim that may be made by its manufacturer, is not guaranteed or endorsed by the publisher.

Supplementary material

The Supplementary Material for this article can be found online at: <https://www.frontiersin.org/articles/10.3389/fendo.2024.1382896/full#supplementary-material>

27. Shannon P, Markiel A, Ozier O, Baliga NS, Wang JT, Ramage D, et al. Cytoscape: a software environment for integrated models of biomolecular interaction networks. *Genome Res.* (2003) 13:2498–504. doi: 10.1101/gr.1239303
28. Davis AP, Grondin CJ, Johnson RJ, Sciaky D, McMorran R, Wiegers J, et al. The comparative toxicogenomics database: update 2019. *Nucleic Acids Res.* (2019) 47: D948–54. doi: 10.1093/nar/gky868
29. Shahid MH, Rashid F, Tauqeer S, Ali R, Farooq M, Aleem N. Change in central macular thickness on OCT after pan retinal photocoagulation. *PJMHS.* (2022) 16:315–7. doi: 10.53350/pjmhs22166315
30. Howell SJ, Lee CA, Zapadka TE, Lindstrom SI, Taylor BE, R. Taylor ZR, et al. Inhibition of CD40-TRAF6-dependent inflammatory activity halts the onset of diabetic retinopathy in streptozotocin-diabetic mice. *Nutr Diabetes.* (2022) 12:46. doi: 10.1038/s41387-022-00225-z
31. Zhou AY, Taylor BE, Barber KG, Lee CA, R. Taylor ZR, Howell SJ, et al. Anti-il17a halts the onset of diabetic retinopathy in type I and II diabetic mice. *Int J Mol Sci.* (2023) 24:1347. doi: 10.3390/ijms24021347
32. Shimada K, Nakamura M, Anai S, De Velasco MA, Tanaka M, Tsujikawa K, et al. A novel human AlkB homologue, ALKBH8, contributes to human bladder cancer progression. *Cancer Res.* (2009) 69:3157–64. doi: 10.1158/0008-5472.can-08-3530
33. Pilżys T, Marcinkowski M, Kukwa W, Garbicz D, Dylewska M, Ferenc K, et al. ALKBH overexpression in head and neck cancer: potential target for novel anticancer therapy. *Sci Rep.* (2019) 9:13249. doi: 10.1038/s41598-019-49550-x
34. Vrijssen S, Besora-Casals L, van Veen S, Zielich J, den Haute CV, Hamouda NN, et al. ATP13A2-mediated endo-lysosomal polyamine export counters mitochondrial oxidative stress. *Proc Natl Acad Sci.* (2020) 117:31198–207. doi: 10.1073/pnas.1922342117
35. Covy JP, Waxman EA. Characterization of cellular protective effects of ATP13A2/PARK9 expression and alterations resulting from pathogenic mutants. *J Neurosci Res.* (2012) 90:2306–16. doi: 10.1002/jnr.23112
36. Mukherjee AB, Appu AP, Sadhukhan T, Casey S, Mondal A, Zhang Z, et al. Emerging new roles of the lysosome and neuronal ceroid lipofuscinoses. *Mol Neurodegeneration.* (2019) 14:4. doi: 10.1186/s13024-018-0300-6



OPEN ACCESS

EDITED BY

Mohd Imtiaz Nawaz,
King Saud University, Saudi Arabia

REVIEWED BY

Asad Ullah Jatoi,
Liaquat University of Medical & Health
Sciences, Pakistan
Adeola Onakoya,
University of Lagos, Nigeria
Junhao Tu,
The First Affiliated Hospital of Nanchang
University, China

*CORRESPONDENCE

Yi Zhang

✉ zhayisn@163.com

Yan Ding

✉ dywzx@163.com

[†]These authors have contributed equally to
this work

RECEIVED 16 January 2024

ACCEPTED 24 April 2024

PUBLISHED 10 May 2024

CITATION

Li B, Zhao X, Xie W, Hong Z, Cao Y, Ding Y
and Zhang Y (2024) Causal association of
circulating metabolites with diabetic
retinopathy: a bidirectional Mendelian
randomization analysis.
Front. Endocrinol. 15:1359502.
doi: 10.3389/fendo.2024.1359502

COPYRIGHT

© 2024 Li, Zhao, Xie, Hong, Cao, Ding and
Zhang. This is an open-access article
distributed under the terms of the [Creative
Commons Attribution License \(CC BY\)](#). The
use, distribution or reproduction in other
forums is permitted, provided the original
author(s) and the copyright owner(s) are
credited and that the original publication in
this journal is cited, in accordance with
accepted academic practice. No use,
distribution or reproduction is permitted
which does not comply with these terms.

Causal association of circulating metabolites with diabetic retinopathy: a bidirectional Mendelian randomization analysis

Bo Li^{1,2†}, Xu Zhao^{3†}, Wanrun Xie¹, Zhenzhen Hong¹, Ye Cao^{4,5},
Yan Ding^{2*} and Yi Zhang^{1*}

¹Department of Endocrinology, Quanzhou First Hospital, Affiliated to Fujian Medical University, Quanzhou, Fujian, China, ²Hubei Key Laboratory of Embryonic Stem Cell Research, Biomedical Research Institute, Hubei University of Medicine, Shiyan, Hubei, China, ³Emergency and Critical Care Center, Renmin Hospital, Hubei University of Medicine, Shiyan, Hubei, China, ⁴Department of Cardiology, Fujian Provincial Hospital, Shengli Clinical Medical College, Fujian Medical University, Fuzhou, Fujian, China, ⁵Department of Cardiology, Renmin Hospital, Hubei University of Medicine, Shiyan, Hubei, China

Introduction: The retina is a highly metabolically active tissue, and there is a lack of clarity about the relationship between metabolites and diabetic retinopathy (DR). This study used two-sample bidirectional Mendelian randomization (MR) analyses to identify causal relationships between metabolites and DR.

Methods: Genetic variants were selected from the open-access Genome-Wide Association Studies (GWAS) summary database as proxies for the 1400 most recently published metabolites. MR analysis was performed to examine associations between these metabolite traits and DR. Single nucleotide polymorphism (SNP) data that were significantly associated with exposure were screened through association analysis. Validated instrumental variables (IVs) were obtained by removing SNPs with linkage disequilibrium (LD) and F-statistic values below 10. MR analyses were performed using the inverse variance weighted (IVW) method as the primary approach. The robustness of the results was verified by sensitivity analyses, including assessments of heterogeneity, horizontal pleiotropy, and the leave-one-out method.

Results: In the IVW approach and in the primary analysis of several sensitivity analyses, genetically determined glycolithocholate sulfate levels, androstenediol (3 beta, 17 beta) monosulfate (1) levels, 1-stearoyl-2-arachidonoyl-GPE (18:0/20:4) levels, 1-oleoyl-2-arachidonoyl-GPE (18:1/20:4) levels, 1-oleoyl-2-linoleoyl-GPE (18:1/18:2) levels, X-26109 levels, N6-methyllysine levels, (N6, N6-dimethyllysine levels), and (N2-acetyl,N6,N6-dimethyllysine levels) were negatively associated with the risk of DR. 5-hydroxymethyl-2-furoylcarnitine levels and the glutamate-to-alanine ratio were positively associated with the risk of DR. No reverse causal association was found between DR and metabolites.

Discussion: This MR study suggests that nine metabolites may have a protective effect in DR, while two metabolites may be associated with an increased risk of DR. However, further research is needed to confirm these findings. Supplementation with beneficial metabolites may reduce DR risk and could potentially be a novel therapeutic approach to DR treatment.

KEYWORDS

diabetic retinopathy, metabolites, causal relationship, diabetes mellitus, MR analysis

Introduction

DR is one of the common complications of diabetes mellitus (DM), which seriously endangers human health and is the leading cause of vision loss and blindness (1). DM is a systemic metabolic disorder in which chronic hyperglycemic exposure causes widespread damage to neurons and vascular cells. Diabetic vision hazards primarily affect the retina (2). Structural and functional changes occur in retinal neurons and blood vessels, along with abnormalities in metabolic immunity, which further disrupt the blood-retinal barrier. Ultimately, these factors lead to neuronal damage. Currently, DR lacks effective early treatment and prevention measures. Exploring the pathogenesis and etiology of the disease is beneficial for early intervention.

The retina is a metabolically highly active tissue that requires the interaction of cells ranging from light-sensitive photoreceptors to neurons that transmit electrochemical signals to the brain (2). Currently, there is a lack of clarity about the relationship between metabolites and DR. Meta-analyses of DR studies have shown that blood pressure, serum total cholesterol, and glycosylated hemoglobin levels are associated with retinopathy. However, these factors account for only 9% of DR progression (3). Metabolomics is an emerging scientific field that has gained popularity in the biomedical community. It is used to diagnose diseases, understand disease mechanisms, and identify new drug targets. It has had a profound impact on unraveling the underlying causes of complex diseases, drug discovery, and precision medicine (4). Approximately 50% of phenotypic differences at metabolite level are attributed to genetic variation (5). This provides an opportunity to make causal inferences from metabolites to diseases. Alleles are randomly assigned at conception, and this randomization process helps eliminate the confounding effect of most risk factors, reducing confounding bias (6).

The Mendelian randomization approach is an epidemiological method that uses genetic variation as an instrumental variable to evaluate causality, while accounting for confounding factors. Genotyping can be a powerful tool for investigating causal relationships between exposure factors and outcomes. To investigate the mechanisms of DR, we hypothesized that there is a correlation between metabolite traits and DR. In our study, we used

a two-sample bidirectional MR analysis to establish the causal relationship between metabolites and DR.

Materials and methods

Study design

We assessed the causal relationship between 1400 metabolite traits and DR using a two-sample MR analysis. SNPs that were significantly associated with exposure were used as exposure proxies, while SNPs in linkage disequilibrium (LD) and weak IVs were excluded from MR analysis. Effective causal inference IVs must satisfy three essential assumptions: (1) IVs must have a direct relationship with the exposure variable; (2) IVs must be independent of potential confounding variables between exposure and outcome; and (3) IVs must not affect outcome through any other pathways than exposure. Ethical consent was previously obtained for GWAS primary studies in each country, and current analyses are based on publicly available summary-level data that do not require additional approval (Figure 1).

GWAS data sources for DR

Summary GWAS data for the DR were obtained from the IEU Open GWAS project (<https://gwas.mrcieu.ac.uk/>). The study analyzed 190,594 European men and women (Ncase = 14,584, Ncontrol = 176,010) and examined 16,380,347 genetic variants.

GWAS metabolites data source

Metabolite data were obtained from 8299 individuals in the Canadian Longitudinal Study of Aging (CLSA) cohort study. The GWAS summary study was performed by aggregating 1,091 blood metabolites and 309 metabolite ratios. 850 Blood metabolites were derived from known superpathways, while 241 metabolites were either unknown or only partially known. Metabolite-gene and gene expression information were integrated to identify genes with significant effects on

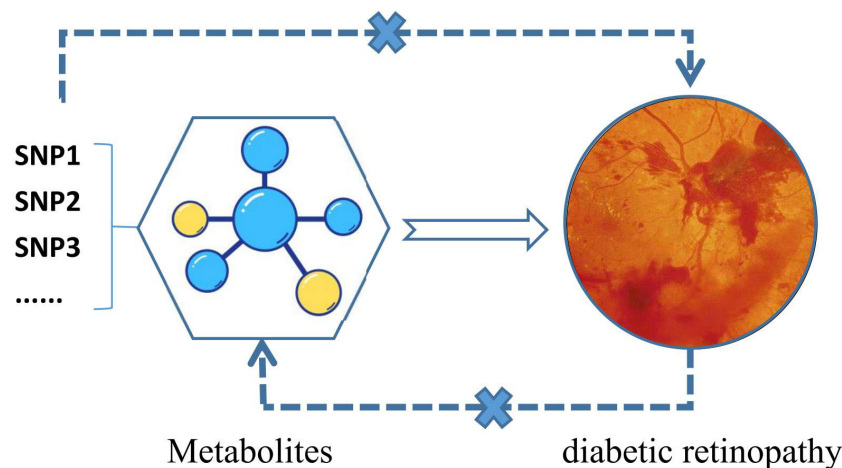


FIGURE 1
Flowchart of bidirectional Mendelian randomization analysis of metabolites and DR.

traits and diseases. Genetic signatures of 109 metabolites and 48 metabolite ratios were ultimately identified as effector genes (6).

Selection of IVs

In the analysis of metabolite-DR associations, we established a correlation threshold of 1×10^{-5} to identify SNPs that are significantly associated with metabolites. The r^2 cutoff clustering was set to 0.001, and the clustering window was set to 10,000 kb to eliminate LD. F-statistics ($F = \frac{N-K-1}{K} \frac{R^2}{1-R^2}$) were calculated for each IV (7), and any F value less than 10 was considered a weak IV and therefore excluded. When exposure and outcome were harmonized, palindromic SNPs with intermediate allele frequencies were removed. For DR and metabolite MR analysis, we set the correlation threshold at 5×10^{-8} to screen for SNPs significantly correlated with DR. We applied the same criteria to screen for IVs.

Statistical analysis

To investigate the causal relationship between 1400 metabolite traits and DR, we used five methods (MR Egger, weighted median, IVW, simple mode, and weighted mode) from the TwoSampleMR package for analysis. The IVW method was used as the primary statistic, and sensitivity analyses were conducted using the weighted mode and weighted median methods. IVW, weighted median, and weighted mode were used to analyze and present the results. Heterogeneity was assessed using funnel plots and Cochran's Q p values from IVW and MR-Egger tests, with $p < 0.05$ indicating heterogeneity. The horizontal pleiotropy of the data and the robustness of the results were assessed using MR-Egger intercepts. A p-value of less than 0.05 indicated that horizontal pleiotropy was excluded (8). Horizontal pleiotropy was also assessed using the MR-PRESSO global test, and peripheral SNPs were excluded by the MR-PRESSO outlier test (9). Finally, leave-one-out and single-SNP analyses were used to determine whether individual SNPs influenced primary causality (10).

In addition, the false positive rate increased due to the large number of exposure factors and multiple exposure phenotypes in GWAS derived from the same sample set. To address this, we applied the false discovery rate ($FDR < 0.2$) to correct MR results.

Ethical consent was obtained prior to the initial GWAS studies in each country, and the current analyses were based on publicly available summary data, which did not require further approval.

TwoSampleMR (version 0.5.6) in R (version 4.2.3) were used for MR analysis.

Results

A total of 34,843 SNPs were screened as IVs for 1,400 metabolites, using IV screening criteria. The association results of 1400 metabolites with DR were obtained using five MR analysis methods, and 94 metabolites were found to be causally associated with DR according to IVW method. The MR results were filtered using the following criteria: $p < 0.05$ and $FDR < 0.2$ in the IVW method, consistency in the direction of β -value across five MR methods, and $p > 0.05$ to account for horizontal pleiotropy. Finally, 11 metabolites were found to be causally associated with DR (Figure 2; Supplementary Figures S1, S2). Reverse MR analysis did not reveal an association between DR and these 11 metabolites.

Effects of metabolites on DR

Glycolithocholate sulfate levels (IVW: $\beta = -0.0578$, OR = 0.944, 95% CI = 0.911–0.987, $p = 0.001$), androstenediol (3 beta, 17 beta) monosulfate (1) levels (IVW: $\beta = -0.109$, OR = 0.897, 95%CI = 0.839–0.959, $p = 0.001$), 1-stearoyl-2-arachidonoyl-GPE (18:0/20:4) levels (IVW: $\beta = -0.067$, OR = 0.935, 95%CI = 0.899–0.971, $p < 0.001$), 1-oleoyl-2-arachidonoyl-GPE (18:1/20:4) levels (IVW: $\beta = -0.084$, OR = 0.920, 95%CI = 0.882–0.960, $p < 0.001$), 1-oleoyl-2-linoleoyl-GPE (18:1/18:2) levels (IVW: $\beta = -0.072$, OR = 0.931, 95%CI = 0.891–

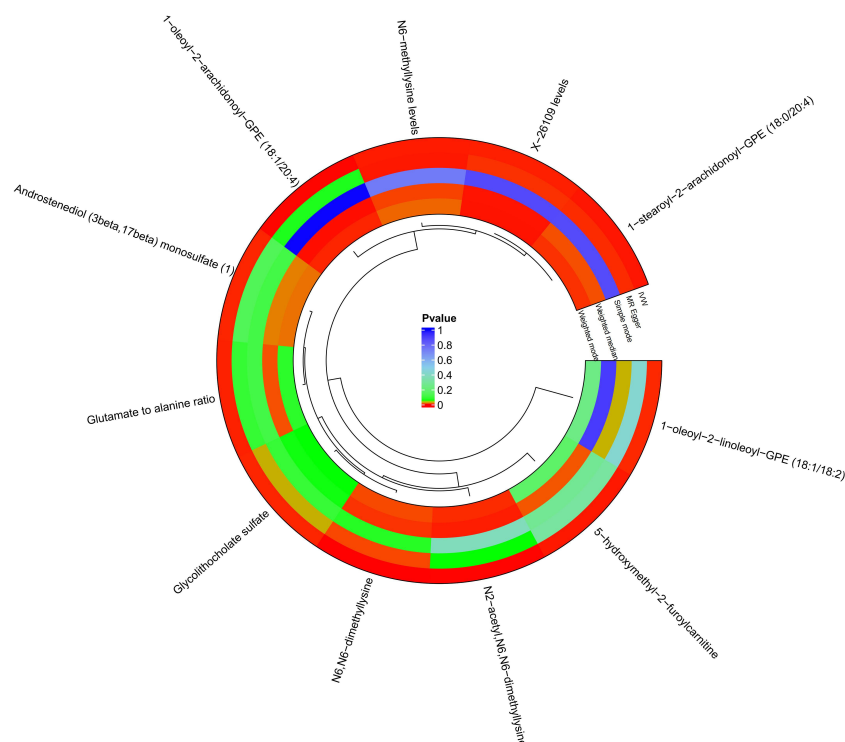


FIGURE 2

Circle plots of five MR analyses of 11 metabolites with significant causal effects with diabetic retinopathy. MR methods with $p < 0.05$ are shown in red.

0.973, $p = 0.002$), X-26109 levels (IVW: $\beta = -0.061$, OR = 0.941, 95% CI=0.907-0.976, $p = 0.001$), N6-methyllysine levels (IVW: $\beta = -0.057$, OR = 0.944, 95%CI=0.913-0.977, $p < 0.001$), N6,N6-dimethyllysine levels (IVW: $\beta = -0.081$, OR = 0.922, 95%CI=0.888-0.957, $p < 0.001$), N2-acetyl,N6,N6-dimethyllysine levels (IVW: $\beta = -0.045$, OR = 0.956, 95%CI=0.935-0.978, $p < 0.001$) were negatively associated with the risk of DR. 5-hydroxymethyl-2-furoylcarnitine levels (IVW: $\beta = 0.100$, OR = 1.105, 95%CI=1.043-1.170, $p < 0.001$) and the glutamate-to-alanine ratio (IVW: $\beta = 0.132$, OR = 1.142, 95%CI=1.054-1.237, $p = 0.001$) were positively associated with the risk of DR (Figure 3).

Pleiotropy and sensitivity analysis

Sensitivity and pleiotropy analyses validated the robustness of the IVW results. IVW and MR-Egger heterogeneity tests showed no heterogeneity in glycolithocholate sulfate levels, androstenediol (3 beta, 17 beta) monosulfate (1) levels, 1-stearoyl-2-arachidonoyl-GPE (18:0/20:4) levels, 1-oleoyl-2-arachidonoyl-GPE (18:1/20:4) levels, 1-oleoyl-2-linoleoyl-GPE (18:1/18:2) levels, X-26109 levels, N6-methyllysine levels, N6,N6-dimethyllysine levels, and N2-acetyl,N6,N6-dimethyllysine levels in MR analysis with DR ($p > 0.05$) (Table 1; Supplementary Figure S3).

The MR-Egger intercept and MR-PRESSO tests showed no evidence of horizontal pleiotropy (Table 1). The robustness and reliability of the causal relationship between metabolites and DR have been further confirmed using sensitivity analyses on leave-one-out (Supplementary Figure S4).

Causal effects of DR onset on metabolites

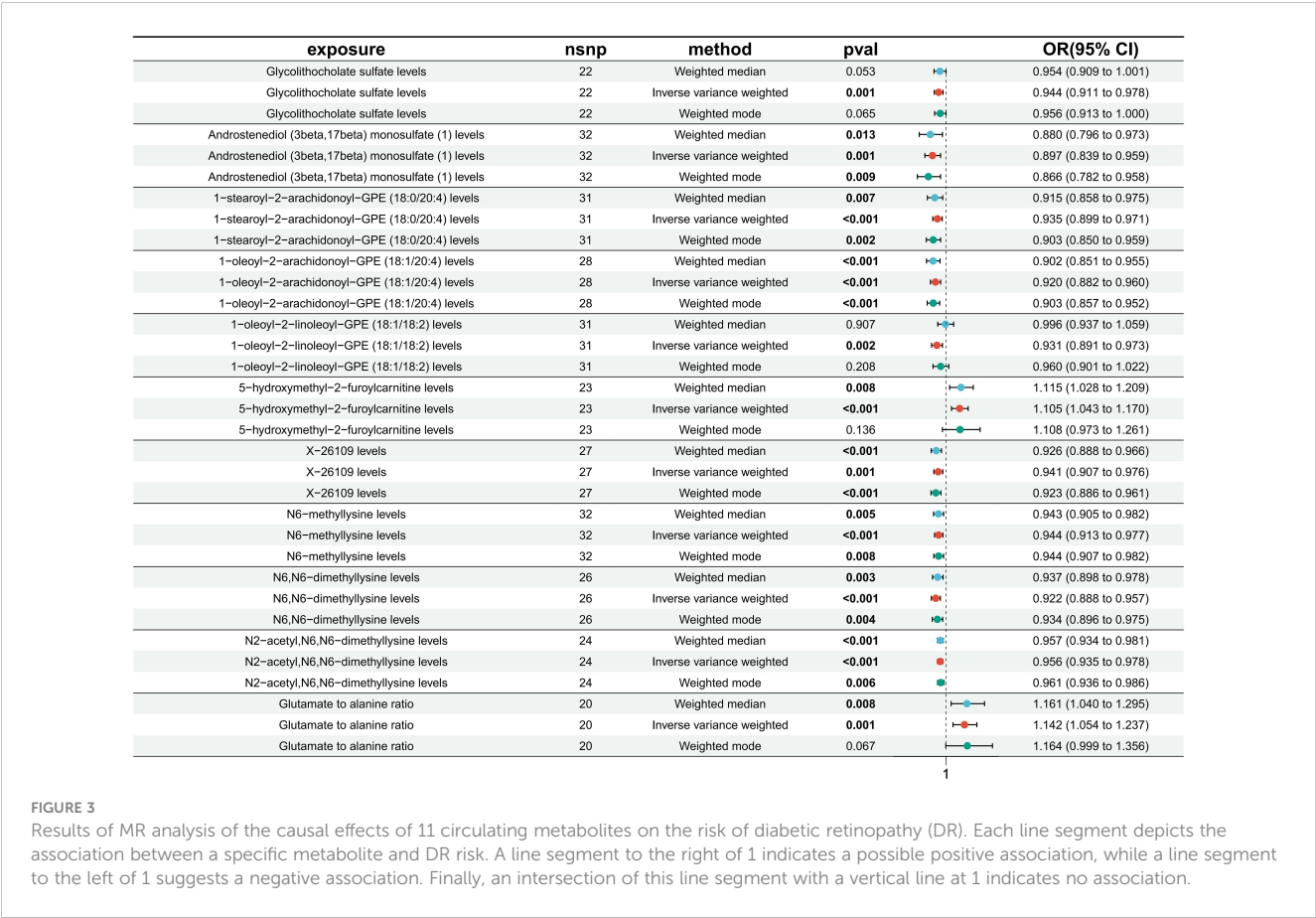
No reverse causal association was found between metabolites and DR (Figure 4).

Effects of metabolites on T2DM

To estimate the causal effect of metabolites with diabetes, we performed MR analysis of 1400 circulating metabolites with T2DM (nCase: 38841, nControl: 451,248, nSNP: 24167560, Dataset:ebi-a-GCST90018926). 24 Metabolites showed a potential causal association (Supplementary Figure S5). Further Venn intersection analysis of DR and T2DM-related metabolites revealed that only 1-oleoyl-2-linoleoyl-GPE (18:1/18:2) levels had a negative phase causal effect with both DR and T2DM (Supplementary Figure S6).

Discussion

DR is a common chronic complication of diabetes that primarily affects the retina of the eye. The retina, which is part of the central nervous system, is characterized by a high metabolism and a demand matched by a large supply of metabolites (11). Despite strict control of risk factors such as blood pressure and glucose that reduce DR risk, many diabetic patients continue to develop DR (12). Metabolic memory has been used to explain this phenomenon, whereby persistent epigenetic modifications induced



by early exposure to hyperglycemia predispose individuals to diabetic complications even when good glycemic control is achieved (13). Metabolites are closely associated with disease onset and progression. Han et al. identified 311 differential metabolites by metabolite analysis of retinal tissues from diabetic and nondiabetic mice, and DR metabolites were significantly enriched in purine metabolic signals. Adenosine, guanine and inosine have higher sensitivity, specificity and accuracy for DR prediction (14), suggesting that metabolic phenotypes (metabolites) associated with disease states may be related to disease mechanisms and pathophysiology, and could be used in individualized medicine or public health (13). Metabolomic analysis of the vitreous

TABLE 1 Results of metabolite and DR heterogeneity and horizontal pleiotropy tests.

| Heterogeneity | | | | Pleiotropy | | |
|---------------|--|--------------|---------|-----------------|---------|-------------|
| ID | Exposure | MR Egger Q_p | IVW Q_p | Egger intercept | Egger P | MR-Presso p |
| GCST90199811 | Glycolithocholate sulfate levels | 0.253 | 0.304 | -0.001 | 0.927 | 0.396 |
| GCST90199872 | Androstenediol (3beta,17beta) monosulfate (1) levels | 0.196 | 0.227 | -0.002 | 0.729 | 0.266 |
| GCST90200045 | 1-stearoyl-2-arachidonoyl-GPE (18:0/20:4) levels | 0.634 | 0.509 | 0.012 | 0.078 | 0.428 |
| GCST90200079 | 1-oleoyl-2-arachidonoyl-GPE (18:1/20:4) levels | 0.305 | 0.350 | -0.002 | 0.794 | 0.396 |
| GCST90200082 | 1-oleoyl-2-linoleoyl-GPE (18:1/18:2) levels | 0.254 | 0.236 | -0.008 | 0.252 | 0.135 |
| GCST90200244 | 5-hydroxymethyl-2-furoylcarnitine levels | 0.865 | 0.890 | 0.004 | 0.662 | 0.902 |
| GCST90200671 | X-26109 levels | 0.276 | 0.228 | 0.008 | 0.171 | 0.286 |
| GCST90200689 | N6-methyllysine levels | 0.918 | 0.816 | 0.011 | 0.057 | 0.862 |
| GCST90200696 | N6,N6-dimethyllysine levels | 0.381 | 0.417 | 0.005 | 0.568 | 0.459 |
| GCST90200697 | N2-acetyl,N6,N6-dimethyllysine levels | 0.851 | 0.818 | -0.007 | 0.223 | 0.857 |
| GCST90200946 | Glutamate to alanine ratio | 0.952 | 0.966 | -0.004 | 0.732 | 0.967 |

Q_p, Cochran's Q p-values.

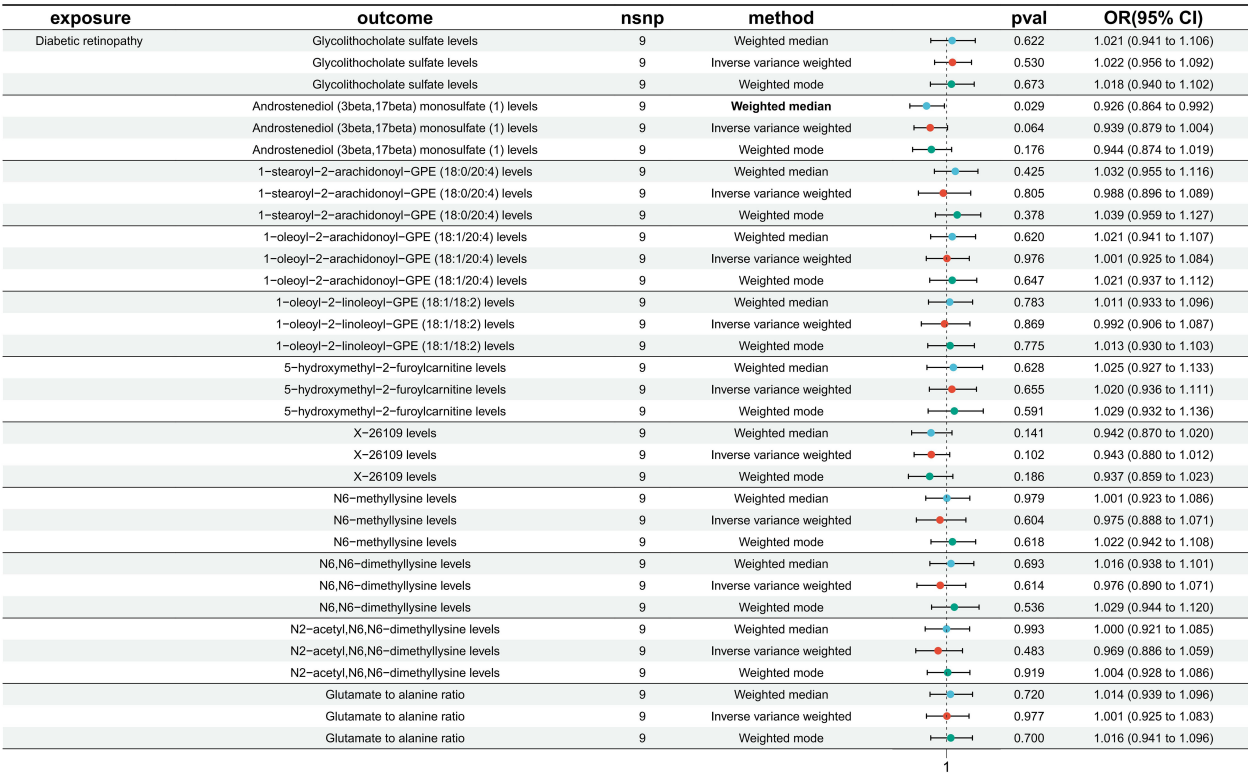


FIGURE 4 Causal effect analysis between DR and 11 metabolites. All lines intersect 1, indicating no reverse causal effect between them.

suggested increased lactate and glucose abundance in value-added DR (PDR) and significant reductions in galactose-pure and ascorbic acid (15). Plasma or serum remains the biofluid of choice in metabolomics studies due to the invasive nature of vitreous sampling limiting the replicable and translational potential of the study (12). Analysis of plasma metabolomics from DR patients showed that plasma metabolites complemented traditional risk factors and facilitated risk stratification of patients in the early stages of DR, and that the plasma metabolic phenotype of DR is unique and not just a continuation of diabetic plasma metabolism (12), and that studying DR metabolomics is valuable for DR prevention and treatment and risk stratification.

DR is a chronic metabolic disease, and dysregulation of retinal metabolism is a key factor in DR pathogenesis (16). Circulating metabolomics analyses have significant translational value in the study of DR mechanisms, risk stratification, and the development of new therapeutic measures (12). Changes in the metabolome represent the interaction of genetic and environmental factors and provide information complementary to genomic, transcriptomic or proteomic data (12). A recent 12-year follow-up on metabolites and DR in Finnish men with type 2 diabetes showed that 17 metabolites were significantly associated with incident DR, among which N-lactoyl isoleucine, N-lactoyl valine, N-lactoyl tyrosine, N-lactoyl phenylalanine, N-(2- furoyl) glycine, N,N,N-trimethyl-5-aminovalerate,carboxylic acid maleate, 3-hydroxypyridine sulfate, 4-vinylphenol sulfate, 4-ethylcatechol sulfate, dimethyl sulfoneand 5-hydroxylysine were associated with an increased risk of DR, and

citrulline, myristoleate (14:1n5), palmitoleate (16. 1n7), Sphingomyelin (d18:2/24:2), and 5-dodecenoate (12:1n7) with a decreased risk of DR (17). Another nested case-control metabolomics study found 11 metabolites (1,5-Anhydroglucitol, 1,5-Gluconolactone, 2-Deoxyribonic acid, 3,4-Dihydroxybutyric acid, Erythritol, Gluconic acid, Lactose/cellobiose, Maltose/ trehalose, Mannose, Ribose, Urea) was associated with DR, and correction for metabolic risk factors and renal function did not significantly affect the results (12). Our results showed that the following metabolites were negatively associated with the risk of DR: glycolithocholate sulfate levels, androstenediol (3 beta, 17 beta) monosulfate (1) levels, 1-stearoyl-2-arachidonoyl-GPE (18:0/20:4) levels, 1-oleoyl-2-arachidonoyl-GPE (18:1/20:4) levels, 1-oleoyl-2-linoleoyl-GPE (18:1/18:2) levels, X-26109 levels, N6-methyllysine levels, N6,N6-dimethyllysine levels, and N2-acetyl,N6,N6-dimethyllysine levels. On the other hand, 5-hydroxymethyl-2-furoylcarnitine levels and glutamate-to-alanine ratios were positively associated with DR risk. No reverse causal effect was found between metabolites and DR. MR analyses from UK Biobank data showed no association of circulating metabolites with fasting glucose and 2-hour glucose, and 19 circulating metabolites were associated with a lower risk of type 2 diabetes (18). However, these metabolites did not intersect with those associated with DR risk in our analysis. This may be related to the different levels of refinement and classificationbolites.

Metabolomics is the omics discipline closest to phenotype and can be used not only to explore important biomarkers of disease,

but also to identify metabolites that may alter the phenotype of a cell or organism (19). The combination of metabolomics and systems biology information can test endogenous metabolites for phenotype-altering functions, and there is growing evidence that metabolites regulate a variety of biological processes (19). Metabolites are important bridges between genes, proteins and phenotypes. They are downstream of gene transcription and translation, and also support and regulate molecules in the microenvironment where gene expression and environmental exposure are regulated (20). Not only does it respond to the health status of the organism, but it can also be an effective window to regulate the state of the organism. Because metabolites are often readily available, especially for multifactorial diseases, they are considered a very powerful instrument with great potential for clinical translation (20). Although there is an increasing number of metabolomics studies in the eye, metabolomics research is still in its early stages and there are still many questions to be solved. Our study provides some theoretical support for DR mechanism research, prevention and risk stratification.

MR analysis methods. Results were robust and unaffected by horizontal pleiotropy or other confounding factors. Our studies have some limitations. The study is based on an individual of European ancestry, so conclusions cannot be extrapolated to the entire population. MR studies of DR in GWAS cohorts from other different ancestry groups (Africans, African Americans, Europeans, Hispanics, and Asians) will provide insights into how different genetic compositions resulting from inter-ethnic diversity and different environments lead to varying degrees of causal effects of circulating metabolites on DR development. Secondly, despite sensitivity analyses, horizontal pleiotropy could not be completely eliminated. Finally, using a lower threshold to assess the causal relationship between metabolite traits and DR may increase the number of false positives, but it allows for a more comprehensive assessment.

In addition, MR analysis predicts trends associated with DR risk and does not reflect metabolite disorders at different stages of disease, so more comprehensive, multimetric assessment strategies are needed to analyze different aspects of metabolite change.

Conclusions

We confirmed a causal relationship between a variety of metabolites and DR through bidirectional MR analysis, highlighting the complex features of the interactions between the metabolites and DR.

Our study significantly reduced the effects of reverse causality, confounding factors that are difficult to exclude, and other factors, providing new ideas for further exploration of the biological mechanisms of DR and some guidance for early treatment and prevention of DR.

Data availability statement

The original contributions presented in the study are included in the article/**Supplementary Material**. Further inquiries can be directed to the corresponding authors.

Author contributions

BL: Conceptualization, Software, Writing – original draft. XZ: Data curation, Investigation, Writing – review & editing. WX: Supervision, Writing – original draft. ZH: Project administration, Validation, Writing – original draft. YC: Resources, Writing – review & editing. YD: Writing – review & editing. YZ: Visualization, Writing – review & editing.

Funding

The author(s) declare financial support was received for the research, authorship, and/or publication of this article. This study was supported by the Research Fund of the Science and Technology Program of Fujian Province (2023J011776).

Acknowledgments

We gratefully acknowledge the researchers who have made GWAS summary data publicly available, as well as the participants who have contributed to these studies.

Conflict of interest

The authors declare that the research was conducted in the absence of any commercial or financial relationships that could be construed as a potential conflict of interest.

Publisher's note

All claims expressed in this article are solely those of the authors and do not necessarily represent those of their affiliated organizations, or those of the publisher, the editors and the reviewers. Any product that may be evaluated in this article, or claim that may be made by its manufacturer, is not guaranteed or endorsed by the publisher.

Supplementary material

The Supplementary Material for this article can be found online at: <https://www.frontiersin.org/articles/10.3389/fendo.2024.1359502/full#supplementary-material>

References

- Ogurtsova K, da Rocha Fernandes JD, Huang Y, Linnenkamp U, Guariguata L, Cho NH, et al. IDF Diabetes Atlas: Global estimates for the prevalence of diabetes for 2015 and 2040. *Diabetes Res Clin Pract.* (2017) 128:40–50. doi: 10.1016/j.diabres.2017.03.024
- Antonetti DA, Silva PS, Stitt AW. Current understanding of the molecular and cellular pathology of diabetic retinopathy. *Nat Rev Endocrinol.* (2021) 17:195–206. doi: 10.1038/s41574-020-00451-4
- Ronald Klein M. *Contemporary diabetes: diabetic retinopathy vol. 1*. Duh EJMD, editor. Clifton, Passaic, New Jersey, United States: Humana Press (2008) p. 67–107. MPH. doi: 10.1007/978-1-59745-563-3
- Wishart DS. Emerging applications of metabolomics in drug discovery and precision medicine. *Nat Rev Drug Discovery.* (2016) 15:473–84. doi: 10.1038/nrd.2016.32
- Hagenbeek FA, Pool R, van Dongen J, Draisma HHM, Jan Hottenga J, Willemsen G, et al. Heritability estimates for 361 blood metabolites across 40 genome-wide association studies. *Nat Commun.* (2020) 11:39. doi: 10.1038/s41467-019-13770-6
- Chen Y, Lu T, Pettersson-Kymmer U, Stewart ID, Butler-Laporte G, Nakanishi T, et al. Genomic atlas of the plasma metabolome prioritizes metabolites implicated in human diseases. *Nat Genet.* (2023) 55:44–53. doi: 10.1038/s41588-022-01270-1
- Pierce BL, Ahsan H, Vanderweele TJ. Power and instrument strength requirements for Mendelian randomization studies using multiple genetic variants. *Int J Epidemiol.* (2011) 40:740–52. doi: 10.1093/ije/dyq151
- Bowden J, Davey Smith G, Burgess S. Mendelian randomization with invalid instruments: effect estimation and bias detection through Egger regression. *Int J Epidemiol.* (2015) 44:512–25. doi: 10.1093/ije/dyv080
- Verbanck M, Chen CY, Neale B, Do R. Detection of widespread horizontal pleiotropy in causal relationships inferred from Mendelian randomization between complex traits and diseases. *Nat Genet.* (2018) 50:693–8. doi: 10.1038/s41588-018-0099-7
- Bowden J, Spiller W, Del Greco MF, Sheehan N, Thompson J, Minelli C, et al. Improving the visualization, interpretation and analysis of two-sample summary data Mendelian randomization via the Radial plot and Radial regression. *Int J Epidemiol.* (2018) 47:1264–78. doi: 10.1093/ije/dyy101
- Country MW. Retinal metabolism: A comparative look at energetics in the retina. *Brain Res.* (2017) 1672:50–7. doi: 10.1016/j.brainres.2017.07.025
- Chen L, Cheng CY, Choi H, Ikram MK, Sabanayagam C, Tan GS, et al. Plasma metabolomic profiling of diabetic retinopathy. *Diabetes.* (2016) 65:1099–108. doi: 10.2337/db15-0661
- Holmes E, Wilson ID, Nicholson JK. Metabolic phenotyping in health and disease. *Cell.* (2008) 134:714–7. doi: 10.1016/j.cell.2008.08.026
- Han X, Zhang L, Kong L, Tong M, Shi Z, Li XM, et al. Comprehensive metabolomic profiling of diabetic retinopathy. *Exp Eye Res.* (2023) 233:109538. doi: 10.1016/j.exer.2023.109538
- Barba I, Garcia-Ramírez M, Hernández C, Alonso MA, Masmiquel L, García-Dorado D, et al. Metabolic fingerprints of proliferative diabetic retinopathy: an 1H-NMR-based metabolomic approach using vitreous humor. *Invest Ophthalmol Vis Sci.* (2010) 51:4416–21. doi: 10.1167/iovs.10-5348
- Yau JW, Rogers SL, Kawasaki R, Lamoureux EL, Kowalski JW, Bek T, et al. Global prevalence and major risk factors of diabetic retinopathy. *Diabetes Care.* (2012) 35:556–64. doi: 10.2337/dc11-1909
- Fernandes Silva L, Hokkanen J, Vangipurapu J, Oravilahti A, Laakso M. Metabolites as risk factors for diabetic retinopathy in patients with type 2 diabetes: A 12-year follow-up study. *J Clin Endocrinol Metab.* (2023) 109:100–6. doi: 10.1210/clinem/dgad452
- Wong THT, Mo JMY, Zhou M, Zhao JV, Schooling CM, He B, et al. A two-sample Mendelian randomization study explores metabolic profiling of different glycemic traits. *Commun Biol.* (2024) 7:293. doi: 10.1038/s42003-024-05977-1
- Guijas C, Montenegro-Burke JR, Warth B, Spilker ME, Siuzdak G. Metabolomics activity screening for identifying metabolites that modulate phenotype. *Nat Biotechnol.* (2018) 36:316–20. doi: 10.1038/nbt.4101
- Lains I, Gantner M, Murinello S, Lasky-Su JA, Miller JW, Friedlander M, et al. Metabolomics in the study of retinal health and disease. *Prog Retin Eye Res.* (2019) 69:57–79. doi: 10.1016/j.preteyeres.2018.11.002



OPEN ACCESS

EDITED BY

Mohd Imtiaz Nawaz,
King Saud University, Saudi Arabia

REVIEWED BY

Mohammad A. Alfihli,
King Saud University, Saudi Arabia
Sara Rezzola,
University of Brescia, Italy

*CORRESPONDENCE

Caiyun You
✉ youcaiyun@126.com

[†]These authors have contributed
equally to this work and share
first authorship

RECEIVED 16 December 2023

ACCEPTED 22 April 2024

PUBLISHED 10 May 2024

CITATION

Ding R, Zeng Y, Wei Z, He Z, Jiang Z, Yu J
and You C (2024) The L-shape relationship
between hemoglobin, albumin,
lymphocyte, platelet score and the risk of diabetic
retinopathy in the US population.
Front. Endocrinol. 15:1356929.
doi: 10.3389/fendo.2024.1356929

COPYRIGHT

© 2024 Ding, Zeng, Wei, He, Jiang, Yu and
You. This is an open-access article distributed
under the terms of the [Creative Commons
Attribution License \(CC BY\)](#). The use,
distribution or reproduction in other forums
is permitted, provided the original author(s)
and the copyright owner(s) are credited and
that the original publication in this journal is
cited, in accordance with accepted academic
practice. No use, distribution or reproduction
is permitted which does not comply with
these terms.

The L-shape relationship between hemoglobin, albumin, lymphocyte, platelet score and the risk of diabetic retinopathy in the US population

Ranran Ding^{1,2†}, Yusong Zeng^{1,2†}, Zhimei Wei^{1,2†}, Zitong He^{1,2},
Zhixin Jiang³, Jinguo Yu¹ and Caiyun You^{1*}

¹Department of Ophthalmology, Tianjin Medical University General Hospital, Heping District,
Tianjin, China, ²Tianjin Medical University, Heping District, Tianjin, China, ³Tianjin Eye Hospital, Nankai
University Affiliated Eye Hospital, Clinical College of Ophthalmology, Tianjin Medical University, Tianjin
Eye Institute, Tianjin Key Laboratory of Ophthalmology and Visual Science, Tianjin, China

Background: The primary aim of this study was to investigate the correlation
between diabetic retinopathy (DR) and the HALP score (hemoglobin, albumin,
lymphocyte, and platelet) in individuals with diabetes within the United
States population.

Methods: This cross-sectional investigation was based on the National Health
and Nutrition Examination Survey (NHANES) database from 2003-2018. The
following module calculated the HALP score: HALP score = [lymphocytes (/L) ×
hemoglobin (g/L) × albumin (g/L)]/platelets (/L). By performing the receiver
operating characteristic (ROC) analysis, the optimal cutoff value of HALP was
ascertained. Restricted cubic splines (RCS), multivariable logistic regression
analysis, sensitivity analysis, and subgroup analysis were conducted to evaluate
the effect of the HALP score on DR patients. Finally, the decision curve analysis
(DCA) and clinical impact curve (CIC) were conducted to estimate the predictive
power and clinical utility of the HALP score with clinical indicators.

Results: According to the cutoff value (42.9) determined by the ROC curve, the
participants were stratified into a lower HALP group (HALP_{low}) and a higher HALP
group (HALP_{high}). An L-shaped relationship between HALP score and DR risk was
presented in the RCS model (P for nonlinearity <0.001). The DR risk sharply
decreased with the increase of HALP, and the decline reached a plateau when
HALP was more than 42.9. After fully adjustment, the multivariate logistic
regression analysis found that HALP_{low} was an independent risk factor for DR
(OR = 1.363, 95% CI: 1.111-1.671, P < 0.001). Besides, sensitivity analysis showed
consistent results. Furthermore, the combination of HALP score and clinical
indicators demonstrated predictive power and clinical utility, as shown by the
ROC curve, DCA, and CIC.

Conclusion: The HALP score has an L-shaped correlation with the risk of DR, and thus, the HALP score may contribute to the timely intervention of diabetes patients.

KEYWORDS

HALP score, diabetic retinopathy, biomarker, NHANES, diabetes complication

Highlights

- Limited studies have focused on the relationship between diabetic retinopathy (DR) and the hemoglobin, albumin, lymphocyte, platelet (HALP) score. We were the first team to demonstrate a negative association between lower HALP score and the prevalence of DR.
- An L-shaped correlation between HALP and DR occurrence was also initially observed in our findings. Moreover, diabetic patients with HALP score <49.2 were found to have a significantly increased risk of DR.
- We examined a large sample size, which represented 19.3 million residents in the United States.

Introduction

Diabetes mellitus (DM) is an escalating worldwide public health concern projected to impact around 700 million individuals by 2045 (1). Diabetic retinopathy (DR), a visually impairing condition associated with DM, remains the primary cause of avoidable vision impairment in the working-age population. It is estimated that approximately 160.5 million people with DM will suffer from DR in 2045 (1). Therefore, exploring new predictors of DR occurrence may help in the early identification and intervention of DR, which will play a crucial role in mitigating the visual impairment or loss associated with DM (2).

Abbreviations: HALP, Hemoglobin, albumin, lymphocyte, platelet score; DM, Diabetes mellitus; DR, Diabetic retinopathy; NHANES, National health and nutrition examination survey; NCHS, National Center for Health Statistics; CDC, Centers for disease control; CBC, Complete blood count; BCP, Bromocresol purple; BMI, Body mass index; HbA1c, Glycosylated hemoglobin A1c; HDL-C, High-density lipoprotein cholesterol; LDL-C, Low-density lipoprotein cholesterol; SE, Standard error; OR, Odds ratio; CI, Confidence intervals; ROC, Receiver operating characteristic; AUC, Area under curve; SD, Standard deviation; RCS, Restricted cubic spline; NLR, Neutrophil-to-lymphocyte ratio; PLR, Platelet-to-lymphocyte ratio; DME, Diabetic macular edema; DCA, Decision curve analysis; CIC, Clinical impact curve.

The etiology of DR is complex and multifaceted, with diverse factors involved, such as dyslipidemia and chronic inflammation (3). Previous evidence demonstrated that combinations of the hematological indices, such as neutrophil-to-lymphocyte ratio (NLR) and platelet-to-lymphocyte ratio (PLR), were regarded as being associated with DR incidence (4, 5). However, there are disagreements in some findings in terms of the correlation between NLR, PLR, and DR (6–9). The inconsistent conclusions make people realize that the use of single parameters representing inflammation status does not meet the requirements of clinical practice; therefore, multi-parameter combinations are necessary to be explored.

Increasing evidence supports that nutrition status also plays a role in the initiation and progression of DR in addition to inflammation (10–12). The combination of hemoglobin, albumin, lymphocyte, and platelet (HALP) score, as a novel immune-nutritional marker, provides insights into the chronic inflammation and immunological condition of the patients (13), which is relatively more stable than single blood parameters. In a cross-sectional study, researchers found that low hemoglobin concentrations are associated with a higher risk of DR (14). Serum albumin, representing nutritional state and metabolic demands (15), was found to have a quantitatively significant negative correlation with DR (16). Recently, much clinical research suggested that a low HALP score was indicative of a poor prognosis in multiple tumors (17–20). The latest studies have suggested that the HALP score is also related to dyslipidemia (21), which is a commonly acknowledged risk factor for DR. Nevertheless, the available evidence concerning the association between the HALP score and the occurrence of DR is extremely restricted.

To fill the research gap, this study investigated the relationships between DR and the HALP scores in a nationally representative sample of individuals with diabetes in the United States.

Materials and methods

Data source

The National Health and Nutrition Examination Survey (NHANES), created by the National Center for Health Statistics

(NCHS), is a series of publicly accessible cross-sectional surveys aiming to be representative of the US general population (<https://www.cdc.gov/nchs/nhanes/>). NCHS granted the study procedures of the Ethics Review Board (Protocol #98-12, #2005-06, #2011-17, #2018-01). Informed consent of the participants was obtained before collecting any data. All interviews and examinations were conducted under the guidance of the NHANES protocol. In this study, eight cycles of the NAHNES database were used (2003-2018), the selection process of which was depicted in Figure 1A. The exclusion criteria were: (a) age < 20 years ($n = 35,522$); (b) pregnant ($n = 941$); (c) without DR self-report ($n = 38,249$); (d) missing data on serum albumin ($n = 589$); and (e) missing lymphocyte, hemoglobin or platelet data ($n = 27$). Finally, 4,984 individuals participated in the investigation.

Measurement of serum albumin and blood lymphocyte, hemoglobin, platelet count

Lymphocytes, hemoglobin, and platelets were derived from the complete blood count (CBC) using the Beckman-Coulter method of sizing and counting. Serum albumin was measured based on the bromocresol purple (BCP) dye approach in the NHANES database. The following module calculated the HALP score: $\text{HALP score} = [\text{lymphocytes (}/\text{L)} \times \text{hemoglobin (g/L)} \times \text{albumin (g/L)}] / \text{platelets (}/\text{L)}$ (22).

Ascertainment of DM and DR

DM was briefly defined by the Standards of Medical Care in Diabetes (23): (a) FPG $\geq 126\text{mg/dL}$ (7.0mmol/L), (b) 2-h OGTT $\geq 200\text{mg/dL}$ (11.1mmol/L), (c) HbA1c $\geq 6.5\%$ (47.5mmol/L), (d) antidiabetic or insulin therapy, (e) who replied “yes” to the question “Did the doctor tell you that you have diabetes?” DR patients were those who replied “yes” to the question, “Has a doctor ever told you that diabetes has affected your eyes or that you had retinopathy?” The diabetes duration was calculated by: the claimed age when interviewing minus the age at first diagnosis of diabetes, and then separated into two categories: ≤ 10 years and > 10 years. Glycemic was assigned as excellent ($\text{HbA1c} < 7\%$) or bad ($\text{HbA1c} \geq 7\%$) glucose management.

Assessment of covariates

The selected demographic variables included age, gender, race, and education level. Examination and laboratory covariates for this study included body mass index (BMI), glycosylated hemoglobin A1c (HbA1c), low-density lipoprotein cholesterol (LDL-C), and high-density lipoprotein cholesterol (HDL-C). Self-reported daily habits and health state were also taken into account, including alcohol consumption, smoking status, and medicine history.

Dyslipidemia is frequently distinguished by three lipid abnormalities (24), namely: (a) increased levels of triglycerides (\geq

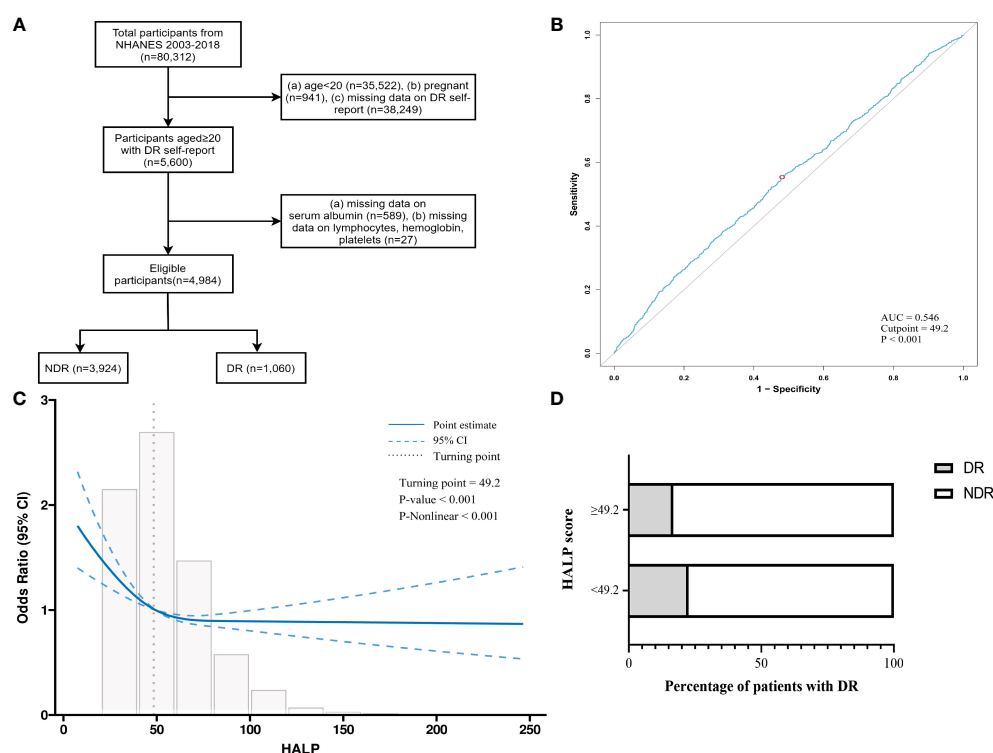


FIGURE 1

Study design and cutoff determination. (A) Flow diagram for research. (B) The cutoff of HALP score for the prediction of DR elevated by receiver operating characteristic curve (AUC=0.546, cutpoint=49.2, $p < 0.001$). (C) The “L-shape” relationship between HALP score and DR based on restricted cubic splines (turning-point=49.2, $p\text{-nonlinear} < 0.001$). (D) Stacked bar graphs of DR proportions in different HALP groups. AUC, Area under curve.

150 mg/dL), (b) increased levels of tiny LDL-C particles (≥ 130 mg/dL), and (c) decreased levels of HDL-C (< 40 mg/dL for men; < 50 mg/dL for women). Besides, people who were prescribed medication for dyslipidemia were also considered. Hypertension was determined as a blood pressure measurement over 140/90 mmHg measured on three consecutive occasions, a related medicine history, or a professional diagnosis.

Smoking history was categorized based on self-report in the following manner: (a) non-smokers: individuals who have never consumed 100 cigarettes during their lives; (b) former smokers: individuals who previously smoked over 100 cigarettes but have quit smoking; (c) current smokers: individuals who have a history of current smoking. Alcohol consumption was assessed by a 24-hour food recall.

Statistical analyses

The analysis of statistics was performed using Stata 16.0, R software (version 4.2.2), and MSTAT software. To ensure that the estimates could be representative of the general U.S. population, weighted samples, as well as the stratification and clustering of the design, were taken into consideration in all analyses conducted in accordance with centers for disease control (CDC) guidelines. To compare the disparities in baseline characteristics between the NDR and DR groups, continuous variables were expressed as means \pm standard error (SE), and categorical variables were presented as proportions. When comparing the differences in continuous variables between patients with NDR and DR, a weighted t-test was applied for continuous variables, while a weighted chi-square test was used for categorical variables. The cutoff value of HALP to predict DR in diabetes subjects was initially determined by the receiver operating characteristic (ROC) curve, and then the HALP score in all the individuals was evaluated by the restricted cubic spline (RCS) curve. Furthermore, three logistic regression analysis models were performed to assess the relationship between HALP and DR prevalence, and sensitivity analysis and subgroup analysis were further carried out. Finally, the decision curve analysis (DCA) and clinical impact curve (CIC) were conducted to estimate the predictive power and clinical utility of the HALP score. A two-sided $p < 0.05$ was considered significant.

Results

Characteristics of the participants at baseline

Totally, 4,984 NHANES diabetes patients were enrolled in this study, representing 19.3 million individuals in the USA. The baseline characteristics of all the eligible individuals were displayed in [Table 1](#), including 3,924 patients without DR and 1,060 patients with DR, and the weighted prevalence of DR was 19.57%. Totally, the average age was 59.6 ± 0.26 years, and 51.51% were males. In particular, in contrast to the NDR group, DR patients were more likely to have lower education level, longer diabetic duration, high levels of HDL-C, and HbA1c. The mean HALP score

was 55.07 ± 0.78 , and the DR patients tended to have lower HALP compared with NDR ones (50.67 ± 1.11 vs. 55.07 ± 0.78 , $P < 0.001$).

While no statistically significant disparity was observed in age, gender, race, body mass index, alcohol consumption, smoking history, hypertension presence, or hyperlipidemia presence among diabetes patients with or without DR.

The relationships of HALP score with diabetic retinopathy

According to the analysis of the ROC curve, the optimal cutoff value for HALP to predict the DR prevalence in diabetes subjects was 49.2 (AUC = 0.546) ([Figure 1B](#)). Additionally, in the restricted cubic spline (RCS) model, a noteworthy nonlinear correlation was observed between HALP and DR risk (P -nonlinear < 0.001). An L-shaped association between HALP score and DR incidence was displayed in [Figure 1C](#), and the inflection point of HALP for DR was also 49.2. Then, the relationships between HALP and DR were further analyzed by segmented logistic regression. The DR risk sharply decreased with the increase of HALP, and the decline reached a plateau when HALP was more than 42.9 ([Supplementary Table 1](#)).

Therefore, patients were categorized into two groups depending on their HALP scores: the higher HALP group ($\text{HALP}_{\text{high}} \geq 49.2$) and the lower HALP group ($\text{HALP}_{\text{low}} < 49.2$). The comparison between DR patients and NDR patients was illustrated in [Figure 1D](#), where the proportion of DR patients in the $\text{HALP}_{\text{high}}$ group was smaller than that in the HALP_{low} group (16.74% vs. 22.53%, $P < 0.001$).

Logistic regression analysis and sensitivity analysis

The results of logistic regression analyses evaluating the associations between HALP_{low} and DR in the diabetes population demonstrated that low HALP was associated with DR, regardless of other known factors ($P < 0.05$) ([Table 2](#)). Specifically, in the crude model (Model 1), a low HALP score was related to an elevated risk of DR (OR = 1.446, 95% CI: 1.188–1.760, $P < 0.001$). After several factors were adjusted (age, gender, race, BMI, education level, diabetic duration, and HbA1c level), a low HALP score was also presented as being related to the elevated risk of DR (OR = 1.364, 95% CI: 1.112–1.672, $P = 0.003$). Considering extrema's potential effects, a sensitivity analysis was performed to check the robustness of our results. After excluding samples with extreme HALP scores, similarly, sensitivity analysis indicated that the HALP_{low} group has a higher risk of DR prevalence in Model 3 (OR = 1.357, 95% CI: 1.107–1.664) ([Table 3](#)).

Stratification analysis of HALP score with diabetic retinopathy

As shown in [Figure 2A](#), further analysis was stratified by gender, diabetic duration, and HbA1c level. The findings from the subgroup

TABLE 1 Baseline of participants with or without DR.

| Characteristics | TOTAL (N=4984) | DR (-) (N=3924) | DR (+) (N=1060) | P-value |
|----------------------------|-------------------|--------------------|--------------------|---------|
| Age, years | 59.94 ± 0.25 | 59.55 ± 0.28 | 59.88 ± 0.56 | 0.885 |
| Gender, % | | | | 0.551 |
| Male | 51.42 | 51.63 | 50.57 | |
| Female | 48.58 | 48.37 | 49.43 | |
| Race/Ethnicity, % | | | | 0.307 |
| Mexican American | 9.26 | 9.29 | 9.13 | |
| Other Hispanic | 5.37 | 5.29 | 5.71 | |
| Non-Hispanic White | 62.27 | 62.91 | 59.65 | |
| Non-Hispanic Black | 14.50 | 14.19 | 15.79 | |
| Other (multi-racial) | 8.59 | 8.32 | 9.73 | |
| Education level | | | | <0.001 |
| Less than 9th grade | 10.89 | 10.34 | 13.61 | |
| 9th-12th grade | 13.41 | 12.93 | 15.41 | |
| High School/GED | 24.81 | 24.27 | 27.06 | |
| Some college/AA | 31.20 | 31.79 | 28.80 | |
| College or above | 19.52 | 20.60 | 15.09 | |
| Missing | 0.07 | 0.08 | 0.03 | |
| Alcohol consumption, g/day | 5.19 ± 0.40 | 5.38 ± 0.43 | 4.41 ± 0.99 | 0.186 |
| Smoking status, % | | | | 0.512 |
| non-smokers | 48.85 | 48.53 | 50.18 | |
| current-smokers | 35.29 | 35.35 | 35.04 | |
| former-smokers | 15.86 | 16.12 | 14.79 | |
| Diabetic duration, years | 11.52 ± 0.23 | 10.28 ± 0.23 | 16.64 ± 0.62 | <0.001 |
| BMI, kg/m ² | 32.89 ± 0.15 | 32.88 ± 0.17 | 32.92 ± 0.34 | 0.896 |
| BMI category | | | | 0.641 |
| Normal (<25) | 11.88 | 11.67 | 12.72 | |
| Overweight (25-30) | 26.04 | 26.03 | 26.09 | |
| Obese (≥ 30) | 62.08 | 62.30 | 61.19 | |
| Hypertension, % | | | | 0.054 |
| Yes | 54.00 | 53.33 | 56.84 | |
| No | 46.00 | 46.68 | 43.16 | |
| Hyperlipidemia, % | | | | 0.789 |
| Yes | 82.10 | 82.03 | 82.40 | |
| No | 17.90 | 17.97 | 17.60 | |
| HbA1c, % | 7.31 ± 0.03 | 7.21 ± 0.03 | 7.71 ± 0.07 | <0.001 |
| HDL-C, mg/dL | 47.59 ± 0.27 | 47.34 ± 0.30 | 48.63 ± 0.59 | 0.010 |
| HALP | 55.07 ± 0.78 | 56.14 ± 0.93 | 50.67 ± 1.11 | <0.001 |

Data was presented as means ± standard error (SE) or proportions.

BMI, Body mass index; HbA1c, Glycosylated hemoglobin A1c; HDL, High density lipoprotein; HALP, hemoglobin, albumin, lymphocyte, and platelet.

TABLE 2 Logistic regression analysis for the association between HALP and DR in various models.

| | Model 1 OR (95%CI) P | Model 2 OR (95%CI) P | Model 3 OR (95%CI) P |
|----------------------|---------------------------|---------------------------|--------------------------|
| HALP _{high} | reference | reference | reference |
| HALP _{low} | 1.446(1.188–1.760) <0.001 | 1.453(1.185–1.781) <0.001 | 1.364(1.112–1.672) 0.003 |
| P trend | <0.001 | <0.001 | <0.001 |

Model 1: crude model, without any adjustments; Model 2: adjusted for age, gender, race; Model 3: based on model 2, further adjusted for diabetic duration, HbA1c, education level, BMI.
OR, Odds ratios; CI, Confidence intervals.

analysis demonstrated persistent and favorable associations between HALP_{low} and DR risk across gender and HbA1c subgroups (P for interaction > 0.05). Notedly, HALP_{low} showed significantly higher prevalence of DR in the subgroups of longer diabetic duration (>10 years) (P for interaction = 0.033), with OR (95% CI) 1.684 (1.286–2.205).

Predictive power of HALP score with clinical indicators for DR

To examine the diagnostic value of the HALP score combined with common clinical indicators for DR, we conducted ROC analysis. As depicted in Figure 2B, a combination of HALP score, HbA1c, and diabetic duration indeed results in a model with increased predictive performance (AUC=0.666). DCA investigated the potential clinical utility of the HALP score in predicting the risk of DR. DR demonstrated a favorable net clinical benefit within a threshold probability range of 7% to 40%, with the highest net benefit observed (Supplementary Figure S1). In addition, CIC was created as a visual tool to evaluate the concordance between prediction and observation of DR occurrences. As presented in Supplementary Figure S2, there were consistently more anticipated

TABLE 3 Sensitivity analysis for the association between HALP and DR in various models.

| | Model 1 OR (95%CI) P | Model 2 OR (95%CI) P | Model 3 OR (95%CI) P |
|----------------------|---------------------------|---------------------------|--------------------------|
| HALP _{high} | reference | reference | reference |
| HALP _{low} | 1.438(1.181–1.751) <0.001 | 1.445(1.178–1.772) <0.001 | 1.357(1.107–1.664) 0.003 |

Model 1: crude model, without any adjustments; Model 2: adjusted for age, gender, race; Model 3: based on model 2, further adjusted for diabetic duration, HbA1c, education level, BMI.
OR, Odds ratios; CI, Confidence intervals.

high-risk patients than real DR patients at the optimal threshold probability, with a satisfactory cost-benefit ratio.

Discussion

To date, this was the first investigation into the potential association between HALP score and DR prevalence in diabetes patients, using the NHANES database based on a nationwide representative population scattered across the United States. The results suggested that a lower HALP score was a significant risk factor for DR, independent of other confounders. The DR risk for diabetes patients in the HALP_{low} group was 36% higher than that in the HALP_{high} group after adjusting for several factors. A similar conclusion was also drawn from sensitivity analysis, which represented that the findings were stable. Significantly, this research was the first to establish an L-shaped correlation between the HALP score and DR risk after adjusting for confounding variables. Additionally, a significant statistical trend was observed only when HALP was below 49.2. Specifically, HALP score showed a hazardous effect on DR occurrence when below 42.9 and then appeared relatively flat. Stratification analysis suggested that HALP_{low} was a reliable predictor of DR risk, thereby potentially aiding in the detection and monitoring of diabetes patients who are

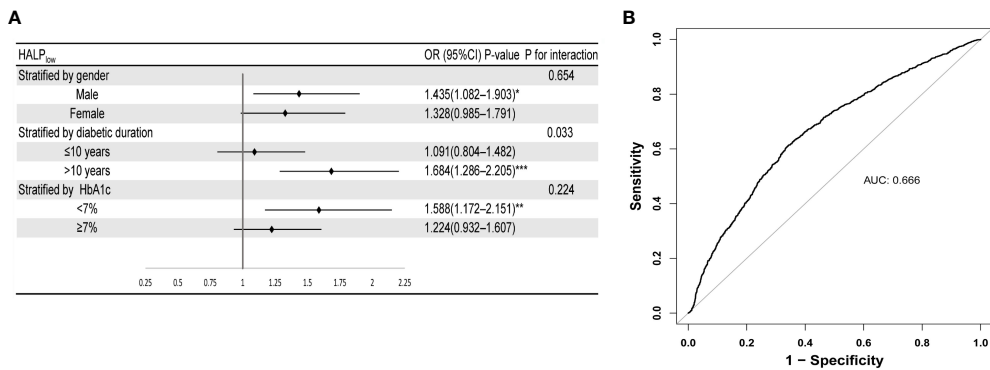


FIGURE 2 Robustness and diagnostic value of HALP. (A) Forest plot of the relationship of DR with HALP in different subgroups (after adjusting age, gender, race, BMI, education level, diabetic duration, and HbA1c level). (B) ROC curve of HALP score combined with clinical indicators (HbA1c level and diabetic duration) for predicting DR. Stratified by diabetes duration, HbA1c and gender. Subgroups were all adjusted for age, gender, race, diabetic duration, HbA1c, education level.

susceptible to DR, especially among patients with over 10 years of diabetic duration. Furthermore, the combination of HALP score and clinical indicators demonstrated predictive power and clinical utility, as shown by the ROC curve, DCA, and CIC.

The pathophysiology of DR is complex and multifactorial, involving chronic inflammation and oxidative stress. Accumulating studies have reported that chronic inflammation contributes to the upregulation of pro-inflammatory cytokines and chemokines, such as interleukin-1 β (IL-1 β) and vascular endothelial growth factor (VEGF), which can exacerbate the pathophysiological progression observed in DR, such as endothelial failure, leukocyte adhesion and infiltration, platelet activation, and neovascularization (25).

As a recognized indicator of inflammation, lymphocytes are actively involved in the elimination and repair of inflammation. Zhu et al. found that a lower lymphocyte percentage might potentially serve as a valuable diagnostic indicator for identifying the onset and progression of diabetic macular edema (DME) (26). Platelets play a crucial role in diabetes patients through heightened adhesion, activation, and aggregation of platelets due to disruptions in multiple signaling pathways and metabolic abnormalities such as hyperglycemia and dyslipidemia (27). Oxidative stress, systemic inflammation, reduced nitric oxide bioavailability, poor calcium metabolism, and increased phosphorylation and glycosylation of cellular proteins contribute to exacerbated platelet activation (28). This, in turn, leads to the occurrence of diabetic complications.

Serum albumin is rich in thiol groups that can effectively neutralize the majority of reactive oxygen in the blood (29), potentially aiding in protecting DR patients from oxidative damage. Furthermore, albumin has the ability to attach to advanced glycation end products (AGEs) formed through non-enzymatic glycation processes in a hyperglycemic environment (30). AGEs are strongly linked to the development of DR (31), and albumin can potentially reduce the harmful impact on the retina by binding to them (32). Hemoglobin, as an oxygen carrier, was correlated with more severe DR when it was in low concentration (33). Compared to red blood cells in the general population, those in diabetic individuals have less deformability and more capillary aggregation, making them more brittle and susceptible to breaking, leading to lower hemoglobin levels and potentially causing anemia (34). Hypoxia caused by anemia triggers the production of inflammatory mediators and vasoproliferative factors like VEGF and erythropoietin (35, 36). These substances can increase retinal vascular permeability and worsen DR (33). Moreover, anemia may lead to ischemia, which is believed to aggravate the progression of retinal hypoxia and further exacerbate the progression of DR (37).

The HALP score, a novel indication, is derived from the integration of the aforementioned four hematological parameters. This finding may be significant because it is cost-effective and easily assesses current inflammation and nutritional status, which can aid physicians in primary hospitals and outpatient clinics in evaluating DR occurrence especially when HALP score is lower than 42.9, and developing suitable treatment strategies through regulating hemoglobin, albumin, lymphocyte, and platelet.

This research exhibited some strengths and weaknesses. As far as our knowledge extends, this was the first investigation that assessed the potential correlation between HALP score and DR in patients with diabetes. Moreover, our study was a large sample size, which represented 19.3 million residents in the United States. Considering its cross-sectional and observational nature, some limitations existed in this study. First, this was a cross-sectional analysis, and causality cannot be extrapolated. Second, the history of DR in NHANES was just self-reported data and failed to involve the classification of DR. Third, the hemoglobin count, serum albumin levels, lymphocyte count, and platelet count were assessed during the examination. However, it failed to demonstrate how the HALP score exhibits dynamic changes over time. Consequently, prospective cohort investigations remain necessary to confirm the conclusions.

Conclusion

The HALP score had an L-shaped association with the risk of diabetic retinopathy, suggesting possible predictive potential. Moreover, diabetes patients with a lower HALP score were more likely to have an increased risk of diabetic retinopathy, particularly among those with over 10 years of diabetic duration. Prospective studies are needed to prove its reliability and clinical utility.

Data availability statement

The original contributions presented in the study are included in the article/**Supplementary Material**. Further inquiries can be directed to the corresponding author.

Ethics statement

The NHANES protocols and testing procedures were all approved by the Institutional Review Board of the Centers for Disease Control and Prevention (Protocol #2005-06, Continuation of Protocol #2005-06, <https://www.cdc.gov/nchs/nhanes/irba98.htm>). All individuals who participated in the survey were provided with informed consent prior to their inclusion. The database included in this study underwent a process of de-identification, ensuring the removal of individually identifiable information and making it appropriate for non-human participant research. Therefore, no further ethical approval or consent to participate is needed.

Author contributions

RD: Data curation, Formal Analysis, Methodology, Software, Writing – original draft. YZ: Investigation, Writing – original draft. ZW: Data curation, Writing – original draft. ZH: Conceptualization, Writing – review & editing. ZJ: Funding acquisition, Writing – review

& editing. JY: Supervision, Writing – review & editing. CY: Funding acquisition, Writing – review & editing.

Funding

The author(s) declare financial support was received for the research, authorship, and/or publication of this article. This study was supported by National Natural Science Foundation of China (32200684), Tianjin Science & Technology Foundation (23JCZJC00140) and Tianjin Science & Technology Foundation (21JCQNJC01030).

Acknowledgments

Thanks to the public databases and the efforts of the authors.

Conflict of interest

The authors declare that the research was conducted in the absence of any commercial or financial relationships that could be construed as a potential conflict of interest.

References

- GBD 2019 Blindness and Vision Impairment Collaborators; Vision Loss Expert Group of the Global Burden of Disease Study. Causes of blindness and vision impairment in 2020 and trends over 30 years, and prevalence of avoidable blindness in relation to VISION 2020: the Right to Sight: an analysis for the Global Burden of Disease Study. *Lancet Glob Health*. (2021) 9:e144–e60. doi: 10.1016/S2214-109X(20)30489-7
- Lin S, Ramulu P, Lamoureux EL, Sabanayagam C. Addressing risk factors, screening, and preventative treatment for diabetic retinopathy in developing countries: a review. *Clin Exp Ophthalmol*. (2016) 44:300–20. doi: 10.1111/ceo.12745
- Wang W, Lo ACY. Diabetic retinopathy: pathophysiology and treatments. *Int J Mol Sci*. (2018) 19(6):1816. doi: 10.3390/ijms19061816
- Zeng J, Chen M, Feng Q, Wan H, Wang J, Yang F, et al. The platelet-to-lymphocyte ratio predicts diabetic retinopathy in type 2 diabetes mellitus. *Diabetes Metab Syndr Obes*. (2022) 15:3617–26. doi: 10.2147/DMSO.S378284
- Rajendrakumar AL, Hapca SM, Nair ATN, Huang Y, Chourasia MK, Kwan RS-Y, et al. Competing risks analysis for neutrophil to lymphocyte ratio as a predictor of diabetic retinopathy incidence in the Scottish population. *BMC Med*. (2023) 21:304. doi: 10.1186/s12916-023-02976-7
- Akdoğan M, Ustundag-Budak Y, Huysal K. The association of hematologic inflammatory markers with atherogenic index in type 2 diabetic retinopathy patients. *Clin Ophthalmol*. (2016) 10:1797–801. doi: 10.2147/OPTH
- Ciray H, Aksoy AH, Ulu N, Cizmecioglu A, Gaipov A, Solak Y. Nephropathy, but not Angiographically Proven Retinopathy, is Associated with Neutrophil to Lymphocyte Ratio in Patients with Type 2 Diabetes. *Exp Clin Endocrinol Diabetes*. (2015) 123:267–71. doi: 10.1055/s-00000017
- Dascau AM, Georgescu A, Costea AC, Tribus L, El Youssoufi A, Serban D, et al. Association between neutrophil-to-lymphocyte ratio (NLR) and platelet-to-lymphocyte ratio (PLR) with diabetic retinopathy in type 2 diabetic patients. *Cureus*. (2023) 15:e48581. doi: 10.7759/cureus.48581
- Onalan E, Gozel N, Donder E. Can hematological parameters in type 2 diabetes predict microvascular complication development? *Pak J Med Sci*. (2019) 35:1511–5. doi: 10.12669/pjms.35.6.1150
- Joussen AM, Poulaki V, Le ML, Koizumi K, Esser C, Janicki H, et al. A central role for inflammation in the pathogenesis of diabetic retinopathy. *FASEB J*. (2004) 18:1450–2. doi: 10.1096/fj.03-1476fje
- Rübsam A, Parikh S, Fort PE. Role of inflammation in diabetic retinopathy. *Int J Mol Sci*. (2018) 19(4):942. doi: 10.3390/ijms19040942
- Sharma Y, Saxena S, Mishra A, Saxena A, Natu SM. Nutrition for diabetic retinopathy: plummeting the inevitable threat of diabetic vision loss. *Eur J Nutr*. (2017) 56:2013–27. doi: 10.1007/s00394-017-1406-2
- Xu S-S, Li S, Xu H-X, Li H, Wu C-T, Wang W-Q, et al. Hemoglobin, albumin, lymphocyte and platelet predicts postoperative survival in pancreatic cancer. *World J Gastroenterol*. (2020) 26:828–38. doi: 10.3748/wjg.v26.i8.828
- Lee M-K, Han K-D, Lee J-H, Sohn S-Y, Jeong J-S, Kim M-K, et al. High hemoglobin levels are associated with decreased risk of diabetic retinopathy in Korean type 2 diabetes. *Sci Rep*. (2018) 8:5538. doi: 10.1038/s41598-018-23905-2
- Oetli K, Reibnegger G, Schmut O. The redox state of human serum albumin in eye diseases with and without complications. *Acta Ophthalmol*. (2011) 89:e174–e9. doi: 10.1111/aos.2011.89.issue-2
- Wang G-X, Fang Z-B, Li J-T, Huang B-L, Liu D-L, Chu S-F, et al. The correlation between serum albumin and diabetic retinopathy among people with type 2 diabetes mellitus: NHANES 2011–2020. *PLoS One*. (2022) 17:e0270019. doi: 10.1371/journal.pone.0270019
- Solmaz S, Uzun O, Sevindik OG, Demirkan F, Ozcan MA, Ozsan GH, et al. The effect of hemoglobin, albumin, lymphocyte and platelet score on the prognosis in patients with multiple myeloma. *Int J Lab Hematol*. (2023) 45:13–9. doi: 10.1111/ijlh.13958
- Wang J, Jiang P, Huang Y, Tu Y, Zhou Q, Li N, et al. Prognostic value of the cutoffs for HALP in endometrial cancer. *Am J Clin Oncol*. (2023) 46:107–13. doi: 10.1097/JCO.0000000000000977
- Sargin ZG, Dusunceli I. The effect of HALP score on the prognosis of gastric adenocarcinoma. *J Coll Physicians Surg Pak*. (2022) 32:1154–9. doi: 10.29271/jcpsp
- Zhao Z, Yin X-N, Wang J, Chen X, Cai Z-L, Zhang B. Prognostic significance of hemoglobin, albumin, lymphocyte, platelet in gastrointestinal stromal tumors: A propensity matched retrospective cohort study. *World J Gastroenterol*. (2022) 28:3476–87. doi: 10.3748/wjg.v28.i27.3476
- Alshuweishi Y, BaSudan AM, Alfaifi M, Daghistani H, Alfahli MA. Association of the HALP score with dyslipidemia: A large, nationwide retrospective study. *Medicina (Kaunas)*. (2023) 59(11):2002. doi: 10.3390/medicina59112002
- Chen X-L, Xue L, Wang W, Chen H-N, Zhang W-H, Liu K, et al. Prognostic significance of the combination of preoperative hemoglobin, albumin, lymphocyte and platelet in patients with gastric carcinoma: a retrospective cohort study. *Oncotarget*. (2015) 6:41370–82. doi: 10.18632/oncotarget.v6i38
- Elsayed NA, Aleppo G, Aroda VR, Bannuru RR, Brown FM, Bruemmer D, et al. 2. Classification and diagnosis of diabetes: standards of care in diabetes-2023. *Diabetes Care*. (2023) 46:S19–40. doi: 10.2337/dc23-S002
- Schwartz SL. Diabetes and dyslipidemia. *Diabetes Obes Metab*. (2006) 8:355–64. doi: 10.1111/j.1463-1326.2005.00516.x

Publisher's note

All claims expressed in this article are solely those of the authors and do not necessarily represent those of their affiliated organizations, or those of the publisher, the editors and the reviewers. Any product that may be evaluated in this article, or claim that may be made by its manufacturer, is not guaranteed or endorsed by the publisher.

Supplementary material

The Supplementary Material for this article can be found online at: <https://www.frontiersin.org/articles/10.3389/fendo.2024.1356929/full#supplementary-material>.

SUPPLEMENTARY FIGURE 1

Decision curve analysis of HALP score prediction model to estimate DR.

SUPPLEMENTARY FIGURE 2

Clinical impact curve of HALP score.

SUPPLEMENTARY TABLE 1

Effect of Standardized HALP Level on DR: Odds Ratios from Segmented Logistic Regression Analysis adjusted. OR: Odds Ratio, CI: Confidence Interval, SD: Standard deviation.

25. Cheung N, Mitchell P, Wong TY. Diabetic retinopathy. *Lancet*. (2010) 376:124–36. doi: 10.1016/S0140-6736(09)62124-3
26. Zhu Y, Cai Q, Li P, Zhou Y, Xu M, Song Y. The relationship between peripheral blood inflammatory markers and diabetic macular edema in patients with severe diabetic retinopathy. *Ann Palliat Med*. (2022) 11:984–92. doi: 10.21037/apm
27. Suslova TE, Sitorzhievskii AV, Ogurkova ON, Kravchenko ES, Kologrivova IV, Anfinogenova Y, et al. Platelet hemostasis in patients with metabolic syndrome and type 2 diabetes mellitus: cGMP- and NO-dependent mechanisms in the insulin-mediated platelet aggregation. *Front Physiol*. (2014) 5:501. doi: 10.3389/fphys.2014.00501
28. El Haouari M, Rosado JA. Platelet signaling abnormalities in patients with type 2 diabetes mellitus: a review. *Blood Cells Mol Dis*. (2008) 41:119–23. doi: 10.1016/j.bcmd.2008.02.010
29. Merlot AM, Kalinowski DS, Richardson DR. Unraveling the mysteries of serum albumin—more than just a serum protein. *Front Physiol*. (2014) 5:299. doi: 10.3389/fphys.2014.00299
30. Twarda-Clapa A, Olczak A, Białkowska AM, Koziolkiewicz M. Advanced glycation end-products (AGEs): formation, chemistry, classification, receptors, and diseases related to AGEs. *Cells*. (2022) 11(8):1312. doi: 10.3390/cells11081312
31. Takayanagi Y, Yamanaka M, Fujihara J, Matsuoka Y, Gohto Y, Obana A, et al. Evaluation of relevance between advanced glycation end products and diabetic retinopathy stages using skin autofluorescence. *Antioxidants (Basel)*. (2020) 9(11):1100. doi: 10.3390/antiox9111100
32. Henning C, Stübner C, Arabi SH, Reichenwallner J, Hinderberger D, Fiedler R, et al. Glycation alters the fatty acid binding capacity of human serum albumin. *J Agric Food Chem*. (2022) 70:3033–46. doi: 10.1021/acs.jafc.1c07218
33. Traveset A, Rubinat E, Ortega E, Alcubierre N, Vazquez B, Hernández M, et al. Lower hemoglobin concentration is associated with retinal ischemia and the severity of diabetic retinopathy in type 2 diabetes. *J Diabetes Res*. (2016) 2016:3674946. doi: 10.1155/2016/3674946
34. Goldstein M, Leibovitch I, Levin S, Alster Y, Loewenstein A, Malkin G, et al. Red blood cell membrane mechanical fluctuations in non-proliferative and proliferate diabetic retinopathy. *Graefes Arch Clin Exp Ophthalmol*. (2004) 242:937–43. doi: 10.1007/s00417-004-0946-3
35. Hernández C, Fonollosa A, García-Ramírez M, Higuera M, Catalán R, Miralles A, et al. Erythropoietin is expressed in the human retina and it is highly elevated in the vitreous fluid of patients with diabetic macular edema. *Diabetes Care*. (2006) 29:2028–33. doi: 10.2337/dc06-0556
36. Simó R, Hernández C. Neurodegeneration in the diabetic eye: new insights and therapeutic perspectives. *Trends Endocrinol Metab*. (2014) 25:23–33. doi: 10.1016/j.tem.2013.09.005
37. Wang J, Xin X, Luo W, Wang R, Wang X, Si S, et al. Anemia and diabetic kidney disease had joint effect on diabetic retinopathy among patients with type 2 diabetes. *Invest Ophthalmol Vis Sci*. (2020) 61:25. doi: 10.1167/iovs.61.14.25



OPEN ACCESS

EDITED BY

Mohd Imtiaz Nawaz,
King Saud University, Saudi Arabia

REVIEWED BY

Guoming Zhang,
Shenzhen Eye Hospital, China
Weihua Yang,
Shenzhen Eye Institute, China
Baoke Hou,
People's Liberation Army General Hospital,
China

*CORRESPONDENCE

Wei Zhou

✉ zyyykzw@tmu.edu.cn

Hua Yan

✉ zyyyanhua@tmu.edu.cn

[†]These authors have contributed equally to this work

RECEIVED 19 January 2024

ACCEPTED 29 April 2024

PUBLISHED 14 May 2024

CITATION

He K, Wei-Zhang S, Li Z, Kaysar P, Yang T, Sun Z, Zhou W and Yan H (2024) Correlation between vessel density and thickness in the retina and choroid of severe non-proliferative diabetic retinopathy patients.
Front. Endocrinol. 15:1373363.
doi: 10.3389/fendo.2024.1373363

COPYRIGHT

© 2024 He, Wei-Zhang, Li, Kaysar, Yang, Sun, Zhou and Yan. This is an open-access article distributed under the terms of the [Creative Commons Attribution License \(CC BY\)](#). The use, distribution or reproduction in other forums is permitted, provided the original author(s) and the copyright owner(s) are credited and that the original publication in this journal is cited, in accordance with accepted academic practice. No use, distribution or reproduction is permitted which does not comply with these terms.

Correlation between vessel density and thickness in the retina and choroid of severe non-proliferative diabetic retinopathy patients

Kai He^{1†}, Selena Wei-Zhang^{1†}, Ziqi Li¹, Parhat Kaysar¹,
Tianjing Yang², Zhiyong Sun¹, Wei Zhou^{1*} and Hua Yan^{1,3,4,5,6*}

¹Department of Ophthalmology, Tianjin Medical University General Hospital, Tianjin, China, ²School of Medicine, Nankai University, Tianjin, China, ³Ministry of Education International Joint Laboratory of Ocular Diseases, Tianjin, China, ⁴Tianjin Key Laboratory of Ocular Trauma, Tianjin, China, ⁵Tianjin Institute of Eye Health and Eye Diseases, Tianjin, China, ⁶China-UK "Belt and Road" Ophthalmology Joint Laboratory, Tianjin, China

Objectives: To explore the correlation between the vessel density (VD) of the retina and choroid vascular plexuses and the thicknesses of their respective retinal layers and choroid membranes in participants with severe non-proliferative diabetic retinopathy (NPDR).

Methods: We retrospectively analyzed the data of 42 eyes of 42 participants with diabetes mellitus (DM) and severe NPDR. In addition, 41 eyes of 41 healthy controls were evaluated. Measurements were taken for both groups using optical coherence tomography angiography (OCTA), including the area and perimeter of the foveal vascular zone (FAZ) and the vascular density (VD) in the superficial capillary plexus (SCP), deep capillary plexus (DCP), and choroid capillary (CC). These measurements were compared with the retinal thickness (RT) of the inner/intermediate retinal layers and choroidal thickness (CT). The study evaluated the correlation between RT or CT and VD in the respective vascular networks, namely superficial capillary plexus (SCP), deep capillary plexus (DCP), or CC.

Results: The inner RT and VD in all plexuses were significantly lower in the severe NPDR group than in the healthy controls. Furthermore, the FAZ area and perimeter were larger in the severe NPDR group. Inner RT was correlated with VD in the SCP group ($r=0.67$ and $r=0.71$ in the healthy control and severe NPDR groups, respectively; $p<0.05$). CT negatively correlated with VD in the CC ($r=-0.697$ and $r=-0.759$ in the healthy control and severe NPDR groups, respectively; $p<0.05$). Intermediate RT significantly correlated with VD in the DCP of the severe NPDR group ($r=-0.55$, $p<0.05$), but not in the healthy control group.

Conclusions: Retinal or choroidal thickness strongly correlated with VD. Therefore, patients with severe NPDR must consider the distinct anatomical and functional entities of the various retinal layers and the choroid.

KEYWORDS

retinal thickness, optical coherence tomography angiography, severe nonproliferative diabetic retinopathy, vessel density, choroidal thickness

1 Introduction

Diabetic retinopathy (DR) is a prevalent complication of DM, particularly in the working-age population, representing a primary cause of blindness (1). Severe NPDR is the severe pathological stage of diabetic retinopathy at which DR is most commonly recommended for clinical treatment (2). Fluorescent angiography and fundus photography have been used to diagnose DR. OCTA is a form of non-invasive examination that can provide elaborate images without dye injection. It is increasingly used for diabetic retinopathy diagnosis and observational studies owing to its high resolution and noninvasiveness.

DR leads to structural and functional changes in the retina, microaneurysm formation, non-perfusion areas, and vascular abnormalities, which are the main pathological features of severe NPDR (3). In this context, OCTA can acquire more information, allowing quantitative analysis of the choroid and retina. The majority of the literature has demonstrated the potential role of OCTA in DR, such as in examining neovascular complexes (4) and non-perfusion areas (5). VD, as well as the FAZ area in the retina of diabetic patients are altered compared with those of healthy people (6, 7). Moreover, the structure of retinal changes, even in diabetic patients who do not have DR (8, 9), included a thinner retinal sublayer, including the ganglion cell layer (GCL), retinal nerve fiber layer (RNFL), and inner plexiform layer (IPL).

Several studies have previously investigated on the correlation between the retinal structure and VD, providing particular insights into diagnosing and treating fundus diseases (10, 11). Some researchers (12) have further demonstrated that the OCTA parameters for the VD and FAZ circularity indices were correlated with the GCL/IPL in diabetic patients with diabetes. Decreased choroidal VD can lead to structural changes in the retina (13). Choroidal VD has been suggested to correlate with retinal thickness. However, relevant studies investigating the correlation between retinal/choroidal thickness and OCTA-related parameters need to be performed, particularly in patients with severe NPDR.

In this study, we focused on identifying changes in VD and retinal sublayer/choroidal thickness, as well as identifying the correlation between thickness and VD in patients with severe NPDR.

2 Materials and method

2.1 Participants

Participants with diabetes who underwent DR-related fundus examinations were admitted to Tianjin Medical University General Hospital between March 2021 and March 2023. Age-matched healthy controls were included in this cross-sectional study. Two ophthalmologists evaluated and graded the fundus images. All participants who were diagnosed as severe NPDR without the presence of diabetic macular edema (DME) were enrolled in this research. Participants who had undergone fundus therapy, such as anti-VEGF therapy and/or laser therapy, or had any other conditions that could affect the microvessels of the choroid and retina, such as retinal vascular obstruction, glaucoma, or proportional retinal disease, were excluded.

Relevant demographic data and clinical information, including age, sex, axial length, body mass index (BMI), smoking status, blood pressure, best-corrected visual acuity (BCVA), and intraocular pressure (IOP), were collected.

This study was conducted in accordance with the principles of the Declaration of Helsinki, and was approved by the Ethics Committee of the Tianjin Medical University General Hospital (approval number (RB2021-YX-048-01). Consent was obtained from the participants, all of whom were made aware of the purpose and potential outcomes of the study and willingly agreed to participate. The participants in this project were well informed about the study's objectives and potential effects, and they willingly provided their consent.

2.2 Swept-source optical coherence tomography and OCTA imaging and measurements

Images derived by Swept-source optical coherence tomography and OCTA were captured by a Zeiss Cirrus (HD-OCT 5000) equipped with an Angioplex (Carl Zeiss Meditec, Dublin, CA, USA). A 3x3 mm scan was created for each eye, focusing on the central part of the foveal area. FastTrac retinal tracking technology (San Francisco, CA, USA) was used to minimize motion artifacts. A

signal strength > 6 out of 10 was accepted. En-face OCTA images were automatically generated using an optical microangiography algorithm of the Angioplex software. The SCP, DCP, and CC were automatically identified using a review software program (Carl Zeiss Meditec). The SCP and DCP were defined as the inner limiting membrane to the inner plexiform layer and from the inner nuclear layer to the outer plexiform layer, respectively (14). CCP was defined as 10 μ m thickness under the complex of retinal pigment epithelium and Bruch membrane (15). The thickness of the central macula was measured manually by an examiner who was unaware of the details. We further determined choroid thickness as the length from the outer border of the retinal pigment epithelium to the sclero-choroidal interface. The thickness of the inner retinal layer was defined from the inner membrane layer to the IPL, whereas that for the intermediate retinal layer was defined from the inner nuclear layer (INL) to the outer plexiform layer (OPL).

2.3 Quantitative OCTA image analysis

As previously mentioned, the binarization processing of the SCP and DCP was conducted using customized Python 3.5 code, provided by The Python Software Foundation (United States) (16). In summary, each image was subjected to a top-hat filter, followed by further processing. Two distinct techniques for binarization were employed: the initial image was processed with a Hessian filter, and subsequently subjected to global thresholding using Huang's fuzzy thresholding approach. A median local thresholding approach was applied to the second image. Combining the two processed images results in the creation of an ultimate binarized image. The foveal circle was surrounded by an annular region. Pixels in both images were exclusively considered when included in the analysis. For the analysis, a combination of automated outlining using review software and manual outlining by two separate investigators was utilized, with manual outlining employed in cases where the algorithm signals were not strong. The diameter of the CC OCTA image was binarized using the Phansalkar method to calculate the VD, which is represented as the percentage of the total vessel area divided by the total measured area (1–3 mm in diameter) (8), as mentioned earlier (15).

2.4 Statistical analysis

The statistical analyses utilized IBM SPSS Statistics for Windows (version 25.0). Categorical variables are described as numbers or percentages. Pearson's chi-square test was conducted on both the healthy control and severe NPDR groups, with continuous variables presented as the mean and standard deviation (SD). Student's *t*-test was conducted to compare two groups. We used a single-factor regression analysis to investigate the correlation between VD and VD in both groups. Statistical significance was set at $p < 0.05$.

TABLE 1 Basic information of healthy controls and severe NPDR patients.

| Characteristic Means \pm SD/ n (%) | Healthy controls (n=41) | Severe NPDR patients (n=42) | p value |
|--------------------------------------|-------------------------|-----------------------------|---------|
| Age, year | 54.6 \pm 12.5 | 52.3 \pm 8.7 | 0.318 |
| BMI, kg/m ² | 25.6 \pm 3.1 | 24.7 \pm 3.0 | 0.202 |
| Blood pressure, mmHg | 143.7 \pm 17.8 | 141.7 \pm 18.9 | 0.619 |
| Axial length, mm | 23.7 \pm 1.4 | 23.5 \pm 1.2 | 0.446 |
| BCVA, logMAR | 0.02 \pm 0.05 | 0.26 \pm 0.25 | <0.001 |
| IOP, mmHg | 16.2 \pm 3.1 | 17.4 \pm 2.5 | 0.061 |
| Sex (male) | 24 (58.5) | 24 (57.1) | 0.89 |
| Smoking (yes) | 16 (39.0) | 16 (38.1) | 0.93 |

BMI, body mass index; BCVA, best-corrected visual acuity; IOP, intraocular pressure; SD, standard deviation; NPDR, nonproliferative diabetic retinopathy.

3 Results

Table 1 summarizes the demographic characteristics of the 83 participants involved in the study. Overall, we examined 41 eyes from 41 healthy controls (age: mean (SD), 54.6 (12.5) years) and 42 eyes from 42 participants with severe NPDR (age: mean (SD), 52.3 (8.7) years). No notable disparities were noted in terms of sex, axial length, BMI, smoking status, blood pressure, or IOP ($p > 0.05$), although the BCVA of the healthy control group (logMAR 0.02 (0.05)) was better than that of the severe NPDR group (LogMAR 0.26 (0.25)) ($p < 0.05$).

Table 2 shows the comparisons between the thickness of the retinal layers (CMT and sublayers) and choroid thickness. In the severe NPDR group, the inner retinal thickness was significantly thinner than that in the healthy control group (107.10 (4.96) vs. 116.0 (4.99), respectively, $p < 0.05$); conversely, the severe NPDR group had a thicker CMT than the healthy control group (277.4 (73.6) vs. 253.5 (18.9)). Furthermore, no significant difference was observed in the intermediate retinal thickness between the two groups (72.00 (10.05) vs. 71.44 (6.18), $p > 0.05$). The severe NPDR group had a thinner choroid than the healthy control group (429.9 (65.7) vs. 464.5 (71.0)).

We further compared the VD and FAZ parameters between the healthy control and severe NPDR groups (Table 2; Figure 1). Overall, the parafoveal VD of SCP and DCP in the severe NPDR group were significantly lower than that in the healthy control group ((28.05 (3.74) vs. 30.23 (2.72), $p < 0.05$, and 26.81 (2.57) vs. 29.30 (1.70), $p < 0.05$, respectively). Additionally, the severe NPDR group had a larger FAZ area and perimeter than the healthy control group (0.56 (0.22) vs. 0.37 (0.10), $p < 0.05$, and 2.84 (0.61) vs. 2.27 (0.30), $p < 0.05$, respectively). The acircularity index of the FAZ was 1.10 (0.07) in the severe NPDR group and 1.59 (0.03) in the healthy control group, with significant difference between the groups ($p < 0.05$).

A strong connection was found in the vascular density of the parafoveal SCP and the thickness of the inner retina in the healthy

TABLE 2 Results of parafoveal VD, FAZ, parafoveal RT, and CT in the two groups.

| Characteristic | Means ± SD | Healthy control (n=41) | Severe NPDR patients (n=42) | p value |
|----------------|---------------------------|------------------------|-----------------------------|---------|
| VD | SCP | 30.23 ± 2.72 | 28.05 ± 3.74 | 0.003 |
| | DCP | 29.30 ± 1.70 | 26.81 ± 2.57 | <0.001 |
| | CC | 64.20 ± 2.40 | 61.7 ± 4.2 | 0.001 |
| FAZ | Area, μm ² | 0.37 ± 0.10 | 0.56 ± 0.22 | <0.001 |
| | Perimeter, μm | 2.27 ± 0.30 | 2.84 ± 0.61 | <0.001 |
| | Acircularity index | 1.59 ± 0.03 | 1.10 ± 0.07 | 0.016 |
| RT | ILM-IPL | 116.0 ± 4.99 | 107.10 4.96 | <0.001 |
| | INL-OPL | 71.44 ± 6.18 | 72.00 10.05 | 0.761 |
| | Central macular thickness | 253.50 ± 18.90 | 277.40 ± 73.60 | 0.049 |
| CT | | 464.50 ± 71.00 | 429.9 ± 65.70 | 0.024 |

Values are expressed as mean ± SD.
CC, choroid capillary; CT, choroidal thickness; VD, vessel density; NPDR, non-proliferative diabetic retinopathy; FAZ, foveal vascular zone; RT, retinal thickness; SCP, superficial capillary plexus; DCP, deep capillary plexus; IPL, inner plexiform layer; ILM, internal limiting membrane; INL, inner nuclear layer; OPL, outer nuclear layer; SD, standard deviation.

control group ($r=0.67$, $p<0.001$; Figure 2A) and severe NPDR groups ($r=0.71$, $p<0.001$; Figure 2B). However, the VD of the parafoveal DCP was not significantly associated with intermediate retinal thickness ($p>0.05$; Figures 2C, D). Analysis of the correlation between choroidal thickness and capillary VD demonstrated negative correlations in both severe NPDR ($r=-0.70$, $p<0.001$; Figure 2E) and healthy control groups ($r=-0.76$, $p<0.001$; Figure 2F). Interestingly, we also found a positive correlation between the FAZ area and the SCP of the VD in the severe NPDR group ($r=0.55$, $p<0.000$; Figure 2G), but not in the healthy control group ($r=0.18$, $p>0.05$; Figure 2H).

4 Discussion

In this study, we examined variations in retinal or choroidal thickness and VD in participants with severe NPDR. We further explored the connection between VD in the retinal plexus or choriocapillaris and the corresponding thickness in the eyes of healthy participants and those with severe NPDR but without DME.

The effect of DM on retinal thickness has been validated in many studies, with results showing that DM affects the RNFL, GCL, and IPL in diabetic patients with (8, 9) or without DR (17). Our results showed that the inner retinal thickness decreased in the severe NPDR group. Kim et al. (18) reported that progressive damage to the mGCIPL affected the progression of patients with early stage DR. Simultaneously, researchers found that patients with DR had lower inner retinal thickness than controls (19). DR is an ischemic disease simultaneously affecting all retinal layers (10, 11). The central retinal vasculature supplied the inner retinal layer. DR causes microvascular dysfunction, leading to chronic retinal

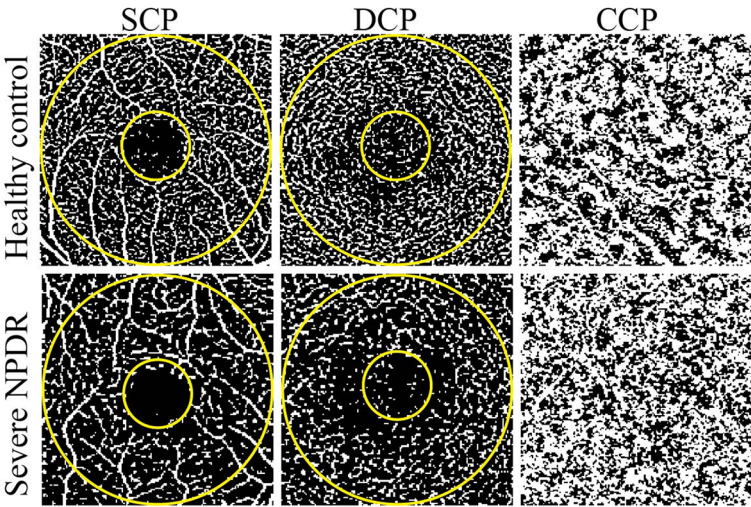


FIGURE 1 Representative OCTA images of healthy control and severe NPDR patients. The left, middle, and right represent OCTA images of the SCP, DCP, and CCP, respectively. The evaluated regions consisted of a circular area with a diameter of 1 mm at the center of the fovea and a donut-shaped area surrounding it, with diameters ranging from 1 to 3 mm.

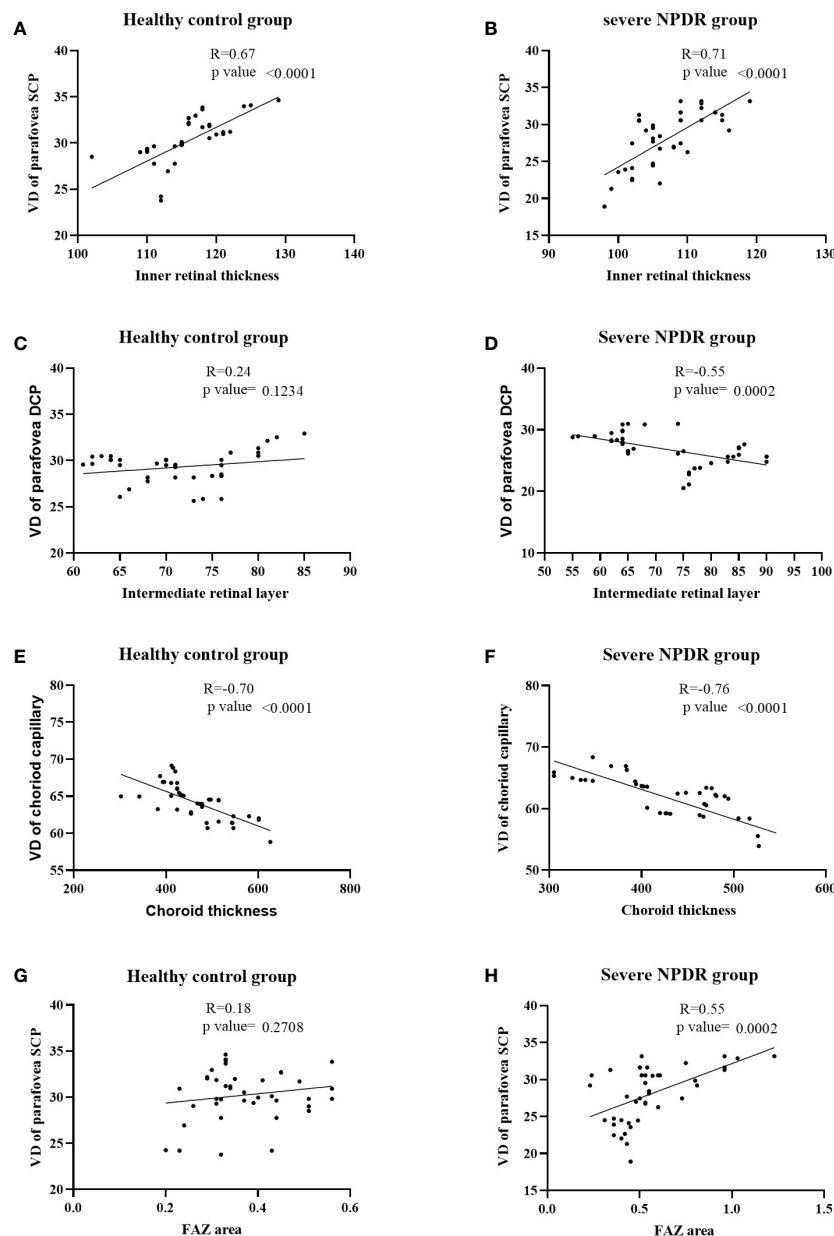


FIGURE 2

Correlations between vessel density and capillary plexuses. (A, B) Correlation between inner retinal thickness and VD of the parafoveal SCP in the healthy control and severe NPDR groups; (C, D) correlation between intermediate retinal thickness and VD of the parafoveal DCP in the healthy control and severe NPDR groups; (E, F) correlation between choroid thickness and VD of choroid capillaries in the healthy control and severe NPDR groups; (G, H) correlation between FAZ area and VD of the parafoveal SCP in the healthy control and severe NPDR groups. VD, vessel density; NPDR, non-proliferative diabetic retinopathy; FAZ, foveal vascular zone; SCP, superficial capillary plexus; DCP, deep capillary plexus.

ischemia. Structural damage to the inner retina is also considered an essential manifestation of DR, as DR causes damage or apoptosis in many cell types in the inner retina (20).

Several studies have reported larger FAZ areas and perimeters in patients with DM (6, 21). OCTA has allowed the capture of detailed images of patients with DM, enabling physicians to make advanced decisions and analysis. Changes in FAZ can be observed in patients with DM, although they do not show signs of DR (6). In our study, the severe NPDR group showed a tendency toward an expanded FAZ area compared to the healthy control group, which has been verified in many studies (6, 7). Although changes in the

FAZ area have been treated as a vital fundus indicator of early DR, they are also considered an essential parameter for measuring DR severity (22). Bresnick et al. (23) reported that FAZ enlargement is caused by capillary loss in the adjacent vessels. Moreover, the severity of microvascular changes and macular ischemia increases with DR progression (24). In addition, we found a positive correlation between the FAZ area and perimeter and retinal VD in the severe NPDR group, but not in the healthy control group. The enlargement of the FAZ area and perimeter is a manifestation of retinal hypoxia. Compared with other DR-related parameters such as VD, spacing between vessels, and perfusion density, the FAZ area

showed lower sensitivity and specificity (21). Based on our results, we believe that changes in the FAZ area, combined with other indicators such as VD, can be used to indicate DR severity.

Several studies have previously demonstrated a correlation between choroidal angiopathy and retinopathy in patients with DR (25, 26). Although indocyanine green angiography can be used to detect choroidal structure and function, OCTA provides real-time imaging with precise anatomical details and quantification of the choroid *in vivo*. In our study, patients with severe NPDR exhibited a thinner choroid than healthy controls and a decrease in CC was observed in the severe NPDR group. Mehreen et al. (27) reported a reduction in the CC of eyes with PDR and DME compared to controls. Regatieri et al. (25) also found that choroidal thickness is altered in diabetes, and may be related to the severity of retinopathy. Choi et al. (13) further found that microvascular abnormalities of the CC occurred in all DR stages. These findings are consistent with our results. In addition, our results showed that both healthy controls and patients with severe NPDR showed a negative correlation between the VD of the CC and choroidal thickness. In support of this, Schocket et al. (28) and Luttly et al. (29) found that the choriocapillaris in eyes with moderate-to-severe DR was closed, which could be the reason for the decrease in the VD of the CC and choroidal thickness. In our study, although only the entire thickness of the choroid and VD of the CC were measured, our findings of decreased choroidal thickness and VD of the CC are consistent with those of Mehreen et al. (27). Although the CC accounts for only 5–10% of the choroid membrane the CC layer accounts for (30), this layer of blood vessels may be involved in the pathological process of DR.

5 Limitations

In this project, we included only a limited number of eyes; thus, the study has limited power. Moreover, this was a retrospective study, and we did not obtain fundus data from patients with severe NPDR before DR occurred.

6 Conclusion

Our study demonstrated a decreasing tendency in retinal or choroidal thickness and VD in patients with severe NPDR, and further showed a correlation between VD and the corresponding thickness. DR affects both the retina and choroid. Our study elucidated the pathological characteristics of the ocular structure in patients with severe NPDR. Numerous OCTA parameters suggest an intrinsic correlation that may provide a new strategy for the pathogenesis and diagnosis of DR.

Data availability statement

The raw data supporting the conclusions of this article will be made available by the authors, without undue reservation.

Ethics statement

The studies involving humans were approved by the ethics committee at Tianjin Medical University. The studies were conducted in accordance with the local legislation and institutional requirements. The participants provided their written informed consent to participate in this study. Written informed consent was obtained from the individual(s) for the publication of any potentially identifiable images or data included in this article.

Author contributions

HY: Funding acquisition, Supervision, Validation, Writing – review & editing. KH: Data curation, Formal analysis, Investigation, Software, Writing – original draft. SW-Z: Data curation, Investigation, Software, Writing – original draft. ZL: Data curation, Investigation, Writing – original draft. PK: Data curation, Investigation, Writing – original draft. TY: Writing – original draft. ZS: Data curation, Investigation, Writing – original draft. WZ: Investigation, Supervision, Validation, Writing – review & editing.

Funding

The author(s) declare financial support was received for the research, authorship, and/or publication of this article. This study was funded by the National Key R&D Program of China (grant 2021YFC2401404) and the National Natural Science Foundation of China (grant 82330031).

Acknowledgments

We would like to thank all subjects participated in the present study.

Conflict of interest

The authors declare that the research was conducted in the absence of any commercial or financial relationships that could be construed as a potential conflict of interest.

Publisher's note

All claims expressed in this article are solely those of the authors and do not necessarily represent those of their affiliated organizations, or those of the publisher, the editors and the reviewers. Any product that may be evaluated in this article, or claim that may be made by its manufacturer, is not guaranteed or endorsed by the publisher.

References

- Cheung N, Mitchell P, Wong TY. Diabetic retinopathy. *Lancet (London England)*. (2010) 376:124–36. doi: 10.1016/S0140-6736(09)62124-3
- Early photocoagulation for diabetic retinopathy. ETDRS report number 9. Early Treatment Diabetic Retinopathy Study Research Group. *Ophthalmology*. (1991) 98:766–85. doi: 10.1016/S0161-6420(13)38011-7
- Wilkinson CP, Ferris FL 3rd, Klein RE, Lee PP, Agardh CD, Davis M, et al. Proposed international clinical diabetic retinopathy and diabetic macular edema disease severity scales. *Ophthalmology*. (2003) 110:1677–82. doi: 10.1016/S0161-6420(03)00475-5
- Khalid H, Schwartz R, Nicholson L, Huemer J, El-Bradey MH, Sim DA, et al. Widefield optical coherence tomography angiography for early detection and objective evaluation of proliferative diabetic retinopathy. *Br J Ophthalmol*. (2021) 105:118–23. doi: 10.1136/bjophthalmol-2019-315365
- Uchitomi D, Murakami T, Dodo Y, Yasukura S, Morino K, Uji A, et al. Disproportion of lamellar capillary non-perfusion in proliferative diabetic retinopathy on optical coherence tomography angiography. *Br J Ophthalmol*. (2020) 104:857–62. doi: 10.1136/bjophthalmol-2019-314743
- de Carlo TE, Chin AT, Bonini Filho MA, Adhi M, Branchini L, Salz DA, et al. Detection of microvascular changes in eyes of patients with diabetes but not clinical diabetic retinopathy using optical coherence tomography angiography. *Retina (Philadelphia Pa)*. (2015) 35:2364–70. doi: 10.1097/IAE.0000000000000882
- Takase N, Nozaki M, Kato A, Ozeki H, Yoshida M, Ogura Y. Enlargement of foveal avascular zone in diabetic eyes evaluated by en face optical coherence tomography angiography. *Retina (Philadelphia Pa)*. (2015) 35:2377–83. doi: 10.1097/IAE.0000000000000849
- Srinivasan S, Dehghani C, Pritchard N, Edwards K, Russell AW, Malik RA, et al. Corneal and retinal neuronal degeneration in early stages of diabetic retinopathy. *Invest Ophthalmol Visual Sci*. (2017) 58:6365–73. doi: 10.1167/iov.17-22736
- El-Fayoumi D, Badr Eldine NM, Esmail AF, Ghalwash D, Soliman HM. Retinal nerve fiber layer and ganglion cell complex thicknesses are reduced in children with type 1 diabetes with no evidence of vascular retinopathy. *Invest Ophthalmol Visual Sci*. (2016) 57:5355–60. doi: 10.1167/iov.16-19988
- Lavia C, Couturier A, Erginay A, Dupas B, Tadayoni R, Gaudric A. Reduced vessel density in the superficial and deep plexuses in diabetic retinopathy is associated with structural changes in corresponding retinal layers. *PloS One*. (2019) 14:e0219164. doi: 10.1371/journal.pone.0219164
- Wang X, Zhu Y, Xu H. Inverted multi-layer internal limiting membrane flap for macular hole retinal detachment in high myopia. *Sci Rep*. (2022) 12:10593. doi: 10.1038/s41598-022-14716-7
- Kim K, Kim ES, Yu SY. Optical coherence tomography angiography analysis of foveal microvascular changes and inner retinal layer thinning in patients with diabetes. *Br J Ophthalmol*. (2018) 102:1226–31. doi: 10.1136/bjophthalmol-2017-311149
- Choi W, Waheed NK, Moulton EM, Adhi M, Lee B, De Carlo T, et al. ultrahigh speed swept source optical coherence tomography angiography of retinal and choriocapillaris alterations in diabetic patients with and without retinopathy. *Retina (Philadelphia Pa)*. (2017) 37:11–21. doi: 10.1097/IAE.0000000000001250
- Chua J, Hu Q, Ke M, Tan B, Hong J, Yao X, et al. Retinal microvasculature dysfunction is associated with Alzheimer's disease and mild cognitive impairment. *Alzheimer's Res Ther*. (2020) 12:161. doi: 10.1186/s13195-020-00724-0
- Spaide RF. Choriocapillaris flow features follow a power law distribution: implications for characterization and mechanisms of disease progression. *Am J Ophthalmol*. (2016) 170:58–67. doi: 10.1016/j.ajo.2016.07.023
- Kim AY, Chu Z, Shahidzadeh A, Wang RK, Puliafito CA, Kashani AH. Quantifying microvascular density and morphology in diabetic retinopathy using spectral-domain optical coherence tomography angiography. *Invest Ophthalmol Visual Sci*. (2016) 57:362–70. doi: 10.1167/iov.15-18904
- Tavares Ferreira J, Proença R, Alves M, Dias-Santos A, Santos BO, Cunha JP, et al. Retina and choroid of diabetic patients without observed retinal vascular changes: A longitudinal study. *Am J Ophthalmol*. (2017) 176:15–25. doi: 10.1016/j.ajo.2016.12.023
- Kim K, Kim ES, Yu SY. Longitudinal relationship between retinal diabetic neurodegeneration and progression of diabetic retinopathy in patients with type 2 diabetes. *Am J Ophthalmol*. (2018) 196:165–72. doi: 10.1016/j.ajo.2018.08.053
- Srinivasan S, Pritchard N, Sampson GP, Edwards K, Vagenas D, Russell AW, et al. Retinal thickness profile of individuals with diabetes. *Ophthalmic Physiol optics: J Br Coll Ophthalmic Opticians (Optometrists)*. (2016) 36:158–66. doi: 10.1111/opo.12263
- King GL, Brownlee M. The cellular and molecular mechanisms of diabetic complications. *Endocrinol Metab Clinics North America*. (1996) 25:255–70. doi: 10.1016/S0889-8529(05)70324-8
- Bhanushali D, Anegondi N, Gadde SG, Srinivasan P, Chidambara L, Yadav NK, et al. Linking retinal microvasculature features with severity of diabetic retinopathy using optical coherence tomography angiography. *Invest Ophthalmol Visual Sci*. (2016) 57:519–25. doi: 10.1167/iov.15-18901
- Johannesen SK, Viken JN, Vergmann AS, Grauslund J. Optical coherence tomography angiography and microvascular changes in diabetic retinopathy: a systematic review. *Acta ophthalmologica*. (2019) 97:7–14. doi: 10.1111/aos.13859
- Bresnick GH, Condit R, Syrtala S, Palta M, Groo A, Korth K. Abnormalities of the foveal avascular zone in diabetic retinopathy. *Arch Ophthalmol (Chicago Ill: 1960)*. (1984) 102:1286–93. doi: 10.1001/archophth.1984.01040031036019
- Wu L, Fernandez-Loaiza P, Sauma J, Hernandez-Bogantes E, Masis M. Classification of diabetic retinopathy and diabetic macular edema. *World J Diabetes*. (2013) 4:290–4. doi: 10.4239/wjd.v4.i6.290
- Regatieri CV, Branchini L, Carmody J, Fujimoto JG, Duker JS. Choroidal thickness in patients with diabetic retinopathy analyzed by spectral-domain optical coherence tomography. *Retina (Philadelphia Pa)*. (2012) 32:563–8. doi: 10.1097/IAE.0B013E31822F5678
- Nagaoka T, Kitaya N, Sugawara R, Yokota H, Mori F, Hikichi T, et al. Alteration of choroidal circulation in the foveal region in patients with type 2 diabetes. *Br J Ophthalmol*. (2004) 88:1060–3. doi: 10.1136/bjo.2003.035345
- Adhi M, Brewer E, Waheed NK, Duker JS. Analysis of morphological features and vascular layers of choroid in diabetic retinopathy using spectral-domain optical coherence tomography. *JAMA Ophthalmol*. (2013) 131:1267–74. doi: 10.1001/jamaophthalmol.2013.4321
- Schocket LS, Brucker AJ, Niknam RM, Grunwald JE, DuPont J, Brucker AJ. Foveolar choroidal hemodynamics in proliferative diabetic retinopathy. *Int Ophthalmol*. (2004) 25:89–94. doi: 10.1023/B:INTE.0000031744.93778.60
- Lutty GA, Cao J, McLeod DS. Relationship of polymorphonuclear leukocytes to capillary dropout in the human diabetic choroid. *Am J Pathol*. (1997) 151:707–14.
- Ramrattan RS, van der Schaft TL, Mooy CM, de Bruijn WC, Mulder PG, de Jong PT. Morphometric analysis of Bruch's membrane, the choriocapillaris, and the choroid in aging. *Invest Ophthalmol Visual Sci*. (1994) 35:2857–64.



OPEN ACCESS

EDITED BY

Mohd Imtiaz Nawaz,
King Saud University, Saudi Arabia

REVIEWED BY

Navneet Mehrotra,
Retina Foundation and Retina Care, India
Haoyu Li,
Central South University, China
Josh J. Wang,
University at Buffalo, United States
Qing Peng,
Tongji University, China

*CORRESPONDENCE

Wei Jin

✉ rm001566@whu.edu.cn

Yiqiao Xing

✉ yiqiao_xing57@whu.edu.cn

RECEIVED 02 January 2024

ACCEPTED 23 May 2024

PUBLISHED 12 June 2024

CITATION

Guo X, Jin W and Xing Y (2024) Levels of asymmetric dimethylarginine in plasma and aqueous humor: a key risk factor for the severity of fibrovascular proliferation in proliferative diabetic retinopathy. *Front. Endocrinol.* 15:1364609. doi: 10.3389/fendo.2024.1364609

COPYRIGHT

© 2024 Guo, Jin and Xing. This is an open-access article distributed under the terms of the [Creative Commons Attribution License \(CC BY\)](#). The use, distribution or reproduction in other forums is permitted, provided the original author(s) and the copyright owner(s) are credited and that the original publication in this journal is cited, in accordance with accepted academic practice. No use, distribution or reproduction is permitted which does not comply with these terms.

Levels of asymmetric dimethylarginine in plasma and aqueous humor: a key risk factor for the severity of fibrovascular proliferation in proliferative diabetic retinopathy

Xinyang Guo, Wei Jin* and Yiqiao Xing*

Eye Center, Renmin Hospital of Wuhan University, Wuhan, Hubei, China

Introduction: Proliferative diabetic retinopathy (PDR) is a common diabetes complication, significantly impacting vision and quality of life. Previous studies have suggested a potential link between arginine pathway metabolites and diabetic retinopathy (DR). Connective tissue growth factor (CTGF) plays a role in the occurrence and development of fibrovascular proliferation (FVP) in PDR patients. However, the relationship between arginine pathway metabolites and FVP in PDR remains undefined. This study aimed to explore the correlation between four arginine pathway metabolites (arginine, asymmetric dimethylarginine[ADMA], ornithine, and citrulline) and the severity of FVP in PDR patients.

Methods: In this study, plasma and aqueous humor samples were respectively collected from 30 patients with age-related cataracts without diabetes mellitus (DM) and from 85 PDR patients. The PDR patients were categorized as mild-to-moderate or severe based on the severity of fundal FVP. The study used Kruskal-Wallis test to compare arginine, ADMA, ornithine, and citrulline levels across three groups. Binary logistic regression identified risk factors for severe PDR. Spearman correlation analysis assessed associations between plasma and aqueous humor metabolite levels, and between ADMA and CTGF levels in aqueous humor among PDR patients.

Results: ADMA levels in the aqueous humor were significantly greater in patients with severe PDR than in those with mild-to-moderate PDR ($P=0.0004$). However, the plasma and aqueous humor levels of arginine, ornithine, and citrulline did not significantly differ between mild-to-moderate PDR patients and severe PDR patients ($P>0.05$). Binary logistic regression analysis indicated that the plasma ($P=0.01$) and aqueous humor ($P=0.006$) ADMA levels in PDR patients were risk factors for severe PDR. Furthermore, significant correlations were found between plasma and aqueous humor ADMA levels ($r=0.263$, $P=0.015$) and between aqueous humor ADMA and CTGF levels ($r=0.837$, $P<0.001$).

Conclusion: Elevated ADMA levels in plasma and aqueous humor positively correlate with the severity of FVP in PDR, indicating ADMA as a risk factor for severe PDR.

KEYWORDS

diabetic retinopathy, fibrovascular proliferation, asymmetric dimethylarginine, targeted metabolomics, plasma, aqueous humor

1 Introduction

With the global prevalence of diabetes on the rise, the incidence of diabetic retinopathy (DR) is also increasing (1). Recent research has revealed a greater incidence of DR in Asian countries than in Western countries (2). Among DR cases, vision-threatening diabetic retinopathy (VTDR) accounts for approximately 10% of cases (2). Proliferative diabetic retinopathy (PDR) is a significant category of VTDR and serves as a crucial cause of visual impairment and potential blindness in working-age diabetic patients. The prognosis of patients with PDR can vary due to the extent of fibrovascular proliferation (FVP) in the fundus. PDR with severe FVP often leads to retinal detachment, while PDR patients with simple vitreous hemorrhage generally have a better prognosis than those with retinal detachment due to severe FVP (3, 4). Moreover, young patients with PDR are more susceptible to severe FVP, resulting in a poorer visual prognosis (5). This condition significantly impacts their quality of life and ability to work, emphasizing the need for extensive attention and care.

Research has demonstrated that the degree of FVP in PDR patients is associated with factors such as renal dysfunction, age, duration of DR, hypertension, and smoking history (6). Furthermore, connective tissue growth factor (CTGF) plays a role in the progression of retinal fibrosis and is a positive correlation with the severity of fundus FVP in patients with DR (7). However, while these risk factors provide some insight, they fail to fully explain the underlying causes and molecular mechanisms involved in the varying degrees of FVP in PDR patients. Therefore, further investigations are necessary to explore the specific bioactive molecules responsible for promoting FVP in the eyes of PDR patients.

In recent years, metabolomics studies have revealed significant upregulation of arginine pathway metabolites in the plasma and aqueous humor of patients with DR, and these metabolites are correlated with the severity of DR (8–10). Research has shown that arginine metabolism promotes skeletal muscle and cardiac fibrosis in patients with muscular dystrophy (11). Additionally, arginine methylation plays a role in regulating epithelial-mesenchymal transition (12). Protein arginine methyltransferase has been shown to promote the progression of fibrosis in conditions such as diabetic nephropathy, idiopathic pulmonary fibrosis, and liver cirrhosis (13). However, the associations between arginine pathway

metabolites and fundal FVP in patients with PDR have not been established. Therefore, this study aimed to investigate the correlation between specific arginine pathway metabolites (L-arginine, ADMA, L-ornithine, and L-citrulline) and the severity of FVP in PDR patients, providing valuable insights into the early warning of intraocular FVP in cases of severe PDR.

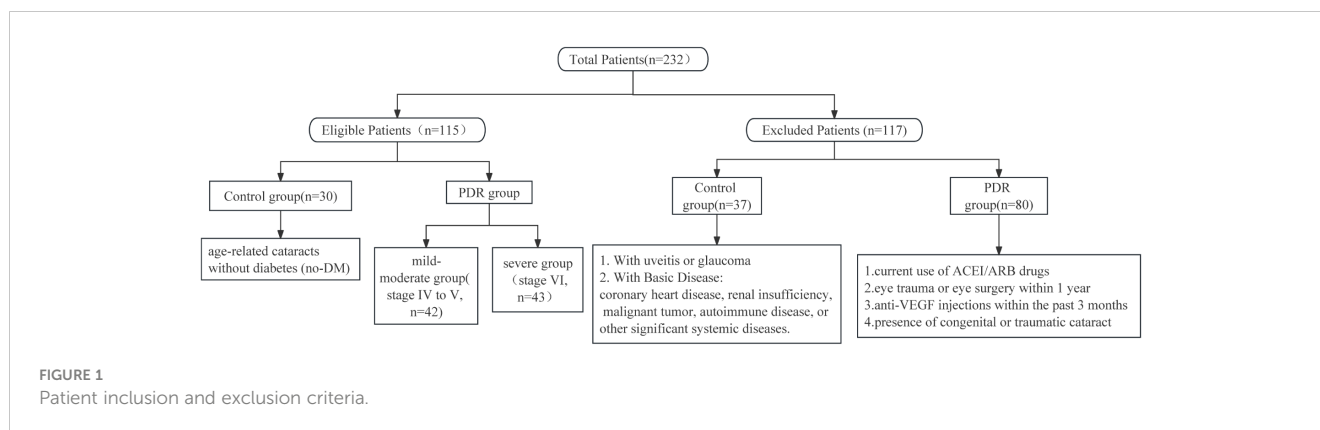
2 Methods

2.1 Ethical statement

The retrospective cross-sectional study involving human participants conducted in this research has undergone thorough review and approval by the Clinical Research Ethics Committee of Renmin Hospital of Wuhan University (WDRY2023-K083). This study strictly adhered to the principles outlined in the Declaration of Helsinki and followed international ethical guidelines, including the Measures for the Ethical Review of Biomedical Research Involving Humans, as well as relevant domestic laws and regulations. The patients provided their written informed consent to participate in this study.

2.2 Patient recruitment

This study randomly recruited a total of 232 patients, aged between 18 and 79 years, from the Eye Center of Renmin Hospital of Wuhan University, during the period from January to July 2023. The inclusion criteria for the PDR group involved meeting the diagnostic criteria for PDR according to the latest guidelines, and additionally, participants needed to exhibit varying degrees of fibrovascular proliferation in the fundus. Patients in the PDR group meeting any of the following criteria were excluded from this study: current use of angiotension converting enzyme inhibitors/angiotensin II receptor blockers (ACEI/ARB), a history of ocular trauma or eye surgery within the past year, or recent use of intravitreal anti-VEGF drug injections within the last 3 months (Figure 1). The inclusion criteria for the control group were defined as patients with age-related cataracts without concurrent diabetes mellitus (DM). Patients in the control group meeting any of the following criteria were excluded: congenital cataract, traumatic



cataract, age-related cataract with uveitis or glaucoma, coronary heart disease, renal insufficiency, malignant tumor, autoimmune disease, and other serious systemic underlying diseases. A total of 115 patients were ultimately included in the study, comprising 85 patients in the PDR group and 30 patients in the control group. To clarify whether the sample size included in the study meets statistical requirements, we conducted a sample size analysis using PASS 2021. Based on preliminary results, the relevant abundance mean of aqueous humor ADMA in the control group was 1, while in the mild PDR group, it was 1.9 with a standard deviation of 0.82, and in the severe PDR group, it was 2.7 with a standard deviation of 0.82. With a two-sided α of 0.05 and a test power ($1-\beta$) of 90%, utilizing Kruskal-Wallis Tests (Simulate), we calculated that each group requires a minimum of 8 subjects, totaling at least 24 subjects. Clinical data collection included gender, age, blood pressure, complications, hemoglobin A1C (HbA1C), and relevant blood biochemistry indicators.

2.3 PDR severity grading

In alignment with the 2019 International Classification of DR by the American Academy of Ophthalmology (14), this study refined the stratification of proliferative diabetic retinopathy (PDR) stages based on the severity of fundal FVP. This was accomplished by referencing the DR grading standard established in 1984 by the Chinese Medical Association. DR was divided into six stages, and PDR corresponded to stages IV-V, which included the early proliferative stage (stage IV), fibroproliferative stage (stage V), and late proliferative stage (stage VI). Neovascularization of the retina (NVE) and neovascularization of the disc (NVD) occur in stage IV (early proliferative stage). Stage V (the fibroproliferative stage) is characterized by the presence of fibrous membranes, which may be accompanied by preretinal or vitreous hemorrhage. In stage VI (the late proliferative stage), traction retinal detachment with a fibrovascular membrane is observed. In this study, the severity of proliferation in PDR patients was evaluated through preoperative fundus ultra-wide-field fundus photography and intraoperative microscopic findings. Based on the aforementioned criteria, PDR patients were classified into two groups: the mild-to-moderate group comprising stages IV to V, and the severe group consisting of stage VI.

2.4 Sample collection

After informed consent was obtained from the patients, fasting whole-blood samples were collected from them using EDTA-containing anticoagulant tubes. The blood was immediately centrifuged at 4500 rpm and 4°C for 15 min, and the resulting supernatant was carefully divided into cryopreservation tubes. After the tubes were briefly exposed to liquid nitrogen for 5 min, they were stored at -80°C. During the surgery, approximately 150 μ L of aqueous humor was collected from one eye in the PDR group. In the control group, approximately 150 μ L of aqueous humor was collected from one eye with a cataract. The aqueous humor samples were then transferred to cryopreservation tubes and rapidly frozen in liquid nitrogen for 5 min before being stored at -80°C for preservation. The interval between the collection of plasma and aqueous humor sample collection was within 2 hours.

2.5 Target metabolite UPLC-MS/MS analysis

Two hundred microliters of acetonitrile containing the internal standard was added to 100 μ L of plasma or aqueous humor. The mixture was vortexed for 30 seconds. The mixture was subsequently centrifuged at 13000 rpm for 15 min at 4°C, after which the supernatant was transferred to a clean tube and dried using a SpeedVac (Labconco, USA). The dried extract was redissolved in 80% acetonitrile and analyzed via ultra-performance liquid chromatography with tandem mass spectrometry (UPLC-MS/MS) conducted on a Waters Acquity UPLC-system coupled with a 5500 QTRAP system (SCIEX). Chromatographic separation was achieved on a Waters Acquity UPLC BEH Amide Column (2.1 mm \times 100 mm, 1.7 μ m, Waters) using a flow rate of 0.3 mL/min at 40°C during an 8 min gradient (0–0.5 min 20% A, 0.5–2 min 20%–80% A, 2–6.5 min 80% A, 6.5–8 min 80%–20% A) using buffer A (5 mM ammonium formate and 0.1% (v/v) formic acid in water) and buffer B (0.1% (v/v) formic acid in acetonitrile).

Mass spectrometry was performed in positive mode with an electrospray source voltage set to 5000 V. The analytes were monitored in multiple reaction monitoring (MRM) mode using precursor-to-product ion transitions of m/z 175.2 \rightarrow 70.0 for arginine, m/z 203.2 \rightarrow 70.0 for ADMA, m/z 176.1 \rightarrow 159.0

for citrulline, m/z 133.1 \rightarrow 70.2 for ornithine and m/z 185.1 \rightarrow 75.0 for arginine-13C6 and 15N4 (IS). The collision energies were 30.0 eV for arginine, 40 eV for ADMA, 15 eV for citrulline, 15 eV for ornithine, and 33.5 eV for IS. Peak determination and area integration were performed using Analyst 1.7.1 (SCIEX) and SCIEX OS1.4.0 software (SCIEX).

2.6 ELISA for CTGF analysis

Detection of CTGF was performed using human-specific ELISA kits (UpingBio, SYP-H0225). In the experiment, wells were designated for standard samples, sample dilution, blanks, and test samples. Standard wells received 50 μ L of standards at different concentrations, sample dilution wells received 50 μ L of sample dilution fluids, blank wells remained empty, and test sample wells received 50 μ L of the samples to be tested. Subsequently, 100 μ L of biotinylated antibody was added to each well and incubated at 37°C for 60 minutes. After washing the plate and patting it dry on absorbent paper, this process was repeated five times. Next, each well received 100 μ L of HRP-conjugated avidin and was incubated at 37°C for 20 minutes. After another five washes, all wells were loaded with 100 μ L of substrate mixture and incubated at 37°C for 15 minutes. Finally, 50 μ L of stop solution was added to each well, and the absorbance (OD values) of each well was read at 450 nm wavelength using an ELISA reader.

2.7 Statistical analysis

The statistical analysis was conducted using SPSS 27.0 software. The normality of the measurement data was assessed using the Shapiro Wilk test. For normally distributed data, the mean \pm standard deviation was used for representation, and the independent sample t test was used for comparing two groups. Non-normally distributed data are represented herein as medians and quartiles. Comparisons between two groups were conducted using the Mann-Whitney U test, while comparisons between three groups were performed using the Kruskal-Wallis test. Categorical data were analyzed using the chi-square test or continuity-corrected chi-square test. Multivariable binary logistic regression was employed for the analysis of risk factors. The correlation analysis was performed using Spearman correlation tests. Using GraphPad Prism 9.0 mapping software, outliers were identified as data points with relevant abundance values outside the 5–95th percentile of metabolite quantification.

3 Results

3.1 Demographic data

This study involved a total of 115 subjects, with 85 individuals in the PDR group and 30 in the group of age-related cataract patients without a history of diabetes. The number and reasons for excluded patients are shown in Figure 1. Table 1 presents the clinical data of

TABLE 1 Demographic data between PDR patients and nondiabetic patients.

| Variables | Non-diabetes | PDR patients | P-Value |
|-------------------|------------------|------------------|----------|
| Sex (% male) | 46.67 | 51.76 | 0.076 |
| Age | 63.80 \pm 8.23 | 52.94 \pm 9.47 | <0.001** |
| SBP (mmHg) | 132 \pm 18 | 137 \pm 20 | 0.238 |
| DBP (mmHg) | 71 \pm 10 | 72 \pm 10 | 0.463 |
| Cr (μ mol/L) | 66 (52,78) | 71(62,89) | 0.102 |
| TCh (mmol/L) | 4.60 \pm 1.11 | 4.65 \pm 0.92 | 0.824 |
| TG(mmol/L) | 1.27 \pm 0.38 | 1.38 \pm 0.57 | 0.319 |

The study groups were compared based on their demographics and comorbidities. To compare the differences between the two groups, A two-sample t tests were used for age, SBP, DBP, TCh, and TG, with the means and standard deviations presented. The Wilcoxon rank sum test was performed for creatinine levels, with the median and interquartile range presented. The chi-squared test was used to compare sex differences. SBP, systolic blood pressure; DBP, diastolic blood pressure; Cr, creatinine; TCh, total cholesterol; TG, triglyceride, ** represents $P < 0.01$.

these subjects. The analysis revealed no significant differences in terms of sex ($P=0.076$), blood pressure (SBP, $P=0.238$; DBP, $P=0.463$), serum creatinine levels ($P=0.102$), or lipid levels (TCh, $P=0.824$; TG, $P=0.319$) between the PDR group and the control group. The age of the individuals in the control group was significantly greater than that of the individuals in the PDR group ($P < 0.001$).

The PDR group was categorized based on the severity of FVP into two subgroups: mild-to-moderate PDR (42 patients) and severe PDR (43 patients). Table 2 presents the clinical data of these subjects. Age ($P=0.333$), sex ($P=0.829$), HbA1c levels ($P=0.512$), and history of hypertension ($P=0.229$) or diabetic nephropathy (DN) ($P=0.052$) did not significantly differ between the mild-to-

TABLE 2 Demographic data between patients with mild-to-moderate PDR and patients with severe PDR.

| Variables | Mild-to-Moderate Diabetes | Severe Diabetes | P Value |
|---------------------|---------------------------|------------------|---------|
| Sex (% male) | 52.38 | 53.49 | 0.829 |
| Age | 53.95 \pm 9.93 | 51.95 \pm 9.00 | 0.333 |
| HbA1c (%) | 8.01 \pm 1.91 | 8.28 \pm 1.76 | 0.512 |
| DM Duration (years) | 12.93 \pm 3.142 | 10.37 \pm 4.39 | 0.003** |
| Cr | 70(62,73) | 73(67,92) | 0.032* |
| HTN | 40.48% | 53.49% | 0.229 |
| DN | 2.38% | 13.95% | 0.052 |

The DR group was divided into mild-to-moderate and severe subgroups based on the severity of PDR. The two subgroups were compared in terms of their demographics and comorbidities. A two-sample t test was used to compare the differences between the subgroups in terms of age, HbA1c level, and duration of diabetes, and the means and standard deviations are presented. The Wilcoxon rank sum test was used to compare the differences in creatinine levels between the two subgroups, and the medians and interquartile ranges are presented. The chi-square test was used to compare sex and comorbidities. HbA1c, glycated hemoglobin A1c; Cr, creatinine; HTN, hypertension; DN, diabetic nephropathy. * represents $P < 0.05$, ** represents $P < 0.01$.

moderate PDR and severe PDR groups. However, significant differences were observed in the duration of diabetes ($P=0.003$) and serum creatinine levels ($P=0.032$). The mild-to-moderate PDR group had a longer duration of diabetes and lower serum creatinine levels than did the severe PDR group. This implies a potential correlation between the duration of diabetes and the severity of PDR. Furthermore, the significant difference in creatinine levels indicates that patients in the severe PDR group exhibit a decline in kidney function compared to those in the mild to moderate PDR group.

3.2 Comparison of the levels of four metabolites

To investigate the differences in these four metabolites among nondiabetic individuals and those with varying severities of PDR, we analyzed the metabolite levels in three distinct patient groups (Figure 2). The plasma levels of ADMA in the mild-to-moderate and severe PDR groups were both significantly greater than those in the nondiabetic group ($P<0.001$). The levels of arginine, ADMA, ornithine, and citrulline in the aqueous humor of the severe PDR group were significantly greater than those in the nondiabetic group

($P=0.0086$, $P<0.0001$; $P<0.0001$; $P=0.0002$). Notably, only the ADMA level in the aqueous humor differed between the mild-to-moderate PDR group and the severe PDR group, with the ADMA level in the severe PDR group being significantly greater than that in the mild-to-moderate PDR group ($P=0.0004$). However, no significant differences were observed in the levels of arginine, ornithine, or citrulline in the aqueous humor between the mild-to-moderate PDR group and the severe PDR group ($P>0.05$).

3.3 Assessment of the correlation of metabolite levels between plasma and aqueous humor in the PDR group

To explore whether the trends in metabolite levels in aqueous humor and plasma are consistent, this study assessed the correlation of the levels of these four metabolites between plasma and aqueous humor (Figure 3). Correlation analysis revealed significant correlations between plasma ADMA levels and aqueous humor ($r=0.263$, $P<0.015$) and between plasma citrulline levels and aqueous humor ($r=0.356$, $P<0.001$). However, we did not observe a significant correlation between the levels of arginine ($P=0.285$) in plasma or aqueous humor or between the levels of ornithine ($P=$

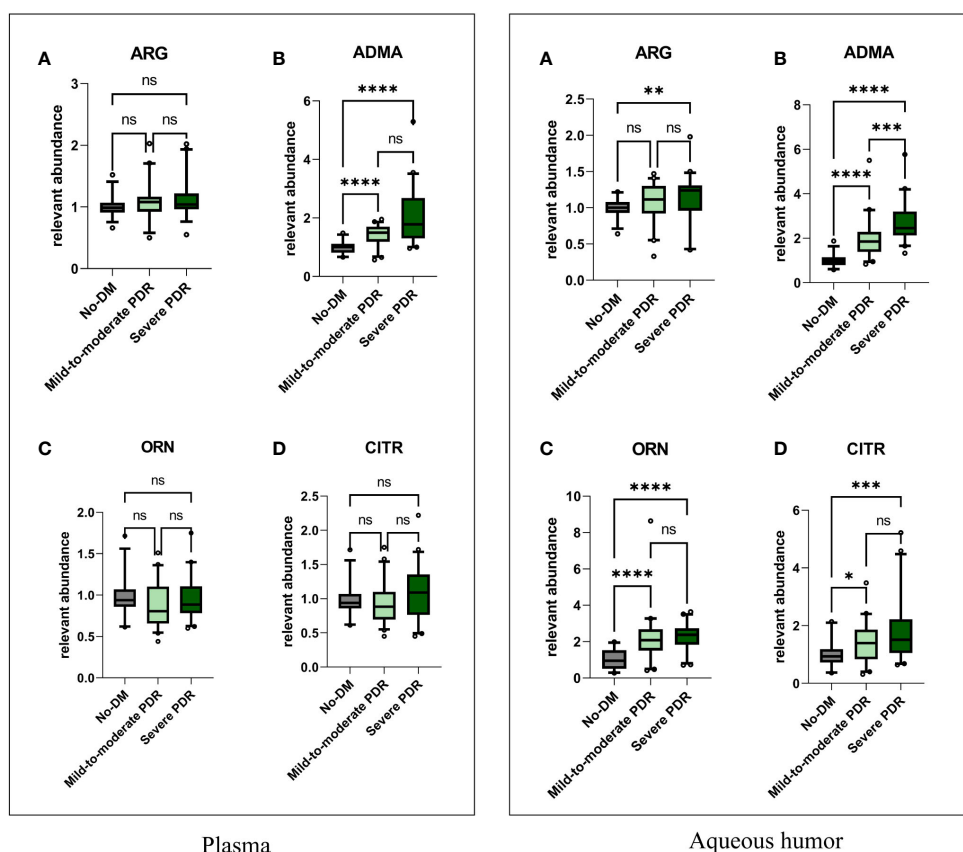


FIGURE 2

The comparisons of plasma and aqueous humor metabolite levels. In the plasma, Figures (A–D) respectively represent the comparison of plasma levels of arginine, ADMA, ornithine, and citrulline among the three groups. In the aqueous humor, Figures (A–D) respectively represent the comparison of aqueous humor levels of arginine, ADMA, ornithine, and citrulline among the three groups. Comparisons between groups were performed using the Kruskal Wallis test. No-DM represents nondiabetic patients. * represents $P<0.05$, ** represents $P<0.01$, *** represents $P<0.001$, and **** represents $P<0.0001$, ns represents $P>0.05$.

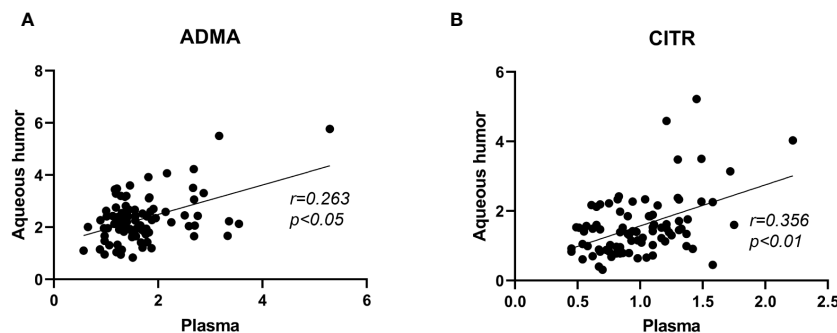


FIGURE 3

Correlation analysis of ADMA and citrulline levels between plasma and aqueous humor samples in PDR patients. Figure (A) represents the correlation analysis of ADMA levels between plasma and aqueous humor. Figure (B) represents the correlation analysis of citrulline levels between plasma and aqueous humor. The correlation analysis was performed using Spearman correlation tests.

0.162) in plasma and aqueous humor (Supplementary Figure 1). Additionally, a significant correlation was found between ADMA and citrulline levels in the plasma ($r=0.469$, $P<0.001$) and in the aqueous humor ($r=0.475$, $P<0.001$; Supplementary Figure 2).

3.4 Binary logistic regression analysis

To further assess whether ADMA levels serve as risk factors for the severity of FVP in PDR patients, we conducted a multivariable binary logistic regression analysis while adjusting for confounding factors such as diabetes duration, HbA1c level, and serum creatinine value (as presented in Table 3). The odds ratio (OR) for plasma ADMA levels was 4.139, with a 95% confidence interval (CI) of 1.402 to 12.214 ($P=0.010$), and the OR for aqueous humor ADMA levels was 3.165, with a 95% CI of 1.402 to 7.148 ($P=0.006$).

3.5 The relationship between the ADMA levels and connective tissue growth factor in the aqueous humor

To further explore the connection between ADMA and the extent of fibrosis in PDR, we conducted a detailed analysis of the correlation between ADMA levels and CTGF in the aqueous humor (Figure 4). Our research findings revealed a positive correlation between the levels of ADMA and CTGF in the aqueous humor ($r=0.837$, $P<0.01$).

TABLE 3 Logistic regression analysis of mild-to-moderate versus severe PDR.

| Variables | OR | CI | P-Value |
|--------------------|-------|--------------|---------|
| Plasma-ADMA | 4.139 | 1.402–12.214 | 0.010* |
| Aqueous humor-ADMA | 3.165 | 1.402–7.148 | 0.006** |

Binary logistic regression analysis was performed with severe PDR as the outcome. The odds ratio is per 1 unit increase in plasma or aqueous humor. * represents $P<0.05$, ** represents $P<0.01$.

4 Discussion

This study aims to investigate the correlation between four arginine pathway metabolites (arginine, ADMA, ornithine, and citrulline) and the severity of FVP in PDR patients. Initially, we analyzed the differences in these metabolites among PDR patients with varying degrees of FVP. Significant differences were observed in the levels of ADMA in the aqueous humor among PDR patients with different severity levels of FVP. Subsequently, we observed a consistent trend in the changes of ADMA levels in both plasma and aqueous humor. Through further analysis, we confirmed ADMA as a risk factor for FVP in PDR patients. Finally, we also found a significant correlation between ADMA in the aqueous humor and CTGF, further indicating the crucial role of ADMA in the occurrence and development of FVP in PDR patients.

In recent years, there has been a notable increase in the occurrence and prevalence of type 2 diabetes mellitus among young individuals (15). Studies suggest that early-onset Type 2 diabetes patients are more likely to develop PDR compared to those

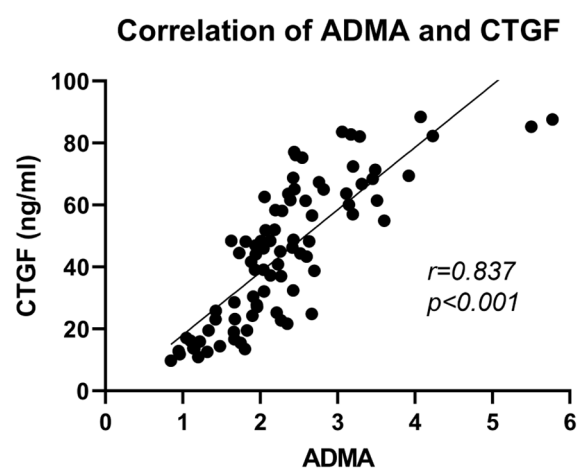


FIGURE 4

Correlation analysis of ADMA and CTGF in the aqueous humor among PDR patients. The correlation analysis was performed using Spearman correlation tests.

with late-onset diabetes (16, 17). A study from Beixinjing found that the incidence of DR significantly increases in patients with diabetes duration of less than 10 years, while it decreases in those with a duration of over 10 years (18). Additionally, younger PDR patients are at higher risk of severe FVP compared to older patients (5). This indicates that individuals diagnosed with diabetes at a younger age are at a higher risk of rapidly developing severe PDR. In this study, we observed that the duration of diabetes in patients with mild-to-moderate PDR was significantly longer than in those with severe PDR. This phenomenon may be attributed to the younger age of onset of diabetes among some PDR patients in this study, leading them to progress to severe PDR within a short period of time. Therefore, early diagnosis and management of diabetes are crucial for preventing the occurrence of severe PDR.

In this study, we utilized age-related cataract patients as the baseline control group and employed their metabolic levels as a reference for the relative quantification of metabolites in the PDR group. However, we observed that age-related cataract patients typically tend to be older compared to PDR patients in clinical settings. Therefore, there is a significant age difference between the control and PDR groups in this study.

Our study observed differences in arginine metabolite levels between the control and PDR groups, which may be age-related. However, our study primarily focused on differences in metabolite levels among PDR patients with varying degrees of severity. There was no statistically significant difference in age between the mild-to-moderate and the severe PDR group. This indicates that age did not influence the comparison of metabolite levels between the mild-to-moderate and severe PDR groups.

In this study, we found that there was no statistically significant difference in ADMA levels in plasma samples between patients with mild-moderate and severe PDR. However, in aqueous humor samples, the ADMA levels in severe PDR patients were significantly higher than those in mild-moderate PDR patients. This suggests that the association between ADMA levels and the severity of FVP in PDR patients is more closely linked in the aqueous humor compared to plasma. This may be attributed to the aqueous humor being an intraocular fluid, providing a more sensitive reflection of metabolic changes within the eye.

Although our results indicate that ADMA levels in plasma do not significantly differ between mild-to-moderate and severe PDR patients, our correlation analysis between aqueous humor and plasma reveals a significant correlation in ADMA levels between these two compartments (Figure 3). This suggests a consistent trend in the changes of ADMA levels in both aqueous humor and plasma, potentially related to aqueous humor circulation. Aqueous humor is generated by the ciliary process and flows into the anterior chamber through the pupil. Subsequently, it traverses the trabecular meshwork, enters the scleral venous system, and eventually enters the systemic circulation (19). The aqueous humor circulation process serves as a pathway for the exchange of substances between intraocular and systemic circulation. Therefore, ADMA within the eye can enter the systemic circulation through the aqueous humor, leading to corresponding changes in ADMA levels in the plasma. Monitoring ADMA levels in the plasma can, to some extent, reflect changes in intraocular ADMA levels.

The ADMA level in the aqueous humor is elevated in severe PDR patients compared to those with mild-to-moderate PDR, suggesting a strong association between ADMA and FVP in PDR patients. Considering the correlation between metabolite levels and patients' renal function (20), we incorporated blood creatinine levels and other potential confounding factors, including diabetes duration and HbA1c, into our multivariate binary logistic regression analysis. The results reveal that elevated plasma and aqueous humor ADMA levels were identified as risk factors for FVP in PDR patients. As the level of ADMA increased, the risk of severe FVP in PDR patients also increased. This implies a positive correlation between ADMA levels and the severity of FVP in PDR patients.

ADMA, an endogenous inhibitor of nitric oxide synthase (NOS), plays a crucial role in inhibiting the production of nitric oxide (NO) (21). In a high glucose environment, the production of ADMA increases while its degradation decreases (22). Elevated ADMA levels, by competitively binding with L-arginine for the active site of NOS, can impede the synthesis of NO, leading to endothelial dysfunction and tissue ischemia and hypoxia (23–25). Tissue hypoxia triggers the upregulation of hypoxia-inducible factor (HIF), activating multiple fibrosis signaling pathways (26). Furthermore, ADMA can induce epithelial/endothelial cell-mesenchymal transition (EMT/EndMT), resulting in the increased generation of myofibroblasts (27). A previous study has also revealed a correlation between the polymorphism of the protein arginine methyltransferase (PRMT1) gene and an increased incidence of PDR (28). PRMT1 is a crucial enzyme involved in ADMA synthesis, highlighting the close association between elevated ADMA levels and PDR. The severity of PDR is closely associated with the FVP in the fundus. Patients with severe PDR typically exhibit a substantial amount of FVP in the fundus. The fibroproliferative membrane formed by FVP can generate tension, further stretching the retina and inducing retinal detachment. ADMA plays a significant role in fostering tissue fibrosis. This may explain why ADMA functions as a risk factor for the severity of FVP in PDR. Further studies are needed to validate and explore the underlying molecular mechanisms involved.

These findings are consistent with the results of previous studies, such as that conducted by Abhary et al., which also reported elevated plasma ADMA levels among individuals with severe DR (29). Similarly, Peters et al. discovered that the plasma ADMA level was notably elevated in PDR patients compared to that in NPDR patients (30). Moreover, previous research has shown that levels of ADMA in the aqueous humor of individuals with severe PDR are significantly higher than those in individuals without diabetes (31). This suggests a crucial role for ADMA in both the occurrence and progression of DR. Nonetheless, earlier research has not established a significant correlation between ADMA levels in plasma and aqueous humor, which might be attributed to variations in detection techniques (31). In our study, we employed UPLC-MS/MS to increase the sensitivity of detection (32). Building on prior research, our study revealed the association between ADMA and the severity of FVP in PDR patients. This provides new insights into the early warning of intraocular FVP in cases of severe PDR.

CTGF plays an important role in basement membrane thickening, extracellular matrix synthesis, angiogenesis, and

fibrosis and is emerging as a crucial biomarker for assessing the extent of ocular fundus fibrosis (33, 34). Our research revealed a significant correlation between the levels of ADMA and CTGF in the aqueous humor. These findings imply that ADMA may cooperate with CTGF or induce the expression of CTGF to promote the formation and development of FVP in PDR. Wang et al. found in their study that ADMA can induce the upregulation of transforming growth factor β (TGF- β), promoting fibrosis in renal glomerular endothelial cells (35). CTGF is a downstream effector molecule of TGF- β , where TGF- β can induce increased expression of CTGF, thereby promoting fibrosis (36). Therefore, ADMA may induce fibrosis in retinal tissue by upregulating CTGF through the TGF- β pathway. Further research is essential to elucidate the specific mechanisms underlying the involvement of ADMA in the FVP of PDR patients.

Previous research indicates that factors such as renal function, and the use of ACE inhibitors may influence the levels of ADMA and CTGF in plasma (20, 37–39). Patients with poorer renal function levels tend to have higher plasma levels of ADMA and CTGF (37, 39). In this study, there was a significant correlation between ADMA and CTGF levels in the aqueous humor of PDR patients. Furthermore, we found a significant correlation between the levels of metabolites in the aqueous humor and plasma. This suggests that renal function may serve as a potential confounding factor influencing ADMA and CTGF levels in the aqueous humor. Further research is necessary to validate this hypothesis.

However, several limitations should be considered in this study. First, the cross-sectional design utilized in this study limits our ability to determine the dynamic changes in metabolite levels and their temporal relationship with the progression of PDR. Employing longitudinal study designs would provide a better understanding of the association between metabolite alterations and disease progression. Secondly, although we observed a significant correlation between ADMA and CTGF levels, further basic experimental and molecular mechanism studies are still needed to elucidate the exact relationship between them and their interaction in the formation and development of FVP in PDR patients.

In conclusion, despite some limitations, this study provides new insights into the warning of intraocular FVP in cases of severe PDR. The study reveals a positive correlation between ADMA levels and the severity of FVP in PDR patients in both plasma and aqueous humor, indicating that ADMA is a risk factor for FVP in PDR patients. Future research can build upon this study by conducting animal or cell model experiments to assess the impact of modulating ADMA levels on PDR development. This will further elucidate the underlying mechanisms, thereby offering theoretical foundations for the prevention and treatment of FVP in PDR patients.

Data availability statement

The raw data supporting the conclusions of this article will be made available by the authors, without undue reservation.

Ethics statement

The studies involving human participants were reviewed and approved by the Clinical Research Ethics Committee of Renmin Hospital of Wuhan University (WDRY2023-K083). The patients provided their written informed consent to participate in this study.

Author contributions

XG: Writing – original draft, Writing – review & editing. WJ: Conceptualization, Funding acquisition, Methodology, Project administration, Writing – review & editing. YX: Resources, Supervision, Validation, Visualization, Writing – review & editing.

Funding

The author(s) declare financial support was received for the research, authorship, and/or publication of this article. This work was supported by the Hubei Provincial Science and Technology Planning Project #1 under Grant number 2019CFB489 and Renmin Hospital of Wuhan University #2 under Grant number JCRCGW-2022-006.

Acknowledgments

We would like to extend our sincere appreciation to Professor Anhuai, Yang for generously providing the samples and data used in this study. Their contribution was invaluable in enabling the progression of our research.

Conflict of interest

The authors declare that the research was conducted in the absence of any commercial or financial relationships that could be construed as a potential conflict of interest.

Publisher's note

All claims expressed in this article are solely those of the authors and do not necessarily represent those of their affiliated organizations, or those of the publisher, the editors and the reviewers. Any product that may be evaluated in this article, or claim that may be made by its manufacturer, is not guaranteed or endorsed by the publisher.

Supplementary material

The Supplementary Material for this article can be found online at: <https://www.frontiersin.org/articles/10.3389/fendo.2024.1364609/full#supplementary-material>

References

- Lin KY, Hsieh WH, Lin YB, Wen CY, Chang TJ. Update in the epidemiology, risk factors, screening, and treatment of diabetic retinopathy. *J Diabetes Investig.* (2021) 12:1322–5. doi: 10.1111/jdi.13480
- Wong TY, Sabanayagam C. Strategies to tackle the global burden of diabetic retinopathy: from epidemiology to artificial intelligence. *Ophthalmologica.* (2020) 243:9–20. doi: 10.1159/000502387
- Lin TZ, Kong Y, Shi C, Eric Pazo E, Dai GZ, Wu XW, et al. Prognosis value of chinese ocular fundus diseases society classification for proliferative diabetic retinopathy on postoperative visual acuity after pars plana vitrectomy in type 2 diabetes. *Int J Ophthalmol.* (2022) 15:1627–33. doi: 10.18240/ijo.2022.10.10
- Lin S-J, Yeh P-T, Huang J-Y, Yang C-M. Preoperative prognostic factors in vitrectomy for severe proliferative diabetic retinopathy. *Taiwan J Ophthalmol.* (2014) 4:174–8. doi: 10.1016/j.tjo.2014.08.005
- Huang C-H, Hsieh Y-T, Yang C-M. Vitrectomy for complications of proliferative diabetic retinopathy in young adults: clinical features and surgical outcomes. *Graefes Arch Clin Exp Ophthalmol.* (2017) 255:863–71. doi: 10.1007/s00417-016-3579-4
- Wu YB, Wang CG, Xu LX, Chen C, Zhou XB, Su GF. Analysis of risk factors for progressive fibrovascular proliferation in proliferative diabetic retinopathy. *Int Ophthalmol.* (2020) 40:2495–502. doi: 10.1007/s10792-020-01428-y
- Ma T, Dong LJ, Du XL, Niu R, Hu BJ. Research progress on the role of connective tissue growth factor in fibrosis of diabetic retinopathy. *Int J Ophthalmol.* (2018) 11:1550–4. doi: 10.18240/ijo.2018.09.20
- Jian Q, Wu Y, Zhang F. Metabolomics in diabetic retinopathy: from potential biomarkers to molecular basis of oxidative stress. *Cells.* (2022) 11:1–19. doi: 10.3390/cells11193005
- Liew G, Lei Z, Tan G, Joachim N, Ho IV, Wong TY, et al. Metabolomics of diabetic retinopathy. *Curr Diabetes Rep.* (2017) 17:102. doi: 10.1007/s11892-017-0939-3
- Hou XW, Wang Y, Pan CW. Metabolomics in diabetic retinopathy: A systematic review. *Invest Ophthalmol Vis Sci.* (2021) 62:4. doi: 10.1167/iovs.62.10.4
- Wehling-Henricks M, Jordan MC, Gotoh T, Grody WW, Roos KP, Tidball JG. Arginine metabolism by macrophages promotes cardiac and muscle fibrosis in mdx muscular dystrophy. *PLoS One.* (2010) 5:e10763. doi: 10.1371/journal.pone.0010763
- Qin J, Xu J. Arginine methylation in the epithelial-to-mesenchymal transition. *FEBS J.* (2022) 289:7292–303. doi: 10.1111/febs.16152
- Yu J, Yu C, Bayliss G, Zhuang S. Protein arginine methyltransferases in renal development, injury, repair, and fibrosis. *Front Pharmacol.* (2023) 14:1123415. doi: 10.3389/fphar.2023.1123415
- Flaxel CJ, Adelman RA, Bailey ST, Fawzi A, Lim JJ, Vemulakonda GA, et al. Diabetic retinopathy preferred practice pattern(R). *Ophthalmology.* (2020) 127:P66–P145. doi: 10.1016/j.ophtha.2019.09.025
- Strati M, Moustaki M, Psaltopoulou T, Vryonidou A, Paschou SA. Early Onset Type 2 Diabetes Mellitus: An Update. *Endocrine.* (2024). doi: 10.1007/s12020-024-03772-w
- Lv X, Ran X, Chen X, Luo T, Hu J, Wang Y, et al. Early-Onset Type 2 Diabetes: A High-Risk Factor for Proliferative Diabetic Retinopathy (Pdr) in Patients with Microalbuminuria. *Medicine (Baltimore).* (2020) 99(19):e20189. doi: 10.1097/md.00000000000020189
- Zou W, Ni L, Lu Q, Zou C, Zhao M, Xu X, et al. Diabetes onset at 31–45 years of age is associated with an increased risk of diabetic retinopathy in type 2 diabetes. *Sci Rep.* (2016) 6:38113. doi: 10.1038/srep38113
- Sabanayagam C, Banu R, Chee ML, Lee R, Wang YX, Tan G, et al. Incidence and progression of diabetic retinopathy: A systematic review. *Lancet Diabetes Endocrinol.* (2019) 7:140–9. doi: 10.1016/S2213-8587(18)30128-1
- Goel M, Picciani RG, Lee RK, Bhattacharya SK. Aqueous humor dynamics: A review. *Open Ophthalmol J.* (2010) 4:52–9. doi: 10.2174/1874364101004010052
- Be'towski J, Kédra A. Asymmetric dimethylarginine (Adma) as a target for pharmacotherapy. *Pharmacol Rep.* (2006) 58:159–78.
- Jarzebska N, Mangoni AA, Martens-Lobenhoffer J, Bode-Boger SM, Rodionov RN. The second life of methylarginines as cardiovascular targets. *Int J Mol Sci.* (2019) 20(18):4592. doi: 10.3390/ijms20184592
- Lin KY, Ito A, Asagami T, Tsao PS, Adimoolam S, Kimoto M, et al. Impaired nitric oxide synthase pathway in diabetes mellitus: role of asymmetric dimethylarginine and dimethylarginine dimethylaminohydrolase. *Circulation.* (2002) 106:987–92. doi: 10.1161/01.cir.0000027109.14149.67
- Cardounel AJ, Cui H, Samouilov A, Johnson W, Kearns P, Tsai AL, et al. Evidence for the pathophysiological role of endogenous methylarginines in regulation of endothelial NO production and vascular function. *J Biol Chem.* (2007) 282:879–87. doi: 10.1074/jbc.M603606200
- Vallance P, Leone A, Calver A, Collier J, Moncada S. Accumulation of an endogenous inhibitor of nitric oxide synthesis in chronic renal failure. *Lancet.* (1992) 339:572–5. doi: 10.1016/0140-6736(92)90865-Z
- Hannemann J, Boger R. Dysregulation of the nitric oxide/dimethylarginine pathway in hypoxic pulmonary vasoconstriction-molecular mechanisms and clinical significance. *Front Med (Lausanne).* (2022) 9:835481. doi: 10.3389/fmed.2022.835481
- Liu M, Ning X, Li R, Yang Z, Yang X, Sun S, et al. Signalling pathways involved in hypoxia-induced renal fibrosis. *J Cell Mol Med.* (2017) 21:1248–59. doi: 10.1111/jcmm.13060
- Zhao WC, Li G, Huang CY, Jiang JL. Asymmetric dimethylarginine: an crucial regulator in tissue fibrosis. *Eur J Pharmacol.* (2019) 854:54–61. doi: 10.1016/j.ejphar.2019.03.055
- Iwasaki H, Shichiri M. Protein arginine N-methyltransferase 1 gene polymorphism is associated with proliferative diabetic retinopathy in a Japanese population. *Acta Diabetol.* (2022) 59:319–27. doi: 10.1007/s00592-021-01808-5
- Abhary S, Kasmeridis N, Burdon KP, Kuot A, Whiting MJ, Yew WP, et al. Diabetic retinopathy is associated with elevated serum asymmetric and symmetric dimethylarginines. *Diabetes Care.* (2009) 32:2084–6. doi: 10.2337/dc09-0816
- Peters KS, Rivera E, Warden C, Harlow PA, Mitchell SL, Calcutt MW, et al. Plasma arginine and citrulline are elevated in diabetic retinopathy. *Am J Ophthalmol.* (2022) 235:154–62. doi: 10.1016/j.ajo.2021.09.021
- Sugai M, Ohta A, Ogata Y, Nakanishi M, Ueno S, Kawata T, et al. Asymmetric dimethylarginine (Adma) in the aqueous humor of diabetic patients. *Endocr J.* (2007) 54:303–9. doi: 10.1507/endocrj.k06-140
- Ortega N, Romero M-P, Macià A, Reguant J, Anglès N, Morelló J-R, et al. Comparative study of uplc-ms/ms and hplc-ms/ms to determine procyanidins and alkaloids in cocoa samples. *J Food Composition Anal.* (2010) 23:298–305. doi: 10.1016/j.jfca.2009.10.005
- Klaassen I, van Geest RJ, Kuiper EJ, van Noorden CJF, Schlingemann RO. The role of ctgf in diabetic retinopathy. *Exp Eye Res.* (2015) 133:37–48. doi: 10.1016/j.exer.2014.10.016
- Kuiper EJ, de Smet MD, van Meurs JC, Tan HS, Tanck MW, Oliver N, et al. Association of connective tissue growth factor with fibrosis in vitreoretinal disorders in the human eye. *Arch Ophthalmol.* (2006) 124:1457–62. doi: 10.1001/archophth.124.10.1457
- Wang L, Zhang D, Zheng J, Feng Y, Zhang Y, Liu W. Actin cytoskeleton-dependent pathways for adma-induced nf-kappab activation and tgfbeta high expression in human renal glomerular endothelial cells. *Acta Biochim Biophys Sin (Shanghai).* (2012) 44:918–23. doi: 10.1093/abbs/gms077
- Yanagihara T, Tsubouchi K, Gholiof M, Chong SG, Lipson KE, Zhou Q, et al. Connective-tissue growth factor contributes to tgfbeta1-induced lung fibrosis. *Am J Respir Cell Mol Biol.* (2022) 66:260–70. doi: 10.1165/rcmb.2020-0504OC
- Gerritsen KG, Abrahams AC, Peters HP, Nguyen TQ, Koeners MP, den Hoedt CH, et al. Effect of gfr on plasma N-terminal connective tissue growth factor (Ctgf) concentrations. *Am J Kidney Dis.* (2012) 59:619–27. doi: 10.1053/j.ajkd.2011.12.019
- Hedayatyanfard K, Khalili A, Karim H, Nooraei S, Khosravi E, Haddadi NS, et al. Potential use of angiotensin receptor blockers in skin pathologies. *Iran J Basic Med Sci.* (2023) 26:732–7. doi: 10.22038/IJBMS.2023.66563.14606
- Said MY, Bollenbach A, Minovic I, van Londen M, Frenay AR, de Borst MH, et al. Plasma adma, urinary adma excretion, and late mortality in renal transplant recipients. *Amino Acids.* (2019) 51:913–27. doi: 10.1007/s00726-019-02725-2



OPEN ACCESS

EDITED BY

Sara Rezzola,
University of Brescia, Italy

REVIEWED BY

Dave Gau,
University of Pittsburgh, United States
Kunbei Lai,
Sun Yat-sen University, China
Josy Augustine,
Queen's University Belfast, United Kingdom
Dario Rusciano,
Consultant, Catania, Italy

*CORRESPONDENCE

Rajashekhar Gangaraju
✉ sgangara@uthsc.edu
Dinesh Upadhy
✉ dinesh.upadhy@manipal.edu

RECEIVED 12 April 2024

ACCEPTED 27 May 2024

PUBLISHED 14 June 2024

CITATION

Reddy SK, Devi V, Seetharaman ATM,
Shailaja S, Bhat KMR, Gangaraju R and
Upadhy D (2024) Cell and molecular
targeted therapies
for diabetic retinopathy.
Front. Endocrinol. 15:1416668.
doi: 10.3389/fendo.2024.1416668

COPYRIGHT

© 2024 Reddy, Devi, Seetharaman, Shailaja,
Bhat, Gangaraju and Upadhy. This is an open-
access article distributed under the terms of
the [Creative Commons Attribution License \(CC BY\)](#). The use, distribution or reproduction
in other forums is permitted, provided the
original author(s) and the copyright owner(s)
are credited and that the original publication
in this journal is cited, in accordance with
accepted academic practice. No use,
distribution or reproduction is permitted
which does not comply with these terms.

Cell and molecular targeted therapies for diabetic retinopathy

Shivakumar K. Reddy¹, Vasudha Devi²,
Amritha T. M. Seetharaman³, S. Shailaja⁴, Kumar M. R. Bhat⁵,
Rajashekhar Gangaraju^{3,6*} and Dinesh Upadhy^{1*}

¹Centre for Molecular Neurosciences, Kasturba Medical College, Manipal, Manipal Academy of Higher Education, Manipal, India, ²Department of Pharmacology, Kasturba Medical College, Manipal, Manipal Academy of Higher Education, Manipal, India, ³Department of Ophthalmology, The University of Tennessee Health Science Center, Memphis, TN, United States, ⁴Department of Ophthalmology, Kasturba Medical College, Manipal, Manipal Academy of Higher Education, Manipal, India, ⁵Department of Anatomy, Kasturba Medical College, Manipal, Manipal Academy of Higher Education, Manipal, India, ⁶Department of Anatomy & Neurobiology, The University of Tennessee Health Science Center, Memphis, TN, United States

Diabetic retinopathy (DR) stands as a prevalent complication in the eye resulting from diabetes mellitus, predominantly associated with high blood sugar levels and hypertension as individuals age. DR is a severe microvascular complication of both type I and type II diabetes mellitus and the leading cause of vision impairment. The critical approach to combatting and halting the advancement of DR lies in effectively managing blood glucose and blood pressure levels in diabetic patients; however, this is seldom achieved. Both human and animal studies have revealed the intricate nature of this condition involving various cell types and molecules. Aside from photocoagulation, the sole therapy targeting VEGF molecules in the retina to prevent abnormal blood vessel growth is intravitreal anti-VEGF therapy. However, a substantial portion of cases, approximately 30–40%, do not respond to this treatment. This review explores distinctive pathophysiological phenomena of DR and identifiable cell types and molecules that could be targeted to mitigate the chronic changes occurring in the retina due to diabetes mellitus. Addressing the significant research gap in this domain is imperative to broaden the treatment options available for managing DR effectively.

KEYWORDS

diabetes, anti-VEGF drugs, neovascularization, apoptosis, inflammation, blood retinal barrier, microaneurysms, leukostasis

Introduction

Uncontrolled blood glucose levels for extended durations are linked with multiple complications such as retinopathy, nephropathy, cardiovascular, cerebrovascular, and peripheral vascular diseases, leading to high morbidity and mortality rates with diabetes mellitus (1, 2). Diabetic retinopathy (DR) is a severe microvascular complication of both type I

and type II diabetes mellitus and the leading cause of vision impairment. Recent systematic review and meta-analysis revealed that approximately 1 in 5 persons with diabetes worldwide have DR, and the total number of people losing vision as a result of DR may continue to rise (3). Multiple studies have recognized that risk factors such as severe hyperglycemia, hypertension, and hyperlipidemia worsen DR.

DR can be broadly categorized into background retinopathy (non-proliferative DR, NPDR) and proliferative DR (PDR) with diabetic macular edema (DME) occurring at any stage of DR. Presently, the primary treatment for NPDR involves anti-vascular endothelial growth factor (anti-VEGF) drugs targeting VEGF, a known cause of DME. However, nearly 30–40% of DR patients do not respond to these anti-VEGF treatments (4–6). In cases where neovascularization leads to PDR, characterized by the formation of abnormal blood vessel growth, photocoagulation stands as the current treatment option. Clinically, neovascularization is identifiable by fine loops or blood vessel networks on the retinal surface extending into the vitreous cavity, often appearing immature and regressing, resulting in ischemia and further neovascularization. The pathophysiology of DR is intricate, involving various cell types and molecules, as evidenced by numerous studies in both human and animal models (Figure 1). This review delves into distinct pathophysiological aspects of DR, along with identifiable cell types and molecules that could serve as targets to alleviate the chronic changes occurring in the retina due to diabetes mellitus. Identifying

additional targets is significant in expanding the range of treatment options available for effectively managing DR.

Blood retinal barrier breakdown in diabetic retinopathy

The blood-retinal barrier (BRB) is the primary defense for the retinal cells against the external factors damaging them. The inner BRB forms tight junctions between retinal capillary endothelial cells, while the outer BRB forms tight junctions between retinal pigment epithelial cells (7). The inner BRB layer contains endothelial cells merged in tight junctions and regulated by pericytes, which regulate transport through retinal capillaries within the inner retina (8, 9). Since BRB is a part of the neurovascular unit, a complex multi-cellular structure consisting of vascular cells (endothelial cells, pericytes), neurons (ganglion, bipolar, horizontal, and amacrine cells), glia (astrocytes, Müller cells, and microglial cells) and smooth muscle cells, maintaining its integrity during highly altered metabolic conditions of diabetes is critical for preventing BRB breakdown (10). Indeed, the loss of BRB integrity is the primary feature of DME. To begin with, in the presence of high levels of mediators that promote inflammation and activated microglia, VEGF is known to be released by macroglia, thus compromising the integrity of the barrier (11). Subsequently, endothelial cells begin to express cell adhesion molecules (CAMs) such as ICAM-1, VCAM-1,

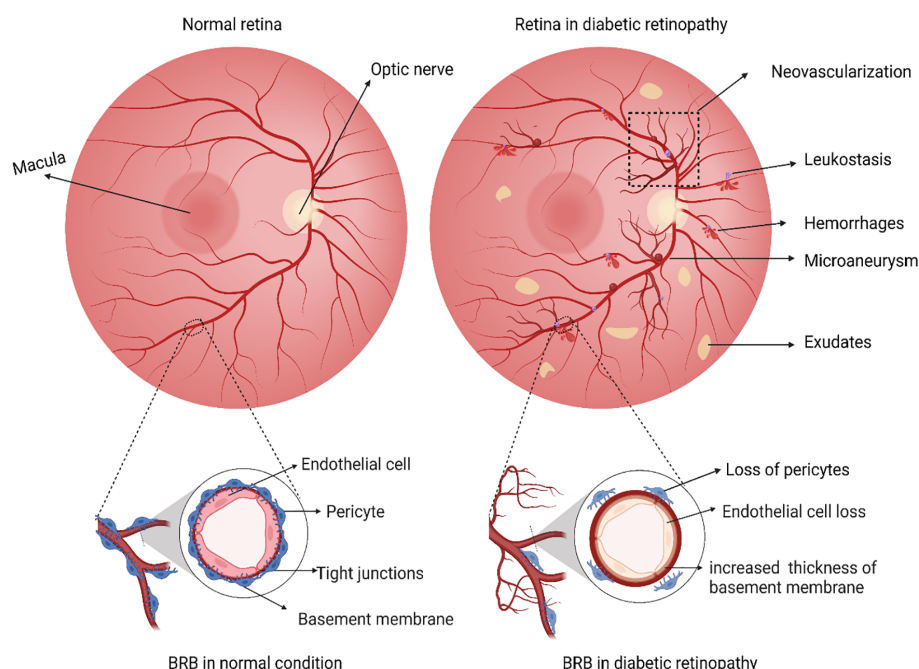


FIGURE 1

Schematic illustration representing differences between a normal retina and a retina with diabetic retinopathy. In the normal retina, a functional inner blood-brain barrier with intact endothelial cells and pericytes, while in diabetic retinopathy, dysfunction of BRB is evident through loss of pericytes and endothelial cells and thickening of the vascular basement membrane. Any loss of such retinal barrier integrity is associated with a cycle of inflammation, vascular damage, and cell death. During the retinal damage, it is likely that activated Microglia and Glial cells release high levels of pro-inflammatory cytokines. These cytokines act on nearby vasculature and neuronal cells, causing further damage. Classical pathological hallmarks of DR such as the formation of microaneurysms, abnormal growth of new blood vessels (neovascularization), microvascular leakages (cotton wool spots, hemorrhages), accumulation of thick yellowish fluids, i.e., exudates and recruitment of leukocytes due to inflammation (leukostasis) are represented. The figure was created using BioRender.

E-selectin, and P-selectin (12), a few of which have been linked to the cause of NPDR (13). On the luminal side of the endothelial cell anchors provided by CAMs, circulating leukocytes bind to the vessel wall through CD11a, CD11b, and CD18 (14) and release pro-inflammatory cytokines. This results in a culmination of cytotoxic mediators adding to the local pro-inflammatory climate (15) and weakening barrier integrity by compromising endothelial tight junction and pericyte-endothelial health (16). Additional studies have shown that loss of integral membrane protein caveolin-1 causes BRB breakdown, venous enlargement, and mural cell alteration (17). A possible target to prevent BRB breakdown is inhibiting cell adhesion molecules or integrins. This is supported by the fact that BRB breakdown significantly decreases when CAMs and integrins are inhibited or genetically deleted (14, 18). Indeed, increased VEGF levels in diabetic mice were shown to be directly correlated with increased levels of ICAM-1 and a loss in BRB, while blockade of VEGF suppressed such BRB breakdown (19). Also, increased VEGF levels activate protein kinase C, which in turn may directly or indirectly increase occludin phosphorylation, leading to its internalization and causing the breakdown of BRB (20).

Blood retinal barrier integrity is safeguarded by suppressing cytokine and chemokine activity (11, 21). The significance of the immune response in BRB breakdown has also been successfully proven in studies that combat inflammatory mediators and the complement system (22, 23). Chronic hyperglycemia polarizes microglia into a proinflammatory subtype through extracellular-signal-regulated kinase 5 (ERK5) (24), the levels of which were shown to be increased in the retina of STZ-induced DR model (25). Such increased ERK5 is known to elicit the production of cytokines such as IL-6, IL-1 β , and VEGF. In turn, these inflammatory markers are known to impair vascular permeability. Thus, blocking the inflammatory pathways downstream of ERK5 through a small molecule inhibitor XMD8-92 prevented retinal inflammation, oxidative stress, VEGF production, and retinal vascular permeability (25). Apart from microglia, other immune cells such as the circulating T helper-17 (Th 17) in the STZ model of DR, induce IL-17A production. Few of the Th17 cells in the circulation were also shown to adhere to the retinal vasculature, thus predicting to be participating in the breakdown of BRB. The IL-17A secreted into the retina binds to their receptors on Müller glial cells and photoreceptors, activating the NF- κ B pathway, Fas-associated death domain (FADD) retinal vascular endothelial cell death, as well as ERK-dependent oxidative stress resulting in retinal vascular impairment and BRB dysfunction (26, 27). The role of photoreceptor cells in maintaining inner BRB in the diabetic retina is another emerging field. Photoreceptors in STZ-induced diabetic mice produce soluble factors, including ICAM1, inducible nitric oxide synthase (iNOS), and cyclooxygenase 2 (COX2), influencing inflammation in the neighboring leukocytes and endothelial cells to produce TNF α . Additionally, photoreceptor cells also release several inflammatory mediators such as IL-1 α , IL-1 β , IL-6, IL-12, TNF- α , chemokine C-X-C motif ligand 1 [CXCL1], CXCL12a, monocyte chemoattractant protein 1 [MCP-1], I-309, and chemokine ligand 25 [CCL25] impairing BRB permeability through partly modulating tight junction protein claudin (28, 29).

The outer BRB, formed at the retinal pigment epithelial (RPE) cell layer, controls the passage of solutes and nutrients from the choroid to the sub-retinal space but also plays a vital role under physiological conditions regulating vitamin A and protecting against oxidative damage. Additionally, RPE releases various growth factors and cytokines, including pigment epithelium-derived factor (PEDF), vascular endothelial growth factor (VEGF), fibroblast growth factor (FGF), insulin-like growth factor-I (IGF-I), tumor necrosis factor α (TNF- α), transforming growth factor β (TGF- β), interleukins (ILs) essential for retinal cell survival and immune privilege (30). Indeed, changes in the expression of these factors lead to destructive inflammation, neovascularization, and immune reactions under pathological conditions (31). For example, the essential role of PEDF, an anti-angiogenic factor in maintaining the integrity of outer BRB without affecting the structure and functionality of normal blood vessels, is known (32). Expectedly, PEDF therapy in diabetic mice reduces microgliosis, boosts tight junction expression, decreases pro-inflammatory mediator production, lowers vascular permeability, and is neuroprotective (8, 33). In addition to growth factors and cytokine release, RPE plays a vital role in solute transport through its tight junctions, occludin-1, claudins, and ZO-1, which are similar to those in other tissues (34). The cytokines released, in particular retinal IL-6 in DR, influence retinal vascular permeability (35) through microglial recruitment to the RPE layers disassembling tight junction complexes, including ZO-1 and occludin proteins (11). Additionally, IL-6-mediated microglial expression of TNF- α is shown to activate NF- κ B and thus reduce levels of ZO-1 in RPE cells. Indeed, STAT 3 inhibition reverses the disintegration of ZO-1, suggesting the essential role of IL-6-STAT 3 pathways in microglial and RPE cells in regulating outer BRB (11). Lastly, the tight junctions, combined with the actin cytoskeleton, provide polarity to the RPE cells to regulate signal transduction and help localize certain proteins to maintain the outer BRB (36). Several studies using RPE cell lines have reported the benefits of maintaining the tight junctions as relevant to DR affecting tight junction permeability (e.g., C-reactive protein and tissue factor) and promoting tight junction formation (e.g., somatostatin, nicotinamide, lysophosphatidic acid, and HIW12-mediated activation of Akt), highlighting their significance for maintaining epithelial phenotype (37). However, the relevance of these studies in animal models remains to be determined. Taken together with outer and inner barrier function, the integrity of the neurovascular unit of the retina is of primary importance to prevent BRB breakdown in preclinical DR and individuals with prolonged diabetes. Future studies exploring targets that could protect BRB will continue to be of interest to the field.

Neovascularization in diabetic retinopathy

Neovascularization refers to the formation of new and abnormal blood vessel growth. It is one of the most common critical pathologies of DR. Clinically, neovascularization could be characterized by fine loops or blood vessel networks on the retinal surface extended into the vitreous cavity (38). Among the various growth factors identified, vascular endothelial growth factor

(VEGF) has been well-established to play a central role in the neovascularization of DR (39).

VEGF is a homodimer glycoprotein that binds to heparin and has a molecular weight of 46 kDa. It is synthesized in human cells through alternative splicing. The transcription factor HIF-1 (hypoxia-inducible transcription factor 1) binds to the hypoxia-responsive enhancer elements (HREs) at the VEGF gene, upregulating transcription, which is physiologically regulated by oxygen tension (40, 41). Apart from enhancing the transcription of VEGF, HIF-1 also helps its stability by preventing VEGF mRNA degradation (42, 43). VEGF is biologically active through tyrosine kinase receptors (RTKs). VEGF family contains VEGF A, B, C, D and PlGF (Placental growth factor). VEGF receptors include VEGFR1, VEGFR2 and VEGFR3. VEGF-A can bind and activate VEGFR1 and VEGFR2, but PlGF and VEGF-B bind only to VEGFR1. VEGFA has 5 isoforms based on splice variants, and VEGF 165 is predominantly expressed in the retina (44). Additionally, it was shown that the transmembrane protein Neuropilin-1 functions as a coreceptor for VEGF-A (45, 46). Increased ischemia or hypoxia enhances VEGF production through hypoxia-inducible factor 1(HIF-1). Apart from endothelial cells, retinal Müller cells also produce significant amounts of VEGF in diabetic mice. This increase is associated with a three-fold increase in leukostasis and two-fold higher levels of ICAM-1 and proinflammatory marker TNF- α , drastic reduction in occludin and ZO-1 levels, ~60% increase in retinal vascular leakage in animal models. Conversely, inhibition of Müller cell-derived VEGF significantly reduces these effects, suggesting that VEGF production from Müller cells could be targeted to control DR (23). The irregular production and secretion of VEGF induce vascular endothelial cell proliferation and migration, increasing vascular permeability (39). Activating endothelial nitric oxide synthase (eNOS) and generating nitric oxide are further components of VEGF-A/VEGFR2's control of vascular permeability and plasma extravasation (47). Multiple VEGF functions, such as survival, proliferation, migration, vascular permeability, and gene expression, have been mediated by activation of the phospholipase C, protein kinase C, Ca²⁺, extracellular signal-regulated protein kinase, mTOR, protein kinase B, Src family kinase, focal adhesion kinase, and calcineurin pathways (48).

Apart from VEGF, other key molecules involved in neovascularization in DR include platelet-derived growth factor (PDGF), placental growth factor (PlGF) and others. Platelet-derived growth factors are secreted by platelets, endothelial cells, activated macrophages and smooth muscle cells and are vital players of DR (49–51); PDGF has 4 polypeptide chains(PDGF-A, PDGF-B, PDGF-C, and PDGF-D) and becomes active by homodimer isoform formation such as PDGF-AA, PDGF-BB, PDGF-CC and PDGF-DD or heterodimeric form PDGF-AB. PDGF ligands will bind to transmembrane tyrosine kinase PDGF receptors, which contain homodimeric and heterodimeric isoforms such as PDGFR- $\alpha\alpha$, PDGFR- $\beta\beta$ and PDGFR- $\alpha\beta$ (50). Retina-specific expression of PDGF-B could lead to neovascularization and retinal detachment (52, 53). In diabetic animal models, PDGF-AA and PDGF-BB levels

were increased during the development of DR (54). Inhibiting PDGF-BB levels could prevent neovascularization (55). PDGF-CC could rescue neurons from apoptosis in the retina by regulating GSK3 β phosphorylation (56).

PlGF belongs to the VEGF family of growth factors. PlGF has 4 isoforms, and all its isoforms bind to VEGFR1 with different affinities than VEGF but do not bind to VEGFR2. Reports suggest that PlGF-1 is highly produced by RPE cells during pathogenesis, while low levels were detected under normal conditions (57–59), while PlGF-2 is produced by retinal endothelial cells and pericytes (60, 61). The 3D structure of PlGF-1 shares 42% similarity in amino acid sequence with VEGF but has a strikingly similar 3D structure (62). Elevated levels of PlGF were observed in the aqueous humor and vitreous samples of DR patients and the levels were associated with retinal ischemia and VEGF-A levels (63, 64). While inhibition of VEGF increases PlGF levels, it also acts as a redundant inducer of neovascularization (65). Expression of PlGF is associated with several early and later features of DR in animal models (66). For example, inhibition of PlGF reduces neovascularization, retinal leakage, and associated inflammation and gliosis while preserving normal vascular development and neuronal architecture (65, 67).

Other than growth factors, Profilin1 (Pfn1), an actin-binding protein, was discovered through bioinformatic analysis to transcriptionally upregulated in vascular cells of patients with PDR and further confirmed in a mouse model that mimics PDR (68). Mechanistically, in the context of vascular development in the retina, the deletion of the Pfn1 gene in vascular endothelial cells postnatally impeded the formation of actin-based filopodial structures, tip cell invasion, vascular sprouting, and overall neovascularization, suggesting a crucial role for Pfn1 in promoting actin polymerization and angiogenesis (68). Inhibiting this Pfn1-actin interaction by a novel compound, C74, indeed proved to be a potential therapeutic target for conditions involving abnormal retinal angiogenesis as in PDR (69). Furthermore, the transcription factor FOXC1 has been found to be essential for normal revascularization processes, crucial for pericyte function, and vital for forming the blood-retinal barrier (BRB). Therefore, FOXC1 is now recognized as a therapeutic target for retinal vascular diseases such as DR. Specifically, the loss of FOXC1 in endothelial cells hindered retinal vascular development by reducing mTOR activity. However, treatment with the mTOR agonist MHY-1485 restored disrupted retinal angiogenesis (70).

Microaneurysms in diabetic retinopathy

Microaneurysms represent a slight expansion of capillary walls, resulting from the excessive growth of endothelial cells (ECs) and depletion of pericytes due to prolonged unregulated high blood sugar levels, weakening blood vessel walls (71, 72). While the mean diameter of the normal capillaries is ~10 μ m (72), the mean diameter of microaneurysms in DR ranges from 43–266 μ m and span over more than one retinal layer (71–74). While intravitreal injection of VEGF into the eyes demonstrated

microaneurysms, single and repeated anti-VEGF treatments reduced the microaneurysm levels significantly (71, 75, 76). Further, nearly 80% of the microaneurysms were identified near the capillary dropouts, representing focal ischemic regions (77). These studies suggest a direct link between focal ischemia, VEGF levels, and microaneurysms. However, microaneurysms are associated with resistance from anti-VEGF therapy as they are densely present in refractory areas, and more importantly, retinal thickness reduction after anti-VEGF treatment is minimal in these areas (78). Additionally, the areas with a higher density of microaneurysms were closely associated with residual edema after anti-VEGF treatment compared to areas with lesser edema (79).

Pericytes, dome-shaped cells found on the outer side of the basement membrane alongside endothelial cells, play crucial roles in maintaining capillary structure and function (74). Pericytes provide mechanical stability to the capillary wall and their recruitment depends on PDGF β (80). Interacting with endothelial cells through paracrine signals and making direct cell-cell contact, pericytes in retinal capillaries assist in preserving barrier function (81). Indeed, pericyte density is higher in retinal vessels than in other capillaries to assist in upholding the barrier integrity (82). Persistent hyperglycemia induces transcription of angiopoietin-2 (Ang-2) mediated by tyrosine kinase receptor Tie-2, which provides signals to increase the number of migrating pericytes from the capillaries (83). Adequate endothelial secretion of PDGF β is essential for pericyte function, as a decrease to less than half the normal pericyte density can lead to microaneurysm formation (84). Microaneurysms with pericytes tend to be smaller, though some contain inflammatory cells. Factors such as capillary nonperfusion, pericyte number (Figure 1), and inflammatory cells were all significant contributors to the size of microaneurysms (63). In animal models, the duration of diabetes correlates with increased acellular capillaries and pericyte loss (85). In DR, hyperglycemia-induced pericyte loss is primarily due to the inhibition of PDGF-BB/PDGF β downstream signaling through the activation of the PKC δ -p38 MAPK-SHP-1 pathway (86).

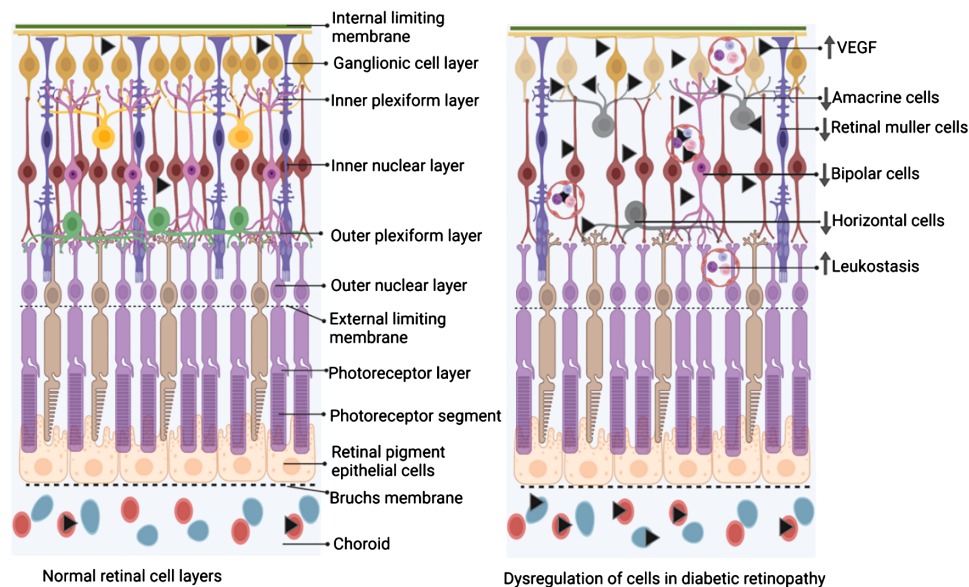
Signals from pericytes may be essential for endothelial cell survival (87). This includes the production of Angiopoietin-1 (ANG1, a heparin binding protein) (88), and VEGF-A (89). In DR, disrupted crosstalk between pericytes and endothelial cells leads to endothelial dysfunction and apoptosis (15). Furthermore, in diabetes, there is an upregulation of cPWWP2A expression in pericytes, affecting pericyte and vascular integrity. This dysregulation is mediated by miR-579 and its target genes, such as angiopoietin 1/occludin/SIRT1 (90). Overall, impaired pericyte-endothelial cell communications could lead to enhanced vascular permeability and leakage, and complications such as microaneurysms, macular edema, and neovascularization. Indeed, preventing early pericyte loss could be a possible approach to prevent complications associated with microaneurysms (90). Additionally, preserving pericyte-endothelial interaction could potentially mitigate neovascularization-induced retinal dysfunction (55, 91) by inhibiting PDGF, which is vital for pericyte function and neovascularization.

Cell death in diabetic retinopathy

Neurodegeneration in the retina precedes vascular abnormalities, possibly leading to visual dysfunction in DR (92). In longitudinal examinations of type 1 and type 2 diabetes patients with no DR or mild NPDR, a progressive inner retinal layer thinning was found (93). The evolution of retinal thinning over time and the increase in the severity of the DR stage were also reported (94). Compared to individuals with normal glucose metabolism, reduced pericentral macula thickness was observed as early as in prediabetes conditions. A statistically significant linear trend was found to link macular thinning to the severity of glucose metabolism status (95). A further study showing thinner inner retinal layers and photoreceptor layers in patients with metabolic syndrome reinforced the notion that retinal neurodegenerative processes begin before the onset of DR (96). Retinal layer thinning may imply that variables other than hyperglycemia-induced thinning, such as insulin resistance and inflammation produced from adipose tissue, could impact neurodegeneration. In type 2 diabetic patients with early-stage DR, diabetes duration was inversely correlated with RNFL thickness, BMI, lipids, HDL, HbA1c, and albumin-creatinine ratio (97). Initial thickening of the macular ganglion cell inner plexiform layer (mGCIPL) and the rate at which the layer thinning was shown to be independent risk factors for developing DR (93). Additionally, a clear positive connection between loss of mGCIPL and decline in vascular density from baseline to 24 months was found in an investigation of eyes with no DR or mild NPDR. Thinner baseline mGCIPL and more considerable mGCIPL thickness reduction were substantially linked with a change in vessel density, according to multivariable regression analysis (93). These findings suggest that retinal microvascular integrity is related to retinal neurodegenerative characteristics.

Neurodegeneration is a prominent aspect of DR (98–100) and may precede the clinical and morphometric vascular changes of diabetes (99). In the early stages of DR progression, apoptosis of retinal neurons reduces the thickness (Figure 2) of the inner retinal layers and the retinal nerve fiber layer (RNFL), as observed in optical coherence tomography (OCT) (101). Various types of retinal cells undergo death in DR (100). Different types of retinal cells undergo distinct forms of cell demise. Endothelial cells primarily experience apoptosis, while pericytes undergo apoptosis and necrosis, whereas Müller cells are expected to succumb to pyroptosis (100, 102–104). Additional mechanisms of endothelial cell death include hyperglycemia-induced reactive oxygen species (104) and excessive amounts of adherent leukocytes in DR (103). Retinal pericyte apoptosis has been linked to hyperglycemia-induced activation of NF- κ B (105) and increased Bax levels, as observed in the human diabetic retina (106). Sorbitol is known to accumulate in the diabetic retina, and severe hyperglycemia-induced increased activity of the polyol pathway promotes retinal neuronal apoptosis and altered expression of GFAP (107).

In animal models, chronic diabetes reduces the thickness of inner plexiform and inner nuclear layers with significant ganglion



Molecular changes in the diabetic retinopathy

FIGURE 2

Schematic diagram depicting the changes in the cellular composition of the retina of diabetic retinopathy compared to the normal retina. On the left is a schematic of the layers of the retina under physiological state demonstrating an intact and significant number of Müller cells, horizontal cells, amacrine cells, bipolar cells, etc., while adherent leukocytes are not seen. On the right is a schematic of the layers of the retina under diabetic retinopathy. Note, a reduced number of Müller cells, horizontal cells, amacrine cells, and bipolar cells, while a significant number of adherent leukocytes are depicted. The figure was created using [BioRender](#).

cell apoptosis even in the early phases of diabetes. This early cell death is also evident in human retinas (99). Also, in the late chronic phase of DR, a significant amount of cell death was observed in untreated DR rats and DR rats treated with anti-VEGF drugs (108). In areas with more significant aggregation of activated microglia, spectral-domain optical coherence tomography found neuronal thinning in the retinas of diabetic rodents, consistent with this manifestation (109, 110). Microglia could destroy neurons and prune synapses, and their activation occurs before neuronal thinning, while they could also phagocytose damaged but functional neurons (111), which may help explain the faster loss of neurons in the early stage of the disease. Caspase activation in the human diabetic retina is well-known (112), and inhibition of caspase activation prevents capillary degeneration in DR (113). Also, inner retinal astrocyte dysfunction was demonstrated during early diabetes with neuronal functional loss (114). Also, prolonged increases in the levels of VEGF induce apoptosis. At the same time, anti-VEGF treatment is concomitant with reduced levels of VEGF and apoptosis (115). In DR, caspase 3 activated the progressive death of retinal ganglionic cells and other retina cell types mostly due to uncontrolled hyperglycemia-induced neurovascular complications (99, 100, 116–119). Retinal cell death in DR is also associated with significantly reducing GABA inhibitory neurotransmitter signaling (120, 121). Treatment with GABA analog pregabalin significantly suppressed retinal IL-1 β , TNF- α , CD11b, caspase 3, oxidative stress, and glutamate levels, suggesting GABA requirement for retaining normal retinal function in DR (121). Direct controlled nano delivery of GABA to the retina for

protecting RGCs in DR needs further evaluation as such deliveries significantly improved GABA deficiency symptoms in the brain (122).

Neurotrophic factors such as nerve growth factor (NGF), Brain-Derived Neurotrophic Factor (BDNF), Ciliary Neurotrophic Factor (CNTF), and Glial Cell-Derived Neurotrophic Factor (GDNF) in the retina are essential for the development and survival of retinal cells (123). NGF levels were significantly elevated in the serum and tear fluid of PDR patients compared to non-diabetic controls and NPDR patients (124). In DR, an increase in proNGF and a decrease in NGF were detected in the retina, correlating with a significant rise in retinal neuronal death (125). In the retinas of diabetic humans and rats, substantial levels of lipid peroxidation, nitrotyrosine, and the pro-apoptotic p75(NTR) receptor were observed. Hyperglycemia-induced peroxynitrite accumulation in the diabetic retina impairs NGF neuronal survival by nitrating the TrkA receptor and increasing the expression of p75(NTR) (126, 127). Peroxynitrite accumulation also hampers the production and activity of matrix metalloproteinase-7 (MMP-7), which extracellularly cleaves proNGF, activates RhoA/p38MAPK, and contributes to neurovascular death in the retina of DR patients and rat models (125). In a mouse model of PDR, early treatment with antagonists of p75(NTR) or proNGF or NGF inhibitors suppressed retinal neuronal cell death and other pathologies, indicating potential additional therapeutic targets for DR (128, 129). Indeed, it was shown that twice-daily treatment with NGF eyedrops in DR rats significantly prevented retinal ganglion cell death (130). Remarkably, a high molecular weight protein like NGF

can be transported from the anterior to the posterior segment to reach the retina and optic nerve, providing protection. Serum and aqueous humor levels of BDNF were significantly lower in diabetes mellitus patients before DR development (131). Additionally, BDNF levels were significantly reduced in the retina of DR rats (132, 133). BDNF protects against neurodegeneration in DR, and the neuroprotection and Müller cell viability it offers are mediated by VEGF (134). Syn3, a BDNF signaling enhancer, significantly reduced retinal ganglion cell loss in DR 10 weeks after intravitreal injection, suggesting a new approach for preventing DR progression (135). However, conflicting reports exist, with studies showing higher levels of NGF, BDNF, GDNF, NT3, NT4, and CNTF in the vitreous of DR patients (136, 137) and elevated levels of NT3 and NT4 in the retina of DR rats (137). In summary, although several neurotrophins in the retina were shown to be essential for the development and survival of retinal cells, the specific roles of individual neurotrophins on retinal cell survival require further investigation.

Leukostasis in diabetic retinopathy

Leukostasis has been documented in both animal models and human subjects with DR (13). Leukostasis involves the closure of the retinal microvasculature and endothelial cell death temporally and spatially associated with adherent leukocytes in DR (103). Leukocyte endothelial interactions, which show the escalating inflammatory response, occur intravascularly during the early phases of DR. Leukostasis is brought about by activating myeloid cells like neutrophils, monocytes, and granulocytes. Leukostasis is identified by immune cells stuck in the narrow retinal blood vessels, leading to blockage and lack of blood flow. In the microcirculation, the presence of rolling and adherent neutrophils, their velocity of movement, and the areas affected by leukostasis worsen with the severity of hyperglycemia (138). Also, increased leukostasis was demonstrated in different animal models of DR with short-term and long-term studies (139). In advanced stages of DR, there is a rise in the systemic neutrophil count, and these cells exhibit heightened expression of myeloperoxidase and produce greater amounts of hydrogen peroxide compared to cells sampled from individuals without diabetes (140).

Leukocyte-endothelium adhesion is characterized by increased production of endothelial cell adhesion molecules and integrins. Leukocytes engage in a multi-step process on the surface of endothelial cells, where they interact with these molecules to stick to the endothelial wall. For example, intercellular adhesion molecule-1 (ICAM-1), vascular cell adhesion molecule-1 (VCAM-1), and selectins, as well as leukocyte β 2-integrins (CD11a, CD11b, and CD18) (E-selectin) were shown to be elevated in DR. In human subjects with DR soluble E-selectin and sVCAM-1 as well as CCL17, CCL19, and TGF- β were shown to be elevated (141). Indeed, the DR severity was correlated to the plasma levels of VCAM-1 and E-selectin (142). In DR rats, a significant increase in the capillary occlusions was noted due to granulocytes and monocytes associated damage to endothelial cells, thus accumulating extravascular leukocytes, neovascularization, and tissue damage (143). Not

surprisingly, diabetic rats demonstrated significantly increased leukostasis in the chronic phase of DR (108).

A variety of molecules and processes have been implicated in higher levels of leukostasis in DR. VEGF has been shown to promote ICAM-1 expression in endothelial cells, thus triggering leukocyte activation and cytokine release, which in turn creates amplifying inflammatory response and increasing VEGF expression. In the early stages of DR progression, the specific endogenous VEGF inhibition has been shown to reduce retinal leukostasis and BRB breakdown, attesting to VEGF's prominent role in leukostasis (19). Additional studies using sulfonated oligosaccharides to inhibit VEGF in the retina in diabetic rats resulted in the inhibition of leukostasis and improved ERG (144). Leukocyte-induced microvascular damage by physically blocking capillaries results in temporary ischemia, resulting in increased VEGF or the release of cytokines and superoxide through the respiratory burst (145). The renin-angiotensin system, oxidative stress, and various other abnormalities associated with diabetes are recognized factors that elevate leukostasis within the retinal blood vessels of diabetic rats, mice, and monkeys. Indeed, enhanced intravascular polymorphonuclear leukocyte counts have been observed around areas of capillary nonperfusion in the retinas of diabetic monkeys (146, 147). In animal models, the deletion of ICAM-1 and CD-18, essential for white blood cell adherence to the endothelium, greatly slowed down diabetes-induced capillary degeneration (103). Leukocytes from diabetic rats, but not control rats, caused *in vitro* endothelial cell death, attesting to the ability of activated leukocytes to damage the endothelial wall (147). The increased Fas (CD95)/Fas-ligand pathway is associated with elevated leukostasis to endothelial dysfunction and BRB impairment. Finally, inducible nitric oxide synthase (iNOS) isoform is demonstrated as a key mediator of leukostasis and BRB breakdown in DR (148).

Retinal inflammation in diabetic retinopathy

Inflammation in the retina is directly linked with the severity of DR (149, 150). However, to date, no single proinflammatory molecule has been exclusively associated with the progression of DR. Using both genetic and induced animal models of DR, it was demonstrated that low-grade subclinical inflammation promotes multiple vascular complications such as pericyte and endothelial cell loss, formation of acellular capillaries, and thickening of the basement membrane of retinal vessels in DR (18, 145). While hyperglycemia is directly linked with increased levels of pro-inflammatory cytokines (151), inflammation in DR is known to persist from the early stages of diabetes to the vision-threatening form of the disease (145).

Tumor necrosis factor (TNF- α), a widely recognized cytokine associated with inflammation, has been demonstrated to have negative implications in DR (152–156). TNF- α triggers alterations in endothelial cells, notably promoting the expression of intercellular adhesion molecule ICAM-1, which is crucial in recruiting leukocytes. Other than TNF- α , elevated levels of pro-

inflammatory cytokines such as IL-1 β , and IL-6 and chemokines like MCP-1, CCL2, and CCL5 were documented in mouse models (153). Not only ICAM-1 but also elevated levels of VCAM-1, draw monocytes and leukocytes and encourage an ongoing inflammatory response (157–159). Inflammatory cells invade, and damage tissues as chronic inflammation builds up, increasing retinal vascular permeability, vasodilation, and retinal thickness in DR subjects. Increased levels of TNF- α , IL - 1 β , IL - 1 α , rantes and MCP-1 were also demonstrated in the serum/aqueous humor of DR patients (160, 161). While the elevated levels of these cytokines might have many downstream effects, increased TNF- α and hyperglycemia are known to cause endoplasmic reticulum (ER) stress in retinal endothelial cells (162). Interestingly, the elevation of ER-specific protein, glucose-regulated protein (GRP78) at the plasma membrane in endothelial cells interacts with the VE-Cadherin, a junction protein in the endothelium that is required for cell-to-cell adhesion in the blood vessels glycosylating VE-Cadherin (GlcNAcylated VE-cadherin), thus increasing transmigration of leukocytes across endothelium and increased permeability creating a perpetual motion of inflammation and ER stress (163).

In both the serum and retinal Müller cells, IL-33 levels are elevated in diabetic conditions (164, 165), whereas IL-35 levels in the vitreous are decreased in diabetic retinopathy (DR) (166). In the peripheral blood mononuclear cells of patients with proliferative diabetic retinopathy (PDR), IL-35 lowers IL-17 levels and inhibits Th17 cell differentiation, offering protection against PDR (167). The proinflammatory cytokine IL-17 is elevated in the plasma and vitreous of diabetic patients, and the worsening of DR is linked to increased retinal IL-17A expression through Act1 signaling, which leads to Müller cell dysfunction (168, 169), and promotes retinal neovascularization (170). In PDR, vitreous IL-17A levels are associated with IL-10, IL-22, and TNF α levels in the aqueous humor and vitreous (171). Administering intravitreal or intraperitoneal injections of anti-IL-17A antibody or anti-IL-17RA antibody to type 1 and type 2 diabetic mice significantly reduces DR pathologies, including Müller cell dysfunction, leukostasis, leakage, downregulation of tight junction proteins, and ganglion cell apoptosis in the retina (27, 172).

Other than pro-inflammatory cytokines, various other molecules are well-known to be involved in DR. For example, in diabetes patients, elevated intracellular glucose levels were known to activate the polyol pathway, which metabolizes glucose (173), resulting in elevated deposition of AGEs. This increased AGEs activates protein kinase C (PKC), AGE receptor upregulation, and overactivity of the hexosamine pathway (174). This, in turn, increases the reactive oxygen species (ROS) within cells, resulting in irreversible cellular damage and chronic inflammatory stress (175). Chemokines that control the leukocyte recruitment and activity play an essential role in the development of DR. To this end, monocyte chemoattractant protein-1 (MCP-1) and macrophage inflammatory protein-1 alpha (MIP-1 α) have been shown to be higher in diabetic individuals (176, 177).

The retinal glial cells, which encompass supportive structural elements such as astrocytes, Müller cells, and microglial cells, play a vital role in maintaining cellular equilibrium. The development and advancement of retinal inflammation in DR are associated with

dysfunction within the retinal neuroglia (178). Research from both laboratory experiments conducted *in vitro* and studies utilizing animal models and human post-mortem samples have indicated that the activation of retinal microglia may play a critical role in modulating cytokine expression. This regulation of cytokine expression by activated retinal microglia could have substantial implications in regulating retinal inflammation associated with diabetes (179). In the presence of hyperglycemia, glial cells exhibit dysfunction, leading to an imbalance in oxidative stress and levels of pro-inflammatory cytokines such as TNF- α , growth factors, IL-1, and IL-6. Retinal evaluation in the early experimental diabetes models also revealed selective and progressive accumulation of FDP-lysine. This, in turn, leads to Müller glial cell dysfunction and upregulation of VEGF, IL-6, and TNF- α , providing evidence of the contribution of advanced lipoxidation end-product formation for the retinal inflammation and pathogenesis of DR (180). Moreover, the pro-inflammatory cytokines released from glial cells contribute to migrating monocytes and T lymphocytes. Persistent inflammation further triggers fibrotic processes, leading to the formation of scar tissue, which can ultimately result in retinal detachment (119). While VEGF is a known inducer of inflammation, various other modulators are also known to enhance retinal inflammation independent of VEGF (181). Equally, inflammation is also known to mediate angiogenesis in DR (182) while the interaction of CD40 Ligand with CD40 is an intermediate step between Inflammation and angiogenesis in DR (183).

Advancing therapies for treating diabetic retinopathy

Over the years, several therapeutic approaches have been developed to manage DR, ranging from conventional treatments to cutting-edge advancements in the field of ophthalmology (Table 1). Some of the main modes of treatment available for DR are photocoagulation, vitrectomy, steroid, and anti-VEGF therapies. Two main types of lasers are used in photocoagulation: pan-retinal photocoagulation (PRP) targets leaking blood vessels, while focal laser therapy targets specific areas of abnormal growth. These procedures can slow DR progression but may not always restore vision. In severe cases such as in PDR with bleeding or scar tissue in the vitreous, vitrectomy may be necessary to remove these obstructions and improve vision. Corticosteroids can reduce inflammation in the retina, while effective in some cases, their use is limited due to potential side effects like cataracts and glaucoma.

Anti-VEGF therapy through intravitreal injections is preferred for treating DME associated with vision loss (196–198). Several anti-VEGF drugs, including Bevacizumab, Ranibizumab, Aflibercept, Faricimab, and Brolucizumab have been used for the treatment of DR. These agents improve visual acuity and reduce retinal thickness due to edema. They continue to be frontline therapies, building on results from landmark trials. Bevacizumab, initially developed for cancer therapy (199), has shown efficacy in treating DR and DME (184, 200). Ranibizumab was the first FDA-approved anti-VEGF protein for treating DME in 2012. It is a 48

TABLE 1 Salient exploratory therapeutic targets for DR.

| Drug/protein/Biologics | Target | Clinical/preclinical studies and indications | References |
|---|--|---|------------|
| Bevacizumab (Avastin) | VEGF-A | Off-label drug for DR, FDA-approved for neovascular (wet) age-related macular degeneration (AMD) and macular edema following retinal vein occlusion | (184) |
| Ranibizumab (Lucentis) | VEGF A | FDA-approved for the treatment of DR in patients with DME and for other eye conditions such as neovascular AMD and macular edema following retinal vein occlusion. | (185) |
| Aflibercept (Eylea) | VEGF B, PIGF 1, PIGF-2 | FDA-approved for DR in patients with DME and other eye conditions such as neovascular AMD and macular edema following retinal vein occlusion. | (186) |
| Faricimab (VABYSMO) | VEGF-A and angiopoietin-2 (Ang-2). | FDA-approved for neovascular (wet) age-related macular degeneration (nAMD) and DME in clinical trials for DR | (187) |
| Brolucizumab (Beovu) | VEGF | FDA-approved for the treatment of neovascular (wet) age-related macular degeneration (AMD) and in clinical trials for DME and DR. | (188) |
| Infliximab | TNF- α | Clinical studies: Decreased macular thickness and improved visual acuity in a diabetic model. | (189) |
| SAR 1118 | antagonist of LFA-1 | Preclinical studies: Reduced leukostasis and retinal vascular leakage. Potential therapeutic for DR or other retinal vascular disorders. | (190) |
| Losartan, an AT1R blocker, or Enalapril, an angiotensin-converting enzyme inhibitor | RAS | Clinical studies: Reduced progression of retinopathy by 70%, while treatment with Enalapril reduced it by 65% in a clinical trial involving type 1 diabetes patients with normotensive and normoalbuminuria. RAS blockade is potentially therapeutic in preventing or delaying the development of DR. | (191) |
| Pigment Epithelium-Derived Factor (PEDF) | PEDF | Preclinical studies: PEDF overexpression prevented neovascularization in a murine adult model of retinopathy, indicating a protective effect against abnormal blood vessel growth in the retina, a hallmark of DR and age-related macular degeneration. | (192) |
| miR-182–5p | angiogenin and BDNF | Preclinical studies: miR-182–5p exerts an inhibitory effect on retinal neovascularization, indicating its regulatory role in the formation of abnormal blood vessels in the retina, which is a characteristic feature of diabetic retinopathy and retinopathy of prematurity | (193) |
| Angiopoietin-like 4 | ANGPTL4 | Preclinical studies: Gene therapy mediated modulation of ANGPTL4 expression, a potential therapeutic approach for stabilizing blood vessels and reducing vascular leakage in diabetic retinopathy. | (194) |
| Syn3 | BDNF enhancer | Preclinical studies: Syn3 demonstrated significant protection against RGC loss in DR | (135) |
| Anti-IL17A | IL 17-A | Preclinical studies: anti IL-17A injection halted diabetes-mediated retinal inflammation, vascular impairment, and the onset of diabetic retinopathy (NPDR) | (27) |
| UPARANT | Urokinase receptor-derived peptide inhibitor | Preclinical studies: Protected the BRB integrity and prevented neovascularization in DR. | (195) |
| XMD8–92 {2-[[2-Ethoxy-4-(4-hydroxy-1-piperidinyl)-5,11-dihydro-5,11-dimethyl-6H-pyrimido[4,5-b] [1,4]benzodiazepin-6-one} | ERK 5 | Preclinical studies: XMD8–92 reduced diabetes mediated retinal inflammation, oxidative stress, vegf production, capillary degeneration and vascular leakage | (25) |

kDa monovalent monoclonal antibody designed for ocular use and binding (201). The small size and lack of the Fc domain of this drug increase the penetration of the drug within the choroid and retina (202, 203). Phase 3 clinical trials showed that patients with monthly ranibizumab gained ≥ 15 letters at 2 years, with higher structural improvement in optical coherence tomography and resolution of leakage. They were also less likely to develop PDR (6, 185). Aflibercept, also known as VEGF trap, is a 115-kDa dimeric glycoprotein and acts as a decoy receptor for VEGF isoforms -A& B and PLGF. Its improved binding properties help to reduce

treatment burden and follow-up visits (186). Faricimab is a humanized antibody that targets both VEGF-A and angiopoietin-2 (Ang-2). This multitarget profile presents intriguing new options for treating exudative retinal disorders. In light of this, Faricimab's Promising data on the use of Faricimab in DME was provided by the phase 2 BOULEVARD study, which demonstrated its superiority over ranibizumab in terms of visual gain (187). Further, in a phase 3, prospective, randomized, double-masked, multicenter study, Brolucizumab demonstrated greater fluid resolution compared with aflibercept (188). Despite the advances

with anti-VEGF therapies, ~40% of cases are refractory with poor response to this treatment (4–6, 196), indicating the requirement of additional dosing or developing new targeting for treating DR. To this end, repeated intravitreal injection of these drugs demonstrated significant improvement in the visual acuity and retinal thickness across studies or delivery of anti-VEGF drugs in nanoformulations reduced the frequency of intravitreal injections in animal studies (108). Apart from VEGF, other growth factors, including placental growth factor (58–60), platelet-derived growth factor (55, 91), and nerve growth factor (204), are known to play important roles in neovascularization and neuronal loss. Individual or combined inhibitions of these growth factors may provide optimal outcomes.

As consistent cell death occurs in different retina layers, neurodegeneration could be a major factor in vision loss. Neuroprotective strategies may be required to maintain the sustained cell density of the retina in DR. Protecting retinal neuronal cells from damage caused by diabetes is another promising area of research. These drugs may help preserve vision even if blood vessel abnormalities persist. For example, diabetic mice demonstrating elevated NLRP3 inflammasome activation and increased production of IL-1 β by Müller glia could be abrogated with Müller glia-specific Regulated in Development and DNA damage 1 (REDD1) deletion, thus improving vision (205). In another example, changes in the microglial immune ligand-receptor CD200-CD200R complex were shown to be associated with neuroinflammation in DR, and CD200Fc, a CD200R agonist, effectively mitigates microglial activity, providing a novel immunotherapeutic target for treating DR (206). Finally, glucagon-like peptide-1 (GLP-1) has been shown to reduce the intracellular overload of Ca²⁺ influx through voltage-gated Ca²⁺ channels, thus protecting RGCs against excitotoxic Ca²⁺ overload in an STZ-induced diabetic animal model (207).

As persistent oxidative stress and inflammation initiate and promote multiple molecular changes, sustained inhibition of molecular pathways to block oxidative stress and inflammation in the retinal tissue could provide an essential avenue in developing therapies. For example, an increase in Takeda G protein-coupled receptor 5 (TGR5) receptor signaling in diabetes is associated with an increase in inflammation and ER stress in the retina and is decreased upon treatment with tauroursodeoxycholic acid (208, 209). ER stress is also known to augment 12/15-LO-induced retinal inflammation in DR via activation of NADPH oxidase and VEGFR2, and thus, perturbation of the 12/15-LO pathway could help develop DR therapies (210). In a clinical investigation including four patients who did not improve after laser photocoagulation treatment, Infliximab, a TNF- α neutralizing antibody, was shown to decrease macular thickness to enhance visual acuity (189). In a diabetic rat model, topical administration of SAR 1118, a minor antagonist of LFA-1 (leukocyte function associated antigen-1) expressed in leukocytes, decreased leukostasis and retinal vascular leakage in a dose-dependent manner (190). Apart from these distinct inflammatory molecules, the AGEs/RAGE pathway is also a potential target for DR due to its prominent role in inducing retinal inflammation. In animal models of DR, soluble RAGE blocking the RAGE activation improved neuronal dysfunction, thus reducing the acellular capillaries and

pericyte ghosts (211). Blockade of RAS with Losartan, an AT1R blocker, or Enalapril, an angiotensin-converting enzyme inhibitor, significantly reduced the progression of retinopathy by 70% and 65%, respectively, in a clinical trial involving type 1 diabetes patients with normotensive and normoalbuminuria (191). Since NADPH oxidase activity is dysregulated in DR and contributes to oxidative stress and inflammatory cascades, blocking NADPH oxidase was shown to reduce oxidative stress, NF- κ B activation, reactive NOS production, and inflammatory responses in retinal cells treated with high glucose (212, 213). Also, intravitreal injection of tissue inhibitor of matrix metalloproteinase-3 (TIMP-3) prevented BRB breakdown in diabetes and downregulated NF- κ B, ICAM-1 and VEGF (214). Urokinase plasminogen activator (uPA)/uPA receptor (uPAR) system is another pathway that was shown to disrupt BRB in DR (215, 216). uPA inhibition with a peptide inhibitor UPARANT significantly protected the BRB integrity and prevented neovascularization in DR rats (195). Additionally, UPARANT also modulates transcription factors responsible for inflammation (217).

Lastly, anti-inflammatory drugs that have demonstrated a significant reduction in inflammation associated with other complications of diabetes mellitus could be evaluated for DR (218, 219). Similarly, regular use of plant-based phytochemicals and dietary supplements with antioxidant and anti-inflammatory properties modulates persistent retinal oxidative stress and chronic inflammation in the retina and prevents DR progression (220–224). Recently, Esculeoside A (ESA), a tomato-derived glycoside, has been shown to alleviate retinopathy in an *in-vivo* rat model of T1DM. The protective mechanism is found to be mediated by the Nrf2/antioxidant axis (225). Overall, research on the drugs that could reduce oxidative stress and inflammation likely help maintain the cellular and molecular integrity of the neurovascular unit, and research along these lines is necessary to prevent complications and vision loss associated with DR.

The research landscape continues to evolve, with promising new avenues, such as gene and cell therapies, which may offer new avenues for managing diabetic eye disease. Gene therapy for diabetic retina employs gene-specific targeted therapy, which is split into two categories based on the pathophysiology of the disease (226): therapies that target pre-existing neovascularization such as the use of sFlt-1, a soluble splice variant of the VEGF receptor 1 (VEGFR-1 or Flt-1), that acts as a decoy VEGF receptor and vascular hyperpermeability (227), and therapies that try to prevent damage to retinal blood vessels such as pigment epithelium-derived factor (PEDF) (192), angiogenin (193), and glial fibrillary acidic protein (GFAP) (228) and those that protect neurons such as the AAV vectors encoding brain-derived neurotrophic factor (BDNF) (229) and erythropoietin (EPO) (230). Some research suggests that modulating ANGPTL4 expression through gene therapy could help stabilize blood vessels and reduce vascular leakage in DR (194). Clinical trials are needed to evaluate the feasibility and effectiveness of this approach. Exploratory cell therapies independent of gene therapies in DR involve the transplantation or manipulation of cells to address the underlying pathology of the disease. Some of these approaches include mesenchymal stem cells (MSCs) (231, 232) or induced

pluripotent stem cells (iPSCs) (233, 234) for their regenerative properties to replace damaged cells, promote tissue repair, or modulate the inflammatory response associated with the disease. Cell therapy approaches involving the transplantation or stimulation of endothelial progenitor cells (EPCs) and/or endothelial colony-forming cells (ECFCs) aim to enhance vascular repair mechanisms and improve blood vessel function in the retina (235). Clinical trials are ongoing to assess the safety and efficacy of EPC-based therapies in DR patients (NCT02119689).

Conclusions and future directions

In summary, the future of DR and DME management looks promising, with ongoing trials aiming to advance treatment options and improve visual outcomes. Despite the tremendous progress in understanding various cell and molecular targets in DR, several challenges need to be addressed soon in the near future. For example, DR involves multifaceted processes, including inflammation, angiogenesis, and neurodegeneration. Pinpointing specific targets within this intricate web of interactions can be challenging. Additionally, DR progresses over time, with varying molecular profiles at different stages. Identifying targets that remain relevant throughout disease progression is essential. Likely, single-target approaches may not suffice. Combining multiple therapies could yield better outcomes. We hope that as research progresses, personalized approaches and innovative treatments may transform the management of this sight-threatening condition.

Author contributions

SR: Writing – original draft, Writing – review & editing. VD: Supervision, Writing – review & editing. ATMS: Writing – original draft, Writing – review & editing. SS: Supervision, Writing – original draft, Writing – review & editing. KMRB: Supervision, Writing – review & editing. RG: Conceptualization, Supervision,

Writing – original draft, Writing – review & editing. DU: Conceptualization, Supervision, Writing – original draft, Writing – review & editing.

Funding

The author(s) declare financial support was received for the research, authorship, and/or publication of this article. This work is supported by funding from the Department of Biotechnology, Govt of India (under Grant BT/PR26814/NNT/28/1476/2017 to DU); National Eye Institute, R01EY034716 (RG); Research to Prevent Blindness (Hamilton Eye Institute). SR is supported by the CSIR (08/0602(13559)/2022-EMR-I) fellowship.

Conflict of interest

RG is a co-founder and holds equity in Cell Care Therapeutics Inc., which is interested in using adipose-derived stromal cells in visual disorders.

The remaining authors declare that the research was conducted in the absence of any commercial or financial relationships that could be construed as a potential conflict of interest.

The author(s) declared that they were an editorial board member of Frontiers, at the time of submission. This had no impact on the peer review process and the final decision.

Publisher's note

All claims expressed in this article are solely those of the authors and do not necessarily represent those of their affiliated organizations, or those of the publisher, the editors and the reviewers. Any product that may be evaluated in this article, or claim that may be made by its manufacturer, is not guaranteed or endorsed by the publisher.

References

- Ali MK, Pearson-Stuttard J, Selvin E, Gregg EW. Interpreting global trends in type 2 diabetes complications and mortality. *Diabetologia*. (2022) 65:3–13. doi: 10.1007/s00125-021-05585-2
- Chakraborty A, Hegde S, Praharaj SK, Prabhu K, Patole C, Shetty AK, et al. Age related prevalence of mild cognitive impairment in type 2 diabetes mellitus patients in the Indian population and association of serum lipids with cognitive dysfunction. *Front Endocrinol (Lausanne)*. (2021) 12:798652. doi: 10.3389/fendo.2021.798652
- Teo ZL, Tham YC, Yu M, Chee ML, Rim TH, Cheung N, et al. Global prevalence of diabetic retinopathy and projection of burden through 2045: systematic review and meta-analysis. *Ophthalmology*. (2021) 128:1580–91. doi: 10.1016/j.ophtha.2021.04.027
- Bressler NM, Beaulieu WT, Glassman AR, Blinder KJ, Bressler SB, Jampol LM, et al. Persistent macular thickening following intravitreal aflibercept, bevacizumab, or ranibizumab for central-involved diabetic macular edema with vision impairment: A secondary analysis of a randomized clinical trial. *JAMA Ophthalmol*. (2018) 136:257–69. doi: 10.1001/jamaophthalmol.2017.6565
- Kodjikian L, Bellocq D, Mathis T. Pharmacological management of diabetic macular edema in real-life observational studies. *BioMed Res Int*. (2018) 2018:8289253. doi: 10.1155/2018/8289253
- Gonzalez-Cortes JH, Martinez-Pacheco VA, Gonzalez-Cantu JE, Bilgic A, de Ribot FM, Sudhakar A, et al. Current treatments and innovations in diabetic retinopathy and diabetic macular edema. *Pharmaceutics*. (2022) 15:122. doi: 10.3390/pharmaceutics15010122
- Campbell M, Humphries P. The blood-retina barrier: tight junctions and barrier modulation. *Adv Exp Med Biol*. (2012) 763:70–84. doi: 10.1007/978-1-4614-4711-5_3
- Pan WW, Lin F, Fort PE. The innate immune system in diabetic retinopathy. *Prog Retin Eye Res*. (2021) 84:100940. doi: 10.1016/j.preteyeres.2021.100940
- Díaz-Coránguez M, Ramos C, Antonetti DA. The inner blood-retinal barrier: Cellular basis and development. *Vision Res*. (2017) 139:123–37. doi: 10.1016/j.visres.2017.05.009
- Lenin R, Thomas SM, Gangaraju R. Endothelial activation and oxidative stress in neurovascular defects of the retina. *Curr Pharm Des*. (2018) 24:4742–54. doi: 10.2174/1381612825666190115122622
- Jo DH, Yun JH, Cho CS, Kim JH, Kim JH, Cho CH. Interaction between microglia and retinal pigment epithelial cells determines the integrity of outer blood-retinal barrier in diabetic retinopathy. *Glia*. (2019) 67:321–31. doi: 10.1002/glia.23542
- Capitão M, Soares R. Angiogenesis and inflammation crosstalk in diabetic retinopathy. *J Cell Biochem*. (2016) 117:2443–53. doi: 10.1002/jcb.25575
- McLeod DS, Lefer DJ, Merges C, Luttly GA. Enhanced expression of intracellular adhesion molecule-1 and P-selectin in the diabetic human retina and choroid. *Am J Pathol*. (1995) 147:642–53.

14. Barouch FC, Miyamoto K, Allport JR, Fujita K, Bursell SE, Aiello LP, et al. Integrin-mediated neutrophil adhesion and retinal leukostasis in diabetes. *Invest Ophthalmol Vis Sci.* (2000) 41:1153–8.
15. Park DY, Lee J, Kim J, Kim K, Hong S, Han S, et al. Plastic roles of pericytes in the blood-retinal barrier. *Nat Commun.* (2017) 8:15296. doi: 10.1038/ncomms15296
16. Ogura S, Kurata K, Hattori Y, Takase H, Ishiguro-Oonuma T, Hwang Y, et al. Sustained inflammation after pericyte depletion induces irreversible blood-retina barrier breakdown. *JCI Insight.* (2017) 2:e90905. doi: 10.1172/jci.insight.90905
17. Gu X, Fliesler SJ, Zhao YY, Stallcup WB, Cohen AW, Elliott MH. Loss of caveolin-1 causes blood-retinal barrier breakdown, venous enlargement, and mural cell alteration. *Am J Pathol.* (2014) 184:541–55. doi: 10.1016/j.ajpath.2013.10.022
18. Joussen AM, Poulaki V, Le ML, Koizumi K, Esser C, Janicki H, et al. A central role for inflammation in the pathogenesis of diabetic retinopathy. *FASEB J.* (2004) 18:1450–2. doi: 10.1096/fj.03-1476fje
19. Ishida S, Usui T, Yamashiro K, Kaji Y, Ahmed E, Carrasquillo KG, et al. VEGF164 is proinflammatory in the diabetic retina. *Invest Ophthalmol Vis Sci.* (2003) 44:2155–62. doi: 10.1167/iov.02-0807
20. Harhaj NS, Felinski EA, Wolpert EB, Sundstrom JM, Gardner TW, Antonetti DA. VEGF activation of protein kinase C stimulates occludin phosphorylation and contributes to endothelial permeability. *Invest Ophthalmol Vis Sci.* (2006) 47:5106–15. doi: 10.1167/iov.06-0322
21. Wang H, Li J, Zhong P, Wang S, Zhang L, Yang R, et al. Blocking CXCR3 with AMG487 ameliorates the blood-retinal barrier disruption in diabetic mice through anti-oxidative. *Life Sci.* (2019) 228:198–207. doi: 10.1016/j.lfs.2019.04.016
22. He J, Wang H, Liu Y, Li W, Kim D, Huang H. Blockade of vascular endothelial growth factor receptor 1 prevents inflammation and vascular leakage in diabetic retinopathy. *J Ophthalmol.* (2015) 2015:605946. doi: 10.1155/2015/605946
23. Wang J, Xu X, Elliott MH, Zhu M, Le YZ. Müller cell-derived VEGF is essential for diabetes-induced retinal inflammation and vascular leakage. *Diabetes.* (2010) 59:2297–305. doi: 10.2337/db09-1420
24. Chen C, Wu S, Hong Z, Chen X, Shan X, Fischbach S, et al. Chronic hyperglycemia regulates microglia polarization through ERK5. *Aging (Albany NY).* (2019) 11:697–706. doi: 10.18632/aging.101770
25. Howell SJ, Lee CA, Batoki JC, Zapadka TE, Lindstrom SI, Taylor BE, et al. Retinal inflammation, oxidative stress, and vascular impairment is ablated in diabetic mice receiving XMD8–92 treatment. *Front Pharmacol.* (2021) 12:732630. doi: 10.3389/fphar.2021.732630
26. Lindstrom SI, Sigurdardottir S, Zapadka TE, Tang J, Liu H, Taylor BE, et al. Diabetes induces IL-17A-Act1-FADD-dependent retinal endothelial cell death and capillary degeneration. *J Diabetes Complications.* (2019) 33:668–74. doi: 10.1016/j.jdiacomp.2019.05.016
27. Zhou AY, Taylor BE, Barber KG, Lee CA, Taylor ZRR, Howell SJ, et al. Anti-IL17A halts the onset of diabetic retinopathy in type I and II diabetic mice. *Int J Mol Sci.* (2023) 24:1347. doi: 10.3390/ijms24021347
28. Tonade D, Liu H, Kern TS. Photoreceptor cells produce inflammatory mediators that contribute to endothelial cell death in diabetes. *Invest Ophthalmol Vis Sci.* (2016) 57:4264–71. doi: 10.1167/iov.16-19859
29. Tonade D, Liu H, Palczewski K, Kern TS. Photoreceptor cells produce inflammatory products that contribute to retinal vascular permeability in a mouse model of diabetes. *Diabetologia.* (2017) 60:2111–20. doi: 10.1007/s00125-017-4381-5
30. Bohley M, Dillinger AE, Tamm ER, Goepferich A. Targeted drug delivery to the retinal pigment epithelium: Untapped therapeutic potential for retinal diseases. *Drug Discovery Today.* (2022) 27:2497–509. doi: 10.1016/j.drudis.2022.05.024
31. Tanihara H, Inatani M, Honda Y. Growth factors and their receptors in the retina and pigment epithelium. *Prog retinal eye Res.* (1997) 16:271–301. doi: 10.1016/S1350-9462(96)00028-6
32. Wang Y, Liu X, Quan X, Qin X, Zhou Y, Liu Z, et al. Pigment epithelium-derived factor and its role in microvascular-related diseases. *Biochimie.* (2022) 200:153–71. doi: 10.1016/j.biochi.2022.05.019
33. Zhang SX, Wang JJ, Gao G, Shao C, Mott R, Ma J. Pigment epithelium-derived factor (PEDF) is an endogenous antiinflammatory factor. *FASEB J.* (2006) 20:323–5. doi: 10.1096/fj.05-4313fje
34. Antonetti DA, Barber AJ, Khin S, Lieth E, Tarbell JM, Gardner TW. Vascular permeability in experimental diabetes is associated with reduced endothelial occludin content: vascular endothelial growth factor decreases occludin in retinal endothelial cells. *Penn State Retina Res Group Diabetes.* (1998) 47:1953–9. doi: 10.2337/diabetes.47.12.1953
35. Yun JH, Park SW, Kim KJ, Bae JS, Lee EH, Paek SH, et al. Endothelial STAT3 activation increases vascular leakage through downregulating tight junction proteins: implications for diabetic retinopathy. *J Cell Physiol.* (2017) 232:1123–34. doi: 10.1002/jcp.25575
36. Rizzolo LJ. Polarity and the development of the outer blood-retinal barrier. *Histol Histopathol.* (1997) 12:1057–67.
37. Caceres PS, Rodriguez-Boulan E. Retinal pigment epithelium polarity in health and blinding diseases. *Curr Opin Cell Biol.* (2020) 62:37–45. doi: 10.1016/j.ccb.2019.08.001
38. Cho H, Alwassia AA, Regatieri CV, Zhang JY, Bauman C, Waheed N, et al. Retinal neovascularization secondary to proliferative diabetic retinopathy characterized by spectral domain optical coherence tomography. *Retina.* (2013) 33:542–7. doi: 10.1097/IAE.0b013e3182753b6f
39. Antonetti DA, Silva PS, Stitt AW. Current understanding of the molecular and cellular pathology of diabetic retinopathy. *Nat Rev Endocrinol.* (2021) 17:195–206. doi: 10.1038/s41574-020-00451-4
40. Holmes DI, Zachary I. The vascular endothelial growth factor (VEGF) family: angiogenic factors in health and disease. *Genome Biol.* (2005) 6:209. doi: 10.1186/gb-2005-6-2-209
41. Gomulka K, Liebhart J, Jaskula E, Lange A, Medrala W. The -2549 -2567 del18 polymorphism in VEGF and irreversible bronchoconstriction in asthmatics. *J Invest Allergol Clin Immunol.* (2019) 29:431–5. doi: 10.18176/jiaci.0369
42. Levy AP, Levy NS, Goldberg MA. Post-transcriptional regulation of vascular endothelial growth factor by hypoxia. *J Biol Chem.* (1996) 271:2746–53. doi: 10.1074/jbc.271.5.2746
43. Levy NS, Chung S, Furneaux H, Levy AP. Hypoxic stabilization of vascular endothelial growth factor mRNA by the RNA-binding protein HuR. *J Biol Chem.* (1998) 273:6417–23. doi: 10.1074/jbc.273.11.6417
44. Penn JS, Madan A, Caldwell RB, Bartoli M, Caldwell RW, Hartnett ME. Vascular endothelial growth factor in eye disease. *Prog Retin Eye Res.* (2008) 27:331–71. doi: 10.1016/j.preteyeres.2008.05.001
45. Sarkar J, Luo Y, Zhou Q, Ivakhniatskaia E, Lara D, Katz E, et al. VEGF receptor heterodimers and homodimers are differentially expressed in neuronal and endothelial cell types. *PLoS One.* (2022) 17:e0269818. doi: 10.1371/journal.pone.0269818
46. Fantin A, Herzog B, Mahmoud M, Yamaji M, Plein A, Denti L, et al. Neuropilin 1 (NRP1) hypomorphism combined with defective VEGF-A binding reveals novel roles for NRP1 in developmental and pathological angiogenesis. *Development.* (2014) 141:556–62. doi: 10.1242/dev.103028
47. Papapetropoulos A, García-Cardeña G, Madri JA, Sessa WC. Nitric oxide production contributes to the angiogenic properties of vascular endothelial growth factor in human endothelial cells. *J Clin Invest.* (1997) 100:3131–9. doi: 10.1172/JCI119868
48. Wang X, Bove AM, Simone G, Ma B. Molecular bases of VEGFR-2-mediated physiological function and pathological role. *Front Cell Dev Biol.* (2020) 8:599281. doi: 10.3389/fcell.2020.599281
49. Praidou A, Klangas I, Papakonstantinou E, Androudi S, Georgiadis N, Karakiulakis G, et al. Vitreous and serum levels of platelet-derived growth factor and their correlation in patients with proliferative diabetic retinopathy. *Curr Eye Res.* (2009) 34:152–61. doi: 10.1080/02713680802585920
50. Shen S, Wang F, Fernandez A, Hu W. Role of platelet-derived growth factor in type II diabetes mellitus and its complications. *Diabetes Vasc Dis Res.* (2020) 17:1479164120942119. doi: 10.1177/1479164120942119
51. Lefevre E, Van Hove I, Sergeys J, Steel DHW, Schlingemann R, Moons L, et al. PDGF as an important initiator for neurite outgrowth associated with fibrovascular membranes in proliferative diabetic retinopathy. *Curr Eye Res.* (2022) 47:277–86. doi: 10.1080/02713683.2021.1966479
52. Freyberger H, Bröcker M, Yakut H, Hammer J, Effert R, Schifferdecker E, et al. Increased levels of platelet-derived growth factor in vitreous fluid of patients with proliferative diabetic retinopathy. *Exp Clin Endocrinol Diabetes.* (2000) 108:106–9. doi: 10.1055/s-2000-5803
53. Mori K, Gehlbach P, Ando A, Dyer G, Lipinsky E, Chaudhry AG, et al. Retina-specific expression of PDGF-B versus PDGF-A: vascular versus nonvascular proliferative retinopathy. *Invest Ophthalmol Vis Sci.* (2002) 43:2001–6.
54. Gong CY, Lu B, Sheng YC, Yu ZY, Zhou JY, Ji LL. The development of diabetic retinopathy in goto-kakizaki rat and the expression of angiogenesis-related signals. *Chin J Physiol.* (2016) 59:100–8. doi: 10.4077/CJP.2016.BAE383
55. Zhou L, Sun X, Huang Z, Zhou T, Zhu X, Liu Y, et al. Imatinib ameliorated retinal neovascularization by suppressing PDGFR- α and PDGFR- β . *Cell Physiol Biochem.* (2018) 48:263–73. doi: 10.1159/000491726
56. Tang Z, Arjunan P, Lee C, Li Y, Kumar A, Hou X, et al. Survival effect of PDGF-CC rescues neurons from apoptosis in both brain and retina by regulating GSK3 β phosphorylation. *J Exp Med.* (2010) 207:867–80. doi: 10.1084/jem.20091704
57. Hollborn M, Tenckhoff S, Seifert M, Köhler S, Wiedemann P, Bringmann A, et al. Human retinal epithelium produces and responds to placenta growth factor. *Graefes Arch Clin Exp Ophthalmol.* (2006) 244:732–41. doi: 10.1007/s00417-005-0154-9
58. Miyamoto N, de Kozak Y, Jeanny JC, Glotin A, Mascarelli F, Massin P, et al. Placental growth factor-1 and epithelial haemato-retinal barrier breakdown: potential implication in the pathogenesis of diabetic retinopathy. *Diabetologia.* (2007) 50:461–70. doi: 10.1007/s00125-006-0539-2
59. Miyamoto N, de Kozak Y, Normand N, Courtois Y, Jeanny JC, Benezra D, et al. PlGF-1 and VEGF-1 pathway regulation of the external epithelial hemato-ocular barrier. A model for retinal edema. *Ophthalmic Res.* (2008) 40:203–7. doi: 10.1159/000119877
60. Zhao B, Cai J, Boulton M. Expression of placenta growth factor is regulated by both VEGF and hyperglycaemia via VEGFR-2. *Microvasc Res.* (2004) 68:239–46. doi: 10.1016/j.mvr.2004.07.004
61. Yonekura H, Sakurai S, Liu X, Migita H, Wang H, Yamagishi S, et al. Placenta growth factor and vascular endothelial growth factor B and C expression in

microvascular endothelial cells and pericytes. Implication in autocrine and paracrine regulation of angiogenesis. *J Biol Chem.* (1999) 274:35172–8. doi: 10.1074/jbc.274.49.35172

62. De Falco S. The discovery of placenta growth factor and its biological activity. *Exp Mol Med.* (2012) 44:1–9. doi: 10.3858/emmm.2012.44.1.025

63. Ando H, Asai T, Koide H, Okamoto A, Maeda N, Tomita K, et al. Advanced cancer therapy by integrative antitumor actions via systemic administration of miR-499. *J Control Release.* (2014) 181:32–9. doi: 10.1016/j.jconrel.2014.02.019

64. Kovacs K, Marra KV, Yu G, Wagley S, Ma J, Teague GC, et al. Angiogenic and inflammatory vitreous biomarkers associated with increasing levels of retinal ischemia. *Invest Ophthalmol Vis Sci.* (2015) 56:6523–30. doi: 10.1167/iops.15–16793

65. Huang H, He J, Johnson D, Wei Y, Liu Y, Wang S, et al. Deletion of placental growth factor prevents diabetic retinopathy and is associated with Akt activation and HIF1 α -VEGF pathway inhibition. *Diabetes.* (2015) 64:200–12. doi: 10.2337/db14–0016

66. Van Bergen T, Etienne I, Cunningham F, Moons L, Schlingemann RO, Feyen JHM, et al. The role of placental growth factor (PlGF) and its receptor system in retinal vascular diseases. *Prog Retin Eye Res.* (2019) 69:116–36. doi: 10.1016/j.preteyeres.2018.10.006

67. Van Bergen T, Hu TT, Etienne I, Reyns GE, Moons L, Feyen JHM. Neutralization of placental growth factor as a novel treatment option in diabetic retinopathy. *Exp Eye Res.* (2017) 165:136–50. doi: 10.1016/j.exer.2017.09.012

68. Gau D, Vignaud L, Allen A, Guo Z, Sahel J, Boone D, et al. Disruption of profilin function suppresses developmental and pathological retinal neovascularization. *J Biol Chem.* (2020) 295:9618–29. doi: 10.1074/jbc.RA120.012613

69. Gau D, Vignaud L, Francoeur P, Koes D, Guillonnet X, Roy P. Inhibition of ocular neovascularization by novel anti-angiogenic compound. *Exp Eye Res.* (2021) 213:108861. doi: 10.1016/j.exer.2021.108861

70. Bhakuni T, Norden PR, Ujije N, Tan C, Lee SK, Tedeschi T, et al. FOXC1 regulates endothelial CD98 (LAT1/4F2hc) expression in retinal angiogenesis and blood-retina barrier formation. *Nat Commun.* (2024) 15:4097. doi: 10.1038/s41467–024-48134–2

71. Pongsachareonont P, Charoenphol P, Hurst C, Somkijrungsroj T. The effect of anti-vascular endothelial growth factor on retinal microvascular changes in diabetic macular edema using swept-source optical coherence tomography angiography. *Clin Ophthalmol.* (2020) 14:3871–388. doi: 10.2147/OPTH.S270410

72. Wang H, Chhablani J, Freeman WR, Chan CK, Kozak I, Bartsch DU, et al. Characterization of diabetic microaneurysms by simultaneous fluorescein angiography and spectral-domain optical coherence tomography. *Am J Ophthalmol.* (2012) 153:861–7. doi: 10.1016/j.ajo.2011.10.005

73. An D, Balaratnasingam C, Heisler M, Francke A, Ju M, McAllister IL, et al. Quantitative comparisons between optical coherence tomography angiography and matched histology in the human eye. *Exp Eye Res.* (2018) 170:13–9. doi: 10.1016/j.exer.2018.02.006

74. An D, Tan B, Yu DY, Balaratnasingam C. Differentiating microaneurysm pathophysiology in diabetic retinopathy through objective analysis of capillary nonperfusion, inflammation, and pericytes. *Diabetes.* (2022) 71:733–46. doi: 10.2337/db21–0737

75. Tolentino MJ, Miller JW, Gragoudas ES, Jakobiec FA, Flynn E, Chatzistefanou K, et al. Intravitreal injections of vascular endothelial growth factor produce retinal ischemia and microangiopathy in an adult primate. *Ophthalmology.* (1996) 103:1820–8. doi: 10.1016/s0161–6420(96)30420–x

76. Sugimoto M, Ichio A, Mochida D, Tenma Y, Miyata R, Matsubara H, et al. Multiple effects of intravitreal aflibercept on microvascular regression in eyes with diabetic macular edema. *Ophthalmol Retina.* (2019) 3:1067–75. doi: 10.1016/j.joret.2019.06.005

77. Takamura Y, Yamada Y, Noda K, Morioka M, Hashimoto Y, Gozawa M, et al. Characteristic distribution of microaneurysms and capillary dropouts in diabetic macular edema. *Graefes Arch Clin Exp Ophthalmol.* (2020) 258:1625–30. doi: 10.1007/s00417–020-04722–8

78. Yamada Y, Takamura Y, Matsumura T, Gozawa M, Morioka M, Inatani M. Regional variety of reduction in retinal thickness of diabetic macular edema after anti-VEGF treatment. *Medicina (Kaunas).* (2022) 58:933. doi: 10.3390/medicina58070933

79. Yamada Y, Takamura Y, Morioka M, Gozawa M, Matsumura T, Inatani M. Microaneurysm density in residual oedema after anti-vascular endothelial growth factor therapy for diabetic macular oedema. *Acta Ophthalmol.* (2021) 99:e876–83. doi: 10.1111/aos.14706

80. Lindahl P, Johansson BR, Levéen P, Betsholtz C. Pericyte loss and microaneurysm formation in PDGF-B-deficient mice. *Science.* (1997) 277:242–5. doi: 10.1126/science.277.5323.242

81. Armulik A, Genové G, Betsholtz C. Pericytes: developmental, physiological, and pathological perspectives, problems, and promises. *Dev Cell.* (2011) 21:193–215. doi: 10.1016/j.devcel.2011.07.001

82. Sims DE. The pericyte—A review. *Tissue Cell.* (1986) 18:153–74. doi: 10.1016/0040-8166(86)90026-1

83. Pfister F, Feng Y, vom Hagen F, Hoffmann S, Molema G, Hillebrands JL, et al. Pericyte migration: a novel mechanism of pericyte loss in experimental diabetic retinopathy. *Diabetes.* (2008) 57:2495–502. doi: 10.2337/db08–0325

84. Enge M, Bjarnegård M, Gerhardt H, Gustafsson E, Kalén M, Asker N, et al. Endothelium-specific platelet-derived growth factor-B ablation mimics diabetic retinopathy. *EMBO J.* (2002) 21:4307–16. doi: 10.1093/emboj/cdf418

85. Toh H, Smolentsev A, Bozadjian RV, Keeley PW, Lockwood MD, Sadjadi R, et al. Vascular changes in diabetic retinopathy—a longitudinal study in the Nile rat. *Lab Invest.* (2019) 99:1547–60. doi: 10.1038/s41374–019-0264–3

86. Gerales P, Hiraoka-Yamamoto J, Matsumoto M, Clermont A, Leitges M, Marete A, et al. Activation of PKC-delta and SHP-1 by hyperglycemia causes vascular cell apoptosis and diabetic retinopathy. *Nat Med.* (2009) 15:1298–306. doi: 10.1038/nm.2052

87. Benjamin LE, Hemo I, Keshet E. A plasticity window for blood vessel remodelling is defined by pericyte coverage of the preformed endothelial network and is regulated by PDGF-B and VEGF. *Development.* (1998) 125:1591–8. doi: 10.1242/dev.125.9.1591

88. Augustin HG, Koh GY, Thurston G, Alitalo K. Control of vascular morphogenesis and homeostasis through the angiopoietin-Tie system. *Nat Rev Mol Cell Biol.* (2009) 10:165–77. doi: 10.1038/nrm2639

89. Darland DC, Massingham LJ, Smith SR, Piek E, Saint-Geniez M, D'Amore PA. Pericyte production of cell-associated VEGF is differentiation-dependent and is associated with endothelial survival. *Dev Biol.* (2003) 264:275–88. doi: 10.1016/j.ydbio.2003.08.015

90. Liu C, Ge HM, Liu BH, Dong R, Shan K, Chen X, et al. Targeting pericyte-endothelial cell crosstalk by circular RNA-cPWWP2A inhibition aggravates diabetes-induced microvascular dysfunction. *Proc Natl Acad Sci U S A.* (2019) 116:7455–64. doi: 10.1073/pnas.1814874116

91. Sadiq MA, Hanout M, Sarwar S, Hassan M, Agarwal A, Sepah YJ, et al. Platelet-derived growth factor inhibitors: A potential therapeutic approach for ocular neovascularization. *Dev Ophthalmol.* (2016) 55:310–6. doi: 10.1159/000438953

92. Archer DB. Bowman Lecture 1998. Diabetic retinopathy: some cellular, molecular and therapeutic considerations. *Eye (Lond).* (1999) 13:497–523. doi: 10.1038/eye.1999.130

93. Kim K, Kim ES, Yu SY. Longitudinal relationship between retinal diabetic neurodegeneration and progression of diabetic retinopathy in patients with type 2 diabetes. *Am J Ophthalmol.* (2018) 196:165–72. doi: 10.1016/j.ajo.2018.08.053

94. Katsuyama A, Kusuhara S, Asahara SI, Nakai SI, Mori S, Matsumiya W, et al. En face slab optical coherence tomography imaging successfully monitors progressive degenerative changes in the innermost layer of the diabetic retina. *BMJ Open Diabetes Res Care.* (2020) 8:e001120. doi: 10.1136/bmjdr-2019–001120

95. De Clerck EEB, Schouten JSAG, Berendschot TTTJM, Goezinne F, Dagnelie PC, Schaper NC, et al. Macular thinning in prediabetes or type 2 diabetes without diabetic retinopathy: the Maastricht Study. *Acta Ophthalmol.* (2018) 96:174–82. doi: 10.1111/aos.13570

96. Karaca C, Karaca Z. Beyond hyperglycemia, evidence for retinal neurodegeneration in metabolic syndrome. *Invest Ophthalmol Vis Sci.* (2018) 59:1360–7. doi: 10.1167/iops.17–23376

97. Shi R, Guo Z, Wang F, Li R, Zhao L, Lin R. Alterations in retinal nerve fiber layer thickness in early stages of diabetic retinopathy and potential risk factors. *Curr Eye Res.* (2018) 43:244–53. doi: 10.1080/02713683.2017.1387669

98. Barber AJ, Lieth E, Khin SA, Antonetti DA, Buchanan AG, Gardner TW. Neural apoptosis in the retina during experimental and human diabetes. Early onset and effect of insulin. *J Clin Invest.* (1998) 102:783–91. doi: 10.1172/JCI2425

99. Sohn EH, van Dijk HW, Jiao C, Kok PH, Jeong W, Demirkaya N, et al. Retinal neurodegeneration may precede microvascular changes characteristic of diabetic retinopathy in diabetes mellitus. *Proc Natl Acad Sci U S A.* (2016) 113:E2655–64. doi: 10.1073/pnas.1522014113

100. Feenstra DJ, Yego EC, Mohr S. Modes of retinal cell death in diabetic retinopathy. *J Clin Exp Ophthalmol.* (2013) 4:298. doi: 10.4172/2155–9570.1000298

101. Scarinci F, Picconi F, Virgili G, Giorno P, Di Renzo A, Varano M, et al. Single retinal layer evaluation in patients with type 1 diabetes with no or early signs of diabetic retinopathy: the first hint of neurovascular crosstalk damage between neurons and capillaries? *Ophthalmologica.* (2017) 237:223–31. doi: 10.1159/000453551

102. Mizutani M, Kern TS, Lorenzi M. Accelerated death of retinal microvascular cells in human and experimental diabetic retinopathy. *J Clin Invest.* (1996) 97:2883–90. doi: 10.1172/JCI118746

103. Joussen AM, Murata T, Tsujikawa A, Kirchhof B, Bursell SE, Adamis AP. Leukocyte-mediated endothelial cell injury and death in the diabetic retina. *Am J Pathol.* (2001) 158:147–52. doi: 10.1016/S0002–9440(10)63952–1

104. Busik JV, Mohr S, Grant MB. Hyperglycemia-induced reactive oxygen species toxicity to endothelial cells is dependent on paracrine mediators. *Diabetes.* (2008) 57:1952–65. doi: 10.2337/db07–1520

105. Romeo G, Liu WH, Asnaghi V, Kern TS, Lorenzi M. Activation of nuclear factor-kappaB induced by diabetes and high glucose regulates a proapoptotic program in retinal pericytes. *Diabetes.* (2002) 51:2241–8. doi: 10.2337/diabetes.51.7.2241

106. Podestà F, Romeo G, Liu WH, Krajewski S, Reed JC, Gerhardinger C, et al. Bax is increased in the retina of diabetic subjects and is associated with pericyte apoptosis in vivo and in vitro. *Am J Pathol.* (2000) 156:1025–32. doi: 10.1016/S0002–9440(10)64970-X

107. Asnaghi V, Gerhardinger C, Hoehn T, Adeboye A, Lorenzi M. A role for the polyol pathway in the early neuroretinal apoptosis and glial changes induced by diabetes in the rat. *Diabetes*. (2003) 52:506–11. doi: 10.2337/diabetes.52.2.506
108. Reddy SK, Ballal AR, Shailaja S, Seetharam RN, Raghu CH, Sankhe R, et al. Small extracellular vesicle-loaded bevacizumab reduces the frequency of intravitreal injection required for diabetic retinopathy. *Theranostics*. (2023) 13:2241–55. doi: 10.7150/thno.78426
109. Alves MRP, Boia R, Campos EJ, Martins J, Nunes S, Madeira MH, et al. Subtle thinning of retinal layers without overt vascular and inflammatory alterations in a rat model of prediabetes. *Mol Vis*. (2018) 24:353–66.
110. van Dijk HW, Verbraak FD, Stehouwer M, Kok PH, Garvin MK, Sonka M, et al. Association of visual function and ganglion cell layer thickness in patients with diabetes mellitus type 1 and no or minimal diabetic retinopathy. *Vision Res*. (2011) 51:224–8. doi: 10.1016/j.visres.2010.08.024
111. Brown GC, Neher JJ. Microglial phagocytosis of live neurons. *Nat Rev Neurosci*. (2014) 15:209–16. doi: 10.1038/nrn3710
112. Mohr S, Xi X, Tang J, Kern TS. Caspase activation in retinas of diabetic and galactosemic mice and diabetic patients. *Diabetes*. (2002) 51:1172–9. doi: 10.2337/diabetes.51.4.1172
113. Vincent JA, Mohr S. Inhibition of caspase-1/interleukin-1 β signaling prevents degeneration of retinal capillaries in diabetes and galactosemia. *Diabetes*. (2007) 56:224–30. doi: 10.2337/db06-0427
114. Ly A, Yee P, Vessey KA, Phipps JA, Jobling AI, Fletcher EL. Early inner retinal astrocyte dysfunction during diabetes and development of hypoxia, retinal stress, and neuronal functional loss. *Invest Ophthalmol Vis Sci*. (2011) 52:9316–26. doi: 10.1167/iov.11-7879
115. Rossino MG, Dal Monte M, Casini G. Relationships between neurodegeneration and vascular damage in diabetic retinopathy. *Front Neurosci*. (2019) 13:1172. doi: 10.3389/fnins.2019.01172
116. Kowluru RA, Koppolu P. Diabetes-induced activation of caspase-3 in retina: effect of antioxidant therapy. *Free Radic Res*. (2002) 36:993–9. doi: 10.1080/1071576021000006572
117. Simó R, Stitt AW, Gardner TW. Neurodegeneration in diabetic retinopathy: does it really matter? *Diabetologia*. (2018) 61:1902–12. doi: 10.1007/s00125-018-4692-1
118. Gardner TW, Davila JR. The neurovascular unit and the pathophysiologic basis of diabetic retinopathy. *Graefes Arch Clin Exp Ophthalmol*. (2017) 255:1–6. doi: 10.1007/s00417-016-3548-y
119. Yang S, Zhang J, Chen L. The cells involved in the pathological process of diabetic retinopathy. *BioMed Pharmacother*. (2020) 132:110818. doi: 10.1016/j.biopha.2020.110818
120. Fang W, Huang X, Wu K, Zong Y, Yu J, Xu H, et al. Activation of the GABA- α receptor by berberine rescues retinal ganglion cells to attenuate experimental diabetic retinopathy. *Front Mol Neurosci*. (2022) 15:930599. doi: 10.3389/fnmol.2022.930599
121. Ali SA, Zaitone SA, Dessouki AA, Ali AA. Pregabalin affords retinal neuroprotection in diabetic rats: Suppression of retinal glutamate, microglia cell expression and apoptotic cell death. *Exp eye Res*. (2019) 184:78–90. doi: 10.1016/j.exer.2019.04.014
122. AB R, SR K, Chandran D, Hegde S, Upadhyay R, Se PK, et al. Cell-specific extracellular vesicle-encapsulated exogenous GABA controls seizures in epilepsy. *Stem Cell Res Ther*. (2024) 15:108. doi: 10.1186/s13287-024-03721-4
123. Kimura A, Namekata K, Guo X, Harada C, Harada T. Neuroprotection, growth factors and BDNF-trkB signalling in retinal degeneration. *Int J Mol Sci*. (2016) 17:1584. doi: 10.3390/ijms17091584
124. Park KS, Kim SS, Kim JC, Kim HC, Im YS, Ahn CW, et al. Serum and tear levels of nerve growth factor in diabetic retinopathy patients. *Am J Ophthalmol*. (2008) 145:432–7. doi: 10.1016/j.ajo.2007.11.011
125. Ali TK, Al-Gayyar MMH, Matragoon S, Pillai BA, Abdelsaid MA, Nussbaum JJ, et al. Diabetes-induced peroxynitrite impairs the balance of pro-nerve growth factor and nerve growth factor, and causes neurovascular injury. *Diabetologia*. (2011) 54:657–68. doi: 10.1007/s00125-010-1935-1
126. Al-Gayyar MM, Matragoon S, Pillai BA, Ali TK, Abdelsaid MA, El-Remessy AB. Epicatechin blocks pro-nerve growth factor (proNGF)-mediated retinal neurodegeneration via inhibition of p75 neurotrophin receptor expression in a rat model of diabetes. *Diabetologia*. (2011) 54:669–80. doi: 10.1007/s00125-010-1994-3
127. Ali TK, Matragoon S, Pillai BA, Liou GI, El-Remessy AB. Peroxynitrite mediates retinal neurodegeneration by inhibiting nerve growth factor survival signaling in experimental and human diabetes. *Diabetes*. (2008) 57:889–98. doi: 10.2337/db07-1669
128. Barcelona PF, Sitaras N, Galan A, Esquivá G, Jmaeff S, Jian Y, et al. p75^{NTR} and its ligand proNGF activate paracrine mechanisms etiological to the vascular, inflammatory, and neurodegenerative pathologies of diabetic retinopathy. *J Neurosci*. (2016) 36:8826–41. doi: 10.1523/JNEUROSCI.4278-15.2016
129. Hammes HP, Federoff HJ, Brownlee M. Nerve growth factor prevents both neuroretinal programmed cell death and capillary pathology in experimental diabetes. *Mol Med*. (1995) 1:527–34. doi: 10.1007/BF03401589
130. Colafrancesco V, Coassin M, Rossi S, Aloe L. Effect of eye NGF administration on two animal models of retinal ganglion cells degeneration. *Ann Ist Super Sanita*. (2011) 47:284–9. doi: 10.4415/ANN_11_03_08
131. Taşlıpınar Uzel AG, Uğurlu N, Toklu Y, Çiçek M, Boral B, Şener B, et al. Relationship between stages of diabetic retinopathy and levels of brain-derived neurotrophic factor in aqueous humor and serum. *Retina*. (2020) 40:121–5. doi: 10.1097/IAE.0000000000002355
132. Kim ST, Chung YY, Hwang HI, Shin HK, Choi R, Jun YH. Differential expression of BDNF and BIM in streptozotocin-induced diabetic rat retina after fluoxetine injection. *In Vivo*. (2021) 35:1461–6. doi: 10.21873/in vivo.12398
133. Seki M, Tanaka T, Nawa H, Usui T, Fukuchi T, Ikeda K, et al. Involvement of brain-derived neurotrophic factor in early retinal neuropathy of streptozotocin-induced diabetes in rats: therapeutic potential of brain-derived neurotrophic factor for dopaminergic amacrine cells. *Diabetes*. (2004) 53:2412–9. doi: 10.2337/diabetes.53.9.2412
134. Le YZ, Xu B, Chucair-Elliott AJ, Zhang H, Zhu M. VEGF mediates retinal müller cell viability and neuroprotection through BDNF in diabetes. *Biomolecules*. (2021) 11:712. doi: 10.3390/biom11050712
135. Li KR, Huan MJ, Yao J, Li JJ, Cao Y, Wang S, et al. Syn3, a newly developed cyclic peptide and BDNF signaling enhancer, ameliorates retinal ganglion cell degeneration in diabetic retinopathy. *Protein Cell*. (2024) 14:pwae028. doi: 10.1093/procel/pwae028
136. Boss JD, Singh PK, Pandya HK, Tosi J, Kim C, Tewari A, et al. Assessment of neurotrophins and inflammatory mediators in vitreous of patients with diabetic retinopathy. *Invest Ophthalmol Vis Sci*. (2017) 58:5594–603. doi: 10.1167/iov.17-21973
137. Abu El-Asrar AM, Mohammad G, De Hertogh G, Nawaz MI, Van Den Eynde K, Siddiquei MM, et al. Neurotrophins and neurotrophin receptors in proliferative diabetic retinopathy. *PloS One*. (2013) 8:e65472. doi: 10.1371/journal.pone.0065472
138. Herdade AS, Silva IM, Calado Â, Saldanha C, Nguyen NH, Hou I, et al. Effects of diabetes on microcirculation and leukostasis in retinal and non-ocular tissues: implications for diabetic retinopathy. *Biomolecules*. (2020) 10:1583. doi: 10.3390/biom10111583
139. Abiko T, Abiko A, Clermont AC, Shoelson B, Horio N, Takahashi J, et al. Characterization of retinal leukostasis and hemodynamics in insulin resistance and diabetes: role of oxidants and protein kinase-C activation. *Diabetes*. (2003) 52:829–37. doi: 10.2337/diabetes.52.3.829
140. Gorudko IV, Kostevich AV, Sokolov AV, Konstantinova EE, Tsapaeva NL, Mironova EV, et al. [Increased myeloperoxidase activity is a risk factor for ischemic heart disease in patients with diabetes mellitus]. *BioMed Khim*. (2012) 58:475–84. doi: 10.18097/pbmc20125804475
141. Dai Y, Wu Z, Wang F, Zhang Z, Yu M. Identification of chemokines and growth factors in proliferative diabetic retinopathy vitreous. *BioMed Res Int*. (2014) 2014:486386. doi: 10.1155/2014/486386
142. Gomulka K, Ruta M. The role of inflammation and therapeutic concepts in diabetic retinopathy-A short review. *Int J Mol Sci*. (2023) 24:1024. doi: 10.3390/ijms24021024
143. Schröder S, Palinski W, Schmid-Schönbein GW. Activated monocytes and granulocytes, capillary nonperfusion, and neovascularization in diabetic retinopathy. *Am J Pathol*. (1991) 139:81–100.
144. Ma P, Luo Y, Zhu X, Ma H, Hu J, Tang S. Phosphomannopentaose sulfate (PI-88) inhibits retinal leukostasis in diabetic rat. *Biochem Biophys Res Commun*. (2009) 380:402–6. doi: 10.1016/j.bbrc.2009.01.092
145. Tang J, Kern TS. Inflammation in diabetic retinopathy. *Prog Retin Eye Res*. (2011) 30:343–58. doi: 10.1016/j.preteyeres.2011.05.002
146. Kim SY, Johnson MA, McLeod DS, Alexander T, Hansen BC, Luty GA. Neutrophils are associated with capillary closure in spontaneously diabetic monkey retinas. *Diabetes*. (2005) 54:1534–42. doi: 10.2337/diabetes.54.5.1534
147. Jousen AM, Poulaki V, Mitsiades N, Cai WY, Suzuma I, Pak J, et al. Suppression of Fas-FasL-induced endothelial cell apoptosis prevents diabetic blood-retinal barrier breakdown in a model of streptozotocin-induced diabetes. *FASEB J*. (2003) 17:76–8. doi: 10.1096/fj.02-0157fje
148. Leal EC, Manivannan A, Hosoya K, Terasaki T, Cunha-Vaz J, Ambrósio AF, et al. Inducible nitric oxide synthase isoform is a key mediator of leukostasis and blood-retinal barrier breakdown in diabetic retinopathy. *Invest Ophthalmol Vis Sci*. (2007) 48:5257–65. doi: 10.1167/iov.07-0112
149. Rübsam A, Parikh S, Fort PE. Role of inflammation in diabetic retinopathy. *Int J Mol Sci*. (2018) 19:942. doi: 10.3390/ijms19040942
150. Forrester JV, Kuffova L, Delibegovic M. The role of inflammation in diabetic retinopathy. *Front Immunol*. (2020) 11:583687. doi: 10.3389/fimmu.2020.583687
151. Esposito K, Nappo F, Marfella R, Giugliano G, Giugliano F, Ciotola M, et al. Inflammatory cytokine concentrations are acutely increased by hyperglycemia in humans: role of oxidative stress. *Circulation*. (2002) 106:2067–72. doi: 10.1161/01.cir.0000034509.14906.ae
152. Spranger J, Meyer-Schwickerath R, Klein M, Schatz H, Pfeiffer A. TNF- α -Spiegel im Glaskörper. Anstieg bei neovaskulären Augenkrankheiten und proliferativer diabetischer Retinopathie [TNF- α level in the vitreous body. Increase in neovascular eye diseases and proliferative diabetic retinopathy]. *Med Klin (Munich)*. (1995) 90:134–7.

153. Armstrong D, Augustin AJ, Spengler R, Al-Jada A, Nickola T, Grus F, et al. Detection of vascular endothelial growth factor and tumor necrosis factor alpha in epiretinal membranes of proliferative diabetic retinopathy, proliferative vitreoretinopathy and macular pucker. *Ophthalmologica*. (1998) 212:410–4. doi: 10.1159/00027378
154. Limb GA, Chignell AH, Green W, LeRoy F, Dumonde DC. Distribution of TNF alpha and its reactive vascular adhesion molecules in fibrovascular membranes of proliferative diabetic retinopathy. *Br J Ophthalmol*. (1996) 80:168–73. doi: 10.1136/bjo.80.2.168
155. Demircan N, Safran BG, Soylu M, Ozcan AA, Sizmaz S. Determination of vitreous interleukin-1 (IL-1) and tumour necrosis factor (TNF) levels in proliferative diabetic retinopathy. *Eye (Lond)*. (2006) 20:1366–9. doi: 10.1038/sj.eye.6702138
156. Behl Y, Krothapalli P, Desta T, DiPiazza A, Roy S, Graves DT. Diabetes-enhanced tumor necrosis factor-alpha production promotes apoptosis and the loss of retinal microvascular cells in type 1 and type 2 models of diabetic retinopathy. *Am J Pathol*. (2008) 172:1411–8. doi: 10.2353/ajpath.2008.071070
157. Soto I, Krebs MP, Reagan AM, Howell GR. Vascular inflammation risk factors in retinal disease. *Annu Rev Vis Sci*. (2019) 5:99–122. doi: 10.1146/annurev-vision-091517-034416
158. Ellis MP, Lent-Schochet D, Lo T, Yiu G. Emerging concepts in the treatment of diabetic retinopathy. *Curr Diabetes Rep*. (2019) 19:137. doi: 10.1007/s11892-019-1276-5
159. Chen W, Esselman WJ, Jump DB, Busik JV. Anti-inflammatory effect of docosahexaenoic acid on cytokine-induced adhesion molecule expression in human retinal vascular endothelial cells. *Invest Ophthalmol Vis Sci*. (2005) 46:4342–7. doi: 10.1167/iovs.05-0601
160. Meleth AD, Agrón E, Chan CC, Reed GF, Arora K, Byrnes G, et al. Serum inflammatory markers in diabetic retinopathy. *Invest Ophthalmol Vis Sci*. (2005) 46:4295–301. doi: 10.1167/iovs.04-1057
161. Chen H, Zhang X, Liao N, Wen F. Assessment of biomarkers using multiplex assays in aqueous humor of patients with diabetic retinopathy. *BMC Ophthalmol*. (2017) 17:176. doi: 10.1186/s12886-017-0572-6
162. Lenin R, Nagy PG, Alli S, Rao VR, Clauss MA, Kompella UB, et al. Critical role of endoplasmic reticulum stress in chronic endothelial activation-induced visual deficits in tie2-tumor necrosis factor mice. *J Cell Biochem*. (2018) 119:8460–71. doi: 10.1002/jcb.27072
163. Lenin R, Nagy PG, Jha KA, Gangaraju R. GRP78 translocation to the cell surface and O-GlcNAcylation of VE-Cadherin contribute to ER stress-mediated endothelial permeability. *Sci Rep*. (2019) 9:10783. doi: 10.1038/s41598-019-47246-w
164. Peng W, Zhang M, Yi X. Systemic inflammatory mediator levels in non-proliferative diabetic retinopathy patients with diabetic macular edema. *Curr eye Res*. (2024) 49:80–7. doi: 10.1080/02713683.2023.2268306
165. Augustine J, Pavlou S, Harkin K, Stitt AW, Xu H, Chen M. IL-33 regulates Müller cell-mediated retinal inflammation and neurodegeneration in diabetic retinopathy. *Dis Models Mech*. (2023) 16:dmm050174. doi: 10.1242/dmm.050174
166. Yan A, You H, Zhang X. Levels of interleukin 27 and interleukin 35 in the serum and vitreous of patients with proliferative diabetic retinopathy. *Ocular Immunol Inflammation*. (2018) 26:273–9. doi: 10.1080/09273948.2016.1203959
167. Yan A, Zhang Y, Wang X, Cui Y, Tan W. Interleukin 35 regulates interleukin 17 expression and T helper 17 in patients with proliferative diabetic retinopathy. *Bioengineering*. (2022) 13:13293–9. doi: 10.1080/21655979.2022.2080367
168. Qiu AW, Bian Z, Mao PA, Liu QH. IL-17A exacerbates diabetic retinopathy by impairing Müller cell function via Act1 signaling. *Exp Mol Med*. (2016) 48:e280. doi: 10.1038/emmm.2016.117
169. Takeuchi M, Sato T, Tanaka A, Muraoka T, Taguchi M, Sakurai Y, et al. Elevated levels of cytokines associated with th2 and th17 cells in vitreous fluid of proliferative diabetic retinopathy patients. *PLoS One*. (2015) 10:e0137358. doi: 10.1371/journal.pone.0137358
170. Taylor BE, Lee CA, Zapadka TE, Zhou AY, Barber KG, Taylor ZRR, et al. IL-17A enhances retinal neovascularization. *Int J Mol Sci*. (2023) 24:1747. doi: 10.3390/ijms24021747
171. Takeuchi M, Sato T, Sakurai Y, Taguchi M, Harimoto K, Karasawa Y, et al. Association between aqueous humor and vitreous fluid levels of Th17 cell-related cytokines in patients with proliferative diabetic retinopathy. *PLoS One*. (2017) 12:e0178230. doi: 10.1371/journal.pone.0178230
172. Qiu A-W, Liu Q-H, Wang J-L. Blocking IL-17A alleviates diabetic retinopathy in rodents. *Cell Physiol Biochem*. (2017) 41:960–72. doi: 10.1159/000460514
173. Tarr JM, Kaul K, Chopra M, Kohner EM, Chibber R. Pathophysiology of diabetic retinopathy. *ISRN Ophthalmol*. (2013) 2013:343560. doi: 10.1155/2013/343560
174. Giacco F, Brownlee M. Oxidative stress and diabetic complications. *Circ Res*. (2010) 107:1058–70. doi: 10.1161/CIRCRESAHA.110.223545
175. Lin WJ, Kuang HY. Oxidative stress induces autophagy in response to multiple noxious stimuli in retinal ganglion cells. *Autophagy*. (2014) 10:1692–701. doi: 10.4161/autophagy.26076
176. Taghavi Y, Hassanshahi G, Kounis NG, Konari I, Khorramdelazad H. Monocyte chemoattractant protein-1 (MCP-1/CCL2) in diabetic retinopathy: latest evidence and clinical considerations. *J Cell Commun Signal*. (2019) 13:451–62. doi: 10.1007/s12079-018-00500-8
177. Scurt FG, Menne J, Brandt S, Bernhardt A, Mertens PR, Haller H, et al. Monocyte chemoattractant protein-1 predicts the development of diabetic nephropathy. *Diabetes Metab Res Rev*. (2022) 38:e3497. doi: 10.1002/dmrr.3497
178. Yue T, Shi Y, Luo S, Weng J, Wu Y, Zheng X. The role of inflammation in immune system of diabetic retinopathy: Molecular mechanisms, pathogenetic role and therapeutic implications. *Front Immunol*. (2022) 13:1055087. doi: 10.3389/fimmu.2022.1055087
179. Zeng HY, Tso MO, Lai S, Lai H. Activation of nuclear factor-kappaB during retinal degeneration in rd mice. *Mol Vis*. (2008) 14:1075–80.
180. Yong PH, Zong H, Medina RJ, Limb GA, Uchida K, Stitt AW, et al. Evidence supporting a role for N-(3-formyl-3,4-dehydropiperidino)lysine accumulation in Müller glia dysfunction and death in diabetic retinopathy. *Mol Vis*. (2010) 16:2524–38.
181. Rezzola S, Guerra J, Krishna Chandran AM, Loda A, Cancarini A, Sacristani P, et al. VEGF-independent activation of müller cells by the vitreous from proliferative diabetic retinopathy patients. *Int J Mol Sci*. (2021) 22:2179. doi: 10.3390/ijms22042179
182. Rezzola S, Corsini M, Chiodelli P, Cancarini A, Nawaz IM, Coltrini D, et al. Inflammation and N-formyl peptide receptors mediate the angiogenic activity of human vitreous humor in proliferative diabetic retinopathy. *Diabetologia*. (2017) 60:719–28. doi: 10.1007/s00125-016-4204-0
183. Abu El-Asrar AM, Nawaz MI, Ahmad A, Dillemans L, Siddiquei M, Allegaert E, et al. CD40 ligand-CD40 interaction is an intermediary between inflammation and angiogenesis in proliferative diabetic retinopathy. *Int J Mol Sci*. (2023) 24:15582. doi: 10.3390/ijms242115582
184. Jhaveri CD, Glassman AR, Ferris FL 3rd, Liu D, Maguire MG, Allen JB, et al. DRCR retina network. Aflibercept monotherapy or bevacizumab first for diabetic macular edema. *N Engl J Med*. (2022) 387:692–703. doi: 10.1056/NEJMoa2204225
185. Nguyen QD, Brown DM, Marcus DM, Boyer DS, Patel S, Feiner L, et al. RISE and RIDE Research Group. Ranibizumab for diabetic macular edema: results from 2 phase III randomized trials: RISE and RIDE. *Ophthalmology*. (2012) 119:789–801. doi: 10.1016/j.ophtha.2011.12.039
186. Heier JS, Korobelnik JF, Brown DM, Schmidt-Erfurth U, Do DV, Midena E, et al. Intravitreal aflibercept for diabetic macular edema: 148-week results from the VISTA and VIVID studies. *Ophthalmology*. (2016) 123:2376–85. doi: 10.1016/j.ophtha.2016.07.032
187. Sahni J, Patel SS, Dugel PU, Khanani AM, Jhaveri CD, Wyckoff CC, et al. Simultaneous inhibition of angiopoietin-2 and vascular endothelial growth factor-A with faricimab in diabetic macular edema: BOULEVARD phase 2 randomized trial. *Ophthalmology*. (2019) 126:1155–70. doi: 10.1016/j.ophtha.2019.03.023
188. Dugel PU, Singh RP, Koh A, Ogura Y, Weissgerber G, Gedif K, et al. HAWK and HARRIER: ninety-six-week outcomes from the phase 3 trials of brolucizumab for neovascular age-related macular degeneration. *Ophthalmology*. (2021) 128:89–99. doi: 10.1016/j.ophtha.2020.06.028
189. Sfrikakis PP, Markomichelakis N, Theodossiadis GP, Grigoropoulos V, Katsilambros N, Theodossiadis PG. Regression of sight-threatening macular edema in type 2 diabetes following treatment with the anti-tumor necrosis factor monoclonal antibody infliximab. *Diabetes Care*. (2005) 28:445–7. doi: 10.2337/diacare.28.2.445
190. Rao VR, Prescott E, Shelke NB, Trivedi R, Thomas P, Struble C, et al. Delivery of SAR 1118 to the retina via ophthalmic drops and its effectiveness in a rat streptozotocin (STZ) model of diabetic retinopathy (DR). *Invest Ophthalmol Vis Sci*. (2010) 51:5198–204. doi: 10.1167/iovs.09-5144
191. Mauer M, Zimman B, Gardiner R, Suissa S, Sinaiko A, Strand T, et al. Renal and retinal effects of enalapril and losartan in type 1 diabetes. *N Engl J Med*. (2009) 361:40–51. doi: 10.1056/NEJMoa0808400
192. Haurigot V, Villacampa P, Ribera A, Bosch A, Ramos D, Ruberte J, et al. Long-term retinal PEDF overexpression prevents neovascularization in a murine adult model of retinopathy. *PLoS One*. (2012) 7:e41511. doi: 10.1371/journal.pone.0041511
193. Li C, Lie H, Sun W. Inhibitory effect of miR-182–5p on retinal neovascularization by targeting angiogenin and BDNF. *Mol Med Rep*. (2022) 25:61. doi: 10.3892/mmr.2021.12577
194. Babapoor-Farrokhran S, Jee K, Puchner B, Hassan SJ, Xin X, Rodrigues M, et al. Angiopoietin-like 4 is a potent angiogenic factor and a novel therapeutic target for patients with proliferative diabetic retinopathy. *Proc Natl Acad Sci U S A*. (2015) 112:E3030–3039. doi: 10.1073/pnas.1423765112
195. Cammalleri M, Locri F, Marsili S, Dal Monte M, Pisano C, Mancinelli A, et al. The urokinase receptor-derived peptide UPARANT recovers dysfunctional electroretinogram and blood-retinal barrier leakage in a rat model of diabetes. *Invest Ophthalmol Visual Sci*. (2017) 58:3138–48. doi: 10.1167/iovs.17-21593
196. Boyer DS, Hopkins JJ, Sorof J, Ehrlich JS. Anti-vascular endothelial growth factor therapy for diabetic macular edema. *Ther Adv Endocrinol Metab*. (2013) 4:151–69. doi: 10.1177/2042018813512360
197. Ahmad A, Nawaz MI. Molecular mechanism of VEGF and its role in pathological angiogenesis. *J Cell Biochem*. (2022) 123:1938–65. doi: 10.1002/jcb.30344
198. Colucciello M. Current intravitreal pharmacologic therapies for diabetic macular edema. *Postgrad Med*. (2015) 127:640–53. doi: 10.1080/00325481.2015.1052523
199. Yang JC, Haworth L, Sherry RM, Hwu P, Schwartzentruber DJ, Topalian SL, et al. A randomized trial of bevacizumab, an anti-vascular endothelial growth factor

- antibody, for metastatic renal cancer. *N Engl J Med.* (2003) 349:427–34. doi: 10.1056/NEJMoa021491
200. Glassman AR, Wells JA 3rd, Josic K, Maguire MG, Antoszyk AN, Baker C, et al. Five-year outcomes after initial aflibercept, bevacizumab, or ranibizumab treatment for diabetic macular edema (Protocol T extension study). *Ophthalmology.* (2020) 127:1201–10. doi: 10.1016/j.optha.2020.03.021
201. Arrigo A, Aragona E, Bandello F. VEGF-targeting drugs for the treatment of retinal neovascularization in diabetic retinopathy. *Ann Med.* (2022) 54:1089–111. doi: 10.1080/07853890.2022.2064541
202. Ferrara N, Damico L, Shams N, Lowman H, Kim R. Development of ranibizumab, an anti-vascular endothelial growth factor antigen binding fragment, as therapy for neovascular age-related macular degeneration. *Retina.* (2006) 26:859–70. doi: 10.1097/01.iae.0000242842.14624.e7
203. Lowe J, Araujo J, Yang J, Reich M, Oldendorf A, Shiu V, et al. Ranibizumab inhibits multiple forms of biologically active vascular endothelial growth factor in vitro and in vivo. *Exp Eye Res.* (2007) 85:425–30. doi: 10.1016/j.exer.2007.05.008
204. Castoldi V, Zerbini G, Maestroni S, Viganò I, Rama P, Leocani L. Topical Nerve Growth Factor (NGF) restores electrophysiological alterations in the Ins2Akita mouse model of diabetic retinopathy. *Exp Eye Res.* (2023) 237:109693. doi: 10.1016/j.exer.2023.109693
205. McCurry CM, Sunilkumar S, Subrahmanian SM, Yerlikaya EI, Toro AL, VanCleave AM, et al. NLRP3 inflammasome priming in the retina of diabetic mice requires REDD1-dependent activation of GSK3 β . *Invest Ophthalmol Vis Sci.* (2024) 65:34. doi: 10.1167/iov.65.3.34
206. Pfeifer CW, Walsh JT, Santeford A, Lin JB, Beatty WL, Terao R, et al. Dysregulated CD200-CD200R signaling in early diabetes modulates microglia-mediated retinopathy. *Proc Natl Acad Sci U.S.A.* (2023) 120:e2308214120. doi: 10.1073/pnas.2308214120
207. Wang YC, Wang L, Shao YQ, Weng SJ, Yang XL, Zhong YM. Exendin-4 promotes retinal ganglion cell survival and function by inhibiting calcium channels in experimental diabetes. *iScience.* (2023) 26:107680. doi: 10.1016/j.isci.2023.107680
208. Lenin R, Jha KA, Gentry J, Shrestha A, Culp EV, Vaithianathan T, et al. Tauroursodeoxycholic Acid Alleviates Endoplasmic Reticulum Stress-Mediated Visual Deficits in Diabetic tie2-TNF Transgenic Mice via TGR5 Signaling. *J Ocul Pharmacol Ther.* (2023) 39:159–74. doi: 10.1089/jop.2022.0117
209. Zhu L, Wang W, Xie TH, Zou J, Nie X, Wang X, et al. TGR5 receptor activation attenuates diabetic retinopathy through suppression of RhoA/ROCK signaling. *FASEB J.* (2020) 34:4189–203. doi: 10.1096/fj.201902496R
210. Elmasry K, Ibrahim AS, Saleh H, Elsherbiny N, Elshafey S, Hussein KA, et al. Role of endoplasmic reticulum stress in 12/15-lipoxygenase-induced retinal microvascular dysfunction in a mouse model of diabetic retinopathy. *Diabetologia.* (2018) 61:1220–32. doi: 10.1007/s00125-018-4560-z
211. Barile GR, Pachydaki SI, Tari SR, Lee SE, Donmoyer CM, Ma W, et al. The RAGE axis in early diabetic retinopathy. *Invest Ophthalmol Vis Sci.* (2005) 46:2916–24. doi: 10.1167/iov.04-1409
212. Al-Shabrawey M, Rojas M, Sanders T, Behzadian A, El-Remessy A, Bartoli M, et al. Role of NADPH oxidase in retinal vascular inflammation. *Invest Ophthalmol Vis Sci.* (2008) 49:3239–44. doi: 10.1167/iov.08-1755
213. Kowluru RA, Koppolu P, Chakrabarti S, Chen S. Diabetes-induced activation of nuclear transcriptional factor in the retina, and its inhibition by antioxidants. *Free Radic Res.* (2003) 37:1169–80. doi: 10.1080/10715760310001604189
214. Abu El-Asrar AM, Ahmad A, Nawaz MI, Siddiquei MM, De Zutter A, Vanbrabant L, et al. Tissue inhibitor of metalloproteinase-3 ameliorates diabetes-induced retinal inflammation. *Front Physiol.* (2022) 12:807747. doi: 10.3389/fphys.2021.807747
215. Navaratna D, Menicucci G, Maestas J, Srinivasan R, McGuire P, Das A. A peptide inhibitor of the urokinase/urokinase receptor system inhibits alteration of the blood-retinal barrier in diabetes. *FASEB J.* (2008) 22:3310–7. doi: 10.1096/fj.08-110155
216. Cammalleri M, Dal Monte M, Pavone V, De Rosa M, Rusciano D, Bagnoli P. The uPAR system as a potential therapeutic target in the diseased eye. *Cells.* (2019) 8:925. doi: 10.3390/cells8080925
217. Cammalleri M, Dal Monte M, Locri F, Marsili S, Lista L, De Rosa M, et al. Diabetic retinopathy in the spontaneously diabetic torii rat: pathogenetic mechanisms and preventive efficacy of inhibiting the urokinase-type plasminogen activator receptor system. *J Diabetes Res.* (2017) 2017:2904150. doi: 10.1155/2017/2904150
218. Awad AM, Elshaer SL, Gangaraju R, Abdelaziz RR, Nader MA. CysLTR1 antagonism by montelukast can ameliorate diabetes-induced aortic and testicular inflammation. *Int Immunopharmacol.* (2023) 125:111127. doi: 10.1016/j.intimp.2023.111127
219. Awad AM, Elshaer SL, Gangaraju R, Abdelaziz RR, Nader MA. Ameliorative effect of montelukast against STZ induced diabetic nephropathy: targeting HMGB1, TLR4, NF- κ B, NLRP3 inflammasome, and autophagy pathways. *Inflammopharmacology.* (2024) 32:495–508. doi: 10.1007/s10787-023-01301-1
220. Rusciano D, Bagnoli P. Pharmacotherapy and nutritional supplements for neovascular eye diseases. *Medicina (Kaunas).* (2023) 59:1334. doi: 10.3390/medicina59071334
221. Shi C, Wang P, Airen S, Brown C, Liu Z, Townsend JH, et al. Nutritional and medical food therapies for diabetic retinopathy. *Eye Vis (Lond).* (2020) 7:33. doi: 10.1186/s40662-020-00199-y
222. Shah J, Cheong ZY, Tan B, Wong D, Liu X, Chua J. Dietary intake and diabetic retinopathy: A systematic review of the literature. *Nutrients.* (2022) 14:5021. doi: 10.3390/nu14235021
223. Milluzzo A, Barchitta M, Maugeri A, Magnano San Lio R, Favara G, Mazzone MG, et al. Do nutrients and nutraceuticals play a role in diabetic retinopathy? A systematic review. *Nutrients.* (2022) 14:4430. doi: 10.3390/nu14204430
224. Matos AL, Bruno DF, Ambrósio AF, Santos PF. The benefits of flavonoids in diabetic retinopathy. *Nutrients.* (2020) 12:3169. doi: 10.3390/nu12103169
225. Alsabaani NA, Amawi K, Eleawa SM, Ibrahim WN, Aldhaban W, Alaraj AM, et al. Nrf-2-dependent antioxidant and anti-inflammatory effects underlie the protective effect of esculetin A against retinal damage in streptozotocin-induced diabetic rats. *Biomed Pharmacother.* (2024) 173:116461. doi: 10.1016/j.biopha.2024.116461
226. Wang JH, Roberts GE, Liu GS. Updates on gene therapy for diabetic retinopathy. *Curr Diabetes Rep.* (2020) 20:22. doi: 10.1007/s11892-020-01308-w
227. Diaz-Lezama N, Wu Z, Adán-Castro E, Arnold E, Vázquez-Membrillo M, Arredondo-Zamarrilla D, et al. Diabetes enhances the efficacy of AAV2 vectors in the retina: therapeutic effect of AAV2 encoding vasoinhibin and soluble VEGF receptor 1. *Lab Invest.* (2016) 96:283–95. doi: 10.1038/labinvest.2015.135
228. Biswal MR, Prentice HM, Dorey CK, Blanks JC. A hypoxia-responsive glial cell-specific gene therapy vector for targeting retinal neovascularization. *Invest Ophthalmol Vis Sci.* (2014) 55:8044–53. doi: 10.1167/iov.14-13932
229. Shiozawa AL, Igarashi T, Kobayashi M, Nakamoto K, Kameya S, Fujishita S, et al. Tyrosine triple mutated AAV2-BDNF gene therapy in an inner retinal injury model induced by intravitreal injection of N-methyl-D-aspartate (NMDA). *Mol Vis.* (2020) 26:409–22.
230. Biswal MR, Wang Z, Paulson RJ, Uddin RR, Tong Y, Zhu P, et al. Erythropoietin gene therapy delays retinal degeneration resulting from oxidative stress in the retinal pigment epithelium. *Antioxid (Basel).* (2021) 10:842. doi: 10.3390/antiox10060842
231. Elshaer SL, Evans W, Pentecost M, Lenin R, Periasamy R, Jha KA, et al. Adipose stem cells and their paracrine factors are therapeutic for early retinal complications of diabetes in the Ins2(Akita) mouse. *Stem Cell Res Ther.* (2018) 9:322. doi: 10.1186/s13287-018-1059-y
232. Rajashekhar G, Ramadan A, Abburi C, Callaghan B, Traktuev DO, Evans-Molina C, et al. Regenerative therapeutic potential of adipose stromal cells in early stage diabetic retinopathy. *PLoS One.* (2014) 9:e84671. doi: 10.1371/journal.pone.0084671
233. Agrawal M, Rasiah PK, Bajwa A, Rajasingh J, Gangaraju R. Mesenchymal stem cell induced foxp3(+) tregs suppress effector T cells and protect against retinal ischemic injury. *Cells.* (2021) 10:3006. doi: 10.3390/cells10113006
234. Park TS, Bhutto I, Zimmerlin L, Huo JS, Nagaria P, Miller D, et al. Vascular progenitors from cord blood-derived induced pluripotent stem cells possess augmented capacity for regenerating ischemic retinal vasculature. *Circulation.* (2014) 129:359–72. doi: 10.1161/CIRCULATIONAHA.113.003000
235. Gil CH, Chakraborty D, Vieira CP, Prasain N, Li Calzi S, Fortmann SD, et al. Specific mesoderm subset derived from human pluripotent stem cells ameliorates microvascular pathology in type 2 diabetic mice. *Sci Adv.* (2022) 8:eabm5559. doi: 10.1126/sciadv.abm5559



OPEN ACCESS

EDITED BY

Sara Rezzola,
University of Brescia, Italy

REVIEWED BY

Kai Jin,
Zhejiang University, China
Qiqin Shi,
Ningbo Hangzhou Bay Hospital, China
Manhong Xu,
Tianjin Medical University Eye Hospital, China

*CORRESPONDENCE

Hong Zhang
✉ Zhanghong@kmmu.edu

[†]These authors have contributed equally to this work

RECEIVED 31 March 2024

ACCEPTED 06 June 2024

PUBLISHED 03 July 2024

CITATION

Liu J, Li J, Tang Y, Zhou K, Zhao X, Zhang J and Zhang H (2024) Transcriptome analysis combined with Mendelian randomization screening for biomarkers causally associated with diabetic retinopathy.
Front. Endocrinol. 15:1410066.
doi: 10.3389/fendo.2024.1410066

COPYRIGHT

© 2024 Liu, Li, Tang, Zhou, Zhao, Zhang and Zhang. This is an open-access article distributed under the terms of the [Creative Commons Attribution License \(CC BY\)](#). The use, distribution or reproduction in other forums is permitted, provided the original author(s) and the copyright owner(s) are credited and that the original publication in this journal is cited, in accordance with accepted academic practice. No use, distribution or reproduction is permitted which does not comply with these terms.

Transcriptome analysis combined with Mendelian randomization screening for biomarkers causally associated with diabetic retinopathy

Junyi Liu^{1†}, Jinghua Li^{1†}, Yongying Tang¹, Kunyi Zhou¹, Xueying Zhao¹, Jie Zhang² and Hong Zhang^{1*}

¹Department of Ophthalmology, The Second Affiliated Hospital of Kunming Medical University, Kunming, China, ²Department of Ophthalmology, Dali Bai Autonomous Prefecture People's Hospital, Dali, China

Background: Diabetic retinopathy (DR) is considered one of the most severe complications of diabetes mellitus, but its pathogenesis is still unclear. We hypothesize that certain genes exert a pivotal influence on the progression of DR. This study explored biomarkers for the diagnosis and treatment of DR through bioinformatics analysis.

Methods: Within the GSE221521 and GSE189005 datasets, candidate genes were acquired from intersections of genes obtained using WGCNA and DESeq2 packages. Mendelian randomization (MR) analysis selected candidate biomarkers exhibiting causal relationships with DR. Receiver Operating Characteristic (ROC) analysis determined the diagnostic efficacy of biomarkers, the expression levels of biomarkers were verified in the GSE221521 and GSE189005 datasets, and a nomogram for diagnosing DR was constructed. Enrichment analysis delineated the roles and pathways associated with the biomarkers. Immune infiltration analysis analyzed the differences in immune cells between DR and control groups. The miRNet and networkanalyst databases were then used to predict the transcription factors (TFs) and miRNAs, respectively, of biomarkers. Finally, RT-qPCR was used to verify the expression of the biomarkers *in vitro*.

Results: MR analysis identified 13 candidate biomarkers that had causal relationships with DR. The ROC curve demonstrated favorable diagnostic performance of three biomarkers (*OSER1*, *HIPK2*, and *DDRGK1*) for DR, and their expression trends were consistent across GSE221521 and GSE189005 datasets. The calibration curves and ROC curves indicated good predictive performance of the nomogram. The biomarkers were enriched in pathways of immune, cancer, amino acid metabolism, and oxidative phosphorylation. Ten immune cell lines showed notable disparities between the DR and control groups. Among them, effector memory CD8+ T cells, plasmacytoid dendritic cells, and activated CD4+ T cells exhibited good correlation with biomarker expression. The TF-mRNA-miRNA network suggested that hsa-mir-92a-3p, *GATA2*, and *RELA* play important roles in biomarker targeting for DR. RT-qPCR

results also demonstrated a notably high expression of *HIPK2* in patients with DR, whereas notably low expression of *OSER1*.

Conclusion: *OSER1*, *HIPK2*, and *DDRGK1* were identified as biomarkers for DR. The study findings provide novel insights into the pathogenesis of DR.

KEYWORDS

diabetic retinopathy, enrichment analysis, immune infiltration, Mendelian randomization, regulatory network

1 Introduction

Diabetic retinopathy (DR) is a disease that causes vision loss in adults aged 20 to 74 years (1). The incidence of visual impairment and blindness caused by DR in low- and middle-income countries has increased significantly due to the increasing incidence of type 2 diabetes (2). About one-third of the 260 million people with diabetes have DR, and one-third of these patients are diagnosed with advanced DR or diabetic macular edema, and most of these patients have severe vision loss and a serious impact on their quality of life (3). In China, the incidence of diabetes is steadily increasing, with projections indicating that by 2045, approximately 174 million individuals will be diagnosed with diabetes (4). The diagnosis of DR mainly depends on history of diabetes and changes in the fundus of the eye as assessed by fundus photography, optical coherence tomography, and fundus fluorescence angiography (5). At present, DR is diagnosed solely based on the clinical manifestations, and the corresponding symptomatic treatment is based on the findings of fundus evaluation, but there is a lack of predictive and effective evaluation methods for DR. Among the many risk factors for DR, the most relevant factors are diabetes progression and poor glycemic control (6). The pathogenesis of DR is complicated, involving multiple molecular and biochemical mechanisms related to the homeostasis of retinal blood vessels and cells. The treatment for DR mainly includes intravitreal drug injection and retinal laser photocoagulation (7). Due to our lack of understanding of DR pathogenesis, there is also a lack of effective clinical treatment options. Therefore, it becomes vital to identify robust biomarkers for DR and further investigate the mechanisms underlying DR pathogenesis. The ideal therapeutic strategy for the clinical identification and management of DR should aim to enhance the patients' quality of life to the fullest.

Mendelian randomization (MR) is a novel epidemiological design tool that follows the genetic law of random distribution of alleles from parents to offspring (8). This tool has been increasingly used for establishing causal relationships between exposure factors and disease risks, made possible through advancements in statistical techniques, availability of extensive datasets, progress in epigenetics

research, and the emergence of various 'omics' technologies (9). Therefore, in this study, we used MR to screen for biomarkers that exhibit a causal relationship with DR.

We hypothesize that certain genes, which are biomarkers, exert a pivotal influence on the progression of DR. In this study, differential expression analysis, weighted gene co-expression network analysis (WGCNA), functional annotation analysis, protein-protein interaction (PPI) network construction, and MR analysis of data related to DR in the Gene Expression Omnibus (GEO) and the Integrative Epidemiology Unit (IEU) Open genome-wide association study (GWAS) databases identified three biomarkers with a causal relationship with DR. Furthermore, functional enrichment analysis, immune infiltration analysis, regulatory network construction, and drug prediction were performed, and the expression levels of these biomarkers were verified in the two datasets by RT-qPCR. Finally, a diagnostic nomogram was constructed, which could provide new insights into the diagnosis and treatment of DR. The flowchart illustrating the entire analysis process was depicted in Figure 1.

2 Materials and methods

2.1 Data source

The GEO database (<https://www.ncbi.nlm.nih.gov/>) was used to acquire mRNA expression profile of the GSE221521 and GSE189005 datasets with the GPL24676 and GPL23126 platforms, respectively. The study included 41 and 50 venous blood samples of DR and normal samples, respectively, in GSE221521 as the training set. GSE189005 consisted of 10 and 9 venous blood samples of DR and normal samples, respectively. The IEU OpenGWAS database (<https://gwas.mrcieu.ac.uk/>) was employed to obtain the GWAS ID and data for exposure factors and DR. DR was considered as the outcome (finn-b-DM_RETINOPATHY). The finn-b-DM_RETINOPATHY dataset comprised of 14,584 DR samples and 16,380,459 single nucleotide polymorphisms (SNPs).

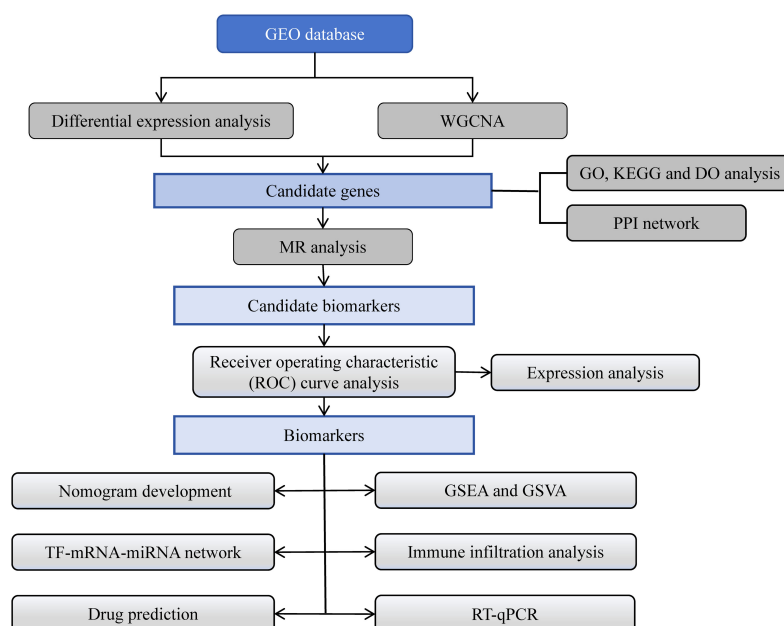


FIGURE 1
The flowchart of entire analysis process.

2.2 Differential expression analysis

In the GSE221521 dataset, DR-differentially expressed genes (DEGs) between DR and normal samples were identified conducted utilizing the DESeq2 package (v 1.34.0) ($|\text{Log2FC}| > 0.5$, $p < 0.05$) (10). The P value was corrected by Benjamini-Hochberg (BH) method. The volcano map and heat map were drawn employing the ggplot2 (v 3.4.1) and ComplexHeatmap (v 2.16.0) packages, respectively (11, 12).

2.3 WGCNA

The WGCNA was implemented to seek DR key module genes. The WGCNA package (v 1.71) was used to perform hierarchical clustering of all samples in the GSE221521 dataset, and outliers were removed (13). Then, the optimal soft threshold (β) was determined by realizing scale-free distribution and setting R^2 above 0.85. Based on the β value, the module was segmented by applying the standard of hybrid dynamic tree cutting algorithm (deepSplit = 2, mergeCutHeight = 0.3), with each module containing at least 100 genes. Modules with an absolute correlation greater than 0.6 with DR were further analyzed, and genes in these module were DR key module genes.

2.4 Identification and functional annotation analysis of candidate genes

The ggVennDiagram package (v 1.2.2) was used to determine the overlap between DR-DEGs and DR key module genes, and candidate genes were identified if there was overlap (14). The clusterProfiler package (v 4.6.0) was used to perform functional annotation analysis, including the Gene Ontology

(GO) functions, Kyoto Encyclopedia of Genes and Genomes (KEGG) pathways, and the disease ontology (DO) enrichment analysis ($p < 0.05$) (15). The STRING database (<https://string-db.org/>) was employed to predict interactions between proteins corresponding to candidate genes with a confidence score threshold of 0.4. The protein-protein interaction (PPI) network was subsequently displayed adopting Cytoscape (v 3.10.0) (16).

2.5 MR analysis

The candidate genes served as exposure factors, and DR was used as the outcome for MR analysis. In MR studies, the following three assumptions were made: (a) the presence of a significant correlation between instrumental variables (IVs) and exposure factors is imperative, (b) IVs should not be affected by confounding factors related to exposure factors or outcome, and (c) IVs can affect the outcome only through exposure factors.

The mv harmonize data function in the TwoSampleMR package (v 0.5.6) was used to unify effect alleles and effect sizes (17). Next, SNPs exhibiting significant correlation with candidate genes were selected as IVs ($p < 5 \times 10^{-8}$), and IVs for linkage disequilibrium (LD) were removed (clump=TRUE, $R^2 = 0.001$, kb=10000). The function extract instruments of TwoSampleMR package (v 0.5.8) was employed for this procedure (17). MR analysis of causality was carried out by five methods—MR Egger, Weighted median, Inverse variance weighted (IVW), Simple mode, Weighted mode), of which results of the IVW were the primary reference ($p < 0.05$) (18–22). Scatter plots, forest plots, and funnel plots were prepared to visualize the results. An odds ratio (OR) greater than 1 indicated that the gene was a risk factor for DR, while the value was less than 1, the gene was considered a protective factor.

2.6 Sensitivity analysis for MR analysis

The reliability of MR analysis was assessed via sensitivity analysis, consisting of heterogeneity and horizontal pleiotropy tests, as well as Leave-One-Out (LOO) analysis. Initially, the Cochran's Q test for heterogeneity was conducted, with $p > 0.05$ indicating the absence of heterogeneity. Subsequently, a horizontal pleiotropy test was performed by employing the MR pleiotropy test function, with $p > 0.05$ indicating that SNPs affected the outcome only through exposure factors. Finally, the LOO analysis was conducted using the MR leave one out function to determine whether a single SNP could significantly alter the overall effects. Genes exhibiting causal relationships with the outcome and passing the sensitivity analysis were identified as potential.

2.7 Receiver operating characteristic curve analysis and nomogram development

The pROC (v 1.18.0) (23) package was employed to plot ROC curves of potential biomarkers in the GSE221521 and GSE189005 datasets, and genes exhibiting area under the curve (AUC) values greater than 0.7 were considered reliable biomarkers. Subsequently, the biomarker expression levels in the GSE221521 and GSE189005 datasets were validated. Based on the expression of biomarkers, the rms package (v 6.5.0) was used to develop a diagnosis nomogram for DR patients (24). Calibration curves and ROC curves were constructed to evaluate the accuracy and reliability of the nomogram predictions. The calibration curve was plotted using the calibrate function and boot method.

2.8 Gene set enrichment analysis and gene set variation analysis

Using c2.cp.kegg.v2023.1.Hs.symbols.gmt as the background gene set, GSEA of biomarkers was conducted with R clusterProfiler (v 4.6.0) ($p < 0.05$) (15). Based on biomarker expression, all samples in the GSE221521 dataset were reorganized into high and low expression groups. The GSVA package (v 1.46.0) was used for GSVA of biomarkers in these two groups (25).

2.9 Immune infiltration analysis

The single sample GSEA (ssGSEA) algorithm was used to assess the abundance of 28 immune cells in the samples of DR and control groups. The Wilcoxon test was used to compare the difference in immune cell infiltration between the two groups ($p < 0.05$). The Spearman correlation coefficient between distinct immune cells, as well as between biomarkers and these cells was computed ($|r| > 0.3$, $p < 0.05$).

2.10 Construction of regulatory network and drug prediction

The miRNA targeting biomarkers were predicted using the miRNet database (<https://www.mirnet.ca>), while the transcription factors (TFs) regulating biomarkers were obtained from the networkanalyst database (<http://www.networkanalyst.ca>). Cytoscape (v 3.10.0) was then used to construct a regulatory network involving TF-mRNA-miRNA interactions (16). In order to explore potential drugs for the treatment of DR, targeted drugs for biomarkers were searched based on Drug Signatures Database (DSigDB) database (<http://tanlab.ucdenver.edu/DSigDB>), and results with $p < 0.05$ were selected.

2.11 Reverse transcription-quantitative polymerase chain reaction

Peripheral venous blood samples were collected from 20 patients in the Second affiliated Hospital of Kunming Medical University, including 10 patients with DR and 10 patients without DR. These samples were divided into two parts, each comprising of five DR samples and five control samples, and RT-qPCR was performed on each part to verify the screened biomarkers. This experiment was approved by the Institutional Review Board of the Second affiliated Hospital of Kunming Medical University (Review -PJ- Research -2024-134). TRIzol (Ambion, Austin, TX) was used to separate total RNA from 10 samples following the manufacturer's instructions. The concentration of RNA was extracted using NanoPhotometer N50 (IMPLEN GmbH), and the purity of RNA was assessed by measuring the ratio of A260/A280. The SureScript-First-strand-cDNA-synthesis-kit (Servicebio, Wuhan, China) was used for reverse transcription of total RNA into cDNA as per the manufacturer's instructions. The temperature was set to 25°C for 5 minutes, followed by 50°C for 15 minutes, then raised to 85°C for a duration of 5 seconds. Finally, maintain the temperature at 4°C during reverse transcription. Subsequently, qPCR analysis was performed using the 2xUniversal Blue SYBR Green qPCR Master Mix (Servicebio) according to the provided manual. The amplification conditions were 95°C for 1min, 95°C for 20s, 55°C for 20s, and 72°C for 30s. The primer sequences for PCR are listed in [Supplementary Table 1](#). Gene expression levels were normalized to GAPDH as an internal reference and calculated using the $2^{-\Delta\Delta Cq}$ method (26). The characteristics of patients are listed in [Supplementary Table 2](#).

2.12 Statistical analysis

R software (v 4.2.1) (<https://www.R-project.org/>) was utilized to process and analyze data. Statistical analysis was performed using the wilcox.test method in R.

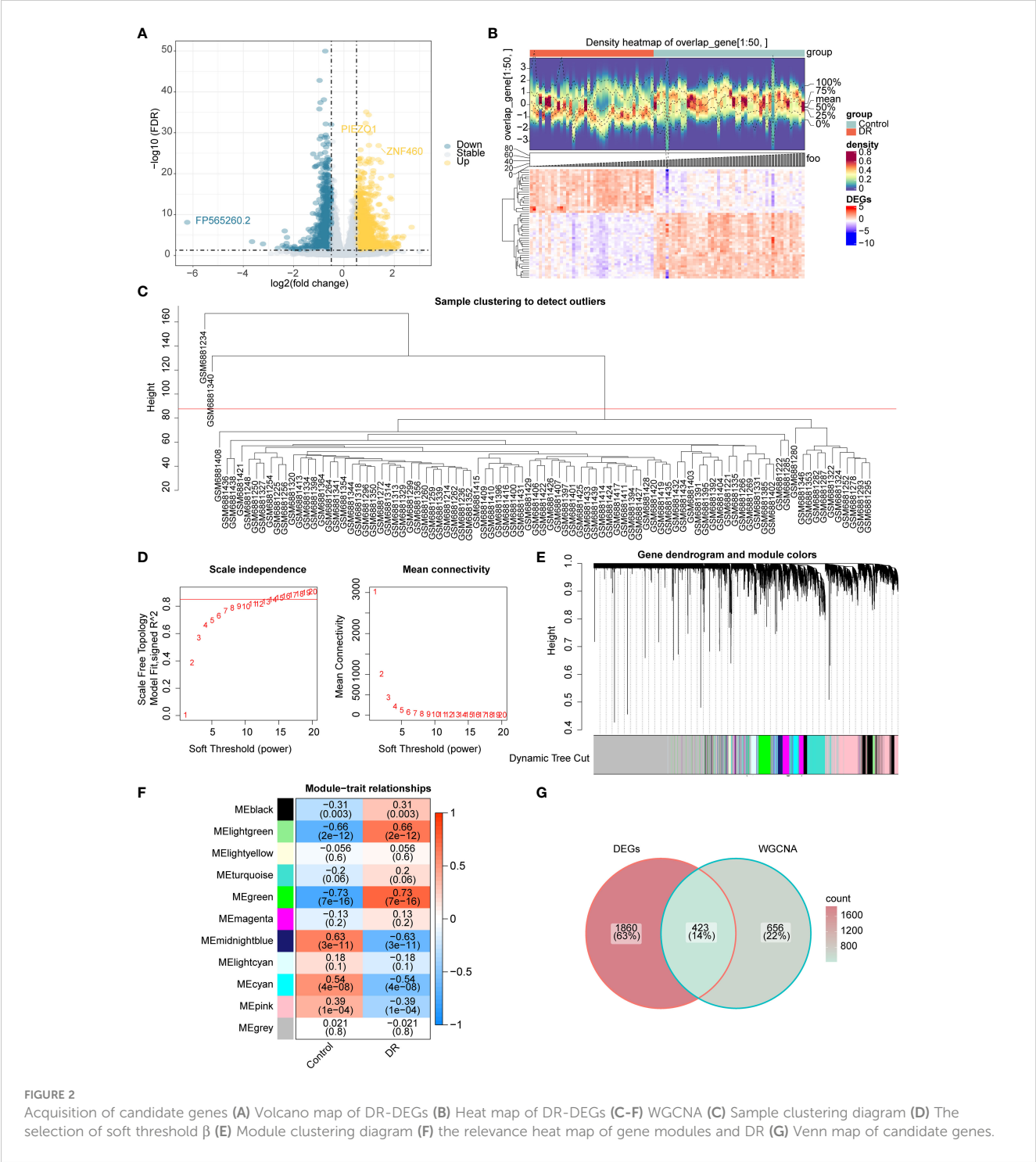
3 Results

3.1 Acquisition of candidate genes

The differential expression analysis between DR and normal samples in GSE221521 yielded 2,283 DR-DEGs, comprising 1,304 upregulated DR-DEGs and 979 downregulated DR-DEGs. The volcano map illustrates both upregulated and downregulated DR-DEGs (Figure 2A). The heatmap displays the expression of the top

50 DR-DEGs, ranked based on *p*.adj values, in the two groups (Figure 2B).

Sample clustering analysis revealed two outliers (GSM6881234 and GSM6881340) in the GSE221521 dataset and were removed for subsequent analysis (Figure 2C). The β value was determined to be 13 by setting a threshold of scale-free R^2 above 0.85 to construct gene modules (Figure 2D). As a result, 10 modules were obtained by the hybrid dynamic tree cutting algorithm (Figure 2E). Subsequently, the correlation between the green ($R=0.73$), light



green ($R=0.66$), and midnight blue ($R=0.63$) module genes with DR were greater than 0.6, and a total of 1,079 DR module genes were obtained from these modules (Figure 2F). Finally, 423 candidate genes were determined based on interaction between 2,283 DR-DEGs and 1,079 DR module genes (Figure 2G).

3.2 Enrichment analysis of candidate genes

In order to understand the functions, diseases, and pathways of candidate genes, enrichment analysis was performed. The GO functions of candidate genes included semaphorin receptor complex, semaphorin-plexin signaling pathway involved in axon guidance, and regulation of cell shape (Figure 3A). The KEGG enrichment analysis showed that candidate genes were markedly enriched in endometrial cancer, basal cell carcinoma, fatty acid biosynthesis, and apoptosis (Figure 3B). The DO enrichment analysis showed that candidate genes were significantly related to meningioma, tuberous sclerosis, intracranial arterial disease, and cerebral arterial disease (Figure 3C).

The PPI network constructed to investigate the interactions among genes contained 324 nodes and 815 edges. *AGO2* had a direct interaction with 18 genes (e.g., *CLCN6*, *UBR4*, *SIDT2*), whereas *ACTG1* interacted with 14 genes (e.g., *SRCAP*, *ITGA3*, *HCLS1*) (Figure 3D).

3.3 Candidate biomarkers exhibiting significant causal relationships with DR

The 423 candidate genes served as exposure factors, with 176 genes exhibiting SNPs, and DR was used as the outcome for the MR analysis. The IVW method was used to identify 13 candidate biomarkers (*OSER1*, *HIPK2*, *DDRKG1*, *PCK2*, *IK*, *IRF5*, *COLGALT1*, *TRPM2*, *SLC38A10*, *TSNARE1*, *PAQR7*, *ZNF142*, and *ARID1A*) that exhibited significant causal relationships with DR ($p<0.05$). Among them, eight candidate biomarkers (*OSER1*, *HIPK2*, *DDRKG1*, *PCK2*, *TRPM2*, *SLC38A10*, *TSNARE1*, and *ZNF142*) exhibited an OR greater than 1 and identified as risk factors for DR. Conversely, five candidate biomarkers (*IK*, *IRF5*, *COLGALT1*, *PAQR7*, and *ARID1A*) demonstrated an OR less than 1 and were considered protective factors for DR (Table 1).

In the scatter plot, the effect of SNPs of *OSER1*, *HIPK2*, *DDRKG1*, *PCK2*, *TRPM2*, *SLC38A10*, *TSNARE1*, and *ZNF142* on DR were positively correlated overall, while the effect of SNPs of *IK*, *IRF5*, *COLGALT1*, *PAQR7*, and *ARID1A* on DR were negatively correlated overall. These results confirmed the above conclusions (Supplementary Figure 1). Consistent with the previous results, the forest map illustrated that the MR effect size of risk factors for DR exceeded 0 and the MR effect sizes of risk factor were less than 0, providing further evidence that IVs exhibit no or weak correlation with outcome (Supplementary Figure 2). At last, the funnel plot illustrated that MR analysis of 13 candidate biomarkers and DR was consistent with Mendel's second random law (Supplementary Figure 3).

Sensitivity analysis results showed that all 13 candidate biomarkers passed the tests of horizontal pleiotropy and

heterogeneity, and LOO analysis affirming the robustness and reliability of our MR analysis (Supplementary Tables 3, 4, Supplementary Figure 4).

3.4 *OSER1*, *HIPK2*, and *DDRKG1* served as dependable biomarkers

The AUC values in ROC curves of *OSER1*, *HIPK2*, and *DDRKG1* were 0.868, 0.815, 0.806, respectively, in GSE221521, and 0.700, 0.833, and 0.722, respectively, in GSE189005 (Figures 4A–F). Given that all the AUC values exceeded 0.7, these three genes could serve as reliable biomarkers. The expression levels of *OSER1*, *DDRKG1* and *HIPK2* were consistent in GSE221521 and GSE189005 (Figures 4G, H). RT-qPCR results also demonstrated a significant high expression of *HIPK2* in patients with DR, whereas *OSER1* exhibited a significant lower expression level (Figures 4I–K, Supplementary Figure S5). A nomogram was constructed based on the expression levels of *OSER1*, *HIPK2*, and *DDRKG1* (Figure 5A). The AUC value for the nomogram was 0.942, and the calibration curve of the nomogram was almost a straight line, indicating a good predictive performance of the nomogram (Figures 5B, C).

3.5 GSEA and GSVA of biomarkers

GSEA analysis demonstrated significant associations between *HIPK2* and *DDRKG1* with ribosome, Parkinson's disease, oxidative phosphorylation, and other pathways. *OSER1* was enriched in spliceosome, neuroactive ligand receptor interaction, and olfactory transduction (Figures 6A–C). The top 20 pathways enriched by *DDRKG1*, *HIPK2* and *OSER1* in GSVA are shown in Figures 6D–F. The first three pathways (glycine serine and threonine metabolism, base excision repair, etc.) of *DDRKG1* were enriched in the high expression group, while the remaining 17 pathways (such as inositol phosphate metabolism and glioma) were enriched in the low expression group. Similarly, the initial 11 pathways (lysine degradation, prostate cancer, etc.) of *HIPK2* were enriched in the high expression group, whereas the remaining nine pathways (glycine serine and threonine metabolism, ribosome, etc.) were enriched in the low expression group. Among pathways related to *OSER1*, the first 14 (beta alanine metabolism, nitrogen metabolism, etc.) were enriched in the high expression group, and the remaining six (glyoxylate and dicarboxylate metabolism, primary immunodeficiency, etc.) were enriched in the low expression group.

3.6 The immune infiltration exhibited notable disparities between the DR and control groups

The distributions of the 28 immune cells in the sample were visualized using a heatmap (Figure 7A). There were 10 immune cell types exhibiting notable disparities between the DR and control groups, such as central memory CD8⁺ T cells, activated CD8⁺ T

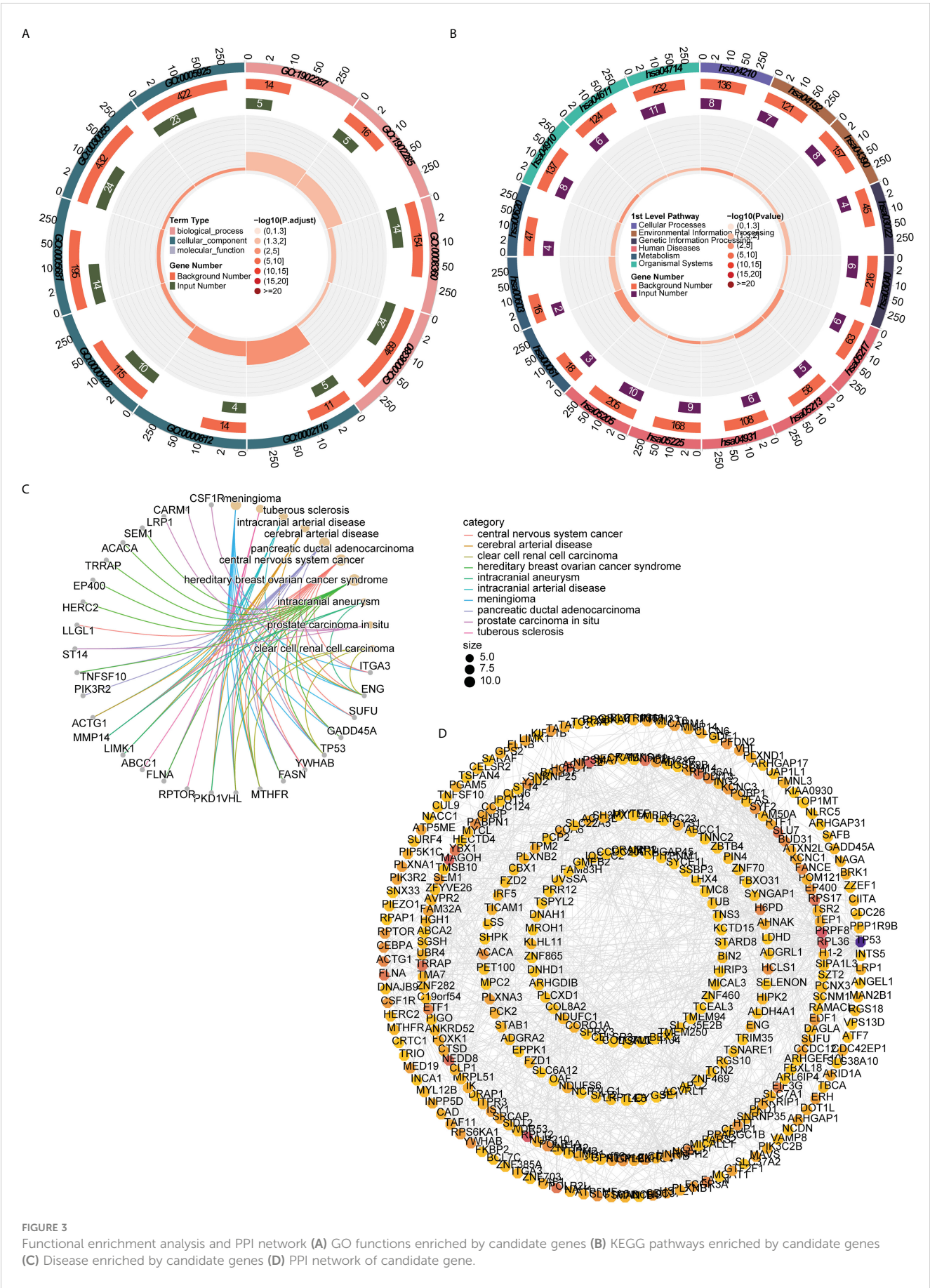


FIGURE 3
Functional enrichment analysis and PPI network (A) GO functions enriched by candidate genes (B) KEGG pathways enriched by candidate genes (C) Disease enriched by candidate genes (D) PPI network of candidate gene.

TABLE 1 MR analysis results (IVW).

| outcome | exposure | gene symbol | Method | P value | OR |
|---------------------------|------------------------|-------------|--------|---------|-------|
| finn-b- DM_RETINOPATHY | eqtl-a-ENSG00000132823 | OSER1 | IVW | 0.04 | 1.052 |
| | eqtl-a-ENSG00000064393 | HIPK2 | IVW | 0.04 | 1.259 |
| | eqtl-a-ENSG00000198171 | DDRKG1 | IVW | 0.022 | 1.064 |
| | eqtl-a-ENSG00000100889 | PCK2 | IVW | 0.002 | 1.078 |
| | eqtl-a-ENSG00000113141 | IK | IVW | 0.039 | 0.926 |
| | eqtl-a-ENSG00000128604 | IRF5 | IVW | 0.003 | 0.925 |
| | eqtl-a-ENSG00000130309 | COLGALT1 | IVW | 0.002 | 0.906 |
| | eqtl-a-ENSG00000142185 | TRPM2 | IVW | 0.043 | 1.09 |
| | eqtl-a-ENSG00000157637 | SLC38A10 | IVW | 0.027 | 1.067 |
| | eqtl-a-ENSG00000171045 | TSNARE1 | IVW | 0.0003 | 1.185 |
| | eqtl-a-ENSG00000182749 | PAQR7 | IVW | 0.003 | 0.893 |
| | eqtl-a-ENSG00000115568 | ZNF142 | IVW | 0.043 | 1.094 |
| | eqtl-a-ENSG00000117713 | ARID1A | IVW | 0.022 | 0.942 |

cells, monocytes, effector memory CD8⁺ T cells, activated CD4⁺ T cells, and myeloid derived suppressor cells (Figure 7B). There was a significant positive association between activated CD8⁺ T cells and activated CD4⁺ T cells (R=0.60). Conversely, a significant negative correlation was identified between monocytes and activated CD4⁺ T cells (R=-0.52) (Figure 7C). *DDRKG1* expression significantly and positively correlated with effector memory CD8⁺ T cells and negatively with plasmacytoid dendritic cells. Activated CD4⁺ T cells correlated significantly and positively with *OSER1* expression. *HIPK2* expression significantly and positively correlated with myeloid derived suppressor cells and negatively with activated CD8⁺ T cells (Figures 7D–F).

3.7 Regulatory relationships with biomarkers

TF-mRNA-miRNA network was composed of 25 TFs, three biomarkers, and 191 miRNAs, with a total of 219 nodes and 233 edges (Figure 8). The hsa-mir-92a-3p linked with all three biomarkers. *GATA2* and *RELA* had strong associations with *HIPK2* and *OSER1*, thereby highlighting their role in the pathogenesis of DR. The target drugs of *HIPK2* mainly included GW5074 (Raf1 Kinase Inhibitor I) MRC, LY-317615 Kinome Scan, and GSK650394A MRC. Furthermore, *OSER1* was primarily targeted by Thioguanosine PC3 UP, Elesclomol CTD 00004602, and Gedunin CTD 00003449 (Table 2).

4 Discussion

DR is a condition affecting the small blood vessels in the retina, commonly seen in individuals with diabetes. It has emerged as a leading cause of visual impairment among middle-aged people

worldwide. Approximately 22.3% of diabetic patients are affected by DR, and about 6.2% experience progressive changes in their retina that can potentially lead to vision loss (27). Timely diagnosis and prompt initiation of treatment can effectively mitigate over 90% of vision loss attributed to DR (28). The occurrence and development of DR are complicated, and its pathogenesis is still unclear. Therefore, it is necessary to investigate further into biomarkers for DR. Bioinformatic analysis techniques, based on the gene expression profiles acquired from databases, have been used to investigate target genes in disease diagnosis (29). For example, inhibition of MAPK3 expression was found through bioinformatics analysis to potentially impact the onset and progression of DR through its regulation of autophagy (30). Likewise, eight potential pyroptosis-related genes involved in the occurrence of DR were analyzed (31). Bioinformatics analysis have allowed us to derive novel insights into the immune mechanisms involved in proliferative diabetic retinopathy, and M2 macrophage-related biomarkers have been recognized to play a role in DR (32). The engagement of hub genes *HMOX1* and *PTGS2*, along with their related TFs and miRNAs, have been shown to potentially play a role in ferroptosis in DR (29).

MR analysis relies on genetic predictors as IVs to investigate the causal association between exposure factors and diseases (33). MR has been used to explore biomarkers of multiple diseases, including diabetes mellitus and DR (34, 35). MR analysis offers crucial evidence regarding the potential causal impacts of numerous alterable exposures, encompassing conventional epidemiological risk factors, lifestyle aspects, and targeted interventions (36).

In this study, based on transcriptome data in the GSE221521 and GSE189005 datasets, candidate genes were identified through differential expression analysis and WGCNA. These candidate genes served as exposure factors, and DR was used as the outcome for MR analysis. A total of 13 candidate biomarkers that exhibited causal relationships with DR were obtained by MR

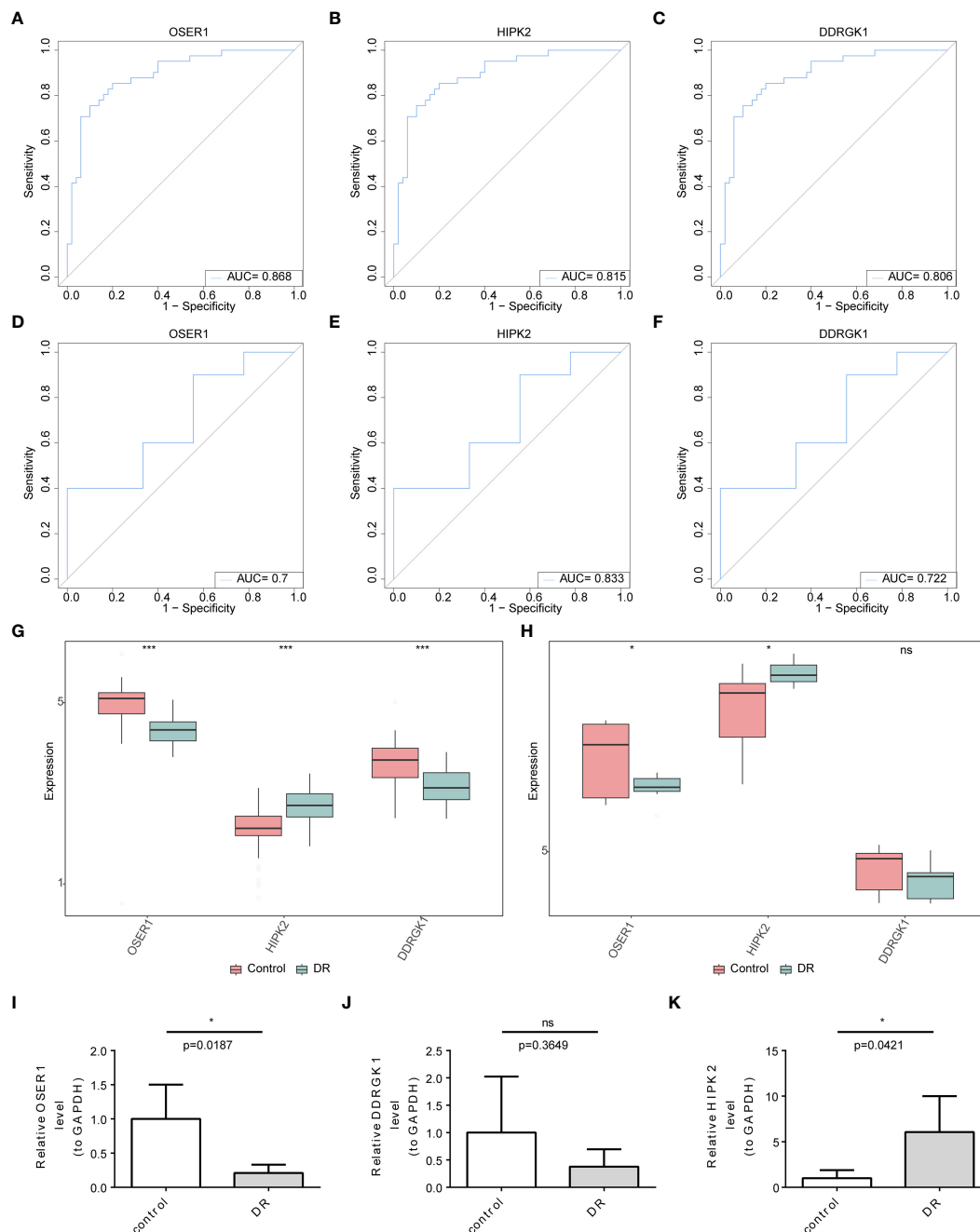


FIGURE 4

Identification and validation of biomarkers (A–F) ROC curve analysis of candidate biomarkers in GSE221521 and GSE189005 datasets (G, H) The expression levels of *OSER1*, *DDRKG1* and *HIPK2* in GSE221521 and GSE189005 datasets (I–K) The expression levels of *OSER1*, *DDRKG1* and *HIPK2* in clinical samples by RT-qPCR. *: $p < 0.5$, ***: $p < 0.001$, ns: not statistically significant.

analysis, and the ROC curve demonstrated favorable diagnostic performance of three biomarkers (*OSER1*, *HIPK2*, and *DDRKG1*) for DR. Enrichment analysis delineated pathways associated with the biomarkers, including oxidative phosphorylation, as well as amino acids and glucose. Immune infiltration analysis showed that biomarkers were associated with pro-inflammatory cells such as activated CD4+ T cells or Tfh cells. Moreover, a TF-mRNA-miRNA network was composed of 25 TFs, three biomarkers, and 191

miRNAs, with a total of 219 nodes and 233 edges. Finally, RT-qPCR verified the expression of the biomarkers *in vitro*. Then, we delve into the in-depth discussion of the roles of *OSER1*, *HIPK2*, and *DDRKG1* in DR.

The long noncoding RNA *OSER1* plays a crucial role in the inflammation and apoptosis of rheumatoid arthritis fibroblasts (37), and its low expression was markedly associated with poor survival of cancer patients (38). In the present study, we found that low

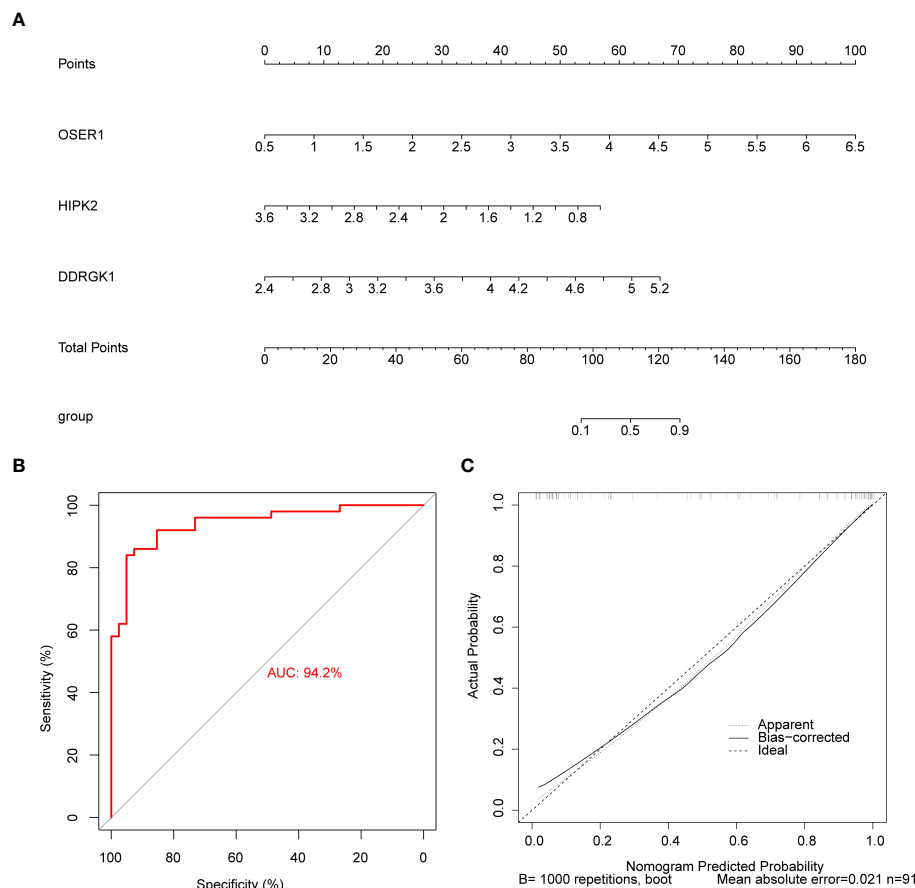


FIGURE 5

Construction and evaluation of the nomogram (A) Construction of the nomogram (B) Calibration curve of nomogram (C) ROC curve of nomogram.

OSER1 expression can also contribute to the pathogenesis of DR. Inflammation is a major driver of DR, and *OSER1* is known to promote the inflammatory cascades (37), thereby triggering DR.

HIPK2 regulates several pro-fibrotic pathways, such as Wnt/ β -catenin, liver and cardiac fibrosis, pulmonary, and renal pathways (TGF- β and Notch signaling) (39). *HIPK2* inhibition can result in cardioprotective effects as it would decrease *EGR3* and *CLEC4D* expression levels through ERK1/2-CREB inhibition in cardiomyocytes, as well as through the suppression of Smad3 phosphorylation in cardiac fibroblasts (40). These findings suggest a close link between *HIPK2* expression and fibrosis. Diabetes-associated fibrosis reflects the repair of primary injury and is involved in the pathogenesis of diabetic nephropathy, cardiomyopathy, and liver dysfunction, as well as the development of DR and neuropathy (41). In the present study, we found that *HIPK2* was upregulated in DR patients, suggesting that *HIPK2* may promote the development of DR by promoting the pathological process of retinal cell fibrosis. miR-423-5p is reported to directly bind to *HIPK2*, and its upregulation in DR patients enhances angiogenesis by inhibiting *HIPK2* expression, thereby activating the HIF1 α /VEGF signaling pathway (42). This is contrary to the results of the present study, and it is speculated that an increase in the level of VEGF may promote the levels of *HIPK2*. It is also possible that the discordant result was because our PCR was based

on blood samples. In order to clarify the exact relationship between *HIPK2* and VEGF, it is necessary to conduct a study using a larger sample size for the extraction and analysis of vitreal fluids.

DDRGK1, a protein containing the *DDRGK* domain, plays a crucial role in the recently identified ufmylation mechanism. Absence of *DDRGK1* leads to significant levels of endoplasmic reticulum (ER) stress (43) and causes a range of conditions, such as malignancies, neurodegenerative disorders, diabetes, and inflammatory disorders (44). Knocking out *DDRGK1* has been observed to trigger ER stress and facilitate apoptosis (45). Due to hyperglycemia and insulin resistance, apoptosis causes DR. Aligning with our finding that low *DDRGK1* expression in DR patients, it is possible that ER stress induced by decreased *DDRGK1* may contribute to the development of DR. However, the large variation in the RT-qPCR results may be related to the small sample size, and more samples are needed for verification of the results.

The present study is the first to demonstrate the association between biomarkers *OSER1* and *DDRGK1* and DR. We found that *HIPK2* may affect fibrosis and VEGF levels through some signaling pathways, suggesting that *HIPK2* serves as reliable biomarkers for DR.

The primary pathophysiological alterations observed in DR are attributed to long-term hyperglycemia, which triggers oxidative stress and inflammation within the microvessels of the retina.

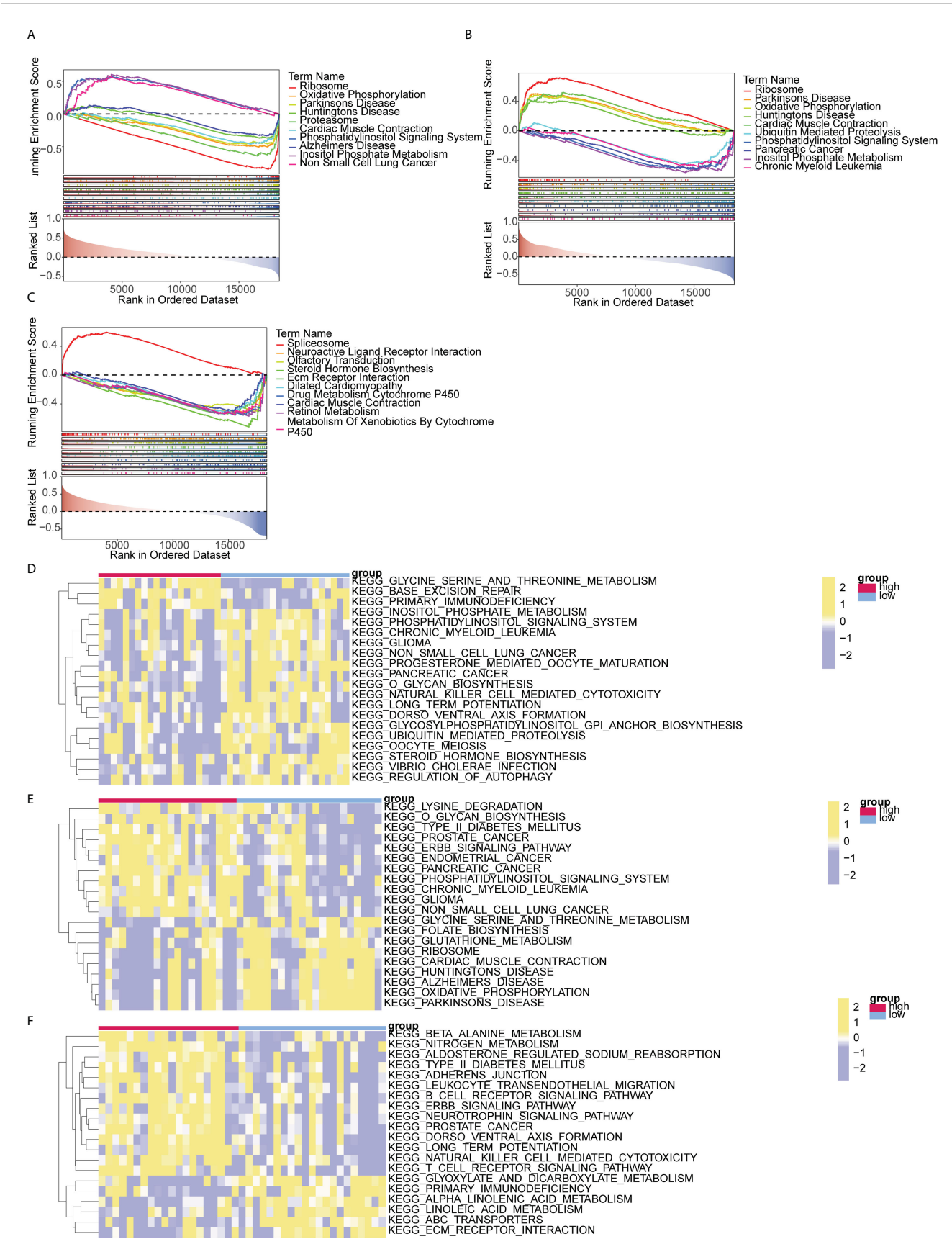


FIGURE 6
GSEA and GSVA analysis of biomarkers (A-C) GSEA analysis of DDRGK1, HIPK2, and OSER1 (D-F) GSVA analysis of DDRGK1, HIPK2, and OSER1.

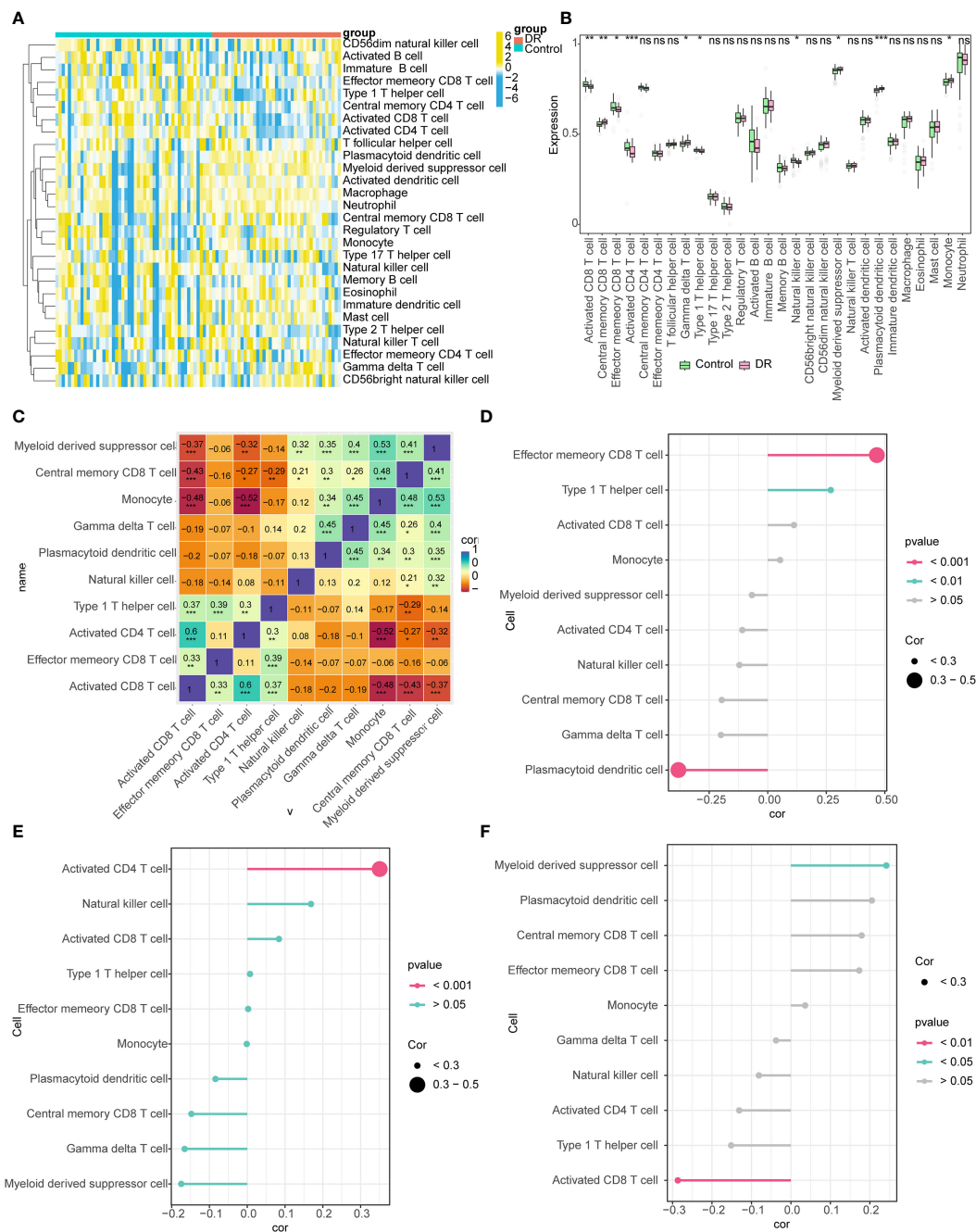


FIGURE 7

Immune infiltration analysis (A) Heat map of the distributions of the 28 immune cells (B) Differences in the abundance of immune cells in DR and Control groups (C) Differential immune cell correlation heat map (* represents the P-value < 0.05, the number represents the correlation coefficient) (D-F) Lollipop chart analysis of correlation between DDRGK1, HIPK2, and OSER1 with differential immune cells (The size of the circle represents correlation, and different colors represent different P-values). *: $p < 0.05$, **: $p < 0.01$, ***: $p < 0.001$, ns, not statistically significant.

Consequently, this leads to thickening of the basement membrane surrounding retinal capillaries, increased permeability of retinal blood vessels, and neovascularization (46). Glycemic control is achieved through the coordinated interaction among glycolysis, the Krebs cycle, and oxidative phosphorylation. Disturbing this equilibrium results in various biochemical and molecular alterations in DR (47). GSEA and GSVA of these three biomarkers provided details of the enrichment between these

genes and related pathways. The biomarkers were enriched in pathways of oxidative phosphorylation, possibly indicating that hyperglycemia disrupts the balance between glycolysis and oxidative phosphorylation, leading to other biochemical and molecular changes in retinal cells that have been linked to the neural and microvascular complications of DR. In summary, the expression of these biomarkers may influence the imbalance between glycolysis and oxidative phosphorylation caused by

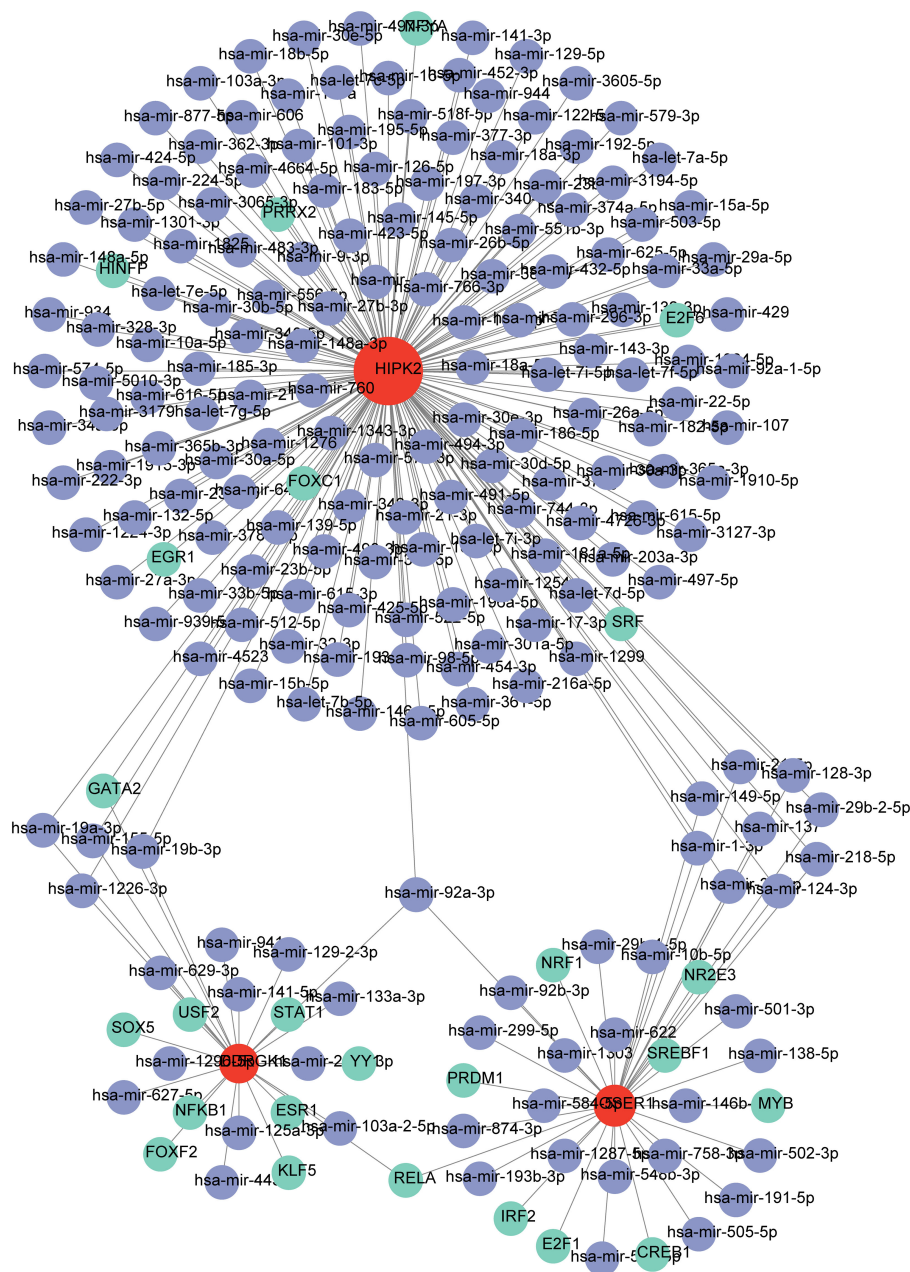


FIGURE 8
TF-mRNA-miRNA regulatory network (Green represents TF, red represents biomarkers, and purple represents miRNA).

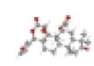
hyperglycemia, potentially leading to retinal microvascular changes associated with DR.

Amino acids play a crucial role in the formation of tissues, specialized proteins, hormones, enzymes, and neurotransmitters. They also contribute to energy metabolism through gluconeogenesis and play important roles in various metabolic pathways (48). Glutamine and arginine levels in the peripheral blood tend to increase in DR patients (49, 50), and methionine level decreases in blood samples of DR patients (48). Therefore, these amino acids can also be used as biomarkers for the early diagnosis of DR. In this study, the pathway of glycine, serine, and threonine metabolism was enriched in the high expression group of *DDRGL1*.

Among *OSER1*-related pathways, beta alanine metabolism, nitrogen metabolism, and other amino acid pathways were enriched in the high expression group. Evidence from previous metabolomics studies and our study suggests that metabolic pathways of many amino acids are involved in the occurrence of DR. Consequently, there may be numerous interactions between metabolic pathways of amino acids and glucose associated with the three biomarkers identified in our study, which require further investigation.

Diabetes is a metabolic disorder, and chronic inflammation plays a vital role in the development of type 2 diabetes. We found 10 immune cell types exhibiting notable disparities between the DR and control groups, including activated CD4⁺ T cells. It is well

TABLE 2 Predicted drugs of biomarkers.

| Target genes | Drugs | Chemical formula | Structure |
|--------------|--------------------------------------|------------------|---|
| HIPK2 | GW5074 (Raf1 Kinase Inhibitor I) MRC | C15H8Br2INO2 |  |
| | LY-317615 Kinome Scan | C32H29N5O2 |  |
| | GSK650394A MRC | / | / |
| OSER1 | Thioguanosine PC3 UP | C10H13N5O4S |  |
| | Elesclomol CTD 00004602 | C19H20N4O2S2 |  |
| | Gedunin CTD 00003449 | C28H34O7 |  |

established that CD4⁺ T cells are involved in inflammation (51), and the accumulation of CD4⁺ T cells, B cells, and macrophages is observed in the vitreous of DR patients (52). Inflammation can also affect retinal vascular pathology in DR through the activation of pro-inflammatory retinal microglia by the innate immune system and the transformation of CD4⁺ T cells into pro-inflammatory Th1 and Th17 cells (53). *OSER1* can affect the inflammatory response in DR patients by affecting activated CD4⁺ T cells, leading to the occurrence of DR. The number of a relatively new subgroup of circulating CD4⁺ T cells i.e., follicular helper T (Tfh) cells, which are located at the germinal center, is reported to increase in DR patients compared to healthy individuals (52, 54). The present study also showed that the number of Tfh cells increases in the DR group. These findings further support our results that the number of activated CD4⁺ T cells significantly and positively correlated with *OSER1* expression, suggesting *OSER1* may promote inflammation and accelerate vascular injury, leading to the development of DR through activated CD4⁺ T cells or Tfh cells.

In conclusion, three biomarkers, namely *OSER1*, *HIPK2*, and *DDRGK1*, were found to play a role in DR pathogenesis. The diagnostic nomogram for DR constructed in this study will help further improve the diagnosis of DR. These three biomarkers are expected to become potential targets for the diagnosis and treatment of DR patients. One limitation of the present study is that the results are based on the bioinformatic analysis of a public database, and further experiments are needed to explore the detailed roles of the biomarkers. Additional clinical studies are needed to validate the results. *OSER1* and *DDRGK1* have not been studied earlier in the context of DR, and additional studies are needed to ascertain their role in DR pathogenesis. Our future studies will focus on these two biomarkers. The relationship between *HIPK2* and DR in the present study was found to be opposite of what has been reported earlier; again, further research is needed to explore these pathways.

Data availability statement

Publicly available datasets were analyzed in this study. This data can be found here: <https://www.ncbi.nlm.nih.gov/>, <https://gwas.mrcieu.ac.uk/>.

Ethics statement

The studies involving humans were approved by Ethics Committee of the Second Affiliated Hospital of Kunming Medical University. The studies were conducted in accordance with the local legislation and institutional requirements. The participants provided their written informed consent to participate in this study.

Author contributions

JYL: Conceptualization, Methodology, Writing – review & editing. JHL: Conceptualization, Methodology, Writing – review & editing. YT: Conceptualization, Methodology, Writing – original draft. KZ: Formal Analysis, Writing – original draft. XZ: Data curation, Writing – review & editing. JZ: Writing – review & editing. HZ: Conceptualization, Methodology, Project administration, Writing – review & editing.

Funding

The author(s) declare financial support was received for the research, authorship, and/or publication of this article. This research was supported by the mechanism of CDKN2A/B hypomethylation regulating TGF-β/Smad signaling pathway in immune cell activation in diabetic retinopathy (202301AC070418) and the Science and Technology Program of Yunnan Provincial Department of Science and Technology-Basic Research Program (202301AC070418).

Acknowledgments

The authors acknowledge the efforts of the consortia in providing high-quality GEO and GWAS resources for researchers. Data and materials are available from the corresponding GWAS consortium. Thanks to all the authors who join in this research.

Conflict of interest

The authors declare that the research was conducted in the absence of any commercial or financial relationships that could be construed as a potential conflict of interest.

References

- Cheung N, Mitchell P, Wong TY. Diabetic retinopathy. *Lancet*. (2010) 376:124–36. doi: 10.1016/S0140-6736(09)62124-3
- Teo ZL, Tham Y-C, Yu M, Chee ML, Rim TH, Cheung N, et al. Global prevalence of diabetic retinopathy and projection of burden through 2045. *Ophthalmology*. (2021) 128:1580–91. doi: 10.1016/j.ophtha.2021.04.027
- Saaddine JB, Honeycutt AA, Narayan KM, Zhang X, Klein R, Boyle JP. Projection of diabetic retinopathy and other major eye diseases among people with diabetes mellitus: United States, 2005–2050. *Arch Ophthalmol*. (2008) 126:1740–7. doi: 10.1001/archophth.126.12.1740
- Sun H, Saeedi P, Karuranga S, Pinkepank M, Ogurtsova K, Duncan BB, et al. IDF Diabetes Atlas: Global, regional and country-level diabetes prevalence estimates for 2021 and projections for 2045. *Diabetes Res Clin Pract*. (2022) 183. doi: 10.1016/j.diabres.2021.109119
- Cai S, Liu TYA. The role of ultra-widefield fundus imaging and fluorescein angiography in diagnosis and treatment of diabetic retinopathy. *Curr Diabetes Rep*. (2021) 21:30. doi: 10.1007/s11892-021-01398-0
- Sabanayagam C, Banu R, Chee ML, Lee R, Wang YX, Tan G, et al. Incidence and progression of diabetic retinopathy: a systematic review. *Lancet Diabetes Endocrinol*. (2019) 7:140–9. doi: 10.1016/S2213-8587(18)30128-1
- Wang W, Lo ACY. Diabetic retinopathy: pathophysiology and treatments. *Int J Mol Sci*. (2018) 19(6). doi: 10.3390/ijms19061816
- Davey Smith G, Ebrahim S. 'Mendelian randomization': can genetic epidemiology contribute to understanding environmental determinants of disease? *Int J Epidemiol*. (2003) 32:1–22. doi: 10.1093/ije/dyg070
- Haycock PC, Burgess S, Wade KH, Bowden J, Relton C, Davey Smith G. Best (but oft-forgotten) practices: the design, analysis, and interpretation of Mendelian randomization studies. *Am J Clin Nutr*. (2016) 103:965–78. doi: 10.3945/ajcn.115.118216
- Love MI, Huber W, Anders S. Moderated estimation of fold change and dispersion for RNA-seq data with DESeq2. *Genome Biol*. (2014) 15(12). doi: 10.1186/s13059-014-0550-8
- Gu Z, Eils R, Schlesner M. Complex heatmaps reveal patterns and correlations in multidimensional genomic data. *Bioinformatics*. (2016) 32:2847–9. doi: 10.1093/bioinformatics/btw313
- Gustavsson EK, Zhang D, Reynolds RH, Garcia-Ruiz S, Ryten M. ggtranscript: an R package for the visualization and interpretation of transcript isoforms using ggplot2. *Bioinformatics*. (2022) 38:3844–6. doi: 10.1093/bioinformatics/btac409
- Langfelder P, Horvath S. WGCNA: an R package for weighted correlation network analysis. *BMC Bioinf*. (2008) 9:599. doi: 10.1186/1471-2105-9-559
- Gao C-H, Yu G, Cai P. ggVennDiagram: an intuitive, easy-to-use, and highly customizable R package to generate Venn diagram. *Front Genet*. (2021) 12. doi: 10.3389/fgene.2021.706907
- Wu T, Hu E, Xu S, Chen M, Guo P, Dai Z, et al. clusterProfiler 4.0: A universal enrichment tool for interpreting omics data. *Innovation (Camb)*. (2021) 2:100141. doi: 10.1016/j.xinn.2021.100141
- Shannon P, Markiel A, Ozier O, Baliga NS, Wang JT, Ramage D, et al. Cytoscape: A software environment for integrated models of biomolecular interaction networks. *Genome Res*. (2003) 13:2498–504. doi: 10.1101/gr.1239303

Publisher's note

All claims expressed in this article are solely those of the authors and do not necessarily represent those of their affiliated organizations, or those of the publisher, the editors and the reviewers. Any product that may be evaluated in this article, or claim that may be made by its manufacturer, is not guaranteed or endorsed by the publisher.

Supplementary material

The Supplementary Material for this article can be found online at: <https://www.frontiersin.org/articles/10.3389/fendo.2024.1410066/full#supplementary-material>

- Hemani G, Zheng J, Elsworth B, Wade KH, Haberland V, Baird D, et al. The MR-Base platform supports systematic causal inference across the human phenome. *eLife*. (2018) 30(7):e34408. doi: 10.7554/eLife.34408
- Burgess S, Thompson SG. Interpreting findings from Mendelian randomization using the MR-Egger method. *Eur J Epidemiol*. (2017) 32:377–89. doi: 10.1007/s10654-017-0255-x
- Bowden J, Davey Smith G, Haycock PC, Burgess S. Consistent estimation in Mendelian randomization with some invalid instruments using a weighted median estimator. *Genet Epidemiol*. (2016) 40:304–14. doi: 10.1002/gepi.21965
- Burgess S, Scott RA, Timpson NJ, Davey Smith G, Thompson SG. Using published data in Mendelian randomization: a blueprint for efficient identification of causal risk factors. *Eur J Epidemiol*. (2015) 30:543–52. doi: 10.1007/s10654-015-0011-z
- Chen X, Kong J, Diao X, Cai J, Zheng J, Xie W, et al. Depression and prostate cancer risk: A Mendelian randomization study. *Cancer Med*. (2020) 9:9160–7. doi: 10.1002/cam4.3493
- Hu J, Song J, Chen Z, Yang J, Shi Q, Jin F, et al. Reverse causal relationship between periodontitis and shortened telomere length: Bidirectional two-sample Mendelian random analysis. *Front Immunol*. (2022) 13. doi: 10.3389/fimmu.2022.1057602
- Robin X, Turck N, Hainard A, Tiberti N, Lisacek F, Sanchez J-C, et al. pROC: an open-source package for R and S+ to analyze and compare ROC curves. *BMC Bioinf*. (2011) 12:77. doi: 10.1186/1471-2105-12-77
- Xu J, Yang T, Wu F, Chen T, Wang A, Hou S. A nomogram for predicting prognosis of patients with cervical cerclage. *Heliyon*. (2023) 9(11). doi: 10.1016/j.heliyon.2023.e21147
- Hänzelmann S, Castelo R, Guinney J. GSEA: gene set variation analysis for microarray and RNA-seq data. *BMC Bioinf*. (2013) 14:7. doi: 10.1186/1471-2105-14-7
- Livak KJ, Schmittgen TD. Analysis of relative gene expression data using real-time quantitative PCR and the 2⁻(Delta Delta C(T)) Method. *Methods*. (2001) 25:402–8. doi: 10.1006/meth.2001.1262
- Tarasiewicz D, Conell C, Gilliam LK, Melles RB. Quantification of risk factors for diabetic retinopathy progression. *Acta Diabetol*. (2023) 60:363–9. doi: 10.1007/s00592-022-02007-6
- Early photocoagulation for diabetic retinopathy. ETDRS report number 9. Early Treatment Diabetic Retinopathy Study Research Group. *Ophthalmology*. (1991) 98:766–85. doi: 10.1016/S0161-6420(13)38011-7
- Huang Y, Peng J, Liang Q. Identification of key ferroptosis genes in diabetic retinopathy based on bioinformatics analysis. *PloS One*. (2023) 18:e0280548. doi: 10.1371/journal.pone.0280548
- Wang N, Wei L, Liu D, Zhang Q, Xia X, Ding L, et al. Identification and validation of autophagy-related genes in diabetic retinopathy. *Front Endocrinol (Lausanne)*. (2022) 13:867600. doi: 10.3389/fendo.2022.867600
- Wang N, Ding L, Liu D, Zhang Q, Zheng G, Xia X, et al. Molecular investigation of candidate genes for pyroptosis-induced inflammation in diabetic retinopathy. *Front Endocrinol (Lausanne)*. (2022) 13:918605. doi: 10.3389/fendo.2022.918605
- Meng Z, Chen Y, Wu W, Yan B, Meng Y, Liang Y, et al. Exploring the immune infiltration landscape and M2 macrophage-related biomarkers of proliferative diabetic retinopathy. *Front Endocrinol (Lausanne)*. (2022) 13:841813. doi: 10.3389/fendo.2022.841813

33. Davey Smith G, Ebrahim S. What can mendelian randomisation tell us about modifiable behavioural and environmental exposures? *Bmj*. (2005) 330:1076–9. doi: 10.1136/bmj.330.7499.1076
34. Su Z, Wu Z, Liang X, Xie M, Xie J, Li H, et al. Diabetic retinopathy risk in patients with unhealthy lifestyle: A Mendelian randomization study. *Front Endocrinol (Lausanne)*. (2022) 13:1087965. doi: 10.3389/fendo.2022.1087965
35. Liu K, Zou J, Fan H, Hu H, You Z. Causal effects of gut microbiota on diabetic retinopathy: A Mendelian randomization study. *Front Immunol*. (2022) 13:930318. doi: 10.3389/fimmu.2022.930318
36. Larsson SC, Butterworth AS, Burgess S. Mendelian randomization for cardiovascular diseases: principles and applications. *Eur Heart J*. (2023) 44:4913–24. doi: 10.1093/eurheartj/ehad736
37. Fu Q, Song MJ, Fang J. LncRNA OSER1-AS1 regulates the inflammation and apoptosis of rheumatoid arthritis fibroblast like synoviocytes via regulating miR-1298–5p/E2F1 axis. *Bioengineered*. (2022) 13:4951–63. doi: 10.1080/21655979.2022.2037854
38. Xie W, Wang Y, Zhang Y, Xiang Y, Wu N, Wu L, et al. Single-nucleotide polymorphism rs4142441 and MYC co-modulated long non-coding RNA OSER1-AS1 suppresses non-small cell lung cancer by sequestering ELAVL1. *Cancer Sci*. (2021) 112:2272–86. doi: 10.1111/cas.14713
39. Garufi A, Pistritto G, D'Orazi G. HIPK2 as a novel regulator of fibrosis. *Cancers (Basel)*. (2023) 15. doi: 10.3390/cancers15041059
40. Zhou Q, Meng D, Li F, Zhang X, Liu L, Zhu Y, et al. Inhibition of HIPK2 protects stress-induced pathological cardiac remodeling. *EBioMedicine*. (2022) 85:104274. doi: 10.1016/j.ebiom.2022.104274
41. Tuleta I, Frangogiannis NG. Diabetic fibrosis. *Biochim Biophys Acta Mol Basis Dis*. (2021) 1867:166044. doi: 10.1016/j.bbdis.2020.166044
42. Xiao Q, Zhao Y, Sun H, Xu J, Li W, Gao L. MiR-423–5p activated by E2F1 promotes neovascularization in diabetic retinopathy by targeting HIPK2. *Diabetol Metab Syndr*. (2021) 13:152. doi: 10.1186/s13098-021-00769-7
43. Cao Y, Li R, Shen M, Li C, Zou Y, Jiang Q, et al. DDRGK1, a crucial player of ufmylation system, is indispensable for autophagic degradation by regulating lysosomal function. *Cell Death Dis*. (2021) 12:416. doi: 10.1038/s41419-021-03694-9
44. Yang X, Zhou T, Wang X, Xia Y, Cao X, Cheng X, et al. Loss of DDRGK1 impairs IRE1 α UFMylation in spondyloepiphyseal dysplasia. *Int J Biol Sci*. (2023) 19:4709–25. doi: 10.7150/ijbs.82765
45. Liu J, Wang Y, Song L, Zeng L, Yi W, Liu T, et al. A critical role of DDRGK1 in endoplasmic reticulum homeostasis via regulation of IRE1 α stability. *Nat Commun*. (2017) 8:14186. doi: 10.1038/ncomms14186
46. Liu K, Gao X, Hu C, Gui Y, Gui S, Ni Q, et al. Capsaicin ameliorates diabetic retinopathy by inhibiting poldip2-induced oxidative stress. *Redox Biol*. (2022) 56:102460. doi: 10.1016/j.redox.2022.102460
47. Yumnamcha T, Guerra M, Singh LP, Ibrahim AS. Metabolic dysregulation and neurovascular dysfunction in diabetic retinopathy. *Antioxidants (Basel)*. (2020) 9. doi: 10.3390/antiox9121244
48. Xia M, Zhang F. Amino acids metabolism in retinopathy: from clinical and basic research perspective. *Metabolites*. (2022) 9(12). doi: 10.3390/metabo12121244
49. Sun Y, Zou H, Li X, Xu S, Liu C. Plasma metabolomics reveals metabolic profiling for diabetic retinopathy and disease progression. *Front Endocrinol (Lausanne)*. (2021) 12:757088. doi: 10.3389/fendo.2021.757088
50. Rhee SY, Jung ES, Park HM, Jeong SJ, Kim K, Chon S, et al. Plasma glutamine and glutamic acid are potential biomarkers for predicting diabetic retinopathy. *Metabolomics*. (2018) 14:89. doi: 10.1007/s11306-018-1383-3
51. DeMaio A, Mehrotra S, Sambamurti K, Husain S. The role of the adaptive immune system and T cell dysfunction in neurodegenerative diseases. *J Neuroinflammation*. (2022) 19:251. doi: 10.1186/s12974-022-02605-9
52. Liu Y, Yang Z, Lai P, Huang Z, Sun X, Zhou T, et al. Bcl-6-directed follicular helper T cells promote vascular inflammatory injury in diabetic retinopathy. *Theranostics*. (2020) 10:4250–64. doi: 10.7150/thno.43731
53. Jerome JR, Deliyanti D, Suphaimol V, Kolkhof P, Wilkinson-Berka JL. Finerenone, a non-steroidal mineralocorticoid receptor antagonist, reduces vascular injury and increases regulatory T-cells: studies in rodents with diabetic and neovascular retinopathy. *Int J Mol Sci*. (2023) 24(3). doi: 10.3390/ijms24032334
54. Xiang X, Huang X, Zhang Z, Gu J, Huang Z, Jiang T. Dysregulation of circulating CD4 + CXCR5 + PD-1+ T cells in diabetic retinopathy. *J Diabetes Complications*. (2023) 37:108420. doi: 10.1016/j.jdiacomp.2023.108420



OPEN ACCESS

EDITED BY

Honghua Yu,
Guangdong Provincial People's Hospital,
China

REVIEWED BY

Qi Feng Liu,
First People's Hospital of Kunshan, China
Kunbei Lai,
Sun Yat-sen University, China

*CORRESPONDENCE

Xin Sun

✉ sunxin77@126.com

Xiandong Zeng

✉ zeng_xiandong1969@163.com

[†]These authors have contributed equally to this work

RECEIVED 22 February 2024

ACCEPTED 08 August 2024

PUBLISHED 27 August 2024

CITATION

Jiang Y, Zhang W, Xu Y, Zeng X and Sun X (2024) Relationship of fibroblast growth factor 21, Klotho, and diabetic retinopathy: a meta-analysis. *Front. Endocrinol.* 15:1390035. doi: 10.3389/fendo.2024.1390035

COPYRIGHT

© 2024 Jiang, Zhang, Xu, Zeng and Sun. This is an open-access article distributed under the terms of the [Creative Commons Attribution License \(CC BY\)](https://creativecommons.org/licenses/by/4.0/). The use, distribution or reproduction in other forums is permitted, provided the original author(s) and the copyright owner(s) are credited and that the original publication in this journal is cited, in accordance with accepted academic practice. No use, distribution or reproduction is permitted which does not comply with these terms.

Relationship of fibroblast growth factor 21, Klotho, and diabetic retinopathy: a meta-analysis

Yanhua Jiang^{1†}, Weilai Zhang^{1†}, Yao Xu², Xiandong Zeng^{1*} and Xin Sun^{3*}

¹Department of Ophthalmology, Fourth People's Hospital of Shenyang, Shenyang, China,

²Department of Ophthalmology, Fourth Affiliated Hospital of Soochow University, Suzhou, China,

³Department of Endocrinology, First Affiliated Hospital of Soochow University, Suzhou, China

Background: Diabetic retinopathy (DR) is a serious microvascular complication of diabetes mellitus. Research has identified a close relationship between fibroblast growth factor 21 (FGF21) and DR. FGF21 is a member of the FGF subfamily, which is activated by the Klotho coenzyme involved in the occurrence of DR. However, the association between FGF21, Klotho, and DR remains controversial.

Aim: To assess FGF21 and Klotho levels in patients with DR.

Methods: A literature search of the Web of Science, Wiley Online Library, PubMed, China National Knowledge Infrastructure and Wanfang databases was performed. The title or abstract search terms "diabetic retinopathy" and "DR" were used in combination with "fibroblast growth factor 21", "FGF21", and "Klotho". Meta-analysis results are presented as standardized mean difference (SMD) with corresponding 95% confidence interval (CI).

Results: Fifteen studies were included in this meta-analysis. FGF21 levels in patients with DR were significantly higher than in non-DR patients with diabetes (SMD: 2.12, 95% CI [1.40, 2.84]). Klotho levels in patients with DR were significantly lower than in non-DR patients with diabetes (SMD: -0.63, 95% CI [-1.22, -0.04]).

Conclusions: This systematic review is the first to evaluate the relationship between FGF21, Klotho levels, and DR. FGF21 levels were significantly higher in patients with DR. Fully elucidating the role of FGF21 will significantly contribute to the treatment of DR.

KEYWORDS

FGF21, Klotho, diabetic retinopathy, fibroblast growth factor 21, DR

Introduction

Diabetes is a common metabolic disease characterized by abnormally high blood glucose levels. Epidemiological studies have reported that diabetes not only has an increasing annual incidence rate, but is also projected to become the seventh leading cause of death worldwide by 2030 (1), posing a serious threat to human health. Diabetic retinopathy (DR) is a serious microvascular complication of diabetes. In 2020, approximately 103 million individuals were affected by DR globally, and this number is projected to increase to 160 million by 2045 (2). DR is an ischemic disease characterized by early stage retinal neurodegeneration, retinal microaneurysms, and bleeding, as well as possible accompanying “cotton wool” patches, venous bead-like changes, and retinal microvascular abnormalities (3). DR is the main cause of visual dysfunction and blindness in working-age adults worldwide and is significantly associated with a risk for future cerebrovascular accidents, myocardial infarction, and congestive heart failure (4). Conventional treatment methods for DR, such as retinal laser photocoagulation, hypoglycemic drugs, and anti-vascular endothelial growth factor (anti-VEGF) therapy, are ineffective and are accompanied by numerous side effects (5). It is clear that DR imposes a significant public health burden worldwide, seriously threatening the vision and quality of life of affected individuals. As such, there is an urgent need to further clarify the precise pathological and physiological mechanisms of DR to improve prevention strategies for DR and develop new treatment strategies.

Recent research has identified a close relationship between fibroblast growth factor 21 (FGF21) and DR, which may be a therapeutic target for pathological vascular growth in patients (6–8). FGF21 is a member of the FGF subfamily, with a coding gene located on chromosome 19 that encodes a long-chain protein comprising 209 amino acids. FGF21 binds to FGF receptors 1–4 under the action of the Klotho coenzyme and enters the bloodstream, producing effects by binding to different receptors (9, 10). FGF21 is expressed in multiple tissues and organs of the human body, mainly in the liver, followed by the pancreas, adipose tissue, myocardial cells, skeletal muscles (11). FGF21, which participates in metabolic regulation in the bloodstream, originates mainly from the liver. However, the association between FGF21, Klotho, and DR remains controversial. The FGF21 and Klotho levels of DR patients were various among studies. To our knowledge, this systematic review is the first to evaluate the relationship between FGF21 and Klotho levels and DR.

Methods

Literature search

A literature search of the Web of Science, Wiley Online Library, PubMed, China National Knowledge Infrastructure (CNKI) and Wanfang databases was performed. The title or abstract search terms “diabetic retinopathy” and “DR” were used in combination with “fibroblast growth factor 21”, “FGF21”, and “Klotho”. The focus of the search period was 1980 to 2024, with publication languages limited to English and Chinese. The reference lists of the retrieved

articles were manually searched to identify additional, potentially eligible studies. To date, no studies have been conducted on this topic. This systematic review and meta-analysis was registered with PROSPERO under accession number CRD42024501425. All items that should be reported for systematic reviews and meta-analyses are listed in the [Supplementary Table 1](#).

Inclusion criteria

Meta-analysis was conducted on studies fulfilling the following criteria: sufficient data regarding FGF21, Klotho levels in DR patients and non-DR patients with diabetes; case-control design; and language limited to English and Chinese.

Data extraction and risk of bias

As part of the preliminary screening process, 2 reviewers independently used the search strategy and read titles and abstracts to exclude studies that did not fulfill the inclusion criteria. To determine whether the studies met the inclusion criteria, the two reviewers methodologically reviewed the full text. If the author’s information is incomplete, they can contact and crosscheck the author. If the conclusions of the two evaluators were inconsistent, the differences were resolved through discussion. If the discussion failed to resolve any differences, it was judged and arbitrated by a third researcher. The Cochrane Collaboration recommends the Newcastle-Ottawa Scale (NOS) as a tool to assess bias in observational studies (12, 13). Studies were rated according to the NOS, which ranged from zero to nine stars, and star scores were used to determine quality. There are three aspects in the NOS: the method for selecting case and control groups, their comparability, and the method for assessing exposure.

Statistical analysis

Heterogeneity among the included studies was assessed using the I^2 statistic, and the data are expressed as standardized mean difference (SMD) and corresponding 95% confidence interval (CI). Fixed-effects models were used if I^2 was < 50% and heterogeneity among studies was low or moderate; otherwise, random-effects models were used if I^2 was > 50%. A sensitivity analysis was performed to evaluate the stability of the results. Begg’s and Egger’s tests were used to detect publication bias. $P < 0.05$ was set as the significance level. Data analysis was performed using Review Manager version 5.3. And the sensitivity analysis and publication bias were performed using Stata version 12.0.

Results

Literature search and study selection

The initial literature search retrieved 85 studies from the Web of Science, Wiley Online Library, PubMed, CNKI and databases. After

screening, 15 studies including 1220 DR cases and 1447 controls were included (6, 7, 14–26). A flow-diagram illustrating the study selection process is presented in Figure 1. The characteristics of each of the included studies are summarized in Table 1. All 15 studies included in this meta-analysis fulfilled the criteria for the Newcastle-Ottawa Scale categories of selection, comparability, and exposure.

Results of meta-analysis

There 10 articles were about FGF21 and DR. While, in these 10 articles, one article used healthy people as control group, not the patients with non-DR diabetes. So, we have performed the analysis in different control groups (non-DR diabetes patients and healthy controls). FGF21 levels were significantly higher in patients with DR than in non-DR patients with diabetes [SMD: 2.12, 95% CI [1.40, 2.84]; $I^2 = 97\%$] (6, 7, 14, 16, 17, 20, 21, 24, 25). Forest plot and funnel plot of FGF21 levels in patients with DR compared to those in non-DR diabetes are presented in Figures 2, 3. It was also found that FGF21 levels in patients with DR were significantly higher than that in healthy controls [SMD: 3.90, 95% CI (2.46, 5.35); $I^2 = 98\%$] (6, 7, 14, 17, 21, 22, 25). In addition, there was no difference in FGF21 levels between patients with non-proliferative DR (NPDR) and those with proliferative DR (PDR) [SMD: 0.89, 95% CI (−1.21, 2.99); $I^2 = 97\%$] (6, 14, 20–22). The Klotho level in patients with DR was significantly lower than that in non-DR patients with diabetes [SMD: −0.63, 95% CI (−1.22, −

0.04); $I^2 = 92\%$] (15, 18, 19, 23, 26). Forest plots and funnel plot of Klotho levels are presented in Figures 4, 5.

Sensitivity analysis and publication bias

Each study was subjected to a sensitivity analysis to determine its influence. Sensitivity analysis showed no significant differences from our previous estimates, indicating that a single study had a marginal impact on the overall estimate (Supplementary Figures 1, 2). Accordingly, the meta-analysis yields stable results. A thorough and comprehensive search of the databases was conducted. Begg's and Egger's tests were conducted to identify whether publication bias was present in the reviewed studies. The results ($P > 0.05$) indicated that there was no publication bias (Supplementary Figures 3–6).

Discussion

This systematic review is the first to evaluate FGF21 and Klotho levels in patients with DR. In our previous research, we found the leptin and chemerin levels in patients with DR were significantly higher than those in non-DR patients (27). In this meta-analysis, fourteen independent studies were included in the meta-analysis. We conclude that FGF21 levels were significantly higher in patients with DR than non-DR patients with diabetes, and that Klotho levels were

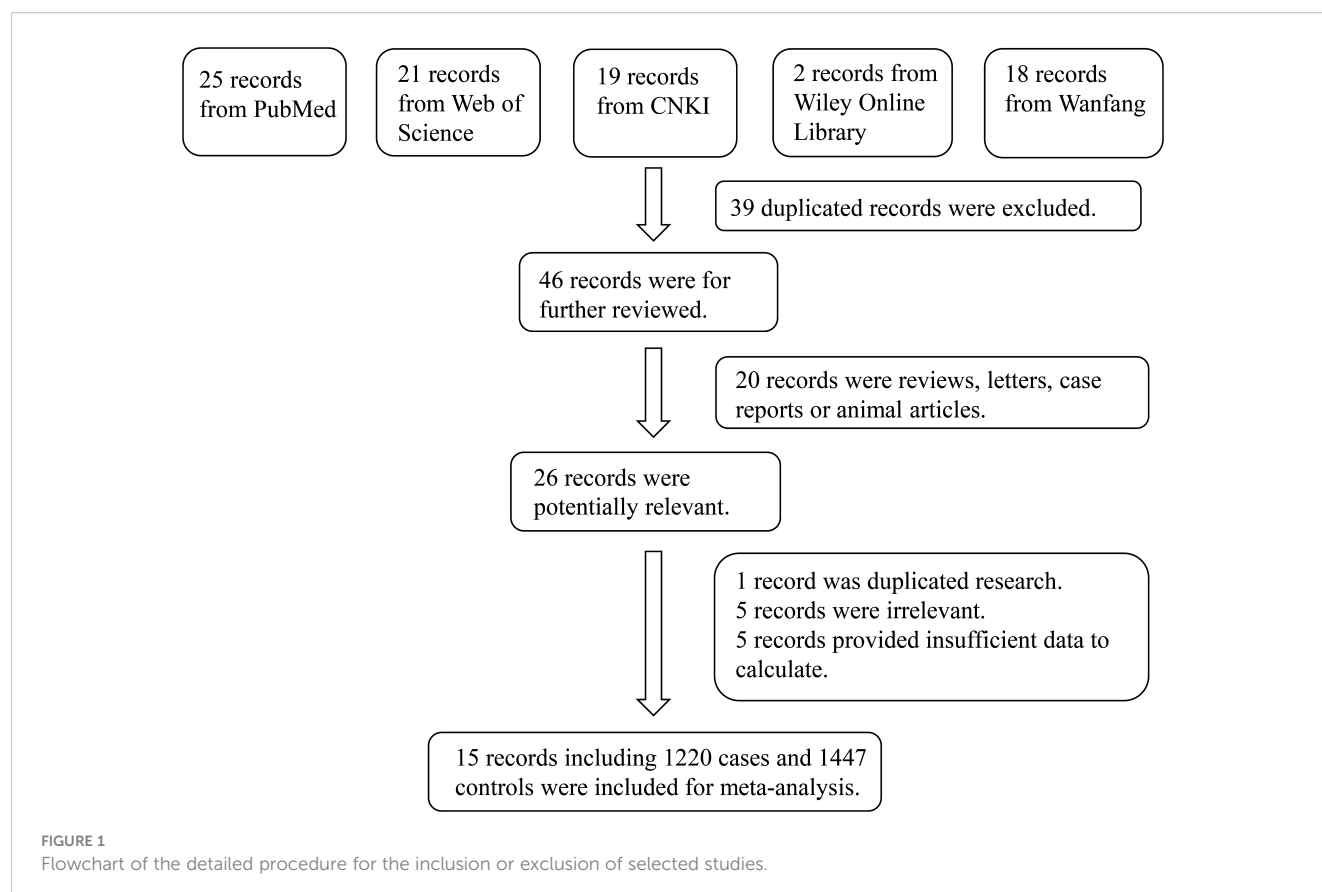
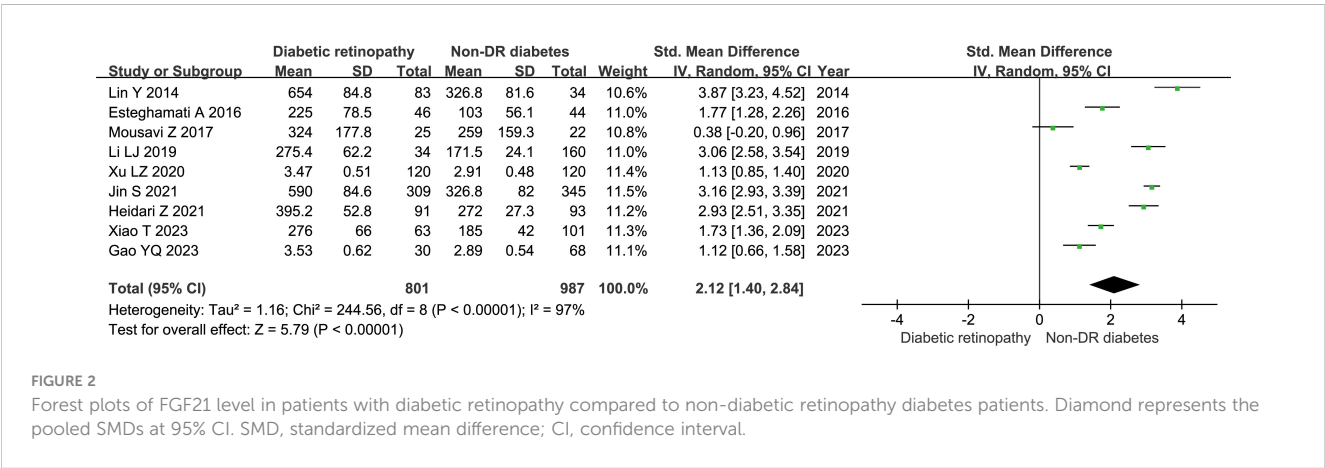
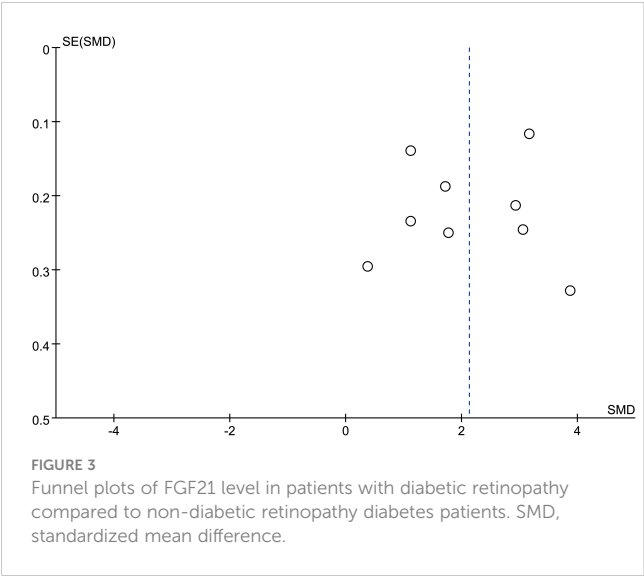


TABLE 1 Study characteristics of the published studies included in the meta-analysis.

| Author | Publication Year | Study Period | Region | Number | | Sex(M/F) | | Age(years) | | Sample | NOS |
|---------------|------------------|----------------------------------|--------|--------|---------|----------|---------|---------------|---------------|--------|-----|
| | | | | Case | Control | Case | Control | Case | Control | | |
| Lin Y | 2014 | October 2009 to May 2012 | China | 83 | 34 | 43/40 | 20/14 | 60.10 ± 11.70 | 59.40 ± 10.20 | FGF21 | 7 |
| Esteghamati A | 2016 | | Iran | 46 | 44 | 17/29 | 21/23 | 56.50 ± 9.00 | 55.00 ± 12.00 | FGF21 | 5 |
| Mousavi Z | 2017 | 2016 to 2017 | Iran | 25 | 22 | 6/19 | 5/17 | 56.00 ± 7.00 | 54.0 ± 6.00 | FGF21 | 6 |
| Zhang L | 2018 | January 2016 to January 2018 | China | 99 | 127 | 48/51 | 59/68 | 52.6 ± 10.25 | 52.9 ± 8.25 | Klotho | 6 |
| Li LJ | 2019 | March 2016 to March 2018 | China | 34 | 160 | 19/15 | 96/64 | 61.35 ± 11.22 | 58.48 ± 13.11 | FGF21 | 6 |
| Xu LZ | 2020 | January 2016 to December 2018 | China | 120 | 120 | 67/53 | 64/56 | 52.14 ± 12.61 | 51.44 ± 11.57 | FGF21 | 6 |
| Ji B | 2020 | November 2015 to November 2016 | China | 33 | 27 | 11/22 | 12/15 | 57.64 ± 6.23 | 58.00 ± 4.70 | Klotho | 6 |
| Corcillo A | 2020 | | UK | 46 | 35 | | | 61.20 ± 8.80 | 60.70 ± 9.30 | Klotho | 5 |
| Jin S | 2021 | January 2018 to October 2019 | China | 309 | 345 | 162/147 | 185/160 | 58.58 ± 10.31 | 57.11 ± 11.99 | FGF21 | 7 |
| Heidari Z | 2021 | | Iran | 91 | 93 | 34/57 | 32/61 | 55.47 ± 9.99 | 54.12 ± 11.27 | FGF21 | 6 |
| Cai LY | 2021 | February 2018 to April 2018 | China | 90 | 85 | 51/39 | 45/40 | 48.36 ± 6.14 | 48.41 ± 6.05 | FGF21 | 6 |
| Wan F | 2022 | January 2017 to December 2019 | China | 106 | 74 | 57/49 | 40/34 | 56.82 ± 10.13 | 56.34 ± 9.20 | Klotho | 5 |
| Hu W | 2022 | November 2020 to October 2021 | China | 45 | 112 | 25/20 | 63/49 | 55.84 ± 10.44 | 52.95 ± 12.01 | Klotho | 6 |
| Xiao T | 2023 | September 2020 to September 2022 | China | 63 | 101 | 33/30 | 52/49 | 53.94 ± 7.49 | 54.10 ± 8.36 | FGF21 | 6 |
| Gao YQ | 2023 | October 2019 to October 2022 | China | 30 | 68 | 16/14 | 38/30 | 53.43 ± 10.37 | 54.01 ± 10.56 | FGF21 | 6 |





significantly lower in patients with DR than non-DR patients with diabetes.

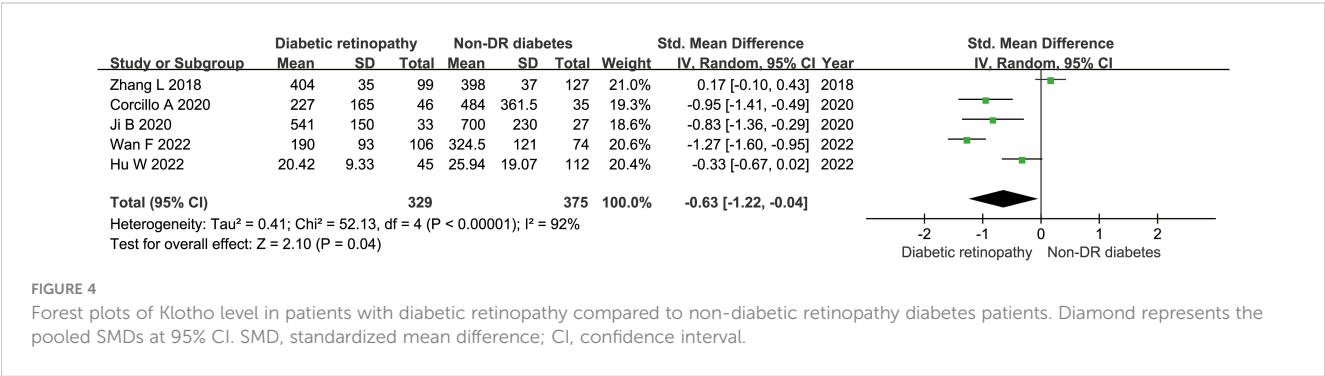
FGF21 is a key regulator of retinal lipid and glucose metabolism. It can metabolize lipoproteins in the adipose tissue and maintain adipocyte phospholipid homeostasis. FGF21 also increases lipid utilization during amino acid starvation. FGF21 acts by regulating the activities of peroxisome proliferator-activated receptors (PPARs) and peroxisome proliferator-activated receptor γ coactivator-1 (PGC-1). FGF21 is crucial in PPAR- α agonists to improve metabolic processes in obese mice (28). FGF21 inhibits the growth of pathological retinal neovascularization through adiponectin (APN). FGF21 promotes APN expression in the blood circulation in a dose-dependent manner (29). Fu et al. reported that APN could inhibit neovascularization of the retina and choroid in mice (30). The use of long-acting FGF21 analogs can increase the concentration of retinal APN in mice, indicating that FGF21 has important effects on metabolic functions (31). To determine whether APN mediates the protective effect of FGF21 on retinal neovascularization, the retinal vascular systems of mice with and without long-acting FGF21 analogs were compared under oxygen-induced retinopathy in APN gene knockout mice. Studies have shown that APN deficiency exacerbates retinal neovascularization and eliminates the beneficial effects of long-acting FGF21 analogs in reducing hypoxic retinal neovascularization. In addition, APN can inhibit retinal neovascularization by reducing the level of tumor

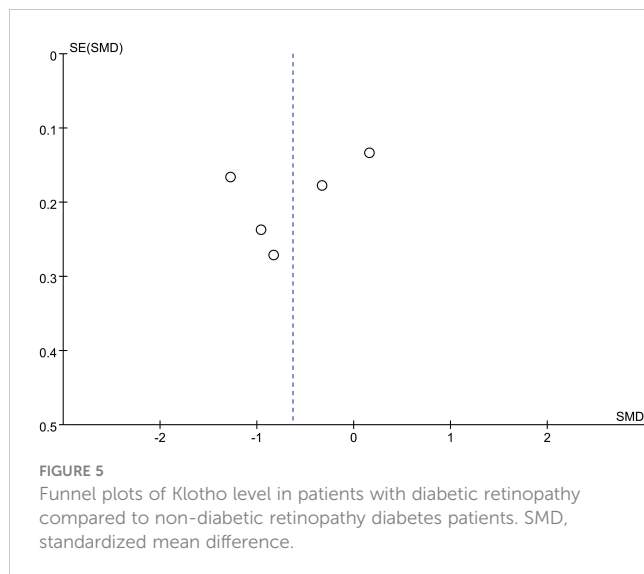
necrosis-alpha (TNF- α) (32). In summary, FGF21 inhibits the growth of pathological retinal neovascularization by targeting APN and reducing TNF- α , which is a key risk factor for hypoxia-induced retinopathy (33).

High blood glucose levels can induce oxidative stress, which is a key factor in DR (34). Photosensitive cells are the most metabolically active cells in the human body and are prone to metabolic disorders and oxidative stress (35). Fu et al. (36) reported that the use of FGF21 in insulin-deficient diabetic mice reversed retinal neuron defects caused by diabetes, improved the function and morphology of photoreceptors, and reduced inflammation of photoreceptors. NRF2 regulates oxidative stress and inflammatory response, and interleukin (IL)-1 β is an inflammatory factor causing retinal neurovascular injury. FGF21 protects photoreceptor cells from oxidative stress by upregulating the expression of the NRF2 protein in the DR retina and decreasing the production of IL-1 β (37, 38). Photosensitive cells can release inflammatory products that stimulate the surrounding cells (39) and cause changes in retinal vascular permeability in diabetic mouse models (40). In addition, the effect of long-term FGF21 administration on the inhibition of retinal vascular leakage in *in vivo* and *in vitro* models has been verified (41). Retinal tissue is highly sensitive to metabolism, and photoreceptors contain the largest number of mitochondria in human cells. Among all cells in the retina, photoreceptors mount the largest response to retinal oxidative stress and inflammation caused by diabetes. In patients with PDR and subsequent retinitis pigmentosa, retinal neovascularization is slow. Therefore, enhancing the levels of antioxidants in photoreceptor cells can prevent neurovascular damage in DR; however, this is, to some extent, independent of the APN-TNF- α pathway (36).

Experimental evidence suggests that FGF21 is beneficial in DR. In the present study, we confirmed that FGF21 levels were significantly higher in patients with DR than in those without DR. It is difficult to explain this phenomenon in patients with DR. Some researchers have named this phenomenon “FGF21 resistance” (42, 43). Although this hypothesis is supported, the mechanism underlying FGF21 resistance has not yet been elucidated. Once the role of FGF21 is fully elucidated, however, we believe that it will contribute significantly to the treatment of DR.

The FGF21 coenzyme Klotho has been found to be expressed in the human retina, optic nerve, and lens (44, 45). Some evidence suggests that Klotho regulates many mechanisms involved in maintaining retinal cell homeostasis and function (44, 46, 47). First, Klotho-knockout mice exhibit several morphological changes





compared with wild-type mice, including reduced pigmentation of the retinal pigment epithelium layer, enlarged choroidal vessels, thinning and deformation of the basement membrane, and signs of degeneration of the outer photoreceptor layer (46). Proteomic analysis has shown that proteins involved in eye development, visual perception, and mitochondrial function are downregulated in Klotho-knockout mice (47). Thus, Klotho-knockout mice have reduced retinal function, with functional defects comparable to those observed in insulin-like growth factor-1 knockout mice (44). Several experimental models have shown that depletion of Klotho negatively affects important functions of retinal cells, including oxidative stress, VEGF-A secretion, and phagocytosis, thereby activating mechanisms that may contribute to the onset and progression of DR. However, there is some evidence that treatment with recombinant Klotho improves retinal function.

The present study had some limitations. First, the duration of diabetes and disease severity varied among the included studies, and data regarding NPDR and PDR were limited. Second, the languages of literature search were limited to English and Chinese. As such, high-quality research investigating the role(s) of FGF21 and Klotho in the treatment of DR is warranted. It is, therefore, important to interpret the results of this meta-analysis cautiously.

Conclusion

This systematic review is the first to evaluate the relationship between FGF21 and Klotho levels and DR. FGF21 levels were significantly higher in patients with DR. Fully characterizing the role of FGF21 will significantly contribute to the treatment of DR.

Data availability statement

The original contributions presented in the study are included in the article/Supplementary Material. Further inquiries can be directed to the corresponding authors.

Author contributions

YJ: Writing – original draft. WZ: Writing – original draft. YX: Writing – original draft. XZ: Data curation, Writing – original draft. XS: Conceptualization, Writing – original draft, Writing – review & editing.

Funding

The author(s) declare that no financial support was received for the research, authorship, and/or publication of this article.

Acknowledgments

We would like to thank Editage (www.editage.cn) for English language editing.

Conflict of interest

The authors declare that the research was conducted in the absence of any commercial or financial relationships that could be construed as a potential conflict of interest.

Publisher's note

All claims expressed in this article are solely those of the authors and do not necessarily represent those of their affiliated organizations, or those of the publisher, the editors and the reviewers. Any product that may be evaluated in this article, or claim that may be made by its manufacturer, is not guaranteed or endorsed by the publisher.

Supplementary material

The Supplementary Material for this article can be found online at: <https://www.frontiersin.org/articles/10.3389/fendo.2024.1390035/full#supplementary-material>

SUPPLEMENTARY TABLE 1

Preferred reporting items for systematic review and meta-analyses (PRISMA) checklist.

SUPPLEMENTARY FIGURE 1

The sensitivity analysis results of FGF21 level in patients with diabetic retinopathy compared to non-diabetic retinopathy diabetes patients.

SUPPLEMENTARY FIGURE 2

The sensitivity analysis results of Klotho level in patients with diabetic retinopathy compared to non-diabetic retinopathy diabetes patients.

SUPPLEMENTARY FIGURE 3

The Begg's test of FGF21 level in patients with diabetic retinopathy compared to non-diabetic retinopathy diabetes patients.

SUPPLEMENTARY FIGURE 4

The Egger's test of FGF21 level in patients with diabetic retinopathy compared to non-diabetic retinopathy diabetes patients.

SUPPLEMENTARY FIGURE 5

The Begg's test of Klotho level in patients with diabetic retinopathy compared to non-diabetic retinopathy diabetes patients.

SUPPLEMENTARY FIGURE 6

The Egger's test of Klotho level in patients with diabetic retinopathy compared to non-diabetic retinopathy diabetes patients.

References

- Choi NH, Shaw JE, Karuranga S, Huang Y, Da RFJ, Ohlrogge AW, et al. IDF Diabetes Atlas: Global estimates of diabetes prevalence for 2017 and projections for 2045. *Diabetes Res Clin Pract.* (2018) 138:271–81. doi: 10.1016/j.diabres.2018.02.023
- Teo ZL, Tham YC, Yu M, Chee ML, Rim TH, Cheung N, et al. Global prevalence of diabetic retinopathy and projection of burden through 2045: systematic review and meta-analysis. *Ophthalmology.* (2021) 128:1580–91. doi: 10.1016/j.ophtha.2021.04.027
- Wong TY, Cheung CM, Larsen M, Sharma S, Simo R. Diabetic retinopathy. *Nat Rev Dis Primers.* (2016) 2:16012. doi: 10.1038/nrdp.2016.12
- Modjtahedi BS, Wu J, Luong TQ, Gandhi NK, Fong DS, Chen W. Severity of diabetic retinopathy and the risk of future cerebrovascular disease, cardiovascular disease, and all-cause mortality. *Ophthalmology.* (2021) 128:1169–79. doi: 10.1016/j.ophtha.2020.12.019
- Olsen TW. Anti-VEGF pharmacotherapy as an alternative to panretinal laser photocoagulation for proliferative diabetic retinopathy. *JAMA.* (2015) 314:2135–6. doi: 10.1001/jama.2015.15409
- Lin Y, Xiao YC, Zhu H, Xu QY, Qi L, Wang YB, et al. Serum fibroblast growth factor 21 levels are correlated with the severity of diabetic retinopathy. *J Diabetes Res.* (2014) 2014:929756. doi: 10.1155/2014/929756
- Esteghamati A, Momeni A, Abdollahi A, Khandan A, Afarideh M, Noshad S, et al. Serum fibroblast growth factor 21 concentrations in type 2 diabetic retinopathy patients. *Ann Endocrinol (Paris).* (2016) 77:586–92. doi: 10.1016/j.ando.2016.01.005
- Tomita Y, Ozawa N, Miwa Y, Ishida A, Ohta M, Tsubota K, et al. Pemafrate prevents retinal pathological neovascularization by increasing FGF21 level in a murine oxygen induced retinopathy model. *Int J Mol Sci.* (2019) 20:5878. doi: 10.3390/ijms20235878
- Nishimura T, Nakatake Y, Konishi M, Itoh N. Identification of a novel FGF, FGF-21, preferentially expressed in the liver. *Biochim Biophys Acta.* (2000) 1492:203–6. doi: 10.1016/S0167-4781(00)00067-1
- Woo YC, Xu A, Wang Y, Lam KS. Fibroblast growth factor 21 as an emerging metabolic regulator: clinical perspectives. *Clin Endocrinol (Oxf).* (2013) 78:489–96. doi: 10.1111/cen.12095
- Keuper M, Haring HU, Staiger H. Circulating FGF21 levels in human health and metabolic disease. *Exp Clin Endocrinol Diabetes.* (2020) 128:752–70. doi: 10.1055/a-0879-2968
- Wells GA, Shea B, O'Connell D, et al. The Newcastle-Ottawa Scale (NOS) for Assessing the Quality of Non randomized Studies in Meta-Analyses. Available online at: http://www.ohri.ca/programs/clinical_epidemiology/oxford.asp (Accessed 2014 Aug 5).
- Higgins JPT, Green S. Cochrane Handbook for Systematic Reviews of Interventions Version 5.1.0. Available online at: <http://www.cochrane-handbook.org> (Accessed 2014 Aug).
- Mousavi Z, Bonakdaran S, Sahebkar A, Yaghoubi G, Yaghoubi MA, Davoudian N, et al. The relationship between serum levels of fibroblast growth factor 21 and diabetic retinopathy. *EXCLI J.* (2017) 16:1249–56. doi: 10.17179/excli2017-672
- Zhang L, Liu T. Clinical implication of alterations in serum Klotho levels in patients with type 2 diabetes mellitus and its associated complications. *J Diabetes Complicat.* (2018) 32:922–30. doi: 10.1016/j.jdiacomp.2018.06.002
- Li LJ, Zhang M, Li ZX, Han XP, Zheng JC. Correlation between serum fibroblast growth factor 21 level and diabetic kidney disease and diabetic retinopathy in type 2 diabetic patients. *Chin J Diabetes.* (2019) 27:812–5. doi: 10.3969/j.issn.1006-6187.2019.11.003
- Xu LZ, Tan HT, Zhang SQ, Liu F. Serum levels of fibroblast growth factor 21 in patients with type 2 diabetic retinopathy and its clinical significance. *Chin J Gen Pract.* (2020) 18:959–61. doi: 10.16766/j.cnki.issn.1674-4152.001402
- Corcillo A, Fountoulakis N, Sohal A, Farrow F, Ayis S, Karalliedde J. Low levels of circulating anti-ageing hormone Klotho predict the onset and progression of diabetic retinopathy. *Diabetes Vasc Dis Res.* (2020) 17:203390146. doi: 10.1177/1479164120970901
- Ji B, Wei H, Ding Y, Liang H, Yao L, Wang H, et al. Protective potential of klotho protein on diabetic retinopathy: Evidence from clinical and *in vitro* studies. *J Diabetes Invest.* (2020) 11:162–9. doi: 10.1111/jdi.13100
- Jin S, Xia N, Han L. Association between serum fibroblast growth factor 21 level and sight-threatening diabetic retinopathy in Chinese patients with type 2 diabetes. *BMJ Open Diabetes Res Care.* (2021) 9:e002126. doi: 10.1136/bmjdr-2021-002126
- Heidari Z, Hasanpour M. The serum fibroblast growth factor 21 is correlated with retinopathy in patients with type 2 diabetes mellitus. *Diabetes Metab Syndr.* (2021) 15:102296. doi: 10.1016/j.dsx.2021.102296
- Cai LY, Luo G. Expression and significance of serum chemokine and fibroblast growth factor 21 in patients with diabetic retinopathy. *J Pract Clin Med.* (2021) 25:76–80. doi: 10.7619/jcmp.20211123
- Wang F, Meng XD, Peng J. Changes of serum Klotho, NEP and Vaspin levels in patients with diabetic retinopathy and their clinical significance. *Int J Lab Med.* (2022) 43:791–5. doi: 10.3969/j.issn.1673-4130.2022.07.005
- Gao YQ, Liang N. Predictive value of serum irisin, FGF-21, TNF- α and IL-6 combined detection for retinopathy in patients with type 2 diabetes mellitus. *Lab Med Clin.* (2023) 20:3037–40. doi: 10.3969/j.issn.1672-9455.2023.20.021
- Xiao T, Cai ZW, Lin J, Gao XL. Correlation between serum fibroblast growth factor 21 and retinal vessel diameter in type 2 diabetes mellitus. *J Chronic Med.* (2023) 24:1064–6. doi: 10.16440/J.CNKI.1674-8166.2023.07.29
- Hu W. *Correlation between Serum FGF23 and Klotho Protein Levels and Microvascular Complications in Type 2 Diabetes Mellitus.* China: Xian Medical University (2022).
- Jiang Y, Fan H, Xie J, Xu Y, Sun X. Association between adipocytokines and diabetic retinopathy: a systematic review and meta-analysis. *Front Endocrinol (Lausanne).* (2023) 14:1271027. doi: 10.3389/fendo.2023.1271027
- Fruchart JC. Pemafrate (K-877), a novel selective peroxisome proliferator activated receptor alpha modulator for management of atherogenic dyslipidemia. *Cardiovasc Diabetol.* (2017) 16:124. doi: 10.1186/s12933-017-0602-y
- Struijk D, Dommerholt MB, Jonker JW. Fibroblast growth factors in control of lipid metabolism: from biological function to clinical application. *Curr Opin Lipidol.* (2019) 30:235–43. doi: 10.1097/MOL.0000000000000599
- Fu Z, Lofqvist CA, Shao Z, Sun Y, Joyal JS, Hurst CG, et al. Dietary ω -3 polyunsaturated fatty acids decrease retinal neovascularization by adipose endoplasmic reticulum stress reduction to increase adiponectin. *Am J Clin Nutr.* (2015) 101:879–88. doi: 10.3945/ajcn.114.099291
- Lin Z, Tian H, Lam KS, Lin S, Hoo RC, Konishi M, et al. Adiponectin mediates the metabolic effects of FGF21 on glucose homeostasis and insulin sensitivity in mice. *Cell Metab.* (2013) 17:779–89. doi: 10.1016/j.cmet.2013.04.005
- Higuchi A, Ohashi K, Kihara S, Walsh K, Ouchi N. Adiponectin suppresses pathological microvessel formation in retina through modulation of tumor necrosis factor- α expression. *Circ Res.* (2009) 104:1058–65. doi: 10.1161/CIRCRESAHA.109.194506
- Kociok N, Radetzky S, Krohne TU, Gavranic C, Jousen AM. Pathological but not physiological retinal neovascularization is altered in TNF-Rp55-receptor-deficient mice. *Invest Ophthalmol Vis Sci.* (2006) 47:5057–65. doi: 10.1167/iovs.06-0407
- Madsen-Bouterse SA, Kowluru RA. Oxidative stress and diabetic retinopathy: pathophysiological mechanisms and treatment perspectives. *Rev Endocr Metab Disord.* (2008) 9:315–27. doi: 10.1007/s11154-008-9090-4
- Kern TS, Berkowitz BA. Photoreceptors in diabetic retinopathy. *J Diabetes Investig.* (2015) 6:371–80. doi: 10.1111/jdi.12312
- Fu Z, Wang Z, Liu CH, Gong Y, Cakir B, Liel R, et al. Fibroblast growth factor 21 protects photoreceptor function in type 1 diabetic mice. *Diabetes.* (2018) 67:974–85. doi: 10.2337/db17-0830
- Wang MX, Zhao J, Zhang H, Li K, Niu LZ, Wang YP, et al. Potential protective and therapeutic roles of the nrf2 pathway in ocular diseases: an update. *Oxid Med Cell Longev.* (2020) 2020:9410952. doi: 10.1155/2020/9410952
- Wooff Y, Man SM, Aggio-Bruce R, Natoli R, Fernando N. IL-1 family members mediate cell death, inflammation and angiogenesis in retinal degenerative diseases. *Front Immunol.* (2019) 10:1618. doi: 10.3389/fimmu.2019.01618
- Tonade D, Liu H, Palczewski K, Kern TS. Photoreceptor cells produce inflammatory products that contribute to retinal vascular permeability in a mouse model of diabetes. *Diabetologia.* (2017) 60:2111–20. doi: 10.1007/s00125-017-4381-5
- Honasoge A, Nudelman E, Smith M, Rajagopal R. Emerging insights and interventions for diabetic retinopathy. *Curr Diabetes Rep.* (2019) 19:100. doi: 10.1007/s11892-019-1218-2
- Tomita Y, Fu Z, Wang Z, Cakir B, Cho SS, Britton W, et al. Long-acting FGF21 inhibits retinal vascular leakage in *in vivo* and *in vitro* models. *Int J Mol Sci.* (2020) 21:1188. doi: 10.3390/ijms21041188
- Liu JJ, Foo JP, Liu S, Lim SC. The role of fibroblast growth factor 21 in diabetes and its complications: A review from clinical perspective. *Diabetes Res Clin Pract.* (2015) 108:382–9. doi: 10.1016/j.diabres.2015.02.032
- So WY, Leung PS. Fibroblast growth factor 21 as an emerging therapeutic target for type 2 diabetes mellitus. *Med Res Rev.* (2016) 36:672–704. doi: 10.1002/med.21390
- Reish NJ, Maltare A, McKeown AS, Laszczyk AM, Kraft TW, Gross AK, et al. The age-regulating protein klotho is vital to sustain retinal function. *Invest Ophthalmol Vis Sci.* (2013) 54:6675–85. doi: 10.1167/iovs.13-12550

45. Zhang Y, Wang L, Wu Z, Yu X, Du X, Li X. The expressions of klotho family genes in human ocular tissues and in anterior lens capsules of age-related cataract. *Curr Eye Res.* (2017) 42:871–5. doi: 10.1080/02713683.2016.1259421
46. Kokkinaki M, Abu-Asab M, Gunawardena N, Ahern G, Javidnia M, Young J, et al. Klotho regulates retinal pigment epithelial functions and protects against oxidative stress. *J Neurosci.* (2013) 33:16346–59. doi: 10.1523/JNEUROSCI.0402-13.2013
47. Zhou S, Hum J, Taskintuna K, Olaya S, Steinman J, Ma J, et al. The anti-aging hormone klotho promotes retinal pigment epithelium cell viability and metabolism by activating the AMPK/PGC-1 α Pathway. *Antioxidants (Basel).* (2023) 12(2):385. doi: 10.3390/antiox12020385



OPEN ACCESS

EDITED BY

Mohd Imtiaz Nawaz,
King Saud University, Saudi Arabia

REVIEWED BY

Ricardo Adrian Nugraha,
Airlangga University, Indonesia
Dorela Doris Shuboni-Mulligan,
Eastern Virginia Medical School, United States

*CORRESPONDENCE

Bin Zheng
✉ 111575@wmu.edu.cn

RECEIVED 29 May 2024

ACCEPTED 29 August 2024

PUBLISHED 16 September 2024

CITATION

Wang Z, Wu M, Li H and Zheng B (2024)
Association between rest-activity rhythm and
diabetic retinopathy among US middle-age
and older diabetic adults.
Front. Endocrinol. 15:1440223.
doi: 10.3389/fendo.2024.1440223

COPYRIGHT

© 2024 Wang, Wu, Li and Zheng. This is an
open-access article distributed under the terms
of the [Creative Commons Attribution License](#)
(CC BY). The use, distribution or reproduction
in other forums is permitted, provided the
original author(s) and the copyright owner(s)
are credited and that the original publication
in this journal is cited, in accordance with
accepted academic practice. No use,
distribution or reproduction is permitted
which does not comply with these terms.

Association between rest-activity rhythm and diabetic retinopathy among US middle-age and older diabetic adults

Zhijie Wang^{1,2}, Mengai Wu^{1,2}, Haidong Li^{1,2} and Bin Zheng^{1,2*}

¹Department of Retina Center, Eye Hospital and School of Ophthalmology and Optometry, Wenzhou Medical University, Hangzhou, China, ²National Clinical Research Center for Ocular Diseases, Eye Hospital, Wenzhou Medical University, Wenzhou, China

Background: The disruption of circadian rhythm has been reported to aggravate the progression of diabetic retinopathy (DR). Rest-activity rhythm (RAR) is a widely used method for measuring individual circadian time influencing behavior. In this study, we sought to explore the potential association between RAR and the risk of DR.

Methods: Diabetic participants aged over 40 from 2011–2014 National Health and Nutrition Examination Survey (NHANES) were enrolled. Data from the wearable device ActiGraph GT3X was used to generate RAR metrics, including interdaily stability (IS), intradaily variability (IV), most active 10-hour period (M10), least active 5-hour period (L5), and Relative amplitude (RA). Weighted multivariable logistic regression analysis and restricted cubic spline analysis were conducted to examine the association between RAR metrics and DR risk. Sensitivity analysis was also conducted to examine the robustness of the findings. An unsupervised K-means clustering analysis was conducted to identify patterns in IV and M10.

Results: A total of 1,096 diabetic participants were enrolled, with a DR prevalence of 20.53%. The mean age of participants was 62.3 years, with 49.57% being male. After adjusting covariates, IV was positively associated with DR (β : 3.527, 95%CI: 1.371–9.073). Compared with the lowest quintile of IV, the highest quintile of IV had 136% higher odds of DR. In contrast, M10 was negatively associated with DR (β : 0.902, 95%CI: 0.828–0.982), with participants in the highest M10 quintile showing 48.8% lower odds of DR. Restricted cubic spline analysis confirmed that these associations were linear. Meanwhile, sensitivity analysis confirmed the robustness. K-means clustering identified three distinct clusters, with participants in Cluster C (high-IV, low-M10) had a significantly higher risk of DR comparing with Cluster A (low-IV, high-M10).

Conclusion: A more fragmented rhythm and lower peak activity level might be associated with an increased risk of DR. These findings indicate that maintaining a more rhythmic sleep-activity behavior might mitigate the development of DR.

Further research is necessary to establish causality and understand the underlying mechanisms, and focus on whether interventions designed to enhance daily rhythm stability and increase diurnal activity level can effectively mitigate the risk of progression of DR.

KEYWORDS

diabetic retinopathy, rest-activity rhythm, circadian rhythm, fragmented rhythm, NHANES

1 Introduction

Diabetic retinopathy (DR), is the leading cause of vision impairment and blindness among work-age adults, characterized by the progressive retina vascular damage as a severe complication of diabetes mellitus. Paralleling the rise of diabetes, the prevalence of DR had been increasing globally. According to a recent meta-analysis, the global prevalence of DR among the diabetic population is 22.27%, and the number of DR is projected to reach 160.50 million by 2045 (1). DR manifests through series of stages, from microaneurysms abnormalities to proliferative DR marked by neovascularization and retinal detachment (2). Understanding the risk factors and pathophysiological mechanisms of DR is crucial for developing effective prevention and treatment strategies.

Circadian rhythm is an intrinsic 24-hour cycle regulating various biological processes in organisms. One critical output of circadian rhythm is the rest-activity rhythm (RAR), which encompasses the patterns of physical activity and rest throughout the day and night (2). Disturbance of RAR, often resulting from irregular sleep patterns, shift work, or exposure to artificial light (3–5), has been implicated in various metabolic diseases and cardiovascular disorders, such as hypertension, diabetes, and so on (2, 6, 7).

Emerging evidence indicates that the disruption of circadian rhythm may also influence the diverse facets of DR, from alterations in clock genes to changes in rhythmic clinical manifestations (8, 9). Notably, a remarkable decrease of a diverse array of clock genes were observed in retina of diabetes rodent model (10, 11). Our recent study revealed that diabetes reshapes the rhythmic profile of retinal transcriptome (12). Aberrant expression or loss of core clock genes could accelerate retinal endothelial dysfunction and increase retinal permeability (13). Furthermore, disturbed rhythms in retinal structures and physiological functions, such as retinal thickness and melatonin rhythm, have been observed in DR (14). A recent cross-sectional study explored alteration of circadian rhythm in DR by examining 24-hour melatonin secretion, intrinsically photosensitive retinal ganglion cell (ipRGC) and RAR (15). The results indicated that DR patients exhibited lower melatonin output and reduced ipRGC function. However, due to the small sample size ($n=25$), no significant change in RAR was observed. In the present study, we aimed to explore the association between RAR metrics and DR

based on a large, population-based cohort, hypothesizing that irregular RAR may be a potential risk factor for the development and progression of DR. This will be investigated through a cross-sectional study among middle-age or older diabetic participants ($\text{age} \geq 40$) within the U.S. National Health and Nutrition Examination Survey (NHANES).

2 Methods

2.1 Study population

NHANES is a complex, multi-staged national survey in the United States, that investigates the health and nutrition status of U.S. civilian population through personal interviews, physical examinations and laboratory tests (16). This survey is conducted in two-year cycles. The NHANES protocols were approved by the NCHS Research Ethics Review Board (Protocol #2011-17), and written consent was received from each participant.

For present study, we limited the participants to those from 2011-2014 cycles of NHANES. Participants with the following characteristics were excluded: a) absence of diabetes mellitus; b) age <40 years old; c) those with fewer than 4 days of valid accelerometer data; d) pregnancy. As shown in Figure 1, a total of 1096 participants met inclusion criteria for the subsequent analysis.

2.2 RAR metrics

According to NHANES protocol, all participants aged 6 years and older were required to wear the physical activity monitor (PAM) ActiGraph GT3X+ accelerometer (Pensacola, FL) for seven consecutive days to collect objective data. The accelerometer data, recorded at a frequency of 80 Hz, and ambient light measurements, taken at 1 Hz, were aggregated on a per-minute basis for each participant, specified in Monitor-Independent Movement Summary (MIMS) units.

The first and last days of accelerometer data were omitted due to the incomplete 24-h periods. According to the previous research, the raw data were pre-processed using *acelmissing* R package (17). A valid day was defined as having more than 16 hours of wearing

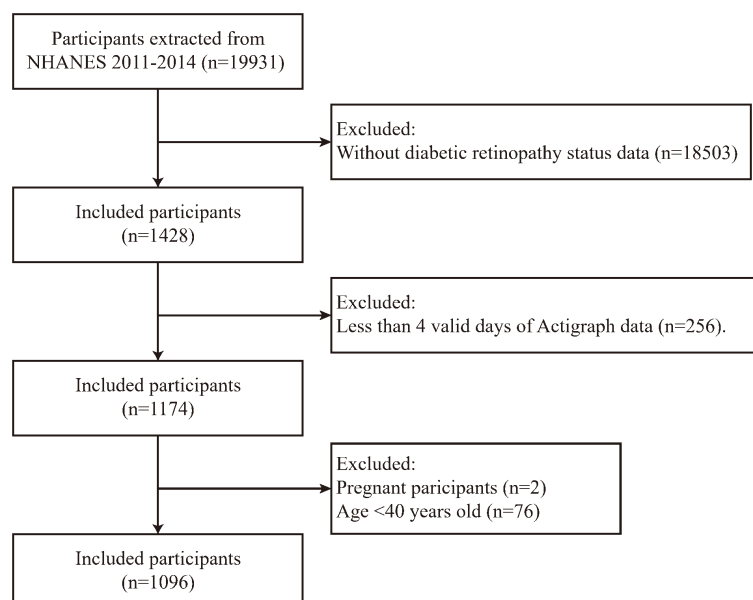


FIGURE 1
Flow chart of the sample screening process.

time, and subjects were required to have at least four valid days of data to be included in the analysis. RAR metrics are reliable variables for quantifying the strength, timing, and regularity of sleep and physical activity patterns, partially reflecting the objective behavioral manifestation of daily rhythm in response to environmental cues (18). In this study, we employed non-parametric methods to generate RAR metrics using nparACT R package (19). The key RAR metrics included: 1) Interdaily Stability (IS), which assesses the consistency of the rest-activity pattern with the 24h light-dark cycle; 2) intradaily variability (IV), which measures the fragmentation of the 24-hour rhythm, with higher IV values indicating greater rhythm fragmentation, commonly associated with frequent snapping or inefficient sleep; 3) Most active 10-hour period (M10), which measures the average activity of ten consecutive hours with the peak activity among 24-hour period; 4) Least active 5-hour period (L5), measures the average activity of five consecutive hour with nadir activity; 5) Relative amplitude(RA), which demonstrates the relative difference between M10 and L5, with higher RA values indicating greater circadian rhythm strength.

2.3 Definition of diabetes mellitus and diabetic retinopathy

Diabetes mellitus is defined according to the following criteria: 1) glycohemoglobin HbA1c $\geq 6.5\%$; 2) fasting glucose $\geq 7.0\text{mmol/L}$; 3) self-reported previous diagnosis of diabetes by a doctor. Participants were classified as having DR if they answered 'yes' to: 'Has a doctor ever informed you that your eyes are affected by diabetes or that you have retinopathy?'

2.4 Covariates

The following covariates were included: age (40-60, >60 years), sex (male, female), marital status (never married, married or living with a partner, widowed/divorced/separated), education level (<high school, high school or equivalent, >high school), poverty income ratio (PIR, <1.3, 1.3-3.5, >3.5) race ethnicity (non-Hispanic white, other), self-reported sleep problems (yes, no), hypertension (yes, no), and hyperlipidemia (yes, no). Missing values for covariates were imputed with multiple imputation by chained equations with the 'mice' R package. We generated five imputed datasets with the random forest imputation algorithm and subsequently pooled the results following Rubin's standard rules.

2.5 Statistical analysis

In the present study, all statistical analyses were conducted with consideration of the survey weights based on the NHANES protocol. Participant characteristics were demonstrated using descriptive statistical analyses based on the presence of DR. Continuous variables were presented as weighted mean \pm SD, and differences between groups were compared using one-way ANOVA. Categorical variables were presented as weighted percentage, and differences were compared using the Rao-Scott chi-square test. To investigate the association between the risk of DR and each RAR metric, weighted logistic regression analysis was conducted. RAR metrics were categorized into quintiles, and the first quintile was set as the reference. Three regression models were generated: Model 1 was the crude model without any adjustments. Model 2 was adjusted for the age, sex, race, marital status, PIR.

Model 3 was further adjusted for hypertension, hyperlipidemia, and sleep problems. In the fully adjusted model, the non-linear relationship was explored using the restricted cubic spline (RCS) method with four knots, setting RAR metrics as the exposure and the risk of DR as the outcome. To identify patterns in IV and M10, an unsupervised K-means clustering analysis was conducted with R.

For subgroup analysis, participants were stratified by age (40-60, >60), sex (male, female), education level (<high school, high school or equivalent, >high school), and race ethnicity (non-Hispanic white, other) in the fully adjusted model. The interaction between RAR metrics and potential modifiers were calculated to examine the differences in effect across subgroups (p for interaction). To assess the robustness of the main findings, sensitivity analysis was performed after excluding the participant with any missing covariates.

All statistical analyses were performed using R (version 4.2.2), and two-side p-value <0.05 was considered statistically significant.

3 Results

3.1 Baseline characteristic

In this study, a total of 1,096 eligible participants with diabetic mellitus were included (Figure 1), representing an estimated weighted population of 16,930,542 in the United States. The mean age of participants was 62.3 years, with 49.57% being male. Detailed characteristics of the participants are summarized in Table 1, covering a variety of social-culture backgrounds in the United States. The prevalence of DR among the valid participants was 20.53%. Notably, the majority of participants were non-Hispanic white (63.27%), and more than (76.16%) had a high school degree or above. In terms of marital status, the percent of married or live with a partner is 60.35% in this cohort. The rest-activity rhythm was quantified into five parameters: IS, IV, RA, L5 and M10. Compare to participants without DR, those with DR had a lower M10 level (p=0.035) and tended to have higher IV level, though this difference was not statistically significant (p=0.065). Additionally, participants with DR were more likely to be never married and had a lower prevalence of hypertension (p=0.044 and 0.048, respectively).

3.2 Association between RAR metrics and DR

To investigate the association between RAR and DR, we conducted weighted multivariable logistic regression analyses on the RAR metrics. As shown in Table 2, after adjusting for a comprehensive set of confounders, the results of Model 3 demonstrated a positive association between IV and the risk of DR (OR=3.527; 95% CI, 1.371-9.073; p=0.011). Additionally, the value of M10 was negatively associated with DR when adjusted for sociodemographic factors and comorbidity (Table 2, Model 3, OR=0.902; 95% CI, 0.828-0.982; p=0.02). Consistently, when we categorized RAR metrics by dividing the values into quintiles, the

TABLE 1 Baseline characteristics of participants in NHANES 2011-2014 (N=1096).

| Characteristic | total (N=1096) | Without DR (N=871) | With DR (N=225) | p |
|-------------------------------------|----------------|--------------------|-----------------|--------|
| Age, n (%) | | | | 0.784 |
| 40-60 | 373(40.49) | 301(40.24) | 72(41.72) | |
| ≥60 | 723(59.51) | 570(59.76) | 153(58.28) | |
| Sex, n (%) | | | | 0.185 |
| Female | 548(50.43) | 452(51.55) | 96(44.92) | |
| Male | 548(49.57) | 419(48.45) | 129(55.08) | |
| Race, n (%) | | | | 0.115 |
| Non-Hispanic White | 387(63.27) | 314(64.44) | 73(57.52) | |
| other | 709(36.73) | 557(35.56) | 152(42.48) | |
| Education level, n (%) | | | | 0.074 |
| < High school | 370(23.83) | 290(22.89) | 80(28.49) | |
| High School Grad/ GED or Equivalent | 256(25.51) | 199(24.53) | 57(30.35) | |
| > High school | 470(50.65) | 382(52.57) | 88(41.17) | |
| Marital status, n (%) | | | | 0.044* |
| Married or living with a partner | 598(60.35) | 485(61.43) | 113(55.04) | |
| Never married | 96(7.96) | 77(6.92) | 19(13.14) | |
| Widowed, divorced, separated | 402(31.69) | 309(31.66) | 93(31.82) | |
| PIR, n (%) | | | | 0.126 |
| <1.3 | 447(28.70) | 347(27.08) | 100(36.66) | |
| 1.3-3.5 | 415(39.69) | 332(40.14) | 83(37.50) | |
| >3.5 | 234(31.61) | 192(32.78) | 42(25.84) | |
| Smoke, n (%) | | | | 0.932 |
| never | 550(48.89) | 444(48.63) | 106(50.18) | |
| former | 393(37.23) | 304(37.51) | 89(35.84) | |
| now | 153(13.88) | 123(13.86) | 30(13.97) | |
| Hypertension, n (%) | | | | 0.048* |
| Yes | 257(23.39) | 216(24.58) | 41(17.54) | |
| No | 839(76.61) | 655(75.42) | 184(82.46) | |
| Hyperlipidemia, n (%) | | | | 0.938 |
| No | 138(9.877) | 112(9.901) | 26(9.758) | |
| Yes | 958(90.123) | 759(90.099) | 199(90.242) | |

(Continued)

TABLE 1 Continued

| Characteristic | total (N=1096) | Without DR (N=871) | With DR (N=225) | p |
|-------------------------|-------------------|--------------------------|-----------------------|--------|
| Sleep problem, n (%) | | | | 0.423 |
| No | 692(59.14) | 553(58.51) | 139(62.26) | |
| Yes | 404(40.86) | 318(41.49) | 86(37.74) | |
| IS, mean ± SD | 0.37 ± 0.00 | 0.37 ± 0.00 | 0.36 ± 0.01 | 0.163 |
| IV, mean ± SD | 0.64 ± 0.01 | 0.64 ± 0.01 | 0.68 ± 0.02 | 0.065 |
| RA, mean ± SD | 0.79 ± 0.01 | 0.80 ± 0.01 | 0.78 ± 0.01 | 0.154 |
| L5, mean ± SD | 1.08 ± 0.04 | 1.09 ± 0.04 | 1.08 ± 0.06 | 0.939 |
| M10, mean ± SD | 9.64 ± 0.14 | 9.76 ± 0.14 | 9.06 ± 0.32 | 0.035* |

PIR, poverty income ratio. IS, interdaily stability. IV, intradaily variability. M10, most active 10-hour period. L5, least active 5-hour period. RA, relative amplitude. *p value<0.05.

participants in the fifth quintile (Q5) of IV were 136% more likely to develop DR than those in the first quintile (Q1) (Table 3, Model 3; OR=2.360; p for trend = 0.047). The risk of DR in the Q5 group of M10 showed significant reductions compared to the Q1 group, with a decrease of 49% (Table 3, Model 3; OR=0.512; p for trend = 0.024). To explore the nonlinear relationship between IV/M10 and the risk of DR, we conducted RCS analysis. No nonlinear association was detected for either IV or M10 (Figure 2, p for nonlinearity = 0.207 and 0.311, respectively). However, as demonstrated in Figure 2, these two curves also do not completely fit a linear relationship. For association between IV and the risk of DR, the curve is relatively stable over most of the range but shows a significant upward trend at high IV values (IV>0.75). For association between IV and the risk of DR, when M10 <9, the OR value decrease significantly as M10 increases, whereas when M10 value exceed 9, this downward trend gradually stabilizes. In summary, as IV value increases and M10 value decreases, the risk of developing DR tends to rise.

TABLE 2 Association between RAR metrics and DR (N=1096).

| 24-h Rest- activity rhythm variables | Model 1 | | Model 2 | | Model 3 | |
|---|--------------------|--------|--------------------|--------|--------------------|--------|
| | OR (95%CI) | p | OR (95%CI) | p | OR (95%CI) | p |
| RA | 0.327(0.074,1.443) | 0.135 | 0.375(0.087,1.610) | 0.178 | 0.366(0.084,1.589) | 0.170 |
| IS | 0.249(0.035,1.786) | 0.160 | 0.292(0.047,1.812) | 0.177 | 0.281(0.044,1.794) | 0.170 |
| IV | 2.971(1.025,8.613) | 0.045* | 3.554(1.373,9.202) | 0.011* | 3.527(1.371,9.073) | 0.011* |
| L5 | 0.993(0.813,1.211) | 0.940 | 0.969(0.787,1.194) | 0.758 | 0.973(0.789,1.199) | 0.787 |
| M10 | 0.916(0.839,1.001) | 0.052 | 0.903(0.830,0.982) | 0.020* | 0.902(0.828,0.982) | 0.020* |

Model 1: crude model, without any adjustment.
Model 2: adjusted for age, sex, education level, marital status, PIR.
Model 3: adjusted for age, sex, education level, marital status, PIR, sleep problem, and hyperlipidemia and hypertension.
OR, odds ratios. CI, confidence interval. RAR, rest-activity rhythm. RA, relative amplitude. IS, interdaily stability. IV, intradaily variability. M10, most active 10-hour period. L5, least active 5-hour period.
*p value<0.05.

3.3 Stratified and sensitivity analyses

To explore the impact of age, sex, race and education level on the findings, we performed the subgroup analysis based on different features (Supplementary Tables 1, 2). The IV quintiles displayed interactions with different education level subgroups (p for interaction = 0.014). The negative association between IV and DR was predominantly significant among the population with a high school education level or below.

In sensitivity analyses, participants with any missing covariates were excluded, and the analysis was re-performed on the remaining 938 participants. The association between IV and M10 and the risk of DR persisted, confirming that the main findings were reliable (Supplementary Table 3).

3.4 Unsupervised cluster analysis of IV and M10 in DR

Subsequently, we performed an unsupervised K-means clustering analysis to cluster 1,096 participants based on their IV and M10 values. As depicted in Figure 3A, three distinct clusters were identified: Cluster A (n=230), Cluster B (n=519) and Cluster C (n=347). These clusters demonstrated significant differences in IV and M10 distribution, with Cluster A exhibiting lower IV and higher M10, while Cluster C had higher IV and lower M10 values (Figures 3B, C).

The baseline characteristics of participants in these three clusters are summarized in Supplementary Table 4. There were significant differences in age, sex, race, education level, PIR and DR risk among the clusters. Notably, participants in Cluster C (high-IV, low-M10) are more prone to have DR.

Logistic regression analyses were conducted to evaluate the association between these clusters and the risk of DR. After adjusting for a comprehensive set of covariates, participants in Cluster C (high-IV, low-M10) were found to be 55% more likely to have DR compared to those in Cluster A (low-IV, high-M10)(p for

TABLE 3 Association between quintiles of RAR metrics and DR.

| 24-h Rest-activity rhythm variables | Model 1 OR (95% CI) | Model 2 OR (95% CI) | Model 3 OR (95% CI) |
|-------------------------------------|---------------------------|---------------------------|---------------------------|
| IS | | | |
| Q1 | ref | ref | ref |
| Q2 | 0.957 (0.512,1.790) | 1.022 (0.538,1.942) | 1.006 (0.530,1.909) |
| Q3 | 1.328 (0.664,2.656) | 1.515 (0.751,3.056) | 1.511 (0.748,3.049) |
| Q4 | 0.435 (0.236,0.800) | 0.470 (0.264,0.838) | 0.466 (0.258,0.842) |
| Q5 | 0.895 (0.480,1.666) | 0.938 (0.538,1.638) | 0.924 (0.521,1.639) |
| p for trend | 0.211 | 0.225 | 0.222 |
| IV | | | |
| Q1 | ref | ref | ref |
| Q2 | 1.471 (0.804,2.693) | 1.737 (0.943,3.198) | 1.737 (0.933,3.232) |
| Q3 | 0.961 (0.501,1.843) | 1.150 (0.571,2.315) | 1.157 (0.575,2.331) |
| Q4 | 1.185 (0.489,2.869) | 1.438 (0.578,3.581) | 1.443 (0.578,3.599) |
| Q5 | 1.949 (1.016,3.738) | 2.368 (1.214,4.621) | 2.360 (1.205,4.621) |
| p for trend | 0.132 | 0.047* | 0.047* |
| M10 | | | |
| Q1 | ref | ref | ref |
| Q2 | 0.686 (0.317,1.483) | 0.696 (0.327,1.481) | 0.696 (0.325,1.488) |
| Q3 | 0.416 (0.193,0.896) | 0.449 (0.213,0.948) | 0.444 (0.207,0.951) |
| Q4 | 0.369 (0.177,0.772) | 0.343 (0.161,0.729) | 0.343 (0.161,0.728) |
| Q5 | 0.593 (0.248,1.419) | 0.518 (0.212,1.263) | 0.512 (0.208,1.260) |
| p for trend | 0.063 | 0.026* | 0.024* |
| L5 | | | |
| Q1 | ref | ref | ref |
| Q2 | 1.247 (0.587,2.652) | 1.233 (0.591,2.574) | 1.233 (0.584,2.603) |
| Q3 | 1.134 (0.496,2.593) | 1.083 (0.503,2.333) | 1.072 (0.495,2.319) |
| Q4 | 1.720 (0.839,3.526) | 1.715 (0.856,3.436) | 1.730 (0.848,3.531) |
| Q5 | 1.190 (0.642,2.205) | 1.102 (0.600,2.022) | 1.113 (0.601,2.059) |
| p for trend | 0.386 | 0.544 | 0.515 |

(Continued)

TABLE 3 Continued

| 24-h Rest-activity rhythm variables | Model 1 OR (95% CI) | Model 2 OR (95% CI) | Model 3 OR (95% CI) |
|-------------------------------------|---------------------------|---------------------------|---------------------------|
| RA | | | |
| Q1 | ref | ref | ref |
| Q2 | 0.885 (0.450,1.741) | 0.905 (0.450,1.821) | 0.905 (0.445,1.840) |
| Q3 | 0.740 (0.420,1.305) | 0.769 (0.442,1.336) | 0.762 (0.438,1.325) |
| Q4 | 0.599 (0.317,1.133) | 0.637 (0.331,1.226) | 0.632 (0.328,1.220) |
| Q5 | 0.595 (0.265,1.336) | 0.608 (0.271,1.365) | 0.602 (0.266,1.363) |
| p for trend | 0.09 | 0.111 | 0.108 |

Model 1: crude model, without any adjustment.
Model 2: adjusted for age, sex, education level, marital status, PIR.
Model 3: adjusted for age, sex, education level, marital status, PIR, sleep problem, and hyperlipidemia and hypertension.
OR, odds ratios. CI, confidence interval. RAR, rest-activity rhythm. RA, relative amplitude. IS, interdaily stability. IV, intradaily variability. M10, most active 10-hour period. L5, least active 5-hour period. Ref, reference. *p value<0.05.

trend=0.014, **Figure 3D**). This result further supports the above finding that the risk of DR increases as M10 decreases and IV increases.

4 Discussion

The present study uncovered the association between DR and RAR parameters in a representative U.S. working-age or older diabetes population. Notably, our findings demonstrated that the risk of DR increases with the higher IV value and lower M10 value. This indicates that fragmented rhythms and lower peak activity are more common among DR participants. These findings highlight the potential advantages of maintaining a regular sleep-activity rhythm and having high activity levels during the daytime in terms of delaying the onset of DR.

It is well documented that circadian rhythm plays a crucial role in regulating glucose homeostasis (20). Previous studies have revealed that the disruptions of circadian rhythm, induced by lifestyle factors such as shift work (21) and social jetlag (22), are associated with type 2 diabetes. Glucose homeostasis is essential for maintaining the normal physiological function of retinal cells. Hyperglycemia triggers a cascade of complex pathophysiological changes in retinal cells (23). For example, chronic hyperglycemia can cause endothelial dysfunction, pericyte loss, and the perturbations of endothelial glycocalyx in the retina (24, 25). In addition, hyperglycemia activates retinal microglia and Müller cell, inducing the release of various inflammatory cytokines and vascular growth factors (26, 27). The production of reactive oxygen species and the formation of advanced glycation end products also increase under poorly controlled blood glucose. These processes exacerbate retinal vascular damage, promote neovascularization, and ultimately lead to the progression of DR (28).

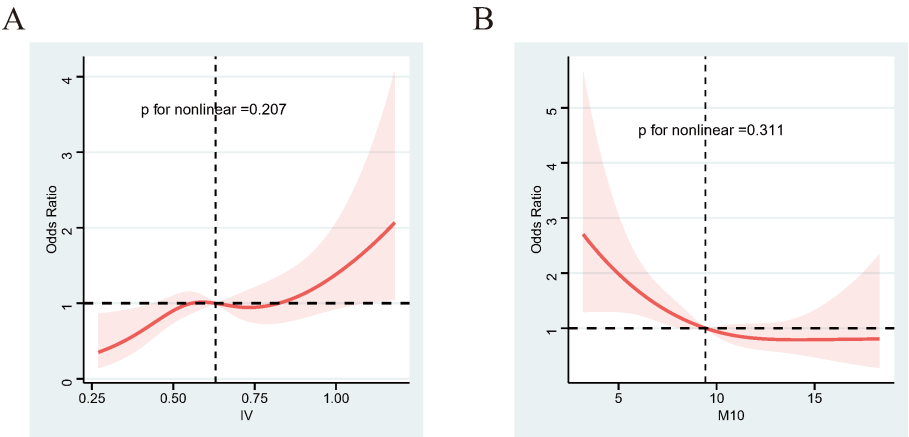


FIGURE 2
RCS results between IV/M10 and DR. **(A)** IV and the risk of DR. **(B)** M10 and the risk of DR. Adjusted for age, sex, race, education level, marital status, PIR, sleep problem, and hyperlipidemia and hypertension. The shaded part represents the 95%CI. RCS, restricted cubic spline.

Additionally, clinical findings and laboratory studies have indicated that circadian rhythm disturbances are directly associated with DR (29). Melatonin, a hormone acting as a dark signal for the retina, was found to be decreased in DR patients (15, 30). Furthermore, DR patients suffer from ipRGC dysfunction (15), which is a crucial component of the light entrainment in synchronization of the central clock to environment cues (31). Our previous study found that circadian oscillations of the transcriptomic profile in the retina were reshaped in streptozocin-induced diabetic mouse model (12). The expression of clock genes was altered in retina

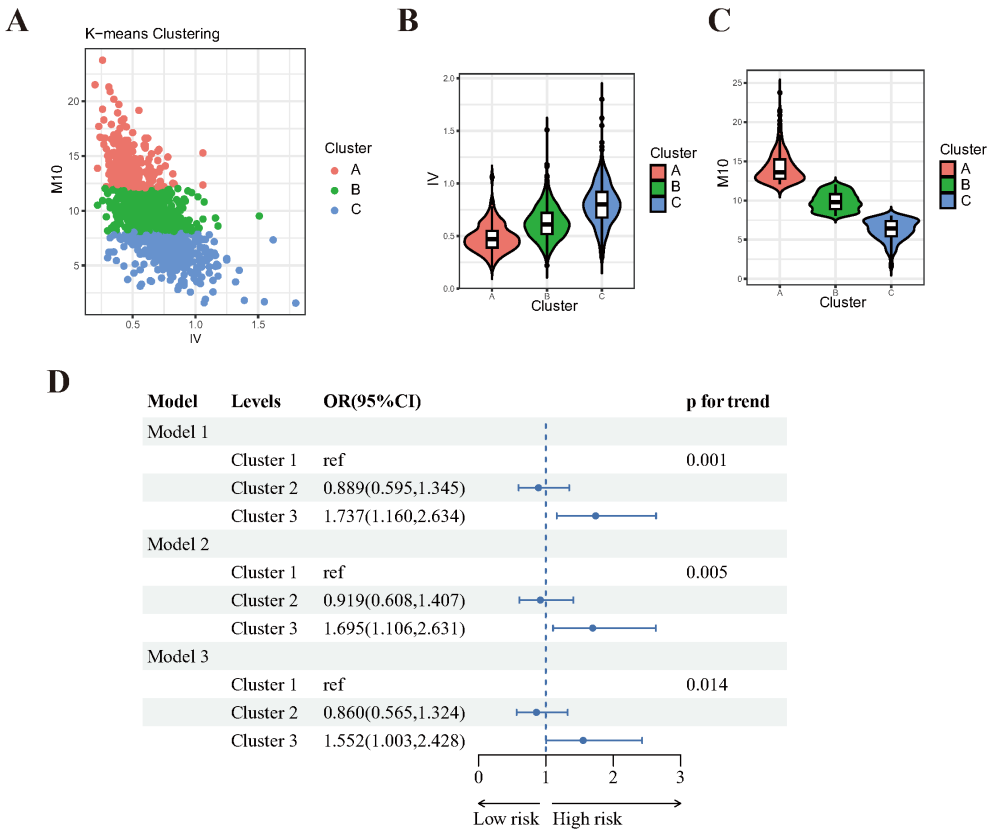


FIGURE 3
Unsupervised Cluster analysis results of IV and M10 in DR. **(A)** three distinct clusters were identified by K-means clustering. **(B)** violin plot of IV distribution among clusters. **(C)** violin plot of IV distribution among clusters. **(D)** Forest plot of clusters and the risk of DR. Model 1: crude model, without any adjustment. Model 2: adjusted for age, sex, education level, marital status, PIR. Model 3: adjusted for age, sex, education level, marital status, PIR, sleep problem, and hyperlipidemia and hypertension.

of diabetic mice (32), and the loss of core clock gene was related to the phenotype of DR. For instance, *Per2* mutant mice showed DR-like retinal vascular, including increased retinal vascular permeability and avascular capillaries (13). Interestingly, deletion of another core clock gene *Bmal1*, reduced neovascularization and vascular leakage, indicating *Bmal1* could drive neovascularization (33). In a summary, circadian rhythm disruption and altered expression of clock genes play crucial roles in the development of DR. The development of wearable device Actigraphy enables individuals to conduct 24-hour sleep and activity monitoring. The introduction of the RAR, generated from Actigraphy data, provides a robust quantification of daily rhythm. Recently, researchers have uncovered the association between RAR and various diseases, such as Parkinson's disease, non-alcoholic fatty liver disease (34, 35). Additionally, it was found that blunted RAR is strongly correlated with biological aging and may negatively affect well-being and longevity (36). However, there are limited studies on relationship between RAR and DR.

Recently, Mayuko et al. examined RAR in relation to common diabetic complications, including DR (37). The findings of our study share similarities with those of Mayuko et al., but also exhibit differences. They stated that the presence of DR was associated with higher IV and lower daytime activity, consistent with our findings. However, Mayuko et al. found that RA and L5 were also significantly associated with DR, which was not observed in our study. The differences could be explained by a few reasons. Firstly, considering the complex survey design, sample weights for each individual was calculated when conducting analysis in our study, whereas Mayuko et al. had a limited sample size. Secondly, Mayuko et al. further graded DR into simple diabetic retinopathy and proliferative diabetic retinopathy, whereas we only considered the presence of DR without considering its severity.

M10, representing the mean activity level during the most active 10-hour period within 24-hour cycle, which is used to analyze activity patterns. In this study, M10 was found to be negatively associated with the risk of DR. It is well known that environmental and lifestyle modifications can alter circadian rhythm (38). Research in animals has shown that db/db mice, a well-acknowledged diabetic mouse model, showed sporadic wheel-running activity with no consistent pattern (39). There is substantial evidence supporting the insight that increasing physical activity alleviates the progression of DR (40). Several prospective cohort studies have reported that higher physical activity is independently associated with a lower incidence of DR (41, 42). The mechanism is speculated to be that physical activity might improve glycemic control and 25-hydroxyvitamin D level (43, 44). It was reported that 25-hydroxyvitamin D could inhibit retinal inflammation and retinal neovascularization *in vivo* and *in vitro* (45–47). Thus, we speculate that subjects with high activity pattern (high M10 value) may have better glycemic control and higher level of 25-hydroxyvitamin D, thereby ameliorating DR-related pathogenesis.

Intradaily variability (IV), refers to fluctuation or change in an individual's activity levels and rest periods within a single day. High IV indicates a less stable or more fragmented rest-activity pattern,

with frequent transitions between activity and rest states. This instability generally results from irregular sleep patterns, inconsistent wake times or frequent napping. A case-control study compared sleep quality among diabetic patients with and without DR, and found that poor sleep, sleep latency and daytime dysfunction were more common in DR patients (48). A recent meta-analysis also reported poor sleep satisfaction was associated with a 2-fold risk of having DR (48). Sirimon et al. found DR patients were more likely to have insomnia and greater sleep variability (49). Melatonin, the primary hormone involved in regulating the sleep-wake cycles, is known that melatonin deficiency is responsible for sleep disorders (50). Melatonin exhibits multiple protective effects that could benefit DR patients, including anti-oxidative, anti-inflammatory and anti-apoptotic properties (51). Accordingly, we speculate that some participants, due to a lack of melatonin, may lose its protective effect on the retina and become more prone to developing DR. Additionally, melatonin-deficient participants are more likely to experience sleep disorders or fragmented rest-activity patterns, as evidenced by elevated IV value in RAR.

The main strength of this study is its nationally representative and diverse population-based cohort, which enhances the generalizability of the findings. However, there are several limitations to consider when interpreting the results. Firstly, due to the cross-sectional study design, causality between RAR metrics and DR cannot be established. Given that advanced stages of DR can cause severe vision loss and dysfunction of ipRGCs, leading to misalignment of circadian photoentrainment, it is possible that blunted RAR is a result of DR. Secondly, the diagnosis of DR was obtained from the self-reports in the medical conditions questionnaire, which could lead to diagnostic omissions. Additionally, in this study, only the presence of DR was available for analysis without considering the severity of DR. Future research should incorporate fundus photo and optical coherence tomography images for more accurate DR diagnosis and grading.

5 Conclusions

We demonstrated that altered RAR parameters are associated with the onset of DR. Notably, the significant associations were observed for IV, reflecting the fragmentation of rhythm, and for M10, reflecting the daytime activity level. These findings indicate that the fragmented rhythm and lower peak activity may increase the risk of DR. Further interventional research aimed at improving circadian rhythm through lifestyle, behavioral and environmental modification should be conducted to elucidate the casual links between circadian disruption and DR.

Data availability statement

The original contributions presented in the study are included in the article/in [Supplementary Material](#). Further inquiries can be directed to the corresponding author.

Ethics statement

The studies involving humans were approved by NCHS Research Ethics Review Board. The studies were conducted in accordance with the local legislation and institutional requirements. The participants provided their written informed consent to participate in this study.

Author contributions

ZW: Writing – original draft, Software, Methodology, Formal analysis, Data curation. MW: Writing – original draft, Formal analysis. HL: Writing – review & editing. BZ: Writing – review & editing, Project administration.

Funding

The author(s) declare financial support was received for the research, authorship, and/or publication of this article. This research was supported by Zhejiang Provincial Natural Science Foundation of China (Grant No. ZCLQ24H1202), and Wenzhou Municipal Science and Technology Bureau (Grant No. Y2023811).

References

- Teo ZL, Tham YC, Yu M, Chee ML, Rim TH, Cheung N, et al. Global prevalence of diabetic retinopathy and projection of burden through 2045: systematic review and meta-analysis. *Ophthalmology*. (2021) 128:1580–91. doi: 10.1016/j.ophtha.2021.04.027
- Yang X, Hu R, Zhu Y, Wang Z, Hou Y, Su K, et al. Meta-analysis of serum vitamin B12 levels and diabetic retinopathy in type 2 diabetes. *Arch Med Res*. (2023) 54:64–73. doi: 10.1016/j.arcmed.2022.12.006
- Canazei M, Weninger J, Pohl W, Marksteiner J, Weiss EM. Effects of dynamic bedroom lighting on measures of sleep and circadian rest-activity rhythm in inpatients with major depressive disorder. *Sci Rep*. (2022) 12:6137. doi: 10.1038/s41598-022-10161-8
- Kim SJ, Lim YC, Kwon HJ, Lee JH. Association of rest-activity and light exposure rhythms with sleep quality in insomnia patients. *Chronobiol Int*. (2020) 37:403–13. doi: 10.1080/07420528.2019.1696810
- Chang WP, Li HB. Influence of shift work on rest-activity rhythms, sleep quality, and fatigue of female nurses. *Chronobiol Int*. (2022) 39:557–68. doi: 10.1080/07420528.2021.2005082
- Yeung CHC, Bauer C, Xiao Q. Associations between actigraphy-derived rest-activity rhythm characteristics and hypertension in United States adults. *J Sleep Res*. (2023) 32:e13854. doi: 10.1111/jsr.13854
- Makarem N, German CA, Zhang Z, Diaz KM, Palta P, Duncan DT, et al. Rest-activity rhythms are associated with prevalent cardiovascular disease, hypertension, obesity, and central adiposity in a nationally representative sample of US adults. *J Am Heart Assoc*. (2024) 13:e032073. doi: 10.1161/JAHA.122.032073
- Liu WJ, Chen JY, Niu SR, Zheng YS, Lin S, Hong Y. Recent advances in the study of circadian rhythm disorders that induce diabetic retinopathy. *BioMed Pharmacother*. (2023) 166:115368. doi: 10.1016/j.biopha.2023.115368
- Bhatwadekar AD, Rameswara V. Circadian rhythms in diabetic retinopathy: an overview of pathogenesis and investigational drugs. *Expert Opin Investig Drugs*. (2020) 29:1431–42. doi: 10.1080/13543784.2020.1842872
- Busik JV, Tikhonenko M, Bhatwadekar A, Opreanu M, Yakubova N, Caballero S, et al. Diabetic retinopathy is associated with bone marrow neuropathy and a depressed peripheral clock. *J Exp Med*. (2009) 206:2897–906. doi: 10.1084/jem.20090889
- Lahouaoui H, Coutanson C, Cooper HM, Bennis M, Dkhissi-Benyahya O. Diabetic retinopathy alters light-induced clock gene expression and dopamine levels in the mouse retina. *Mol Vis*. (2016) 22:959–69.
- Ye S, Wang Z, Ma JH, Ji S, Peng Y, Huang Y, et al. Diabetes reshapes the circadian transcriptome profile in murine retina. *Invest Ophthalmol Vis Sci*. (2023) 64:3. doi: 10.1167/iovs.64.13.3
- Bhatwadekar AD, Yan Y, Qi X, Thinschmidt JS, Neu MB, Li Calzi S, et al. Per2 mutation recapitulates the vascular phenotype of diabetes in the retina and bone marrow. *Diabetes*. (2013) 62:273–82. doi: 10.2337/db12-0172
- Polito A, Del Borrello M, Polini G, Furlan F, Isola M, Bandello F. Diurnal variation in clinically significant diabetic macular edema measured by the Stratus OCT. *Retina*. (2006) 26:14–20. doi: 10.1097/00006982-200601000-00003
- Reutrakul S, Park JC, McAnany JJ, Chau FY, Danielson KK, Prasad B, et al. Dysregulated 24 h melatonin secretion associated with intrinsically photosensitive retinal ganglion cell function in diabetic retinopathy: a cross-sectional study. *Diabetologia*. (2024) 67:1114–21. doi: 10.1007/s00125-024-06118-3
- Chen TC, Parker JD, Clark J, Shin HC, Rammon JR, Burt VL. National health and nutrition examination survey: estimation procedures, 2011–2014. *Vital Health Stat* 2. (2018) 177:1–26.
- Xu Y, Su S, McCall WV, Wang X. Blunted rest-activity rhythm is associated with increased white blood-cell-based inflammatory markers in adults: an analysis from NHANES 2011–2014. *Chronobiol Int*. (2022) 39:895–902. doi: 10.1080/07420528.2022.2048663
- Li J, Somers VK, Lopez-Jimenez F, Di J, Covassin N. Demographic characteristics associated with circadian rest-activity rhythm patterns: a cross-sectional study. *Int J Behav Nutr Phys Act*. (2021) 18:107. doi: 10.1186/s12966-021-01174-z
- Blume C, Santhi N, Schabus M. 'nparACT' package for R: A free software tool for the non-parametric analysis of actigraphy data. *MethodsX*. (2016) 3:430–5. doi: 10.1016/j.mex.2016.05.006
- Qian J, Scheer F. Circadian system and glucose metabolism: implications for physiology and disease. *Trends Endocrinol Metab*. (2016) 27:282–93. doi: 10.1016/j.tem.2016.03.005
- Pan A, Schernhammer ES, Sun Q, Hu FB. Rotating night shift work and risk of type 2 diabetes: two prospective cohort studies in women. *PloS Med*. (2011) 8:e1001141. doi: 10.1371/journal.pmed.1001141
- Parsons MJ, Moffitt TE, Gregory AM, Goldman-Mellor S, Nolan PM, Poulton R, et al. Social jetlag, obesity and metabolic disorder: investigation in a cohort study. *Int J Obes (Lond)*. (2015) 39:842–8. doi: 10.1038/ijo.2014.201

Conflict of interest

The authors declare that the research was conducted in the absence of any commercial or financial relationships that could be construed as a potential conflict of interest.

Publisher's note

All claims expressed in this article are solely those of the authors and do not necessarily represent those of their affiliated organizations, or those of the publisher, the editors and the reviewers. Any product that may be evaluated in this article, or claim that may be made by its manufacturer, is not guaranteed or endorsed by the publisher.

Supplementary material

The Supplementary Material for this article can be found online at: <https://www.frontiersin.org/articles/10.3389/fendo.2024.1440223/full#supplementary-material>

23. Wong TY, Cheung CM, Larsen M, Sharma S, Simo R. Diabetic retinopathy. *Nat Rev Dis Primers*. (2016) 2:16012. doi: 10.1038/nrdp.2016.12
24. Kaur G, Harris NR. Endothelial glycocalyx in retina, hyperglycemia, and diabetic retinopathy. *Am J Physiol Cell Physiol*. (2023) 324:C1061–C77. doi: 10.1152/ajpcell.00188.2022
25. Gui F, You Z, Fu S, Wu H, Zhang Y. Endothelial dysfunction in diabetic retinopathy. *Front Endocrinol (Lausanne)*. (2020) 11:591. doi: 10.3389/fendo.2020.00591
26. Hu A, Schmidt MHH, Heinig N. Microglia in retinal angiogenesis and diabetic retinopathy. *Angiogenesis*. (2024) 27:311–31. doi: 10.1007/s10456-024-09911-1
27. Yang S, Qi S, Wang C. The role of retinal Muller cells in diabetic retinopathy and related therapeutic advances. *Front Cell Dev Biol*. (2022) 10:1047487. doi: 10.3389/fcell.2022.1047487
28. Yumnamcha T, Guerra M, Singh LP, Ibrahim AS. Metabolic dysregulation and neurovascular dysfunction in diabetic retinopathy. *Antioxidants (Basel)*. (2020) 9:1244. doi: 10.3390/antiox9121244
29. Wang Z, Zhang N, Lin P, Xing Y, Yang N. Recent advances in the treatment and delivery system of diabetic retinopathy. *Front Endocrinol (Lausanne)*. (2024) 15:1347864. doi: 10.3389/fendo.2024.1347864
30. Wan WC, Long Y, Wan WW, Liu HZ, Zhang HH, Zhu W. Plasma melatonin levels in patients with diabetic retinopathy secondary to type 2 diabetes. *World J Diabetes*. (2021) 12:138–48. doi: 10.4239/wjdv12.i2.138
31. LeGates TA, Fernandez DC, Hattar S. Light as a central modulator of circadian rhythms, sleep and affect. *Nat Rev Neurosci*. (2014) 15:443–54. doi: 10.1038/nrn3743
32. Vancura P, Oebel L, Spohn S, Frederiksen U, Schafer K, Sticht C, et al. Evidence for a dysfunction and disease-promoting role of the circadian clock in the diabetic retina. *Exp Eye Res*. (2021) 211:108751. doi: 10.1016/j.exer.2021.108751
33. Jidigam VK, Sawant OB, Fuller RD, Wilcots K, Singh R, Lang RA, et al. Neuronal Bmal1 regulates retinal angiogenesis and neovascularization in mice. *Commun Biol*. (2022) 5:792. doi: 10.1038/s42003-022-03774-2
34. Brooks C, Shaafi Kabiri N, Mortazavi F, Auerbach S, Bonato P, Erb MK, et al. Variations in rest-activity rhythm are associated with clinically measured disease severity in Parkinson's disease. *Chronobiol Int*. (2020) 37:699–711. doi: 10.1080/07420528.2020.1715998
35. Gu W, Han T, Sun C. Association of 24 h Behavior Rhythm with Non-Alcoholic Fatty Liver Disease among American Adults with Overweight/Obesity. *Nutrients*. (2023) 15:2101. doi: 10.3390/nu15092101
36. Chen L, Zhao Y, Liu F, Chen H, Tan T, Yao P, et al. Biological aging mediates the associations between urinary metals and osteoarthritis among U. S. adults. *BMC Med*. (2022) 20:207. doi: 10.1186/s12916-022-02403-3
37. Kadono M, Nakanishi N, Yamazaki M, Hasegawa G, Nakamura N, Fukui M. Various patterns of disrupted daily rest-activity rhythmicity associated with diabetes. *J Sleep Res*. (2016) 25:426–37. doi: 10.1111/jsr.12385
38. Ruan W, Yuan X, Eltzschig HK. Circadian rhythm as a therapeutic target. *Nat Rev Drug Discovery*. (2021) 20:287–307. doi: 10.1038/s41573-020-00109-w
39. Alex A, Luo Q, Mathew D, Di R, Bhatwadekar AD. Metformin corrects abnormal circadian rhythm and kir4.1 channels in diabetes. *Invest Ophthalmol Vis Sci*. (2020) 61:46. doi: 10.1167/iops.61.6.46
40. Praidou A, Harris M, Niakas D, Labiris G. Physical activity and its correlation to diabetic retinopathy. *J Diabetes Complications*. (2017) 31:456–61. doi: 10.1016/j.jdiacomp.2016.06.027
41. Kuwata H, Okamura S, Hayashino Y, Tsujii S, Ishii H, Diabetes D, et al. Higher levels of physical activity are independently associated with a lower incidence of diabetic retinopathy in Japanese patients with type 2 diabetes: A prospective cohort study, Diabetes Distress and Care Registry at Tenri (DDCRT15). *PLoS One*. (2017) 12: e0172890. doi: 10.1371/journal.pone.0172890
42. Yan X, Han X, Wu C, Shang X, Zhang L, He M. Effect of physical activity on reducing the risk of diabetic retinopathy progression: 10-year prospective findings from the 45 and Up Study. *PLoS One*. (2021) 16:e0239214. doi: 10.1371/journal.pone.0239214
43. Boniol M, Dragomir M, Autier P, Boyle P. Physical activity and change in fasting glucose and HbA1c: a quantitative meta-analysis of randomized trials. *Acta Diabetol*. (2017) 54:983–91. doi: 10.1007/s00592-017-1037-3
44. Scott D, Blizzard L, Fell J, Ding C, Winzenberg T, Jones G. A prospective study of the associations between 25-hydroxy-vitamin D, sarcopenia progression and physical activity in older adults. *Clin Endocrinol (Oxf)*. (2010) 73:581–7. doi: 10.1111/j.1365-2265.2010.03858.x
45. Imanparast F, Javaheri J, Kamankesh F, Rafiei F, Salehi A, Mollaaliakbari Z, et al. The effects of chromium and vitamin D(3) co-supplementation on insulin resistance and tumor necrosis factor-alpha in type 2 diabetes: a randomized placebo-controlled trial. *Appl Physiol Nutr Metab*. (2020) 45:471–7. doi: 10.1139/apnm-2019-0113
46. Lazzara F, Longo AM, Giurandella G, Lupo G, Platania CBM, Rossi S, et al. Vitamin D(3) preserves blood retinal barrier integrity in an *in vitro* model of diabetic retinopathy. *Front Pharmacol*. (2022) 13:971164. doi: 10.3389/fphar.2022.971164
47. Gverovic Antunica A, Znaor L, Ivankovic M, Puzovic V, Markovic I, Kastelan S. Vitamin D and diabetic retinopathy. *Int J Mol Sci*. (2023) 24:12014. doi: 10.3390/ijms241512014
48. Dutta S, Ghosh S, Ghosh S. Association of sleep disturbance with diabetic retinopathy. *Eur J Ophthalmol*. (2022) 32:468–74. doi: 10.1177/1120672120974296
49. Reutrakul S, Crowley SJ, Park JC, Chau FY, Priyadarshini M, Hanlon EC, et al. Relationship between intrinsically photosensitive ganglion cell function and circadian regulation in diabetic retinopathy. *Sci Rep*. (2020) 10:1560. doi: 10.1038/s41598-020-58205-1
50. Poza JJ, Pujol M, Ortega-Albas JJ, Romero O. Insomnia Study Group of the Spanish Sleep S. Melatonin in sleep disorders. *Neurologia (Engl Ed)*. (2022) 37:575–85. doi: 10.1016/j.nrl.2018.08.002
51. Dehdashtian E, Mehrzadi S, Yousefi B, Hosseinzadeh A, Reiter RJ, Safa M, et al. Diabetic retinopathy pathogenesis and the ameliorating effects of melatonin; involvement of autophagy, inflammation and oxidative stress. *Life Sci*. (2018) 193:20–33. doi: 10.1016/j.lfs.2017.12.001



OPEN ACCESS

EDITED BY

Sara Rezzola,
University of Brescia, Italy

REVIEWED BY

Peter D. Westenskow,
Roche, Switzerland
Qingjian Ou,
Tongji University, China

*CORRESPONDENCE

Domitilla Mandatori
✉ domitilla.mandatori@unich.it

RECEIVED 09 July 2024

ACCEPTED 24 September 2024

PUBLISHED 15 October 2024

CITATION

Pelusi L, Hurst J, Detta N, Pipino C, Lamolinara A, Conte G, Mastropasqua R, Allegretti M, Di Pietrantonio N, Romeo T, El Zarif M, Nubile M, Guerricchio L, Bollini S, Pandolfi A, Schnichels S and Mandatori D (2024) Effects of mesenchymal stromal cells and human recombinant Nerve Growth Factor delivered by bioengineered human corneal lenticule on an innovative model of diabetic retinopathy.
Front. Endocrinol. 15:1462043.
doi: 10.3389/fendo.2024.1462043

COPYRIGHT

© 2024 Pelusi, Hurst, Detta, Pipino, Lamolinara, Conte, Mastropasqua, Allegretti, Di Pietrantonio, Romeo, El Zarif, Nubile, Guerricchio, Bollini, Pandolfi, Schnichels and Mandatori. This is an open-access article distributed under the terms of the [Creative Commons Attribution License \(CC BY\)](#). The use, distribution or reproduction in other forums is permitted, provided the original author(s) and the copyright owner(s) are credited and that the original publication in this journal is cited, in accordance with accepted academic practice. No use, distribution or reproduction is permitted which does not comply with these terms.

Effects of mesenchymal stromal cells and human recombinant Nerve Growth Factor delivered by bioengineered human corneal lenticule on an innovative model of diabetic retinopathy

Letizia Pelusi¹, Jose Hurst², Nicola Detta³, Caterina Pipino⁴, Alessia Lamolinara⁵, Gemma Conte³, Rodolfo Mastropasqua⁵, Marcello Allegretti⁶, Nadia Di Pietrantonio⁴, Tiziana Romeo⁶, Mona El Zarif¹, Mario Nubile⁷, Laura Guerricchio⁸, Sveva Bollini⁸, Assunta Pandolfi⁴, Sven Schnichels² and Domitilla Mandatori^{4*}

¹Department of Medicine and Aging Science, Center for Advanced Studies and Technology-CAST, University G. d'Annunzio of Chieti-Pescara, Chieti, Italy, ²University Eye Hospital, Centre for Ophthalmology, University of Tübingen, Tübingen, Germany, ³Dompé Farmaceutici SpA, Napoli, Italy, ⁴Department of Medical, Oral and Biotechnological Sciences, Center for Advanced Studies and Technology-CAST, University G. d'Annunzio of Chieti-Pescara, Chieti, Italy, ⁵Department of Neuroscience, Imaging and Clinical Sciences, University G. d'Annunzio of Chieti-Pescara, Chieti, Italy, ⁶Dompé Farmaceutici SpA, L'Aquila, Italy, ⁷Ophthalmology Clinic, Department of Medicine and Aging Science, "G. d'Annunzio" of Chieti-Pescara, Chieti, Italy, ⁸Department of Experimental Medicine, University of Genova, Genova, Italy

Introduction: Diabetic retinopathy (DR) is a microvascular complication of diabetes in which neurodegeneration has been recently identified as a driving force. In the last years, mesenchymal stromal cells (MSCs) and neurotrophins like Nerve Growth Factor (NGF), have garnered significant attention as innovative therapeutic approaches targeting DR-associated neurodegeneration. However, delivering neurotrophic factors directly in the eye remains a challenge. Hence, this study evaluated the effects of MSCs from human amniotic fluids (hAFSCs) and recombinant human NGF (rhNGF) delivered by human corneal lenticule (hCL) on a high glucose (HG) induced *ex vivo* model simulating the molecular mechanisms driving DR.

Methods: Porcine neuroretinal explants exposed to HG (25 mM for four days) were used to mimic DR *ex vivo*. hCLs collected from donors undergoing refractive surgery were decellularized using 0.1% sodium dodecyl sulfate and then bioengineered with hAFSCs, microparticles loaded with rhNGF (rhNGF-PLGA-MPs), or both simultaneously. Immunofluorescence (IF) and scanning electron microscopy (SEM) analyses were performed to confirm the hCLs bioengineering process. To assess the effects of hAFSCs and rhNGF, bioengineered hCLs were co-cultured with HG-treated neuroretinal explants and following four days RT-PCR and cytokine array experiments for inflammatory, oxidative, apoptotic, angiogenic and retinal cells markers were performed.

Results: Data revealed that HG-treated neuroretinal explants exhibit a characteristic DR-phenotype, including increased level of NF- κ B, NOS2, NRF2 GFAP, VEGFA, Bax/Bcl2 ratio and decreased expression of TUBB3 and Rho. Then, the feasibility to bioengineer decellularized hCLs with hAFSCs and rhNGF was demonstrated. Interestingly, co-culturing hAFSCs- and rhNGF- bioengineered hCLs with HG-treated neuroretinal explants for four days significantly reduced the expression of inflammatory, oxidative, apoptotic, angiogenic and increased retinal markers.

Conclusion: Overall, we found for the first time that hAFSCs and rhNGF were able to modulate the molecular mechanisms involved in DR and that bioengineered hCLs represents a promising ocular drug delivery system of hAFSCs and rhNGF for eye diseases treatment. In addition, results demonstrated that porcine neuroretinal explants treated with HG is a useful model to reproduce *ex vivo* the DR pathophysiology.

KEYWORDS

diabetic retinopathy, mesenchymal stromal cells, rhNGF, corneal lenticule, ocular delivery

1 Introduction

Diabetic retinopathy (DR) is a leading cause of vision impairment and blindness in working-age populations worldwide (1). This is considered one of the most frequent complications of diabetes mellitus (DM) related to hyperglycemia and may occur in approximately 27% of patients with diabetes (2). Of note, high glucose concentration, a common characteristic of poorly controlled diabetes, plays a defining role in activating the mechanisms that cause DR, including genetic and epigenetic factors, inflammation, heightened production of free radicals, oxidative stress and vascular endothelial growth factor (VEGF), which induce vascular endothelial cell proliferation, migration, and increased vascular permeability (3–6).

Clinically, DR can be divided into two stages: non-proliferative (NPDR) and proliferative (PDR) (4). NPDR is asymptomatic and characterized by inflammation, loss of endothelial and neuronal cells, and retinal microvasculature abnormalities. As the disease progresses in PDR, neovascularization is characterized by the presence of fragile vessels, which can easily break and hemorrhage into the vitreous, leading to sudden vision loss and often retinal detachment (3).

Although for several years DR has been considered a microvascular complication of DM, recently growing evidence suggests that the vascular phase of DR might be preceded by a diabetes-driven neurodegenerative process, which particularly interests the retinal ganglion cells (RGC) (7). These findings led to the definition of DR as a highly specific neurovascular complication (8, 9).

Currently, in addition to controlling blood glucose, blood pressure, and serum cholesterol levels, various therapeutic

approaches have become the standard for managing DR (10). These encompass laser photocoagulation, intravitreal injection of triamcinolone acetonide (IVTA) or anti-VEGF agents and intravitreal steroid implants (11). However, these options are principally used to target the late PDR stages, when vision is already significantly impaired (12). In addition, despite the discovery of therapeutic applications that have revolutionized the handling of DR, different side effects are related to its use, including endophthalmitis, intraocular inflammation, rhegmatogenous retinal detachment, tractional retinal detachment, intraocular pressure elevation, ocular hemorrhage, and ghost cell glaucoma (4). Thus, there is a strong need to develop novel treatments, particularly targeted at the initial phase of DR, where neurodegeneration is the driving force. From this perspective, there has been growing interest in stem cell (SCs) therapy and neurotrophins, with particular attention being paid to mesenchymal stromal cells (MSCs) owing to their modulatory potential. This is based on secreted soluble factors, including growth factors, cytokines, and chemokines, which are primarily responsible for therapeutic benefits through paracrine effects (13). Among the different cell sources, human SCs from amniotic fluid appear to be promising for the treatment of DR. Indeed, as reported by Costa et al., the secretome of fetal and perinatal human amniotic fluid SCs (hAFSCs) is enriched in immunomodulatory, anti-inflammatory, anti-fibrotic, and neurotrophic factors (14).

Neurotrophins, a family of structurally and functionally related growth factors, have gained attention for DR management because they are essential for the growth, differentiation, and survival of several cell types, including retinal neurons and glial cells. Among these, one of the main members is the nerve growth factor (NGF),

which plays a key role in neurodegeneration, inflammation, vascular permeability, and injury processes involved in DR pathogenesis (15).

While numerous studies (16–21) have highlighted the positive effect of MSCs and NGF in *in vitro* and *in vivo* DR models, the delivery of these factors directly in the eye remains a challenge. Concerning this, we recently demonstrated the feasibility of using human corneal lenticules (hCLs), a thin and disc-shaped part of the cornea obtained and discarded during refractive surgery, as an ocular drug delivery system. In fact, we have proven that hCLs can be bioengineered with polylactic-co-glycolic-acid (PLGA) microparticles loaded with rhNGF (rhNGF-PLGA-MPs), and that active rhNGF is sustainably released from such bioengineered hCLs for up to 1 month (22). In addition, Gary Hin-Fai Yam emphasized the reinnervation potential of decellularized hCLs in grafted chick dorsal root ganglion models in the presence of NGF (23).

It is well established that tissue culture models have the advantage of preserving the different cell types within the tissue structure (24–26). However, to transfer experiments from animal models or animal tissues to humans, it is crucial to consider the anatomical, physiological, and morphological differences between species and humans when selecting a model organism (27). In this context, pigs are used as experimental model in various medical fields because of their anatomical and morphological similarities to humans (15, 28). In particular, the pig eye has a high morphological similarity to the human eye, especially in terms of size, retinal structure, and histology, making it suitable as a retinal DR model (27, 29–31).

Based on these assumptions, the present study aimed to evaluate the effects of hAFSCs and rhNGF, delivered by hCLs, on the molecular mechanisms underlying DR using an *ex vivo* model represented by porcine neuroretinal explants treated with high glucose (HG). In particular, by using the entire neuroretina, we can mimic the DR *milieu* across all retinal tissues cell types, enabling a thorough assessment of how HG treatment, as well as hAFSCs and rhNGF, could influence the entire retinal structure and its cellular components.

2 Materials and methods

2.1 Pig eyes handling, isolation and cultivation of retinal explants

Eyes were obtained from 6-month-old pigs euthanized by electrocution at a local abattoir and transported at 4°C to the laboratory within 3 h of animal death. After arrival at the laboratory, the eyes were washed and disinfected prior to neuroretinal explant isolation. According to established procedure (32, 33), retinas were pierced with a dermal punch ($\varnothing = 8$ mm; Pmf medical AG, Germany) on the previously generated clover-leaf-like structures. These were placed in a petri dish with neurobasal medium (Neurobasal-A medium; Thermo Fisher Scientific, Karlsruhe, Germany) and neuroretinal explants were removed with a spoon and placed on a 12-well Millicell culture insert (Merck, Germany, with a pore size of 4 μ m) containing 100 μ L of

retina culture medium per insert and 1 mL per well (50 mL Neurobasal-A medium supplemented with 2% B27 (Thermo Fisher Scientific, Karlsruhe, Germany), 1% N2 (Thermo Fisher Scientific, Karlsruhe, Germany), 1% penicillin/streptomycin (P/S), 0.5 μ L ciliary neurotrophic factor (CNTF; Merck, Darmstadt, Germany), and 0.5 μ L brain-derived neurotrophic factor (BDNF; Merck, Darmstadt, Germany) with the ganglion layer (GCL) facing up. Neuroretinal explants were placed in an incubator at 5% CO₂ and 37°C for 3 h.

2.2 HG *ex vivo* model

3 h after explantation, the 8 mm neuroretinal explants were exposed to HG concentration for 96 h. To this end, retinal culture medium was replaced by a basal medium (1:1 retina culture medium and α -MEM with 10% of fetal bovine serum, Gibco-Life Technologies, Waltham, MA, USA, 1% L-glutamine and 1% penicillin/streptomycin (Sigma-Aldrich, St. Louis, MO, USA) added with D-glucose (HG-medium; SIGMA, St. Louis, MO, USA; G8270-100G) at a final concentration of 25 mM. After 48 h, HG medium was completely replaced with fresh medium. The same concentration of mannitol (25 mM) was added to 1:1 basal medium as the osmotic control.

2.3 hCLs collection and decellularization

The hCLs obtained from the cornea of healthy patients undergoing to small-incision lenticule extraction (SMILE) refractive surgical procedure were collected in accordance with the Declaration of Helsinki and following the “G. d’Annunzio” of Chieti-Pescara University’s Institutional Review Board and Ethical Committee approval (authorization n.: 03/07-02-2019). To obtain a human corneal keratocytes-free scaffold, hCLs were decellularized, as previously described (22). Briefly, the tissues were washed in phosphate buffer solution (PBS 1X, Sigma-Aldrich) and incubated in a 0.1% sodium dodecyl sulfate (SDS) solution for 24 h under 300 rpm agitation at room temperature (RT).

2.4 hAFSCs isolation

hAFSC were isolated from leftover samples of human amniotic fluid (hAF) collected by amniocentesis during II trimester prenatal diagnosis screening from the Fetal and Perinatal Medical and Surgery Unit and the Human Genetics Laboratory at IRCCS Istituto Gaslini hospital (Genova, Italy), following written informed consent and according to local ethical committee authorization (as obtained from Comitato Etico Territoriale Liguria, protocol P.R. 428REG2015). Donor’s age of AF ranged from 36 to 41 years, with an average age of 37.42 ± 0.32 . hAF were processed as previously described (34–36) by centrifugation at 1200 rpm for 5 min to retrieve cellular components. The pellet was seeded on a glass coverslip in Chang Medium C (Irvine Scientific) supplemented with 1% L-glutamine and 1% penicillin/streptomycin

(Gibco, Thermo Fisher Scientific) and cultured in an incubator at 37°C with a 5% CO₂ and 20% O₂ atmosphere. hAFSC were isolated from a population of adherent amniotic fluid mesenchymal stromal cells by immunomagnetic sorting for c-KIT expression (CD117 MicroBead Kit, Miltenyi Biotechnology). c-KIT⁺ hAFS were further expanded in Minimal Essential Medium (MEM)-alpha with 15% fetal bovine serum (FBS; Gibco - Thermo Fisher Scientific), 20% Chang Medium C (Irvine Scientific) with 1% L-glutamine, and 1% penicillin/streptomycin (Gibco - Thermo Fisher Scientific), in an incubator at 37°C with 5% CO₂ and 20% O₂ atmosphere. hAFSC were cultured and expanded to 3-4 passages before cryopreservation in liquid nitrogen until further application.

2.5 rhNGF-MPs preparation

PLGA microparticles (MPs) loaded with rhNGF were synthesized following a previously described customized double emulsion solvent evaporation technique (22). The MPs produced had an average size of 5 µm, and the encapsulation efficiency of rhNGF exceeded 65%.

2.6 hCLs bioengineering

Decellularized hCLs (Decell_hCL) were dehydrated for 2 h at 60°C and then bioengineered (BioE_hCL) in three different ways as follows:

with hAFSCs (BioE_hCL_A): Decell_hCLs were incubated for 72 h in a 96 well plate with 200 µL suspension of c-KIT⁺ hAFSCs (80 × 10³ cells/hCL; 5% CO₂, 37°C).

with rhNGF-PLGA-MPs (BioE_hCL_B): rhNGF-PLGA-MPs were suspended in 0.175 mL of 0.9% NaCl (highest saturation degree). One Decell_hCL per tube was incubated with MPs solutions for 3h at RT with orbital shaking at 200 rpm. Following the incubation time, samples were finally washed 10 times in 0.4 mL of 0.9% NaCl. Fluo-PLGA-MPs (Cat. LGFG20K; Sigma-Aldrich). Louis, MO, USA) were used as controls for the bioengineering process with PLGA-MPs (BioE_hCL_Fluo-PLGA-MPs).

with hAFSCs and rhNGF-PLGA-MPs (BioE_hCL_C): For a double bioengineering, Decell_hCLs were first incubated with rhNGF-MPs solutions, as reported above. Subsequently, hCLs bio-engineered with rhNGF-MPs were incubated for 24 h with 200 µL of the hAFSCs suspension (80 × 10³ cells/hCL; 96 well plate).

All bioengineering processes were confirmed by immunofluorescence (IF) and scanning electron microscopy (SEM) analyses.

2.7 Immunofluorescence and histological analyses

For IF experiments neuroretinal samples were cryoprotected using Tissue Tek (Sakura, Umkirch, Germany) and frozen in liquid nitrogen. Neuroretinal explants were then cut on cryostat (10 µm sections) and fixed with 4% PFA. 1 h of 5% BSA blocking was

performed. After washing, neuroretinal explants slices were stained with monoclonal Purified Mouse Anti-GFAP Cocktail (1:200; BD PharmingenTM, Franklin Lakes, New Jersey, USA, cat. 556330), Anti-Rhodopsin antibody (1:1000; Cambridge, UK, cat. ab98887), Anti-Nerve Growth Factor Receptor antibody (NGFR p75, 1:50; Sigma-Aldrich, St. Louis, MO, USA, cat. S-N5408), and Trka monoclonal primary antibody (1:50; Danvers, Massachusetts, USA cat. 2505S). Cy3 anti-mouse (1:200; Jackson ImmunoResearch, Laboratories, cat. 111-165-144), Alexa Fluor 488 anti-rabbit (1:500; Invitrogen, Thermo Fisher Scientific, Waltham, MA, USA, cat. A11034) and Alexa Fluor 546 anti-mouse (1:500; Invitrogen, Thermo Fisher Scientific, Waltham, MA, USA, cat. A-11030) were used as the secondary antibodies. Counterstaining with DAPI (4'6'-diamidino-2-phenylindole; Thermo Fisher Scientific, Karlsruhe, Germany) was performed. The slices were mounted using FluorSafe (Merck, Darmstadt, Germany). Images were captured using a confocal microscope (Zeiss LSM-800; Carl Zeiss Meditec AG, Oberkochen, Germany). Staining intensity of GFAP and Rho were measured by using ImageJ software (NIH, United States ImageJ software, public domain available at: <http://rsb.info.nih.gov/ni-image/>).

To evaluate retinal tissue morphology, cryosections (10 µm) of control and HG-treated neuroretinal explants, were stained with Hematoxylin and Eosin (H&E). The sections were photographed under light microscopy objectives (10X and 20X) using the slide scanner system NanoZoomer. Quantification analyses was performed with Qu-Path 0.3.2 software using cell detection tool.

To confirm the bioengineering process, Decell_hCL and the three different BioE_hCLs were fixed in 4% paraformaldehyde (PFA; 10 min, RT) and blocked for 1 h at RT with 1% of albumin bovine serum (BSA) (SIGMA, St.Louis, MO, USA). Louis, MO, USA, A4503). hCLs were stained with paxillin (5 µg/mL; Thermo Fisher Scientific, Waltham, MA, USA, cat. MA5-13356) or phalloidin-rhodamine-conjugated primary antibody (1:300; Invitrogen, Thermo Fisher Scientific, Waltham, MA, USA, cat. R415). FITC-goat anti-mouse was used as secondary antibody (1:100; Jackson ImmunoResearch Europe Ltd., Cambridge House, St. Thomas' Place, cat. 115-095-006). DAPI staining was used to determine the nuclei.

2.8 Scanning electron microscopy

Decell_hCLs and the three different BioE_hCLs were fixed and dehydrated using an ascending ethanol series (50%, 70%, and 100%), followed by immersion in hexamethyldisilazane and air drying at RT in a desiccator. The dried samples were then mounted onto SEM stubs and sputter-coated with gold layers (150 Å thick). Samples were examined using a Phenom XL microscope (Alfatest, Phenom World).

2.9 Co-culture of neuroretinal explants with BioE_hCL_Fluo-MPs

Control (CTRL) neuroretinal explants were placed in direct contact with BioE_hCL_Fluo-PLGA-MPs to assess the possible

release of Fluo-PLGA-MPs from hCLs and their incorporation into the retinal layers. In detail, after four days of co-cultivation, BioE_hCL_Fluo-PLGA-MPs were removed from the co-culture system. Then, the neuroretinal explants were collected, cryoprotected and cut as described in 2.7 for the subsequent IF analyses performed with the Zeiss LSM-800 (Carl Zeiss Meditec AG, Oberkochen, Germany). Counterstaining with DAPI was performed to visualize retinal cells and layers.

2.10 Co-culture of HG-treated neuroretinal explants with BioE_hCLs

HG-treated neuroretinal explants were placed in direct contact with Decell_hCLs or with each of the three different BioE_hCLs to evaluate the effects of neurotrophic and regenerative factors. Specifically, hCLs were placed over the HG-treated neuroretinal explants. HG medium was completely replaced with fresh medium after 48 h of co-culture. After four days of co-cultivation, the BioE_hCL were removed from the co-culture system. Finally, neuroretinal explants were collected and processed for subsequent real-time PCR.

2.11 Real-time PCR

RNA isolation from neuroretinal explants was conducted using TRIzol reagent (Thermo Fisher Scientific, Waltham, MA, USA) according to previously established protocols (Pelusi L., 2022) following the manufacturer's instructions. The quality and concentration of the total RNA were assessed using a NanoDrop 2000c spectrophotometer (Thermo Fisher Scientific, Waltham, MA, USA). A high-capacity cDNA Reverse Transcription Kit (Thermo Fisher Scientific, Waltham, MA, USA) was used for cDNA synthesis. The TaqMan Universal PCR Master Mix (Thermo Fisher Scientific, Waltham, MA, USA) and TaqMan Gene Expression Assay (Thermo Fisher Scientific, Waltham, MA, USA) probes for glyceraldehyde-3-phosphate dehydrogenase (GAPDH; Ss03375629_u1), glial fibrillar acid protein (GFAP; Ss03373547_m1), Cyclin Dependent Kinase Inhibitor 1A (p21; Ss06866662_m1), Nuclear factor erythroid 2-related factor 2 (NRF2; Ss06886078_m1), Nitric oxide synthase 2 (NOS2; Ss03374886_u1), Bcl2-associated X protein (Bax; Ss03375842_u1), B-Cell Leukemia/Lymphoma 2 (Bcl-2; Ss03375167_s1), nuclear factor kappa B subunit 1 (NF-kB1; Ss03388575_m1); Tubulin Beta 3 Class III (TUBB3; Ss06898264_g1) RHO, VEGFA (Ss03393990_m1) were used according to the manufacturer's instructions. All samples were analyzed in duplicate. The relative expression of the target genes in each group was expressed as the fold change in mRNA expression by means of by $2^{-\Delta\Delta C_t}$ considering GAPDH as housekeeping.

2.12 Cytokine array

Conditioned media derived from HG-treated neuroretinal explants co-cultivated with each of the three BioE_hCLs were

pulled ($n \geq 6$) and analyzed using a semi-quantitative Cytokine Array (RayBiotech, Inc. Parkway Lane, GA, cat. AAP-CYT-1-8), according to the manufacturer's instructions. After blocking the membranes, samples were pipetted into each well and incubated for 5 h at RT. After two washes, the biotinylated antibody cocktail was pipetted into each well and incubated overnight at 4°C. Afterwards, 1X HRP-Streptavidin was added and incubated for 2 h at RT. The immune complexes were visualized using the Detection Buffer (1:1 C+D) provided by the array kit. Data were processed using the UVITEC Alliance software, and spot signal intensities were quantified using the ImageJ software.

2.13 Statistical analyses

Statistical significance was analyzed using GraphPad Prism Software Analysis (version 9, San Diego, USA). D'Agostino and Pearson normality tests were performed. Then, data were analyzed via unpaired Student's t-test or Mann-Whitney test for comparison between two groups. While, to compare more than two groups one-way ANOVA or Kruskal-Wallis followed by *post hoc* tests (Tukey or Dunn). Data are shown as the mean \pm standard error (SEM). The value of *p* was set at 0.05.

3 Results

3.1 Effect of HG on porcine neuroretinal explants

mRNA expression of markers associated to a pre-stage step of the DR-*ex vivo* model was evaluated to assess molecular changes associated to four days HG treatment (25 mM) in neuroretinal explants. Interestingly, HG treatment induced an upregulation of the inflammatory and oxidative stress processes, as shown by the significant increase of *NFkB*, *NOS2* and *NRF2*. In addition, *GFAP* expression was significantly increased by HG and as expected, this was accomplished with a significant enhance in *VEGFA*. Furthermore, induction of apoptosis was also observed following HG treatment, as evidenced by the notable increase in *BAX/Bcl-2*-ratio expression. This was accompanied by a significant decrease in the expression of *TUBB3* and a trend in downregulation of *RHO*, typical markers for retinal ganglion cells (RGCs) and photoreceptors respectively, indicating a reduction in their functionality (Figure 1). To validate the mRNA expression analyses, IF for GFAP and Rho protein expression were performed. As showed by the representative IF images and by the histograms in Figure 2, HG treatment induced a significant increase in GFAP expression, confirming the activation of an inflammatory process. While the reduction of Rho expression highlighted a retinal cells structure alteration (Figure 2). In support of this, the histological analyses of retinal morphology evaluated through H&E staining (Figure 3A) revealed tissue structure alterations in HG treated neuroretinal explants, primarily affecting the inner plexiform layer (IPL). Of note, the quantification analyses (Figure 3B) showed that HG treatment caused a significant reduction in the cells number of ganglion cell layer (GCL) and inner nuclear

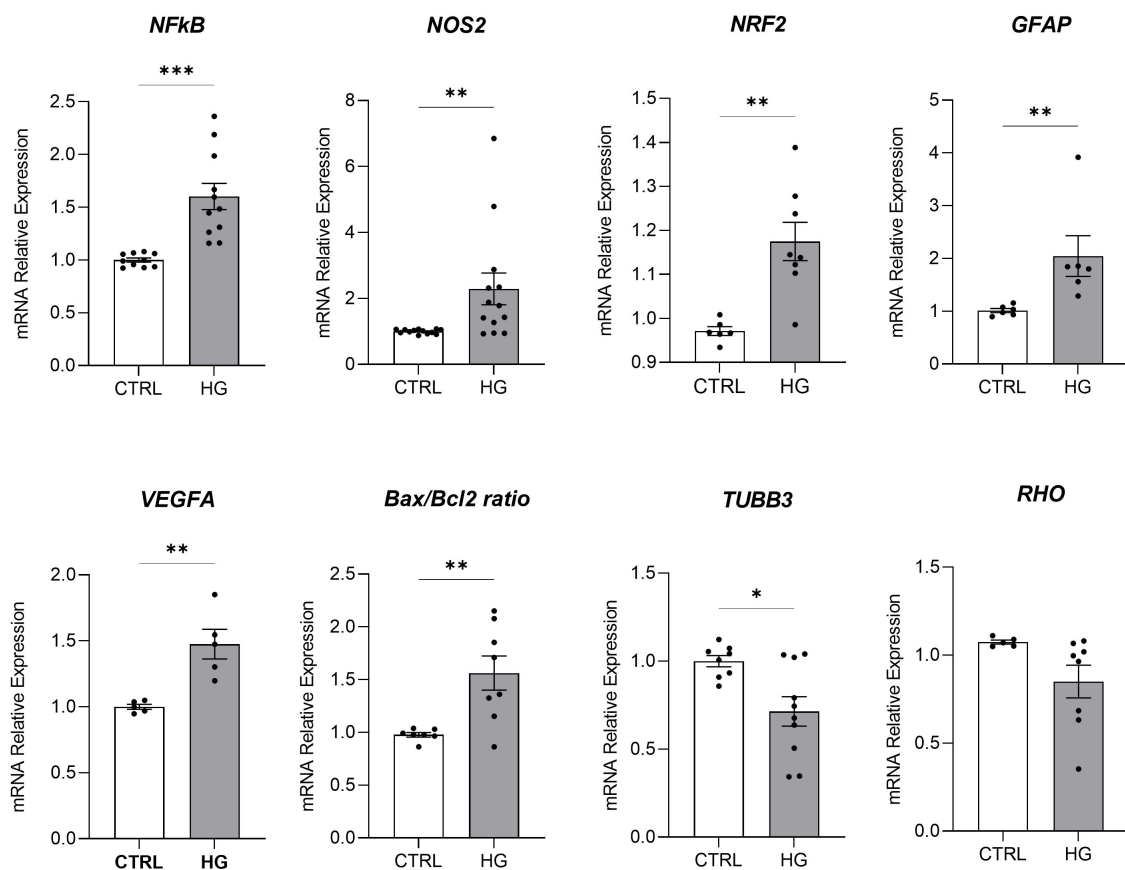


FIGURE 1

Molecular analyses of HG-treated porcine neuroretinal explants. mRNA levels of inflammatory/oxidative (*NFkB*, *NOS2*, *NRF2*, and *GFAP*), pro-angiogenic (*VEGFA*), apoptotic (*Bax/Bcl-2*), and retinal (*TUBB3* and *Rho*) markers in porcine neuroretinal explants cultured for 4 days in the presence or absence of HG (25 mM). Results are shown as the mean \pm error standard (SEM) ($n \geq 5$); * $p < 0.05$; ** $p < 0.01$; *** $p < 0.001$.

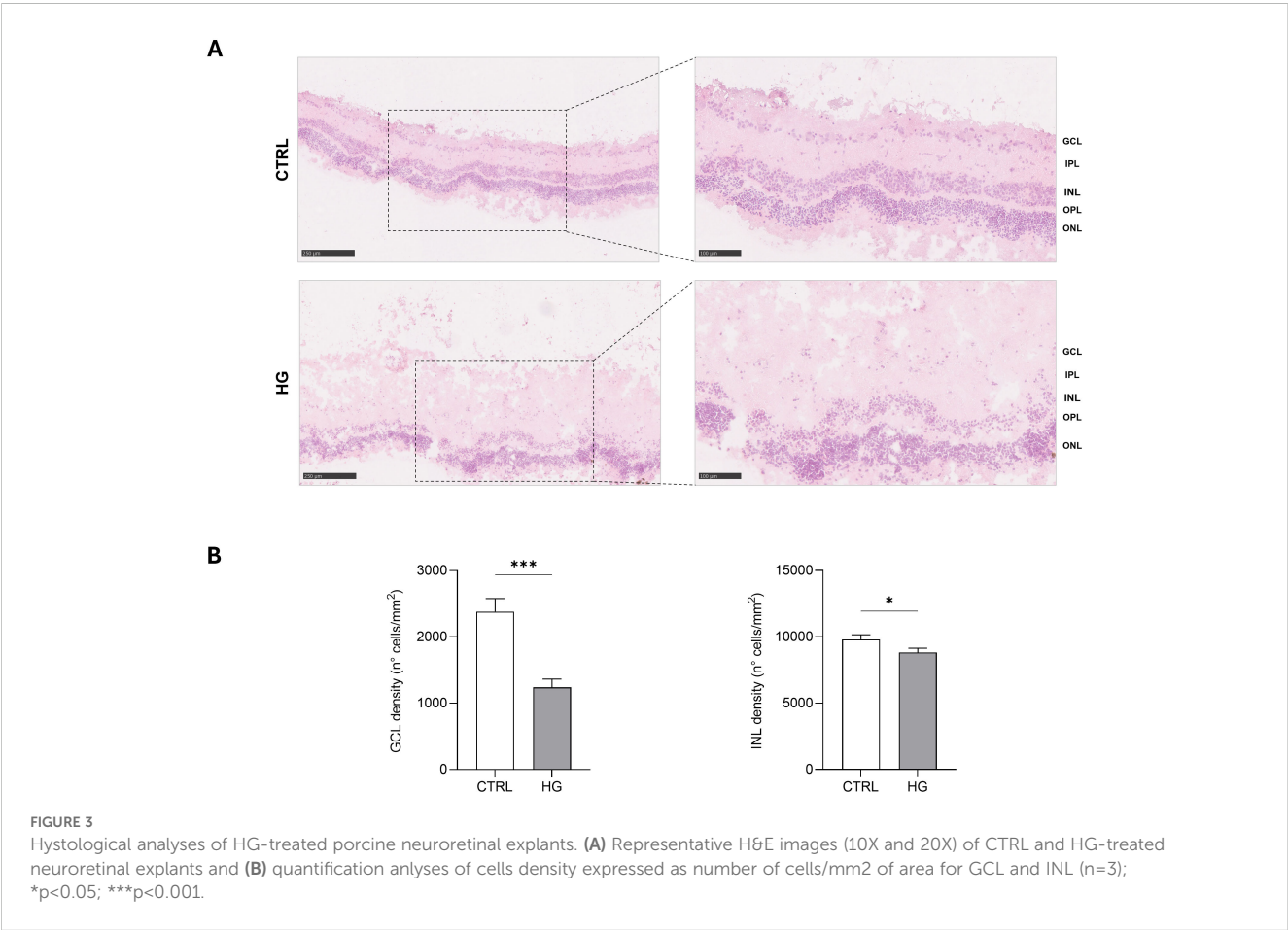
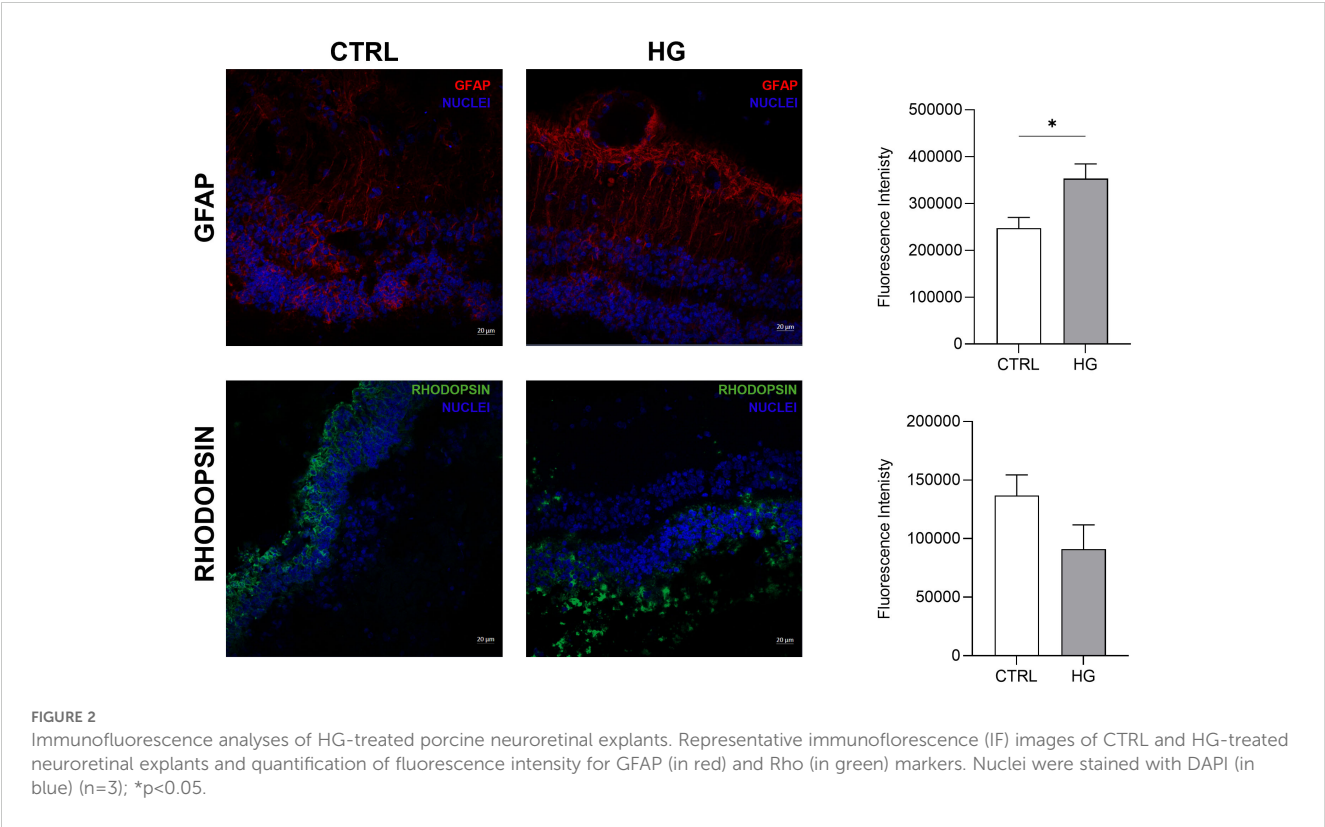
layer (INL). Finally, to confirm that the observed effects were specifically induced by HG treatment, neuroretinal explants were treated with mannitol (MANN; 25 mM) as an osmolarity control.

Treatment with mannitol did not induce any significant changes in the expression of *NOS2*, *NFkB*, *TUBB3*, and *GFAP*, thus confirming the specificity of the HG treatment, which was able to reproduce the DR scenario in *ex vivo* neuroretinal explants (Supplementary Figure S1).

3.2 Analyses of bioengineered hCLs

The bioengineering processes of hCLs were demonstrated using IF and SEM analyses. The efficacy of 0.1% SDS in removing from untreated control hCL (CTRL_hCL) both cellular and nuclear material derived from human corneal keratocytes, was firstly confirmed through the IF staining of Decell_hCLs for phalloidin (intracellular F-actin) and DAPI (nucleic acids) (Figure 4, Decell_hCL image in IF panel). This result was corroborated by the SEM images which showed how the surface of Decell_hCLs (Figure, Decell_hCL image in SEM panel) appears smooth when compared to the surface of untreated control hCLs (Figure 4,

CTRL_hCL image in SEM panel). Subsequently, the feasibility of bioengineering hCLs with hAFSCs (BioE_hCL_A condition) was proven. To this end, Decell_hCLs were incubated for 72 h with hAFSCs and then IF staining for the nuclei and F-actin revealed the ability of hAFSCs cells to repopulate the surface of Decell_hCLs (Figure 4, BioE_hCL_A image in IF panel). Of note, the presence of focal adhesions of hAFSCs was also found as evidenced by the presence of paxillin localized along the cell periphery and interacting with F-actin on the plasma membrane (Figure 3, BioE_hCL_A image in IF panel). In support of this, SEM images clearly displayed the monolayer of hAFSCs and their close adherence on Decell_hCL surface (Figure 4, BioE_hCL_A image in SEM panel). Then, the BioE_hCL_B condition was firstly verified in IF incubating Decell_hCLs with a suspension of Fluo-PLGA-MPs, which were used as bioengineering process control. In detail, confirming our previous findings (22), the IF images confirmed that Fluo-PLGA-MPs are able to attach the hCLs surface (Figure 4, BioE_hCL_B image in IF panel). While the bioengineering process with rhNGF-PLGA-MPs was confirmed by SEM analyses which highlighted the attachment of rhNGF-PLGA-MPs to the collagen fibers of Decell_hCLs surface (Figure 4, BioE_hCL_B image in SEM panel).



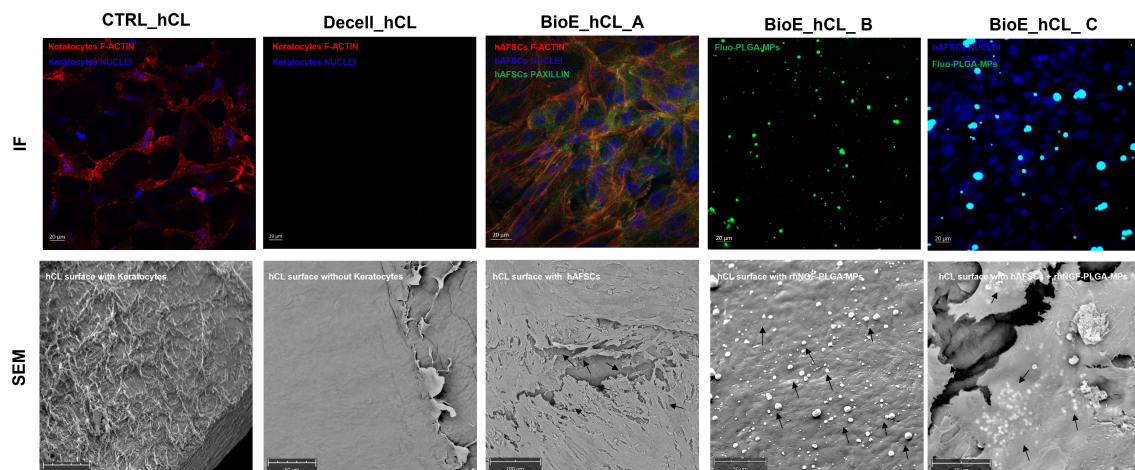


FIGURE 4

Analyses of BioE_hCLs. Representative immunofluorescence (IF) and scanning electron microscope (SEM) images: hCLs (CTRL_hCL); decellularized hCLs with SDS 0.1% (Decell_hCL); Decell_hCL bioengineered with hAFSCs (BioE_hCL_A); Decell_hCL bioengineered with Fluo-PLGA-MPs or rhNGF-PLGA-MPs (BioE_hCL_B); Decell_hCL bioengineered with hAFSCs and Fluo-PLGA-MPs or rhNGF-PLGA-MPs (BioE_hCL_C).

Finally, the feasibility of double-bioengineering Decell_hCLs with hAFSCs and rhNGF-PLGA-MPs was investigated. In particular, for IF analyses, Decell_hCLs were first incubated with Fluo-PLGA-MPs solutions and then with hAFSCs. Of note, IF images demonstrated that both Fluo-PLGA-MPs and hAFSCs are simultaneously able to adhere and attach hCLs surface (Figure 4, BioE_hCL_C image in IF panel). These results were validated by SEM analyses which showed the presence of rhNGF-PLGA-MPs below the hAFSCs monolayer in the doubly bioengineered hCL thus demonstrating for the first time the successful development of a doubly bioengineered hCL (Figure 4, BioE_hCL_C image in SEM panel).

3.3 Expression of NGF receptor and release of Fluo-MPs from BioE_hCLs in the neuroretinal explant

Before assessing the effect of BioE_hCLs on our *ex vivo* model, we evaluated the expression of NGF receptors (NGFR p75 and TrkA) in the neuroretinal explants and the possible release of Fluo-PLGA-MPs from BioE_hCLs in the retina layers.

Regarding NGF receptor expression, representative IF images revealed that both NGF receptors are expressed in porcine retinal cells. In particular, TrkA was highly expressed in the Inner Plexiform Layer (IPL), whereas NGFR p75 was expressed in the Outer Nuclear Layer (ONL) (Figure 5A).

Our previous results (22) demonstrated that hCL bioengineered with rhNGF-PLGA-MPs sustained the release of active rhNGF for up to one month. Hence here we investigated whether the growth factors and MPs, probably released from BioE_hCL, were able to reach the neuroretinal explants. This was achieved by using Fluo-PLGA-MPs as a control delivery and thus co-culturing the neuroretinal explants with BioE_hCLs_Fluo-PLGA-MPs.

Representative IF images (Figure 5B) showed that Fluo-PLGA-MPs were released from BioE_hCLs and subsequently incorporated into the retinal layers, particularly into the IPL.

3.4 Effect of hAFSCs and rhNGF released from BioE_hCLs on the *ex vivo* DR model: mRNA expression analyses

HG-treated neuroretinal explants were placed in direct contact with BioE_hCL for four days. Interestingly, depending on the markers analyzed, we observed different effects after co-culturing with each of the three BioE_hCL (Figure 6).

Regarding *NFKB*, *NOS2*, *NRF2*, and *Bax/Bcl-2*, the co-culture with each of the three BioE_hCLs reduced their expression. However, statistical significance was only achieved with BioE_hCLs_B and BioE_hCLs_C, suggesting that the inflammatory and oxidative stress processes induced by HG treatment may be mainly modulated by the release of rhNGF.

The co-culture with BioE_hCL_B and BioE_hCL_C also reduced the expression of *GFAP* in the HG-treated neuroretinal explant. On the contrary, *GFAP* levels were improved following the co-culture with BioE_hCL_A. This condition also significantly increased *VEGFA* expression, probably due to the release of pro-angiogenic factors from hAFSCs. Of note, this pro-angiogenic effect was significantly reverted in the BioE_hCL_B and BioE_hCL_C conditions compared to the HG and BioE_hCL_A ones.

Regarding the retinal cell's markers, a similar pattern was observed for *TUBB3* and *RHO*. Although no difference was found in BioE_hCL_A and BioE_hCL_B compared to HG treatment, the reduction of *TUBB3* and *RHO* induced by HG treatment was significantly reversed in BioE_hCL_C, indicating a synergistic effect between rhNGF and hAFSCs in the double bioengineered hCL.

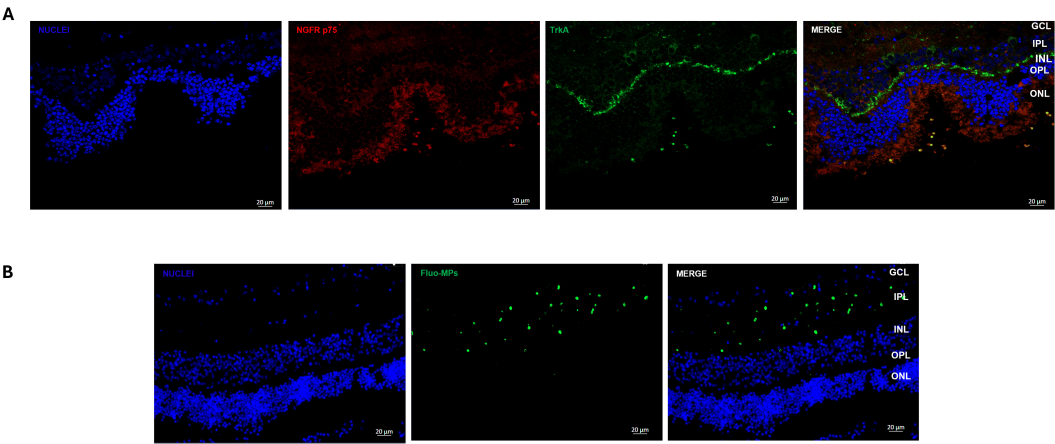


FIGURE 5 Immunofluorescence analyses of NGF receptor and Fluo-MPs in porcine neuroretinal explants. Representative immunofluorescence (IF) images of (A) NGF receptors in porcine neuroretinal explants. Alexa Fluor 576 was used to stain NGFR p75 and Alexa Fluor 488 for TrkA, and (B) Fluo-PLGA-MPs were incorporated into the porcine neuroretina layers after release from BioE_hCL.

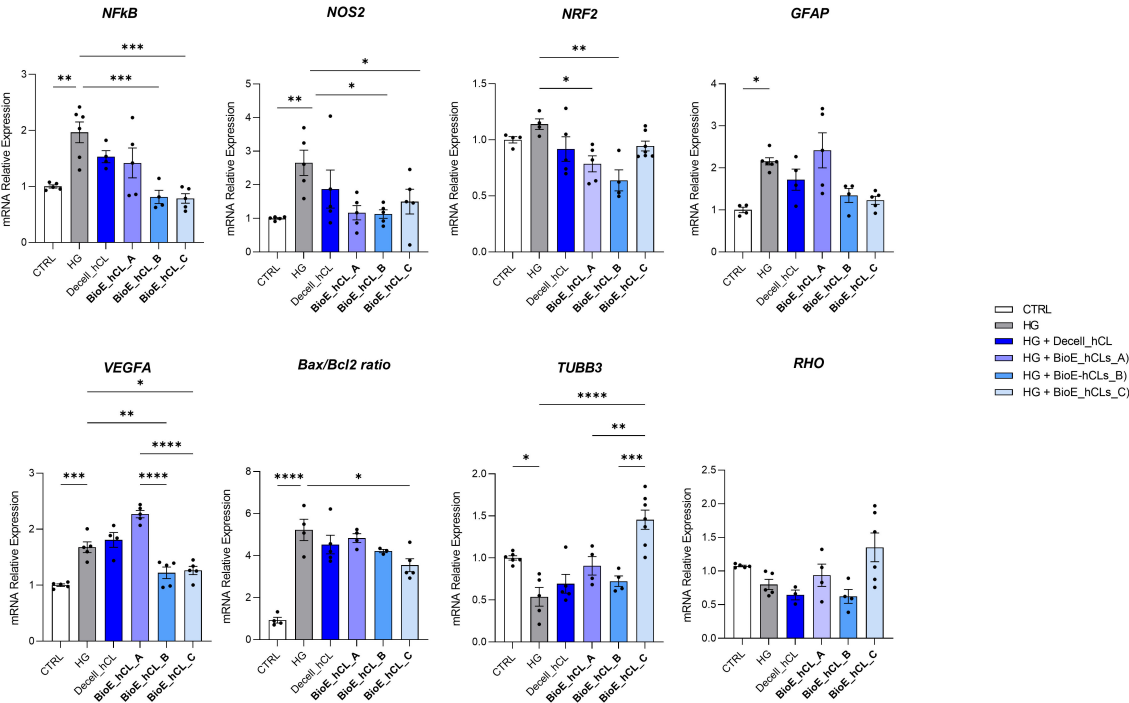


FIGURE 6 Molecular analyses of HG-treated porcine neuroretinal explants co-cultured with BioE_hCL. mRNA levels of inflammatory/oxidative (*NF- κ B*, *NOS2*, *NRF2*, and *GFAP*), pro-angiogenic (*VEGFA*), apoptotic (*Bax/Bcl-2*), and retinal (*TUBB3* and *Rho*) markers in HG-treated porcine neuroretinal explants co-cultured with each of the three BioE_hCL. Results are shown as the mean \pm error standard (SEM) ($n \geq 4$); * $p < 0.05$; ** $p < 0.01$; *** $p < 0.001$; **** $p < 0.0001$.

To better appreciate this synergic effect on our DR-*ex vivo* model, we normalized the computed values of BioE_hCL_C versus the HG condition (Table 1). Notably, this comparison highlighted that co-culture with BioE_hCL_C significantly reduced

inflammatory (*NFkB*, *NOS2*, *GFAP*), oxidative (*NRF2*), angiogenic (*VEGF*), apoptotic (*Bax/Bcl-2*), and retinal cell (*TUBB3* and *RHO*) markers, reinforcing the assumption that hAFSCs and rhNGF have a synergistic effect.

TABLE 1 HG-treated porcine neuroretinal explants co-cultured with BioE_hCL_C.

| Markers | HG | BioE_hCL_C | p-value | Sig. level |
|-----------------|-------------|--------------|---------|------------|
| <i>NFkB</i> | 1.00 ± 0.00 | 0.41 ± 0.099 | 0.0001 | *** |
| <i>NOS2</i> | 1.00 ± 0.00 | 0.59 ± 0.32 | 0.006 | ** |
| <i>NRF2</i> | 1.00 ± 0.00 | 0.77 ± 0.1 | 0.03 | * |
| <i>GFAP</i> | 1.00 ± 0.00 | 0.57 ± 0.99 | 0.02 | * |
| <i>VEGFA</i> | 1.00 ± 0.00 | 0.76 ± 0.099 | 0.0026 | ** |
| <i>Bax/Bcl2</i> | 1.00 ± 0.00 | 0.69 ± 0.13 | 0.0002 | *** |
| <i>TUBB3</i> | 1.00 ± 0.00 | 3.017 ± 0.62 | <0.0001 | **** |
| <i>RHO</i> | 1.00 ± 0.00 | 1.72 ± 0.66 | 0.004 | * |

Normalized computed values of BioE_hCL_C versus HG condition. *p<0.05; **p<0.01; ***p<0.001; ****p<0.0001.

3.5 Effect of hAFSCs and rhNGF released from BioE_hCLs on the *ex vivo* HG-model: cytokine release analyses

To strengthen the mRNA expression results, conditioned media collected from each experimental condition were analyzed using a 48-cytokine array.

In general, as reported by the heatmap in Figure 7A, a modulation of cytokines involved in inflammation, angiogenesis, and cell growth was observed. Notably, the values of the principal markers of interest were extrapolated and plotted.

As expected, the dot plots shown in Figure 7B disclosed that HG treatment activated an inflammatory process in the neuroretina explants, as revealed by the increased release of pro-inflammatory cytokines such as granulocyte-macrophage colony-stimulating factor (GM-CSF), interleukin 1 β (IL-1 β), and interleukin 1 Receptor Antagonist (IL-1 ra) and by the decrease of the anti-inflammatory cytokine IL-10.

Notably, the release of pro-inflammatory cytokines was reduced in HG-treated neuroretinal explants co-cultured with each of the three BioE_hCLs. In contrast, IL-10 levels increased only in BioE_hCL_B and BioE_hCL_C. In addition, HG induced an increase in platelet-derived growth factor-BB (PDGF-BB), indicating activation of the neovascularization process. This was successively reversed in the HG-*ex vivo* neuroretinal explants treated with BioE_hCL_B and BioE_hCL_C. Interestingly, we also observed a decrease in INSULIN levels in HG-treated neuroretinal explants, confirming that HG reduced the levels of this important neuroprotective factor (37). Notably, co-culture with BioE_hCL_B and BioE_hCL_C restored INSULIN levels.

4 Discussion

DR is a complex ocular disease affecting a high percentage of diabetic patients (38). Even though it is considered a microvascular complication of DM, recent studies define DR as a tissue-specific neurovascular impairment of multiple retinal cells, including neurons, glial cells, and vascular cells that constitute the

neurovascular units (NVUs) (8, 39). Therefore, the development of new therapeutic approaches for the management of DR associated neurodegeneration requires in depth investigation of the underlying molecular mechanisms (40).

In this context, several *in vitro* and *in vivo* experimental models of DR have been developed over the years which, however, are affected by different drawbacks (40–44). Cell culture models fail to replicate *in vivo* conditions because they lack a tissue microenvironment, which can significantly influence cellular responses. Likewise, *in vivo* models encounter growing ethical and regulatory challenges in the animals use (25). Therefore, tissue culture models have been highlighted as promising alternatives, especially in the field of ocular disease such as DR (25, 27, 45–48). However, although the anatomy of pig eye is highly similar to that of the human eye (29), no studies have explored the feasibility of replicating the DR *milieu* in porcine neuroretinal explants.

In light of this, in the present study, porcine neuroretinal explants were collected and treated with HG (25 mM), allowing us to evaluate the effects of HG in all retinal cell types thus replicating the diabetic *milieu* on the entire retinal structure. Notably, HG treated neuroretinal explants showed elevated expression of *NFkB*, implying the onset of a pro-inflammatory state, the initiation of a pro-apoptotic program leading to DNA damage through the increase of reactive oxygen species (ROS) production (49, 50). Additionally, in our *ex vivo* model, HG caused an increase in the *Bax/Bcl-2* ratio and *Nrf2* levels, supporting the relationship between *NFkB* activation and cell apoptosis. Indeed, it is known that both factors work together to maintain redox homeostasis in healthy cells and this regulation may be disrupted under DR condition (51–56).

Among the pro-inflammatory and oxidative stress mediators involved in the early stage of DR, *NOS2* plays a critical role in tissue injury, neurodegeneration, and cell apoptosis. According to the state of the art (57–60), we found a significant increase of the *NOS2* level following the HG treatment.

Moreover, in line with the study of Lechner and colleagues (61), our DR model also underlined the activation of a neurodegenerative process revealed by the GFAP modulation, confirmed also by the IF analyses performed on cryosections of control and HG-treated neuroretinal samples.

Furthermore, although we also observed a modulation of the vascular markers VEGF, we were unable to evaluate the microvascular changes typical of DR. Indeed, in our model, the porcine neuroretinal explants were treated with HG for four days, which is a relatively short period and likely insufficient to observe significant microvascular changes. Furthermore, despite the porcine eye being represents an excellent research model, largely due to its anatomical and vascular similarities to the human eye (29), there are important differences that must be acknowledged. Unlike humans, where the central retinal artery and vein travel within the optic nerve before reaching the optic disc, pigs have retinal vessels that originate from chorioretinal arteries and veins at the optic disc periphery (62). For these reasons and since from the start of the enucleation process there is probably a rapid degeneration of vascular components, principally due to the lack of blood flow and biomechanical tissue support, it was difficult to study microvascular changes in our model, shifting the focus mainly to neural damage.

In addition to the markers discussed above, a decreased expression of *TUBB3* and *RHO* was found confirming that, RGCs and

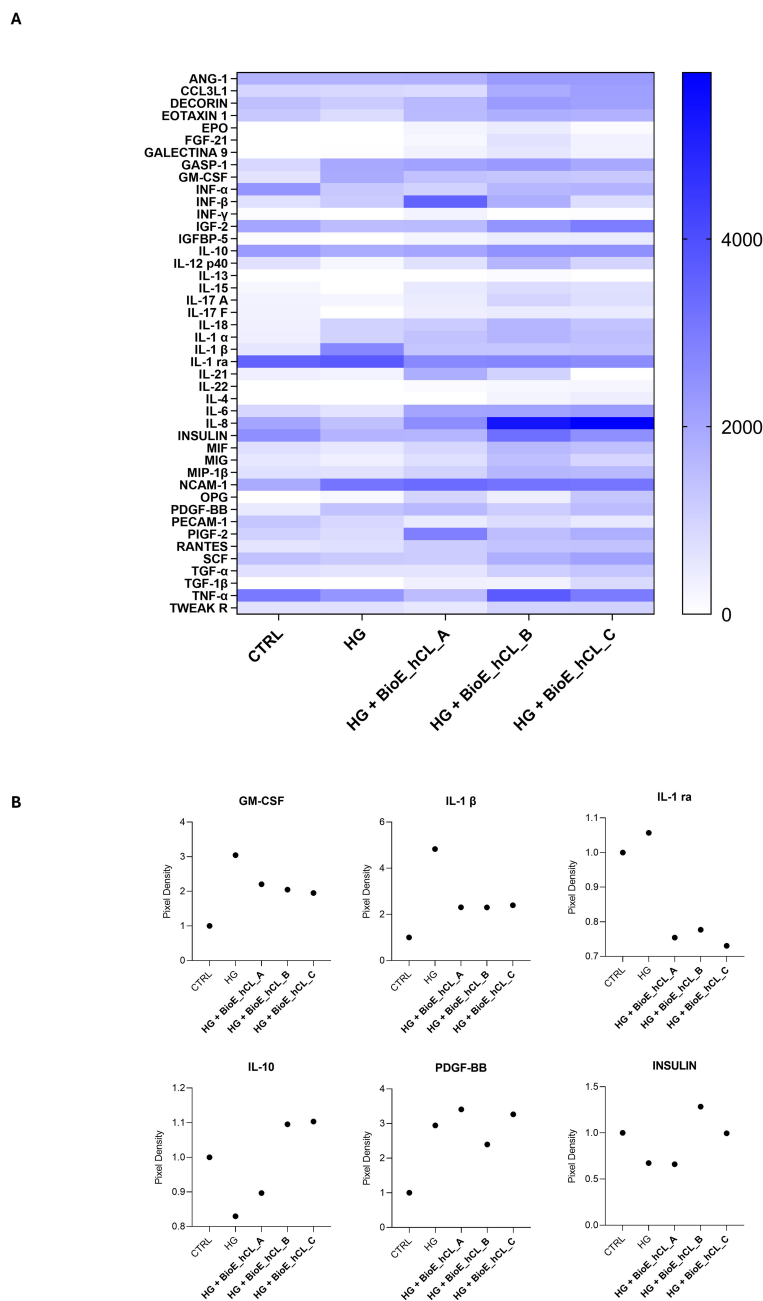


FIGURE 7

Cytokine array analyses of HG-treated porcine neuroretinal explants co-cultured with BioE_hCL. Cytokine release **(A)** Heatmap and **(B)** scatter dot plot showing the release of pro-inflammatory (GM-CSF, IL-1 β , and IL-1 ra), anti-inflammatory (IL-10), pro-angiogenic (PDGF-BB), and neuroprotective (INSULIN) cytokines in conditioned media of CTRL and HG-treated porcine neuroretinal explants co-cultured with each of the three BioE_hCL. ($n \geq 6$ for pooled conditioned media).

photoreceptors respectively, were affected to the HG treatment (63). In support of this, in line with Jeong JS and colleagues (64) H&E staining also revealed evident morphological changes in HG treated neuroretinal explants which mainly interest the IPL. Interestingly, compared to the CTRL group, a reduction in the numbers of nuclei in the GCL and INL were observed in HG treated samples, thus supporting the gene expression data.

Despite these observations, to note is that just the severing of the optic nerve initiates a degenerative program which primarily affect the RGCs (27, 65). This could influence the interpretation of

RGC state, representing a limit of our model. However, although the model cannot fully discriminate the effects of HG treatment from the impact of optic nerve severing due to the enucleation process, the observed differences between the CTRL neuroretinal explants (basal condition) and the HG treated ones suggest that HG significantly contributes to worsen retinal damage. Considering the neurodegenerative signature of DR, recently gained attention has been focused on the development of new therapeutic approaches based on the use of MSCs and the replacement of neurotrophic factors (15).

MSCs therapy has been recognized as one of the most effective treatments for various degenerative diseases, including DR conditions (66, 67). It is well established that MSCs release several factors, such as insulin-like growth factor (IGF), VEGF, basic fibroblast growth factor (bFGF), BDNF, ciliary neurotrophic factor (CNTF), and NGF, which exert anti-apoptotic, angiogenic, pro-regenerative, and anti-fibrotic effects. Several studies demonstrated that intravitreal injections of different sources of MSCs promote in DR models the downregulation of GFAP, IL-1 β , TNF- α , IL-10, and VEGF protein expression (18, 68, 69). While for the use of neurotrophic factors, experimental evidence has proven the effectiveness of NGF treatment in degenerative diseases of the retina, such as glaucoma, retinitis pigmentosa, and diabetic retinopathy (70–72). However, the direct delivery of these factors to the eye remains a challenge.

As regard of this, we previously demonstrated the feasibility of using hCLs as a natural ocular drug delivery system able of releasing rhNGF-PLGA-MPs for one month (22). In particular, Decell_hCL, through a phenomenon of ‘soaking’ allows the rhNGF-PLGA-MPs to adhere uniformly to the hCL surface and incorporated within its stroma. Consequently, rhNGF-PLGA-MPs do not form covalent bonds but rather adhere to the hCL surface due to the polymeric and mucoadhesive properties of PLGA, which facilitate interaction with the collagen fibers of the hCLs. Thus, the mucoadhesive property of PLGA resulted particularly advantageous as allows to rhNGF-PLGA-MPs to adhere to the collagen fibers on the surface of the hCL, preventing them from falling off even after the washing phase of the procedure also allowing the sustained release over time of rhNGF. Furthermore, recently it has also been shown that hCLs can be recellularized with primary human stromal fibroblasts or with MSCs (73–75). In the wake of these studies, we demonstrated the feasibility of bioengineering hCLs with both hAFSCs and rhNGF-PLGA-MPs and their effect on the *ex vivo* DR model. Interestingly, by co-culturing each of the three BioE_hCLs here developed with HG-treated porcine neuroretina, we observed that hAFSCs and rhNGF ameliorate the HG induced damaged status. Nevertheless, a closer investigation showed that depending on the markers analyzed, the three BioE_hCLs displayed different patterns.

Among the existing sources, we selected hAFSCs thanks to their secretome enriched in proregenerative and neuroprotective factors (14). In detail, we found that hCLs bioengineered with only hAFSCs (BioE_hCLs_A) did not restore the increased levels of *GFAP* and *VEGF* in the HG-treated neuroretinal explant. While it reduced HG induced inflammation, oxidative stress, and apoptosis probably due to the release of well-known anti-inflammatory, immunomodulatory, and neurotrophic factors present in the hAFSCs secretome. Therefore, assuming that the effects are mediated by the release of paracrine factors from hAFSCs, it would be interesting to evaluate in the future the possibility of bioengineering hCLs with EVs derived from hAFSCs, thereby overcoming the current limitations in the clinical application of these cells.

As regard the replacement of neurotrophic factors, it was found that in DR rats model the retrobulbar injection of NGF attenuates visual damage by reducing RGCs apoptosis (20). However, ST-induced diabetic rats treated with NGF eye drops showed a non-significant trend toward protecting ganglion cells from diabetes-induced degeneration (76, 77). Interestingly, our data strikingly concurs with these results since the rhNGF released from BioE_hCLs_B significantly

decreased inflammation, oxidative stress, neovascularization, and apoptosis. Probably, the rhNGF binding to its high affinity TrkA receptor, activating pathways like Ras-MAPK, ERK, PI3K-Akt, and PLC- γ (78–80). However, rhNGF did not improve the levels of retinal markers such as *TUBB3* and *RHO*.

To confirm that these results were due to the release of rhNGF from BioE_hCLs, we co-cultured neuroretinal samples with BioE_hCL_Fluo_PLGA-MPs, as delivery control. Interestingly, we provided evidence that Fluor-PLGA-MPs were released by BioE_hCL_Fluo-PLGA-MPs and that these were internalized into the retinal layer. This confirmed our previous results (22) and allowed us to hypothesize that BioE_hCLs were also able to release hAFSC-derived paracrine factors.

Although various studies have investigated the effects of MSCs and NGF on DR-model, none have explored the potential synergistic effect that could arise from their simultaneous release. Here, for the first time, we propose that they might have synergistic beneficial effects. Indeed, when BioE_hCLs_C were co-cultured with HG-treated neuroretinal explants a better effect was displayed compared to BioE_hCLs_A and BioE_hCLs_B, since a significant decrease of *Nfkb*, *NOS2*, *VEGFA*, and *Bax/Bcl2* and an increased in *TUBB3* expression was observed. Additionally, a trend in the downregulation of *Nrf2* and *GFAP* and in the upregulation of *RHO* were detected. In accordance with Zha et al. (81) we hypothesis that the rhNGF released stimulates hAFSCs paracrine factor production through the TrkA-MSCs receptor interaction thus resulting in a synergistic effect.

Although the results obtained are promising, the study here reported has some limitations. Firstly we considered a sample size of neuroretinal explants equal to or greater than five ($n \geq 5$) external factors such as the time of animal euthanasia as per day or night, which may affect photoreceptor activation, as well as the variability among animals often make it difficult to achieve statistical significance. Furthermore, the present study mainly focused on profiling the modulation of mRNA expression. A significant technical challenge we encountered was performing IF or histological analyses on neuroretinal explants following co-culture with BioE_hCLs. Indeed, due to the close contact between BioE_hCLs and the retinal explants, removing the BioE_hCLs could potentially cause a damage in the neuroretinal tissue structure, making the protein markers analyses performed directly *ex vivo* on the retina difficult. However, to support our mRNA expression results, we analyzed the conditioned medium of neuroretinal explants co-cultured with BioE_hCLs to quantify the levels of 48 cytokines involved in the processes of inflammation, oxidative stress and neovascularization. This evidenced the reduced release of GM-CSF, IL-1 β , IL-1 α , and PDGF-BB, along with the increased levels of IL-10 and INSULIN. An additional limit is the difficulty in maintaining neuroretinal explants in *ex vivo* culture for extended periods, as they tend to undergo spontaneous degeneration through programmed cell death, including apoptosis and necroptosis (82). This did not allow us to observe the long-term effects of HG, especially the factors released by BioE_hCLs.

Nevertheless overall, our results are encouraging and provide compelling evidence that hAFSCs and rhNGF can modulate the molecular mechanisms underlying DR following their release from BioE_hCLs, which might be proposed as a valuable ocular delivery system. Notably, we also successfully demonstrated the feasibility of mimicking DR *ex vivo* by treating porcine neuroretinal explants with

HG concentrations, thereby replicating the disease's *milieu*. This innovative approach not only sets the stage for more detailed studies but also paves the way for transitioning to an *in vivo* experimental model that will enable us to confirm the effects of hAFSCs and rhNGF on DR. Furthermore, the employment of an *in vivo* experimental model will allow us to identify the optimal implantation site for BioE_hCL, ensuring sufficient exposure and release of neurotrophic and regenerative factors to the retina providing us a better guidance on the subsequent treatment planning to move forward to possible clinical studies. Indeed, this is a proof-of-concept study that does not currently support the feasibility and efficacy of this transplant approach in DR patients. Therefore, further studies will be needed to assess its potential for clinical application.

Data availability statement

The original contributions presented in the study are included in the article/**Supplementary Material**. Further inquiries can be directed to the corresponding author.

Ethics statement

The studies involving humans were approved by hCL collection: University's Institutional Review Board and Ethical Committee (Approval number: 03/07-02-2019); hAFSCs isolation and collection: Regional Ethic Committee with the authorization P.R. 428REG2015 released on 11 November 2019. The studies were conducted in accordance with the local legislation and institutional requirements. The participants provided their written informed consent to participate in this study. Ethical approval was not required for the study involving animals in accordance with the local legislation and institutional requirements because a local slaughterhouse donated discarded pigs' eyes after processing the animals for food consumption.

Author contributions

LP: Formal analysis, Methodology, Investigation, Data curation, Writing – review & editing, Writing – original draft, Conceptualization. JH: Visualization, Writing – review & editing, Writing – original draft, Data curation, Conceptualization. ND: Investigation, Methodology, Writing – original draft. CP: Visualization, Writing – original draft. AL: Methodology, Investigation, Writing – review & editing. GC: Investigation, Methodology, Writing – original draft. RM: Writing – review & editing, Validation. MA: Funding acquisition, Writing – review & editing, Validation. NDP: Investigation, Writing – original draft, Methodology. TR: Validation, Writing – review & editing. ME: Writing – review & editing. MN: Validation, Writing – review & editing. LG: Investigation, Writing – original draft, Methodology. SB: Validation, Writing – review & editing. AP: Funding acquisition, Writing – original draft, Validation, Conceptualization, Writing –

review & editing. SS: Writing – review & editing, Writing – original draft, Validation, Conceptualization, Methodology. DM: Methodology, Formal analysis, Validation, Supervision, Data curation, Writing – review & editing, Writing – original draft, Conceptualization.

Funding

The author(s) declare financial support was received for the research, authorship, and/or publication of this article. This publication has emanated from research conducted with the financial support of: PON-MISE Sustainable Growth Funding-DD27 September 2018 (grant no. 21, F/180021/03/X43).

Acknowledgments

DM is a researcher (code n. 53-I-14751-1) supported by PON R&I “Ricerca e Innovazione” 2014–2020, Action IV.4 “Doctorates and research contracts on innovation issues”, DM 1061/2021, funded by the Ministry of University and Research (MUR), Italy, FSE REACT-EU. LP is a post-doc fellowship and MEZ is a doctoral fellowship both supported by PNRR-MR1-2022-12376561. We would also like to thank Dr. Pamela Di Tomo, Francesco Del Pizzo and Samuele Faieta for technical assistance. Dr. Erminia D'Ugo for her support on stromal lenticule samples collection.

Conflict of interest

The authors ND, GC, MA, and TR are employed by Dompé Farmaceutici SpA. ND, MA, MN, AP, and DM are authors of European Patent n° 20179055.7-1109, 09/06/2020, “New Drug Delivery System for Ophthalmic Use”.

The remaining authors declare that the research was conducted in the absence of any commercial or financial relationships that could be construed as a potential conflict of interest.

The author(s) declared that they were an editorial board member of Frontiers, at the time of submission. This had no impact on the peer review process and the final decision.

Publisher's note

All claims expressed in this article are solely those of the authors and do not necessarily represent those of their affiliated organizations, or those of the publisher, the editors and the reviewers. Any product that may be evaluated in this article, or claim that may be made by its manufacturer, is not guaranteed or endorsed by the publisher.

Supplementary material

The Supplementary Material for this article can be found online at: <https://www.frontiersin.org/articles/10.3389/fendo.2024.1462043/full#supplementary-material>

References

- Ellis MP, Lent-Schochet D, Lo T, Yiu G. Emerging concepts in the treatment of diabetic retinopathy. *Curr Diabetes Rep.* (2019) 19:137. doi: 10.1007/s11892-019-1276-5
- Thomas RL, Halim S, Gurudas S, Sivaprasad S, Owens DR. IDF Diabetes Atlas: A review of studies utilising retinal photography on the global prevalence of diabetes related retinopathy between 2015 and 2018. *Diabetes Res Clin Pract.* (2019) 157:107840. doi: 10.1016/j.diabres.2019.107840
- Selvaraj K, Gowthamarajan K, Karri VV, Barauah UK, Ravisankar V, Jojo GM. Current treatment strategies and nanocarrier based approaches for the treatment and management of diabetic retinopathy. *J Drug Targeting.* (2017) 25:386–405. doi: 10.1080/1061186X.2017.1280809
- Gaddam S, Periasamy R, Gangaraju R. Adult stem cell therapeutics in diabetic retinopathy. *Int J Mol Sci.* (2019) 20:4876. doi: 10.3390/ijms20194876
- Arrigo A, Teussink M, Aragona E, Bandello F, Battaglia Parodi M. MultiColor imaging to detect different subtypes of retinal microaneurysms in diabetic retinopathy. *Eye (Lond).* (2021) 35:277–81. doi: 10.1038/s41433-020-0811-6
- Di Fulvio P, Pandolfi A, Formoso G, Silvestre S, Tomo P, Giardinelli A, et al. Features of endothelial dysfunction in umbilical cord vessels of women with gestational diabetes. *Nutr Metab Cardiovasc Dis.* (2014) 24:1337–45. doi: 10.1016/j.numecd.2014.06.005
- Zerbini G, Maestroni S, Leocani L, Mosca A, Godi M, Paleari R, et al. Topical nerve growth factor prevents neurodegenerative and vascular stages of diabetic retinopathy. *Front Pharmacol.* (2022) 13:1015522. doi: 10.3389/fphar.2022.1015522
- Solomon SD, Chew E, Duh EJ, Sobrin L, Sun JK, VanderBeek BL, et al. Diabetic retinopathy: A position statement by the american diabetes association. *Diabetes Care.* (2017) 40:412–8. doi: 10.2337/dc16-2641
- Simo R, Simo-Servat O, Bogdanov P, Hernandez C. Diabetic retinopathy: role of neurodegeneration and therapeutic perspectives. *Asia Pac J Ophthalmol (Phila).* (2022) 11:160–7. doi: 10.1097/APO.0000000000000510
- Lin KY, Hsieh WH, Lin YB, Wen CY, Chang TJ. Update in the epidemiology, risk factors, screening, and treatment of diabetic retinopathy. *J Diabetes Investig.* (2021) 12:1322–5. doi: 10.1111/jdi.13480
- Kutluturk Karagoz I, Allahverdiyev A, Bagirova M, Abamor ES, Dinparvar S. Current approaches in treatment of diabetic retinopathy and future perspectives. *J Ocul Pharmacol Ther.* (2020) 36:487–96. doi: 10.1089/jop.2019.0137
- Simo R, Stitt AW, Gardner TW. Neurodegeneration in diabetic retinopathy: does it really matter? *Diabetologia.* (2018) 61:1902–12. doi: 10.1007/s00125-018-4692-1
- Kim KS, Park JM, Kong T, Kim C, Bae SH, Kim HW, et al. Retinal angiogenesis effects of TGF- β 1 and paracrine factors secreted from human placental stem cells in response to a pathological environment. *Cell Transplant.* (2016) 25:1145–57. doi: 10.3727/096368915X688263
- Costa A, Ceresa D, Palma A, Rossi R, Turturo S, Santamaria S, et al. Comprehensive profiling of secretome formulations from fetal- and perinatal human amniotic fluid stem cells. *Int J Mol Sci.* (2021) 22:3713. doi: 10.3390/ijms22073713
- Stitt AW, Curtis TM, Chen M, Medina RJ, McKay GJ, Jenkins A, et al. The progress in understanding and treatment of diabetic retinopathy. *Prog Retin Eye Res.* (2016) 51:156–86. doi: 10.1016/j.preteyeres.2015.08.001
- Kong JH, Zheng D, Chen S, Duan HT, Wang YX, Dong M, et al. A comparative study on the transplantation of different concentrations of human umbilical mesenchymal cells into diabetic rats. *Int J Ophthalmol.* (2015) 8:257–62. doi: 10.3980/j.issn.2222-3959.2015.02.08
- He Y, Zhang Z, Yao T, Huang L, Gan J, Lv H, et al. Extracellular vesicles derived from human umbilical cord mesenchymal stem cells relieves diabetic retinopathy through a microRNA-30c-5p-dependent mechanism. *Diabetes Res Clin Pract.* (2022) 190:109861. doi: 10.1016/j.diabres.2022.109861
- Gu C, Zhang H, Gao Y. Adipose mesenchymal stem cells-secreted extracellular vesicles containing microRNA-192 delays diabetic retinopathy by targeting ITGA1. *J Cell Physiol.* (2021) 236:5036–51. doi: 10.1002/jcp.30213
- Mysona BA, Al-Gayyar MM, Matragoon S, Abdelsaid MA, El-Azab MF, Saragovi HU, et al. Modulation of p75(NTR) prevents diabetes- and proNGF-induced retinal inflammation and blood-retina barrier breakdown in mice and rats. *Diabetologia.* (2013) 56:2329–39. doi: 10.1007/s00125-013-2998-6
- Wang QC, Sheng W, Yi CJ, Lv H, Cheng B. Retrobulbarly injecting nerve growth factor attenuates visual impairment in streptozotocin-induced diabetes rats. *Int Ophthalmol.* (2020) 40:3501–11. doi: 10.1007/s10792-020-01537-8
- Elsherbiny NM, Abdel-Mottaleb Y, Elkazaz AY, Atef H, Lashine RM, Youssef AM, et al. Carbamazepine alleviates retinal and optic nerve neural degeneration in diabetic mice via nerve growth factor-induced PI3K/akt/mTOR activation. *Front Neurosci.* (2019) 13:1089. doi: 10.3389/fnins.2019.01089
- Mastropasqua L, Nubile M, Acerra G, Detta N, Pelusi L, Lanzini M, et al. Bioengineered human stromal lenticule for recombinant human nerve growth factor release: A potential biocompatible ocular drug delivery system. *Front Bioeng Biotechnol.* (2022) 10:887414. doi: 10.3389/fbioe.2022.887414
- Yam GH, Bandeira F, Liu YC, Devarajan K, Yusoff N, Htoon HM, et al. Effect of corneal stromal lenticule customization on neurite distribution and excitatory property. *J Adv Res.* (2022) 38:275–84. doi: 10.1016/j.jare.2021.09.004
- Murali A, Ramlogan-Steel CA, Andrzejewski S, Steel JC, Layton CJ. Retinal explant culture: A platform to investigate human neuro-retina. *Clin Exp Ophthalmol.* (2019) 47:274–85. doi: 10.1111/ceo.13434
- Hurst J, Fietz A, Tsai T, Joachim SC, Schnichels S. Organ cultures for retinal diseases. *Front Neurosci.* (2020) 14:583392. doi: 10.3389/fnins.2020.583392
- Schnichels S, Kiebler T, Hurst J, Maliha AM, Loscher M, Dick HB, et al. Retinal organ cultures as alternative research models. *Altern Lab Anim.* (2019) 47:19–29. doi: 10.1177/0261192919840092
- Schnichels S, Paquet-Durand F, Loscher M, Tsai T, Hurst J, Joachim SC, et al. Retina in a dish: Cell cultures, retinal explants and animal models for common diseases of the retina. *Prog Retin Eye Res.* (2021) 81:100880. doi: 10.1016/j.preteyeres.2020.100880
- Lai AK, Lo AC. Animal models of diabetic retinopathy: summary and comparison. *J Diabetes Res.* (2013) 2013:106594. doi: 10.1155/2013/106594
- Guduric-Fuchs J, Ringland LJ, Gu P, Dellett M, Archer DB, Cogliati T. Immunohistochemical study of pig retinal development. *Mol Vis.* (2009) 15:1915–28.
- Slijkerman RW, Song F, Astuti GD, Huynen MA, van Wijk E, Stieger K, et al. The pros and cons of vertebrate animal models for functional and therapeutic research on inherited retinal dystrophies. *Prog Retin Eye Res.* (2015) 48:137–59. doi: 10.1016/j.preteyeres.2015.04.004
- Quiroz J, Yazdanyar A. Animal models of diabetic retinopathy. *Ann Transl Med.* (2021) 9:1272. doi: 10.21037/atm-20-6737
- Fietz A, Corsi F, Hurst J, Schnichels S. Blue Light Damage and p53: Unravelling the Role of p53 in Oxidative-Stress-Induced Retinal Apoptosis. *Antioxid (Basel).* (2023) 12:2072. doi: 10.3390/antiox12122072
- Fietz A, Schnichels S, Hurst J. Co-cultivation of primary porcine RPE cells and neuroretina induces inflammation: a potential inflammatory AMD-model. *Sci Rep.* (2023) 13:19345. doi: 10.1038/s41598-023-46029-8
- Balbi C, Lodder K, Costa A, Moimas S, Moccia F, Herwaarden Tv, et al. Supporting data on *in vitro* cardioprotective and proliferative paracrine effects by the human amniotic fluid stem cell secretome. *Data Brief.* (2019) 25:104324. doi: 10.1016/j.dib.2019.104324
- Balbi C, Piccoli M, Barile L, Papait A, Armirotti A, Principi E, et al. First characterization of human amniotic fluid stem cell extracellular vesicles as a powerful paracrine tool endowed with regenerative potential. *Stem Cells Transl Med.* (2017) 6:1340–55. doi: 10.1002/sctm.16-0297
- Costa A, Balbi C, Garbati P, Palama MEF, Reverberi D, Palma A, et al. Investigating the paracrine role of perinatal derivatives: human amniotic fluid stem cell-extracellular vesicles show promising transient potential for cardiomyocyte renewal. *Front Bioeng Biotechnol.* (2022) 10:902038. doi: 10.3389/fbioe.2022.902038
- Ipp E. Diabetic retinopathy and insulin insufficiency: beta cell replacement as a strategy to prevent blindness. *Front Endocrinol (Lausanne).* (2021) 12:734360. doi: 10.3389/fendo.2021.734360
- Saeedi P, Petersohn I, Salpea P, Malanda B, Karuranga S, Unwin N, et al. Global and regional diabetes prevalence estimates for 2019 and projections for 2030 and 2045: Results from the International Diabetes Federation Diabetes Atlas, 9(th) edition. *Diabetes Res Clin Pract.* (2019) 157:107843. doi: 10.1016/j.diabres.2019.107843
- Soni D, Sagar P, Takkar B. Diabetic retinal neurodegeneration as a form of diabetic retinopathy. *Int Ophthalmol.* (2021) 41:3223–48. doi: 10.1007/s10792-021-01864-4
- Sadikhan MZ, Abdul Nasir NA, Lambuk L, Mohamud R, Reshidan NH, Low E, et al. Diabetic retinopathy: a comprehensive update on *in vivo*, *in vitro* and *ex vivo* experimental models. *BMC Ophthalmol.* (2023) 23:421. doi: 10.1186/s12886-023-03155-1
- Olivares AM, Althoff K, Chen GF, Wu S, Morrisson MA, DeAngelis MM, et al. Animal models of diabetic retinopathy. *Curr Diabetes Rep.* (2017) 17:93. doi: 10.1007/s11892-017-0913-0
- Yin Y, Xu R, Ning L, Yu Z. Bergein alleviates Diabetic Retinopathy in STZ-induced rats. *Appl Biochem Biotechnol.* (2023) 195:5299–311. doi: 10.1007/s12010-022-03949-x
- Ly K, Ying H, Hu G, Hu J, Jian Q, Zhang F. Integrated multi-omics reveals the activated retinal microglia with intracellular metabolic reprogramming contributes to inflammation in STZ-induced early diabetic retinopathy. *Front Immunol.* (2022) 13:942768. doi: 10.3389/fimmu.2022.942768
- Rakieten N, Rakieten ML, Nadkarni MV. Studies on the diabetogenic action of streptozotocin (NSC-37917). *Cancer Chemother Rep.* (1963) 29:91–8.
- Amato R, Biagioni M, Cammalleri M, Monte MD, Casini G. VEGF as a survival factor in *ex vivo* models of early diabetic retinopathy. *Invest Ophthalmol Vis Sci.* (2016) 57:3066–76. doi: 10.1167/iovs.16-19285

46. Gucciardo E, Loukovaara S, Korhonen A, Lehti K. An *ex vivo* tissue culture model for fibrovascular complications in proliferative diabetic retinopathy. *J Vis Exp.* (2019) 143. doi: 10.3791/59090
47. Rezzola S, Belleri M, Ribatti D, Costagliola C, Presta M, Semeraro F. A novel *ex vivo* murine retina angiogenesis (EMRA) assay. *Exp Eye Res.* (2013) 112:51–6. doi: 10.1016/j.exer.2013.04.014
48. Alarautalahti V, Ragauskas S, Hakkarainen JJ, Uusitalo-Jarvinen H, Uusitalo H, Hyttinen J, et al. Viability of mouse retinal explant cultures assessed by preservation of functionality and morphology. *Invest Ophthalmol Vis Sci.* (2019) 60:1914–27. doi: 10.1167/iov.18-25156
49. Ding X, Sun Z, Guo Y, Tang W, Shu Q, Xu G. Inhibition of NF-kappaB ameliorates aberrant retinal glia activation and inflammatory responses in streptozotocin-induced diabetic rats. *Ann Transl Med.* (2023) 11:197. doi: 10.21037/atm-22-2204
50. Kowluru RA, Koppolu P, Chakrabarti S, Chen S. Diabetes-induced activation of nuclear transcriptional factor in the retina, and its inhibition by antioxidants. *Free Radic Res.* (2003) 37:1169–80. doi: 10.1080/10715760310001604189
51. Ganesh Yerra V, Negi G, Sharma SS, Kumar A. Potential therapeutic effects of the simultaneous targeting of the Nrf2 and NF-kappaB pathways in diabetic neuropathy. *Redox Biol.* (2013) 1:394–7. doi: 10.1016/j.redox.2013.07.005
52. Taguchi K, Motohashi H, Yamamoto M. Molecular mechanisms of the Keap1-Nrf2 pathway in stress response and cancer evolution. *Genes Cells.* (2011) 16:123–40. doi: 10.1111/j.1365-2443.2010.01473.x
53. Kensler TW, Wakabayashi N, Biswal S. Cell survival responses to environmental stresses via the Keap1-Nrf2-ARE pathway. *Annu Rev Pharmacol Toxicol.* (2007) 47:89–116. doi: 10.1146/annurev.pharmtox.46.120604.141046
54. Zhong Q, Kowluru RA. Regulation of matrix metalloproteinase-9 by epigenetic modifications and the development of diabetic retinopathy. *Diabetes.* (2013) 62:2559–68. doi: 10.2337/db12-1141
55. Kowluru RA. Cross talks between oxidative stress, inflammation and epigenetics in diabetic retinopathy. *Cells.* (2023) 12:300. doi: 10.3390/cells12020300
56. Zhong Q, Mishra M, Kowluru RA. Transcription factor Nrf2-mediated antioxidant defense system in the development of diabetic retinopathy. *Invest Ophthalmol Vis Sci.* (2013) 54:3941–8. doi: 10.1167/iov.13-11598
57. Mishra A, Newman EA. Inhibition of inducible nitric oxide synthase reverses the loss of functional hyperemia in diabetic retinopathy. *Glia.* (2010) 58:1996–2004. doi: 10.1002/glia.21068
58. Othman R, Vaucher E, Couture R. Bradykinin type 1 receptor - inducible nitric oxide synthase: A new axis implicated in diabetic retinopathy. *Front Pharmacol.* (2019) 10:300. doi: 10.3389/fphar.2019.00300
59. Toda N, Nakanishi-Toda M. Nitric oxide: ocular blood flow, glaucoma, and diabetic retinopathy. *Prog Retin Eye Res.* (2007) 26:205–38. doi: 10.1016/j.preteyeres.2007.01.004
60. Pandolfi A, De Filippis EA. Chronic hyperglycemia and nitric oxide bioavailability play a pivotal role in pro-atherogenic vascular modifications. *Genes Nutr.* (2007) 2:195–208. doi: 10.1007/s12263-007-0050-5
61. Lechner J, Medina RJ, Lois N, Stitt AW. Advances in cell therapies using stem cells/progenitors as a novel approach for neurovascular repair of the diabetic retina. *Stem Cell Res Ther.* (2022) 13:388. doi: 10.1186/s13287-022-03073-x
62. Simoens P, Schaepdrijver L, Lauwers H. Morphologic and clinical study of the retinal circulation in the miniature pig. A: Morphology of the retinal microvasculature. *Exp Eye Res.* (1992) 54:965–73. doi: 10.1016/0014-4835(92)90161-k
63. Ren J, Zhang S, Pan Y, Jin M, Li J, Luo Y, et al. Diabetic retinopathy: Involved cells, biomarkers, and treatments. *Front Pharmacol.* (2022) 13:953691. doi: 10.3389/fphar.2022.953691
64. Jeong JS, Lee WK, Moon YS, Kim NR. Early changes in retinal structure and BMP2 expression in the retina and crystalline lens of streptozotocin-induced diabetic pigs. *Lab Anim Res.* (2017) 33:216–22. doi: 10.5625/lar.2017.33.3.216
65. Buccarello L, Dragotto J, Hassanzadeh K, Maccarone R, Corbo M, Feligioni M. Retinal ganglion cell loss in an *ex vivo* mouse model of optic nerve cut is prevented by curcumin treatment. *Cell Death Discovery.* (2021) 7:394. doi: 10.1038/s41420-021-00760-1
66. Saha B, Roy A, Beltramo E, Sahoo OS. Stem cells and diabetic retinopathy: From models to treatment. *Mol Biol Rep.* (2023) 50:4517–26. doi: 10.1007/s11033-023-08337-0
67. Fiori A, Terlizzi V, Kremer H, Gebauer J, Hammes HP, Harmsen MC, et al. Mesenchymal stromal/stem cells as potential therapy in diabetic retinopathy. *Immunobiology.* (2018) 223:729–43. doi: 10.1016/j.imbio.2018.01.001
68. Sun F, Sun Y, Zhu J, Wang X, Ji C, Zhang J, et al. Mesenchymal stem cells-derived small extracellular vesicles alleviate diabetic retinopathy by delivering NEDD4. *Stem Cell Res Ther.* (2022) 13:293. doi: 10.1186/s13287-022-02983-0
69. Abdel-Kawi SH, Hashem KS. Administration of melatonin in diabetic retinopathy is effective and improves the efficacy of mesenchymal stem cell treatment. *Stem Cells Int.* (2022) 2022:6342594. doi: 10.1155/2022/6342594
70. Castoldi V, Zerbini G, Maestroni S, Viganò I, Rama P, Leocani L. Topical Nerve Growth Factor (NGF) restores electrophysiological alterations in the Ins2(Akita) mouse model of diabetic retinopathy. *Exp Eye Res.* (2023) 237:109693. doi: 10.1016/j.exer.2023.109693
71. Lambiasi A, Aloe L, Centofanti M, Parisi V, Bao SN, Mantelli F, et al. Experimental and clinical evidence of neuroprotection by nerve growth factor eye drops: Implications for glaucoma. *Proc Natl Acad Sci U S A.* (2009) 106:13469–74. doi: 10.1073/pnas.0906678106
72. Rocco ML, Calza L, Aloe L. NGF and retinitis pigmentosa: structural and molecular studies. *Adv Exp Med Biol.* (2021) 1331:255–63. doi: 10.1007/978-3-030-74046-7_17
73. Aghamollaei H, Hashemian H, Safabakhsh H, Halabian R, Baghersad M, Jadidi K. Safety of grafting acellular human corneal lenticule seeded with Wharton's Jelly-Derived Mesenchymal Stem Cells in an experimental animal model. *Exp Eye Res.* (2021) 205:108451. doi: 10.1016/j.exer.2021.108451
74. Yam GH, Yusoff NZ, Goh TW, Setiawan M, Lee XW, Liu YC, et al. Decellularization of human stromal refractive lenticules for corneal tissue engineering. *Sci Rep.* (2016) 6:26339. doi: 10.1038/srep26339
75. Alio del Barrio JL, Chiesa M, Garagorri N, Garcia-Urquía N, Fernandez-Delgado J, Bataille L, et al. Acellular human corneal matrix sheets seeded with human adipose-derived mesenchymal stem cells integrate functionally in an experimental animal model. *Exp Eye Res.* (2015) 132:91–100. doi: 10.1016/j.exer.2015.01.020
76. Colafrancesco V, Coassin M, Rossi S, Aloe L. Effect of eye NGF administration on two animal models of retinal ganglion cells degeneration. *Ann Ist Super Sanita.* (2011) 47:284–9. doi: 10.4415/ANN_11_03_08
77. Shityakov S, Nagai M, Ergun S, Braunger BM, Forster CY. The protective effects of neurotrophins and microRNA in diabetic retinopathy, nephropathy and heart failure via regulating endothelial function. *Biomolecules.* (2022) 12:1113. doi: 10.3390/biom12081113
78. Aloe L, Rocco ML, Bianchi P, Manni L. Nerve growth factor: from the early discoveries to the potential clinical use. *J Transl Med.* (2012) 10:239. doi: 10.1186/1479-5876-10-239
79. Klesse LJ, Meyers KA, Marshall CJ, Parada LF. Nerve growth factor induces survival and differentiation through two distinct signaling cascades in PC12 cells. *Oncogene.* (1999) 18:2055–68. doi: 10.1038/sj.onc.1202524
80. Reichardt LF. Neurotrophin-regulated signalling pathways. *Philos Trans R Soc Lond B Biol Sci.* (2006) 361:1545–64. doi: 10.1098/rstb.2006.1894
81. Zha K, Yang Y, Tian G, Sun Z, Yang Z, Li X, et al. Nerve growth factor (NGF) and NGF receptors in mesenchymal stem/stromal cells: Impact on potential therapies. *Stem Cells Transl Med.* (2021) 10:1008–20. doi: 10.1002/sctm.20-0290
82. Puertas-Neyra K, Galindo-Cabello N, Hernandez-Rodriguez LA, Gonzalez-Perez F, Rodriguez-Cabello JC, Gonzalez-Sarmiento R, et al. Programmed cell death and autophagy in an *in vitro* model of spontaneous neuroretinal degeneration. *Front Neuroanat.* (2022) 16:812487. doi: 10.3389/fnana.2022.812487



OPEN ACCESS

EDITED BY

Mohd Imtiaz Nawaz,
King Saud University, Saudi Arabia

REVIEWED BY

Viktor Kravchenko,
National Academy of Sciences of Ukraine,
Ukraine
Tong Yue,
University of Science and Technology of
China, China

*CORRESPONDENCE

Wei Yan
✉ yanwei_jlu@163.com

RECEIVED 21 January 2024

ACCEPTED 25 September 2024

PUBLISHED 21 October 2024

CITATION

Ouyang J, Zhou L, Wang Q and Yan W (2024)
Genetically mimicked effects of thyroid
dysfunction on diabetic retinopathy risk: a 2-
sample univariable and multivariable
Mendelian randomization study.
Front. Endocrinol. 15:1374254.
doi: 10.3389/fendo.2024.1374254

COPYRIGHT

© 2024 Ouyang, Zhou, Wang and Yan. This is
an open-access article distributed under the
terms of the [Creative Commons Attribution
License \(CC BY\)](#). The use, distribution or
reproduction in other forums is permitted,
provided the original author(s) and the
copyright owner(s) are credited and that the
original publication in this journal is cited, in
accordance with accepted academic
practice. No use, distribution or reproduction
is permitted which does not comply with
these terms.

Genetically mimicked effects of thyroid dysfunction on diabetic retinopathy risk: a 2-sample univariable and multivariable Mendelian randomization study

Junlin Ouyang¹, Ling Zhou², Qing Wang¹ and Wei Yan^{3*}

¹China–Japan Union Hospital of Jilin University, Department of Endocrinology, Jilin, China, ²China–Japan Union Hospital of Jilin University, Department of Obstetrics and Gynecology, Jilin, China, ³China–Japan Union Hospital of Jilin University, Emergency Department, Jilin, China

Background: Thyroid dysfunction exhibits a heightened prevalence among people with diabetes compared to those without diabetes. Furthermore, TD emerges as a notable correlated risk factor for the onset of diabetic retinopathy.

Methods: Using data from the FinnGen database (R9), we investigated the causal relationship between thyroid dysfunction (TD) and four stages of diabetic retinopathy (DR). A two-sample univariable Mendelian randomization (UVMR) approach was employed to estimate the total causal effect of TD on four stages of DR, while multivariable Mendelian randomization (MVMR) was used to assess the direct causal effect. The meta-analysis was conducted to summarize the collective effect of TD on four stages of DR. The inverse variance weighted (IVW) method was the primary approach for Mendelian randomization analysis, with heterogeneity, horizontal pleiotropy, and leave-one-out sensitivity analyses performed to validate the robustness of the findings.

Results: In UVMR analysis, thyrotoxicosis (TOS) was significantly associated with an increased risk of diabetic retinopathy across four stages (OR, 1.10–1.19; $P < 0.025$). However, MVMR analysis, after adjusting for Graves' disease (GD) and/or rheumatoid arthritis (RA), revealed no significant association between TOS and the four stages of diabetic retinopathy. The Meta-analysis demonstrated the collective effect of TOS on diabetic retinopathy across all stages [OR=1.11; 95% CI (1.08–1.15); $P < 0.01$]. In UVMR analysis, the estimates for hypothyroidism (HPT) and GD were similar to those for TOS. In the MVMR analysis, after adjusting for RA, the significant effect of HPT on DR and non-proliferative diabetic retinopathy (NPDR) remained. Additionally, MVMR analysis suggested that the estimates for GD on DR were not affected by TOS, except for GD-proliferative diabetic retinopathy (PDR). However, no significant correlation persisted after adjusting for RA, including for GD-PDR.

Conclusion: Our study demonstrated a significant association between thyroid dysfunction TD and DR, with the relationship being particularly pronounced in HPT-DR.

KEYWORDS

thyroid dysfunction, diabetic retinopathy, Mendelian randomization, meta-analysis, gene

1 Introduction

Diabetic retinopathy(DR), a prominent microvascular complication of diabetes, stands as a leading cause of adult blindness (1). Recent investigations highlight a global prevalence of 34.6% for DR (2). The pathophysiological spectrum of DR encompasses two primary categories: proliferative DR(PDR) and nonproliferative DR(NPDR). In cases where PDR or macular edema with central involvement manifests, intravitreal anti-vascular endothelial growth factor(VEGF) therapy proves efficacious. However, the challenge of rapid recurrence upon drug discontinuation remains a noteworthy concern (3). Nevertheless, due to cost-effectiveness, it remains unrecognized for the treatment of NPDR. DR has garnered growing public concern owing to its widespread prevalence, expensive treatment modalities, and adverse impact on health. Consequently, it is a rising imperative to investigate etiological factors to avert the development of DR. Recent studies have reported that thyroid dysfunction(TD) may elevate the prevalence of DR (4).

TD, encompassing thyrotoxicosis(TOS), hypothyroidism(HPT), and autoimmune thyroid diseases. Diabetes mellitus(DM) and TD are prevalent endocrine system maladies in clinical practice, exhibiting an inherent connection (5). Blood glucose plays a pivotal role in regulating the hypothalamic-pituitary-thyroid axis and the release of thyroid-stimulating hormone(TSH) from the pituitary. Simultaneously, it influences the conversion of thyroxine to triiodothyronine in peripheral tissues (5). Concurrently, numerous observational studies highlight a higher prevalence of TD in diabetic populations compared to non-diabetic counterparts, particularly in type 1 diabetes mellitus, suggesting a robust shared genetic susceptibility. Serum levels of TSH represent an independent risk factor for DR (6). Despite this, the role of TD remains insufficiently emphasized in the context of DR prevention and treatment. Consequently, the paper aims to investigate the potential relationship between TD and diabetic retinopathy.

Nevertheless, existing evidence regarding the link between TD and diabetic retinopathy primarily stems from observational studies, introducing challenges such as confounding bias and reverse causality. To more accurately assess the potential causal relationships between TD, including TOS, HPT and Graves' disease (GD), and various stages of DR, genetic approaches have surfaced as a reliable alternative for assessing causality. The approach helps circumvent interference from

confounding or reverse causality (7). Mendelian randomization(MR) stands out as a robust analytical method for accomplishing this objective. Grounded in Mendel's laws, MR is less susceptible to confounding factors. Its emphasis lies in investigating the causal relationship between the exposures and the outcomes through the utilization of genetic variants that meet three fundamental assumptions as instrumental variables(IVs) (8).

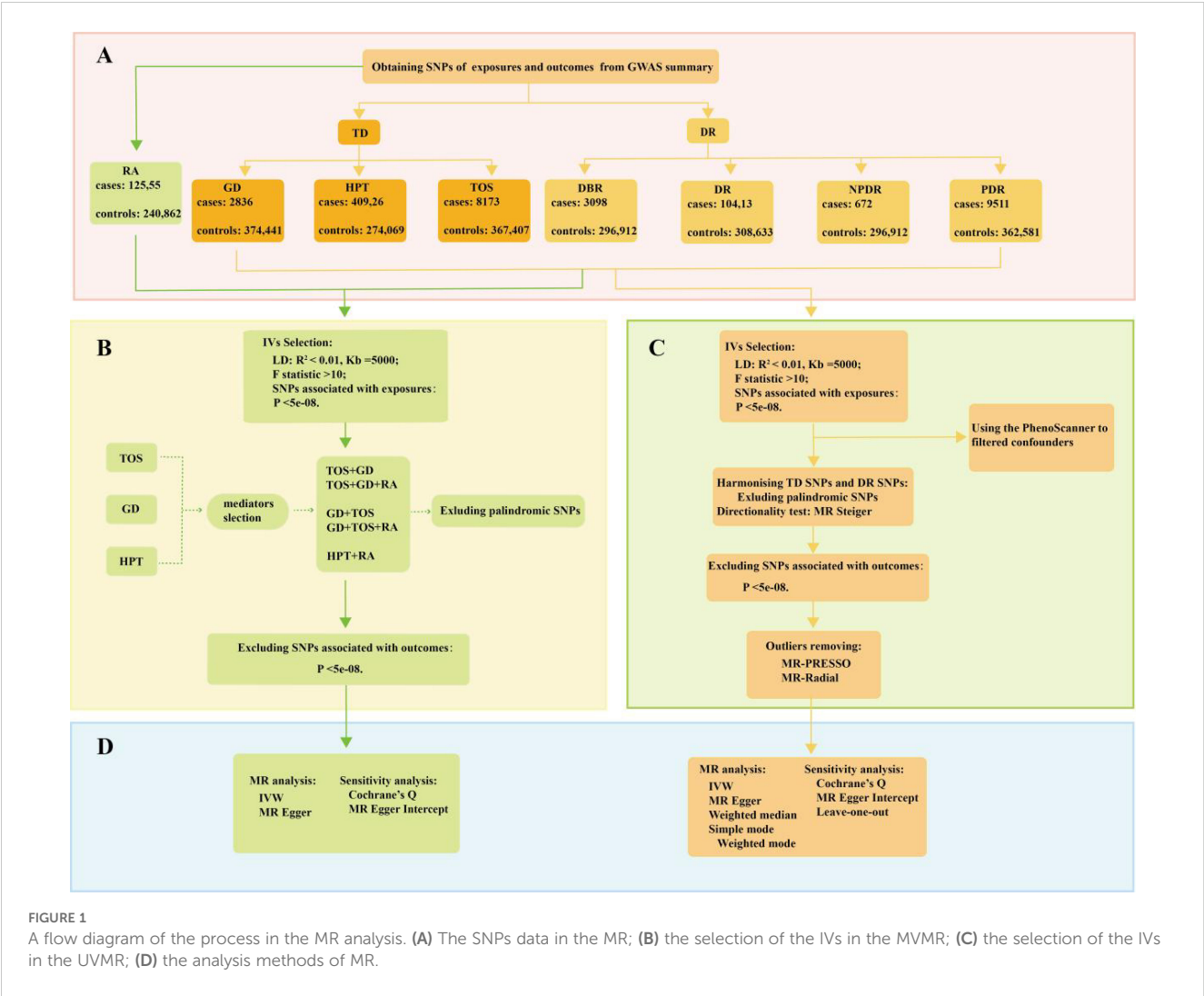
2 Materials and methods

2.1 Study design

As illustrated in [Figure 1](#), the study design was based on the latest genome-wide association studies from the FinnGen database (R9) focusing on TD, rheumatoid arthritis (RA), and four stages of DR: background diabetic retinopathy (DBR), DR, NPDR, and PDR. Pooled data were analyzed using two-sample univariable Mendelian randomization (UVMR) to estimate the total causal effect of each exposure and multivariable Mendelian randomization (MVMR) to assess the direct causal effects of multiple exposures simultaneously. Meta-analysis was conducted for the pooled analysis. Additionally, a series of sensitivity analyses were performed to evaluate potential biases, including heterogeneity and horizontal pleiotropy, within the MR framework. The implementation of MR analysis relies on three critical assumptions, constituting an indispensable prerequisite for conducting analyses (9, 10): (1) Correlation: A robust correlation must exist between genetic variants and exposures; (2) Independence: Genetic variation should demonstrate independence from confounding factors; (3) Exclusion restriction: Genetic variation should exclusively influence the outcome through the targeted exposure factors. The present reporting and analysis procedures adhered to the STROBE-MR guidelines (11). [Table 1](#) provides a concise overview of the characteristics of the data sources utilized for the MR analysis, all of which are publicly accessible.

2.2 Instrumental variables

In the study, we queried the FinnGen(R9) database to identify key single-nucleotide polymorphisms(SNPs) serving as IVs, guided



by three fundamental hypotheses (Figure 1). Firstly, we evaluated the correlation of IVs with exposures using genome-wide significance levels ($P < 5e-08$) and an F statistic (>10) (12). The F statistic was computed using the following formula:

$$F = (R^2/k)/[(1 - R^2)/(n - k - 1)]$$

R^2 is defined as the ability of the genetic variance to explain the exposure; k is the number of IVs used in the model; and n is the sample size.

TABLE 1 Descriptive details of the sources of TD and DR.

| Phenotype | TOS ^{Ia} | HPT ^{II} | GD ^{Ib} | RA ^{VII} | DR ^{III} | DBR ^{IV} | NPDR ^V | PDR ^{VI} |
|-------------------------|-------------------|-------------------|------------------|-------------------|-------------------|-------------------|-------------------|-------------------|
| ncases | 8173 | 40926 | 2836 | 12555 | 10413 | 3098 | 672 | 9511 |
| Female gender (%) | 79.0 | 80.0 | 84.5 | 67.3 | 43.9 | 45.8 | 41.1 | 47.9 |
| Age at diagnosis (mean) | 51.72 | 51.76 | 49.0 | 52.1 | 57.02 | 49.7 | 46.7 | 55.8 |
| Data source | the FinnGen | | | | | | | |

^{I-VII}Data from the FinnGen all consist of European cohorts.
^{Ia}GWAS ID: finngen_R9_THYROTOXICOSIS;
^{II}GWAS ID: finngen_R9_E4_HYTHY_AI_STRICT;
^{Ib}GWAS ID: finngen_R9_E4_GRAVES_STRICT;
^{III}GWAS ID: finngen_R9_DM_RETINOPATHY_EXMORE;
^{IV}GWAS ID: finngen_R7_DM_BCKGRND_RETINA;
^VGWAS ID: finngen_R7_DM_BCKGRND_RETINA_NONPROLIF;
^{VI}GWAS ID: finngen_R9_DM_RETINA_PROLIF;
^{VII}GWAS ID: finngen_R9_M13_RHEUMA.

Secondly, linkage disequilibrium (LD) was employed to guarantee the independence of IVs from other genes ($kb = 5000$, $r^2 = 0.01$) (13, 14). Proxy SNPs were not used in cases where there were no SNPs associated with exposures in the outcomes. Additionally, we harmonized genetic variation by merging exposures and outcomes, concurrently eliminating palindromic SNPs. Lastly, SNPs significantly linked to outcomes ($P < 5e-08$) were also excluded.

2.3 Mendelian randomization

In the UVMR analysis, several MR methods were employed to substantiate total causal effect between TD and four stages of DR (Figure 1). These methods encompassed inverse variance weighting (IVW), MR-Egger, weighted median(WM), Simple mode, and Weighted mode (15). Among these, IVW, grounded on the equilibrium assumption of horizontal pleiotropy of IVs, stands out for its ability to disregard IVs' heterogeneity, rendering it the most frequent approach in MR analysis (16). Other MR methods were employed to offer supplementary evaluations. The MR-Egger method, akin to IVW, differs primarily in considering the presence of intercept term in the regression. Furthermore, WM estimates furnish a reliable evaluation of causality even when only 50% of the IVs are valid (17). In MVMR analyses, the estimation of the direct causal effect of TD on four stages of DR predominantly relies on IVW and MR-Egger regression (Figure 1).

2.4 Sensitivity analyses

Subsequent to detecting causal effects through the aforementioned methods, we conducted sensitivity analyses to scrutinize the robustness of the MR findings, encompassing tests for heterogeneity and horizontal pleiotropy (Figure 1). In UVMR analyses, the identification of outliers is significantly reliant on the MR-PRESSO test and the RadialMR (9). Cochran's Q statistic ($P > 0.05$) and MR-Egger Intercept ($P > 0.05$) were separately employed in the study to assess the heterogeneity and horizontal pleiotropy (18). Furthermore, we evaluated the impact of individual SNP on the pooled causal estimates using the leave-one-out method, aiming to discern the presence of potentially pleiotropic SNPs that might influence the causal estimates (19). Statistical power for the UVMR study was calculated using the mRnd online tool (<https://shiny.cnsgenomics.com/mRnd/>). We employed the MR Steiger directionality test to evaluate the directionality of UVMR causal estimates. The TwoSampleMR and MendelianRandomization packages were utilized to identify potential confounders. In MVMR analyses, Cochran's Q statistic was primarily used to assess study heterogeneity, and MR-Egger intercept was employed to evaluate horizontal pleiotropy.

2.5 Statistical analyses

The TwoSampleMR package and the RadialMR package were employed for UVMR analyses within the R (version 4.2.3) (20, 21). For MVMR analyses, we utilized the MendelianRandomization

package. Meta-analyses were conducted using the Meta package. A significance threshold of $P < 0.05$ was established for statistical significance. Bonferroni correction was applied to redefine the threshold of statistical significance ($P < 0.05/n$) to account for multiple testing, where n denotes the number of MR tests (14). The adjusted p-value for the TD-diabetic retinopathy (DBR/DR/NPDR/PDR) analysis was set at 0.025. Similarly, the MVMR analyses also employed an adjusted p-value (0.025). The OR, beta values and their respective 95% confidence intervals were utilized to furnish estimates of relative risk.

3 Results

The UVMR study examined the total causal effect between TD and DR using three different exposures and four stages of outcomes. All IVs were significantly associated with the exposures ($P < 5e-08$) and had F-statistics greater than 10 (Supplementary Tables 1–12), indicating a strong association with the exposure. Additionally, outliers were eliminated by MR-PRESSO (Supplementary Table: MR results sum1-12) and the RadialMR (Supplementary Figures 1–3), and each SNP was not associated with the outcome ($P > 5e-08$) (Supplementary Tables 1–12). Given GD is a known etiology of TOS, the pleiotropic effects of TOS and GD may violate the exclusion restriction hypothesis. Our analysis using the Phenoscanner package identified RA as a potentially influential confounder or mediator (Supplementary Table: potential confounders), with SNPs associated with RA detailed in Supplementary Table 13. Furthermore, prior reports have hinted at ambiguous associations of RA with both diabetic retinopathy and TD (22–24). Consequently, we employed MVMR to adjust for TOS, GD, and RA.

3.1 Sensitivity analyses

The results of the UVMR analyses passed Cochran's Q test (Tables 2, 3). With the exception of the GD-NPDR analysis, all UVMR analyses passed the MR-Egger intercept test (Tables 2, 3). Leave-one-out analyses confirmed that the causality observed in the UVMR analyses was not driven by any single SNP (Supplementary Figures 4–6). Additionally, the MR Steiger directionality test results supported the accuracy of our causal direction estimates (Supplementary Tables 1–12), further validating the robustness of the UVMR findings. The statistical power of the UVMR studies, as calculated using the web tool, was all greater than 0.9. Although the heterogeneity test ($P < 0.05$) indicated some heterogeneity in the MVMR analyses, no horizontal pleiotropy was detected ($P > 0.05$). The meta-analysis showed heterogeneity in both the overall and partial subgroup analyses, therefore, the random-effects model was used to combine the effect sizes.

3.2 Univariable Mendelian randomization

In populations of European ancestry (EA), IVW analyses indicated a potential causal relationship between genetically

TABLE 2 MR results of TOS on DBR/DR/NPDR/PDR.

| Exposures | Outcomes | Method | NSNP | OR | 95%CI | P value | Cochrane's Q | MR-Egger test | |
|-----------|----------|----------|------|------|-----------|---------|--------------|---------------|---------|
| | | | | | | | p-value | Intercept | p-value |
| TOS | DBR | MR Egger | 32 | 1.39 | 1.06-1.82 | 0.03 | 0.10 | -0.02 | 0.27 |
| | | WM | 32 | 1.09 | 0.96-1.22 | 0.18 | | | |
| | | IVW | 32 | 1.19 | 1.09-1.31 | 0.00009 | 0.09 | | |
| | DR | MR Egger | 27 | 1.19 | 1.00-1.40 | 0.05 | 0.11 | -0.01 | 0.34 |
| | | WM | 27 | 1.07 | 1.00-1.15 | 0.05 | | | |
| | | IVW | 27 | 1.10 | 1.04-1.16 | 0.001 | 0.11 | | |
| | NPDR | MR Egger | 37 | 1.58 | 1.04-2.42 | 0.0396 | 0.52 | -0.05 | 0.16 |
| | | WM | 37 | 1.20 | 0.96-1.50 | 0.0933 | | | |
| | | IVW | 37 | 1.19 | 1.03-1.37 | 0.0218 | 0.47 | | |
| | PDR | MR Egger | 32 | 1.10 | 0.97-1.25 | 0.14 | 0.64 | 0.00 | 0.94 |
| | | WM | 32 | 1.06 | 1.00-1.13 | 0.06 | | | |
| | | IVW | 32 | 1.10 | 1.05-1.15 | 2.8E-05 | 0.69 | | |

predicted TOS and DBR/DR/NPDR/PDR (Table 2). However, WM and MR-Egger did not provide similar evidence in the TOS-DBR/DR/NPDR/PDR analyses ($P>0.025$). Notably, the OR values from both WM and MR-Egger were all greater than 1 (Table 2), and the scatter plot suggested a positive correlation between TOS and DBR/DR/NPDR/PDR (Supplementary Figure 7), indicating consistency in the directionality of the results. Sensitivity analyses showed no evidence of bias, supporting the validity of the findings. Similarly, in the HPT-DR analyses, IVW indicated that genetically predicted HPT was potentially causally related to DBR/DR/NPDR/PDR

(Table 3). In the MR results for HPT-DR/PDR, MR-Egger did not provide supporting evidence ($P>0.025$). However, WM provided consistent estimates, and the ORs from MR-Egger and WM were all greater than 1 (Table 3). The scatter plot further demonstrated a potential positive correlation between HPT and DR/PDR (Supplementary Figures 8B, D), which aligns with our overall interpretation of the MR results.

In contrast to the previous findings, IVW, WM, and MR-Egger all indicated a potential causal relationship between genetically predicted GD and DR/DBR/NPDR/PDR (Table 4).

TABLE 3 MR results of HPT on DBR/DR/NPDR/PDR.

| Exposures | Outcomes | Method | NSNP | OR | 95%CI | P value | Cochrane's Q | MR-Egger test | |
|-----------|----------|----------|------|------|-----------|---------|--------------|---------------|---------|
| | | | | | | | p-value | Intercept | p-value |
| HPT | DBR | MR Egger | 152 | 1.49 | 1.21-1.84 | 0.0002 | 0.73 | -0.0026 | 0.73 |
| | | WM | 152 | 1.38 | 1.23-1.54 | 1.8E-08 | | | |
| | | IVW | 152 | 1.44 | 1.34-1.55 | 8.4E-24 | 0.75 | | |
| | DR | MR Egger | 144 | 1.09 | 0.97-1.23 | 0.16 | 0.63 | 0.01 | 0.14 |
| | | WM | 144 | 1.14 | 1.07-1.22 | 4.2E-05 | | | |
| | | IVW | 144 | 1.19 | 1.14-1.24 | 6.4E-16 | 0.61 | | |
| | NPDR | MR Egger | 179 | 2.22 | 1.50-3.29 | 9.0E-05 | 0.83 | -0.02 | 0.09 |
| | | WM | 179 | 1.58 | 1.29-1.94 | 1.2E-05 | | | |
| | | IVW | 179 | 1.62 | 1.42-1.86 | 3.1E-12 | 0.80 | | |
| | PDR | MR Egger | 175 | 1.10 | 0.99-1.23 | 0.09 | 0.41 | 0.00 | 0.42 |
| | | WM | 175 | 1.13 | 1.07-1.21 | 4.5E-05 | | | |
| | | IVW | 175 | 1.15 | 1.11-1.19 | 7.6E-13 | 0.42 | | |

TABLE 4 MR results of GD on DBR/DR/NPDR/PDR.

| Exposures | Outcomes | Method | NSNP | OR | 95%CI | P value | Cochrane's Q | MR-Egger test | |
|-----------|----------|----------|------|------|-----------|---------|--------------|---------------|---------|
| | | | | | | | p-value | Intercept | p-value |
| GD | DBR | MR Egger | 11 | 1.59 | 1.3-1.94 | 0.001 | 0.52 | -0.02 | 0.51 |
| | | WM | 11 | 1.48 | 1.32-1.66 | 3.7E-11 | | | |
| | | IVW | 11 | 1.49 | 1.38-1.62 | 2.7E-23 | 0.57 | | |
| | DR | MR Egger | 11 | 1.29 | 1.16-1.44 | 0.001 | 0.79 | -0.01 | 0.66 |
| | | WM | 11 | 1.26 | 1.19-1.34 | 1.5E-13 | | | |
| | | IVW | 11 | 1.26 | 1.20-1.32 | 1.2E-24 | 0.84 | | |
| | NPDR | MR Egger | 16 | 2.47 | 1.77-3.46 | 0.0001 | 0.60 | -0.15 | 0.01 |
| | | WM | 16 | 1.51 | 1.23-1.84 | 5.6E-05 | | | |
| | | IVW | 16 | 1.50 | 1.28-1.76 | 4.2E-07 | 0.11 | | |
| | PDR | MR Egger | 17 | 1.24 | 1.11-1.38 | 0.0013 | 0.11 | -0.02 | 0.19 |
| | | WM | 17 | 1.17 | 1.11-1.24 | 6.4E-09 | | | |
| | | IVW | 17 | 1.16 | 1.11-1.21 | 1.1E-10 | 0.07 | | |

3.3 Multivariable Mendelian randomization

When accounting for GD and/or RA, both IVW and MR-Egger analyses suggested that genetically predicted TOS did not significantly increase the risk of DBR/DR/NPDR/PDR, though the results were not statistically significant (Tables 5, 6).

When RA was considered, both IVW and MR-Egger analyses suggested that genetically predicted HPT could still increase the risk of developing DR (DR/NPDR) (Tables 5, 6). However, for DBR, genetically predicted HPT was found to be non-significant after adjusting for RA in both IVW and MR-Egger analyses (Tables 5, 6). While IVW analysis indicated that genetically predicted HPT was not

TABLE 5 MVMR results (IVW) of TD on DBR/DR/NPDR/PDR.

| Items | Model 1 | | | Model 2 | | |
|-------|---------|--------------|---------|---------|-------------|---------|
| | β | 95%CI | P-value | β | 95%CI | P-value |
| TOS | | | | | | |
| DBR | -0.56 | -1.24, 0.12 | 0.104 | -0.05 | -0.71, 0.61 | 0.873 |
| DR | -0.31 | -0.74, 0.12 | 0.153 | -0.05 | -0.48, 0.39 | 0.836 |
| NPDR | -0.54 | -1.32, 0.23 | 0.17 | -0.02 | -0.71, 0.68 | 0.96 |
| PDR | -0.10 | -0.38, 0.19 | 0.515 | 0.06 | -0.24, 0.37 | 0.681 |
| HPT | | | | | | |
| DBR | 0.16 | -0.02, 0.35 | 0.088 | – | – | – |
| DR | 0.18 | 0.06, 0.30 | 0.005 | – | – | – |
| NPDR | 0.29 | 0.07, 0.52 | 0.012 | – | – | – |
| PDR | 0.09 | -0.001, 0.18 | 0.052 | – | – | – |
| GD | | | | | | |
| DBR | 0.79 | 0.27, 1.30 | 0.003 | 0.23 | -0.31, 0.76 | 0.406 |
| DR | 0.42 | 0.10, 0.74 | 0.011 | 0.13 | -0.23, 0.48 | 0.476 |
| NPDR | 0.85 | 0.26, 1.44 | 0.005 | 0.23 | -0.33, 0.79 | 0.412 |
| PDR | 0.21 | -0.01, 0.42 | 0.062 | 0.02 | -0.23, 0.26 | 0.887 |

Model 1^{TOS} adjusted for: GD; Model 1^{HPT} adjusted for: RA; Model 1^{GD} adjusted for: TOS. Model 2^{TOS} adjusted for: GD and RA; Model 2^{GD} adjusted for: TOS and RA.

TABLE 6 MVMR results (MR-egger) of TD on DR (DBR/DR/NPDR/PDR).

| Items | Model 1 | | | Model 2 | | |
|-------|---------|-------------|---------|---------|-------------|---------|
| | β | 95%CI | P-value | β | 95%CI | P-value |
| TOS | | | | | | |
| DBR | -0.58 | -1.51, 0.36 | 0.229 | 0.14 | -0.62, 0.89 | 0.718 |
| DR | -0.27 | -0.85, 0.31 | 0.362 | 0.06 | -0.44, 0.57 | 0.810 |
| NPDR | -0.11 | -1.18, 0.96 | 0.838 | 0.19 | -0.62, 0.99 | 0.646 |
| PDR | -0.02 | -0.40, 0.37 | 0.931 | 0.18 | -0.17, 0.53 | 0.318 |
| HPT | | | | | | |
| DBR | 0.35 | -0.05, 0.74 | 0.087 | – | – | – |
| DR | 0.51 | 0.23, 0.78 | 0.000 | – | – | – |
| NPDR | 0.56 | 0.08, 1.03 | 0.022 | – | – | – |
| PDR | 0.31 | 0.12, 0.50 | 0.002 | – | – | – |
| GD | | | | | | |
| DBR | 0.79 | 0.27, 1.31 | 0.003 | 0.27 | -0.27, 0.81 | 0.329 |
| DR | 0.42 | 0.09, 0.74 | 0.012 | 0.15 | -0.21, 0.51 | 0.408 |
| NPDR | 0.87 | 0.28, 1.45 | 0.004 | 0.27 | -0.29, 0.84 | 0.343 |
| PDR | 0.21 | -0.01, 0.42 | 0.063 | 0.04 | -0.21, 0.29 | 0.747 |

Model 1^{TOS} adjusted for: GD; Model 1^{HPT} adjusted for: RA; Model 1^{GD} adjusted for: TOS. Model 2^{TOS} adjusted for: GD and RA; Model 2^{GD} adjusted for: TOS and RA.

significantly associated with PDR after adjusting for RA (Table 5), MR-Egger analysis suggested that genetically predicted HPT could still increase the risk of PDR (Table 6), with both MR-Egger and IVW analyses showing a positive association. Therefore, the study concludes that HPT may still increase the risk of PDR after adjusting for RA.

When considering TOS, both IVW and MR-Egger analyses indicated that genetically predicted GD could still increase the risk of developing DBR/DR/NPDR (Tables 5, 6). However, when both TOS and RA were considered, genetically predicted GD was no longer associated with DBR/DR/NPDR/PDR (Tables 5, 6).

3.4 Meta-analysis

In UVMR analysis, this study assessed the effect of TD on diabetic retinopathy across its four stages. A meta-analysis, conducted using R software, summarized the overall impact of TD on DBR/DR/NPDR/PDR based on UVMR results. As shown in Figure 2, the effect of GD and HPT on DBR/DR/NPDR/PDR was greater than that of TOS, with the difference being statistically significant (P<0.01). Although the meta-analysis showed significance in both subgroup and overall analyses (P<0.01), substantial heterogeneity was noted in the HPT/GD subgroup as well as in the overall estimates.

4 Discussion

The two-sample UVMR study demonstrated that genetically predicted TD, particularly HPT, can increase the risk of diabetic

retinopathy in patients with DM, with the robustness of the analytical procedure confirmed. In MVMR analysis, no significant association was found between TOS and diabetic retinopathy after adjusting for GD. However, GD remained significantly associated with diabetic retinopathy, except for GD-PDR, after adjusting for TOS. This observed difference is thought-provoking. The study by Lin D et al. (6) provides a plausible explanation for the discrepancy. They found that bovine TSH (b-TSH) promotes glucose-induced mitochondrial apoptosis in human peripapillary retinal cells, whereas blocking TSHR significantly inhibits mitochondrial apoptosis in a high-glucose environment (6). In thyrotoxicosis, elevated levels of thyroxine and triiodothyronine inhibit TSH production via negative feedback on the hypothalamic-pituitary-thyroid axis. In contrast, in GD, thyroid-stimulating antibodies (TSAb) mimic the effects of TSH by binding to TSHR, which may explain the observed difference. In contrast, hypothyroidism involves positive feedback activation of the hypothalamic-pituitary-thyroid axis. Both univariate and multivariate MR analyses indicated a significant association between HPT and diabetic retinopathy, aligning with a prior meta-analysis of observational studies that reported a significant correlation between hypothyroidism and diabetic retinopathy (OR=2.13, 95% CI=1.41–3.23, P<0.001) (25). A subsequent meta-analysis reached a similar conclusion (26). Additionally, a case-control study demonstrated a significant association between hypothyroidism and an increased prevalence of diabetic retinopathy in DM patients, even after adjusting for age, gender, diabetes duration, glycosylated hemoglobin, BMI, hypertension, and LDL cholesterol (27). Furthermore, higher thyrotropic hormone levels have been

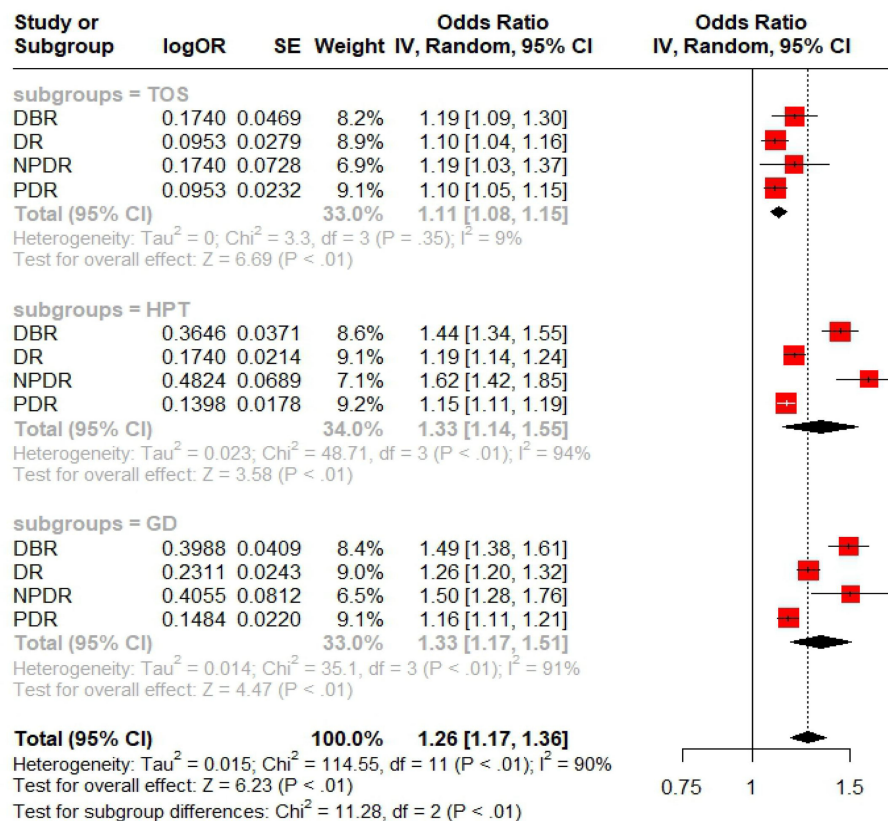


FIGURE 2
Forest plots of Meta analysis on TD-DBR/DR/NPDR/PDR.

linked to narrower retinal arterioles and lower arteriovenous indices in patients with hypothyroidism compared to those with normal thyroid function (28). In the pooled analysis, we observed that the overall effect of HPT on diabetic retinopathy was greater than that of TOS or GD. While our findings, along with previous studies, seem to implicate TSH as the key factor driving the increased risk of diabetic retinopathy associated with TD. But is this really the case? A retrospective study in a Caucasian population, for instance, found no significant association between TSH levels or hypothyroidism and diabetic retinopathy (29). Moreover, UVMR analysis suggested the presence of horizontal pleiotropy in GD-NPDR, but after adjusting for TOS, the pleiotropy disappeared, and both MR analyses indicated that GD could increase the risk of developing NPDR. This result seems to imply that thyrotoxicosis alone plays a role in the GD-NPDR axis. However, an MR study on thyroid hormones and microvascular complications in diabetes suggested that elevated thyroid hormone levels do not increase the risk of developing DR (30). This may be due to the fact that the study, when selecting IVs, focused solely on hormone levels and overlooked the disease itself. Additionally, variations in the sources of exposure-related IVs may have contributed to the differences in the analytical results.

Diabetic retinopathy constitutes a significant microvascular complication of diabetes (1), wherein microvascular injury plays a pivotal role in its pathogenesis. Various factors contribute to

microvascular injury, including hypoxia, endothelial damage, oxidative stress, inflammatory response, and fibrovascular proliferation. In individuals with TD, both TOS and HPT are associated with elevated serum C-reactive protein levels, indicating a heightened systemic inflammatory response (5). Furthermore, conditions such as GD and Hashimoto thyroiditis can all result in increased serum VEGF levels (31). Individuals with HPT exhibit increased activity of plasma malondialdehyde, a specific indicator of oxidative stress levels (5). Moreover, thyroid hormones play a significant role in the normal development of retinal cellular structures, as evidenced by researchers discovering low levels of sirtuin2 in the retinal ganglion cell layer of hypothyroid mice (32). Therefore, the impact of TD on diabetic retinopathy may not solely be attributed to the level of TSH and thyroid hormone but rather the combined influence of numerous factors.

Compared to observational studies, the MR study can significantly mitigate confounding effects. However, the current MR design possesses both its own strengths and inherent limitations, primarily stemming from three essential assumptions that must be satisfied. Firstly, the correlation assumption was supported by the genome-wide significance level ($P < 5e-08$) in the GWAS. Additionally, the UVMR studies are less susceptible to weak instrument bias, as we exclusively incorporated SNPs with substantial instrumental strength ($F > 10$) while excluding those in linkage disequilibrium. Nevertheless, MVMR analyses exclusively

considered SNPs with genome-wide significance levels ($P < 5 \times 10^{-8}$) and eliminated those in linkage disequilibrium. Secondly, the MR-Egger Intercept evaluated the horizontal pleiotropy in the UVMR analysis, indicating an absence of horizontal pleiotropy. However, during confounder screening, we identified RA as potentially influencing the causal chain of TD on diabetic retinopathy. Consequently, confounding was addressed through the MVMR analysis. Nevertheless, violations may persist, and alternative pleiotropic pathways from IVs to diabetic retinopathy remain unexplored in this study, necessitating investigation in future research. Thirdly, the genetic variant data predominantly relied on GWAS from European ancestry. The approach has the drawback of lacking the ability to fully represent the entire population. However, it offers the advantage of minimizing the risk of population-based confounding. Additionally, heterogeneity was observed in the MVMR analysis, but we employed the IVW with a random-effects model to evaluate the MVMR results. Lastly, given the presence of heterogeneity, the meta-analysis utilized a random-effects model to amalgamate effect sizes.

5 Conclusion

In conclusion, our study demonstrated a significant correlation between TD and diabetic retinopathy, with a particularly strong association for HPT. In the HPT-DBR/DR/NPDR/PDR MVMR analysis, HPT remained significantly associated with DBR/DR/NPDR/PDR even after adjusting for RA, suggesting that the impact of HPT on diabetic retinopathy is independent of RA.

Data availability statement

The original contributions presented in the study are publicly available. This data can be found here: <https://github.com/ling-98/TD-DR-MR-analyses.git>.

Author contributions

JO: Writing – review & editing, Writing – original draft, Software, Methodology, Investigation, Formal analysis, Data

curation, Conceptualization. LZ: Writing – review & editing, Writing – original draft, Software, Methodology, Investigation, Formal analysis, Data curation, Conceptualization. QW: Writing – review & editing, Writing – original draft. WY: Writing – review & editing, Writing – original draft.

Funding

The author(s) declare that no financial support was received for the research, authorship, and/or publication of this article.

Acknowledgments

We sincerely appreciate for all the GWAS data provided by the FinnGen.

Conflict of interest

The authors declare that the research was conducted in the absence of any commercial or financial relationships that could be construed as a potential conflict of interest.

Publisher's note

All claims expressed in this article are solely those of the authors and do not necessarily represent those of their affiliated organizations, or those of the publisher, the editors and the reviewers. Any product that may be evaluated in this article, or claim that may be made by its manufacturer, is not guaranteed or endorsed by the publisher.

Supplementary material

The Supplementary Material for this article can be found online at: <https://www.frontiersin.org/articles/10.3389/fendo.2024.1374254/full#supplementary-material>

References

- Cheung N, Mitchell P, Wong TY. Diabetic retinopathy. *Lancet*. (2010) 376:124–36. doi: 10.1016/S0140-6736(09)62124-3
- Yau JW, Rogers SL, Kawasaki R, Lamoureux EL, Kowalski JW, Bek T, et al. Global prevalence and major risk factors of diabetic retinopathy. *Diabetes Care*. (2012) 35:556–64. doi: 10.2337/dc11-1909
- Tan TE, Wong TY. Diabetic retinopathy: Looking forward to 2030. *Front Endocrinol (Lausanne)*. (2023) 13:1077669. doi: 10.3389/fendo.2022.1077669
- Prinz N, Tittel SR, Bachran R, Birnbacher R, Brückel J, Dunstheimer D, et al. Characteristics of patients with type 1 diabetes and additional autoimmune disease in the DPV registry. *J Clin Endocrinol Metab*. (2021) 106:e3381–9. doi: 10.1210/clinem/dgab376
- Stefanowicz-Rutkowska MM, Baranowska-Jurkun A, Matuszewski W, Bandurska-Stankiewicz EM. Thyroid dysfunction in patients with diabetic retinopathy. *Endokrynol Pol*. (2020) 71:176–83. doi: 10.5603/EP.a2020.0013
- Lin D, Qin R, Guo L. Thyroid stimulating hormone aggravates diabetic retinopathy through the mitochondrial apoptotic pathway. *J Cell Physiol*. (2022) 237:868–80. doi: 10.1002/jcp.30563
- Burgess S, Timpson NJ, Ebrahim S, Davey Smith G. Mendelian randomization: where are we now and where are we going? *Int J Epidemiol*. (2015) 44:379–88. doi: 10.1093/ije/dyv108
- Davies NM, Holmes MV, Davey Smith G. Reading Mendelian randomisation studies: a guide, glossary, and checklist for clinicians. *BMJ*. (2018) 362:k601. doi: 10.1136/bmj.k601

9. Xian W, Wu D, Liu B, Hong S, Huo Z, Xiao H, et al. Graves disease and inflammatory bowel disease: A bidirectional Mendelian randomization. *J Clin Endocrinol Metab.* (2023) 108:1075–83. doi: 10.1210/clinem/dgac683
10. Ishigaki K, Akiyama M, Kanai M, Takahashi A, Kawakami E, Sugishita H, et al. Large-scale genome-wide association study in a Japanese population identifies novel susceptibility loci across different diseases. *Nat Genet.* (2020) 52:669–79. doi: 10.1038/s41588-020-0640-3
11. Skrivankova VW, Richmond RC, Woolf BAR, Davies NM, Swanson SA, VanderWeele TJ, et al. Strengthening the reporting of observational studies in epidemiology using mendelian randomisation (STROBE-MR): explanation and elaboration. *BMJ.* (2021) 375:n2233. doi: 10.1136/bmj.n2233
12. Burgess S, Thompson SG, CRP CHD Genetics Collaboration. Avoiding bias from weak instruments in Mendelian randomization studies. *Int J Epidemiol.* (2011) 40:755–64. doi: 10.1093/ije/dyr036
13. Magnus MC, Miliku K, Bauer A, Engel SM, Felix JF, Jaddoe VVW, et al. Vitamin D and risk of pregnancy related hypertensive disorders: mendelian randomisation study. *BMJ.* (2018) 361:k2167. doi: 10.1136/bmj.k2167
14. Zhou Z, Zhang H, Chen K, Liu C. Iron status and obesity-related traits: A two-sample bidirectional Mendelian randomization study. *Front Endocrinol (Lausanne).* (2023) 14:985338. doi: 10.3389/fendo.2023.985338
15. Liang Z, Zhao L, Lou Y, Liu S. Causal effects of circulating lipids and lipid-lowering drugs on the risk of epilepsy: a two-sample Mendelian randomization study. *QJM.* (2023) 116:421–8. doi: 10.1093/qjmed/hcad048
16. Bowden J, Del Greco MF, Minelli C, Davey Smith G, Sheehan N, Thompson J. A framework for the investigation of pleiotropy in two-sample summary data Mendelian randomization. *Stat Med.* (2017) 36:1783–802. doi: 10.1002/sim.7221
17. Bowden J, Davey Smith G, Haycock PC, Burgess S. Consistent estimation in Mendelian randomization with some invalid instruments using a weighted median estimator. *Genet Epidemiol.* (2016) 40:304–14. doi: 10.1002/gepi.21965
18. Burgess S, Thompson SG. Interpreting findings from Mendelian randomization using the MR-Egger method. *Eur J Epidemiol.* (2017) 32:377–89. doi: 10.1007/s10654-017-0255-x
19. Zheng C, Wei X, Cao X. The causal effect of obesity on diabetic retinopathy: A two-sample Mendelian randomization study. *Front Endocrinol (Lausanne).* (2023) 14:1108731. doi: 10.3389/fendo.2023.1108731
20. Hemani G, Zheng J, Elsworth B, Wade KH, Haberland V, Baird D, et al. The MR-Base platform supports systematic causal inference across the human genome. *Elife.* (2018) 7:e34408. doi: 10.7554/eLife.34408
21. Bowden J, Spiller W, Del Greco MF, Sheehan N, Thompson J, Minelli C, et al. Improving the visualization, interpretation and analysis of two-sample summary data Mendelian randomization via the Radial plot and Radial regression. *Int J Epidemiol.* (2018) 47:1264–78. doi: 10.1093/ije/dyy101
22. Bartels CM, Wong JC, Johnson SL, Thorpe CT, Barney NP, Sheibani N, et al. Rheumatoid arthritis and the prevalence of diabetic retinopathy. *Rheumatol (Oxford).* (2015) 54:1415–9. doi: 10.1093/rheumatology/kev012
23. Powell ED, Field RA. Diabetic retinopathy and rheumatoid arthritis. *Lancet.* (1964) 2:17–8. doi: 10.1016/s0140-6736(64)90008-x
24. Conigliaro P, D'Antonio A, Pinto S, Chimenti MS, Triggianese P, Rotondi M, et al. Autoimmune thyroid disorders and rheumatoid arthritis: A bidirectional interplay. *Autoimmun Rev.* (2020) 19:102529. doi: 10.1016/j.autrev.2020.102529
25. Wu J, Yue S, Geng J, Liu L, Teng W, Liu L, et al. Relationship between diabetic retinopathy and subclinical hypothyroidism: a meta-analysis. *Sci Rep.* (2015) 5:12212. doi: 10.1038/srep12212
26. Han C, He X, Xia X, Li Y, Shi X, Shan Z, et al. Subclinical hypothyroidism and type 2 diabetes: A systematic review and meta-analysis. *PLoS One.* (2015) 10:e0135233. doi: 10.1371/journal.pone.0135233
27. Yang JK, Liu W, Shi J, Li YB. An association between subclinical hypothyroidism and sight-threatening diabetic retinopathy in type 2 diabetic patients. *Diabetes Care.* (2010) 33:1018–20. doi: 10.2337/dc09-1784
28. Ittermann T, Dörr M, Völzke H, Tost F, Lehmphul I, Köhrle J, et al. High serum thyrotropin levels are associated with retinal arteriolar narrowing in the general population. *Thyroid.* (2014) 24:1473–8. doi: 10.1089/thy.2014.0190
29. Ramis JN, Artigas CF, Santiago MA, Mañes FJ, Canonge RS, Comas LM. Is there a relationship between TSH levels and diabetic retinopathy in the Caucasian population? *Diabetes Res Clin Pract.* (2012) 97:e45–7. doi: 10.1016/j.diabres.2012.05.015
30. Li H, Li M, Dong S, Zhang S, Dong A, Zhang M. Assessment of the association between genetic factors regulating thyroid function and microvascular complications in diabetes: A two-sample Mendelian randomization study in the European population. *Front Endocrinol (Lausanne).* (2023) 14:1126339. doi: 10.3389/fendo.2023.1126339
31. Ahmed A, Waris A, Naheed A, Anjum A. Diabetic retinopathy and its correlation with thyroid profile and anti thyroid antibodies. *IOSR-JDMS.* (2017) 16:96–8. doi: 10.9790/0853-1601079698
32. Kocaturk T, Ergin K, Cesur G, Evlicoglu GE, Cakmak H. The effect of methimazole-induced postnatal hypothyroidism on the retinal maturation and on the Sirtuin 2 level. *Cutan Ocul Toxicol.* (2016) 35:36–40. doi: 10.3109/15569527.2015.1007509



OPEN ACCESS

EDITED BY

Mohd Imtiaz Nawaz,
King Saud University, Saudi Arabia

REVIEWED BY

Ricardo Adrian Nugraha,
Airlangga University, Indonesia
Salvatore Di Lauro,
Hospital Clínico Universitario de Valladolid,
Spain

*CORRESPONDENCE

Zhentao Zhu

✉ jshayyzt@163.com

Weihua Yang

✉ benben0606@139.com

Gaoen Ma

✉ 15757826611@163.com

†These authors have contributed
equally to this work and share
first authorship

RECEIVED 26 May 2024

ACCEPTED 14 March 2025

PUBLISHED 16 April 2025

CITATION

Zhang Q, Gong D, Huang M, Zhu Z,
Yang W and Ma G (2025) Recent
advances and applications of optical
coherence tomography angiography
in diabetic retinopathy.
Front. Endocrinol. 16:1438739.
doi: 10.3389/fendo.2025.1438739

COPYRIGHT

© 2025 Zhang, Gong, Huang, Zhu, Yang and
Ma. This is an open-access article distributed
under the terms of the [Creative Commons
Attribution License \(CC BY\)](#). The use,
distribution or reproduction in other forums
is permitted, provided the original author(s)
and the copyright owner(s) are credited and
that the original publication in this journal is
cited, in accordance with accepted academic
practice. No use, distribution or reproduction
is permitted which does not comply with
these terms.

Recent advances and applications of optical coherence tomography angiography in diabetic retinopathy

Qing Zhang^{1,2†}, Di Gong^{3†}, Manman Huang⁴, Zhentao Zhu^{5*},
Weihua Yang^{3*} and Gaoen Ma^{1,2*}

¹Department of Ophthalmology, The Third Affiliated Hospital of Xinxiang Medical University, Xinxiang Medical University, Xinxiang, Henan, China, ²Department of Ophthalmology, The First Affiliated Hospital of Hainan Medical University, Haikou, Hainan, China, ³Shenzhen Eye Hospital, Shenzhen Eye Medical Center, Southern Medical University, Shenzhen, Guangdong, China, ⁴Zhengzhou University People's Hospital, Henan Eye Institute, Henan Eye Hospital, Henan Provincial People's Hospital, Zhengzhou, Henan, China, ⁵Department of Ophthalmology, Huaian Hospital of Huaian City, Huaian, Jiangsu, China

Introduction: Optical coherence tomography angiography (OCTA), a noninvasive imaging technique, is increasingly used in managing ophthalmic diseases like diabetic retinopathy (DR). This review examines OCTA's imaging principles, its utility in detecting DR lesions, and its diagnostic advantages over fundus fluorescein angiography (FFA).

Methods: We systematically analyzed 75 articles (2015–2024) from the Web of Science Core Collection, focusing on OCTA's technical principles, clinical applications in DR diagnosis, and its use in diabetes mellitus (DM) without DR and prediabetes. The use of artificial intelligence (AI) in OCTA image analysis for DR severity evaluation was investigated.

Results: OCTA effectively identifies DR lesions and detects early vascular abnormalities in DM and prediabetes, surpassing FFA in noninvasiveness and resolution. AI integration enhances OCTA's capability to diagnose, evaluate, and predict DR progression.

Discussion: OCTA offers significant clinical value in early DR detection and monitoring. Its synergy with AI holds promise for refining diagnostic precision and expanding predictive applications, positioning OCTA as a transformative tool in future ophthalmic practice.

KEYWORDS

optical coherence tomography angiography, diabetic retinopathy, grading, lesion recognition, artificial intelligence

1 Background

Optical coherence tomography angiography (OCTA) is a noninvasive imaging technique that captures detailed images of the retinal and choroidal microvasculature. This method exploits the reflectivity of laser light from the surface of moving red blood cells. Although OCTA cannot directly display the vascular structures, it can detect the presence of blood flow in different regions and layers of the retina (1). Optical coherence tomography (OCT), another retinal imaging technique, uses multiple A-scans to generate a B-scan, providing valuable information on the retina's structural characteristics in a cross-sectional view (2). OCTA detects and compares changes in blood flow by taking multiple images at different time points, rather than directly measuring blood flow velocity. These time-series images enable OCTA to distinguish regional variations in different blood flow rates (3).

Diabetic retinopathy (DR) is the most common and significant ocular complication among individuals with diabetes. Approximately one-third of diabetics show signs of DR, with some experiencing vision-threatening retinopathy or macular edema (4). DR results from diabetes-related damage to the eye's tiny blood vessels and can progress from non-proliferative diabetic retinopathy (NPDR) to proliferative diabetic retinopathy (PDR). Diabetic macular edema (DME), characterized by increased blood vessel permeability, thickening, and hard exudates in the macula, frequently occurs regardless of the DR stage (5, 6). OCTA, an emerging imaging modality, enables the detection of effects in various layers of the retina in DR, the impact of different treatment modalities on retinal microvasculature and blood flow, and the correlation between functional levels and anatomical and vascular indicators. As a widely used method, OCTA aids in diagnosing DR and its complications, assisting in DR grading and early detection, particularly in diabetic patients who have not yet developed the condition (7). OCTA's imaging modality can reveal more profound changes that ophthalmologists' funduscopy may not detect, helping predict and detect pre-diabetic retinopathy stage changes. In clinical applications and DR research, OCTA can identify promising and sensitive biomarkers under different modalities, offering new insights into the early-stage pathophysiology and treatment and screening of DR (8).

2 History of OCTA

Since its introduction in 2014, OCTA has gained significant traction in clinical practice and has witnessed extensive utilization for various ocular diseases (9). The two most commonly employed OCTA devices are Spectral-domain OCTA (SD-OCTA) and Swept-source OCTA (SS-OCTA), both utilizing Fourier domain detection techniques. However, in SD-OCTA instruments, a broadband near-infrared superluminescent diode serves as the light source, currently

operating at a center wavelength of approximately 840 nm, with a spectrometer as the detector. With the advancement of the SD-OCTA device, the clinical application of the prototype 1.0 micrometer SD-OCTA has also been reported. In contrast, SS-OCTA instruments adopt a tunable swept laser with a central wavelength of around 1050 nm and a single photodiode detector (10). SS-OCTA offers the advantage of faster scanning speed compared to SD-OCTA, enabling denser scan patterns and wider scan areas within a given acquisition time. Additionally, the use of longer wavelength in SS-OCTA leads to reduced sensitivity roll-off and improved light penetration through the retinal pigment epithelium (RPE) for better detection of signals from deeper layers. Moreover, the longer wavelength used in SS-OCTA ensures greater safety for the eye, allowing for higher laser power to be employed. The combination of higher power and reduced sensitivity roll-off enhances the ability to detect weaker signals from deeper layers, thus overcoming the barrier posed by the RPE in SS-OCT systems (11). The OCTA algorithm segments the resulting image (ranging from 3 mm²–12 mm²) into four zones, as per the standard: the superficial retinal plexus, deep retinal plexus, outer retina, and choriocapillaris. When applied to an optical disk, this encompasses the entire depth of the disk (12). While ultra-wide-field OCTA (UWF-OCTA) images have been developed and employed in clinical research, their practical clinical application may be limited due to factors such as longer acquisition time and image quality (13).

3 Methods of literature retrieval

This paper aimed to present an overview of OCTA for DR applications. We obtained all the literature from the Web of Science Core Collection (WoSCC), a leading global database of scholarly information founded in 1985. The WoSCC contains both authoritative and influential journals from a wide range of disciplines. We used the WoS core set of journals indexed to the Science Citation Index and combined titles and subjects to search for subject terms to maximize accuracy while maintaining search sensitivity. Our search formula was as follows: TS= ("Optical coherence tomography angiography" and "diabetic retinopathy") OR ("OCTA" and "diabetic retinopathy") OR ("Optical coherence tomography angiography" and "DR") OR ("OCTA" and "DR") OR TI= ("Optical coherence tomography angiography" and "diabetic retinopathy") OR ("OCTA" and "diabetic retinopathy") OR ("Optical coherence tomography angiography" and "DR") OR ("OCTA" and "DR") AND (DT= ("ARTICLE") AND LA= ("ENGLISH")). Within our search formula, TS=Topic, TI=Title, DT=Document type, LA=Language. We restricted the documents to essays and review papers, limited the language to English, and excluded documents outside the year of the OCTA application.

A search of literatures revealed a total of 885 articles published in the field over the last decade. 75 articles were mentioned in this review after being screened by ophthalmic

imaging specialists and retinal disease specialists. In this review, many research directions within the field of OCTA in DR applications are mentioned. The Literature Search and Review Roadmap is shown in Figure 1.

4 Basic imaging features of OCTA

OCTA can produce a signal that reveals the impact of motor blood flow on retinal and choroidal vessels, providing a clear view of the superficial capillary network (SCN) in the ganglion cell layer (GCL), deep capillary network (DCN), and choriocapillaris (CC) in the outer plexiform layer. With its high sensitivity and specificity, OCTA effectively detects neovascularization even in the presence of blood flow (14). OCTA enables the detection of blood vessel shape and distribution in various retina regions, the mean artery count is 7.0 ± 1.2 , and the mean vein count is 6.9 ± 1.2 in the $3 \text{ mm} \times 3 \text{ mm}$ retina OCTA (15, 16).

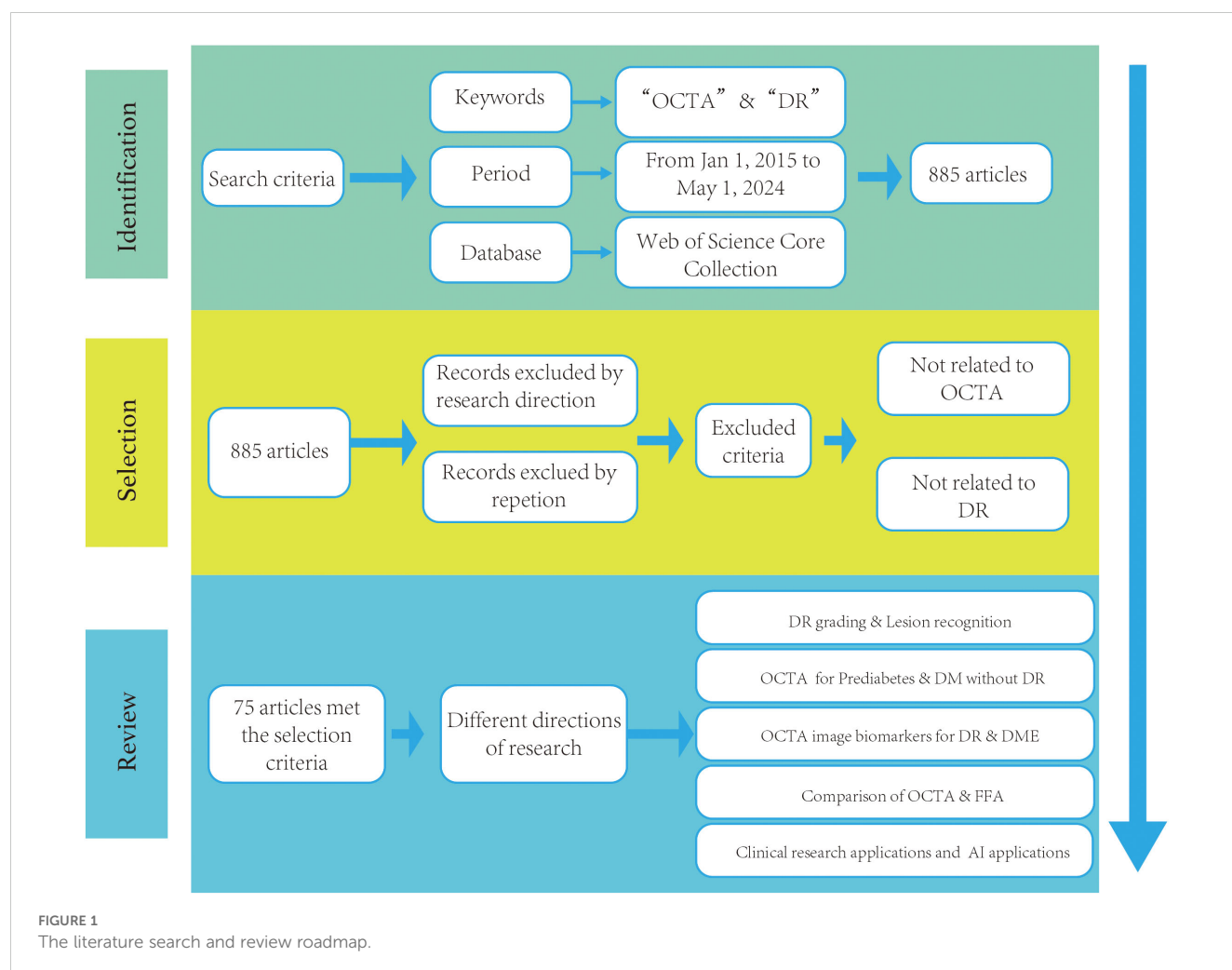
OCTA's capabilities extend beyond the detection of neovascularization, as it also allows for the measurement of the foveal avascular zone (FAZ) size and identification of areas without blood flow in patients who exhibit no visible clinical symptoms. Additionally,

OCTA facilitates a more detailed examination of the choroid's perfusion status, identification of choroidal capillaries, and detection of neovascular complexes in certain non-exudative lesions (17).

5 The application of OCTA in DR

5.1 DR grading

DR, a potentially vision-threatening condition, poses three primary threats to visual health: vitreous hemorrhages resulting from neovascularization, retinal detachment that can cause substantial vision loss, and localized damage to the macula or fovea, leading to the loss of central vision (4). Historically, the classification and grading of DR severity have been based on visible signs of increasing severity under the color fundus photograph, progressing from no retinopathy to non-proliferative or pre-proliferative stages, and finally to advanced proliferative disease. The grading of DR is crucial in guiding and preventing clinical management of the disease. Precise DR grading can assist patients in better managing the condition, thereby reducing the risk of vision loss. However, this grading system may not accurately represent functionally severe disease, as maculopathy with significant



visual loss can occur with moderate ophthalmoscopic signs. This has necessitated the need for disease monitoring. By clearly visualizing key DR pathological features—microaneurysms (MAs), retinal nonperfusion, intraretinal microvascular abnormalities (IRMAs), and retinal neovascularizations (RNVs)—OCTA has been endorsed in expert consensus guidelines as a critical adjunct assessment tool for clinical staging and treatment decision-making in DR management (18, 19).

5.2 Lesion recognition

OCTA is employed in clinical practice for the diagnosis of DR, frequently to identify the characteristic lesions of various stages of DR. This complements the diagnosis and grading of DR, such as MAs, IRMAs, and RNVs, as shown in Figure 2 above.

5.2.1 Microaneurysm

Retinal microaneurysms (MAs) serve as an early symptom of DR, with the type of MA correlating with visual acuity, DR duration, and severity (20). The identification and study of MAs are of interest because their morphological features and turnover are associated with the risk of DR complications and adverse visual outcomes. OCTA techniques can reliably classify retinal MAs (21). Studies have identified various morphological types of MAs, such as focal bulge, saccular/pedunculated, fusiform, and mixed types, and found that these different typologies may correspond to DR progression at varying stages. This understanding allows for the assessment of the relationship between MAs and the progression of clinical stages of DR.

5.2.2 Intraretinal microvascular abnormalities

Intraretinal microvascular abnormalities (IRMAs) were first observed in the eyes of diabetic patients with severe NPDR and PDR. It was initially unclear whether these vascular anomalies indicated the development of new intraretinal blood vessels or the expansion of existing ones (22). IRMAs are characterized by abnormal branching or dilation of existing retinal capillaries, and

their presence correlates with the severity and progression of DR (23). These abnormalities may be a consequence of ongoing ischemia.

OCTA images reveal IRMAs as abnormal, branching, and dilated retinal vessels that do not extend into the vitreous cavity (24). OCTA enables the visualization of morphological changes in IRMAs both before and after pan-retinal photocoagulation (PRP), which aids in classifying IRMAs into more specific types. Monitoring these morphological changes in IRMAs can facilitate the early detection of severe signs of DR, potentially leading to earlier treatment interventions (25).

5.2.3 Retinal neovascularization

Retinal neovascularization (RNV) is a critical clinical feature of PDR, representing a pathophysiological alteration resulting from retinal ischemia in DR. This abnormal formation of blood vessels signifies the progression of DR to PDR (26). RNV increases the risk of severe vision loss due to complications such as vitreous hemorrhage or traction retinal detachment. Early detection and timely treatment of RNV are crucial for preventing disease progression and subsequent vision loss (27).

Ophthalmologic funduscopy can reveal RNV as irregular red blood columns in the optic nerve head and retina. However, the direct visualization of neovascularization is limited by the retinal structure and laser spots formed after treatment. Although OCTA has poor ability to detect NVD or NVE by the lack of detection of leakage from RNV. On OCTA images, the most common neovascular lesions are irregular hyperplasia of fine blood vessels, while some RNVs appear as filamentous neovascular loops (28).

The identification of characteristic lesions of DR, as described, often relies on OCTA as complementary information for DR diagnosis. RNV identification was rigorously performed using B-scan flow analysis, where neovascularization confirmation required detectable flow signals above the internal limiting membrane (ILM), thereby distinguishing true RNV from IRMA. Nevertheless, OCTA has limitations; it cannot detect hard exudates, which are due to the extravasation of lipids and proteins following the breakdown of the blood-retina barrier, nor can it accurately identify vessels with low blood flow velocities or hemodynamically abnormal capillaries.

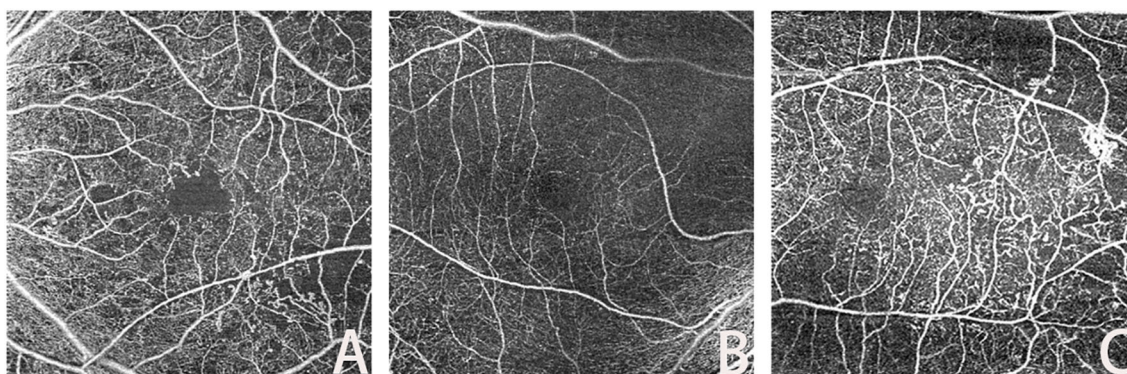


FIGURE 2
Lesions in OCTA ((A): MA; (B): IRMAs; (C): RNV).

5.3 OCTA imaging biomarkers for diabetes mellitus patients without DR

In patients with diabetes mellitus (DM) without DR, OCTA imaging parameters can detect potential microvascular and neurological changes that may not be observable during fundoscopic examination. A prospective study analyzing OCTA data from patients with type 1 diabetes, in conjunction with clinical data, found that metabolic markers and other patient data influenced OCTA results (29). Several studies have indicated that microvascular changes, such as enlargement and remodeling of the FAZ and capillary nonperfusion zone, may begin before the clinical signs of DR become apparent. OCTA is used to identify diabetic patients at risk for retinopathy and to provide rapid, noninvasive screening for diabetes prior to a systematic diagnosis (30). Retinal microvascular abnormalities, including capillary dropout, dilated capillary loops, tortuous capillary branches, patches of reduced capillary perfusion, irregular FAZ contours, FAZ enlargement, and focal or diffuse choriocapillaris flow impairment, have been observed in some diabetic eyes without retinopathy. These abnormalities may serve as early signs of DR and could potentially act as biomarkers for early detection and monitoring of the disease (31).

OCTA metrics have proven valuable in anticipating the advancement of DR in individuals with type 2 DM through the assessment of thickness measurements, retinal nerve fiber layer, and plexiform layer thickness measurements within the ganglion cell layer. Changes in retinal vascular parameters in participants were identified by OCTA measurements of retinal avascular zones, including area, circumference, circularity, vascular density (VD), and macular perfusion (MP) (29, 32, 33). In individuals diagnosed with type 1 diabetes without any signs of DR, it was observed that the VD of the superficial capillary plexus (SCP), deep capillary plexus (DCP), and choroidal ciliary body was lower compared to that of healthy individuals, indicating an earlier impact on both retinal and choroidal circulation before the manifestation of DR (34). Furthermore, patients with diabetes exhibited a reduced vessel density in the superficial and deep retinas surrounding the central fovea (35). However, various studies have reported conflicting findings regarding changes in the size of the FAZ in the early stages of DR. Some studies suggest a significant increase in FAZ size among patients with diabetes (30), while others found no notable differences in FAZ size between the SCP and DCP regions (36). Given the considerable variability in the FAZ region among healthy individuals, its association with DR requires further investigation and verification (37).

In diabetic patients without DR, there is an association between early changes in the morphology of blood vessels around the optic nerve and the density of blood vessels in the retinal choroid capillaries. These changes are linked to a decrease in the thickness of the nerve fiber layer. Notably, alterations in surface vessel density are more commonly observed in the peripapillary region than in the macular area. It is important to note that patients with diabetes may experience early damage to both neurons and small blood vessels, even before clinical signs of DR are present (38). Furthermore, individuals with diabetes exhibit a reduced vascular response to

flash stimuli, and there is a decrease in perfusion density in the deep capillary layer in those without DR (37). OCTA imaging reveals damage in the retinal microvasculature, and it has been observed that patients with type 2 diabetes who have microalbuminuria but do not yet have DR exhibit changes in retinal microcirculation. These alterations could potentially serve as an early monitoring tool for tracking microvascular complications in such patients (39, 40).

RNV can arise from IRMAs. Early detection of IRMAs may serve as a reliable method to predict the progression of PDR. Regular use of OCTA to monitor the occurrence of IRMAs may aid in the timely diagnosis of PDR (41). Identifying alterations in OCT and OCTA parameters in specific diabetic patients at an early stage may serve as an indicator of subsequent overt retinopathy (42). A decrease in macular CC perfusion could potentially act as an initial marker for clinically undetectable diabetic vasculopathy (43). The analysis of intercapillary areas (ICAs) involves measuring the distance between surrounding vessels and each pixel in the intercapillary region. Consequently, employing OCTA in DM patients without existing DR holds promise for early detection and prediction of DR development (44). It is imperative to enhance the quantification of retinal ischemia through various perspectives and integrate OCTA imaging into routine clinical and scientific practices. The adoption of standardized and device-independent image analysis methods becomes essential in this regard (45). OCTA has demonstrated remarkable potential in the management of prevalent ocular complications among DM patients. The use of imaging tests for preventing and controlling DR is particularly crucial for DM patients with existing DR.

5.4 Prediabetes OCTA imaging biomarkers recognition

Prediabetes, also known as impaired glucose regulation (IGR), is a pathological condition characterized by blood glucose levels that are higher than normal but have not yet reached the diagnostic criteria for diabetes. According to the World Health Organization (WHO), prediabetes is classified into two types: impaired fasting glucose (IFG) and abnormal glucose tolerance (IGT) (46). The risk of DR may be related to prediabetes. During examination by direct ophthalmoscopy, vascular changes, such as a lower arteriole-to-venule ratio and increased retinal arteriole or venular caliber, were found in the retinas of patients with prediabetes, which may be associated with the pre-diabetic state (47). The current application of the OCTA technique for monitoring blood flow in normoglycemia versus prediabetes shows that the paravascular density in the SCP and DCP layers of the retina was reduced in the prediabetes group compared with that in the normoglycemia group (48).

5.5 OCTA imaging biomarkers of DR

In the application of OCTA for DR, several image markers can be utilized to predict the severity of the disease and provide

complementary information for DR diagnosis and management. These markers include metrics for the FAZ and vascular and perfusion densities, which have been extensively studied as clinically interpretable features to gauge the severity of DR.

5.5.1 The foveal avascular zone

Foveal avascular zone (FAZ) corresponds to the region of the human retina with the highest concentration of cone photoreceptors and oxygen consumption (49). Researchers have extensively studied the correlation between FAZ changes and various ocular diseases (50). As DR progresses, the fovea, which is responsible for central vision, can be affected. In such cases, abnormalities in the size and shape of the FAZ can contribute to vision loss (51). OCTA assessment of the FAZ area in patients with type 2 diabetes enables early detection of macular changes that precede findings from conventional retinography and SD-OCT examinations (52). One study conducted an assessment of neurological dysfunction in pre-diabetic individuals using multifocal electroretinography (mfERG), analysis of neurodegeneration, and measurement of retinal layer thickness with SD-OCT. Additionally, quantitative parameters such as FAZ area, vessel area density (VAD), vessel length fraction (VLF), vessel diameter index (VDI), and fractal dimension (FD) were measured using OCTA. It should be noted that the association between pre-diabetic neurodegeneration and early microvascular damage is not yet fully understood. However, a glycemic threshold was identified for pre-diabetic patients with observable retinopathy (53, 54).

5.5.2 Vessel density

Vessel density (VD) was defined as the proportion of the vascular area in the image to the total measured area and was used to indicate microvascular perfusion (55, 56). The VD must be corrected for the thickness of the retinal layers during analysis, such as the macular ganglion cell inner plexiform layer (35). Moreover, VD is related to scanning signal strength (57). During clinical applications, poor-quality images should be deleted.

5.5.3 Vascular length density/skeleton density

Vascular length density (VLD)/skeleton density (SD) serves as a metric similar to VD. However, because VD only considers the density per unit area of the vascular area, VLD is deemed to be more sensitive than VD to changes in perfusion at the capillary level (3).

5.5.4 Vessel diameter index

The vessel diameter index (VDI) and the average vessel caliber (AVC) were determined by analyzing binarized and skeletonized images. This metric quantifies the average size of blood vessels in terms of their vascular caliber (54), increased VDI may be associated with higher fasting blood glucose levels (58).

5.5.5 Fractal dimension

Fractal dimension (FD), an indicator of vascular network complexity calculated via methods like box-counting or circular mass-radius in OCTA images, reflects the self-similarity of the

retinal capillary network, notably in the superficial (SCP) and deep capillary plexus (DCP), and is automatically computed by artificial intelligence (AI) as a potential biomarker for DR progression (59). Research shows FD typically decreases in DR patients compared to healthy controls and diabetics without DR, especially in the DCP, with Singh et al. (2021) noting a significant reduction using the circular mass-radius method (60), and Zahid et al. (2016) confirming lower FD in DR versus controls and non-DR diabetics (60), suggesting vascular simplification due to capillary dropout. The FD variation pattern differs across DR stages: in diabetic patients without clinical DR signs, FD may align with healthy controls (60), yet a 2022 study found it already lower, hinting at early changes (61); in NPDR, FD drops below normal and non-DR diabetic levels, particularly in the DCP, reflecting capillary dropout-induced simplification (62); in PDR, FD further declines, with DCP FD lower than in NPDR (60), likely due to intensified capillary loss, though neovascular complexity in PDR may not be fully captured by standard FD measures despite new vessel growth.

5.5.6 Other OCTA imaging biomarkers of DR

OCTA has the capability to identify and objectively detect diseases through alternative biomarkers, such as the VDI, vessel perimeter index (VPI), and vessel skeleton density (VSD) (63). These biomarkers have been further detailed in the context of detecting and categorizing DR during regular care for patients with PDR (64). To quantify the extent of retinal ischemia, the intercapillary area (ICA) is analyzed by measuring the distance between each intercapillary pixel and adjacent vessels (45). The capillary nonperfusion area (NPA) serves as a critical biomarker for assessing DR progression by OCTA, with its distribution varying among patients with different severities of DR (65). Certain OCTA biomarkers and parameters are essential assessment criteria in clinical studies of anti-VEGF drugs, although signal attenuation artifacts can pose challenges to accurate quantification (66, 67). Among these biomarkers, the extrafoveal avascular area (EAA) correlates well with DR severity and demonstrates high sensitivity in differentiating between diabetic and healthy populations (68). In the management of diabetic maculopathy, OCTA can detect changes in reflectance at different stages of progression, which aids in understanding the characteristics of microaneurysms and improves the timing of treatment for diabetic maculopathy lesions, facilitating a more individualized treatment plan (69). OCTA's potential in managing patients with diabetic macular degeneration has been highlighted by a study showing that some patients with early DR macular degeneration (characterized by microaneurysms, leakage, neovascularization, and internal microvascular abnormalities) exhibit more pronounced changes in the FAZ, despite a relatively normal clinical presentation (52).

5.6 OCTA in DME

Utilizing OCTA, the identification and structural assessment of DME now extend beyond merely delineation of internal morphological disruptions. This enhanced investigative modality

also affords a nuanced in-depth visual interrogation of the macular microvasculature in DME and enables precise monitoring of dynamic alterations using quantifiable OCTA parameters (70).

5.6.1 Diabetic Macular Ischemia (DMI) and its role in DME progression

The progression of DME is intrinsically linked to the development of DMI. Clinically, DMI presents with enlargement and irregularity in the FAZ, along with the loss of retinal capillaries, predominantly in regions not directly bordering the macula (71). Analysis of outcomes through Fundus fluorescein Angiography (FFA) and OCTA revealed consistent observations, thereby substantiating the gradability of DMI via OCTA (72).

5.6.2 Prognostication and quantitative assessment for DME

Underpinning studies on Diabetic Macular Ischemia have elucidated a predictive capacity within OCTA, particularly through the evaluation of SCP and DCP. This allows for the prognostic discrimination of DME's advancement. Severe presentations of DME exhibit irregular FAZ morphology and extensive vascular damage within the Deep Vascular Plexus (DVP), compounding vision impairment ancillary to escalated degrees of DME severity, expanded FAZ regions, and accentuated central macular thickness (73). Furthermore, VD has been demonstrated to bear potential in managing DME. Among individuals with DME, there exists a statistically significant decrease in DCP's VD compared to those without evidence of DME (74).

5.6.3 Role of OCTA in anti-VEGF Therapy for DME

OCTA applications within research about anti-VEGF treatment for DME have been pivotal. By quantifying changes within macular microvasculature through OCTA parameters, enhanced insight and evaluation of the anti-VEGF therapy's efficacy are facilitated. The integrity of the DCP is closely correlated with the treatment outcomes concerning VEGF inhibitors in DME management. The extent of DCP has been identified as a significant predictor of the response to anti-VEGF therapies (75). A comparative analysis between DME patients and those without DME highlights a distinct deterioration in visual function across multiple quadrants for those with DME. Particularly, after treatment with VEGF inhibitory agents, a superior post-treatment visual prognosis is observed in patients with higher visual deficits in both the SCP and DCP (76).

5.7 Impact of age on OCTA parameters in DR assessment

In the assessment of DR using OCTA, age significantly influences the baseline values of parameters such as VD, fractal dimension (FD), and NPA. In healthy populations, VD and FD exhibit a physiological decline with age—for instance, macular VD decreases by approximately 1.5–2.0% per decade (77)—whereas in

DR patients, pathological changes superimpose upon age-related degeneration, increasing the complexity of clinical interpretation. In younger patients (<50 years), OCTA parameters are more sensitive to early microvascular changes, with VD reductions reaching 10–12% during the NPDR stage (78), though rapid disease progression can confound results. In older patients (≥60 years), vascular network degeneration may obscure early ischemic signs, and systemic factors such as hypertension often exacerbate parameter heterogeneity—for example, peripapillary vessel tortuosity increases by 15% (79).

6 Comparison of OCTA and FFA in DR

OCTA is capable of accurately detecting changes in the retinal vasculature, although it has limitations in identifying specific lesions in clinical practice. Primarily, OCTA provides supplementary information for the management and diagnosis of patients with DR. FFA, an essential diagnostic tool for evaluating the clinical fundus characteristics of DR, can detect primary vasculopathy and vascular anomalies, such as venous bead-like changes and retinal microvascular anomalies, during the development of vasculopathy in DR. In cases of retinal nonperfusion, characterized by dark areas surrounded by large blood vessels, neovascularization is often marked by significant leakage of fluorescent dye into the vitreous cavity on FFA (80). The FFA procedure involves injecting a fluorescent dye into the anterior vein, typically via a short posterior ciliary artery, which then reaches the optic and choroid regions 8 to 12 seconds later. The choroid circulation appears as choroidal flush, a patchy, mottled hyperfluorescence, as the choroid lobules fill (81). Retinal circulation occurs 1 to 3 seconds later (11–18 seconds after injection). Early arteriovenous malformation (AVM) is associated with the filling of the retinal arteries, arterioles, and capillaries, followed by an advanced arteriovenous or laminar venous phase as the dye fills the veins in a laminar fashion. After about 10 minutes, the complete emptying of the dye occurs, and during this phase, the optic disc, Bruch's membrane, choroid, and sclera are stained (82). The normal stages of FFA include: 1. choroidal phase; 2. arterial phase; 3. arteriovenous phase; 4. venous phase; and 5. recirculation phase. The features of DR, as identified by OCTA and FFA, are summarized in Table 1.

FFA offers a wider field of view and can dynamically display retinal blood flow. In contrast, OCTA provides a clearer visualization of dynamic blood flow at various retinal levels under different parameters, although it may be slightly less effective in detecting specific lesions with inaccessible or localized blood turbulence (80). The primary clinical disadvantage of FFA is its invasiveness and time-consuming nature. The contrast agent used in FFA can cause several potential side effects, including nausea, vomiting, hives, seizures, allergic reactions, and even death (83). Therefore, the benefits of FFA must be weighed against the potential risks and the availability of less invasive imaging procedures in clinical practice, as presented in Figure 3 below.

As a noninvasive, dye-free method for ocular vascular visualization, OCTA complements other diagnostic investigations

TABLE 1 Comparison of OCTA and FFA.

| Lesion type | Etiology | OCTA | FFA |
|-------------|--|---|--|
| MA | Elevation of capillary pressure due to loss of perivascular and endothelial cells and smooth muscle cells, etc., leading to focal dilatation of capillaries. | Demarcated, saccular or fusiform shapes of focally dilated capillary vessels in the superficial and deep plexuses. | Early stage shows hyperfluorescent pinpoint dots; late stage shows focal leakage. |
| IRMA | Remodeling of retinal capillaries due to retinal hypoxia. | Clusters of irregular tortuous vessels or dilation of existing capillaries, without proliferative changes. Intraretinal flow below ILM. | Can be distinguished from neovascularization by no or less profuse leakage on FFA. These vessels do not extend over vascular branches. |
| RNV | Proliferation of fibroblasts due to hypoxia after localized closure of retinal capillaries. | Lesions show retinal new vessels breaching the ILM. | Early stage is strongly fluorescent abnormal vascular network; late fluorescent leakage is clumped strong fluorescence. |
| DME | Accumulation of fluid, lipids, and proteins in the retina that occurs after rupture of the blood-retinal barrier. | / | Hyperfluorescent areas. |

MA, Microaneurysm; IRMA, Intraretinal Microvascular Abnormalities; RNA, Retinal Neovascularization; DME, Diabetic Macular Edema; FFA, Fundus Fluorescein Angiography.

in diagnosing, screening, and managing patients with DR. The advent and development of UWF-OCTA have partially addressed the limitations of OCTA’s small-image recognition area. UWF-OCTA can detect a broader range of retinal images during the actual acquisition process, but its longer image acquisition time may result in more artifacts and lower resolution. Thus, it is crucial to find the optimal balance between scanning area and parameter settings for UWF-OCTA under different circumstances (13, 84).

When assessing the severity of DR, UWF-OCTA has demonstrated promising results in evaluating DR retinal blood flow status. It captures more detailed information about retinal blood flow operations at once compared to standard OCTA due to its larger image range (40, 85). Furthermore, when used as input

data for artificial intelligence (AI) analysis, UWF-OCTA reflects the significant potential of integrating AI with clinical applications, as it contains richer image information (86).

7 OCTA in DR-related clinical researches

In clinical studies, OCTA imaging modalities facilitate the identification of complications that may lead to retinal ischemia and assess the natural course and progression of retinal ischemia in DR, emphasizing the importance of prevention (87). However, in certain cases where patients have background retinal structures and

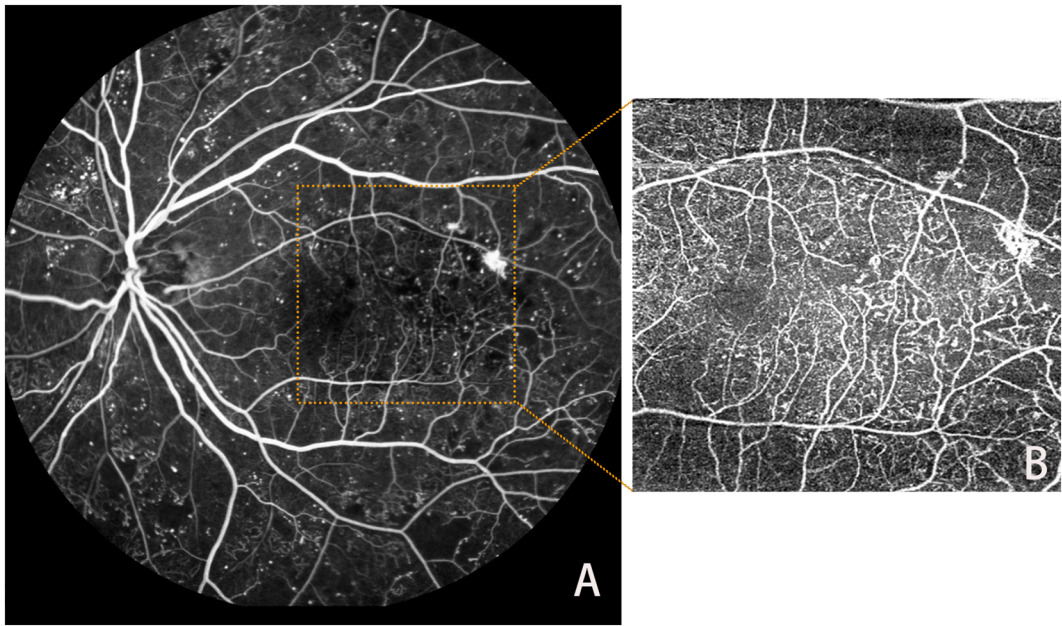


FIGURE 3
Lesions in FFA (A) and OCTA (B).

laser scars, the detailed manifestation of the disease may not be visualized solely through color fundus photograph examination. OCTA has proven effective in accurately detecting various types of neovascularization, particularly beneficial for monitoring patients with a history of retinal surgery (28). OCTA is extensively used in diverse clinical studies, such as assessing retinal inner layer (DRIL) and ellipsoid zone (EZ) losses, leading to the identification of biomarkers that contribute to visual function evaluation in patients' eyes (88).

The assessment of GCL and inner plexiform layer (IPL) thickness for detecting retinal neurodegenerative changes has revealed a correlation between retinal vascular closure and the advancement of DR severity in patients with NPDR. This suggests that OCTA vascular closure measurements can serve as an indicator of DR progression severity. Post-analysis of OCTA images has shown that retinal neurodegeneration exhibits consistent and stable progression, potentially due to a reduction in vessel density, including vessel closure, caused by alterations in the DCP (89, 90). The analysis of biomarkers, such as VAD, VLF, and VDI, provides quantitative insights into neuronal damage observed in DR patients, indicating that it cannot be attributed solely to microvascular damage (42). The increasing use of OCTA in clinical research underscores its growing significance in advanced ophthalmic studies, including investigating potential retinal microvascular damage caused by different treatment modalities. This technique effectively assesses the number and circulatory condition of peripapillary microvessels, evaluating surgical outcomes and prognoses in clinical settings. For example, OCTA can be used when evaluating the efficacy and follow-up of surgical procedures like pars plana vitrectomy (PPV) combined with ILM peeling for epiretinal membrane (ERM) cases (91). It can also be applied in combination with certain drugs in proliferative DR and various neovascularization-related retinal diseases (92), assessing the efficacy of drug application in DR patients, and comparing the efficacy and safety after different drug applications (93). When applied to DR, OCTA parameters have been found to be good predictors of the efficacy of anti-VEGF drugs (ranibizumab (94), bevacizumab (95)) and also play a role in observing the therapeutic efficacy of other fundus implants (e.g., drug nanoparticles) (96). OCTA has played a crucial role in assessing retinal nerve damage and microvascular changes in several experimental studies (97).

Compared to other imaging techniques, such as FFA, OCTA is more accurate in detecting specific lesions in clinical research and has gained broader application due to its noninvasive, user-friendly, and harmless nature.

8 AI for OCTA in DR

The diagnosis of DR and the selection of treatment approaches and timing heavily depend on digital imaging data, encompassing OCT and FFA. Targeted feature extraction and objective feature quantification present significant opportunities for biomarker discovery, disease burden assessment, and prediction of treatment response. With the recent advancements in AI in ophthalmic applications, AI-assisted image analysis and OCTA data acquisition, generation, and collection can be technologically integrated. Machine learning-based techniques are particularly well-suited for leveraging OCTA to gather a vast amount of information. AI can transform the generation of OCTA images from a motion-contrast measurement to an image transformation problem, potentially reducing artifacts that are challenging to manage in traditional OCTA image formation (98). For diabetic patients without overt DR signs, OCTA's quantitative vascular metrics (e.g., vessel density and morphological parameters) serve as tools for early screening and follow-up (99). The application of AI in analyzing and processing various biomarkers derived from OCTA has revealed the potential of specific biomarkers to serve as new imaging biomarkers for the early detection of DR (Table 2).

8.1 AI for OCTA quantitative parameter analysis

The FAZ, a central avascular region in the macula, typically enlarges in DR due to capillary dropout, with studies showing significantly higher median FAZ area in DR patients, especially in severe NPDR and PDR stages (105). AI, via deep learning (DL) automates FAZ quantification; Guo et al. (2021) demonstrated strong consistency with manual measurements (68), underscoring AI's precision in measuring FAZ area as a potential DR severity biomarker.

TABLE 2 Performance summary of AI techniques in OCTA application.

| Reference | AI Technique Used | Performance Metrics | Journal/Conference |
|--------------------------------------|---|--|---|
| Le D, et al. (2020) (100) | Transfer learning with VGG16 CNN | Cross-val Acc 87.27%, Ext-val Acc 70.83% | Translational Vision Science & Technology |
| Eladawi N, et al. (2018) (101) | ANN with blood vessel reconstruction | Acc 94.3%, Spec 87%, Sens 97.9% | Medical Physics |
| Xu X, et al. (2023) (102) | AV-casNet neural network for segmentation | Arteriole Acc 94.2%, Venule Acc 93.5% | IEEE Trans Med Imaging |
| Afarid M, et al. (2022) (61) | Feature analysis using radiomics features | AUROC 0.87 for FAZ area | BMC Ophthalmol |
| Schottenhamml J, et al. (2021) (103) | Computational method for segmentation (graph-based) | Mean absolute error: ~0.91 pixel | Biomed Opt Express |
| Ryu G, et al. (2021) (104). | Deep Learning (CNN) | AUC 0.976, Sens 96%, Spec 98% | Scientific Reports |

Acc, Accuracy; Spec, Specificity; Sens, Sensitivity; AUROC, Area Under the Receiver Operating Characteristic Curve; Cross-val, Cross-validation; Ext-val, External validation.

Vessel density, reflecting overall retinal vascular density, decreases in DR progression, notably in superficial and deep capillary plexuses, indicating vascular loss. Research highlights a marked VD reduction with increasing DR severity, particularly post-VEGF inhibitor treatment (106). AI employs DL for vessel segmentation and density quantification, with Wang et al. (2020) validating high consistency with manual measurements (107), affirming AI's efficacy in assessing VD as a DR progression marker.

FD measures vascular complexity, with varying findings in DR. Some studies report reduced FD in DR patients, reflecting network simplification; Hashmi et al. (2021) found significantly lower FD using the circular mass-radius method (108), supported by Zahid et al. (2019) in the deep capillary layer (60). Conversely, early DR may show FD increases due to abnormal vessels or microaneurysms, though OCTA-specific evidence is limited. AI rarely measures FD directly, relying on image processing algorithms, but may implicitly learn FD-related features for DR classification. These parameters, analyzed via AI, serve as potential biomarkers for DR severity and progression, though FD variability warrants further investigation.

AI enhances DR detection accuracy through parameter analysis. Kim et al. (2021) achieved an AUC of 0.976, sensitivity of 96%, and specificity of 98% using a CNN model (104). Le et al. (2020) reported a cross-validation accuracy of 87.27% with VGG16 transfer learning, dropping to 70.83% in external validation, highlighting generalization issues (100). Eladawi et al. (2018) used support vector machines (SVM) to extract FAZ area and VD features, achieving 94.3% accuracy (101).

8.2 Intelligent classification of DR

The rapid advancement of AI has revolutionized DR classification through convolutional neural networks (CNNs) and transfer learning models. Studies demonstrate high diagnostic accuracy, such as Kim et al.'s CNN model achieving an AUC of 0.976 with 96% sensitivity and 98% specificity using 6×6 mm² OCTA images (104). However, generalization challenges persist, exemplified by Le et al.'s VGG16 transfer learning model showing an 87.27% cross-validation accuracy that dropped to 70.83% in external validation (109).

AI algorithms predict DR severity by analyzing biomarkers including NPA, macular ganglion cell/inner plexiform layer thickness, retinal arteriole/venule conditions, and extrafoveal vessel density (102). CNN-based approaches further classify DR into five stages (Normal to PDR) by processing OCTA parameters, enhancing grading precision (85). Despite these advancements, variability in imaging protocols and instrument settings underscores the need for standardized acquisition parameters to ensure broader clinical applicability.

8.3 Other AI applications for OCTA in DR

In the application of AI to OCTA images of DR patients, motion correction techniques can be employed to eliminate artifacts caused by eye movements, thereby enhancing the clarity of images, DR characteristic retinopathy, and surrounding features

(110). During the collection and processing of information by AI, it is advisable to construct a standard computer-aided diagnostic (CAD) system as defined in each learning model. OCTA, as part of ophthalmic imaging examinations, has demonstrated significant effectiveness in retinal assessment when combined with DL and machine learning (ML) methods, along with other patient imaging data (111). Some studies suggest that collaborative DL can yield comparable outcomes to conventional DL, achieved by utilizing jointly learned models and merging databases for microvessel segmentation and DR classification. These findings highlight the potential applicability of jointly learned models across various domains in OCT and OCTA data (112).

Enhancing the objectivity of OCTA image interpretation in future research, longitudinal tracking, and the integration of computational models to create automated diagnostics and clinical decision-support systems can augment their practical applications. Advances in computational technologies, including DL and radiomics, offer the possibility of developing distinct imaging phenotypes. The construction of these ocular imaging phenotypes can facilitate personalized disease management and increase opportunities for precision medicine. These quantifiable biomarkers and automated methods can be applied to individualized medicine, where treatments are tailored to patient-specific, longitudinally trackable biomarkers, and response monitoring can be achieved with high accuracy. Despite the integration of AI with OCTA image information in DR research, a standardized CAD system remains elusive. The evaluation criteria for learning models across different AI clinical studies are not well-defined. It is crucial to assess these models based on uniform and standardized criteria to enhance the overall proficiency of AI clinical studies in DR applications using OCTA (113).

9 Shortcomings of OCTA in DR

OCTA has several limitations, including a limited field of view and an inability to visualize certain DR-characteristic lesions such as vascular leakage, as well as increased susceptibility to artifacts during the technique's application, such as blinking, motion, and vascular reimaging. Additionally, OCTA cannot detect blood flow below the slowest detectable flow rate (66). Traditional markers for DR diagnostic grading, such as blood-retinal barrier disruption and vascular leakage, lack clear diagnostic markers in OCTA. The standardization of output from different OCTA instruments also significantly impacts the subsequent processing of image data. Current OCTA imaging also faces challenges, such as the inability to detect some ischemic vessels, specific blood flow rate requirements, low imaging efficiency for larger resolution images, and the inevitable formation of noise and artifacts due to subject eye movements during the imaging process. OCTA has a limitation in effectively identifying detailed lesion structures and comprehending the overall architecture of the retinal vasculature in DR.

Further research is needed to determine the utility of OCTA in clinical settings, given its relatively short history of clinical application, and to explore its potential for detailed visualization of the retinal vasculature. Subsequently, OCTA parameters and

settings need to be standardized, and standardized guidelines based on the application of OCTA for DR diagnostic grading should be developed. Despite these disadvantages, OCTA offers the advantage of being noninvasive and capable of obtaining volume scans segmented to a specific depth within seconds. Future advancements should focus on obtaining a larger field of view, faster scanning speeds, and higher resolution.

While AI demonstrates high accuracy (100), automation, and potential for early screening in resource-limited settings, its clinical application faces challenges: 1) High-cost dependency on large annotated datasets for training robust models; 2) Limited generalizability, exemplified by Le et al.'s (2020) external validation accuracy of 70.83% (114); 3) Reduced clinical trust due to the black-box nature of DL; 4) Misclassification risks from artifacts (e.g., projection artifacts, motion artifacts); 5) Widespread neglect of age-stratified corrections in current models, leading to misdiagnosis of age-related VD/FD decline as DR progression or underestimation of early pathological signs in younger patients.

Future advancements should prioritize: developing interpretable AI frameworks with age-adaptive feature decoupling to distinguish physiological aging from pathological changes; establishing multicenter age-stratified cohort validation systems and age-specific reference standards; optimizing artifact correction through interdisciplinary collaboration; and promoting standardized CAD systems (115) for unified evaluation. Despite challenges in data scalability, model generalizability, and image quality dependency, the synergy of AI and OCTA holds transformative potential for precise DR management (116). Crucially, AI should be positioned as a clinical aid to enhance diagnostic objectivity, not as a replacement for expert judgment.

10 Conclusion

Since the advent of OCTA imaging technology, numerous clinical studies have explored its applications. OCTA is a common noninvasive method for examining retinal diseases, offering simplicity and convenience. Its advantages—noninvasiveness, dye-free imaging, rapid processing, and accurate blood flow localization—have led to its swift adoption in ocular examinations.

Initially, OCTA was primarily an auxiliary imaging tool for DR due to its unique imaging capabilities. However, as clinical studies progressed and the technology evolved, OCTA has increasingly been used to assess retinal nerve and vascular function in DR. It is particularly sensitive in detecting subtle lesions indicative of DR and DM before they manifest. OCTA aids in diagnosing and classifying established DR and can predict and manage retinal conditions in DM patients without DR. It can also identify retinal microcirculation states in prediabetic patients, which is beneficial for community screening and managing DM-related ocular complications.

Recent advances in OCTA for DR have focused on enhancing image resolution and improving software algorithms to better visualize microvascular changes. These improvements allow for earlier DR detection, detailed retinal vasculature mapping, and non-invasive DR progression monitoring. Enhanced OCTA

technology also facilitates more accurate treatment efficacy assessments, improving patient management and outcomes. OCTA has the potential to serve as an independent predictor of DR. In clinical applications, OCTA is commonly used as a supplementary diagnostic tool for DR grading. Current technological developments aim to collect high-resolution, wide-field OCTA images faster, leveraging AI's powerful processing capabilities. Further exploration is needed to standardize OCTA outputs and terminology across different instruments to fully realize its potential in diagnosing, evaluating, and predicting DR.

Although OCTA is not yet a standalone diagnostic criterion for DM in ocular imaging, the emergence of UWF-OCTA and AI integration in ophthalmology has identified more diagnostic and clinically relevant OCTA biomarkers. Despite the lack of standardized grading and interpretation methods for DR assessment, ongoing clinical research and advanced AI models are expected to establish Diagnostic Classification Guidelines for OCTA in DR soon. OCTA will continue to explore new biomarkers and practical applications, playing an increasingly significant role in the prediction, diagnosis, and management of DR across various scenarios.

Data availability statement

The original contributions presented in the study are included in the article/supplementary material. Further inquiries can be directed to the corresponding authors.

Author contributions

QZ: Writing – original draft, Writing – review & editing, Data curation. DG: Writing – original draft, Writing – review & editing, Data curation. MH: Writing – original draft. ZZ: Writing – review & editing, Conceptualization, Validation. WY: Writing – review & editing, Conceptualization, Supervision, Validation, Funding acquisition. GM: Writing – review & editing, Conceptualization, Funding acquisition, Validation.

Funding

The author(s) declare that financial support was received for the research and/or publication of this article. This research was funded by the Introduction Plan of High-Level Foreign Experts (G2022026027L), Major Program of Medical Science Challenging Plan of Henan province (SBGJ202102190) and Sanming Project of Medicine in Shenzhen (SZSM202311012).

Conflict of interest

The authors declare that the research was conducted in the absence of any commercial or financial relationships that could be construed as a potential conflict of interest.

Publisher's note

All claims expressed in this article are solely those of the authors and do not necessarily represent those of their affiliated

organizations, or those of the publisher, the editors and the reviewers. Any product that may be evaluated in this article, or claim that may be made by its manufacturer, is not guaranteed or endorsed by the publisher.

References

- Koustenis A Jr., Harris A, Gross J, Januleviciene I, Shah A, Siesky B. Optical coherence tomography angiography: an overview of the technology and an assessment of applications for clinical research. *Br J Ophthalmol*. (2017) 101:16–20. doi: 10.1136/bjophthalmol-2016-309389
- Fingler J, Readhead C, Schwartz DM, Fraser SE. Phase-contrast OCT imaging of transverse flows in the mouse retina and choroid. *Invest Ophthalmol Vis Sci*. (2008) 49:5055–9. doi: 10.1167/iops.07-1627
- Spaide RF, Klancnik JM Jr., Cooney MJ. Retinal vascular layers imaged by fluorescein angiography and optical coherence tomography angiography. *JAMA Ophthalmol*. (2015) 133:45–50. doi: 10.1001/jamaophthalmol.2014.3616
- Cheung N, Mitchell P, Wong TY. Diabetic retinopathy. *Lancet*. (2010) 376:124–36. doi: 10.1016/S0140-6736(09)62124-3
- Davis MD, Fisher MR, Gangnon RE, Barton F, Aiello LM, Chew EY, et al. Risk factors for high-risk proliferative diabetic retinopathy and severe visual loss: Early Treatment Diabetic Retinopathy Study Report 18. *Invest Ophthalmol Vis Sci*. (1998) 39:233–52.
- Mohamed Q, Gillies MC, Wong TY. Management of diabetic retinopathy: a systematic review. *Jama*. (2007) 298:902–16. doi: 10.1001/jama.298.8.902
- Vujosevic S, Cunha-Vaz J, Figueira J, Löwenstein A, Midena E, Parravano M, et al. Standardization of optical coherence tomography angiography imaging biomarkers in diabetic retinal disease. *Ophthalmic Res*. (2021) 64:871–87. doi: 10.1159/000518620
- Liu K, Zhu T, Gao M, Yin X, Zheng R, Yan Y, et al. Functional OCT angiography reveals early retinal neurovascular dysfunction in diabetes with capillary resolution. *BioMed Opt Express*. (2023) 14:1670–84. doi: 10.1364/BOE.485940
- Spaide RF, Fujimoto JG, Waheed NK, Sadda SR, Staurengi G. Optical coherence tomography angiography. *Prog Retin Eye Res*. (2018) 64:1–55. doi: 10.1016/j.preteyeres.2017.11.003
- Lains I, Wang JC, Cui Y, Katz R, Vingopoulos F, Staurengi G, et al. Retinal applications of swept source optical coherence tomography (OCT) and optical coherence tomography angiography (OCTA). *Prog Retin Eye Res*. (2021) 84:100951. doi: 10.1016/j.preteyeres.2021.100951
- Miller AR, Roisman L, Zhang Q, Zheng F, Rafael de Oliveira Dias J, Yehoshua Z, et al. Comparison between spectral-domain and swept-source optical coherence tomography angiographic imaging of choroidal neovascularization. *Invest Ophthalmol Vis Sci*. (2017) 58:1499–505. doi: 10.1167/iops.16-20969
- Spaide RF, Curcio CA. Evaluation of segmentation of the superficial and deep vascular layers of the retina by optical coherence tomography angiography instruments in normal eyes. *JAMA Ophthalmol*. (2017) 135:259–62. doi: 10.1001/jamaophthalmol.2016.5327
- Zhu Y, Cui Y, Wang JC, Lu Y, Zeng R, Katz R, et al. Different scan protocols affect the detection rates of diabetic retinopathy lesions by wide-field swept-source optical coherence tomography angiography. *Am J Ophthalmol*. (2020) 215:72–80. doi: 10.1016/j.ajo.2020.03.004
- Querques L, Giuffrè C, Corvi F, Zucchiatti I, Carnevali A, De Vitis LA, et al. Optical coherence tomography angiography of myopic choroidal neovascularisation. *Br J Ophthalmol*. (2017) 101:609–15. doi: 10.1136/bjophthalmol-2016-309162
- Bonnin S, Mané V, Couturier A, Julien M, Paques M, Tadayoni R, et al. New insight into the macular deep vascular plexus imaged by optical coherence tomography angiography. *Retina*. (2015) 35:2347–52. doi: 10.1097/IAE.0000000000000839
- Savastano MC, Lumbroso B, Rispoli M. *In vivo* characterization of retinal vascularization morphology using optical coherence tomography angiography. *Retina*. (2015) 35:2196–203. doi: 10.1097/IAE.0000000000000635
- Huang D, Jia Y, Rispoli M, Tan O, Lumbroso B. Optical coherence tomography angiography of time course of choroidal neovascularization in response to Anti-Angiogenic treatment. *Retina*. (2015) 35:2260–4. doi: 10.1097/IAE.0000000000000846
- Amoaku WM, Ghanchi F, Bailey C, Banerjee S, Banerjee S, Downey L, et al. Diabetic retinopathy and diabetic macular oedema pathways and management: UK Consensus Working Group. *Eye (Lond)*. (2020) 34:1–51. doi: 10.1038/s41433-020-0961-6
- Lee J, Rosen R. Optical coherence tomography angiography in diabetes. *Curr Diabetes Rep*. (2016) 16:123. doi: 10.1007/s11892-016-0811-x
- Pappuru RKR, Ribeiro L, Lobo C, Alves D, Cunha-Vaz J. Microaneurysm turnover is a predictor of diabetic retinopathy progression. *Br J Ophthalmol*. (2019) 103:222–6. doi: 10.1136/bjophthalmol-2018-311887
- Fukuda Y, Nakao S, Kaizu Y, Arima M, Shimokawa S, Wada I, et al. Morphology and fluorescein leakage in diabetic retinal microaneurysms: a study using multiple en face OCT angiography image averaging. *Graefes Arch Clin Exp Ophthalmol*. (2022) 260:3517–23. doi: 10.1007/s00417-022-05713-7
- Goldberg MF, Jampol LM. Knowledge of diabetic retinopathy before and 18 years after the Airline House Symposium on Treatment of Diabetic Retinopathy. *Ophthalmology*. (1987) 94:741–6. doi: 10.1016/S0161-6420(87)33524-9
- Sabanayagam C, Banu R, Chee ML, Lee R, Wang YX, Tan G, et al. Incidence and progression of diabetic retinopathy: a systematic review. *Lancet Diabetes Endocrinol*. (2019) 7:140–9. doi: 10.1016/S2213-8587(18)30128-1
- Pan J, Chen D, Yang X, Zou R, Zhao K, Cheng D, et al. Characteristics of neovascularization in early stages of proliferative diabetic retinopathy by optical coherence tomography angiography. *Am J Ophthalmol*. (2018) 192:146–56. doi: 10.1016/j.ajo.2018.05.018
- Shimouchi A, Ishibazawa A, Ishiko S, Omae T, Ro-Mase T, Yanagi Y, et al. A proposed classification of intraretinal microvascular abnormalities in diabetic retinopathy following panretinal photocoagulation. *Invest Ophthalmol Vis Sci*. (2020) 61:34. doi: 10.1167/iops.61.3.34
- de Carlo TE, Bonini Filho MA, Bauman CR, Reichel E, Rogers A, Witkin AJ, et al. Evaluation of preretinal neovascularization in proliferative diabetic retinopathy using optical coherence tomography angiography. *Ophthalmic Surg Lasers Imaging Retina*. (2016) 47:115–9. doi: 10.3928/23258160-20160126-03
- Wong TY, Sun J, Kawasaki R, Ruamviboonsuk P, Gupta N, Lansingh VC, et al. Guidelines on diabetic eye care: the international council of ophthalmology recommendations for screening, follow-up, referral, and treatment based on resource settings. *Ophthalmology*. (2018) 125:1608–22. doi: 10.1016/j.ophtha.2018.04.007
- Ishibazawa A, Nagaoka T, Yokota H, Takahashi A, Omae T, Song YS, et al. Characteristics of retinal neovascularization in proliferative diabetic retinopathy imaged by optical coherence tomography angiography. *Invest Ophthalmol Vis Sci*. (2016) 57:6247–55. doi: 10.1167/iops.16-20210
- Wysocka-Mincewicz M, Baszyńska-Wilk M, Gołębiewska J, Olechowski A, Byczyńska A, Hautz W, et al. Influence of metabolic parameters and treatment method on OCT angiography results in children with type 1 diabetes. *J Diabetes Res*. (2020) 2020:4742952. doi: 10.1155/2020/4742952
- de Carlo TE, Chin AT, Bonini Filho MA, Adhi M, Branchini L, Salz DA, et al. Detection of microvascular changes in eyes of patients with diabetes but not clinical diabetic retinopathy using optical coherence tomography angiography. *Retina*. (2015) 35:2364–70. doi: 10.1097/IAE.0000000000000882
- Choi W, Waheed NK, Moulton EM, Adhi M, Lee B, De Carlo T, et al. Ultrahigh speed swept source optical coherence tomography angiography of retinal and choriocapillaris alterations in diabetic patients with and without retinopathy. *Retina*. (2017) 37:11–21. doi: 10.1097/IAE.0000000000001250
- Srinivasan S, Sivaprasad S, Rajalakshmi R, Anjana RM, Malik RA, Kulothungan V, et al. Association of OCT and OCT angiography measures with the development and worsening of diabetic retinopathy in type 2 diabetes. *Eye (Lond)*. (2023) 37(18):3781–6. doi: 10.1038/s41433-023-02605-w
- Wang XN, Gai X, Li TT, Long D, Wu Q. Peripapillary vessel density and retinal nerve fiber layer thickness changes in early diabetes retinopathy. *Int J Ophthalmology*. (2022) 15:1488–95. doi: 10.18240/ijo.2022.09.12
- Cao D, Yang D, Huang Z, Zeng Y, Wang J, Hu Y, et al. Optical coherence tomography angiography discerns preclinical diabetic retinopathy in eyes of patients with type 2 diabetes without clinical diabetic retinopathy. *Acta Diabetol*. (2018) 55:469–77. doi: 10.1007/s00592-018-1115-1
- Dimitrova G, Chihara E, Takahashi H, Amano H, Okazaki K. Quantitative retinal optical coherence tomography angiography in patients with diabetes without diabetic retinopathy. *Invest Ophthalmol Vis Sci*. (2017) 58:190–6. doi: 10.1167/iops.16-20531
- Scarinci F, Picconi F, Giorno P, Boccassini B, De Geronimo D, Varano M, et al. Deep capillary plexus impairment in patients with type 1 diabetes mellitus with no signs of diabetic retinopathy revealed using optical coherence tomography angiography. *Acta Ophthalmol*. (2018) 96:e264–e5. doi: 10.1111/aos.2018.96.issue-2
- Sacconi R, Casaluci M, Borrelli E, Mulinacci G, Lamanna F, Gelormini F, et al. Multimodal imaging assessment of vascular and neurodegenerative retinal alterations in type 1 diabetic patients without fundoscopic signs of diabetic retinopathy. *J Clin Med*. (2019) 8(9):1409. doi: 10.3390/jcm8091409

38. Vujosevic S, Muraca A, Gatti V, Masoero L, Brambilla M, Cannillo B, et al. Peripapillary microvascular and neural changes in diabetes mellitus: an OCT-angiography study. *Invest Ophthalmol Vis Sci.* (2018) 59:5074–81. doi: 10.1167/iovs.18-24891
39. Cankurtaran V, Inanc M, Tekin K, Turgut F. Retinal microcirculation in predicting diabetic nephropathy in type 2 diabetic patients without retinopathy. *Ophthalmologica.* (2020) 243:271–9. doi: 10.1159/000504943
40. Wang F, Saraf SS, Zhang Q, Wang RK, Rezaei KA. Ultra-widefield protocol enhances automated classification of diabetic retinopathy severity with OCT angiography. *Ophthalmol Retina.* (2020) 4:415–24. doi: 10.1016/j.oret.2019.10.018
41. Russell JF, Shi Y, Scott NL, Gregori G, Rosenfeld PJ. Longitudinal angiographic evidence that intraretinal microvascular abnormalities can evolve into neovascularization. *Ophthalmol Retina.* (2020) 4:1146–50. doi: 10.1016/j.oret.2020.06.010
42. Pilotto E, Torresin T, Leonardi F, Gutierrez De Rubalcava Doblas J, Midena G, Moretti C, et al. Retinal microvascular and neuronal changes are also present, even if differently, in adolescents with type 1 diabetes without clinical diabetic retinopathy. *J Clin Med.* (2022) 11(14):3982. doi: 10.3390/jcm11143982
43. Dai Y, Zhou H, Chu Z, Zhang Q, Chao JR, Rezaei KA, et al. Microvascular changes in the choriocapillaris of diabetic patients without retinopathy investigated by swept-source OCT angiography. *Invest Ophthalmol Vis Sci.* (2020) 61:50. doi: 10.1167/iovs.61.3.50
44. Sarabi MS, Khansari MM, Zhang J, Kushner-Lenhoff S, Gahm JK, Qiao Y, et al. 3D retinal vessel density mapping with OCT-angiography. *IEEE J BioMed Health Inform.* (2020) 24:3466–79. doi: 10.1109/JBHI.6221020
45. Lauermann P, van Oterendorp C, Storch MW, Khattab MH, Feltgen N, Hoerauf H, et al. Distance-thresholded intercapillary area analysis versus vessel-based approaches to quantify retinal ischemia in OCTA. *Transl Vis Sci Technol.* (2019) 8:28. doi: 10.1167/tvst.8.4.28
46. Tabák AG, Herder C, Rathmann W, Brunner EJ, Kivimäki M. Prediabetes: a high-risk state for diabetes development. *Lancet.* (2012) 379:2279–90. doi: 10.1016/S0140-6736(12)60283-9
47. Nguyen TT, Wang JJ, Wong TY. Retinal vascular changes in pre-diabetes and prehypertension: new findings and their research and clinical implications. *Diabetes Care.* (2007) 30:2708–15. doi: 10.2337/dc07-0732
48. Santos AR, Ribeiro L, Bandello F, Lattanzio R, Egan C, Frydkjaer-Olsen U, et al. Functional and structural findings of neurodegeneration in early stages of diabetic retinopathy: cross-sectional analyses of baseline data of the EUROCONDOR project. *Diabetes.* (2017) 66:2503–10. doi: 10.2337/db16-1453
49. Yu DY, Cringle SJ, Su EN. Intraretinal oxygen distribution in the monkey retina and the response to systemic hyperoxia. *Invest Ophthalmol Vis Sci.* (2005) 46:4728–33. doi: 10.1167/iovs.05-0694
50. Conrath J, Giorgi R, Raccah D, Ridings B. Foveal avascular zone in diabetic retinopathy: quantitative vs qualitative assessment. *Eye (Lond).* (2005) 19:322–6. doi: 10.1038/sj.eye.6701456
51. Alipour SH, Rabbani H, Akhlaghi M, Dehnavi AM, Javanmard SH. Analysis of foveal avascular zone for grading of diabetic retinopathy severity based on curvelet transform. *Graefes Arch Clin Exp Ophthalmol.* (2012) 250:1607–14. doi: 10.1007/s00417-012-2093-6
52. Stana D, Potop V, Istrate SL, Eniceicu C, Mihalcea AR, Pașca IG, et al. Foveal avascular zone area measurements using OCT angiography in patients with type 2 diabetes mellitus associated with essential hypertension. *Rom J Ophthalmol.* (2019) 63:354–9. doi: 10.22336/rjo.2019.55
53. Kirthi V, Reed KI, Alattar K, Zuckerman BP, Bunce C, Nderitu P, et al. Multimodal testing reveals subclinical neurovascular dysfunction in prediabetes, challenging the diagnostic threshold of diabetes. *Diabetes Med.* (2023) 40:e14952. doi: 10.1111/dme.14952
54. Frizziero L, Midena G, Longhin E, Berton M, Torresin T, Parrozzani R, et al. Early retinal changes by OCT angiography and multifocal electroretinography in diabetes. *J Clin Med.* (2020) 9(11):3514. doi: 10.3390/jcm9113514
55. You Q, Freeman WR, Weinreb RN, Zangwill L, Manalastas PIC, Saunders LJ, et al. Reproducibility of vessel density measurement with optical coherence tomography angiography in eyes with and without retinopathy. *Retina.* (2017) 37:1475–82. doi: 10.1097/IAE.0000000000001407
56. Shen Q, Ao R, Niu YL, Xin L, Zhang YS, Liu CY, et al. Reproducibility of macular perfusion parameters in non-proliferative diabetic retinopathy patients by two different OCTA sweep modes. *Int J Ophthalmology.* (2022) 15:1483–7. doi: 10.18240/ijo.2022.09.11
57. Lim HB, Kim YW, Kim JM, Jo YJ, Kim JY. The importance of signal strength in quantitative assessment of retinal vessel density using optical coherence tomography angiography. *Sci Rep.* (2018) 8:12897. doi: 10.1038/s41598-018-31321-9
58. Tang FY, Ng DS, Lam A, Luk F, Wong R, Chan C, et al. Determinants of quantitative optical coherence tomography angiography metrics in patients with diabetes. *Sci Rep.* (2017) 7:2575. doi: 10.1038/s41598-017-02767-0
59. Uji A, Balasubramanian S, Lei J, Baghdasaryan E, Al-Sheikh M, Sadda SR. Impact of multiple en face image averaging on quantitative assessment from optical coherence tomography angiography images. *Ophthalmology.* (2017) 124:944–52. doi: 10.1016/j.ophtha.2017.02.006
60. Zahid S, Dolz-Marco R, Freund KB, Balaratnasingam C, Dansingani K, Gilani F, et al. Fractal dimensional analysis of optical coherence tomography angiography in eyes with diabetic retinopathy. *Invest Ophthalmol Vis Sci.* (2016) 57:4940–7. doi: 10.1167/iovs.16-19656
61. Afarid M, Mohsenipoor N, Parsaei H, Amirmoezzi Y, Ghofrani-Jahromi M, Jafari P, et al. Assessment of macular findings by OCT angiography in patients without clinical signs of diabetic retinopathy: radiomics features for early screening of diabetic retinopathy. *BMC ophthalmology.* (2022) 22:281. doi: 10.1186/s12886-022-02492-x
62. Kim AY, Chu Z, Shahidzadeh A, Wang RK, Puliafito CA, Kashani AH. Quantifying microvascular density and morphology in diabetic retinopathy using spectral-domain optical coherence tomography angiography. *Invest Ophthalmol Visual Sci.* (2016) 57:OCT362 – OCT70. doi: 10.1167/iovs.15-18904
63. Schwartz R, Khalid H, Sivaprasad S, Nicholson L, Anikina E, Sullivan P, et al. Objective evaluation of proliferative diabetic retinopathy using OCT. *Ophthalmol Retina.* (2020) 4:164–74. doi: 10.1016/j.oret.2019.09.004
64. Le D, Dadzie A, Son T, Lim JJ, Yao X. Comparative analysis of OCT and OCT angiography characteristics in early diabetic retinopathy. *Retina.* (2023) 43(6):992–8. doi: 10.1097/IAE.0000000000003761
65. Kawai K, Murakami T, Mori Y, Ishihara K, Dodo Y, Terada N, et al. Clinically significant nonperfusion areas on widefield OCT angiography in diabetic retinopathy. *Ophthalmol Sci.* (2023) 3:100241. doi: 10.1016/j.xops.2022.100241
66. Choi KE, Yun C, Cha J, Kim SW. OCT angiography features associated with macular edema recurrence after intravitreal bevacizumab treatment in branch retinal vein occlusion. *Sci Rep.* (2019) 9:14153. doi: 10.1038/s41598-019-50637-8
67. Guo Y, Hormel TT, Xiong H, Wang B, Camino A, Wang J, et al. Development and validation of a deep learning algorithm for distinguishing the nonperfusion area from signal reduction artifacts on OCT angiography. *BioMed Opt Express.* (2019) 10:3257–68. doi: 10.1364/BOE.10.003257
68. Guo Y, Hormel TT, Gao L, You Q, Wang B, Flaxel CJ, et al. Quantification of nonperfusion area in montaged widefield OCT angiography using deep learning in diabetic retinopathy. *Ophthalmol Sci.* (2021) 1:100027. doi: 10.1016/j.xops.2021.100027
69. Vujosevic S, Toma C, Villani E, Brambilla M, Torti E, Leporati F, et al. Subthreshold micropulse laser in diabetic macular edema: 1-year improvement in OCT/OCT-angiography biomarkers. *Transl Vis Sci Technol.* (2020) 9:31. doi: 10.1167/tvst.9.10.31
70. Mané V, Dupas B, Gaudric A, Bonnin S, Pedinielli A, Bousquet E, et al. Correlation between cystoid spaces in chronic diabetic macular edema and capillary nonperfusion detected by optical coherence tomography angiography. *Retina.* (2016) 36 Suppl 1:S102–s10. doi: 10.1097/IAE.0000000000001289
71. Kassoff A, Goodman AD, Buehler J, Garza D, Mehu M, Locatelli J, et al. Grading diabetic retinopathy from stereoscopic color fundus photographs—an extension of the modified Airlie House classification. ETDRS report number 10. Early Treatment Diabetic Retinopathy Study Research Group. *Ophthalmology.* (1991) 98:786–806. doi: 10.1016/S0161-6420(13)38012-9
72. Bradley PD, Sim DA, Keane PA, Cardoso J, Agrawal R, Tufail A, et al. The evaluation of diabetic macular ischemia using optical coherence tomography angiography. *Invest Ophthalmol Vis Sci.* (2016) 57:626–31. doi: 10.1167/iovs.15-18034
73. Han R, Gong R, Liu W, Xu G. Optical coherence tomography angiography metrics in different stages of diabetic macular edema. *Eye Vis (Lond).* (2022) 9:14. doi: 10.1186/s40662-022-00286-2
74. AttaAllah HR, Mohamed AAM, Ali MA. Macular vessels density in diabetic retinopathy: quantitative assessment using optical coherence tomography angiography. *Int Ophthalmol.* (2019) 39:1845–59. doi: 10.1007/s10792-018-1013-0
75. Lee J, Moon BG, Cho AR, Yoon YH. Optical coherence tomography angiography of DME and its association with anti-VEGF treatment response. *Ophthalmology.* (2016) 123:2368–75. doi: 10.1016/j.ophtha.2016.07.010
76. Sorour OA, Sabrosa AS, Yasin Alibhai A, Arya M, Ishibazawa A, Witkin AJ, et al. Optical coherence tomography angiography analysis of macular vessel density before and after anti-VEGF therapy in eyes with diabetic retinopathy. *Int Ophthalmol.* (2019) 39:2361–71. doi: 10.1007/s10792-019-01076-x
77. You QS, Chan JCH, Ng ALK, Choy BKN, Shih KC, Cheung JJC, et al. Macular vessel density measured with optical coherence tomography angiography and its associations in a large population-based study. *Invest Ophthalmol Vis Sci.* (2019) 60:4830–7. doi: 10.1167/iovs.19-28137
78. Rodrigues TM, Marques JP, Soares M, Simão S, Melo P, Martins A, et al. Macular OCT-angiography parameters to predict the clinical stage of nonproliferative diabetic retinopathy: an exploratory analysis. *Eye (Lond).* (2019) 33:1240–7. doi: 10.1038/s41433-019-0401-7
79. Li Y, Choi WJ, Wei W, Song S, Zhang Q, Liu J, et al. Aging-associated changes in cerebral vasculature and blood flow as determined by quantitative optical coherence tomography angiography. *Neurobiol Aging.* (2018) 70:148–59. doi: 10.1016/j.neurobiolaging.2018.06.017
80. Ishibazawa A, Nagaoka T, Takahashi A, Omae T, Tani T, Sogawa K, et al. Optical coherence tomography angiography in diabetic retinopathy: A prospective pilot study. *Am J Ophthalmol.* (2015) 160:35–44.e1. doi: 10.1016/j.ajo.2015.04.021
81. Zen QZ, Li SY, Yao YO, Jin EZ, Qu JF, Zhao MW. Comparison of 24x20 mm² swept-source OCTA and fluorescein angiography for the evaluation of lesions in diabetic retinopathy. *Int J Ophthalmol.* (2022) 15:1798–805. doi: 10.18240/ijo.2022.11.10

82. Rabb MF, Burton TC, Schatz H, Yannuzzi LA. Fluorescein angiography of the fundus: a schematic approach to interpretation. *Surv Ophthalmol.* (1978) 22:387–403. doi: 10.1016/0039-6257(78)90134-0
83. Kornblau IS, El-Annan JF. Adverse reactions to fluorescein angiography: A comprehensive review of the literature. *Surv Ophthalmol.* (2019) 64:679–93. doi: 10.1016/j.survophthal.2019.02.004
84. Cui Y, Zhu Y, Wang JC, Lu Y, Zeng R, Katz R, et al. Imaging artifacts and segmentation errors with wide-field swept-source optical coherence tomography angiography in diabetic retinopathy. *Transl Vis Sci Technol.* (2019) 8:18. doi: 10.1167/tvst.8.6.18
85. Yu TT, Ma D, Lo J, Ju MJ, Beg MF, Sarunic MV. Effect of optical coherence tomography and angiography sampling rate towards diabetic retinopathy severity classification. *BioMed Opt Express.* (2021) 12:6660–73. doi: 10.1364/BOE.431992
86. Hirano T, Hoshiyama K, Takahashi Y, Murata T. Wide-field swept-source OCT angiography (23 × 20 mm) for detecting retinal neovascularization in eyes with proliferative diabetic retinopathy. *Graefes Arch Clin Exp Ophthalmol.* (2023) 261:339–44. doi: 10.1007/s00417-022-05878-1
87. Mohite AA, Perais JA, McCullough P, Lois N. Retinal ischaemia in diabetic retinopathy: understanding and overcoming a therapeutic challenge. *J Clin Med.* (2023) 12(6):2406. doi: 10.3390/jcm12062406
88. Tsai WS, Thottarath S, Gurudas S, Pearce E, Giani A, Chong V, et al. Characterization of the structural and functional alteration in eyes with diabetic macular ischemia. *Ophthalmol Retina.* (2023) 7:142–52. doi: 10.1016/j.oret.2022.07.010
89. Marques IP, Kubach S, Santos T, Mendes L, Madeira MH, de Sistiernes L, et al. Optical coherence tomography metrics monitor severity progression of diabetic retinopathy-3-year longitudinal study. *J Clin Med.* (2021) 10(11):2296. doi: 10.3390/jcm10112296
90. Marques IP, Ferreira S, Santos T, Madeira MH, Santos AR, Mendes L, et al. Association between neurodegeneration and macular perfusion in the progression of diabetic retinopathy: A 3-year longitudinal study. *Ophthalmologica.* (2022) 245:335–41. doi: 10.1159/000522527
91. Yoon K, Park JB, Kang MS, Kim ES, Yu SY, Kim K. Peripapillary microvasculature changes after vitrectomy in epiretinal membrane via swept-source OCT angiography. *BMC Ophthalmol.* (2023) 23:50. doi: 10.1186/s12886-023-02793-9
92. Silva Tavares Neto JED, Cyrino FVR, Lucena MM, Scott IU, Messias AMV, Jorge R. Intravitreal bevacizumab plus propranolol for neovascular age-related macular degeneration (the BEVALOL study): a phase I clinical trial. *Int J Retina Vitreous.* (2023) 9:28. doi: 10.1186/s40942-023-00460-1
93. Parravano M, Scarinci F, Parisi V, Giorno P, Giannini D, Oddone F, et al. Citicoline and vitamin B(12) eye drops in type 1 diabetes: results of a 3-year pilot study evaluating morpho-functional retinal changes. *Adv Ther.* (2020) 37:1646–63. doi: 10.1007/s12325-020-01284-3
94. Hsieh YT, Alam MN, Le D, Hsiao CC, Yang CH, Chao DL, et al. OCT angiography biomarkers for predicting visual outcomes after ranibizumab treatment for diabetic macular edema. *Ophthalmol Retina.* (2019) 3:826–34. doi: 10.1016/j.oret.2019.04.027
95. Hunt M, Teper S, Wylęgała A, Wylęgała E. Response to 1-year fixed-regimen bevacizumab therapy in treatment-naïve DME patients: assessment by OCT angiography. *J Diabetes Res.* (2022) 2022:3547461. doi: 10.1155/2022/3547461
96. Carnota-Méndez P, Méndez-Vázquez C, Pérez-Gavella C. OCT-angiography changes in patients with diabetic macular edema treated with intravitreal dexamethasone implant. *Clin Ophthalmol.* (2022) 16:247–63. doi: 10.2147/OPTH.S345947
97. Korobelnik JF, Gaucher D, Baillif S, Creuzot-Garcher C, Kodjikian L, Weber M. Optical coherence tomography angiography in diabetic macular edema treated with intravitreal aflibercept: A 48-week observational study (the DOCTA study). *Ophthalmologica.* (2023) 246:71–80. doi: 10.1159/000528426
98. Hormel TT, Hwang TS, Bailey ST, Wilson DJ, Huang D, Jia Y. Artificial intelligence in OCT angiography. *Prog Retin Eye Res.* (2021) 85:100965. doi: 10.1016/j.preteyeres.2021.100965
99. Rajesh AE, Davidson OQ, Lee CS, Lee AY. Artificial intelligence and diabetic retinopathy: AI framework, prospective studies, head-to-head validation, and cost-effectiveness. *Diabetes Care.* (2023) 46:1728–39. doi: 10.2337/dci23-0032
100. Le D, Alam M, Yao CK, Lim JI, Hsieh YT, Chan RVP, et al. Transfer learning for automated OCTA detection of diabetic retinopathy. *Transl Vis Sci Technol.* (2020) 9:35. doi: 10.1167/tvst.9.2.35
101. Eladawi N, Elmogy M, Khalifa F, Ghazal M, Ghazi N, Aboelfetouh A, et al. Early diabetic retinopathy diagnosis based on local retinal blood vessel analysis in optical coherence tomography angiography (OCTA) images. *Med Physics.* (2018) 45:4582–99. doi: 10.1002/mp.2018.45.issue-10
102. Xu X, Yang P, Wang H, Xiao Z, Xing G, Zhang X, et al. AV-casNet: fully automatic arteriole-venule segmentation and differentiation in OCT angiography. *IEEE Trans Med Imaging.* (2023) 42:481–92. doi: 10.1109/TMI.2022.3214291
103. Schottenhamml J, Moulton EM, Ploner SB, Chen S, Novais E, Husvogt L, et al. OCT-OCTA segmentation: combining structural and blood flow information to segment Bruch's membrane. *BioMed Opt Express.* (2021) 12:84–99. doi: 10.1364/BOE.398222
104. Ryu G, Lee K, Park D, Park SH, Sagong M. A deep learning model for identifying diabetic retinopathy using optical coherence tomography angiography. *Sci Rep.* (2021) 11:23024. doi: 10.1038/s41598-021-02479-6
105. Mastropasqua R, Toto L, Mastropasqua A, Aloia R, De Nicola C, Mattei PA, et al. Foveal avascular zone area and parafoveal vessel density measurements in different stages of diabetic retinopathy by optical coherence tomography angiography. *Int J Ophthalmol.* (2017) 10:1545–51. doi: 10.18240/ijo.2017.10.11
106. Cheong KX, Lee SY, Ang M, Teo KYC. Vessel density changes on optical coherence tomography angiography after vascular endothelial growth factor inhibitor treatment for diabetic macular edema. *Turk J Ophthalmol.* (2020) 50:343–50. doi: 10.4274/tjo.galenos.2020.81592
107. Wang Y, Shen Y, Yuan M, Xu J, Yang B, Liu C, et al. A deep learning-based quality assessment and segmentation system with a large-scale benchmark dataset for optical coherence tomographic angiography image. *Arxiv.* (2021), 2107.10476. doi: 10.2139/ssrn.4073651
108. Hashmi S, Lopez J, Chiu B, Sarrafpour S, Gupta A, Young J. Fractal dimension analysis of OCTA images of diabetic retinopathy using circular mass-radius method. *Ophthalmic Surg Lasers Imaging Retina.* (2021) 52:116–22. doi: 10.3928/23258160-20210302-01
109. Le D, Alam M, Taeyoon S, Lim JI, Xincheng Y. Deep learning artery-vein classification in OCT angiography. *Proc SPIE - Prog Biomed Optics Imaging.* (2021) 11623:116231B. doi: 10.1117/12.2577304
110. Athwal A, Balaratnasingam C, Yu DY, Heisler M, Sarunic MV, Ju MJ. Optimizing 3D retinal vasculature imaging in diabetic retinopathy using registration and averaging of OCT-A. *BioMed Opt Express.* (2021) 12:553–70. doi: 10.1364/BOE.408590
111. Elsharkawy M, Elrazaz M, Sharafeldien A, Alhalabi M, Khalifa F, Soliman A, et al. The role of different retinal imaging modalities in predicting progression of diabetic retinopathy: A survey. *Sensors (Basel).* (2022) 22(9):3490. doi: 10.3390/s22093490
112. Lo J, Yu TT, Ma D, Zang P, Owen JP, Zhang Q, et al. Federated learning for microvasculature segmentation and diabetic retinopathy classification of OCT data. *Ophthalmol Sci.* (2021) 1:100069. doi: 10.1016/j.xops.2021.100069
113. Yang WH, Shao Y, Xu YW. Guidelines on clinical research evaluation of artificial intelligence in ophthalmology (2023). *Int J Ophthalmol.* (2023) 16:1361–72. doi: 10.18240/ijo.2023.09.02
114. Eladawi N, Elmogy M, Ghazal M, Fraiwan L, Aboelfetouh A, Riad A, et al. Diabetic retinopathy grading using 3D multi-path convolutional neural network based on fusing features from OCTA scans, demographic, and clinical biomarkers. *2019 IEEE International Conference on Imaging Systems and Techniques (IST).* (2019), 1–6. doi: 10.1109/IST48021.2019
115. Vujosevic S, Limoli C, Nucci P. Novel artificial intelligence for diabetic retinopathy and diabetic macular edema: what is new in 2024? *Curr Opin Ophthalmol.* (2024) 35:472–9. doi: 10.1097/ICU.0000000000001084
116. Lupidi M, Gujar R, Cerquaglia A, Chablani J, Fruttini D, Muzi A, et al. OCT-Angiography as a reliable prognostic tool in laser-treated proliferative diabetic retinopathy: The RENOCTA Study. *Eur J Ophthalmol.* (2021) 31:2511–9. doi: 10.1177/1120672120963451

Frontiers in Endocrinology

Explores the endocrine system to find new therapies for key health issues

The second most-cited endocrinology and metabolism journal, which advances our understanding of the endocrine system. It uncovers new therapies for prevalent health issues such as obesity, diabetes, reproduction, and aging.

Discover the latest Research Topics

[See more →](#)

Frontiers

Avenue du Tribunal-Fédéral 34
1005 Lausanne, Switzerland
frontiersin.org

Contact us

+41 (0)21 510 17 00
frontiersin.org/about/contact

